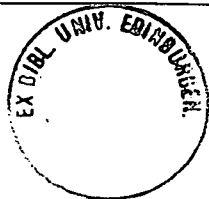


SEDIMENTOLOGY, NEOTECTONICS AND GEOMORPHOLOGY  
RELATED TO TECTONIC UPLIFT AND SEA-LEVEL CHANGE:  
QUATERNARY OF CYPRUS.

ANDREW JOHN POOLE

THESIS SUBMITTED FOR THE DEGREE OF  
DOCTOR OF PHILOSOPHY  
DEPARTMENT OF GEOLOGY AND GEOPHYSICS  
UNIVERSITY OF EDINBURGH  
1992



**Declaration:**

**This thesis is my own work, except where specifically stated.**

**Andrew J. Poole (10th March 1992).**

## **Abstract.**

A combination of northward underthrusting of the African plate and serpentinite diapirism has resulted in rapid uplift of southern Cyprus during the latest Pliocene-Quaternary; this uplift marks the culmination of a sedimentary sequence that indicates progressively shallower environments from the Upper Cretaceous through to the Recent. The Quaternary uplift was associated with the development of a succession of alluvial fans and marine terraces. Marine terraces in coastal southern Cyprus are developed at 350-360m, 110-100m, 60-50m, 11-8m and 2-3m above the present sea-level.

The marine sediments within each terrace reflect transgressive and then regressive conditions, with the deposition of sedimentary sequences in sub-littoral, littoral and finally subaerial environments. Shallow marine carbonate sequences crop out within the preserved terraces at locations outwith the influence of the major drainage systems, whereas the preserved deltaic and siliciclastic littoral successions mark the continuum of the onshore fluvial sequences offshore.

Alluvial fans of the Faglomerate Group, correlatable with the early marine terraces, crop out on the northern flanks of the Troodos Massif, forming extensive, dissected, peneplaned terraces. Later uplift resulted in the formation of channel fans and river terraces. Proximal sheetflood conglomerates pass distally into channelised braidplain environments. On the southern margin of the Troodos Massif the Faglomerate Group comprises braided, channelised and floodplain sequences, although much of the sediment bypassed continental environments and was deposited as shallow marine facies.

Provenance studies indicate that uplift and resulting erosion of Cyprus was centred on Mount Olympus, in the Troodos Massif. Field evidence indicates that neotectonic faulting has played a limited role during the Quaternary period, the development of the Polis-Paphos graben, in south-west Cyprus, is a notable exception. Uranium-series dates and amino-acid data reveal that uplift of the island was reasonably uniform during the latest Quaternary, with a maximum rate of uplift of c.10cm/ka. over the last 185ka. The available age data and geomorphological and sedimentological evidence indicate that uplift of the southern portion of Cyprus was most rapid in the early and middle Pleistocene, i.e. an average rate of c.20cm/ka. In the Late Pleistocene, when the rate of uplift was reduced, eustatic sea-level changes dominated. Anthropogenic induced modifications and local submergence of southern coastal areas have effected Cyprus during the Holocene.

The formation and preservation of Quaternary sediments, geomorphological and tectonic features in southern Cyprus, represents the interaction of tectonic uplift, isostatic effects, eustatic sea-level changes and climate variations.

## Contents

|                        |     |
|------------------------|-----|
| Declaration .....      | i   |
| Abstract .....         | ii  |
| Contents .....         | iii |
| Acknowledgements ..... | ix  |

### Chapter One: Introduction.

|                                                                       |    |
|-----------------------------------------------------------------------|----|
| 1.1 Objectives and rationale .....                                    | 1  |
| 1.2 Tectonic setting of Cyprus.....                                   | 2  |
| 1.3 Geological history and structural setting of Cyprus.....          | 3  |
| 1.3.1 Cyprus terranes .....                                           | 9  |
| 1.3.1.1 The Troodos and Mamonia terranes .....                        | 9  |
| 1.3.1.2 The Kyrenia terrane .....                                     | 12 |
| 1.3.2 Late Cretaceous to pre-Quaternary sedimentary history .....     | 12 |
| 1.4 Processes causing uplift.....                                     | 16 |
| 1.5 Previous work .....                                               | 19 |
| 1.5.1 Cyprus .....                                                    | 21 |
| 1.5.2 Comparable studies world-wide .....                             | 22 |
| 1.6 The Quaternary: definitions and problems .....                    | 22 |
| 1.6.1 Definitions.....                                                | 22 |
| 1.6.2 Quaternary sea-level changes.....                               | 23 |
| 1.7 Thesis organisation and techniques used.....                      | 23 |
| 1.7.1 Organisation .....                                              | 23 |
| 1.7.2 Techniques .....                                                | 25 |
| 1.8 Stratigraphy.....                                                 | 26 |
| 1.8.1 Mediterranean and previous Cyprus Quaternary stratigraphy ..... | 26 |
| 1.8.2 Stratigraphy used in this thesis.....                           | 32 |

### Chapter Two: Geomorphology.

|                                                                                                              |    |
|--------------------------------------------------------------------------------------------------------------|----|
| 2.1 Introduction.....                                                                                        | 33 |
| 2.2 Drainage patterns .....                                                                                  | 33 |
| 2.2.1 Introduction .....                                                                                     | 35 |
| 2.2.2 Radial drainage pattern around the Troodos Massif.....                                                 | 36 |
| 2.2.3 The lateral, east-west, drainage pattern through the centre of the Mesaoria Plain.....                 | 36 |
| 2.2.4 The nature of the drainage pattern along the southern coast of the island.....                         | 37 |
| 2.2.5 The effect of pre-existing tectonic structures and topographical features on the drainage pattern..... | 42 |
| 2.2.6 Evidence for river capture.....                                                                        | 44 |
| 2.2.7 The formation of gorges associated with the development of the Quaternary drainage pattern.....        | 47 |
| 2.3 Erosion surfaces .....                                                                                   | 48 |
| 2.3.1 North Troodos margin.....                                                                              | 48 |
| 2.3.2 Southern coastal areas.....                                                                            | 56 |
| 2.3.3 South-eastern Cyprus .....                                                                             | 58 |
| 2.3.4 The Polis-Paphos graben.....                                                                           | 60 |
| 2.4 Coastal geomorphology.....                                                                               | 60 |
| 2.4.1 Introduction .....                                                                                     | 60 |
| 2.4.2 Palaeo-clifflines and associated features in south-west Cyprus.....                                    | 62 |
| 2.4.3 Palaeo-clifflines and associated features in south-east Cyprus.....                                    | 64 |
| 2.4.3.1 Beach ridges of south-east Cyprus .....                                                              | 66 |
| 2.4.4 Palaeo-clifflines and associated features in south Cyprus.....                                         | 66 |
| 2.4.5 Palaeo-clifflines and associated features in the Polis-Paphos graben and along                         |    |

|                                                                                                                          |    |
|--------------------------------------------------------------------------------------------------------------------------|----|
| the north coast of the island .....                                                                                      | 68 |
| 2.4.6 Bathymetric data .....                                                                                             | 69 |
| 2.4.7 Dune development .....                                                                                             | 69 |
| 2.4.8 The effects of sea-level change on the development of the geomorphology of southern Cyprus: two case studies ..... | 71 |
| 2.4.9 Karst .....                                                                                                        |    |
| 2.5 Colluvium .....                                                                                                      | 72 |
| 2.6 Interpretation, discussion and conclusions .....                                                                     | 72 |
| 2.6.1 Drainage pattern .....                                                                                             | 72 |
| 2.6.2 Erosion surfaces .....                                                                                             | 74 |
| 2.6.3 Coastal geomorphology .....                                                                                        | 77 |
| 2.6.4 Discussion .....                                                                                                   | 78 |
| 2.6.5 Conclusions .....                                                                                                  | 81 |

### Chapter Three: Quaternary biostratigraphy and geochronology.

|                                                   |     |
|---------------------------------------------------|-----|
| 3.1 Introduction .....                            | 82  |
| 3.2 Palaeontology .....                           | 85  |
| 3.2.1 Micropalaeontology .....                    | 85  |
| 3.2.2 Invertebrate palaeontology .....            | 86  |
| 3.2.3 Vertebrate palaeontology .....              | 88  |
| 3.2.3.1 Introduction .....                        | 88  |
| 3.2.3.2 Occurrence .....                          | 89  |
| 3.2.3.3 Fauna .....                               | 89  |
| 3.3 Geochronological dating methods .....         | 90  |
| 3.3.1 Uranium series disequilibrium method .....  | 90  |
| 3.3.1.1 Introduction .....                        | 90  |
| 3.3.1.2 Sampling and analytical techniques .....  | 95  |
| 3.3.1.3 Results of analysis .....                 | 96  |
| 3.3.2 Amino-acid racemization/epimerization ..... | 98  |
| 3.3.2.1 Introduction .....                        | 98  |
| 3.3.2.2 Analytical methods .....                  | 100 |
| 3.3.2.3 Results .....                             | 100 |
| 3.3.3 Radiocarbon method .....                    | 107 |
| 3.3.3.1 Introduction .....                        | 107 |
| 3.3.3.2 Methodology .....                         | 108 |
| 3.3.3.3 Results .....                             | 108 |
| 3.4 Discussion and conclusions .....              | 109 |
| 3.4.1 Discussion .....                            | 109 |
| 3.4.2 Conclusions .....                           | 115 |

### Chapter Four: Neotectonics.

|                                                                     |     |
|---------------------------------------------------------------------|-----|
| 4.1 Introduction .....                                              | 117 |
| 4.2 Seismic studies .....                                           | 117 |
| 4.3 Earthquake data and borehole stress studies .....               | 120 |
| 4.4 Field evidence for Quaternary faulting in southern Cyprus ..... | 120 |
| 4.5 Discussion and conclusions .....                                | 128 |

### Chapter Five: The Fonglomerate Group.

|                                                              |     |
|--------------------------------------------------------------|-----|
| 5.1 Introduction .....                                       | 129 |
| 5.1.1 Nomenclature .....                                     | 129 |
| 5.1.2 Previous work .....                                    | 129 |
| 5.2 Geographical distribution and thickness variations ..... | 131 |
| 5.3 Sedimentary facies .....                                 | 134 |
| 5.3.1 The north Troodos margin .....                         | 134 |

|                                                                                                        |     |
|--------------------------------------------------------------------------------------------------------|-----|
| 5.3.1.1 Introduction .....                                                                             | 134 |
| 5.3.1.2 The F1 and F2 Fanglomerate units (lower-middle Pleistocene) .....                              | 134 |
| 5.3.1.3 The F3 Fanglomerate unit (early Late Pleistocene) .....                                        | 145 |
| 5.3.1.4 The F4 Fanglomerate unit (late Late Pleistocene) .....                                         | 146 |
| 5.3.2 South-eastern Cyprus .....                                                                       | 148 |
| 5.3.3 The south coast between Larnaca and the Akrotiri Peninsula .....                                 | 149 |
| 5.3.3.1 Introduction .....                                                                             | 149 |
| 5.3.3.2 The F1 and F2 Fanglomerate units (lower-middle Pleistocene) .....                              | 150 |
| 5.3.3.3 The F3 Fanglomerate unit (early late Pleistocene) .....                                        | 151 |
| 5.3.3.4 The F4 Fanglomerate unit and Recent fluvial sediments (late Late Pleistocene<br>-Recent) ..... | 153 |
| 5.3.4 South-western Cyprus .....                                                                       | 155 |
| 5.3.4.1 Introduction .....                                                                             | 155 |
| 5.3.4.2 The F1 Fanglomerate unit (lower Pleistocene) .....                                             | 156 |
| 5.3.4.3 Channellised F1 Fanglomerate unit sequences .....                                              | 156 |
| 5.3.4.4 The F1 and F2 Fanglomerate units cropping out in the Paphos area (lower<br>Pleistocene) .....  | 159 |
| 5.3.4.5 The F3 and F4 Fanglomerate units in south-west Cyprus (Late Pleistocene) .....                 | 159 |
| 5.3.4.6 Floodplain sequences of south-west Cyprus .....                                                | 161 |
| 5.3.5 The Fanglomerate units of the Polis-Paphos graben .....                                          | 161 |
| 5.3.6 The Fanglomerate units in the Kato Pyrgos area .....                                             | 163 |
| 5.3.7 The Fanglomerate units of the Kyrenia Range .....                                                | 165 |
| 5.4 Palaeocurrent studies .....                                                                        | 165 |
| 5.4.1 Introduction .....                                                                               | 165 |
| 5.4.2 Palaeocurrent data from the north Troodos margin .....                                           | 165 |
| 5.4.3 Coastal southern Cyprus .....                                                                    | 165 |
| 5.4.4 The north coast .....                                                                            | 168 |
| 5.5 Provenance studies .....                                                                           | 168 |
| 5.5.1 Clast analysis within the Fanglomerate Group .....                                               | 168 |
| 5.5.1.1 North Troodos margin .....                                                                     | 168 |
| 5.5.1.2 Clast analysis in south-east Cyprus .....                                                      | 171 |
| 5.5.1.3 The south coast region: Larnaca to Limassol .....                                              | 171 |
| 5.5.1.4 South-west Cyprus, the Polis-Paphos graben and the Kato Pyrgos area .....                      | 173 |
| 5.5.1.5 Fanglomerate units of the Kyrenia Range .....                                                  | 174 |
| 5.5.2 X-ray diffraction studies .....                                                                  | 176 |
| 5.5.2.1 Borehole samples .....                                                                         | 176 |
| 5.5.2.2 X-ray diffraction analysis of bone bed samples from the Fanglomerate Group ..                  | 180 |
| 5.5.3 X-ray fluorescence studies .....                                                                 | 180 |
| 5.6 Interpretation, discussion and conclusions .....                                                   | 182 |
| 5.6.1 Thickness variation .....                                                                        | 182 |
| 5.6.2 Sedimentology .....                                                                              | 186 |
| 5.6.2.1 Introduction .....                                                                             | 186 |
| 5.6.2.2 North Troodos margin .....                                                                     | 188 |
| 5.6.2.3 Model of deposition in coastal southern Cyprus .....                                           | 190 |
| 5.6.3 Palaeocurrents .....                                                                             | 193 |
| 5.6.4 Provenance .....                                                                                 | 194 |
| 5.6.4.1 North Troodos margin .....                                                                     | 194 |
| 5.6.4.2 South-east Cyprus .....                                                                        | 196 |
| 5.6.4.3 The south coast .....                                                                          | 196 |
| 5.6.4.4 South-west Cyprus .....                                                                        | 197 |
| 5.6.5 Summary .....                                                                                    | 197 |

## Chapter Six: Siliciclastic shallow marine sediments.

|                                                                                                               |     |
|---------------------------------------------------------------------------------------------------------------|-----|
| 6.1 Introduction.....                                                                                         | 199 |
| 6.2 Geographical distribution and age of siliciclastic shallow marine sequences .....                         | 199 |
| 6.3 Description of the Quaternary deltaic sequences.....                                                      | 201 |
| 6.3.1 South-east Cyprus.....                                                                                  | 201 |
| 6.3.1.1 The Dhekelia area .....                                                                               | 201 |
| 6.3.1.2 Ormidhia area.....                                                                                    | 201 |
| 6.3.1.3 Outcrops west of Cape Pyla .....                                                                      | 206 |
| 6.3.2 Southern Cyprus .....                                                                                   | 206 |
| 6.3.2.1 Sedimentary units .....                                                                               | 206 |
| 6.3.2.2 Provenance data.....                                                                                  | 210 |
| 6.3.2.3 Palaeocurrent data.....                                                                               | 210 |
| 6.3.3 The Polis-Paphos graben.....                                                                            | 210 |
| 6.3.3.1 Sedimentary units .....                                                                               | 210 |
| 6.3.4 Deltaic sequences of south-west Cyprus.....                                                             | 213 |
| 6.4 Siliciclastic beach sequences .....                                                                       | 214 |
| 6.4.1 Introduction .....                                                                                      | 213 |
| 6.4.2 F3 and F4 siliciclastic beach sequences of south-east Cyprus.....                                       | 214 |
| 6.4.2.1 Coarse conglomerate lag .....                                                                         | 214 |
| 6.4.2.2 Coarse and medium conglomerate .....                                                                  | 216 |
| 6.4.2.3 Fine conglomerate and coarse sand.....                                                                | 219 |
| 6.4.2.4 Sand units .....                                                                                      | 219 |
| 6.4.2.5 Sub-aerial and shelly hash units .....                                                                | 220 |
| 6.5 Interpretation, discussion and conclusions .....                                                          | 220 |
| 6.5.1 Deltaic sequences of south-east Cyprus.....                                                             | 220 |
| 6.5.1.1 Dhekelia .....                                                                                        | 220 |
| 6.5.1.2 Ormidhia .....                                                                                        | 221 |
| 6.5.1.3 Cape Pyla .....                                                                                       | 222 |
| 6.5.1.4 Model of deposition of the deltaic sequence in south-east Cyprus .....                                | 222 |
| 6.5.2 Deltaic sequences of the south coast and the Polis-Paphos graben.....                                   | 223 |
| 6.5.2.1 The south coast .....                                                                                 | 223 |
| 6.5.2.2 The Polis-paphos graben.....                                                                          | 226 |
| 6.5.2.3 Deltaic sequences of south-west Cyprus.....                                                           | 228 |
| 6.5.2.4 Models of deposition of the deltaic sediments of the south coast and the Polis<br>-Paphos graben..... | 229 |
| 6.5.3 Southern beach sequences.....                                                                           | 230 |
| 6.5.3.1 South-east Cyprus .....                                                                               | 230 |
| 6.5.4 Summary .....                                                                                           | 232 |

## Chapter Seven: Carbonate littoral and sub-littoral sediments.

|                                                                           |     |
|---------------------------------------------------------------------------|-----|
| 7.1 Introduction.....                                                     | 233 |
| 7.2 Geographical distribution .....                                       | 233 |
| 7.3 Sedimentology of the carbonate sequences.....                         | 234 |
| 7.3.1 Introduction .....                                                  | 234 |
| 7.3.2 The F0 carbonate sequences (upper Pliocene-lower Pleistocene) ..... | 234 |
| 7.3.3 The F1 carbonate sequences (lower-middle Pleistocene).....          | 236 |
| 7.3.3.1 Introduction .....                                                | 236 |
| 7.3.3.2 Sedimentary facies .....                                          | 237 |
| 7.3.4 The F2 carbonate sequences (Middle Pleistocene) .....               | 237 |
| 7.3.4.1 Introduction .....                                                | 237 |
| 7.3.4.2 Sedimentary facies.....                                           | 238 |
| 7.3.5 The F3 carbonate sequences (early Late Pleistocene).....            | 244 |
| 7.3.5.1 Introduction .....                                                | 244 |
| 7.3.5.2 Cape Greco.....                                                   | 244 |

|                                                                                        |     |
|----------------------------------------------------------------------------------------|-----|
| 7.3.5.3 Larnaca .....                                                                  | 246 |
| 7.3.5.4 Akrotiri Peninsula .....                                                       | 247 |
| 7.3.5.5 West coast of Cyprus .....                                                     | 247 |
| 7.3.5.6 The north coast between Polis and Kato Pyrgos .....                            | 252 |
| 7.3.5.7 Deposition of F3 carbonate sediments on wave cut platforms .....               | 254 |
| 7.3.6 The F4 carbonate sequences (late Late Pleistocene) .....                         | 254 |
| 7.3.6.1 Introduction .....                                                             | 254 |
| 7.3.6.2 South-east Cyprus .....                                                        | 255 |
| 7.3.6.3 Akrotiri .....                                                                 | 257 |
| 7.3.6.4 Paphos .....                                                                   | 258 |
| 7.3.7 Summary of the components of the carbonate sequences .....                       | 261 |
| 7.4 Petrology and diagenesis .....                                                     | 261 |
| 7.4.1 Introduction .....                                                               | 261 |
| 7.4.2 Petrographic analysis of the carbonate littoral and sub-littoral sequences ..... | 262 |
| 7.4.3 Summary .....                                                                    | 268 |
| 7.4.4 Diagenesis .....                                                                 | 269 |
| 7.5 Interpretation, discussion and conclusions .....                                   | 272 |
| 7.5.1 Introduction .....                                                               | 272 |
| 7.5.2 Interpretation .....                                                             | 273 |
| 7.5.2.1 The basal unconformity surface and conglomerate lag sequence .....             | 273 |
| 7.5.2.2 Coral and coralline algal framebuilders .....                                  | 273 |
| 7.5.2.3 Grainstones .....                                                              | 278 |
| 7.5.2.4 Sub-aerial deposits .....                                                      | 279 |
| 7.5.2.5 Diagenetic data .....                                                          | 279 |
| 7.5.3 Summary .....                                                                    | 279 |

### Chapter Eight: Aeolianite formations.

|                                                           |     |
|-----------------------------------------------------------|-----|
| 8.1 Introduction .....                                    | 282 |
| 8.2 Geographical distribution .....                       | 282 |
| 8.3 Lithological description .....                        | 284 |
| 8.4 Petrology .....                                       | 286 |
| 8.4.1 The mixed clastic aeolianites .....                 | 286 |
| 8.4.2 Carbonate aeolianites .....                         | 289 |
| 8.5 Palaeocurrent data .....                              | 291 |
| 8.6 Recent dune formation .....                           | 294 |
| 8.7 Discussion and conclusions .....                      | 295 |
| 8.8 Model of formation of the carbonate aeolianites ..... | 296 |

### Chapter Nine: Quaternary caliche and palaeosols: their formation and development.

|                                                              |     |
|--------------------------------------------------------------|-----|
| 9.1 Introduction .....                                       | 299 |
| 9.2 Distribution of caliche in Cyprus .....                  | 300 |
| 9.3 Caliche development on Cyprus .....                      | 303 |
| 9.4 Petrology and geochemistry of the caliche horizons ..... | 304 |
| 9.4.1 Caliche petrology .....                                | 305 |
| 9.4.2 X-ray diffraction data .....                           | 305 |
| 9.4.3 X-ray fluorescence data .....                          | 307 |
| 9.5 Speed and degree of formation of Recent caliche .....    | 312 |
| 9.6 Models of formation of the caliche .....                 | 312 |
| 9.6.1 Pedogenic caliche .....                                | 312 |
| 9.6.2 Mature crust .....                                     | 313 |
| 9.7 Palaeosol development .....                              | 315 |
| 9.7.1 Palaeosol characteristics .....                        | 315 |
| 9.7.2 Interpretation .....                                   | 316 |
| 9.8 Conclusions .....                                        | 317 |



## Chapter Ten: Discussions and conclusions

|                                                                                                                             |     |
|-----------------------------------------------------------------------------------------------------------------------------|-----|
| 10.1 Evolution of Cyprus during the Quaternary period.....                                                                  | 319 |
| 10.1.1 Upper Pliocene-lower Pleistocene: early uplift.....                                                                  | 319 |
| 10.1.2 Lower Pleistocene-middle Pleistocene (F1 and F2): main phase of uplift.....                                          | 319 |
| 10.1.3 Early Late Pleistocene (F3): further uplift.....                                                                     | 321 |
| 10.1.4 Late Late Pleistocene-Holocene (F4): slightly lowered base levels, submergence<br>and anthropogenic influences ..... | 322 |
| 10.2 Discussion.....                                                                                                        | 323 |
| 10.2.1 Tectonic uplift versus isostatic effects.....                                                                        | 323 |
| 10.2.2 Uplift versus sea-level change.....                                                                                  | 324 |
| 10.2.3 Nature of tectonic control .....                                                                                     | 326 |
| 10.3 Conclusions.....                                                                                                       | 328 |
| 10.3.1 Geomorphology .....                                                                                                  | 328 |
| 10.3.2 Sedimentology.....                                                                                                   | 329 |
| 10.3.3 Neotectonics.....                                                                                                    | 331 |
| 10.3.4 General .....                                                                                                        | 331 |
| 10.3.5 Summary .....                                                                                                        | 332 |
| 10.4 Further work.....                                                                                                      | 332 |
| References .....                                                                                                            | 334 |

**Appendix A: sample collection in store at the Department of Geology and Geophysics, Edinburgh University.**

**Appendix B: locations cited in the text**

**Appendix C: method for radiocarbon and uranium series disequilibrium dating**

**Appendix D: the occurrence of Plio-Pleistocene molluscs from Cyprus, with comparison of the age ranges of these fauna in the south-east and western Mediterranean (after Moshkovitz, 1968)**

**Appendix E: X-ray diffraction and fluorescence data**

**Appendix F: published papers**

## Acknowledgements.

This thesis is dedicated to my parents for their unswerving support and their belief in the impossible!

I acknowledge the receipt of an N.E.R.C. award and the University of Edinburgh for permission to use their facilities. I would like to thank my supervisors: Alastair Robertson, Claudio Vita-Finzi and Geoffrey Boulton, who provided constant guidance, encouragement and enthusiasm during the evolution of this study.

I thank those people in Cyprus who have made my field seasons enjoyable and constructive. The staff at the Geological Survey Department in Nicosia and especially Costas Xenophontos who assisted me throughout my time in the field, with lively discussion and unlimited technical and logistical support. Stuart Swiney, Vathi Moustaki and everybody else at C.A.R.R.I. provided me with a haven in Nicosia, a most congenial place even at the worst times. The following who provided accomodation, enlightened discussion and light relief from the fieldwork are thanked: Chris and Linda Houlin, John and Sheri Leonard, Murray McClennan and Co., diggers at Kalavastos, Eddie Peltenberg, Gordon, Paul and Louise *et al.* in Kissonerga, Mr. Michales in Marathounda, and Costas and Andriane Loizou in Mitsero. A special mention must go to Geoff, Kath, Sarah and Simon Morley and the "lads" for introducing me to the delights of service life. The warmth of the people and the beauty of the island of Cyprus will stay with me for a longtime.

This study has benefited from the experience of many people beyond Edinburgh, distilled through invaluable discussion with them:

Brian Rosen and Paul Taylor at the British Museum, London, Alan Lord and Liam Gallagher at University College London and Shimon Moshkovitz at the Israeli Geological Survey (palaeontology),  
 Dave Rothery at the Open University and Ian Dowman at University College London (remote sensing),  
 Paul Hearty at Duke University, North Carolina, U.S.A. and David Bowen and Gerald Sykes at Aberystwyth (amino-acid analysis),  
 Claudio Vita-Finzi ( $^{14}\text{C}$  analysis),  
 David Reese at the Field Museum, Chicago (dwarf mammal fauna),  
 and finally Basil Gomez (Indiana State University), Gilbert Kelling (Keele University), Martyn Pedley (Hull University), Dorit Sivan (Israeli Geological Survey) and all those post-grads who have spent time discussing this work.

The assistance and involvement of many people in Edinburgh ensured that this work was completed:

Graham Shimmield, Francis Lindsay, Steve Mowbray and Mike Saunders in the radiochemistry laboratory,  
 Dodie James and Godfrey Fitton for assistance with the X-ray fluorescence studies,  
 Geoff Angel for assistance with the X-ray diffraction studies,  
 Chris Clarke for showing me how to push buttons on the GEMS satellite imagery equipment,

Mike Baillie, Bob Cheeney, Cliff Ford, Richard Hindmarsh and John Miller for aid with computing,  
Diane Baty for aid with drafting and photography,  
Peder Aspen, John Dixon, Dick Kroon, Dave Priestley, Terry Scoffin and Sandy Tudhope for general advice and discussion,  
and finally the super secs, Denise, Heather, Helena and Patricia, to whom I owe a thousand thanks for their happy approach to life and their continuous help and advice.

I am very deeply indebted to Paul Degnan, Karen Dobbie, Ed Follows, Jean McCallum, Alastair Robertson and Sandy Tudhope who struggled through the earlier drafts of this thesis and my father for proof reading the final product, although I alone am responsible for any errors in this work.

My office mates, flat mates, fellow Cyprus and Tethyan fieldworkers and post-grads, unfortunately too numerous to mention, are all thanked for their support, never ending distractions, and especially their patience and humour. Sandra Brown and Neil Stewart proved to be sound flatmates, allowing me to retreat into madness whenever necessary. I am also deeply indebted to Sandra Brown for her sterling work with the production of photographic plates. I would like to thank Pete, Den, Irene and Martin at DFR, Lowestoft for their patience and help over the last nine months. Finally to Jan, thanks for all your support, help and food - I hope it was worth it.

Ed Follows is owed special thanks for saving me from the clutches of the Klirou Police, keeping me sane (well nearly), nabbing my accomodation, introducing me to the delights of Ayia Napa, and finally departing for Brunei before he could finish reviewing this thesis!

# **Chapter One: Introduction.**

## **1.1 OBJECTIVES AND RATIONALE.**

Many of the previous studies of the geology of Cyprus have focused on the evolution and emplacement of the Troodos ophiolite. Far fewer studies have examined the Upper Cretaceous-Recent sedimentary cover sequence, which documents the syn- and post-ophiolite emplacement history. Recent theses (Eaton, 1987; McCallum, 1989; Follows, 1990) have examined the Neogene sedimentology and the relationship between this and the regional tectonic framework. However, the Quaternary uplift of the island, which has resulted in Mount Olympus standing at 1951m above present sea-level, has only been described in general terms (Robertson, 1977; McCallum, 1989) and only limited studies have focused on the Quaternary evolution of Cyprus. Active neotectonic faulting has occurred along the Cyprus Arc and on Cyprus during the Quaternary and Recent (Kempler & Ben-Avraham, 1987; Ward & Robertson, 1987) but the relationship between this faulting and the tectonic uplift of Cyprus has not been examined.

Previous studies of the Quaternary sedimentary sequence have been limited to the coarse fluvial conglomerates that crop out on the Mesaoria Plain but there are also other Quaternary sedimentary environments. What is the relationship between these and the fluvial conglomerates and how do these sediments vary, both temporally and spatially, throughout the Quaternary? What is the relationship between uplift and Quaternary climate changes? The Quaternary sediments should possess some evidence that sheds light on the unroofing and uplift of the Troodos ophiolite and southern Cyprus.

Quaternary geomorphological features have been identified in various parts of Cyprus in the past (De Vaumas, 1959, 1961, 1962; Ducloz, 1965; Dreghorn, 1978) but these features have not been correlated throughout the island and therefore the effects of neotectonics and the relationship between geomorphology and the Quaternary sediments has not been studied.

Quaternary eustatic sea-level changes have interacted with tectonic uplift and isostatic changes. The role of eustatic sea-level changes and the relative importance of these changes compared to tectonic uplift and isostasy and their relation to the geomorphology and patterns of sedimentation have not been considered in the past.

The aim of this work is to build on the immediately preceding research of McCallum (1989) and Follows (1990), with the following specific objectives:

- i) to establish a Quaternary stratigraphy that unifies previous work in local areas and can be applied to all geographical areas of southern Cyprus but is not dependent on varied sedimentary environments and geomorphological features,
- ii) to detail the Quaternary geomorphology and sedimentology in all areas of southern Cyprus,
- iii) to relate the pattern of geomorphology and sedimentology to uplift of the island and climatic and eustatic sea-level changes,
- iv) to examine in detail provenance, drainage and palaeocurrent data, seeking evidence for progressive unroofing of the Troodos ophiolite,
- v) to study the evidence for neotectonic faulting and discern what effect faulting has had on the evolving pattern of sedimentology and geomorphology,
- vi) to complete absolute dating of the fossil marine terraces to deduce rates of coastal uplift and so allow any differential uplift around the coast to be discerned,
- vii) to compare and contrast the late Pliocene to early Pleistocene and Recent evolution of Cyprus,
- viii) to examine the Quaternary environmental changes (i.e. climate and eustatic sea-level changes) and consider whether these can be distinguished and deduce the relative importance of eustatic sea-level changes and tectonic uplift,
- ix) and, most importantly, to provide a framework covering the whole of the Quaternary of southern Cyprus upon which future studies (geological, geographical or archaeological) can build.

As limited work had been carried out in a number of areas throughout southern Cyprus and whole of southern Cyprus has undergone uplift it was decided to correlate the previous work using the whole of southern Cyprus as the field area in an attempt to determine the Quaternary evolution of this portion of the island. It was decided at the outset of this work that a detailed process orientated approach to the sedimentology would not be feasible due to the extent of the proposed field area and the aims of the project (see above). Fieldwork was not possible in the Turkish-occupied portion of the island, i.e. near to, or north of the Greenline. Studies of the Quaternary sediments of the Polis-Paphos graben were minimised as these formed part of a project that was originally being undertaken by L.C. Ward but now forms part of a project by Ann Payne (Edinburgh University).

## **1.2 TECTONIC SETTING OF CYPRUS.**

The Eastern Mediterranean has had a complex tectonic history, with multiple plate interactions resulting from the closure of the Tethys Ocean during the late Palaeozoic, and subsequent opening and closure of small ocean basins during the

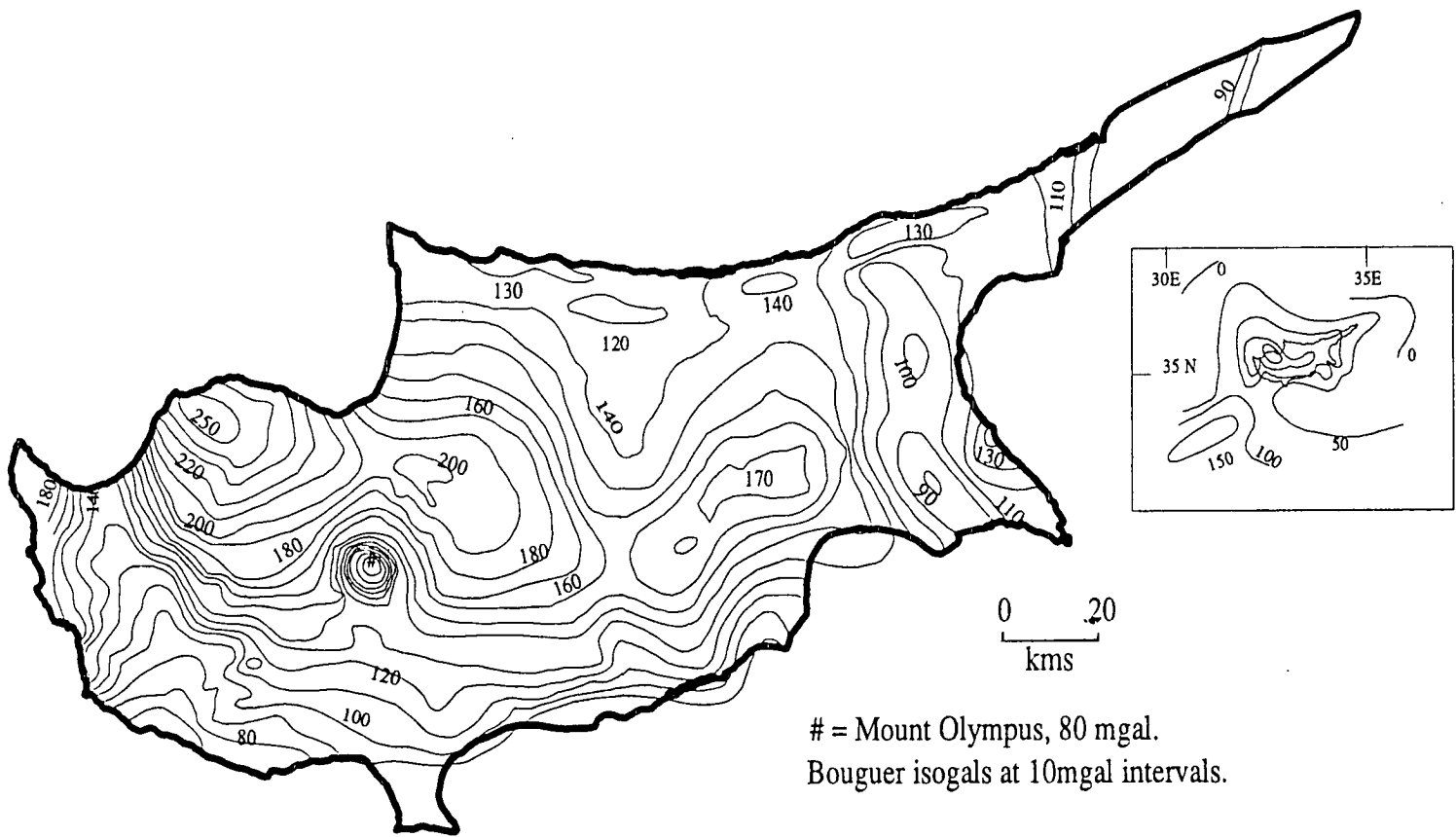
Mesozoic and Cenozoic (Robertson & Dixon, 1984). This tectonic activity has resulted in the coupling of many macro- and micro-plates to form a complex mosaic of terranes, i.e. a discrete tectonic unit with a distinct geological history (Coney *et al.*, 1980), in the Eastern Mediterranean. An intricate zone of convergence (Fig.1.1) now exists between the African and Arabian plates to the south and the Eurasian and Turkish/Anatolia plates to the north (Rotstein, 1984; Dercourt *et al.*, 1985; Dewey *et al.*, 1986).

Cyprus, set in the Levantine Basin of the eastern Mediterranean (Fig.1.1) is situated just to the north of a present day northward-dipping oceanic subduction zone, delineated by the Cyprus Arc. This arc forms the boundary between the African and Eurasian plates which have undergone collision and accretion in the past, as reflected by the presence of ophiolites and allochthonous terranes. High positive Bouguer gravity anomalies (Fig.1.2; Woodside & Bowin, 1970; Woodside, 1976) and evidence for high crustal seismic velocities (Makris *et al.*, 1983), magnetic anomalies and heat flow characteristics suggest that oceanic or transitional crust is still present in the area.

Kempler & Ben-Avraham (1987) divide the Cyprus Arc into three distinct units (Fig.1.1): the western segment extends west to the Hellenic Arc following the line of the Giermann Fault, passing to the north of the Eratosthenes Seamount along the Florence Rise (Fig.1.1). The Giermann Fault delineates an inferred plate boundary (Kempler & Ben-Avraham, 1987) which is thought to be undergoing oblique subduction at present (Rotstein & Kafka, 1982). Disturbed bathymetry, earthquake hypocentres (shallow and intermediate), with the seismic belt in this area following the Mediterranean Ridge, and a positive Bouguer gravity anomaly, support subduction of the African plate to the north, under the Eurasian plate (Rotstein & Kafka, 1982). Finetti (1976) suggests that the Mediterranean ridge is an integral part of the plate boundary and possibly an accretionary wedge of sediments. Many workers (Gass & Masson-Smith, 1963; McKenzie, 1970, 1972; Dewey *et al.*, 1973; Nur & Ben-Avraham, 1978; Dewey & Sengor, 1979) believe that the western end of the Cyprus Arc meets the Hellenic Arc as a cusp with the apex in south-west Turkey.

In the central zone of the Cyprus Arc the Eratosthenes seamount, a possible oceanic plateau (Rotstein, 1984; Ben-Avraham & Nur, 1986) or micro-continental block (Kempler & Ben-Avraham, 1987), is at present approaching the Cyprus Arc and is thought to be preventing subduction. Magnetic data suggest that the sub-surface extent of the seamount is considerable (Makris *et al.*, 1983); this may suggest contact with the subduction zone at present. The seamount is at present undergoing intense faulting as a possible precursor to future continued subduction (Kempler & Ben-Avraham, 1987) similar to that seen in the Hellenic Arc (Stride *et al.*, 1977) and Japan trench (Le Pichon





# = Mount Olympus, 80 mgal.  
 Bouguer isogals at 10mgal intervals.

Fig. 1.2. Bouguer anomaly gravity map of Cyprus (after Gass & Masson-Smith, 1963).  
 Note: the local gravity "low" (80mgals.) associated with Mount Olympus.



*et al.*, 1987). Seismic data (Rotstein & Kafka, 1982) suggest a subduction zone under central Cyprus, dipping at 25-30° towards the north-north-west.

There is little evidence of a plate boundary in the eastern zone of the Cyprus Arc, e.g. undeformed sediments, or an arc continuing to the east into the Levant (Neev, 1975; Nur & Ben-Avraham, 1978). However, many authors (McKenzie, 1970, 1976, 1978; Dewey *et al.*, 1973; Angelier, 1978; Sengor, 1979; Rotstein & Kafka, 1982) believe that there is a boundary to the east that continues into the Amamus mountains and beyond. Kempler & Ben-Avraham (1987) note that plate geometry in the north-east Mediterranean is ambiguous and the relative plate motions are uncertain. It has been suggested that strike-slip faulting is taking place in this area (Neev, 1975; Nur & Ben-Avraham 1978) similar to that seen in the eastern segment of the Hellenic Arc. However, Rotstein & Kafka (1982) suggest that the available data are "inconsistent with a major transform fault in the Cyprus Arc east of Cyprus". A great amount of uncertainty still exists, therefore, concerning the relative plate motions along the eastern segment of the Cyprus Arc.

The relative position and timing of subduction along the plate boundary in the Cyprus area has attracted much discussion (McKenzie, 1970; Lort, 1971; North, 1974; Le Pichon & Angelier, 1979; Robertson & Woodcock, 1980). Robertson and Woodcock (1980) proposed that a northward dipping Benioff zone south of Cyprus was initiated in the early Neogene. Earthquake hypocentres support this view (Kempler & Ben-Avraham, 1987). Robertson (1990) and McCallum (1989) suggest a supra-subduction zone setting from the Oligocene to Late Pliocene with possible pulsed underthrusting of oceanic and continental fragments. Associated normal faulting and subsidence, consistent with the possible southward migration of the subduction zone, is also noted. Robertson *et al.* (1991) suggest that only limited subduction of Neotethyan ocean has taken place since the Oligocene, with slow and/or episodic subduction. Stable palaeomagnetic inclinations recorded in the mid- to late Miocene chalks of southern Cyprus correspond to those in the Pliocene marls of Cyprus; these in turn being equivalent to a 35°N position seen today (Clube, 1985; Clube & Robertson, 1986; Abrahamsen & Schonharting, 1987). These palaeomagnetic data lead to an inference that convergence during the Neogene took place to the north of Cyprus. Eaton (1987) suggests that northward dipping subduction continued through the Lower Miocene with the formation of a series of sub-basins (Fig.1.3; Maroni, Eaton, 1987; Pissouri, Elion, 1983; Polemi, Orszag-Sperber *et al.*, 1980; Polis, Baroz *et al.*, 1978, Orszag-Sperber *et al.*, 1989) and sub-parallel, compressional lineaments (Fig.1.3; Ayia Mavri, Yerasa, Akrotiri; Bear & Morel, 1960; Eaton, 1987; Robertson *et al.*, 1991) in southern Cyprus. Associated intense deformation, uplift and folding during the lower Miocene has been attributed to renewed

underthrusting and/or associated accretion to the south of the island. This Miocene convergence is possibly comparable to the inferred motion witnessed today resulting from the probable collision of a proto-seamount with southern Cyprus (Robertson, 1990). Underthrusting of oceanic crust was apparently reactivated in late Miocene times as a result of reorganised stress regimes caused by the final collision of the African and Eurasian plates to the east (Robertson, 1990).

In northern Cyprus, a plate boundary between the Troodos and Kyrenia mountains is inferred to have existed from the Late Cretaceous to Late Eocene (Robertson & Woodcock, 1986). Pliocene subsidence and the almost undeformed nature of the Pliocene to Recent sediments in the Mesaoria Plain to the north of the Troodos Massif suggests that this plate boundary in northern Cyprus has been inactive since Oligocene times (Robertson & Woodcock, 1986; Kempler & Ben-Avraham, 1987). The Kyrenia Range exhibits tilted terraces (Dreghorn, 1978) which formed as a result of north-south compression; the terraces on the southern flank of the mountain also display east-west warping, with a decreasing altitude to the east and west, away from the Central Range (Dreghorn, 1978). The dramatic Pleistocene uplift of Mount Olympus (Robertson, 1977) has been attributed to large scale serpentinite diapirism (Moores & Vine, 1971). However, this dramatic uplift is thought to be superimposed on a basal ridge causing regional uplift that extends north into the Kyrenia Range and the Misis Mountains of southern Turkey, affecting a large area (Robertson, 1990).

Cyprus has acted as a single structural unit since the beginning of the Quaternary period (Robertson, 1990). The lack of subduction at present is thought to result from the proximity of the Eratosthenes Seamount with Cyprus (Kempler & Ben-Avraham, 1987), but Robertson (1990) postulates that subduction is very likely to continue in the future with true continental collision resulting. The presence of an active margin type of coast, i.e. rugged shorelines, irregular sea cliffs, coastal mountains and elevated sea terraces, with former wave-cut platforms (Kennet, 1986), in Cyprus is suggestive of compressional tectonics, or a zone of coastal collision (Kennett, 1986).

### **1.3 GEOLOGICAL HISTORY AND STRUCTURAL SETTING OF CYPRUS.**

The following introduction to the geology of Cyprus is split into two sections:

- i) a summary of the three tectonic terranes that constitute the island, i.e. the Troodos, Mamonnia and Kyrenia (Fig.1.3 and Table 1.1),
- ii) an outline of the sedimentary cover of Upper Cretaceous to Recent age that preceded the initial amalgamation of the Troodos and Mamonnia terranes, and obduction of the Troodos ophiolite (Tables 1.2 and 1.3).

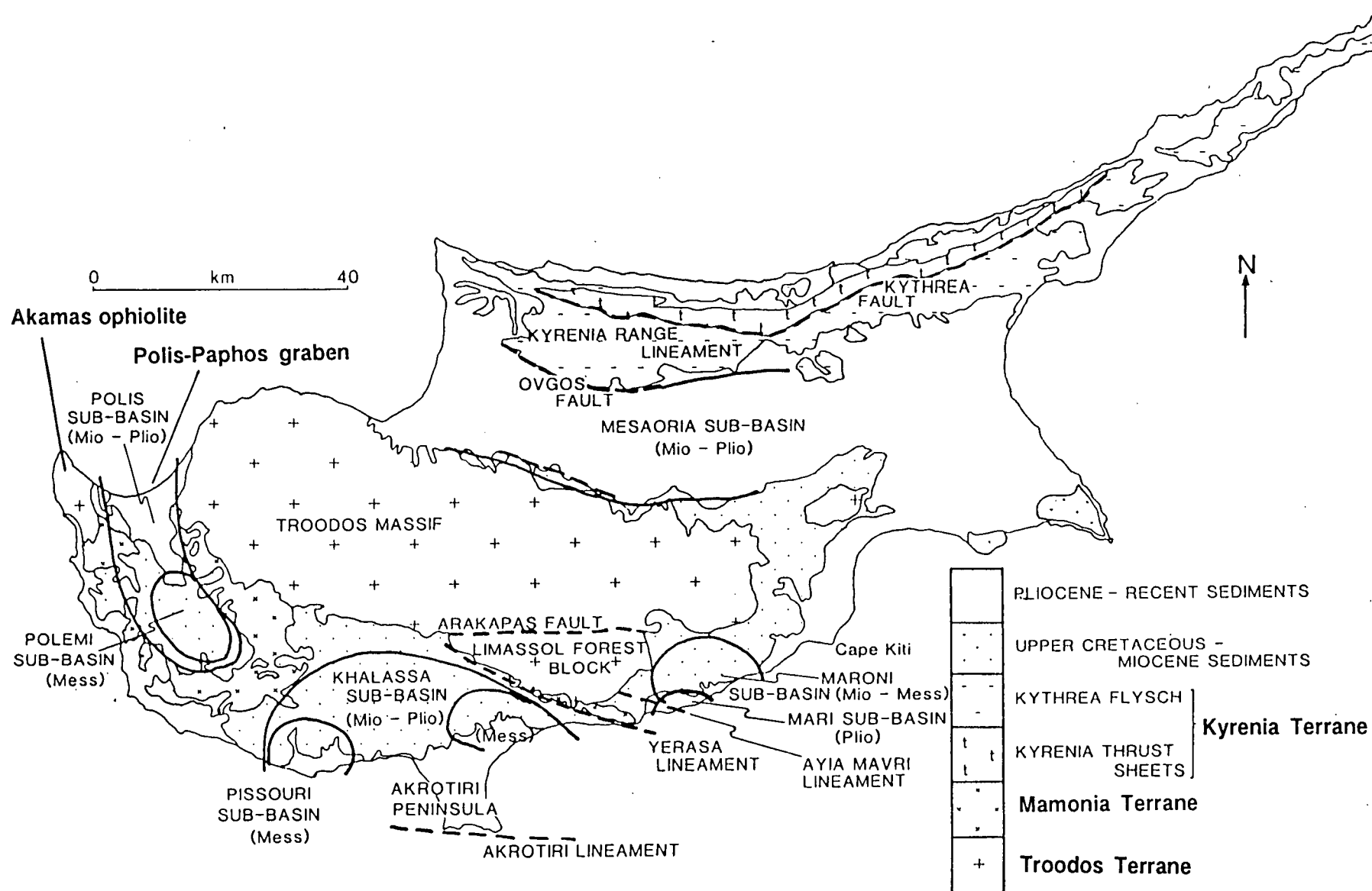


Fig.1.3. Major structural elements of Cyprus (after Robertson *et al.*, 1991).

### **1.3.1 Cyprus terranes.**

#### **1.3.1.1 The Troodos and Mamonia terranes.**

The Troodos terrane, a Late Cretaceous (92-85Ma., Mukasa & Ludden, 1987) ophiolite complex (Gass & Masson-Smith, 1963), dominates the island, forming an elongate west-north-west to east-south-east body rising to 1951m on Mount Olympus. The whole ophiolite stratigraphy is exposed with deep structural levels (ultramafic and mafic units) cropping out in the centre of the Troodos Massif (Fig.1.4). The diabase dyke complex and pillow lavas lie at respectively greater distances from the ultramafic core forming a concentric outcrop pattern.

The Troodos ophiolite is thought to have formed in a supra-subduction zone setting (Pearce *et al.*, 1984; Clube & Robertson, 1986; Gass, 1990; Murton, 1990; Robertson, 1990), with genesis having taken place at a spreading centre above a young intra-oceanic subduction zone. Subsequent collision/subduction caused the detachment and rotation of the Troodos microplate (Clube & Robertson, 1986) relative to the areas to the south of the Arakapas fault belt (Fig.1.3; Allerton & Vine, 1990; Bonhommet *et al.*, 1988), which is a fossil transform fault belt (Moores & Vine, 1971; Simonian & Gass, 1978; Murton, 1986; Murton & Gass, 1986). Rotation of the Troodos microplate continued until the Early Eocene (Clube & Robertson, 1986) and totalled 90° anticlockwise motion, relative to the zones to the south. Rotation along structurally weak strike-slip lineaments brought the Troodos terrane into contact with the continental margin of the Troodos ocean, i.e. the Mamonia terrane (Figs.1.3 and 1.4). Rotation of the Troodos terrane caused slivers of the ophiolite stratigraphy to be caught between the Mamonia and Troodos terranes in south-west Cyprus (Robertson, 1990).

The Mamonia terrane is apparently underlain by a crust of lower density and different origin to that of the adjacent Troodos terrane (Gass & Masson-Smith, 1963; Vine *et al.*, 1973; Clube & Robertson, 1986) and is thought to have formed due to rifting along the north margin of Gondwana (Lapierre, 1975; Lapierre & Rocci, 1976), which resulted in the formation of a Red Sea-type oceanic basin (Robertson & Woodcock, 1979). Within plate-type alkaline lavas of the Dhiarizos Group form the exposed structural basement (Swarbrick 1979, 1980) of the Mamonia terrane. A series of extrusives (Swarbrick, 1979; Swarbrick & Robertson, 1980) are overlain and interbedded with a sedimentary sequence that has been interpreted as forming in a passive margin setting (Robertson & Woodcock, 1979). During Late Triassic to mid-Cretaceous sedimentation took place relatively close to a continental margin (Swarbrick &

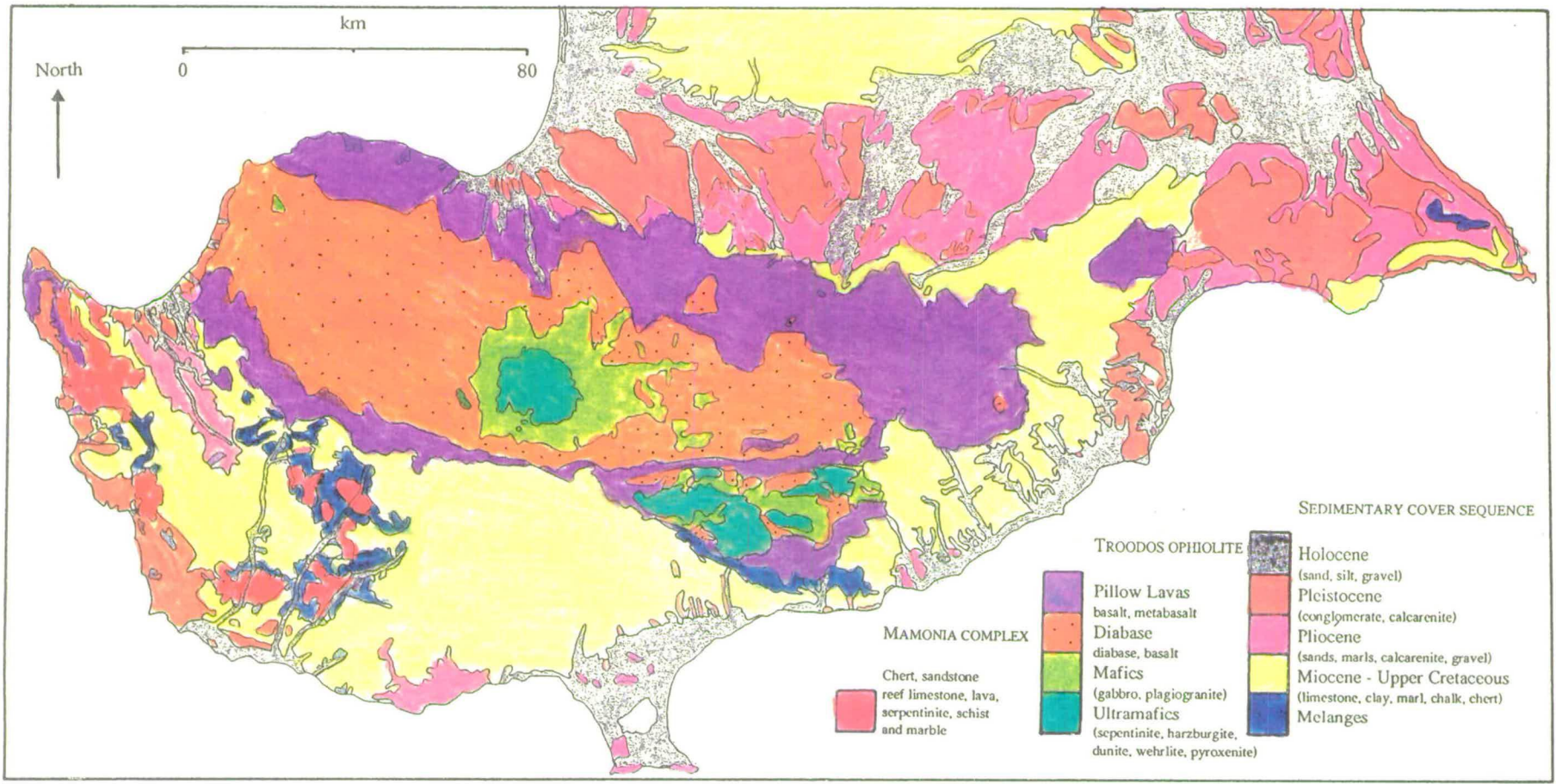


Fig.1.4. Geological map of southern Cyprus (after Pantazis, 1979).

Table 1.1. Summary of the pre-Pliocene geological history of Cyprus (from Robertson, 1977, 1990; Robertson & Woodcock, 1986; Clube & Robertson, 1986).

| TROODOS TERRANE |                                                                                                                                                                                                                                                                                                                                                                                                             | KYRENIA TERRANE  |                                                                                                                                                                                                                                                           | MAMONIA TERRANE    |                                                                                                                                                                                                                                                     |
|-----------------|-------------------------------------------------------------------------------------------------------------------------------------------------------------------------------------------------------------------------------------------------------------------------------------------------------------------------------------------------------------------------------------------------------------|------------------|-----------------------------------------------------------------------------------------------------------------------------------------------------------------------------------------------------------------------------------------------------------|--------------------|-----------------------------------------------------------------------------------------------------------------------------------------------------------------------------------------------------------------------------------------------------|
| U. Mio.         | Evaporites deposited as Messinian salinity crisis affects Mediterranean; tectonism dwindles in S. Cyprus, but N. of Troodos gypsum is deposited in small basins, localised by active normal faults                                                                                                                                                                                                          | U. Mio.          | Kyrenia lineament begins to rise along growth faults; clastic input from the north diminishes and mudstones and marls are deposited prior to gypsum accumulation during the Messinian crisis.                                                             |                    |                                                                                                                                                                                                                                                     |
| Olig.-M.Mio.    | Deposition of chalks, with increasing marl content, (U. Lefkara Fmn.) and marls, calciturbidites and conglomerates, with reef and igneous clasts, (Pakhna Fmn.) signal uplift of the Troodos ophiolite and emergence related to subduction S. of Cyprus; in M. Mio. tectonic shoaling of basement results in narrow deformation belts in S. Cyprus, while extensional faulting starts to affect N. Troodos. | Olig.-M.Mio.     | Kyrenia lineament subsides drastically in extensional setting; thick turbidite sequence (Kythrea Flysch), derived from Turkey, deposited unconformably over lineament; active growth faulting in the Miocene.                                             |                    | Mamonia terrane amalgamated with Troodos terrane.                                                                                                                                                                                                   |
| U. Cret.-Eo.    | Troodos microplate is detached and rotates 90°; a thick sequence of pelagic chalks (L.-M. Lefkara Fmn.), now locally replaced by chert, is deposited as Troodos crust remains in deep carbonate depositing seas; in S. Cyprus some deformation of chalks occurs along inferred S. edge of microplate.                                                                                                       | Eo.              | Major S-directed thrusting, associated with continental collision to the N. slices Kyrenia area into a series of thrust sheets and creates elongate deformation belt; variety of syntectonic sediments.                                                   |                    |                                                                                                                                                                                                                                                     |
| U. Cret-        | Thin unit of metalliferous sediments, radiolarites and mudstones deposited over irregular Troodos crust (Perapedhi Fmn.).<br><br>Crust of Troodos ophiolite generated in small, Neotethyan, ocean basin.                                                                                                                                                                                                    | U.Cret.-I. Tert. | Metamorphosed platform subsides and is covered with pelagic carbonates; bimodal volcanics are extruded and breccias are shed from active fault belts as Kyrenia area comes under transensional stress associated with rotation of the Troodos microplate. | U. Cret.           | Bentonitic clays, radiolarites and volcanoclastics, including olistostromes (Kathikas Fmn.) shed from area to NW. Cyprus during active strike-slip faulting, associated with rotation of the Troodos microplate, are juxtaposed with Mamonia units. |
|                 |                                                                                                                                                                                                                                                                                                                                                                                                             | M.-U. Cret.      | Carbonates brecciated and interleaved with metamorphic slivers as platform is juxtaposed with Troodos-type crust during subduction.                                                                                                                       |                    |                                                                                                                                                                                                                                                     |
|                 |                                                                                                                                                                                                                                                                                                                                                                                                             | L. Cret.-Perm.   | Shallow marine limestones and dolomites deposited on gently subsiding carbonate platform.                                                                                                                                                                 | L. Cret.-U. Trias. | Disrupted assemblage of continental margin lithologies (redeposited mature sandstones and carbonates, lime mudstone and radiolarite) in tectonic contact with oceanic crustal units.                                                                |

Robertson, 1980). Amalgamation of the Troodos and Mamonia terranes occurred in the Late Cretaceous as a result of gravity sliding (Robertson & Woodcock, 1979) and/or underthrusting (Clube & Robertson, 1986), with the Mamonia terrane being juxtaposed with the lavas of the Troodos terrane along strike-slip faults.

Small ophiolites are also present to the south of the Arakapas Fault Belt (the Limassol Forest area; "anti-Troodos Ophiolite") and in north-west Cyprus (the Akamas Ophiolite; Fig.1.3). Tectonized plutonic and depleted ophiolitic extrusive units crop out in areas of the Limassol Forest close to the transform zone (Murton, 1986), part of the transfer zone. Further south, in the "anti-Troodos Ophiolite", extrusives similar to those of the main Troodos ophiolite crop out (MacLeod, 1990).

### **1.3.1.2 The Kyrenia terrane.**

The Kyrenia terrane forms the northern backbone of Cyprus today. A complex lineament, the Kyrenia terrane contains the oldest stratigraphic units cropping out on Cyprus - the Permian Kantara Formation (Ducloz, 1972; Baroz, 1979; Robertson & Woodcock, 1986). The sedimentary, igneous and metamorphic units that constitute this terrane range from Lowest Permian to Recent (Table 1.1; Robertson, 1990). Initial amalgamation with the Troodos terrane probably took place in the Lower Cretaceous coincidental with the amalgamation of the Troodos and Mamonia terranes, but bounding faults remained active until the Pleistocene (McCallum, 1989; Robertson, 1990). The Kyrenia terrane was strongly deformed in the Eocene as a compressional front migrated southwards, uplifting and thrusting the Kyrenia terrane to the south (Robertson & Woodcock, 1986), with the resultant formation of a foreland basin. Rapid subsidence followed in the Oligocene with the deposition of unconformable, fluvial conglomerates and terrigenous turbidites in the lowest Miocene. By the Late Miocene uplift of the Kyrenia Lineament to the north of the Kythrea Fault (Fig.1.3) was taking place (McCallum, 1989). The uplift of the Kyrenia Lineament resulted in affiliated subsidence to the south with the onset of the evolution of the Mesaoria Basin.

### **1.3.2 Late Cretaceous to pre-Quaternary sedimentary history.**

The Late Cretaceous, Palaeogene and Neogene sedimentary history of Cyprus is dominated by the deposition of carbonate sediments, i.e. chalks, limestones, calcareous marls and calcarenites. An overall shallowing of sedimentary environments supports the hypothesis that uplift and emergence of the Troodos Massif, specifically, and the whole of the island, generally, has taken place during this period (Robertson, 1977).

Table 1.2. Stratigraphy and age of the Cretaceous to Tertiary Troodos sedimentary cover sequence.



| Age (Ma.) | Period             |        | Stratigraphy                                                                                     | Lithology                                                                                      |
|-----------|--------------------|--------|--------------------------------------------------------------------------------------------------|------------------------------------------------------------------------------------------------|
| 2.0       | Pleistocene        |        | Fanglomerate Group<br>Apalos Formation                                                           | Conglomerates and sandstones                                                                   |
| 5.2       | Pliocene           |        | Kakkaristra Formation<br>Athalassa Formation<br>Nicosia Formation                                | Calcarenites, sandstones and conglomerates<br>Marls, silts, muds, sandstones and conglomerates |
| 23.4      | Miocene            | Upper  | Kalavastos Formation                                                                             | Evaporites                                                                                     |
|           |                    |        | Koronia Member  | Reefal and bioclastic limestone                                                                |
|           |                    | Middle | Pakhna Formation                                                                                 | Pelagic chalks, marls, calcarenites and conglomerates                                          |
|           |                    | Lower  | Terra Member  | Reefal and bioclastic limestone                                                                |
| 35.4      | Oligocene          |        | Upper Lefkara                                                                                    | Pelagic chalk and minor shale                                                                  |
| 54.9      | Eocene             |        | Middle Lefkara                                                                                   | Pelagic chalk and replacement cherts                                                           |
| 65.0      | Palaeocene         |        |                                                                                                  |                                                                                                |
| 73.0      | Maestrichtian      |        | Lower Lefkara                                                                                    | Pelagic chalks                                                                                 |
| 83.0      | Campanian          |        | Kathikas Formation                                                                               | Matrix-supported conglomerates                                                                 |
|           |                    |        | Kannaviou Formation                                                                              | Bentonitic clay and tuffaceous sandstone                                                       |
|           |                    |        | Perapedhi Formation                                                                              | Umber and radiolarian chert                                                                    |
| 91.0      | Santonian-Turonian |        |                                                                                                  |                                                                                                |



Table 1.3. Plio-Pleistocene sediments and tectonic history of the Mesaoria and Mari Basins, Cyprus (after McCallum, 1989).

| Age                                 | Mesaoria Basin                       |                                                                                                       | Mari Basin                                           |                                                         | Tectonics                 |                                                                                                                                                                                                                         |
|-------------------------------------|--------------------------------------|-------------------------------------------------------------------------------------------------------|------------------------------------------------------|---------------------------------------------------------|---------------------------|-------------------------------------------------------------------------------------------------------------------------------------------------------------------------------------------------------------------------|
|                                     | Formation                            | Facies                                                                                                | Formation                                            | Facies                                                  | Uplift vs. peneplanation* | Comments                                                                                                                                                                                                                |
| Pleistocene to Recent               | Fanglomerate Series                  | Coarse, angular conglomerate sheets.                                                                  | Fanglomerate Series and Older River Terrace Deposits | Coarse, angular conglomerate sheets.                    |                           | Drastic uplift as compression and ? serpentinization occurs.                                                                                                                                                            |
|                                     | Apalos and Upper Athalassa Fmn.      | Mud-rich alluvial fans, minor conglomerate and sands. Shallow marine to coastal carbonate sands.      | -----                                                | -----                                                   |                           | Period of relative stability as compression and uplift wane.                                                                                                                                                            |
| Upper Pliocene to Lower Pleistocene | Kakkaristra and Lower Athalassa Fmn. | Shelf-fan delta, shallow marine sand bodies, slumped silts and minor fan-delta intercalations.        | Vasilikos Fmn.                                       | Braided fluvial deposits.                               |                           | Start of compression of the whole of Cyprus due to subduction of a microcontinental block; Troodos Massif and Kyrenia Lineament uplifted.                                                                               |
| Lower to Upper Pliocene             | Nicosia Fmn.                         | Marine silts; conglomeratic fan-delta intervals along south margin pass up into sandy intercalations. | -----                                                | -----                                                   |                           | Period of relative stability                                                                                                                                                                                            |
| Miocene                             | Pakhna Fmn. and Kalavastos Fmn.      | Marl, chalky debris flows, evaporites.                                                                | Nicosia Fmn.<br>Kalavastos Fmn.                      | Marine silts overlain by fan-delta facies<br>Evaporites |                           | Subsidence of Mesaoria half graben as a result of tectonic readjustment in the wake of collision in the Bitlis zone; ? induces extension behind the Cyprus Arc. Possible migration of the subduction zone to the south. |

\* = A wider column indicates greater uplift, a narrower column indicates greater peneplanation.

The basal sediments, the metalliferous umbers (Boyle, 1984) and radiolarian cherts of the Perapedhi Formation (Upper Cretaceous) are overlain by the 1000m thick pelagic chalks and replacement cherts of the Lower and Middle Lefkara Formation (Maastrichtian to Early Miocene - Mantis, 1970; Robertson, 1977). Benthic foraminiferal, bioturbated and reworked chalks with increased proportions of marl indicate shallower marine environments during the deposition of the Upper Lefkara Formation (Robertson, 1977). The first evidence of emergence of the Troodos Massif is found within the Miocene Pakhna Formation (Henson *et al.*, 1949) which contains ophiolite-derived clasts (Eaton, 1987; Robertson *et al.*, 1991). The Pakhna Formation consists of marls, calciturbidites, chalks and calcarenites.

Renewed subduction that is inferred to have taken place during this time resulted in the activation of three sub-parallel basement lineaments along the southern margin of the Troodos terrane (Ayia Mavri, Yerasa, Akrotiri; Bear & Morel, 1960; Eaton, 1987; Robertson *et al.*, 1991). These lineaments are thought to have resulted from underthrusting and/or the collision of a seamount, similar to the Eratosthenes Seamount (Fig.1.1). Coincidental extension taking place to the north of the Troodos Mountains resulted in the formation of the Mesaoria basin (Fig.1.3). Extension (Robertson *et al.*, 1991) is thought to have resulted from "roll-back", i.e. the subduction zone moved further south (Dewey, 1980; Carlson & Melia, 1984), along the subducting slab under the island. Uplifting fault blocks associated with the formation of these structures became sites for the deposition of a variety of sedimentary facies (Follows, 1990, 1991; Follows & Robertson, 1990; Robertson *et al.*, 1991) with reef colonization and off-reef facies being recorded (Follows, 1990, 1991). The Mediterranean-wide, Messinian salinity crisis (Hsu *et al.*, 1978) resulted in the formation of the evaporites of the Kalavassos Formation. Recent work (McCallum, 1989; McCallum & Robertson, 1990; Follows, 1990, 1991; Follows & Robertson, 1990; Robertson, 1990; Robertson *et al.*, 1991) shows that deformation continued throughout the Upper Miocene and Pliocene with the Pliocene sequences of the Mesaoria Plain being deposited in a subsiding basin (McCallum, 1989; McCallum & Robertson, 1990).

The Lower Pliocene marine transgression that followed the Messinian salinity crisis caused flooding and the deposition of the first of c.900m of Pliocene sediments. The Lower and Middle Pliocene (Table 1.3) sediments consist of a series of marls and calcarenites, i.e. the Nicosia Formation (Ducloz, 1965; McCallum, 1989; McCallum & Robertson, 1990; Robertson *et al.*, 1991). The Mesaoria and Mari Basins (Fig.1.3) to the north and south of the Troodos Massif, respectively, display a regressive sedimentary sequence with the marls of the Nicosia Formation being succeeded by calcarenite and fan-delta sequences in the north, i.e. the Athalassa and Kakkaristra Formations

respectively (Ducloz, 1965), and fluvial sediments to the south, i.e. the Vasilikos Formation (McCallum, 1989); these in turn are overlain by fluvial facies of the Apalos Formation (Ducloz, 1965; McCallum, 1989; McCallum & Robertson, 1990) and the Quaternary Funglomerate Series (Ducloz, 1965).

The Quaternary period saw the onset of accelerating uplift of the Troodos Massif and Kyrenia Range. This uplift resulted in the deposition of aeolian and alluvial fan sediments, delta, littoral and sub-littoral sequences, and the formation of a great variety of geomorphological features. Studies concentrating on the uplift of the Troodos Massif and the resultant sedimentary, geomorphological and neotectonic features constitute this thesis.

#### **1.4 PROCESSES CAUSING UPLIFT.**

Gradual uplift of Cyprus and the eastern Mediterranean region has occurred throughout the Tertiary; a proposition supported by regressive carbonate sequences and emergence (Carr & Bear, 1960; Follows & Robertson, 1990) in the Middle Miocene (Robertson, 1977), as well as Pliocene marine sediments that crop out 750m above the present day sea-level (ASL) (Harrison, 1955). Dramatic, pulsed Pleistocene uplift (Robertson, 1977) is thought to have been caused by diapiric serpentinite protrusion, superimposed on this regional Tertiary uplift. Other examples of this uplift phenomenon, related to past subduction, are found in the Coastal Ranges of California where a mobile serpentinite protrusion has taken place (Dickinson, 1966; Carlson, 1984). Diapirism and uplift associated with the Troodos Massif has apparently shifted westward to centre on Mount Olympus today (De Vaumas, 1961).

Uplift resulted in the formation of at least three continental erosive phases (De Vaumas, 1959, 1961, 1962). Bear (1960) first suggested that a large hydrated serpentinite diapir centred on Mount Olympus had driven the Troodos up into a dome, dragging the rest of the island up with it. It has previously been suggested that an erosion surface that crops out at Mount Olympus is of Pontian age, i.e. Lower Pliocene (De Vaumas, 1961; Gass & Masson-Smith, 1963), suggesting that uplift has taken place since this time. Gass & Masson-Smith (1963) also suggest that the serpentinite was a forced solid state intrusion. Moores & Vine (1971) oppose solid state intrusion, stating that remnant magnetism indicates that the serpentinite has been remobilised resulting in randomly orientated remnant vectors, unlike the remnant vectors seen in the non-remobilised harzburgites and dunites. The process of serpentinitization can result in a large volume increase. The presence of brucite in oceanic serpentinites suggests that an isochemical change has taken place with a resultant volume increase (Fig.1.5; Dmitriev, 1975;

Bonatti, 1976); this aids intrusion along weak structural zones (Mumpton & Thompson, 1975). The heavy oxygen and hydrogen isotope signatures in the Troodos serpentinite suggest that the water that caused hydration of the serpentinite was meteoric, charged with evaporitic and meteoric fluids, not sea water (Magaritz & Taylor, 1974).

Messinian evaporites found in the Mediterranean Sea to the south of Cyprus (Kidd & Benoulli, 1978) are thought to have contributed to the 50% thicker than normal crust (Woodside & Bowin, 1970; Makris *et al.*, 1983). The lack of a distinct magnetic anomaly (Woodside & Bowin, 1970) suggests that large amounts of sediment and not igneous rocks account for the thick crust, although continental crust does appear to exist beneath Cyprus (Makris *et al.*, 1983). The Messinian evaporites are thought to have been thrust/subducted under Cyprus, mixed with the circulating waters (Robertson, 1990), so increasing the density difference between the serpentinite and overlying units. If this was the case, as sediment dewatering by compaction and dessication of hydrated products takes place at depths of less than 6km (Burst, 1976; Pittman, 1979), serpentinitization is likely to have occurred before this depth of subduction was reached, even though serpentinitization takes place down to depths of approximately 30km (500°C; Bonatti, 1976). Coleman (1977) has suggested that serpentinitization follows obduction of an ophiolite when diapiric movement of the parental ultramafic rock takes place near the basal detachments. Robertson (1990) postulates that the trigger for Quaternary uplift of the serpentinite was the subduction of a large wedge of continental crust under Cyprus. A similar situation has been reported from the Mariana forearc, in the west Pacific Ocean, where the emplacement of serpentinite is thought to represent a tectonic response to the subduction of seamounts (Fryer *et al.*, 1985). Fragments of continental crust are inferred within the present day Mediterranean, as well as underlying Cyprus (Makris *et al.*, 1983); these are thought to have been present in the past (Eaton, 1987). Robertson & Woodcock (1984A, B) have also identified continental fragments that have been emplaced along the northern edge of the Mesozoic Tethys in the Antalya terrane of south-west Turkey.

In summary, diapirism and underthrusting of the mantle wedge have facilitated the Quaternary uplift of Cyprus. Bonatti (1976) estimates that uplift rates of serpentinite bodies are in the order of 0.1cm/year. Harrison (1955) suggests that submergence, in the order of 1cm/year, of Cyprus, should have taken place to maintain isostatic equilibrium, as indicated by the pronounced gravity anomaly (Fig.1.2; c.+250 mgal over the Troodos Massif), but this does not take the reduced Mount Olympus anomaly into account (c.+80 mgal). The uplift of the island has obviously involved a number of geological processes, which will be discerned here.

Fig.1.5. Density (in g/cm<sup>3</sup>) of rock recovered from the ocean floor which represents the common constituents of the oceanic crust (after Bonatti, 1976).

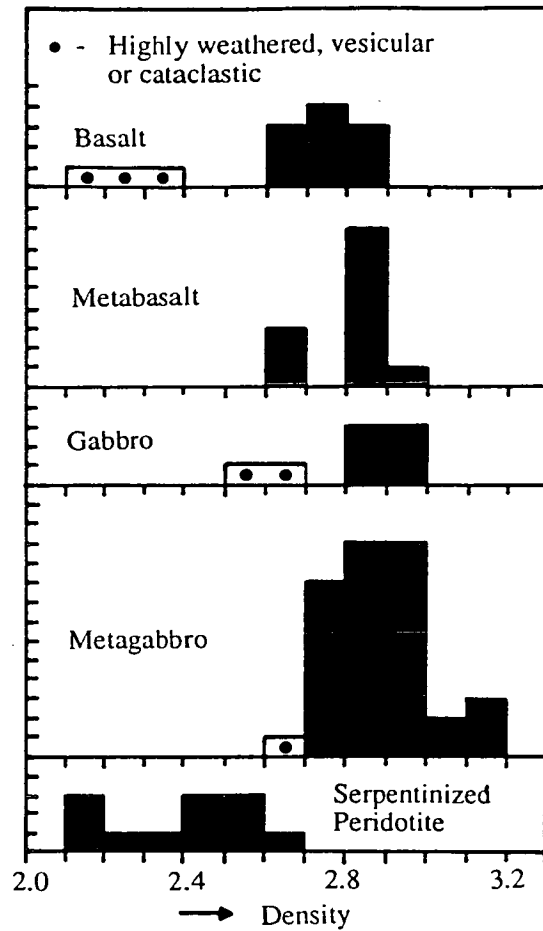
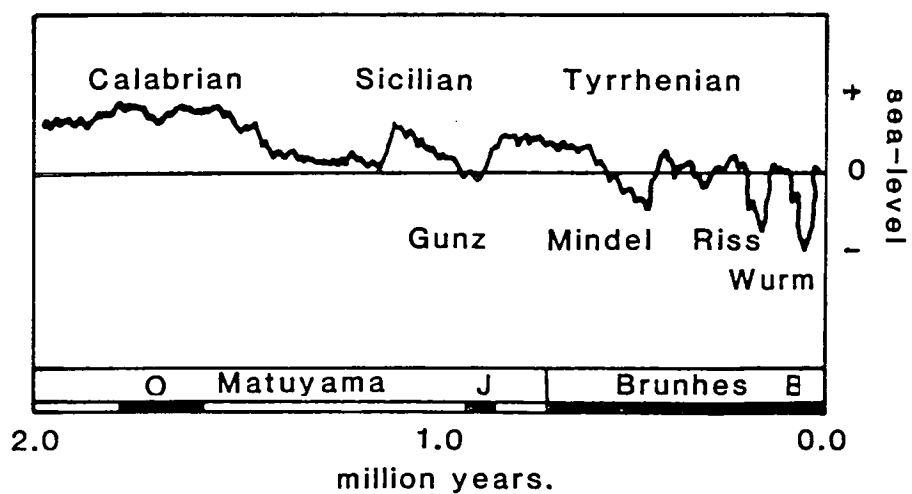


Fig.1.6. A Quaternary sea-level curve and the associated palaeomagnetic reversal boundaries.

Note: a) Mediterranean marine stage names; b) European glacial chronology.



## **1.5 PREVIOUS WORK.**

### **1.5.1 Cyprus.**

Bellamy & Jukes-Browne (1905) and then subsequently Cowper-Reed (1930) recognised coarse sheet conglomerates, i.e. the Fanglomerate Series, forming on hill tops south of Nicosia. Henson *et al.* (1949) first described a tufa-leaf bed in the Kyrenia Range, littoral deposits of the Larnaca and Limassol coastal plains, and stacked marine terraces, noting that some relative emergence had occurred. De Vaumas (1959, 1961, 1962) recognised a number of marine terraces on the flanks of the Kyrenia Range; he also noted the asymmetry on the flanks of the Troodos mountains, with deep rejuvenated valleys and high ridges and concluded that the Troodos range had been peneplaned since the Pliocene, with the most important erosion surface dating from the Pontian, i.e. Lower Pliocene. De Vaumas (1959, 1961, 1962) also inferred that uplift of the island was spasmodic with three or four erosive, epicyclic phases; he also suggested that the Troodos and Kyrenia terraces can be correlated, the difference in terrace height being a consequence of faulting and not Quaternary eustatic sea-level changes. Studies on the northern flanks of the Troodos Massif identified a number of terraces related to the uplift of the ophiolite complex, the different terrace sets being identified by means of altimetry (Ducloz, 1965). Lithological variations could not be used as the terraces have the same field characteristics, e.g. massive conglomerates, secondary limestone and red soils. Ducloz (1965) introduced a stratigraphic column for the Plio-Pleistocene. This was subsequently revised by Turner (1971; *vid.* Table 1.4), who attempted to correlate the Quaternary of Cyprus with circum-Mediterranean events and a world-wide glacial chronology. Palaeontological work by Moshkovitz (1968) presents evidence for faunal changes throughout the Plio-Pleistocene and also concludes that early Quaternary uplift had taken place. Published memoirs by the Geological Survey Department also record evidence of Quaternary Fanglomerate Series and raised beach units (Bagnall, 1960; Bear, 1960; Carr & Bear, 1960; Bear & Morel, 1960; Gass, 1960; Moore, 1960; Pantazis, 1967; Wilson, 1958). Pantazis (1966) also mapped terraces of apparent Tyrrhenian age in the Larnaca area of south-east Cyprus.

Turner (1971) correlated the heights of the marine terraces seen in the Paphos District with those of the Lebanon and Israel and also noted that fan-delta deposits exist in the Polis-Paphos graben of north-west Cyprus. Robertson (1977) first suggested that the Pleistocene was the main period of "drastic uplift" and that a period of relative quiescence exists today.

Table 1.4. Correlation of the Quaternary formations of Cyprus with the Mediterranean stages and glacial periods (after Ducloz, 1965; Turner, 1971).

| PERIOD<br>EPOCH |             | AGE            | PHASE       | CENTRAL<br>MESAORIA | ELEVATION<br>OF SHORE<br>(m) | GLACIAL<br>CHRONOLOGY |
|-----------------|-------------|----------------|-------------|---------------------|------------------------------|-----------------------|
| QUATERNARY      | HOLOCENE    | VERSILIAN      |             | ALLUVIUM            | 0-4                          | HOLOCENE              |
|                 | PLEISTOCENE | TYRRHENIAN III | continental |                     | 4-6                          | WURM I-II             |
|                 |             |                | marine      |                     |                              |                       |
|                 |             | TYRRHENIAN II  | continental | XERI ALLUVIUM       | 12-21                        | WURM I                |
|                 |             |                | marine      |                     |                              |                       |
|                 |             | TYRRHENIAN I   | continental | LAXIA GRAVEL        | 36-43                        | RISS                  |
|                 |             |                | marine      |                     |                              |                       |
|                 |             | MILAZZIAN      | continental | ?                   | 49-75                        | MINDEL                |
|                 |             |                | marine      |                     |                              |                       |
|                 |             | SICILIAN       | continental | KAMBIA GRAVEL       | 61-91                        | GUNZ                  |
|                 |             |                | marine      |                     |                              |                       |
|                 | PLIOCENE    | CALABRIAN      | continental | KANTARA<br>GRAVEL   | 183-244                      | DANUBE                |
| marine          |             |                |             |                     |                              |                       |

Work on the Kyrenia mountains supports the view that rapid Quaternary uplift has taken place, with a suite of six terraces cropping out (Ducloz, 1968, 1972; Dreghorn, 1978; Baroz, 1979), the marine terraces becoming progressively more tilted with increasing altitude. Dreghorn (1978) further showed that micropalaeontological data supports the existence of Pliocene, as well as Quaternary marine terraces on the Kyrenia Range.

Little recent work has been carried out on the problem of uplift in Cyprus. Flemming (1978) studied the changes in Holocene shorelines of the north-eastern Mediterranean and a study of the Late Quaternary shorelines of western Cyprus was made by Giangrande *et al.* (1987). The Quaternary alluvial sediments of the Vasilikos Valley have been studied by Gomez (1987). Vita-Finzi (1990) utilised the  $^{14}\text{C}$  method in an attempt to quantify the Quaternary uplift of western Cyprus.

### **1.5.2 Comparable studies world-wide.**

The approach to previous studies of tectonic uplift and neotectonics in the Mediterranean have been varied. Richards (1982) used intertidal molluscs as sea-level indicators, Butzer & Cuerda (1962) used regressive events on Mallorca to support a eustatic sea-level curve related to Quaternary glacial episodes, whereas Hearty & Hollin (1986) and Hearty (1987) based their work on amino-acid geochronology, linked with uranium series data. Vita-Finzi & King (1985) related landforms and seismicity in time and space in the Corinth area of Greece and concluded that relative altimetry should not be used as an indicator of absolute age of terraces. More recently attempts have been made to model the products of uplift and distinguish between eustatic sea-level and tectonic effects (Keraudren & Sorel, 1987; Collier, 1990); Collier (1990) concluded that transgressive, cyclic sediment resulted from rises in the sea-level, which are subsequently preserved as a result of tectonic uplift. So a high sea-level cuts a coastline which is subsequently uplifted and therefore preserved. Peters *et al.* (1985) showed that late Neogene subsidence in Crete was followed by Quaternary uplift; this resulted in both continental and littoral deposits. Crete is of particular interest as it is located in a fore-arc setting, similar to Cyprus.

Leeder *et al.* (1990), in the Corinth area of Greece, and Maizels (1987, 1988) in Oman, have both recently identified pulsed continental infill and deposition in lacustrine and fluvial environments. Leeder *et al.* (1990) infers tectonic controls, whereas Maizels (1987, 1988) suggests that climatic, eustatic sea-level and hydrologic variations, superimposed on the regional tectonics in the Quaternary, controlled the deposition of the Sharqiya alluvial fan. Satellite imagery has been used to map alluvial terraces along the



Batinah coast of Oman where it has been suggested that seven terrace levels crop out (Abrams *et al.*, 1988); it has been postulated that the formation of these terraces has been controlled by Quaternary climatic changes as uplift has been negligible and sea-level changes have had little effect, as terrace gradients appear to have remained unchanged (Abrams *et al.*, 1988).

Chappell (1974, 1983) and Chappell & Veeh (1978) in Papua New Guinea; Bull (1985) and Bull & Cooper (1986) in New Zealand and others (see Morisawa & Hack, 1985) have all examined the product and processes of Quaternary uplift, with the common aim of fixing uplift both temporally and spatially, to allow the tectonic products to be unravelled from eustatic sea-level changes and other effects (e.g. geoidal and climatic variations).

## **1.6 THE QUATERNARY: DEFINITIONS AND PROBLEMS.**

### **1.6.1 Definitions.**

The Quaternary, a sub-era (Harland *et al.*, 1989) is divided into two epochs, the Pleistocene and Holocene, which stretch from approximately 2Ma. B.P. to the present day. The Pliocene-Quaternary boundary is artificial, as no faunal changes occur. Bowen (1978) states that climatic changes are the dominant characteristic (*sic*) of the Quaternary, with oxygen isotope and palaeontological studies stressing the differences between the Quaternary and older Pliocene period. The Quaternary has experienced approximately 30 glacial episodes, eustatic sea-level oscillations with amplitudes in the order of 100-130m (Shepard, 1963) and large scale latitude displacements resulting from climatic variations (Kennett, 1986).

The Pleistocene epoch was originally defined by Lyell (1839) and refined by Forbes (1846) as the "time distinguished by severe climatic conditions throughout the greater part of the northern hemisphere". The location of the boundary between the Pliocene and Pleistocene has proved to be problematic; it was originally fixed at the base of the Calabrian. Absolute age estimates for this boundary have varied from 1.6Ma. to 2.0Ma.. A date of about 2.0Ma. (Selli *et al.*, 1977) has now been chosen for the boundary; the stratotype is in Vrica, southern Italy. This boundary does not, therefore, correlate with the start of the Olduvai palaeomagnetic reversal (Fig.1.6). The Pleistocene-Holocene boundary is now well established, corresponding to the latest glacial/postglacial and European Pollen Zones III/IV boundaries (Morner, 1976A)

### **1.6.2 Quaternary sea-level changes.**

The large scale, relative, Quaternary eustatic sea-level changes are thought to have been caused and controlled by orbital forcing, i.e. Milankovitch Cycles (Croll, 1875; Berger *et al.*, 1984), but isostatic changes and tecto-eustatic changes should also be considered. Morner (1976B) has argued that geoidal variations have caused relative sea-level changes in the Quaternary, citing a present day example where the Maldives Islands and coast of Papua New Guinea show a difference in actual sea-level of 180m. Because the majority of work relating to sea-level curves has focused on glacial cycles and not hydro-isostasy and the visco-elastic nature of the earth's crust, Kidson (1982) in a review of sea-level changes in the Holocene epoch suggests that these variables need to be examined before accurate sea-level curves for tectonically stable areas can be produced. Unfortunately at present, the change and rate of change of the geoid is poorly understood and therefore its relative importance in affecting the relative sea-level in the Quaternary is uncertain. Models seeking to represent eustatic, isostatic and tensional thinning of the crust have been produced (Tanner, 1968). The visco-elastic rheology of the crust resulting from deglaciation has been modelled to calculate the dependent relative sea-level changes (Clark *et al.*, 1978). Post glacial sea-level changes have been predicted from this model with Cyprus falling into group II or III (Fig.1.7). Kennett (1986) argues that Quaternary absolute sea-level curves cannot be produced on a regional, or global scale. The author agrees with this argument and suggests, however, that local, absolute, Quaternary eustatic sea-level curves are valid in tectonically stable areas. Relative curves in tectonically active areas, where absolute dating of deposits has taken place, are also of importance as they can distinguish between tectonic uplift and eustatic sea-level change.

## **1.7 THESIS ORGANISATION AND TECHNIQUES USED.**

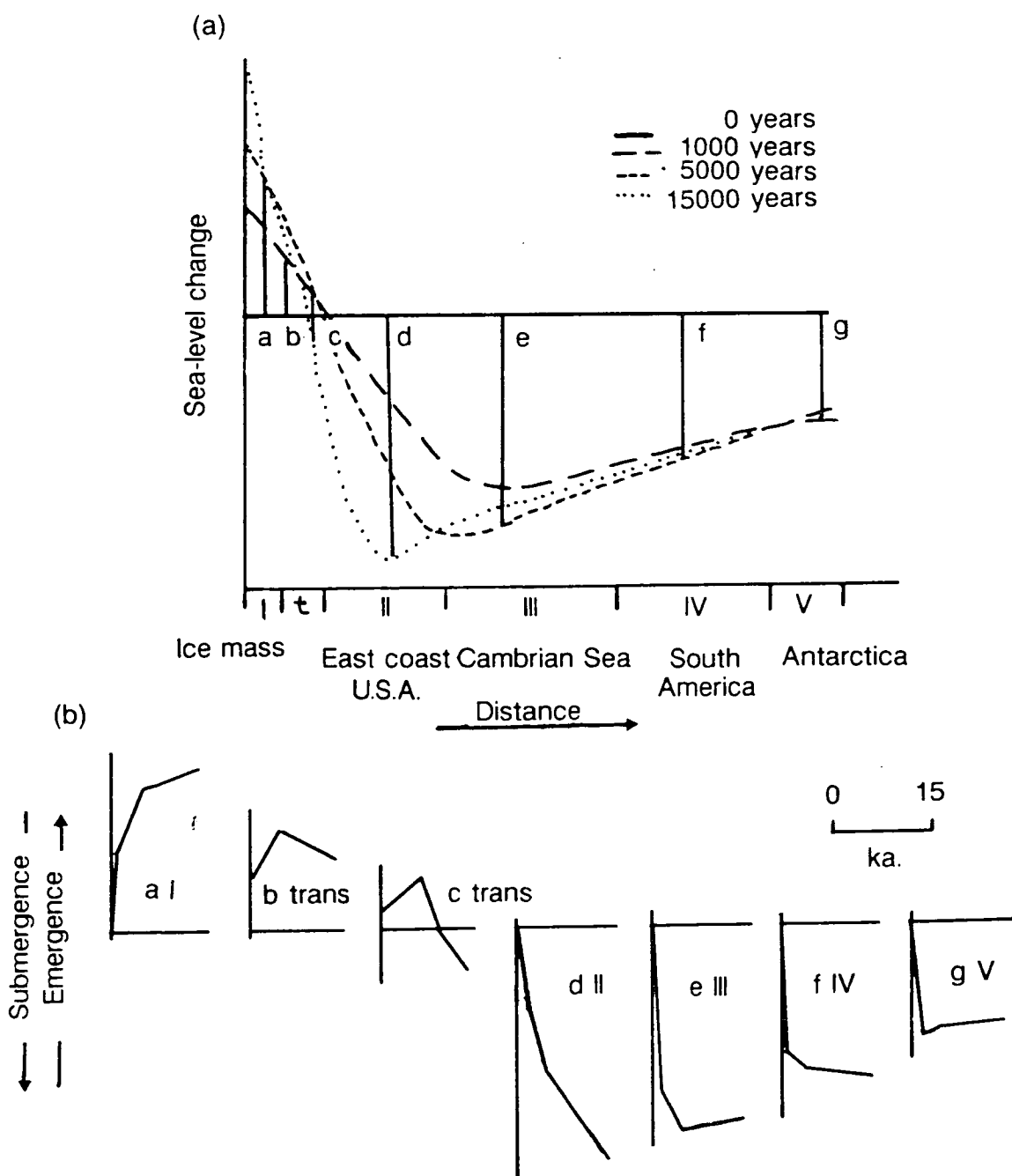
### **1.7.1 Organisation.**

The full range of data obtained during the course of this research is presented in separate chapters; discussion and interpretation of these data form the final section of each chapter. The discussion and conclusions from the work as a whole are recorded in Chapter 10. Published papers and raw data form the appendices. Details of the collection available in the Department of Geology and Geophysics at Edinburgh University are located in Appendix A.

References to other chapters and sections in the thesis are made in parenthesis, e.g. Chapter 7, or Section 6.8. Grid references and 1:50,000 scale Land Survey

Fig.1.7. A schematic representation of the Heaviside Green function (after Clark et al., 1978).

Note: a) the distortion of a reference shoreline up to 15ka. after the melting of a point ice mass; b) the sea-level change relative to an initial reference shoreline. Cyprus probably falls in the region of group II or III. Note: t - transition.



Department 1973 Ordnance Survey map numbers of the locations and samples mentioned in the text, are recorded in Appendix B. All village and town names, cited in the text, follow the spellings recorded on the 1:50,000 Ordnance Survey maps. The use of the term southern Cyprus, in the text, refers to the whole of Greek portion of the island, whereas south Cyprus refers to the portion of Cyprus to the south of the Troodos Massif, to the east of Paphos and the west of Larnaca.

### **1.7.2 Techniques.**

This thesis is based on extensive fieldwork in southern Cyprus. Standard field techniques, following the methods set out in Collinson & Thompson (1982), and Tucker (1988) were employed. Trace fossil identification through the thesis is made with the aid of Lindholm (1987). Clast analysis utilised visual roundness and sphericity tables (Krumbein, 1941; Rittenhouse, 1943) and standard techniques (Pettijohn, 1980); roundness, or sphericity figures recorded in the text of this thesis refer to the tables of Krumbein (1941) and Rittenhouse (1943). Reference to the "L" axis of a clast implies the longest axis of that clast. The provenance and clast analysis studies employed randomly positioned, 50cm square quadrants. 1:50,000 scale topographic maps were used in the field and these were supplemented with 1:5000 scale maps for more detailed studies. Field studies were guided by the 1:250,000 scale Geological Map of Cyprus (Pantazis, 1979) and the Memoirs of the Geological Survey Department of Cyprus accompanied by 1:30,000 scale maps. The map produced by Ducloz (Fig.5.1; 1965) was also of tremendous help whilst working on the central and eastern portion of the Mesaoria Plain.

Fieldwork has been supplemented with petrological studies involving thin section and acetate peel analysis. Routine staining of carbonate thin sections was made, using the method laid out by Dickson (1965). The friable and generally poorly consolidated nature of the sediments led to the vacuum impregnation of the samples, with an Epotek resin stained with a blue dye being used as a standard preparation technique. Sediment samples were also examined using standard sieve techniques. Thin section identification of fauna, e.g. coralline algae, was achieved with the help of Scholle (1978). X-ray diffraction and X-ray fluorescence methods were employed to study clay mineralogy and sediment chemistry in more detail. Preparation of the samples to gain standard sample fraction for X-ray diffraction analysis followed the technique laid out in Hardy & Tucker (1988) and used a Phillips PW 1800 X-ray diffractometer, with CuK alpha radiation. Clay and silt samples taken from Geological Survey Department boreholes were dried and orientated X-ray diffraction samples were produced; each sample was then analysed four times using air dried, glycolated and heated samples (at 375°C and 550°C), so enabling identification of smectite and kaolinite. X-ray fluorescence preparation followed the

techniques laid out in Fitton *et al.* (1984) and Norrish & Hutton (1969). Samples were analysed on a Phillips PW 1450 and a Phillips PW 1480 X-ray spectrometer.

Nannofossil analyses was undertaken by Dr. A. Lord and Dr. L. Gallagher at University College, London. Studies of molluscs and coral were undertaken at the British Museum of Natural History, under the supervision of Dr. J. Taylor and Dr. B. Rosen respectively.

Satellite image studies utilised Landsat Thematic Mapper, Multispectral Scanner (using a Gemstone system in Edinburgh) and S.P.O.T (Satellite Probatoire pour L'Observation de la Terre) data. Air photographs were viewed stereoscopically. Images and data have supplemented fieldwork and aided the study of the geomorphology. Admiralty 1:100,000 scale bathymetric charts and studies of seismic data (using B.G.S and Shell data; after McCallum, 1989) have enabled a limited study of the off-shore regions to the south of the island.

Various dating techniques have been employed to try and determine the timing of events in the Quaternary evolution of Cyprus. These are  $^{14}\text{C}$  method (in Professor C. Vita-Finzi's laboratory at University College, London), the uranium series disequilibrium method (using Dr. G. Shimmield's laboratory in the Department of Geology and Geophysics, Edinburgh) and the amino-acid racemization technique (in Dr. P. Hearty's laboratory in Beaufort, North Carolina, U.S.A. and Professor D. Bowen's laboratory at Royal Holloway and New Bedford College). The detailed procedures involved in the  $^{14}\text{C}$  and uranium series techniques are described in Appendix C.

## **1.8 STRATIGRAPHY.**

### **1.8.1 Mediterranean and previous Cyprus Quaternary stratigraphy.**

The Quaternary stratigraphy used in this study is based on the work of Butzer and others from Mallorca. This stratigraphic column (Table 1.5) will form the backbone of the following discussion of previous Quaternary stratigraphic tables that have been used in Cyprus. The synthesized Mallorcan stratigraphy including: oxygen isotope stages (Shackleton, 1975; Table 1.6); amino-acid zones (Hearty, 1987; Hearty & Hollin, 1986) and European loess and glacial cycles (Kukla, 1975) will form the basis of the stratigraphic column shown in Section 1.8.2.

Table 1.5. Quaternary stratigraphy of Mallorca including inferred Oxygen isotope stages (after Butzer, 1975, 1983; Hearty, 1987; Kukla, 1975; Shackleton, 1975).

| Marine : Continental cycle | Elevation (metres) | Faunal Characteristics (continental facies)                                           | Radiometric Age (ka = 1000 years) | Inferred Oxygen Isotope Stage (a) | Amino Acid Zone (b) | Loess Cycle (c) |
|----------------------------|--------------------|---------------------------------------------------------------------------------------|-----------------------------------|-----------------------------------|---------------------|-----------------|
| Z A                        | +2 to 4            | (Dunes, Early Roman)<br>Common fauna, prehistoric to Medieval.                        | Post-Roman                        | 1                                 | A                   | B-1             |
| Y3 B                       | +0.5 to 3          | (Aeolianite, 3 generations)<br>Rudimentary thermopile fauna (Argillic palaeosol ASL1) | 80 ± 5 ka                         | 2-4<br>5a<br>5b                   | 5a-5c=C             | L-B<br>5=B-3    |
| Y2                         | +1.5 to 2          | Partial <i>Strombus</i> fauna                                                         | 110 ± 5 ka                        | 5c                                |                     |                 |
| Y1                         | +9 to 15           | Partial <i>Strombus</i> fauna                                                         | 125 ± 10 ka                       | 5e                                | E                   |                 |
| X2 C                       | +6.5 to 8.5        | (Aeolianite, 2 generations)<br>Impoverished <i>Strombus</i> fauna                     | 190 ± 10 ka                       | 6<br>7a                           | 7a-7c=F             | L-C<br>7=B-5    |
| X1                         | +2 to +4.5         | Full <i>Strombus</i> fauna                                                            | 210 ± 10 ka                       | 7c                                |                     |                 |
| W2 D                       | +4 to 8            | (Aeolianite, 2 generations)<br>Common fauna                                           | >250 ka                           | 8<br>9(?)                         | G                   | L-D<br>B-7      |
| W1                         | +22 to 25          | (Argillic palaeosol ASL)<br><i>Patella ferruginea</i> fauna                           | ?                                 | (?)                               |                     |                 |
| V E                        | (below +11)        | (Aeolianite, 5 generations)<br>(No data)                                              | ?                                 |                                   |                     | L-E<br>B-9      |
| U F                        | +14 to 15          | (Aeolianite, 3 generations)<br><i>Patella ferruginea</i> (large subspecies fauna)     | ?                                 |                                   |                     | L-F<br>B-11     |
| T G                        | +15- 19            | (Aeolianite, 2 generations)<br><i>Patella longicosta</i>                              |                                   |                                   |                     |                 |

(a) After Shackleton, 1975; (b) after Hearty, 1987; (c) after Kukla (1975). Where an = sign is used (i.e. 7a-7c=F) this signifies that all the preceding zones/cycles are equivalent to the zone following the = sign.

Table 1.6. Age of isotope stage boundaries and terminations from core V28-239. Ages are interpolated from data from core V28-238 assuming constant sedimentation rates (after Shackleton & Opdyke, 1976).

| Boundary | Age (years BP) | Boundary | Age (years BP) |
|----------|----------------|----------|----------------|
| 1-2      | 13 000         | 10-11    | 367 000        |
| 2-3      | 32 000         | 11-12    | 440 000        |
| 3-4      | 64 000         | 12-13    | 472 000        |
| 4-5      | 75 000         | 13-14    | 502 000        |
| 5-6      | 128 000        | 14-15    | 542 000        |
| 6-7      | 195 000        | 15-16    | 592 000        |
| 7-8      | 251 000        | 16-17    | 627 000        |
| 8-9      | 297 000        | 17-18    | 647 000        |
| 9-10     | 347 000        | 18-19    | 688 000        |
|          |                | 19-20    | ?              |

The Quaternary stratigraphy in Cyprus has previously been based on the Mediterranean marine stages and linked to the classic glacial stages: Gunz, Mindel, Riss and Wurm (Table 1.4). Ducloz (1965) produced the first Plio-Pleistocene stratigraphic column for southern Cyprus based on the Fanglomerate Series, which crops out on the Mesaoria Plain. This stratigraphic column has been used in subsequent work and has been amended by McCallum (1989; Table 1.7). Gomez (1987) in has recently produced a local

Table 1.8. The stratigraphy of the fluvial sequences from the Mesaoria Plain, the Kyrenia Range and the lower Vasilikos Valley (after Ducloz, 1965, 1972; Gomez, 1987 respectively).

| Central Mesaoria Plain<br>(Ducloz, 1965) | Central Kyrenia Range<br>Ducloz, 1972) | Lower Vasilikos Valley<br>(Gomez, 1987) |
|------------------------------------------|----------------------------------------|-----------------------------------------|
| Xeri Alluvium                            | Kyrenia Terrace                        | Argakitis Kamilas Terrace               |
| Laxia Gravels                            | Ayios Epikitos Terrace                 | Kalavastos Terrace                      |
| Kambia Gravels                           | Trapeza Terrace                        | Mitsinjites Terrace                     |
| Kantara Gravels                          | Klepini Terrace                        | Phalakros Terrace                       |

Table 1.7. Plio-Quaternary stratigraphy of Cyprus (after previous work identified at the top of each column).

|             | All Cyprus           |                | Mesaoria Plain |               |                 | North Cyprus                  |                           | South Cyprus                      |                 |                 |
|-------------|----------------------|----------------|----------------|---------------|-----------------|-------------------------------|---------------------------|-----------------------------------|-----------------|-----------------|
|             | Henson et al (1949)  | Geol. map*     | Bear (1960)    | Ducloz (1965) | McCallum (1989) | Baroz (1979)                  | Moore (1960)              | Bagnall (1960)                    | Pantazis (1967) | McCallum (1989) |
| Holocene    | Alluvium             | Alluvium       | Alluvium       | Recent        | (not studied)   | Recent beach                  | marine and river terraces | Alluvium                          | Alluvium, dunes | (not studied)   |
|             |                      |                |                | Xeri Alluvium |                 |                               |                           | 40' RB                            |                 |                 |
| Pleistocene | Fang. marine terrace | marine terrace | Fang.          | Laxia Gr.     | Fang.           | six marine and river terraces | Fang.                     | shelly Larnaca sand 120' RB Fang. | Fang.           | 40' RB Fang.    |
|             |                      | Fang.          |                | Kambia Gr.    |                 |                               |                           |                                   |                 |                 |
|             |                      |                |                | marine Fang.  |                 |                               |                           |                                   | Kantara Gr.     |                 |
|             |                      |                |                |               |                 |                               |                           |                                   | Apalos Fmn.     |                 |
| Pliocene    | Ath. Fmn.            | Ath. Fmn.      | Nic. Fmn.      | Nic. Fmn.     | Nic. Fmn.       | Potami Fmn.                   | Nic. Fmn.                 | Ath. Fmn.                         | Ath. Fmn.       | Vasilikos Fmn.  |
|             | Nic. Fmn.            | Nic. Fmn.      | Myrtou Marl    | Nic. Fmn.     | Nic. Fmn.       | Myrtou Marl                   | Myrtou Marl               | Ath. Fmn.                         | Ath. Fmn.       | missing         |
|             | Myrtou Marl          |                |                |               |                 |                               |                           |                                   |                 | Nic. Fmn.       |

\* - 1973 Cyprus Geological Survey Map. Nic. - Nicosia, Ath. - Athalassa, Kak. - Kakkaristra, Kk. - Karka, Fang. - Fanglomerate, R.B. - Raised beach, Fmn - Formation, Gr. - Gravels. This table is not to scale. = interdigitation, = unconformable contact.,



Table 1.9. Summary of the Quaternary stratigraphy and age data from Cyprus.

|                             | Central Mesaoria Plain<br>(Ducloz, 1965) | Central Kyrenia Range<br>(Ducloz, 1972) | Lower Vasilikos Valley<br>(Gomez, 1987) | Continental correlation <sup>(1)</sup><br>(this work) | Climate <sup>(2)</sup><br>(Issar, 1979)                                  | Inferred oxygen isotope stage <sup>(3)</sup> | Height of marine terrace<br>(m ASL) | Age<br>(ka) |
|-----------------------------|------------------------------------------|-----------------------------------------|-----------------------------------------|-------------------------------------------------------|--------------------------------------------------------------------------|----------------------------------------------|-------------------------------------|-------------|
| Holocene                    |                                          |                                         |                                         |                                                       | Present day fauna                                                        | 1                                            |                                     |             |
| Late Pleistocene            | Xeri Alluvium                            | Kyrenia Terr.                           | Argakitis Kamilas Terr.                 | F4                                                    | Tyrrhenian<br>( <i>Strombus</i> fauna)                                   | 2<br>3-4<br>5<br>6<br>7<br>8-14              | < 3                                 | 116-134 ±10 |
|                             | Laxia Gravel                             | Ayios Epikitos Terr.                    | Kalavastos Terr.                        | F3                                                    |                                                                          |                                              | 8-11                                | 185-204 ± 8 |
| Middle to Early Pleistocene | Kambia Gravel                            | Trapeza Terr.                           | Mitsinjites Terr.                       | F2                                                    | Calabro-Sicilian<br>(cold marine fauna, i.e<br><i>Artica islandica</i> ) | ?<br>?<br>?<br>?                             | 50-60                               | ?           |
|                             | Kantara Gravel                           | Klepini Terr.                           | Phalakros Terr.                         | F1                                                    |                                                                          |                                              | 100-110                             | ?           |
|                             | Apalos Formation                         |                                         |                                         |                                                       |                                                                          |                                              |                                     |             |

(1) Note: the numerical F1-F4 nomenclature used in this work.

(2) See Chapter 3 for details.

(3) after Shackleton (1975).

Table 1.10. A summary of the components of the Quaternary evolution of Cyprus.

Note: a) the correlation with oxygen isotope stages.

| Age                                | Height of cliffline (m) | Height of preserved marine terrace (m) | Southern Cyprus correlation | Oxygen isotope stage | Sea-level + (max) - (min) | Facies types onshore on Cyprus                                | Postulated tectonic events + uplift - | Examples of locations in southern Cyprus                       |
|------------------------------------|-------------------------|----------------------------------------|-----------------------------|----------------------|---------------------------|---------------------------------------------------------------|---------------------------------------|----------------------------------------------------------------|
| Holocene                           |                         |                                        | Recent                      | 1                    |                           | Recent alluvium                                               | /                                     |                                                                |
|                                    |                         |                                        |                             | 2                    |                           | Onset of F4 erosion                                           | /                                     |                                                                |
|                                    |                         |                                        |                             | 3                    |                           | F4 fluvial and aeolian sequences                              | /                                     | Zygi; north Troodos margin; Akrotiri                           |
|                                    |                         |                                        |                             | 4                    |                           | F4 carbonate and siliciclastic                                | /                                     | Cape Greco; Limassol area; Paphos                              |
| Late Pleistocene                   | 8-11m                   | <3m                                    | F4                          | 5                    |                           | marine sequences                                              | /                                     | Dhokkita; Akrotiri                                             |
|                                    |                         |                                        |                             |                      |                           | Onset of F3 erosion                                           | /                                     |                                                                |
|                                    |                         |                                        |                             | 6                    |                           | F3 fluvial and aeolian sequences                              | /                                     | North Troodos margin; Limassol area; Tersephanou               |
|                                    |                         |                                        |                             | 7                    |                           | F3 carbonate and siliciclastic deltaic and littoral sequences | /                                     | Mazotos; Polis; Cape Greco; Larnaca; Coral Bay; Petounda Point |
|                                    | 50-60m                  | 8-11m                                  | F3                          |                      |                           | Onset of F2 erosion                                           | /                                     |                                                                |
|                                    |                         |                                        |                             | 8                    |                           | F2 fluvial and aeolian sequences                              | /                                     | Paphos area; Limassol area; north Troodos margin               |
| Middle - Early Pleistocene         | 100-110m                | 50-60m                                 |                             | ?                    |                           | F2 carbonate and siliciclastic littoral sequences             | /                                     | Ormidhia area; Paphos area                                     |
|                                    |                         |                                        | F2                          | ?                    |                           | Onset of F1 erosion                                           | /                                     | North Troodos margin                                           |
|                                    |                         |                                        |                             | ?                    |                           | F1 fluvial sequences                                          | /                                     | North Troodos margin                                           |
|                                    | 350-360m                | 100-110                                | F1                          | ?                    |                           | F1 marine sequences                                           | /                                     | Paphos area                                                    |
|                                    |                         |                                        |                             | ?                    |                           | Onset of F0 erosion                                           | /                                     |                                                                |
| Upper Pliocene - Early Pleistocene |                         | 350-360m                               | F0                          | ?                    |                           | Apalos Formation                                              | /                                     | North Troodos margin                                           |
|                                    |                         |                                        |                             | ?                    |                           | F0 marine sequences                                           | /                                     | Mesoyi; Marathounda                                            |

stratigraphy for the Vasilikos Valley (Table 1.8) in southern Cyprus, where sequences from both the central Mesaoria Plain (Ducloz, 1965) and central Kyrenia Range (Ducloz, 1972) were correlated with that seen in the Vasilikos Valley.

Ducloz (1972), Dreghorn (1978) and Baroz (1979) all produced stratigraphic columns for the Kyrenia Range. Unlike those columns produced for the southern portion of the island, these all show a dovetailed correlation between coastal terraces and continental facies.

### **1.8.2 Stratigraphy used in this thesis.**

The stratigraphic column used in this thesis has combined that produced previously in southern Cyprus (Ducloz, 1965; Turner, 1971; Gomez, 1987; McCallum, 1989), with the detailed stratigraphy that has been built up in Mallorca (Table 1.5). A tentative correlation with the northern portion of the island has been made using Gomez (1987). Absolute dates from this piece of work have allowed greater control, thus allowing a link to the oxygen isotope stages of Shackleton (1975) and the amino-acid zones of Hearty (1987). By linking the stratigraphy to absolute dates and the oxygen isotope stages it is hoped to move away from the vague Mediterranean stage terms that have been used previously. This will allow accurate correlation to be made between Cyprus and other parts of the Mediterranean, as well as other areas of the world. The use of isotope stages will enable a more accurate distinction between eustatic sea-level change and tectonic uplift, on Cyprus, to be made. The proposed stratigraphy used in this thesis is shown in Table 1.9.

A summary table of stratigraphy, terrace height, sea-level and tectonic effects, and the timing and variety of sediments (Table 1.10) is introduced at this point, to clarify the relationships that will be described in the succeeding chapters.

## **Chapter Two: Geomorphology.**

### **2.1 INTRODUCTION.**

De Vaumas (1959, 1961, 1962) first examined the geomorphology of Cyprus, with further work documented in the memoirs of the Cyprus Geological Survey Department (e.g. Bear, 1960; Bagnall, 1960; Gass, 1960; Moore, 1960), continued with studies by Ducloz (1965, 1972) and Dreghorn (1978). Gomez (1987) recently examined the terraces of the lower Vasilikos Valley and correlated these with those on the central Mesaoria Plain and the Kyrenia Range (Table 1.8).

De Vaumas (1959, 1961, 1962) produced the first geomorphological map of Cyprus illustrating that the Troodos Massif is asymmetric. The slopes of the Troodos Massif, and therefore the mature erosion surfaces, are twice as wide on the north, than seen to the south. De Vaumas (1959, 1961, 1962) considered that the Troodos Massif was peneplaned on at least three occasions prior to the Quaternary period:

- i) during the Upper Cretaceous;
- ii) before the Miocene transgression;
- iii) prior to the Pliocene marine incursion.

Erosion of the Troodos Massif was undoubtedly taking place during the Miocene and Pliocene as Troodos-derived clasts are present within in sedimentary units dating from this time (Eaton, 1987; McCallum, 1989; Follows, 1990).

This chapter will examine the field evidence for the Quaternary geomorphological features and data collected from remote sources, including: air photogrammetry, satellite imagery and Ordnance Survey maps. These features are grouped within sections, examining in turn: the drainage patterns, erosional surfaces, the coastal geomorphology and colluvium, with discussion of their correlation and formation.

### **2.2 DRAINAGE PATTERNS.**

#### **2.2.1 Introduction.**

The drainage pattern occurring in Cyprus today (Fig.2.1) consists of five major trends:

- i) a radial pattern of drainage centred on the Troodos Massif, locally concentrated on the area around Mount Olympus (Fig.2.1; Plate 2.1);



## PLATE 2.1.

E - Thematic mapper satellite image of southern Cyprus.

Note: the Troodos ophiolite (dark in the centre of the plate),  
the Arakapas Fault Belt on the southern margin of the Troodos massif  
(Fig1.3),  
the outline of fans developed on the north Troodos margin,  
the radial drainage pattern feeding off the Troodos Massif (Fig.2.1),  
the development of the drainage parallel to the Polis-Paphos graben in  
the north-west of the island (Fig.2.1).

F - Multispectral scanner image of the north Troodos margin displaying the  
development of the drainage feeding from the ultramafic core of the  
ophiolite to the north-north-west into Morphou Bay (Fig2.1).

Note: the dark spot in the centre of the plate marks the an area just to the  
south of Mount Olympus, i.e. the area where the ultramafic units crop out.

G - Thematic mapper satellite image of the south Troodos Massif displaying  
the area of capture of the Kryos River by the Kouris Rvier (Fig.2.3; Plate  
2.3).

Note: the F1 erosion surface picked out north of Limassol (Fig.2.19).

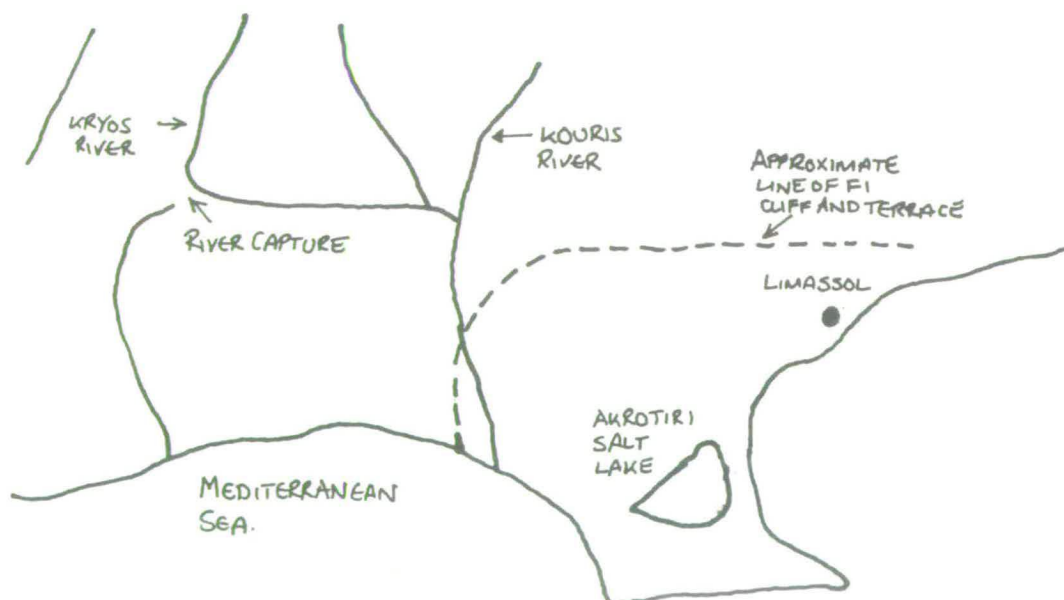
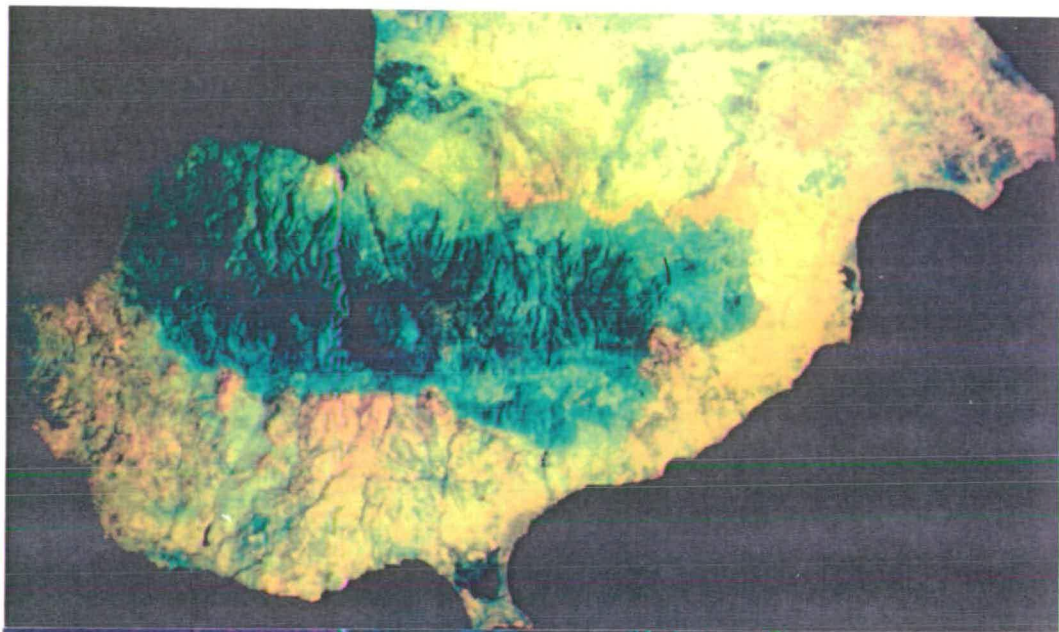
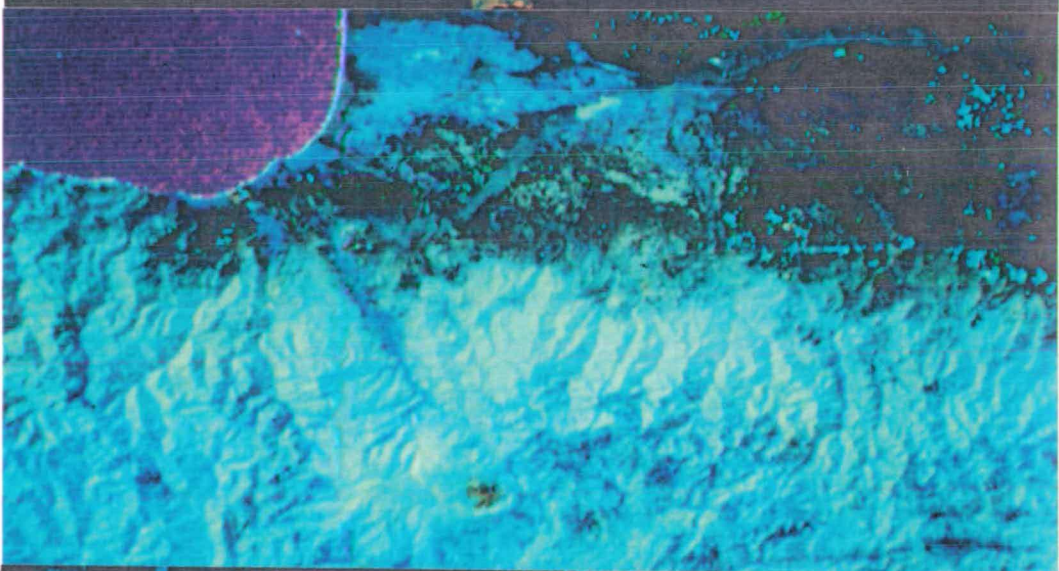


Plate 2.1

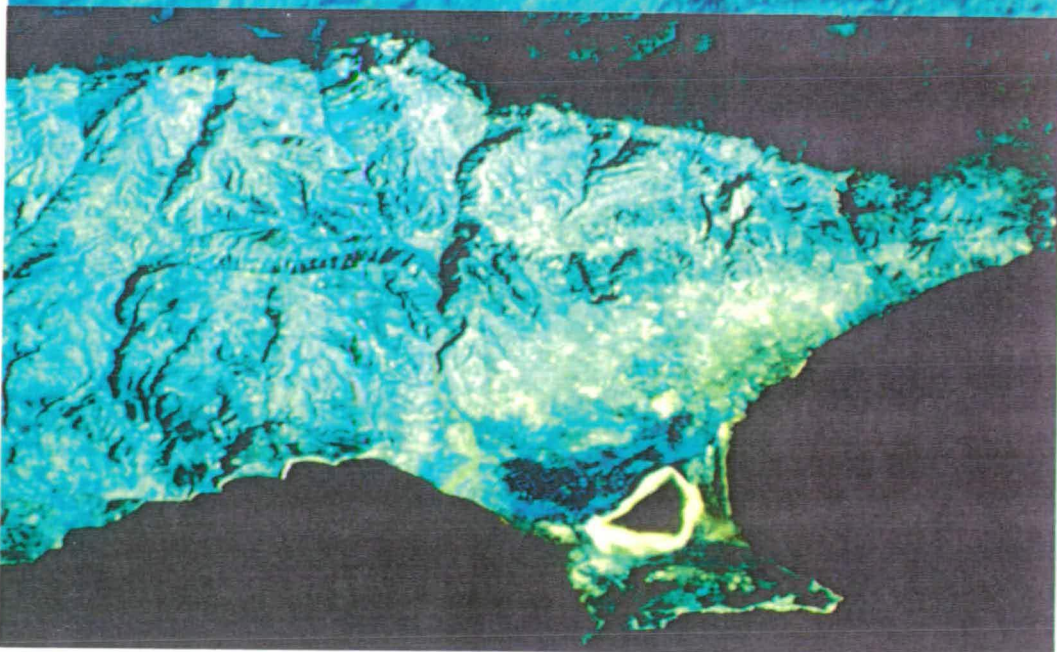
E



F



G



- ii) a lateral, approximately east to west, trend seen in the centre of the Mesaoria Plain, comprising the major rivers (e.g. Pedieos, Serakhis, Yialias, Ovgos; Fig.2.1) that drain out into Morphou Bay in the west and Famagusta Bay to the east (Plate 2.1);
- iii) straight-coursed rivers that drain out to the south and south-west of the island (Plate 2.1);
- iv) a trend that has been affected by pre-existing structure and topography (e.g. the Polis-Paphos graben in the west of the island; Plate 2.1);
- v) a component that represents the effects of river capture, as a result of erosion, during the Quaternary-Recent (Plate 2.1).

Each component of the drainage pattern, and gorge development, will now be described in more detail, dealing with each group of features in turn. An interpretation of the components of the south Cyprus drainage pattern will be made in light of the classification laid down by Howard (1967).

### **2.2.2 Radial drainage pattern around the Troodos Massif.**

The drainage associated with the Troodos Massif forms a radial pattern (Fig.2.1). The rivers to the west of the Karyotis River feed straight off the Troodos Massif into Morphou Bay, e.g. the Atsas River (Fig.2.1). Rivers further east feed onto the Mesaoria Plain and, to the south of the Troodos Massif, on to the southern coastal plain (Fig.2.1). Provenance studies based on clasts taken from the Fanglomerate Group along the north Troodos margin (Section 5.5), suggest that this radial pattern of drainage existed since the ultramafic core of the Troodos ophiolite was unroofed, as clasts derived from this small portion of the ophiolite (Fig.2.1) are only found associated with the rivers feeding from the core of the ophiolite (Fig.2.1). Satellite imagery data (Plate 2.1) and field observations along the north Troodos margin support this argument and suggest that major alluvial sedimentation took place, along this margin, during the Quaternary. Proximal facies pass into distal facies from south to north across the plain in all cases (Section 5.3), this lack of south to north variation in the sedimentary facies<sup>through time</sup> reflects little obvious change in the drainage pattern.

The view that little or no change in the drainage pattern occurred during the Quaternary does not agree with De Vaumas (1959, 1961, 1962) who suggested that the focus of uplift of the Troodos Massif shifted from the east towards a present position beneath Mount Olympus. The hypothesis was supported by the presence of the most dissected portion of the piedmont in the eastern portion of the Mesaoria Plain and by the direction of the origin of the alluvial fans converging on a point east of Mount Olympus, similar to that seen on the north Troodos margin during the Miocene, when the eastern



part of the Troodos Massif was being faulted and uplifted (Follows, 1990). De Vaumas's (1959, 1961, 1962) evidence, however, may reflect some pre-existing variation in the altitude of the Mesaoria Plain, resulting from previous faulting, and not a shift in the highest point on the Troodos Massif.

### **2.2.3 The lateral, east-west, drainage pattern through the centre of the Mesaoria Plain.**

The onset of fluvial sedimentation (with sub-aerial conditions) occurred in the Apalos Formation (McCallum, 1989). Thus the Apalos Formation is interpreted to mark the initiation of the east-west drainage in the centre of the Mesaoria Plain. The pattern of drainage through the centre of the Mesaoria Plain suggests that an east-west watershed exists to the west of Nicosia at the lowest north-south, and highest east-west, point in the Mesaoria Plain. This results in rivers running parallel to the north margin of the Troodos Massif and the southern margin of the Kyrenia Range, forming an axial drainage pattern (Fig.2.2). This component of the drainage pattern has persisted through to the present (Fig.2.1).

The drainage pattern to the west appears to be quite simple (Fig.2.1). By contrast, in the east, Troodos-derived gabbroic clasts are found in shallow marine siliciclastic and fluvial conglomerates in the vicinity of Dhekelia (Fig.2.1; location 3-32; *vid.* Chapters 5 and 6). The presence of these sediments indicates that capture of drainage occurred and/or the drainage pattern in the south-east of the island was more extensive during the Lower and Middle Pleistocene. On the plains of southern and eastern Cyprus present day major rivers appear to be unable to reach the sea due to possible climatic variations, a lack of bedload, low river gradients, or mans influence with the construction of dams.

### **2.2.4 The nature of the drainage pattern along the southern coast of the island.**

Many of the rivers that drain the southern coast of the island show a sub-dendritic passing into parallel drainage pattern, with feeder streams perpendicular to the <sup>main</sup> valleys (Fig.2.3). In south-west Cyprus, data from S.P.O.T. satellite imagery suggests that the large linear drainage systems fed extensive outwash plains that formed beneath 300m ASL. The S.P.O.T. data also highlights the contrast between the northern and southern Troodos margins. In the north, deeply incised V-shaped and hanging valleys are seen, e.g on the eastern side of the Karyotis River, north of Tembria, suggesting rapid downcutting. By contrast, on the southern Troodos margin, the river channels have a youthful drainage pattern proximal to the southern Troodos margin passing into a mature drainage pattern with wide U-shaped valleys further south (Yeropotos and Dhiarizos

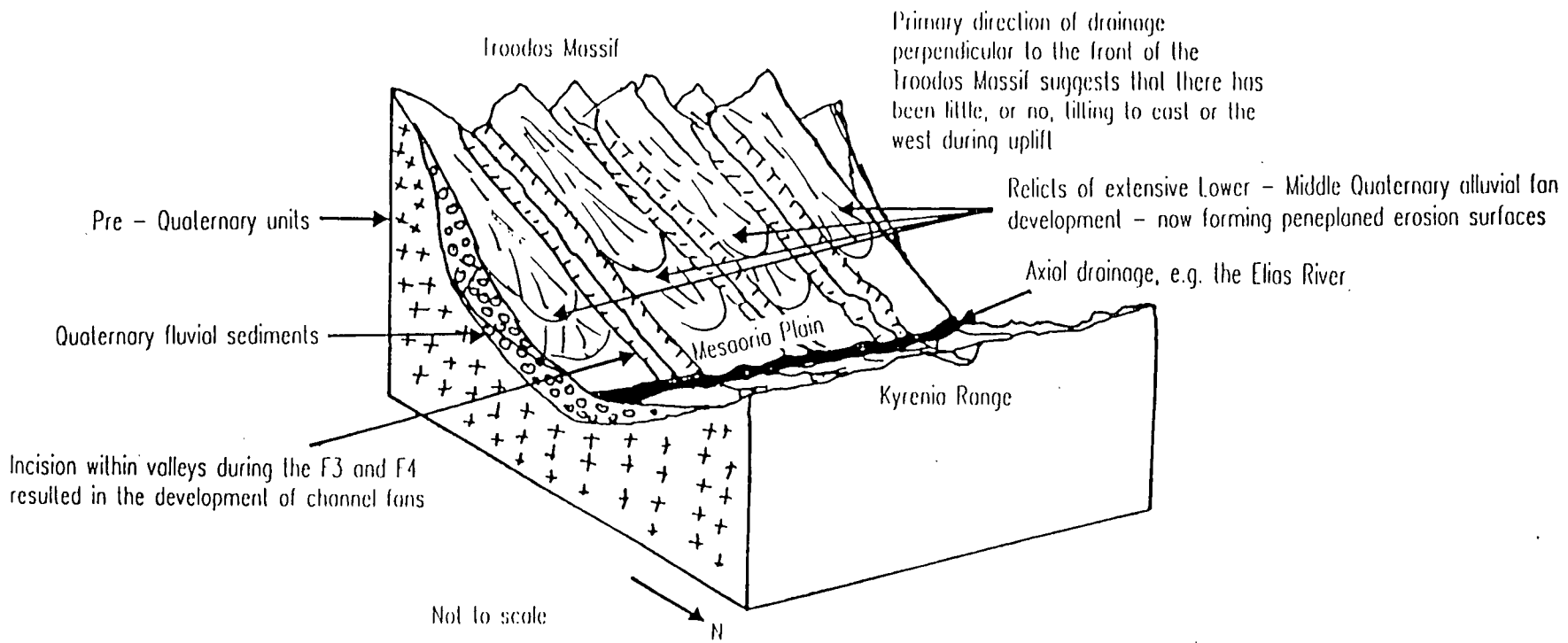


Fig.2.2. Schematic block diagram showing the F2 erosion surface and the development of the F3 and F4 channel fan systems on the north Troodos margin and the axial drainage pattern developed between the Troodos Massif and the Kyrenia Range.

Note: the drainage direction is constant throughout, arguing against the effects of differential block movement from east to west across the Mesaoria Plain.

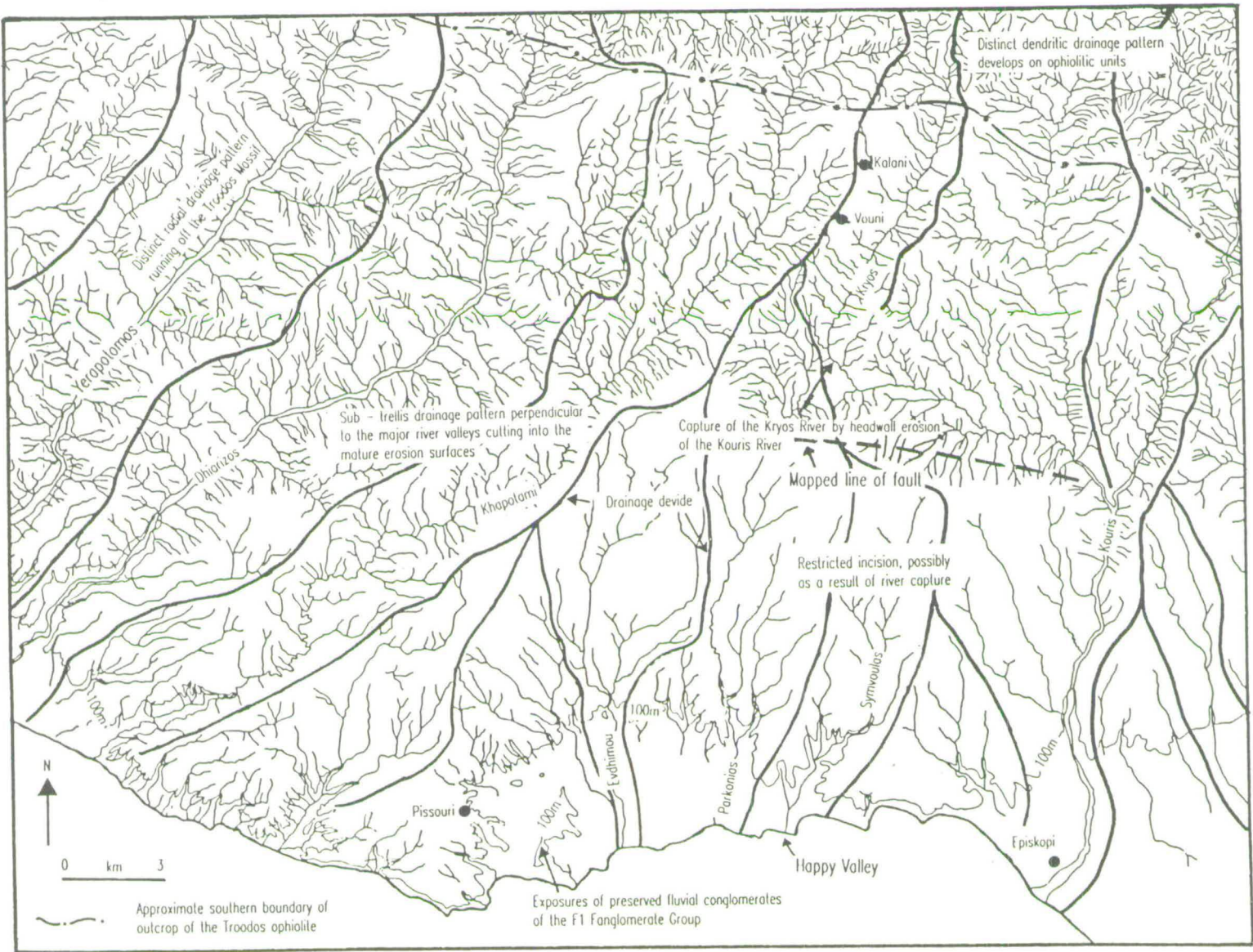


Fig. 2.3. Mapped detail of the rivers that form the subject of Plates 2.2 and 2.3. This diagram also details the capture of the Kryos River and shows the trellis-sub-trellis pattern of drainage seen along the parallel valleys east and west of the area of capture. Drainage divides and erosion surfaces, where present, are highlighted.

Note: see Fig. 2.7 for details of location of this area within southern Cyprus.

Rivers; Fig.2.3). This downcutting preserved channel linearity through a variety of ophiolite and sedimentary lithologies and structural features (Plate 2.1; Fig.2.4). Increased downcutting and rejuvenation of the drainage resulting from base level fall can be identified, as seen at Pissouri (Fig.2.5) and in the Ezousa and Yerapotomos Rivers of south-west Cyprus.

The Yermasoyia River cuts straight across the Limassol Forest Block and the Arakapas Fault belt (Figs.1.3 and 2.1). Rivers feeding the Yermasoyia, however, have utilised the inherent weakness associated with the Arakapas Fault belt with channels cutting courses parallel to the fault belt, i.e. east-west rather than north-south. The Vasilikos Valley (Fig.2.1), by contrast, exploited the weakness of the Arakapas Fault belt with valleys feeding into this area from the north and the south (Fig.2.1). Thus field and satellite evidence show that pre-existing tectonic structures did not play a major role in the development of the drainage pattern along the coast of the island (Plate 2.1).

The rivers that feed from the Troodos Massif into the southern coastal areas of Cyprus cut through a variety of rock types, e.g. chalks, melange, cherts, sandstones and serpentinite, yet this does not affect their course. Faults marked on the 1:250,000 geological map (Pantazis, 1979) are reported to control the position of some of the valleys in the southern coast area, e.g. the Yerapotomos River, but other rivers, e.g. the Dhiarizos River, cut similar courses without mapped tectonic control (Fig.2.4).

Houghton *et al.* (1990) dated the fauna in channel sediments within the Maroni River valley (Fig.2.6), that have cut down through the Miocene sequence at Khirokitia, and concluded that the nannofossil and foraminiferal assemblage is Upper Pliocene in age. This suggests that at least part of the drainage along the southern coast of the island could have arisen as submarine channels before sub-aerial exposure of this area. Similar submarine channels transported debris flow deposits southwards during the Miocene (Eaton, 1987). The Maroni channel system has been mapped (Fig.2.6) indicating that the line of the Pliocene channel conforms with the orientation of the present day drainage. The Pliocene channel was also incised during the Quaternary, resulting in the deposition of Quaternary fluvial sediments of the Fanglomerate Group in the present Maroni River valley.

The nature of the drainage pattern here, and along other areas of the coast, suggests that the uplift of the Troodos Massif relative to base level changes was rapid and possibly episodic (geomorphological studies on river valleys, C. Vita-Finzi, *pers. comm.*, 1989). This uplift caused deep downcutting, back cutting and the initiation of a sub-dendritic pattern on the Troodos Massif, with a steep linear drainage pattern on the

Fig.2.4. The detailed geology of the Dhiarizos River valley, displaying the wide U-shaped valley and the lack of impression that the lithological changes, and structures, have had on altering the course of the river (base map after Lapierre, 1971).

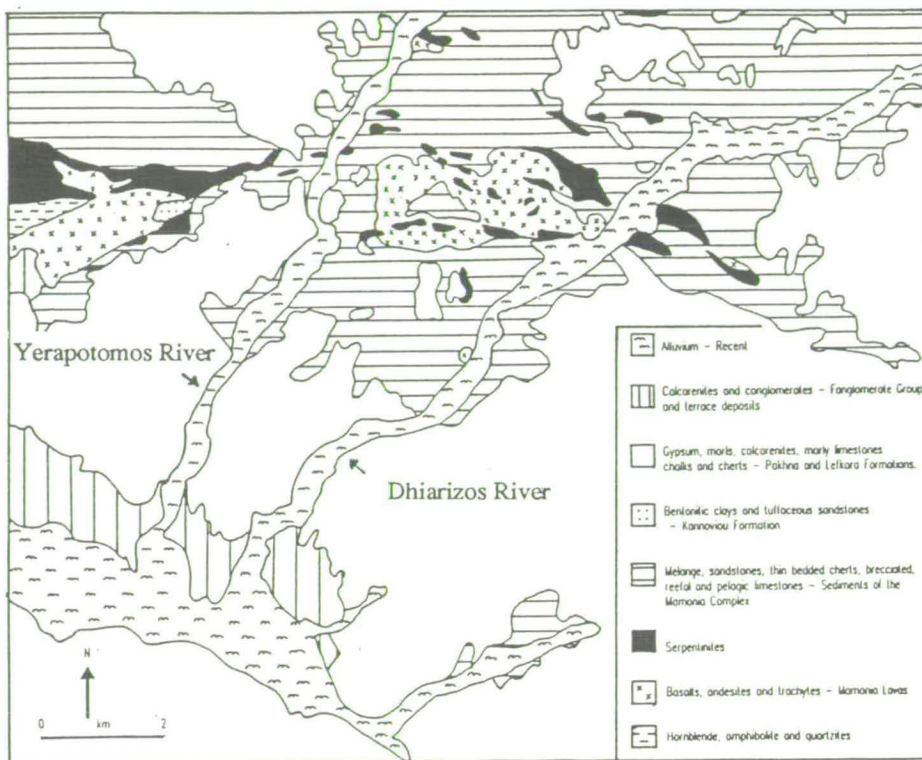


Fig.2.5. Detail of the Pissouri Bay area of southern Cyprus, illustrating features interpreted to represent rejuvenation as a result of a fall in the base level, i.e. uplift and/or sea-level fall.

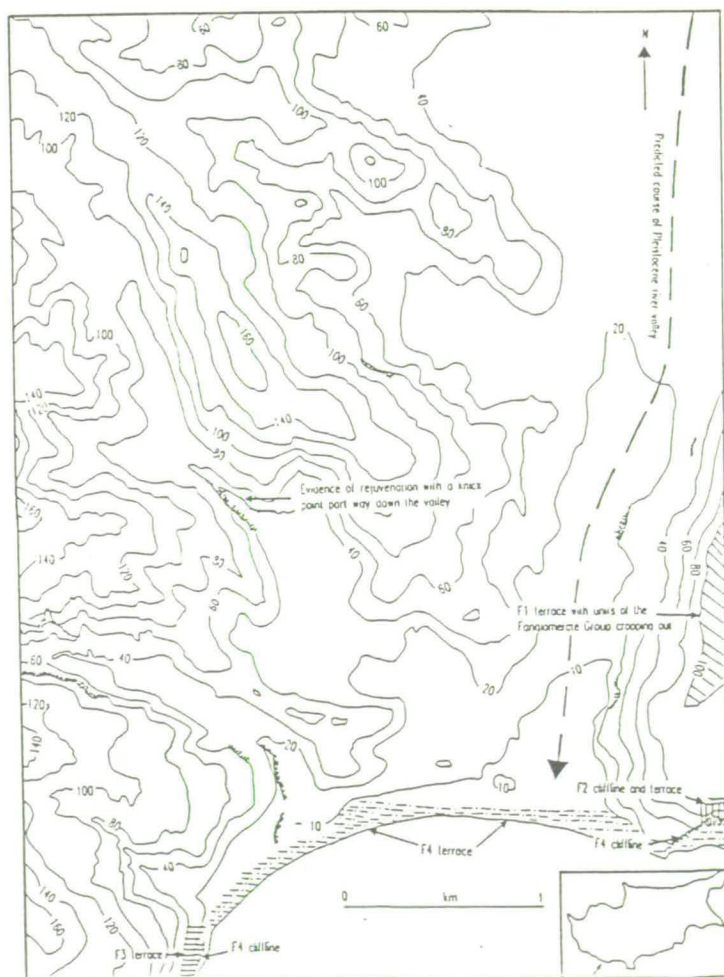
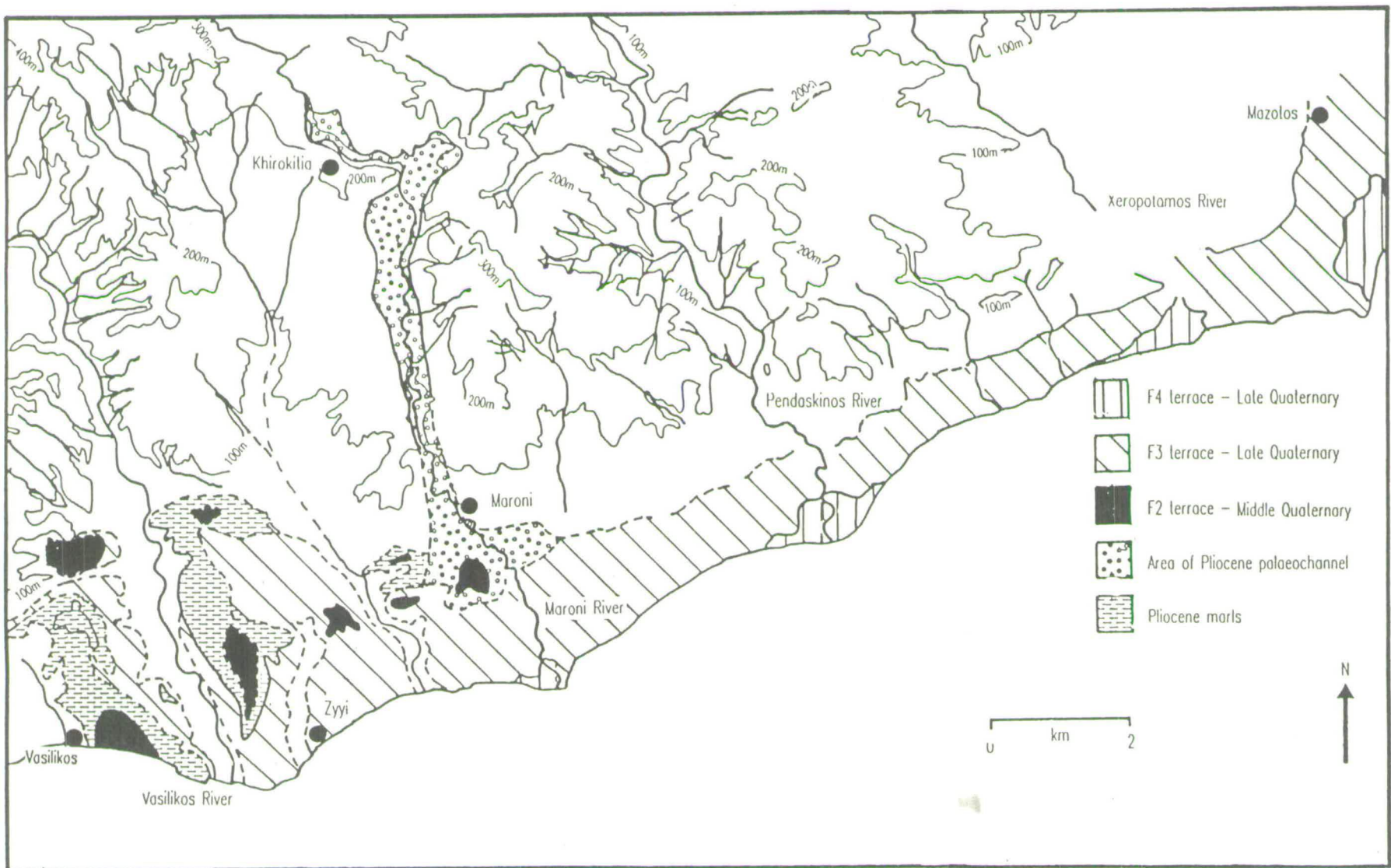


Fig.2.6. A detailed map of the Quaternary sequences in and around the Maroni River valley, southern Cyprus.



Note: details of the location of this map within southern Cyprus are shown in Fig.2.7.

margins of the Troodos Massif. Subsequent uplift of the island resulted in renewed downcutting. There is no evidence to support the view that neotectonic or palaeo-tectonic structures dictated the pattern of drainage. Seismic data (McCallum, 1989) allow the Quaternary sediments to be recognised offshore. This evidence, coupled with the drainage pattern seen on the south coast, suggests that much of the deposition associated with the erosion of the Troodos Massif and Troodos cover sediments took place quite some distance away from the major source areas along the present coastal plain area. Some drainage even by-passed this area, depositing sediment offshore (McCallum *et al.*, 1991).

The major control on the drainage pattern in southern Cyprus was undoubtedly the uplift of the island, and more specifically, the rising Troodos Massif.

### **2.2.5 The effect of pre-existing tectonic structures and topographical features on the drainage pattern.**

The Mesaoria Plain existed as a half graben and depo-centre in Pliocene times (McCallum, 1989), influencing the development of subsequent drainage patterns during the Quaternary. Similarly the Polis-Paphos graben (Fig.2.1) controls the drainage pattern in west Cyprus. The Khrysokhou River initially flows towards the south-west, but later runs north-west down the axis of the graben (Fig.2.1), resulting in the deposition of sediments of the Fanlomerate Group. There is no evidence of capture during the Quaternary period suggesting that from the onset of fluvial action the graben controlled the pattern of drainage in this area. Many rivers feed back into the western limb of the graben, e.g. Akamas Peninsula (Fig.2.7), but have not yet breached this structure. S.P.O.T. satellite data reveals a major drainage divide at Polemi which is not obvious in the field.

De Vaumas (1959, 1961, 1962) identified a strong rectilinear pattern of drainage in the area of the Arakapas Fault belt (Figs.1.3 and 2.1), where the streams are aligned parallel to the fault belt. This is another example of the drainage influenced by tectonic structures, yet, as seen with the Polis-Paphos graben, there is little evidence to suggest that the structure has actually caused the drainage pattern to deviate. Large-scale active fault movement, e.g. in the Polis-Paphos graben and along Arakapas Fault Belt, took place between the Late Cretaceous and Late Tertiary (Robertson, 1990). The Quaternary drainage pattern later took advantage of these lines of weakness, or topographic lows, created as a result of these tectonic events.

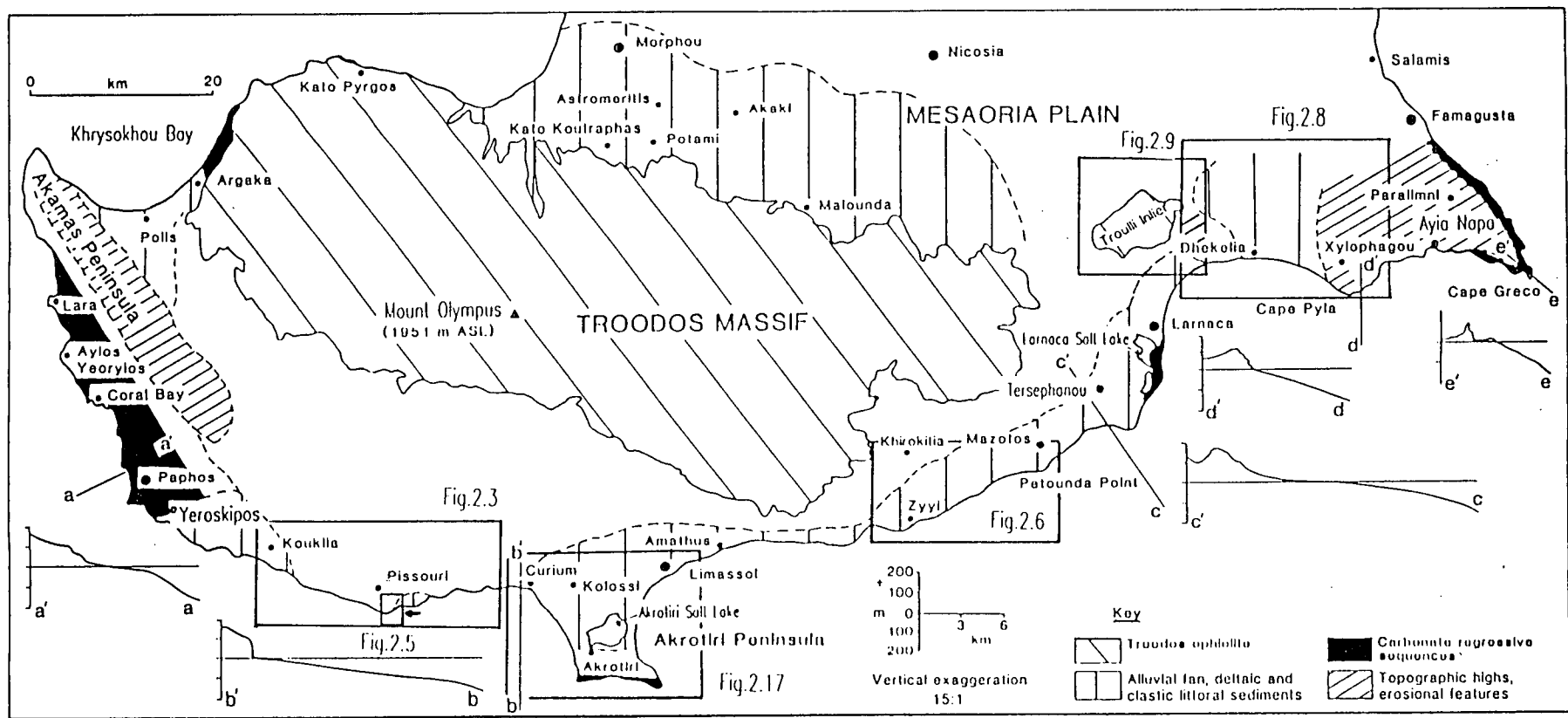


Fig. 2.7. Outline map of southern Cyprus showing the variation in Quaternary sediments and selected topographic sections.  
 Note: boxes indicating the location of other figures cited in the text.



There are only three large areas in southern Cyprus, other than the Troodos Massif, where pre-existing Pleistocene topography affects the drainage pattern seen. In the south-east of the island, a topographic "high" occurs to the south and east of Xylophagou (Fig.2.8). This feature is mainly formed of Miocene limestones (Follows, 1990), which are generally resistant to erosion, and has prevented rivers draining out to the far south-east of the island. The Xylophagou high was complemented by the Troulli topographic "high" to the east (Fig.2.8). The Troulli high is an inlier of both Troodos ophiolite and its sedimentary cover sequence. The Troulli Inlier and the Pano Lefkara area (Allerton & Gomez, 1989) further west are areas of high ground that reflect the palaeo-relief and the configuration of the Troodos ophiolite during its formation at a mid-ocean ridge spreading centre in the Tethys Ocean. Quaternary uplift of the island resulted in these features becoming areas of high relief, e.g. the off-axis horst that now constitutes the mountain Stavrovouni Monastery stands on, north-west of Larnaca (Allerton & Gomez, 1989), linked by Lefkara chalks to the eastern margin of the Troodos Massif. This area of raised relief caused the drainage flowing east across the Mesaoria Plain to diverge and flow to the north and east into Famagusta Bay, or south between the areas of high relief into Larnaca Bay. Rivers from the Troulli inlier flow in a radial pattern, with those rivers flowing to the south subsequently cutting back into the inlier resulting in the pattern seen today, with a narrow ridge separating those rivers flowing to the north and east from those flowing to the south (Fig.2.9). Rivers flowing from the Xylophagou high ground generally run perpendicular to the coast, forming a simple youthful drainage pattern. An exception to this pattern exists south of Ormidhia (Fig.2.10) where a more mature channel system has cut down through the pre-Pleistocene sedimentary units. This resulted in the development of a "ria" flooding the channel during, and prior to, the last inter-glacial. Similar embayments are seen at Pissouri (Fig.2.5; Plate 2.2) and at Happy Valley, in the Episkopi garrison area (Fig.2.3). These, south Cyprus embayments have no major rivers running into them today. A modern analogue to these examples is the flooded rivers valleys to the west of Ayia Napa (location 1-136; Plate 2.2).

### **2.2.6 Evidence for river capture.**

The capture by the Garyllis River of the headwaters of the Vathia River at Phasoula and the Mersina River at Spitali is recorded by Bear & Morel (1960). Drainage capture is also seen in the area north-west of Limassol, where the Kryos River turns sharply east, and then links with the Kouris River (Fig.2.3). The Cyprus geological map (Pantazis, 1979) suggests that a fault in this area was responsible (marked on Fig.2.3), but there is no field evidence to support this argument. An oblique aerial view of this area taken from 5,000m (Plate 2.3), satellite imagery data (Plate 2.1) and field evidence (Plate 2.2) indicate that similar erosion surfaces are present on both the Paramali River (that

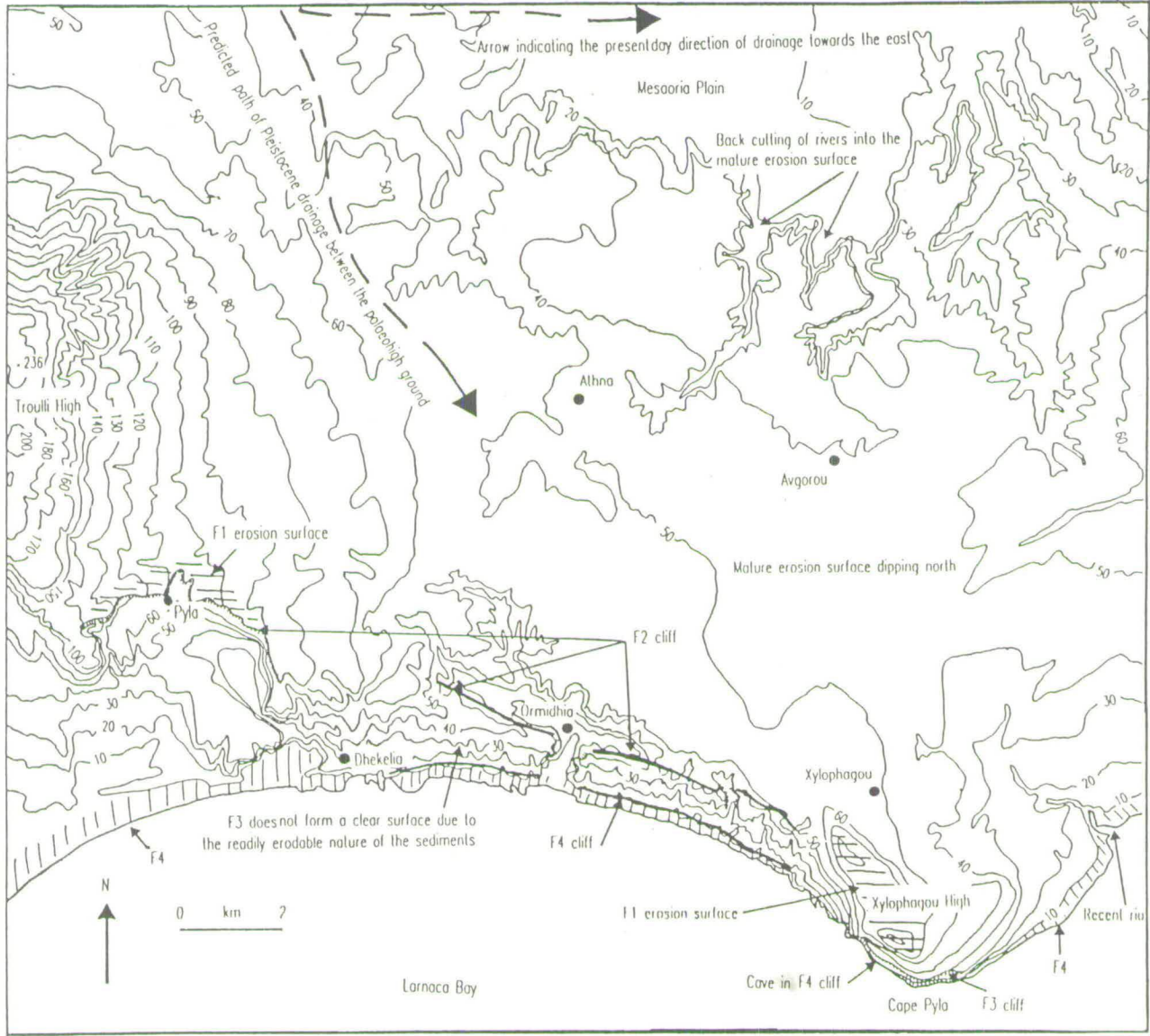


Fig.2.8. Map of the area to the east of Larnaca detailing the location of the Troulli and Xylophagou "highs", with associated drainage trends and terrace patterns.

Note: see Fig.2.7 for details of the location of this map within southern Cyprus.

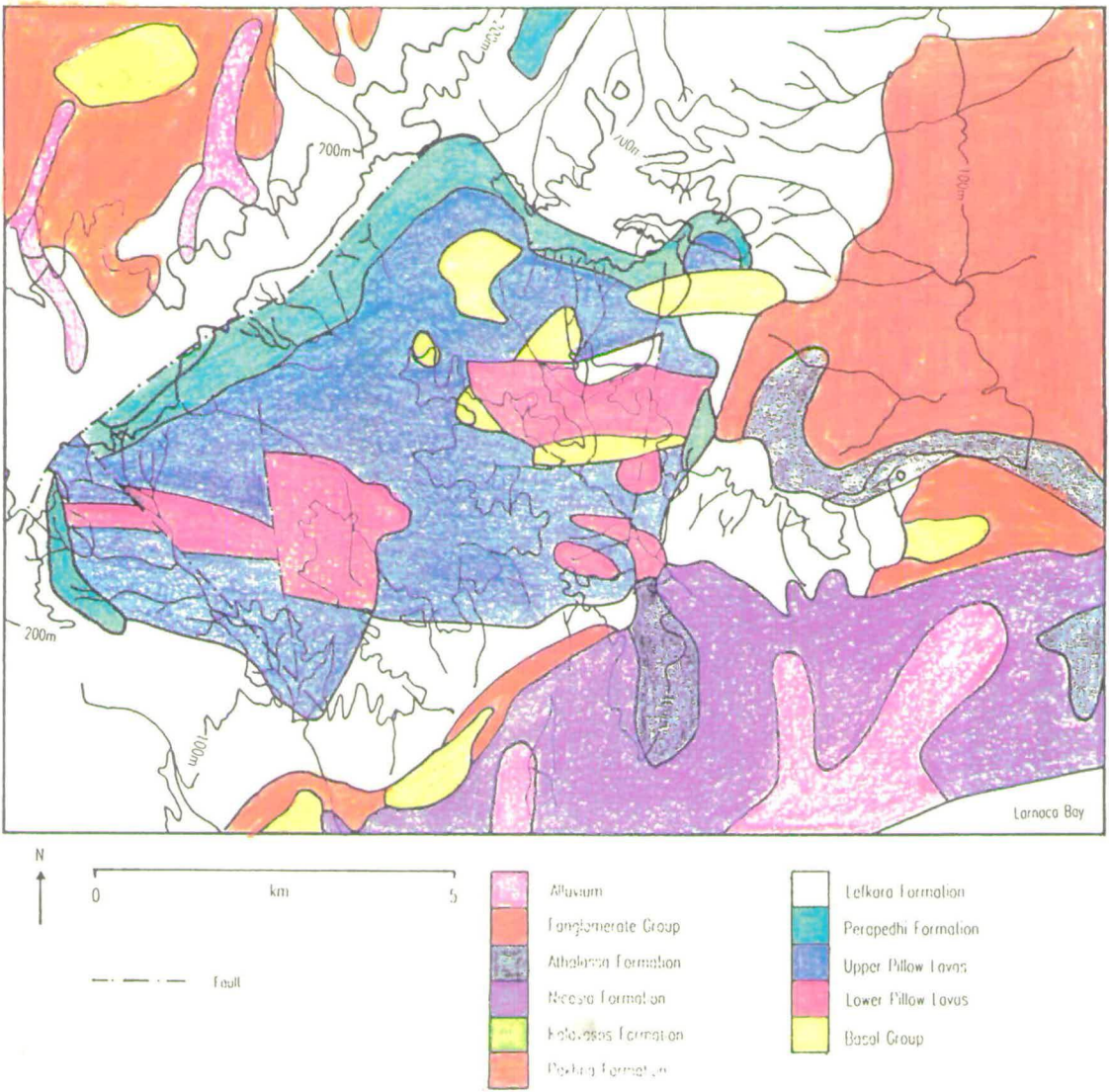


Fig.2.9. The detailed geology, drainage pattern and topography in the area around the Trovili Inlier, south-east Cyprus.

Note: details of setting within southern Cyprus are shown in Fig.2.7.

**PLATE 2.2.**

- E - View of the Pissouri Bay area, looking west, revealing the mature erosion surface capping the opposite hill and the development of the F3 (b) and F4 (a) terraces within the preserved overdeepened embayment.
- F - A present day flooded river valley located to the west of Ayia Napa.
- G - A panoramic view of the F1 (along the crests of the hills) and F2 (bowl shaped) erosion surfaces preserved above the course of the Kryos River, which has been captured by the Kouris River, southern Cyprus.

## Plate 2.2

E



F



G



runs south of the point of capture) and on the north arm of the Kryos River before it turns sharply east (equivalent surfaces can also be seen in the Khapotami River valley to the west; Plate 2.3). However, these erosion surfaces are not found in the east to west linking portion of the Kryos River (Plate 2.3). Evidence from Pissouri (location 3-30) shows that Troodos-derived clasts are found in the Quaternary fluvial channel sediments of this area (Section 5.5), yet no rivers drain back onto the Troodos Massif from here today. This evidence points to capture of the upper reaches of the rivers that feed to the south and west, parallel to the Khapotami River, during the Lower and Middle Pleistocene.

The capture of the Kryos River probably resulted from headwall erosion of a feeder valley to the Kouris River which cut to the west (Fig.2.3). As subsequent uplift took place the present-day Kryos River, instead of continuing to cut down to the south, breached the drainage divide causing a switch in the drainage from the south to the east. This resulted in the development of a more youthful drainage pattern to the south of the east-west Kryos-Kouris link (Fig.2.3), with more mature deep U-shaped valleys to the east and west of this area.

### **2.2.7 The formation of gorges associated with the development of the Quaternary drainage pattern.**

Gorges in the Kyrenia Range result from the rapid downcutting of drainage (Dreghorn, 1978). Steep valleys and gorges are also present in the Troodos Massif and where major channels feed from the Troodos Massif to the south, e.g. near Paphos. The most spectacular series of gorges in southern Cyprus are found on the western flank of the Akamas Peninsula, east of Lara (Fig.2.7), cutting down from a mature erosion surface of resistant limestones and Quaternary fluvial conglomerates, at c.350m ASL (Plate 2.4). These features are identifiable on S.P.O.T. satellite imagery and run out onto the terraces found at c.100m ASL. There is no evidence that these gorges are fault-controlled (Plate 2.4). The field and S.P.O.T. data show that there was no deep incision of the drainage beneath 100m ASL.

A phase of deep channel and river down cutting in south-west and south Cyprus resulted in the formation of gorges and sub-surface drainage, which is related to rapid uplift of the island at that time. Sea-level changes could have played a role in the initial formation of these erosional features, but a lack of evidence for a subsequent rise in sea-level suggests that uplift of the island was the dominant control. An example of sub-surface drainage is seen at Tremithousa (location 3-35; 280m ASL) where a small tunnel has formed. The top of the tunnel, 4-5m in diameter, is found within a few metres of the higher portion of the F1 mature erosion surface (Section 2.3.2). The tunnel is only about

Plate 2.4

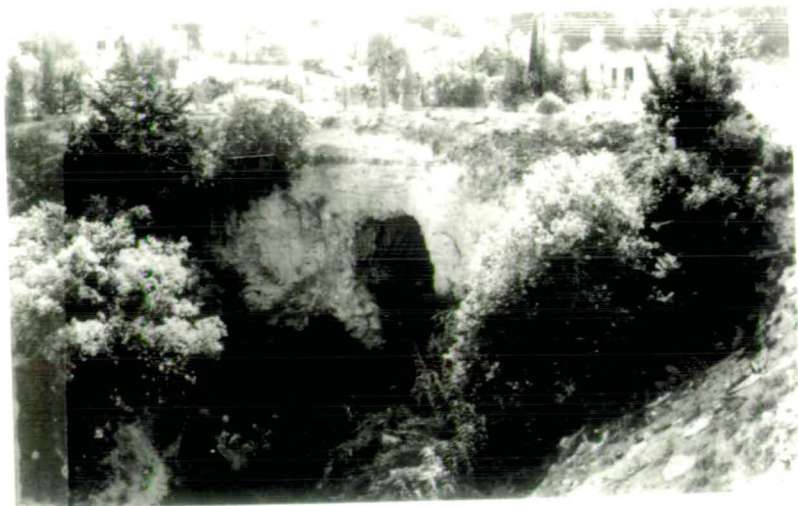
E



F



G



20m long (Plate 2.4) and drops steeply into a gorge in the Koshinas River valley. The channel that formed the cave has cut down through a sequence of marine and fluvial sediments in response to a drop in base level.

## **2.3 EROSION SURFACES.**

### **2.3.1 North Troodos margin.**

A series of fluvial terraces and mature geomorphological surfaces extend across the Mesaoria Plain (Plates 2.5 and 2.6). The plain dips gently to the north at approximately 3-5°. These erosion surfaces were recognised by De Vaumas (1959, 1961, 1962), Bear (1960), Gass (1960) and Moore (1960) who created the following stratigraphy for the Pleistocene of the Mesaoria Plain: the Fanglomerate Series (now replaced by the Fanglomerate Group; *vid.* Chapter 5); young and older river terraces; and Recent alluvium. Ducloz (1965) replaced the earlier Pleistocene stratigraphy of the Mesaoria Plain with a hierarchy based on the analysis of the Fanglomerate Group erosion surfaces in the eastern portion of the Mesaoria Plain; this results in four Pleistocene units and the Recent alluvium above the Apalos Formation (Tables 1.4, 1.7 and 1.9). All previous authors (De Vaumas, 1959, 1961, 1962; Bear, 1960; Gass, 1960; Moore, 1960; Ducloz, 1965) agree that the erosion surfaces on the Mesaoria Plain are related to uplift of the Troodos Massif.

Erosion surfaces on the north Troodos margin were observed using data collected on a number of different scales, e.g. field evidence, air photos and satellite imagery (Section 1.7.2). Sedimentological data relevant to the formation of the Fanglomerate Group are presented in Chapter 5.

Field evidence shows that terraces and erosion surfaces in proximal localities (i.e. close to the northern margin of the Troodos Massif) can be correlated with those mapped by Ducloz (1965) further to the east. By contrast, mature erosion surfaces in distal localities away from the north Troodos margin do not show the same distinct terrace development. Here, the highest terraces preserved today are located within 10's of metres of the present valley floor (location 1-12).

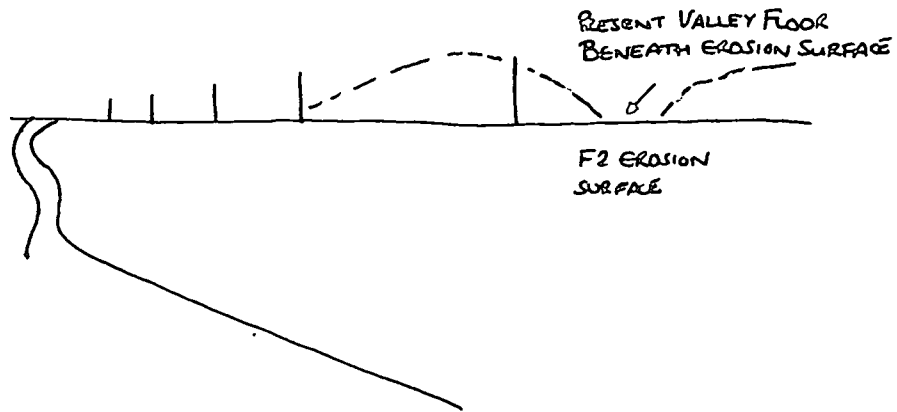
The F1 erosion surface (Kantara Gravels; Ducloz, 1965), that has a patchily developed <sup>ment</sup> in the eastern portion of the Mesaoria Plain, is thought to be largely absent in the west. The F1 erosion surface is at a greater elevation than the plain in the east (Fig.2.11) this is likely to be the case in the west too. The F1 erosion surface is identified close to the summit of Mount Olympus where it is deeply incised by the F2 and later



PLATE 2.5.

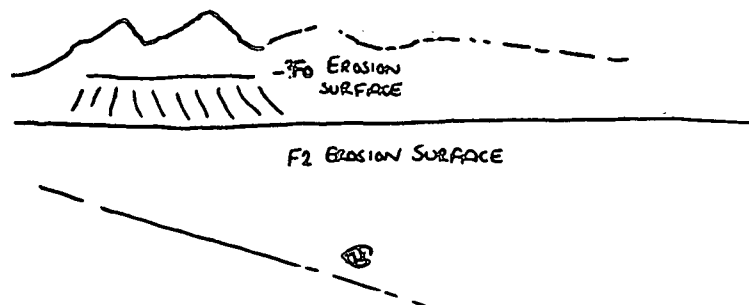
E - A view looking south across, the F2 erosion surface, on the Mesaoria Plain towards the Troodos Massif.

Note: the very shallow dip of the surface and the evidence of the present valley floors being lower than the erosion surface.



F - A view across the F2 erosion surface, looking north, towards the Kyrenia Range.

Note: the shallow dip of the erosion surface and the ?F0 erosion surface preserved at the foot of the Kyrenia Range.



G - The F2 erosion surface on the northern edge of the Troodos Massif overlying the Lefkara Formation and the Pillow Lavas of the Troodos ophiolite.

H - The F1 erosion surface at Koraka Hill (location 1-9) standing proud of the F2 erosion surface that makes up the plain in the foreground.

Plate 2.5

E



F



G



H



## **PLATE 2.6.**

E - A view looking west across the Akaki River valley on the Mesaoria Plain revealing the development of the F2 (a), F3 (b) and F4 (c) erosion surfaces and terraces.

F - A view looking west towards Kreatos Hill revealing the dissected F2 (a) and F3 (b) erosion surfaces.

G - The concave F3 erosion surface on the west of the Mesaoria Plain near Astromeritis (location 1-27).

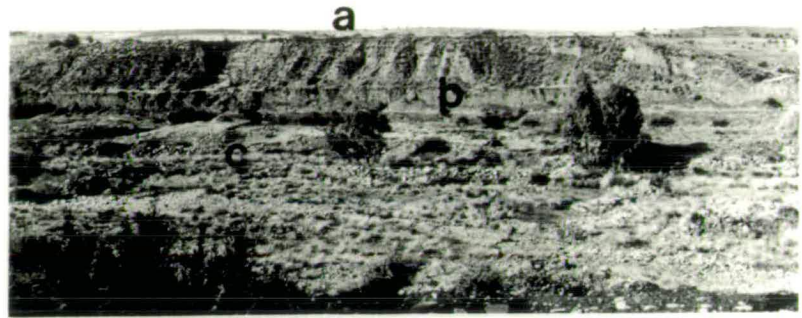
Note: the gently dipping F2 erosion surface intersecting the concave F3 surface.

H - A view looking east towards the F2 erosion surface capping mesa hills near Pera (location 1-97).

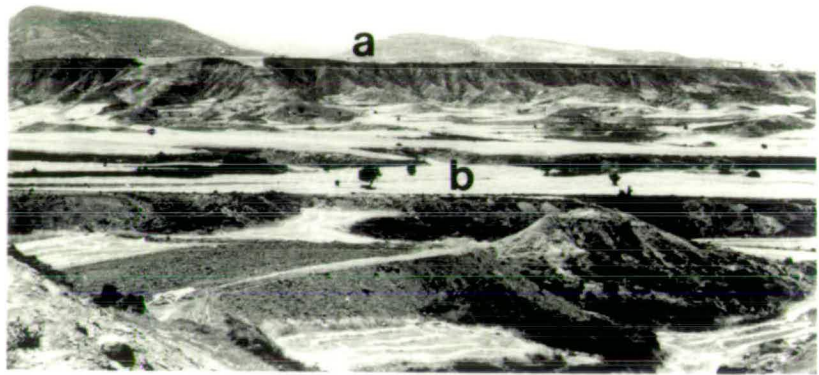
Note: the dark shade of the Fanglomerate Group conglomerates capping the marls of the Nicosia Formation near the top of the mesas.

# Plate 2.6

E



F



G



H



terraces. In the area of Koraka Hill (location 1-9) the F1 erosion surface crops out at 409m ASL. Conglomerates at a similar height, probably related to this surface, are also seen on Kreatos Hill, just east of Mitsero. The F1 surface lies between 30-40m above the F2 surface in proximal localities close to the north Troodos margin; this difference decreases to the north and east. The F1 and F2 terraces do not intersect (Fig.2.11) and the height of the projected F1 terrace at grid line 90 is higher than the elevation of the majority of the Mesaoria Plain. Mount Olympus stands at 1951m ASL (Figs.2.7 and 2.12). If the F1 trace from Fig.2.11 is continued south, as a straight line, to the latitude of Mount Olympus, i.e. grid line 65, then the resulting elevation of the F1 erosion surface is c.800m ASL. The actual presence of the F1 erosion surface close to the summit of Mount Olympus (c.1900m ASL) indicates that this surface is not flat but concave, similar to the surfaces of De Vaumas (1961; Fig.2.13). The presence of the F1 erosion surface close to the summit of Mount Olympus indicates that Quaternary uplift of Mount Olympus was in the order of 1900m, much greater than the equivalent uplift on the Mesaoria Plain. Although this agrees with Robertson (1977), it contradicts De Vaumas (1959, 1961, 1962), who identified this erosion surface as being of Pontian age (Lower Pliocene; surface S3 in Fig.2.13). There is no evidence for the presence of Quaternary marine sediments on the plain and the highest point on the Mesaoria Plain today is only 200m ASL. Thus, the uplift ratio (the uplift ratio = the absolute uplift of Mount Olympus/the absolute uplift of the Mesaoria Plain) was greater than 1:1, and possibly in the order of 9-10:1. This difference in uplift possibly accounts for the intersection of the F1 and F2 erosion surfaces, and the apparent merger of terraces to the north of the Troodos Massif, although it has been assumed that the segment of the erosion surfaces on the Mesaoria Plain are planar.

The F2 (Kambia Gravels; Ducloz, 1965) F1 conglomerate unit, developed on the western portion of the Mesaoria Plain, is the most extensive erosion surface preserved today. Satellite imagery (Plate 2.1), supported by field studies, show that extensive alluvial fan development occurred with the F2 phase of the Quaternary evolution of southern Cyprus. Deflation has, however, resulted in the formation of the flat erosion surface seen today. Palaeocurrent and borehole data from the F1 conglomerate Group on the north Troodos margin (Chapter 5) show that alluvial fans prograded north from the Troodos Massif and then laterally, to both the east and west, across the Mesaoria Plain. Although this interpretation is supported by satellite imagery and field work, only one phase of major alluvial fan development is preserved today. No cross-cutting fans were developed. This implies that much of the F1 surface was either never deposited, or has been extensively eroded, and channel fan development took place after the development of the F2 alluvial fans, during the later part of the Quaternary. Air photographs detail a similar pattern to the satellite data, with small channels running across the F2 erosion

Fig.2.10. A "ria" channel south of Ormidhia probably formed during the last two interglacial periods, down cutting through sedimentary units creating an overdeepened channel, mapped from air photographs, 6" to the mile.

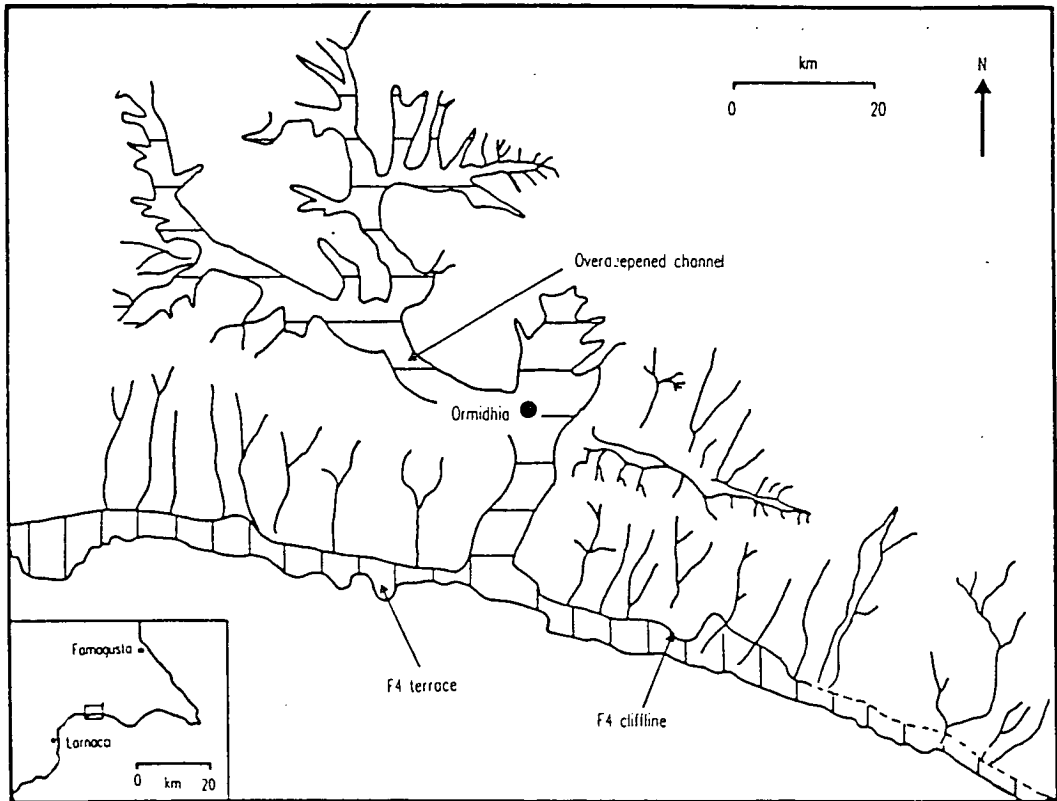


Fig.2.11. Relative slopes of the three erosion surfaces associated with the F1, F2 and F3 events on the northern margin of the Troodos Massif. It is noted that the F3 represents a shallower gradient, perhaps indicative of uplift at a reduced magnitude relative to the F1 and F2.

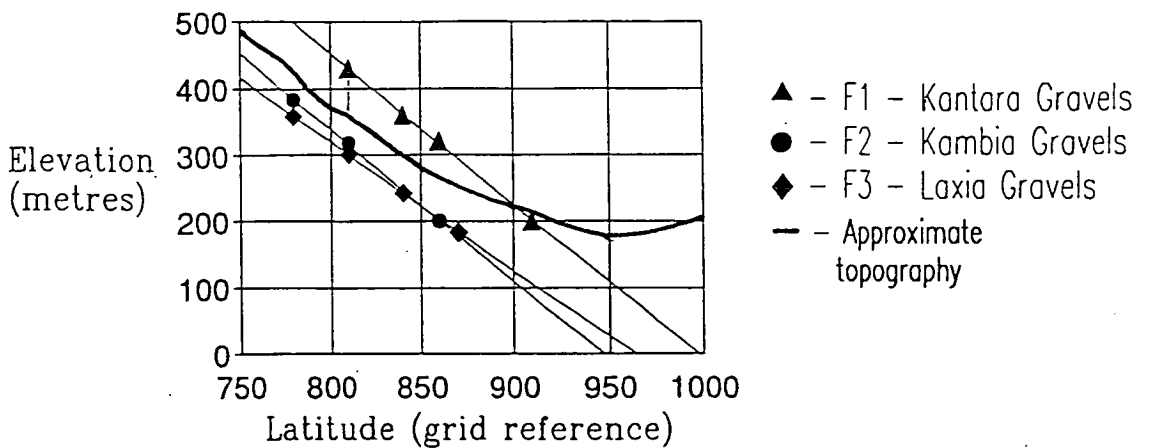


Fig.2.12. 3-d interpolated surface topographic map of southern Cyprus, viewed from the south-west at an angle of 5°, with the contour map from which it was derived.

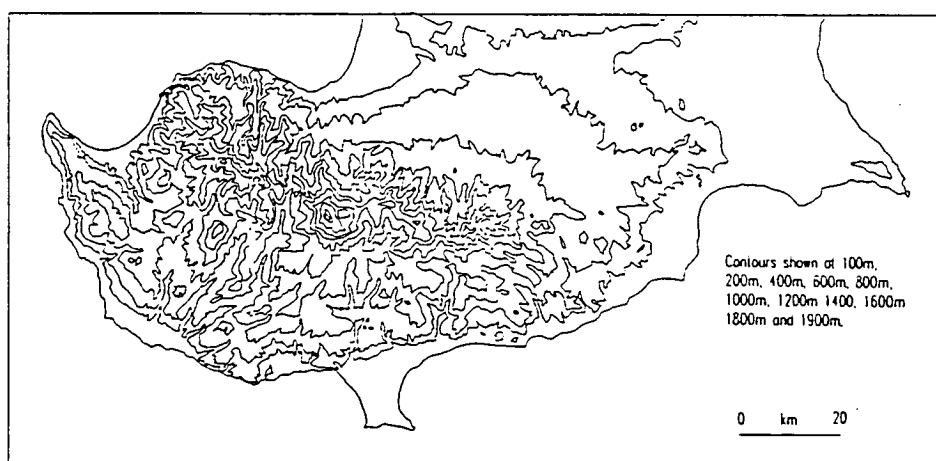
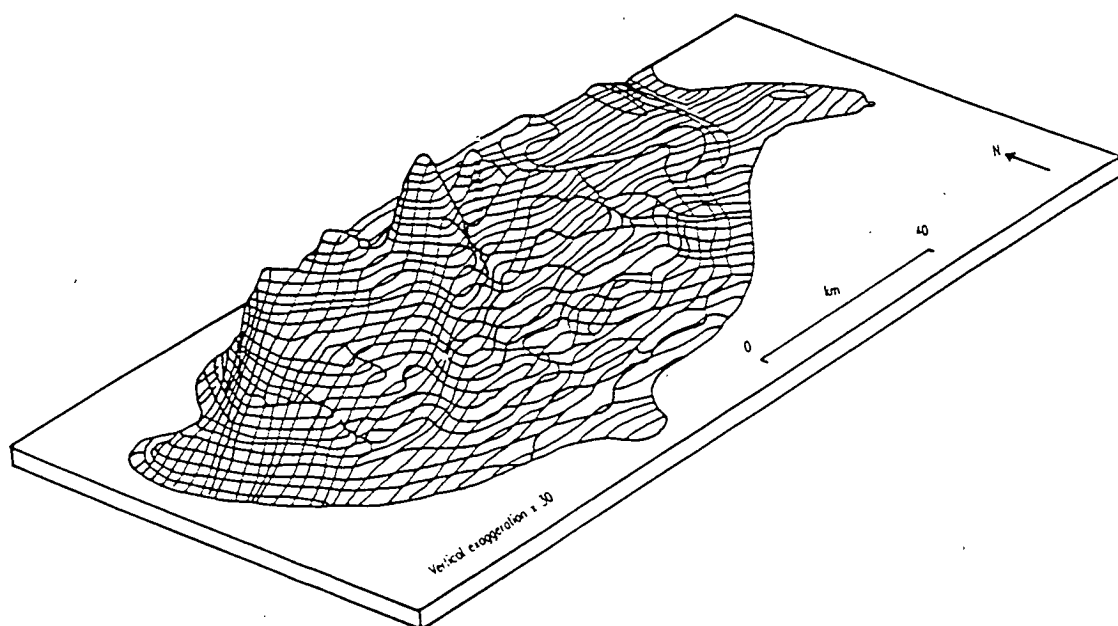
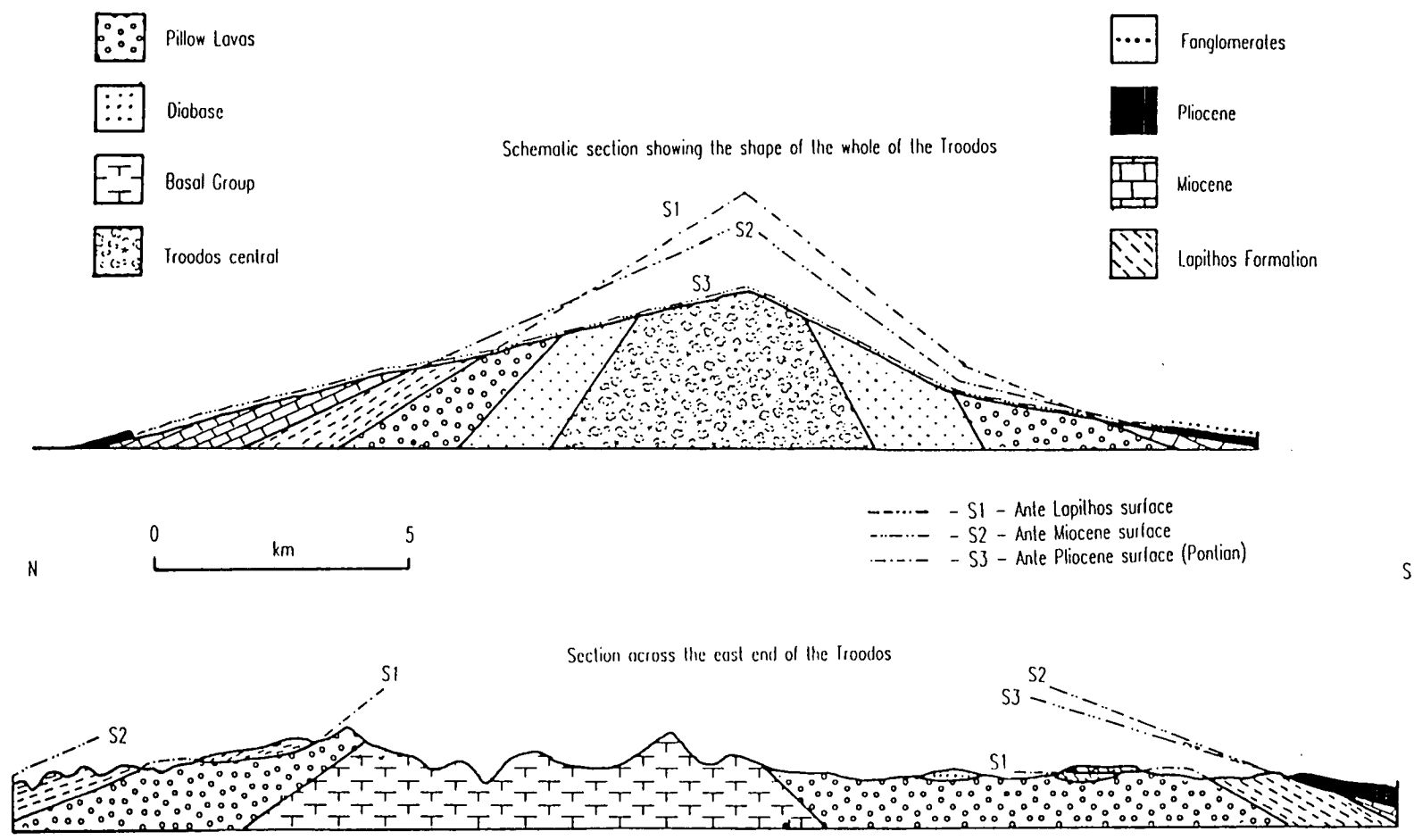


Fig. 2.13. Schematic sections across the Troodos Massif displaying erosion surfaces interpreted as being of Lapilthos age (Upper Cretaceous-Lower Miocene), Miocene and Lower Pliocene in age (after De Vaumas, 1961).





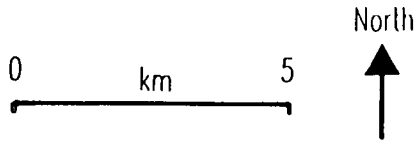
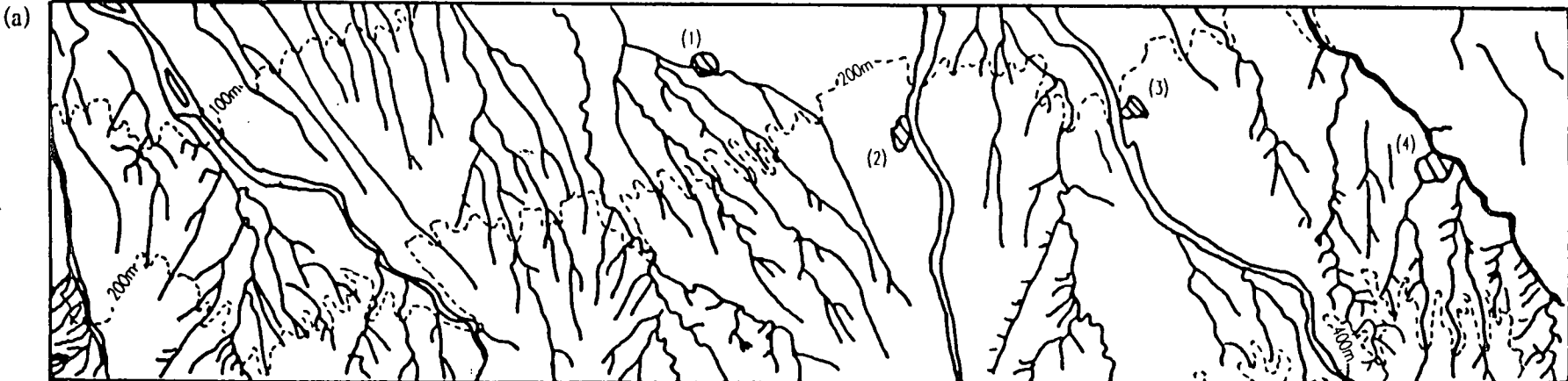
surface, but there is no evidence of major channel switching (Fig.2.14). This suggests that the drainage pattern that existed on the north Troodos margin during the early Quaternary (Section 2.2), reflects that seen today (Fig.2.1). The F2 surfaces are generally more continuously preserved in the west than in the east. In the east, the discontinuous F2 erosion surface is commonly picked out above thin conglomerate caps on buttes and mesa-type hills, e.g. Pera, (location 1-97 and 1-98; Plate 2.6). The caps of the Fonglomerate Group conglomerates have extensively eroded soft Pliocene sediments.

The F3 Fonglomerate surfaces on the north Troodos margin form less extensive features at a lower level than the F2 surfaces. The F3 erosion surfaces make up a series of paired terraces that can be correlated across and between valleys in proximal-intermediate areas, e.g. between Kato Moni, Orounda and Malounda (Fig.2.15), but do not form extensive fan sequences. The F3 surfaces were documented as forming concave slopes and mature erosion surfaces in the eastern part of the Mesaoria Plain (Ducloz, 1965). Similar concave surfaces were also recognised during this study, in the western portion of the Mesaoria Plain at Potami (location 1-118) and west of Astromeritis (location 1-27; cf. Plate 2.6; Fig.2.15). The F3 terraces can be correlated with the Laxia Gravels (Ducloz, 1965) and the Older Fill described by Bear (1960), Gass (1960) and Moore (1960), and are commonly found within 15m of the present day river channels, e.g. Tembria in the Karyotis Valley (location 3-61). Away from the Troodos margin the F3 terraces also converge with the F2 surfaces to the north (location 3-1), the height difference varying from 50m near Aredhiou in the south, to 6m north-east of Kato Lakatamia further north (Ducloz, 1965).

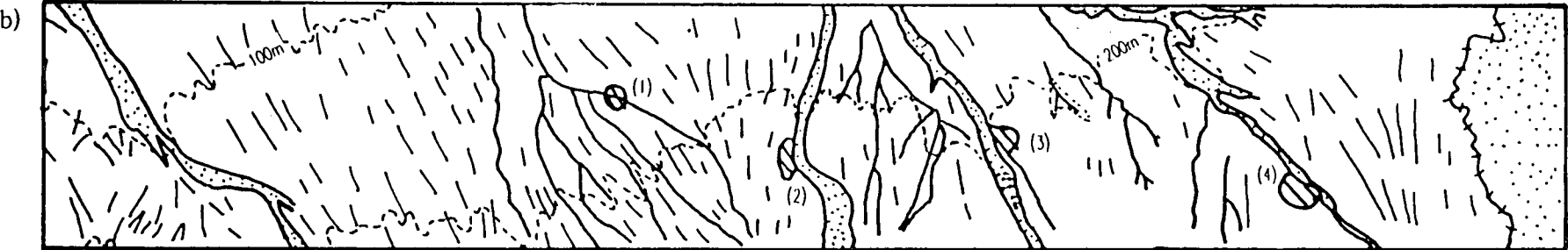
The Xeri Alluvium (Ducloz, 1965) was identified as being correlatable with the F4 erosion surface on the Mesaoria Plain. The F4 unit also forms paired terraces that correlate with the Younger River Terrace of Bear (1960), Gass (1960) and Moore (1960). In the Astromeritis area the F4 terrace crops out 10m above the present day channel (Moore, 1960). The Pedieos River has cut the deepest incision recorded in the Xeri Alluvium (26m near Pera; Ducloz, 1965) into the underlying basement.

Stable, vegetated bars are identified as the F4 surfaces on the Mesaoria Plain; these surfaces are located above the present day channels and within the area confined by the F3 terraces and erosion surfaces. These bars are commonly found within 2-5m of the present day valley floor, e.g. north of Ayios Ioannis (location 3-2).

Fig. 2.14. a) topographic and detailed drainage map of the central and western Mesaoria Plain: displaying the present development of marginal streams and larger ephemeral rivers; b) lineations across the F2 erosion surface on the central and western Mesaoria Plain (mapped from a 6" to the mile air photograph).



- (1) Astromerilis (2) Peristerona
- (3) Akaki (4) Paleometokho



- lineations
- drainage
- F3/F4 terrace development

Fig.2.16. Schematic sketch section of the relationship between pre-Quaternary sequences, aeolian sediments, units of the Fanglomerate Group and deltaic sequences at Tersephanou (location 3-16), along the south coast of Cyprus.

Note: see Fig.2.7. for the location of Tersephanou.

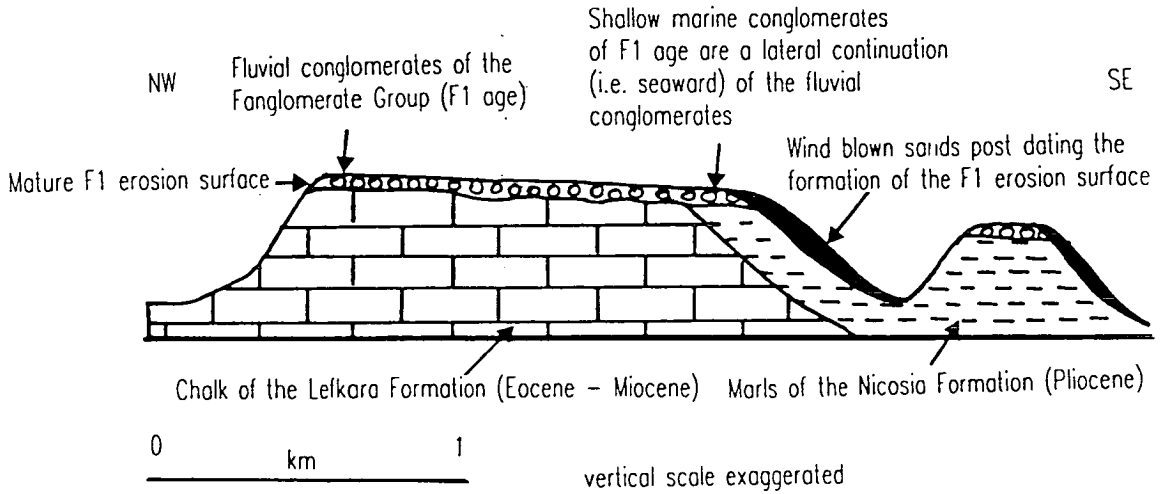
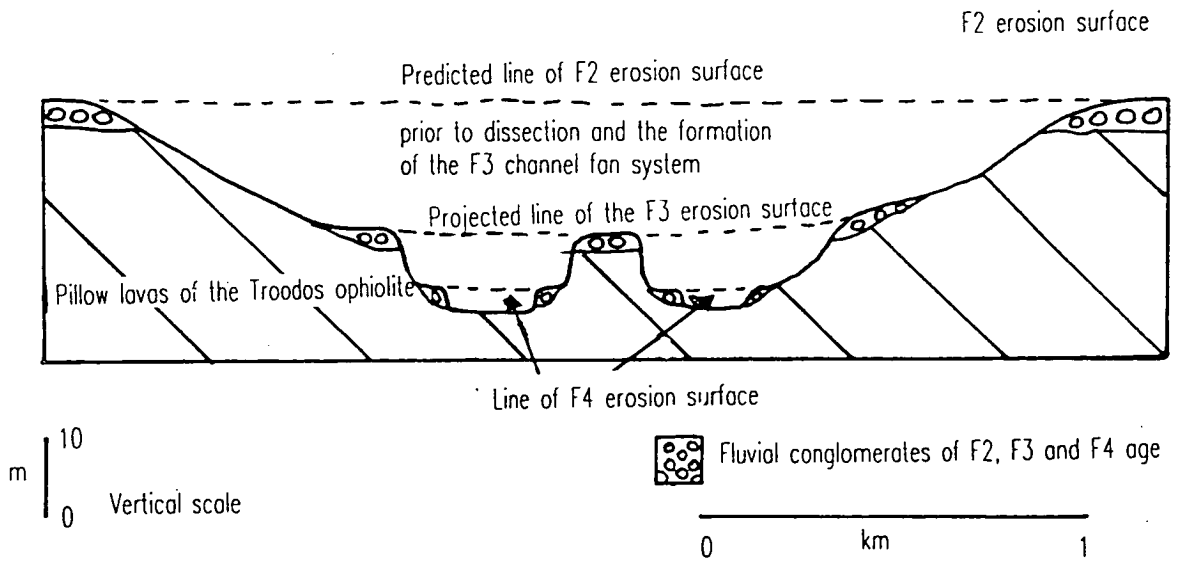


Fig.2.15. Schematic sketch section across the F2 and F3 erosion surfaces displaying the development of paired terraces on the north Troodos margin.



### **2.3.2 Southern coastal areas.**

Correlation of the erosion surfaces of southern Cyprus has depended on generally unfossiliferous lithologies, similar to those seen on the north Troodos margin. Consequently, a terminology similar to that seen on the north Troodos margin has developed, with Fanglomerates, Older and Younger River Gravels and Recent Alluvium (e.g. Bagnall, 1960; Pantazis, 1966). Gomez (1987) introduced a local stratigraphy for the lower Vasilikos Valley (Fig.2.1) and tentatively correlated this with the north Troodos margin and the central Kyrenia Range (Ducloz, 1965, 1972; Table 1.8). McCallum (1989) introduced the term Vasilikos Formation for a series of fluvial sediments that crop out in a quarry at Vasilikos (Fig.2.6), correlating these sediments with the Pliocene Kakkaristra Formation (Table 1.3); she also identified the Fanglomerate, the Older and Younger River Gravels and Recent Alluvium in the Vasilikos area.

The oldest known erosion surface in southern Cyprus lies at approximately 500m ASL along the Akamas Peninsula (Fig.2.7). A corresponding erosion surface, the "Pontian" surface of De Vaumas (1959, 1961, 1962), located on the southern flank of the Troodos Massif, may be equivalent to, or possibly older than this. A firm correlation is not possible. The erosion surfaces along the coastal areas of southern Cyprus do not dip steeply and are not tilted. The seawards dip, of  $6^{\circ}$  or less, of most of the coastal terraces in southern Cyprus may reflect the depositional dip, with exceptions occurring where the cliffs and terraces were overlain by later aeolian deposits (Section 2.4.7; Chapter 8). By contrast, the erosion surfaces related to the Kyrenia Range appear to be tilted, showing a steeper angle of inclination with increased altitude (Dreghorn, 1978). These data suggest that the coastal terraces of southern Cyprus were not subject to extensive tilting during their formation, unlike those in the Kyrenia Range (Dreghorn, 1978).

Erosion surfaces are found lying above all the marine clifflines identified in Section 2.4. These erosion surfaces in southern Cyprus cut down into both the Troodos sedimentary cover sequence and Quaternary marine and fluvial sediments. Similar surfaces are not present around the whole of the southern coast which suggests that the coastline may have been eroded, or that subsequent changes in base level have removed evidence of their existence. The river valleys in these areas, e.g. Dhiarizos River (Fig.2.4) do, however, show evidence of these features with paired terraces and the presence of knick points and rejuvenation features, as outlined in Section 2.2.4.

Erosion surfaces are seen in the area between Lamaca and Paphos. One of these is the F1 Quaternary surface, identified in the Vasilikos Valley (Gomez, 1987), which has

undergone extensive dissection and now comprises minor remnants that dip off the Troodos Massif. Though this surface is a strath feature, i.e. eroding bedrock, close to the Troodos Massif, it overlies Quaternary fluvial deposits in coastal areas, e.g. Pissouri (location 3-30; Fig.2.5). The F1 erosion surface at Pissouri is seen at 100m ASL on the coast and rises to 120m ASL inland, similar to the F1 surface to the north-west of Tersephanou (location 3-16; Fig.2.16).

The F2 surface is the most clearly recognised upper surface along the southern coast, similar to those seen on the north Troodos margin. The F2 terrace forms a series of longitudinal ridges that dip gently seawards (Plates 2.3 and 2.7) and has been greatly dissected by rivers and associated feeder streams (Fig.2.3). The F2 surface is very well developed in the area between Vouni and north-west of Kilani (Fig.2.3), where it lies between 1110m ASL and 700m ASL, dipping to the south at c.1°.

The F3 surfaces cut down into the F2, with the formation of paired terraces and concave erosion surfaces, e.g. in the Khapotami and north Kryos River valleys (Plates 2.2 and 2.3). The F3 features in the south can be correlated with those F3 features present on the north Troodos margin, and mark the development of channels within channels, similar to the channel fans of the north Troodos margin. The F3 surfaces are both erosive and form a surface over depositional sequences, e.g. Limassol (location 3-27) and on the northern portion of the Akrotiri Peninsula (location 3-28). The F3 erosion surface is seen 10-15m above the present valley floor on the Akrotiri Peninsula.

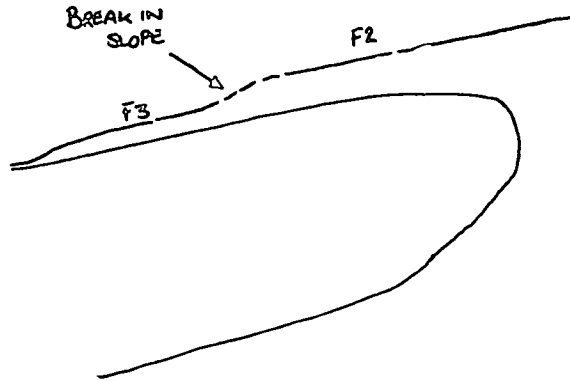
The F4 terraces are commonly found in the broad valleys along the southern coastal margin, e.g. the 2m terrace in the Tremithios River valley, near Larnaca (Gifford, 1978), within a few metres of the present valley floors. The F4 terraces mark the erosion through the F3 conglomerates and underlying basement, e.g. channels have cut down through the Athalassa Formation (location 3-28). The F4 features are small scale and of limited occurrence cropping out above the Recent valley fill that forms vegetated, stable bars. These F4 surfaces have prograded to a position occupied by the present day sea-level, forming small promontories, e.g. the Pendaskinos River (Fig.2.6). The F4 promontories are now being eroded following a reduction in the sediment supply to these areas during the Holocene, e.g. in the Larnaca area (Gifford, 1978). The rivers along the south coast quite commonly do not reach the coast today; interpreted to reflect the development of the F4 coastline during the oxygen isotope 5e sea-level high (Tables 1.9 and 1.10) that followed the formation of the F3 fluvial sequences and erosion surfaces.

The Kouris River braidplain (Plate 2.7; Fig.2.17) and associated sediments along the south coast of the island, e.g. Zyvi (Fig.2.6), and the Larnaca and Akrotiri salt lakes

PLATE 2.7.

E - The F2 erosion surface dipping seaward at Cape Dolos.

Note: the development of a break in slope with the F3 terrace beneath.



F - A view from Curium looking south-east across the Akrotiri Peninsula, the F4 terrace and the Kouris River braidplain.

G - Looking north-east from the western limb of the Polis-Paphos graben across the F0 (a) and, bowl shaped, F1 (b) erosion surfaces.

# Plate 2.7

E



F



G



(Fig.2.7) formed during the latest Pleistocene and Holocene. Archaeological artifacts (Early Bronze Age to Late Roman; I. Todd, *pers. comm.*, 1989) are found within the lowest F4 erosion surface 2m ASL today (location 3-70). Similarly a terrace within 2m ASL was cut into the Tremithios River in the Larnaca lowlands (Gifford, 1978). Gomez (1987) identified 6m of downcutting in the Vasilikos Valley, followed by aggradation and alluviation between 5540 and 5010 B.C.. The fluvial sediments deposited at this time are generally finer-grained than those seen in the lower and middle Pleistocene, i.e. F1-F2. Active erosion of this coast is taking place today with the erosion of archaeological sites at Zyyi (I. Todd, *pers. comm.*, 1989).

### **2.3.3 South-eastern Cyprus.**

Erosion surfaces are less conspicuous in the south-eastern portion of the island. The subdued nature of the surfaces may result from a combination of soft underlying sediments, i.e. marls and calcarenites of Pliocene age, and distance from the Troodos Massif (compared with the development of distal terraces on the north Troodos margin; Section 2.3.1). The mature erosion surfaces seen in the south-east are generally associated with coastal features and deposition of the Faglomerate Group did not take place. This is interpreted to be a consequence of the extensive F1 erosion surface at Xylophagou, which prevented rivers from the Troodos Massif draining out in this area. Rivers were diverted to the north into Famagusta Bay, or west of Xylophagou into Larnaca Bay (Section 2.2.5; Figs.2.1 and 2.8). Erosion surfaces cap the Faglomerate Group sediments in the Dhekelia area (location 3-32) and Athalassa Formation sediments at Pyla (Fig.2.8). The F2 and F3 surfaces are not clearly discernible in this area, possibly as a consequence of the unconsolidated nature of the sediments which makes their preservation potential low. The F4 erosional surface is preserved in the area to the west of Dhekelia (Fig.2.8) and in coastal areas between Dhekelia and Xylophagou (Section 2.4.3). Evidence from all phases of the Quaternary evolution, i.e. F1-F4, are present in the south-east of the island (Section 2.4.3) but a complete sequence is only seen in coastal areas.

Erosion surfaces are associated with the development of the Faglomerate Group to the north and west of Xylophagou. The F1 erosion surface to the north of Dhekelia and Pyla is a shallow-dipping, mature surface, covered by caliche and red soils, with only minor incision, e.g. north of Avgorou (Fig.2.8). The F1 surface marks the easternmost extent of any northward-dipping erosion surface cut into the Mesaoria Plain. The maximum height of the F1 erosion surface dipping to the north in this area is 98m, at Cape Pyla, so a change in altitude from 98m to 30m over 13km would cause the slope to change from  $0^{\circ}$  to  $<1^{\circ}$  during the early part of the Quaternary. Incision is seen from 30m down to 10m north of Avgorou (Fig.2.8). The variation reflects uplift that can be



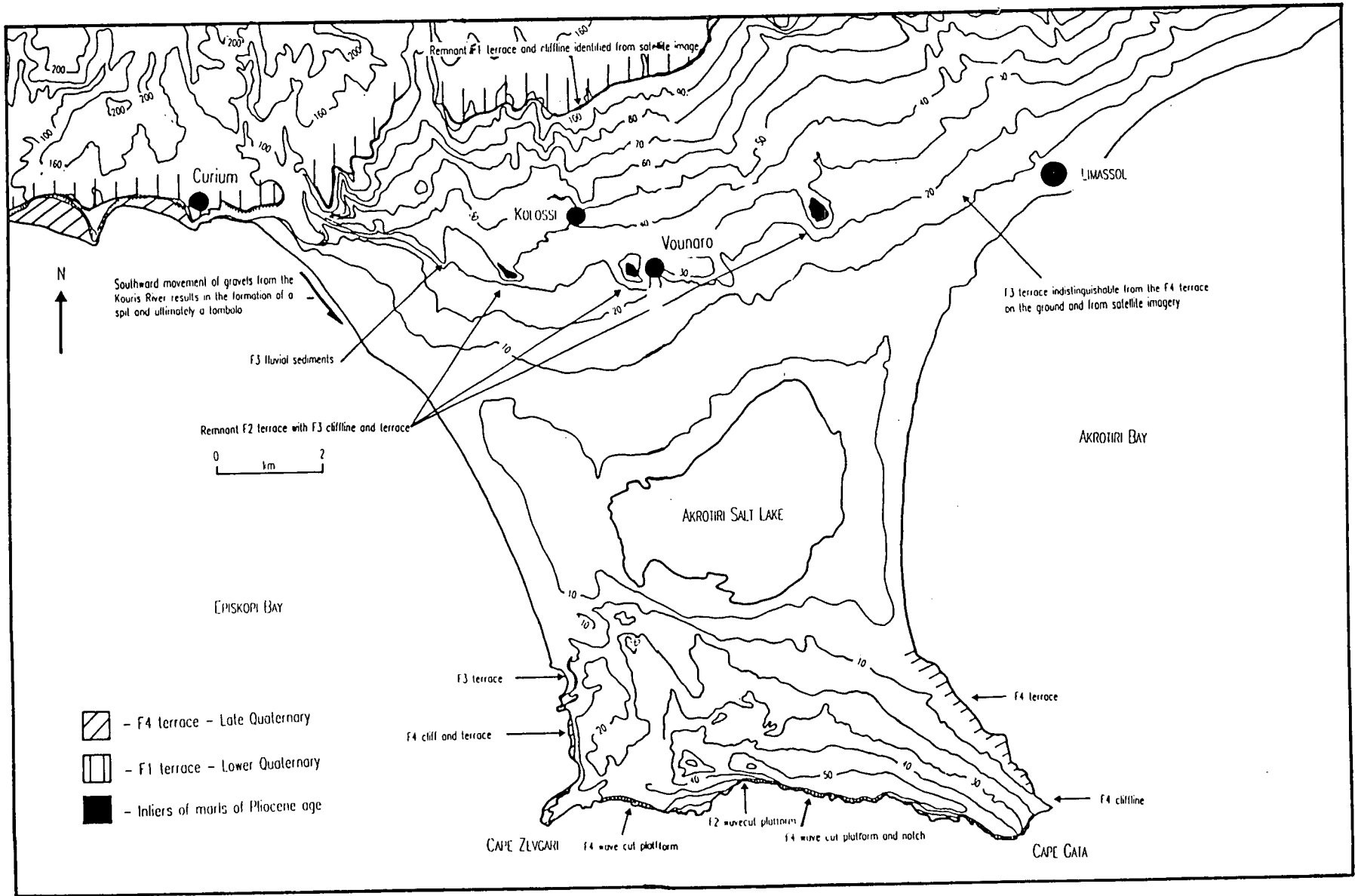


Fig. 2.17. A map of the marine terraces and palaeocliffines developed on, and to the north of, the Akrotiri Peninsula.

correlated with the F2 or F3. The erosion surface to the north, beneath the 10m contour, undulates slightly reaching sea-level 9km away, near Famagusta (Fig.2.7).

### **2.3.4 The Polis-Paphos graben.**

The region enclosed by the Polis-Paphos graben forms a fourth contrasting area for the development of erosion surfaces during the Quaternary period. The main period of graben development took place between the Upper Miocene and the earlier Pliocene (A.H.F. Robertson, *pers. comm.*, 1989; Follows, 1990). Local lower Quaternary footwall uplift (Chapter 4) was superimposed on regional uplift. The footwall uplift is largely absent from later sediments although some active faults are seen in the southern part of the graben, cutting sediments of the Faglomerate Group (Ward & Robertson, 1987).

The Polis-Paphos graben facilitated the formation of a concave bowl-shaped erosional surface which strikes north-west to south-east, parallel to its uplifted flanks. This bowl-shaped erosion surface represents the F1 surface in the graben (Plate 2.7). The surface dips quite steeply at its eastern and western extents, shallowing towards the centre of the graben. This has resulted in convergence and intersection of the F1, F2 and F3 surfaces, with each other, at lower altitudes (Fig.2.18). The F1 and succeeding erosion surfaces have been influenced by sea-level changes at the northern end of the graben (Section 2.4.2).

The F1 surface underwent extensive incision leaving the minor remnants of this surface present today, preserved as a series of hills dipping towards the centre of the graben, i.e. at between 300-400m on the east side of the graben near the village of Philousa. The F2 surface cut into the underlying marl, resulting in limited preservation. The F3 forms longitudinal terraces in the major channels along the northern portion of the graben, parallel to the Khrysokhou River (Fig.2.1). The terraces can be most clearly distinguished in the centre of the graben, where paired terraces of F4 age are also seen.

## **2.4 COASTAL GEOMORPHOLOGY.**

### **2.4.1 Introduction.**

Cowper-Reed (1930) and then Henson *et al.* (1949) made the first references to marine terraces in coastal Cyprus. The memoirs of the Geological Survey Department (Bagnall, 1960; Bear & Morel, 1960; Pantazis, 1967) documented these features in more detail, citing the development of 3 marine terraces at 13m, 40m and approximately 85-100m ASL along the coast between Larnaca and Limassol. The most extensive terrace

Fig.2.18. Schematic east-west section across the Polis-Paphos graben displaying: erosion surfaces and terraces; the effects of normal faults on the erosion surfaces; and sites where colluvium is likely to develop.

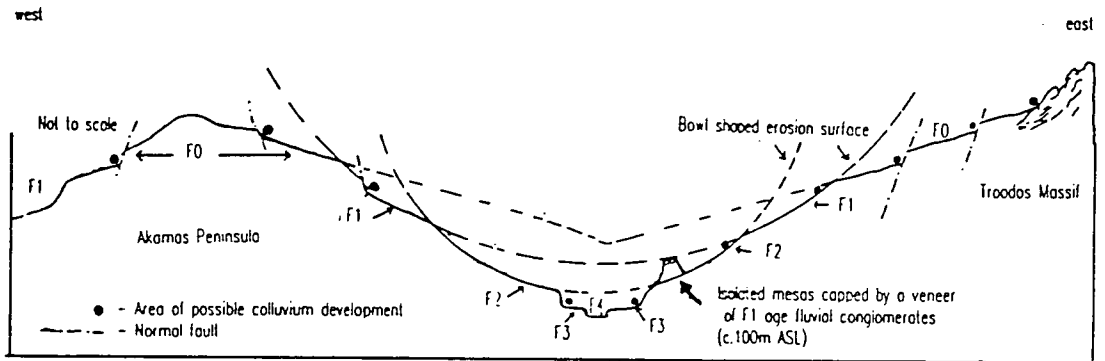
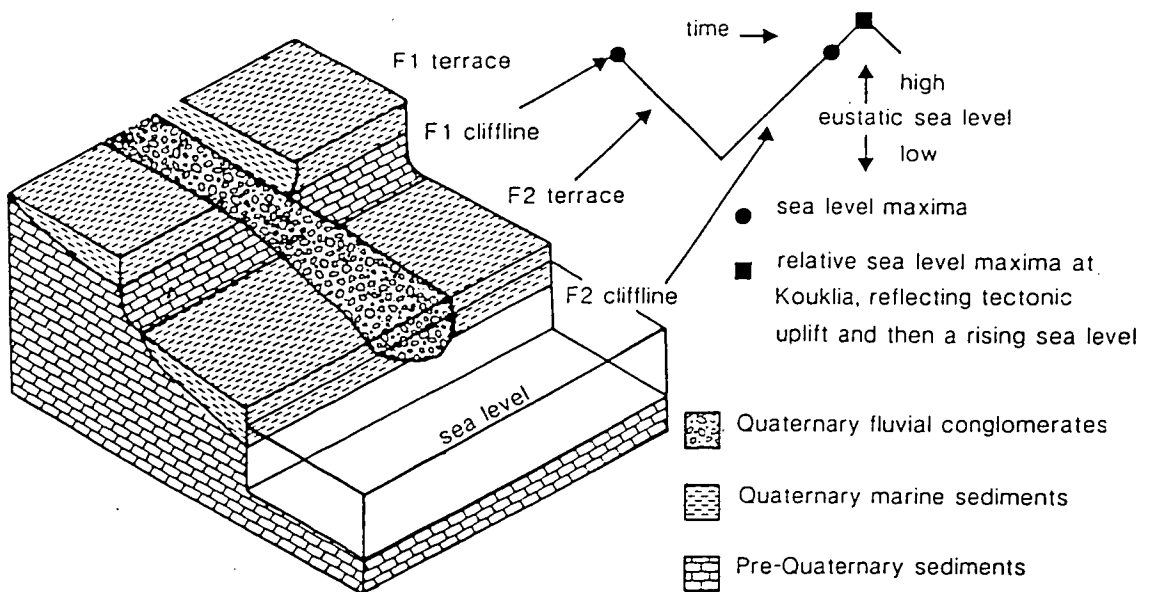


Fig.2.19. Schematic summary of the evolution of the F2 terrace at Koukليا, south-west Cyprus, providing a typical example of terrace and cliff evolution. The diagram depicts the coast as it would have looked in post F2 times, prior to the F3 evolution.



was found at 13m ASL. Turner (1971) identified a series of horizontal terraces at 366m, 200m, 100, 43m, 23m, 13m and 3m west of the village of Kathikas on the Akamas Peninsula. Turner (1971) also reported the presence of a series of terraces in the Polis region, with the highest terraces at between 504-610m with others at 61-91m, 36-43m, 12-21m, 5m, 3-4m and 2m ASL. Ducloz (1972) and Dreghorn (1978) documented similar features from the north flanks of the Kyrenia Range but none are seen in the Mesaoria Plain area.

Geomorphological features including fluvial terraces and associated littoral sediments represent the interaction of sea-level changes and tectonic uplift in the earliest Quaternary (Fig.2.19). Later Quaternary erosion resulted in cliffs, wave cut terraces and stepped coastal plains, e.g. the area to the north and west of Limassol.

#### **2.4.2 Palaeo-cliffines and associated features in south-west Cyprus.**

Outcrops of marine terraces can be grouped into a suite using SPOT satellite data, air photographs and field observations in south-west Cyprus close to Paphos. These exposures represent the most continuous sequence of marine terraces along the south coast of Cyprus. The terraces crop out at 350-360m, 100-110m, 50-60m, 8-11m and less than 3m ASL (Fig.2.20; Plates 2.8 and 2.9), overlying a Quaternary marine sequence which in turn unconformably overlies Pliocene and older sediments (Chapter 7). A suite of corresponding terraces can also be traced along portions of the west coast of the island. Here, the terraces are obscured by later aeolian dunes that have transgressed across them (Section 2.4.7). An exception to the typical pattern occurs at Ayios Yeoryios (location 2-27) where a terrace crops out c.25m ASL; this terrace could either be of F2 age, if faulting has taken place, or more likely F3 age as the F3 cliffline, i.e. exposing the F2 carbonate sequence, in the Paphos area (see below) crops out at between 50-60m ASL. Absolute age data is needed to unravel this doubt.

The Quaternary terrace related sediments, similar to those seen on the north Troodos margin, have been peneplaned during exposure to form generally flat, mature erosion surfaces. Caves associated with the formation of the marine terraces and palaeo-cliffines are found throughout south-west Cyprus, with examples seen cutting into the F2 cliff at Anavagos (location 2-1), associated with the formation of the 100-110m terrace. This erosion and peneplanation results from a change in relative base level, i.e. either uplift and/or a sea-level fall. Absolute uplift took place with a subsequent rise in sea-level allowing the formation of a cliffline, and hence a terrace (Fig.2.20). Therefore, the formation of the 100-110m cliffline can be correlated with the sediments now preserved

Fig. 2.20. 3-d interpolated surface of the topography of the Paphos area, south-west Cyprus, with accompanying contour map showing the marine terrace surfaces.

Note: the 3-d surface is viewed from the south-east at  $10^\circ$ , the vertical exaggeration is x40.

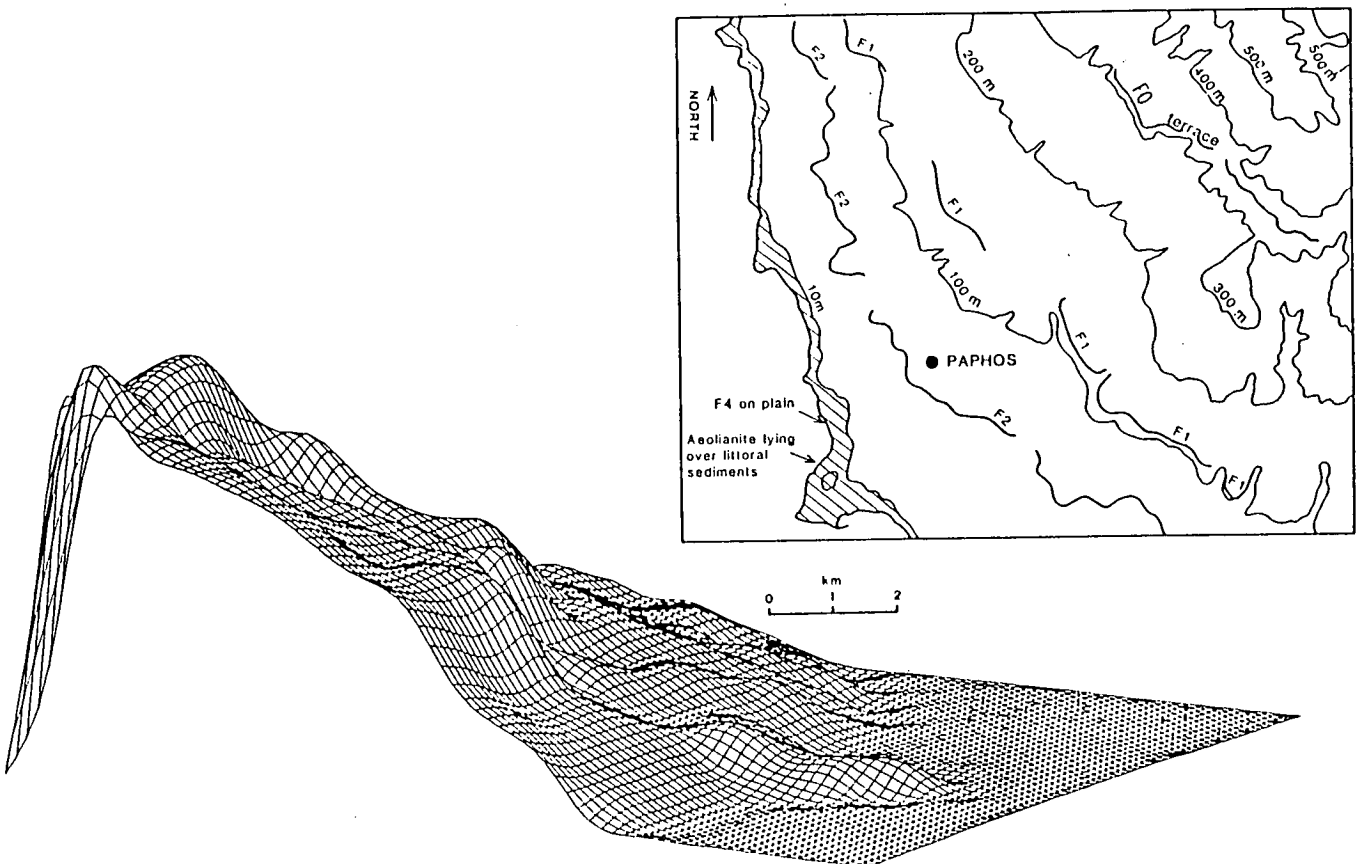


PLATE 2.8.

E - A view, looking north-east, of the F1 (a) and F2 (b) marine terraces and associated clifflines taken from the F3 terrace beneath Yeroskipos, south-west Cyprus.

F - Looking towards Paphos from the north showing the F1 (c), F2 (b) and F3/F4 (a) terraces.

Note: the cliffline identified by the break in slope to the left of (a).

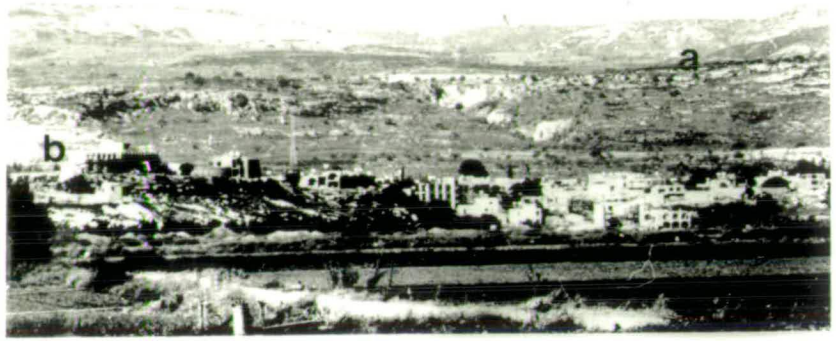
G - The F1 terrace (b) with the F2 cliffline and the F2 terrace (a) above Paphos (location 2-3).

Note: the Quaternary sequence (dark) lying unconformably above chalks of Miocene age (white) in the cliff beneath (b).

H - An F2/F3 marine notch cut into limestones of Miocene age, south-west of Peyia, south-west Cyprus.

# Plate 2.8

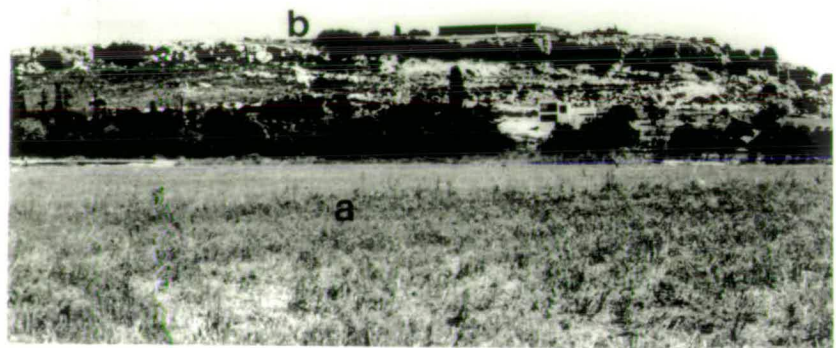
E



F



G



H



## **PLATE 2.9.**

E - The F4 marine terrace north of Paphos.

Note: the mature erosion surface sloping off the western limb of the Polis-Paphos graben.

F - The dipping erosion surfaces on the western flanks of the Polis-Paphos graben between Lara and Paphos, frequently capped by aeolianite.

Note: the F4 cliffline cutting into F3 aeolianites in the embayment in the middle of the plate.

G - The F3 marine terrace capping slumped Miocene chalks at Petounda Point (location 3-11), southern Cyprus.

H - The F3/F4 marine terrace at Cape Greco, south-east Cyprus.

Note: the hummocky relief resulting from the formation of aeolian dunes.



# Plate 2.9

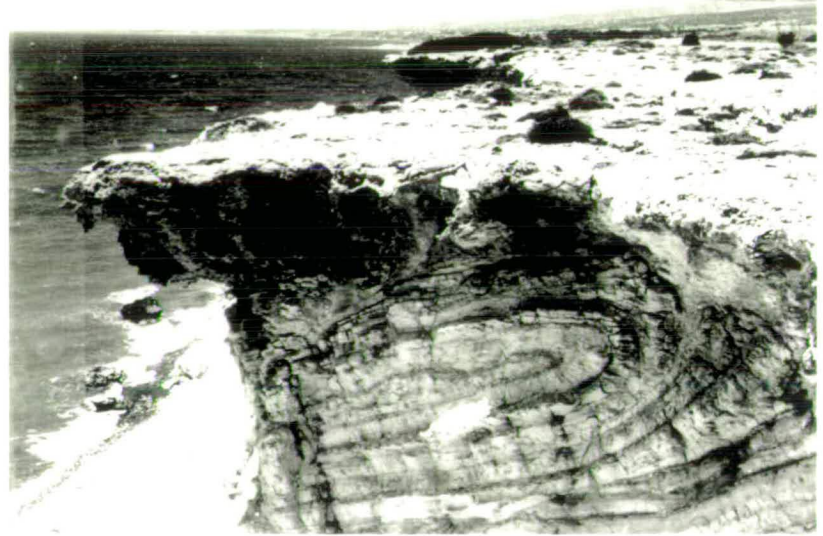
E



F



G



H



in the 50-60m cliffline. On this basis, the following correlations can be made in south-west Cyprus:

- i) the Pliocene erosion surface can be correlated with the sediments of the 350-360m cliffline,
- ii) the F1 cliffline is seen at 350-360m ASL; the F1 erosion surface extends between 350m ASL and 110m ASL; correlatable sediments are preserved in the 100-110m cliffline,
- iii) the F2 cliffline is seen at 100-110m ASL; the F2 erosion surface extends from 100m ASL to 60m ASL; correlatable sediments are preserved in the 50-60m cliffline,
- iv) the F3 cliffline is seen at 50-60m ASL; the F3 erosion surface extends from 50m-11m ASL; correlatable sediments are preserved in the 8-11m terrace,
- v) the F4 cliffline is commonly absent as the F3 terraces typically form part of the present day coastline; the erosion surface extends from 3m to sea-level; correlatable sediments are preserved in coastal terraces at <3m ASL.

#### **2.4.3 Palaeo-cliffines and associated features in south-east Cyprus.**

A suite of terraces correlated with those seen in south-west Cyprus was developed in the far south-east of the island. In the area from Xylophagou eastwards, four erosion surfaces and associated cliffines are seen, best exposed at Cape Greco and Cape Pyla (Figs.2.8, 2.10 and 2.21; Plates 2.9 and 2.10):

- i) F1 erosion surface at 80-90m ASL,
- ii) F2 erosion surface at 30-40m ASL,
- iii) F3 erosion surface at 8-11m ASL,
- iv) F4 erosion surface to within 3m ASL.

The F1 and F2 terraces in south-east Cyprus are slightly lower than those seen in the Paphos area. The terrace sediments in south-eastern Cyprus crop out above Quaternary and pre-Quaternary sediments (location 1-125) and erosional surfaces have cut into pre-Quaternary sediments (location 1-136). The two highest terraces are commonly erosional, cut into the resistant Miocene limestones, whilst Quaternary sedimentary sequences are frequently found on the lower two terraces. This pattern is similar to that seen in south-west Cyprus. Caves at <3m ASL at Cape Pyla, wave-cut notches at Cape Pyla and the development of solution hollows on the erosion surfaces at Cape Greco support a marine origin for these terraces.

A complete suite of terraces is not seen in the area west of Xylophagou around the coast towards Larnaca. As mentioned previously, this may relate to the unconsolidated nature of the underlying basement lithologies (Section 2.3.3). The F1, F2 and F4 erosion

Fig.2.21. 3-d interpolated surface of the topography in the Cape Greco area of south-east Cyprus, with accompanying contour map showing the marine terrace and cliffs.

Note: a). is viewed from the west at 15°, with a vertical exaggeration of c.x30; b) is viewed from the east at 30°, with a vertical exaggeration of c.x35.

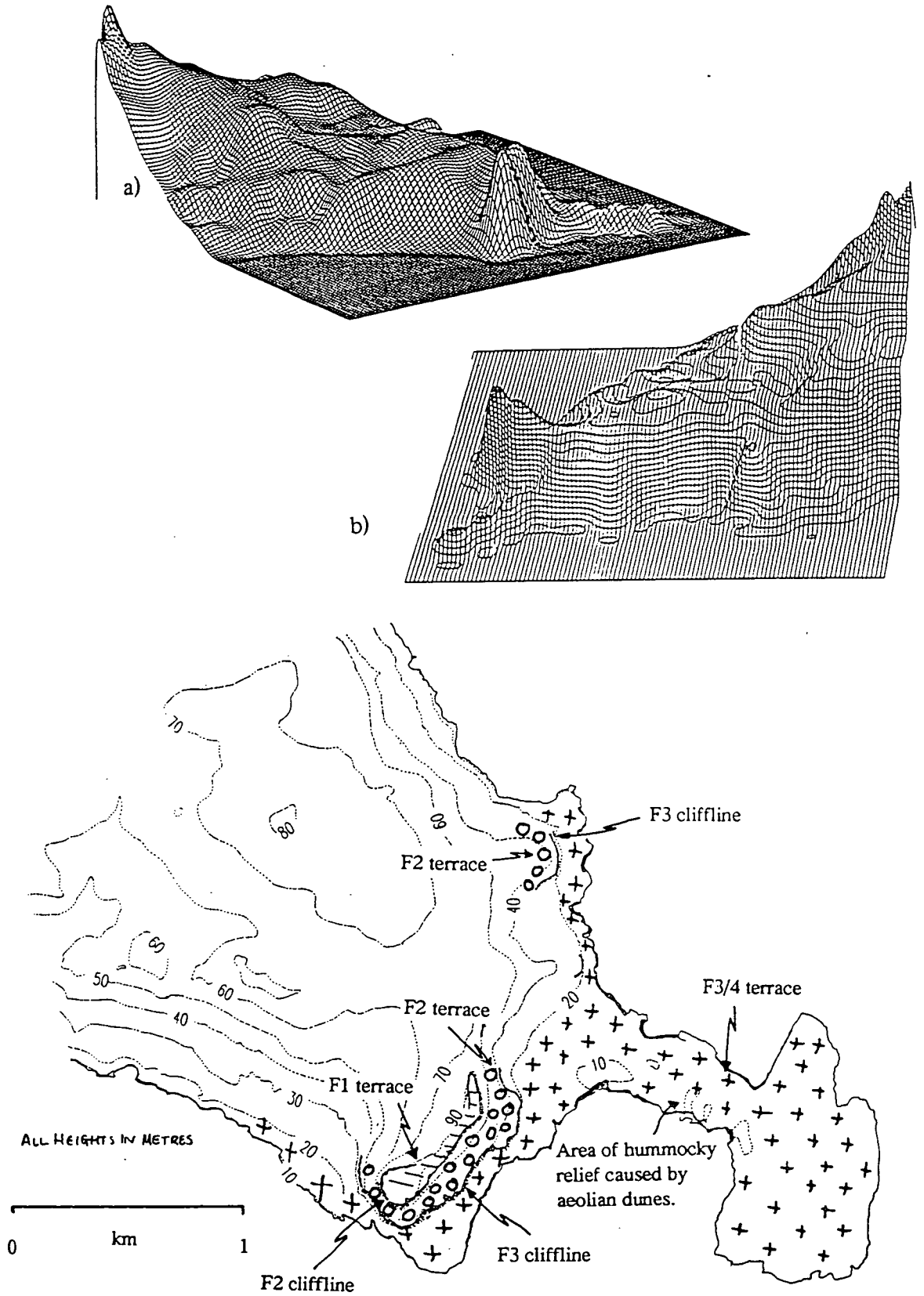
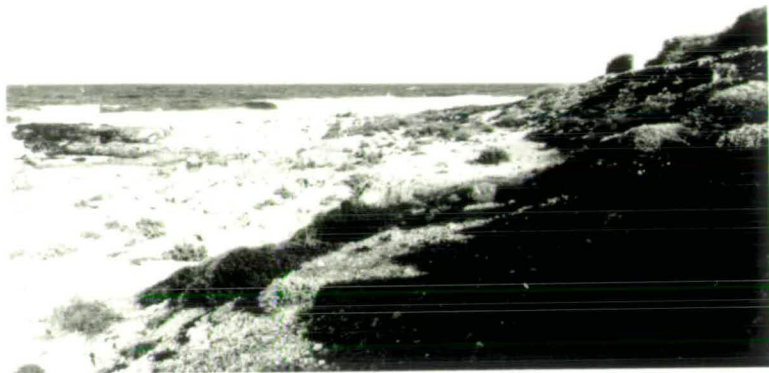


PLATE 2.10.

- E - The F4 marine terrace preserved just above present day sea-level near Paralimni, south-east Cyprus (location 1-120).
- F - An F3/F4 age marine terrace passing back to an F3 age cliffline and F2 age marine terrace near Cape Greco, south-east Cyprus.
- G - The cliffs along the south coast of the Akrotiri Peninsula with evidence for an F4 age wave cut platform and associated notch (a).

Plate 2.10

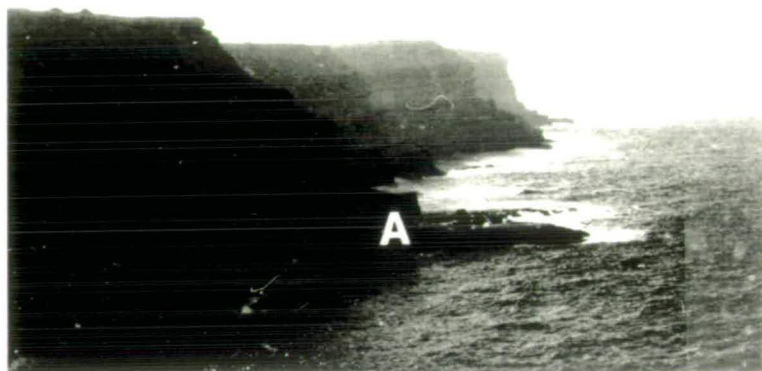
E



F



G



surfaces are seen, but the F3 does not appear (Fig.2.8). The F1 cliffline has actually cut the pre-existing topography perpendicular to the strike of the contours (Fig.2.8). This is the only place where this is seen, reflecting the local importance of the uplifted Troulli Inlier during the latest Pliocene and early Pleistocene. The Troulli Inlier local topographic high influenced the drainage pattern in this area during F1 and F2 times when large quantities of fluvial, Troodos-derived sediment were deposited. These sediments support an argument for a major channel running between the F1 surfaces of Troulli to the west and Xylophagou to the east during F1 and F2 times. The F2 surface is marked by a ridge, south of Ormidhia (Fig.2.8), that trends approximately north-east to south west. The F3 is probably represented by the dry channel feeding southward from Ormidhia although no terrace or cliffline is preserved today. The F4 surface and cliffline, like those seen for the F1 and F2, was cut by wave action, resulting in the formation of marine clastic, e.g. Ormidhia (location 1-129), and carbonate sequences, e.g. Cape Greco (location 1-125), which dip at 4-6° towards the south-west, i.e. seawards. The only obvious terraces and clifflines preserved to the west of Dhekelia, south of Pyla, are correlatable with the F1 and F4 terraces of south-western and south-eastern Cyprus.

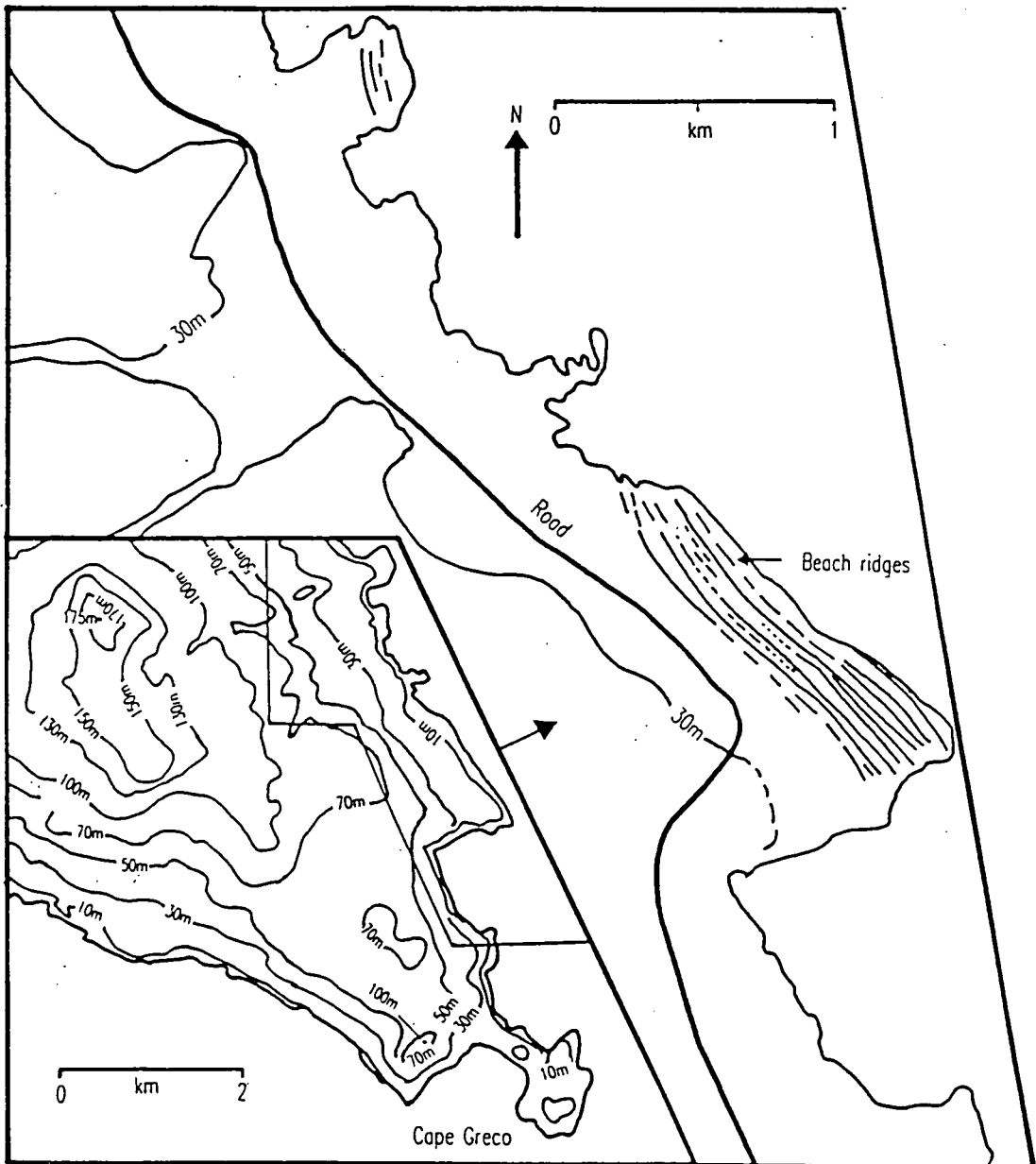
#### **2.4.3.1 Beach ridges of south-east Cyprus.**

Air photographs show the development of beach ridges to the north-west of Cape Greco (Fig.2.22). The ridges dip at 5-10° to the north-north-east and run parallel to the bathymetry on this part of the coast (Fig.2.23). The ridges are found associated the F4 erosion surface but also show evidence for more recent erosion, probably during and succeeding the Holocene sea-level rise. These features are interpreted as resulting from foredune migration associated with a longshore current interacting with sea-level changes (Goldsmith, 1985). Similar modern features are seen in Tasmania and south-east Australia (Davies, 1980; Short, 1988).

#### **2.4.4 Palaeo-cliffines and associated features in south Cyprus.**

The marine terraces that crop out along the south coast of the island are predominantly cut into fluvial sedimentary sequences (*vid.* location 1-162), similar to that seen in the Dhekelia area. This contradicts the views of Bagnall (1960). Locally at Akrotiri (location 3-97) and Larnaca (location 1-130), an F3 terrace made up of carbonate sediments is cut to form an F4 cliff. The marine terraces (Fig.2.6) crop out at the same heights as those in the south-east of the island. The F1 terrace and the associated F2 cliffline, identified by satellite imagery (Plate 2.1; Fig.2.17), can be traced from Curium (Fig.2.17) to the east of Limassol, a distance of 20km. The F2 terrace now forms isolated erosional remnants on top of the Pliocene sediments of the Athalassa Formation at

Fig.2.22. Sketch of the distinct beach ridges occurring in the Cape Greco area of south-east Cyprus, based on air photos, 6" to the mile.



Vounaro (Fig.2.17) and south of Kolossi (Fig.2.17). The F3 terrace also formed above Pleistocene sediments of the Faglomerate Group but is not well preserved, fringing the F2 terraces at Vounaro (Fig.2.17). The F4 terrace and cliffline is exposed beneath the cliffs at Curium (Plate 2.7) and extends across the Akrotiri Peninsula (Fig.2.17). A large coastal plain existed along the southern coast of the island throughout the Quaternary period stretching from south of Larnaca round to the western side of the Akrotiri Peninsula.

The marine terraces and clifflines on the south coast of the Akrotiri Peninsula were predominantly cut into the Mio-Pliocene and Quaternary marine carbonate sediments. The F4 terrace formed a wave cut platform and notch in the pre-Quaternary sequence (Plate 2.10) along much of the southern Akrotiri coast (location 3-96a). Some limited F4 sedimentary sequences are also present with an associated cliffline cutting the F3 sediments at Cape Zevgari (location 3-96) to the west and Cape Gata (location 3-97; Fig.2.17) to the east. A high terrace has an erosion surface capping the Akrotiri peninsula at 50-60m ASL and caves have formed in the soft Pliocene Athalassa Formation at c.30m ASL. These two features could reflect the F1 and F2 phases respectively.

A suite of terraces crop out to the south of Pissouri village are similar to those seen at Tersephanou (location 3-16), to the north-west of Larnaca. The F1 terrace, situated on the east side of Pissouri Bay (Fig.2.5), planed the F1 Faglomerate unit and the earlier ?Pliocene fan-delta deposits. An erosional bench is located at 50-60m ASL. The F3 and F4 terraces are clearly visible on the west side of the bay (Plate 2.2), with the F4 terrace above the Recent storm beach, as well as forming the valley floor cover (Fig.2.5). However, there is no evidence to support a large, coastal plain in this area during the Quaternary, although the bathymetry points to the presence of a submerged plain (Fig.2.23), similar to that identified along the southern coast of the island, east of Limassol (McCallum *et al.*, 199<sup>2</sup>).

#### **2.4.5 Palaeo-cliffines and associated features in the Polis-Paphos graben and along the north coast of the island.**

Marine, wave-cut terraces and clifflines have developed along the northern coast of the island. A series of terraces crop out on both the western and eastern edges of Khrysokhou Bay (Fig.2.7). Four dominant cliffines flank the eastern side of Akamas Peninsula on the west side of the Polis-Paphos graben. The high terraces at about 500m ASL and 320m ASL mirror those seen in the Paphos area, with the 320m terrace correlatable with the Pliocene terrace to the south. In the west, the F1 terrace cuts into basement Miocene and older sediments at c.100m ASL, and the equivalent terrace in the



east has cut down into the pillow lavas of the Troodos ophiolite. There is no evidence of an F2 terrace. The F3 terrace lies on Quaternary fluvial, deltaic and littoral sediments in the centre and eastern portion of the bay but passes onto an erosional bench cutting into Pliocene and then progressively older basement to the west. The F3 terrace, which crops out at its lowest extent at 10m ASL, cuts into the pillow lavas of the Troodos ophiolite to the east of Argaka. The F3 terrace was cut to form the F4 cliffline and terrace within metres of sea-level. The F4 terrace appears to be mainly erosional although the large quantity of overlying Recent beach conglomerate, around much of Khrysokhou Bay, masks its appearance.

F2 and F3 terraces, as well as the F4 cliff, are present in the area between Polis and Kato Pyrgos, eroded into the Troodos ophiolite. Locally these features are associated with carbonate littoral, e.g. Argaka (location 3-93), and fluvial, e.g. Limni (location 1-166), deposition. The steeply dipping margin of the Troodos ophiolite causes a rapid increase in water depth offshore (Fig.2.23) that precludes the development of a coastal plain in this area.

#### **2.4.6 Bathymetric data.**

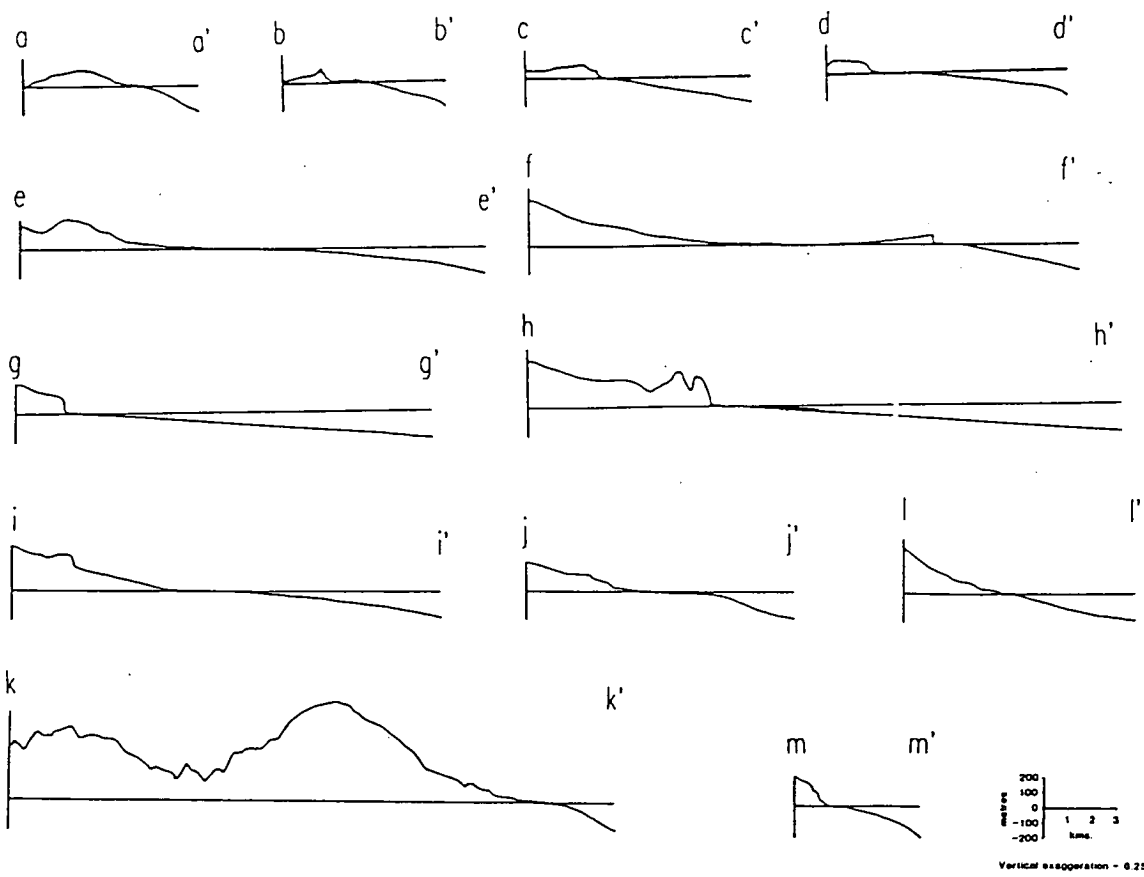
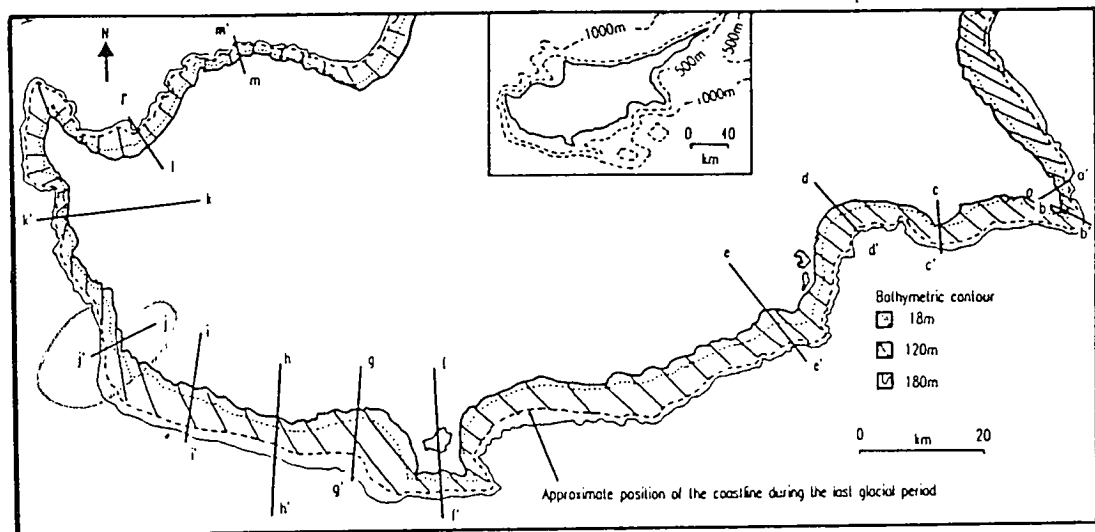
Bathymetric data indicate the presence of an offshore terrace around the south coast of the island to a depth of c.110m (Fig.2.23). This figure equals the inferred drop in sea-level during the last glacial period (40-10ka.; Dansgaard *et al.*, 1982) proposed for the Central and Western Mediterranean by Shackleton *et al.* (1984) and is also supported by seismic records from coastal southern Cyprus (McCallum *et al.*, 1991<sup>2</sup>).

#### **2.4.7 Dune development.**

Aeolian sediments were deposited throughout coastal Cyprus during the Quaternary (Chapter 8). The dunes preserved at Cape Greco (location 1-125) in the south-east, and at Kato Paphos (location 1-57) in the south-west form a hummocky relief above the F3 and F4 erosion surfaces (Fig.2.20; Plates 2.9 and 2.11). Dunes banking up against and over the top of clifflines, are seen on the south coast at Akrotiri (location 3-96a), near Kolossi (location 3-28; Fig.9.5) and at Tersephanou (location 3-17). A similar depositional sequence existed along much of the west coast of the island, between Paphos and Lara (Fig.2.7), creating a more steeply dipping erosion surface (Plate 2.9). The modification of the landscape resulted in aeolian sediments enveloping clifflines and terraces, with the development of an erosion surface that reflects dune formation and not tectonic uplift and sea-level changes. The aeolian sediments modified the coastal geomorphology of southern Cyprus as a result of their mobility prior to cementation.

**Fig.2.23.** This map locates a series of representative topographic profiles of the southern Cyprus coast.

Note: the approximate position of the coastline during the last glacial period, i.e. c.110m bathymetric contour.





#### **2.4.8 The effects of sea-level change on the development of the geomorphology of southern Cyprus: two case studies.**

The Akrotiri Peninsula preserves a good example of the interplay of sea-level change with fluvial systems, which is not seen along the north Troodos margin. The Akrotiri Peninsula and salt lake was first interpreted as forming as result of spit and then subsequent tombolo development (Bear & Morel, 1960; Plate 2.7). The cliffs beneath Curium (Fig.2.17) formed during the last eustatic sea-level highstand (Chapter 3), during which time the Kouris and Garyllis Rivers deposited sediment into a shallow marine environment, i.e. onto the present day Akrotiri Peninsula, (Fig.2.17; Chapter 6). As the sea-level dropped during the last glacial the rivers prograded south out onto the Akrotiri Peninsula and into Episkopi Bay; this resulted in the formation of an offshore terrace (Fig.2.23) and the gravels found in the seismic lines shot along the south coast of the island (McCallum *et al.*, 1991). As sea-level rose to present levels (not the levels recorded for the last inter-glacial, 5-8m ASL; Mesolella *et al.*, 1969; Bloom *et al.*, 1974; Chappell, 1974; Stearns, 1976), spits prograded out from the Kouris and Garyllis Rivers; these eventually formed tombolos that joined the mainland to the Akrotiri high (Fig.2.17). The shallow isolated patch of water caught between the tombolos developed into the Akrotiri Salt Lake. The presence of the F2 and F3 clifflines, both of which are within 60m of the present day sea-level, suggest that the Akrotiri high had been previously attached to the mainland during part of the Late Quaternary. This attachment would have occurred when the sea-level was c.100m lower, during previous low sea-level stands, i.e. glacial periods.

The second case study comes from the Kouklia area 15km east of Paphos (Fig.2.7). The Kouklia terrace can be correlated with the F2 terrace found in the Paphos area. The Kouklia terrace comprises fluvial conglomerates, unlike the F2 terrace seen at Yeroskipos (Fig.2.7) which is made up of marine sediments. The Kouklia conglomerates prograded out over a "shelf" area during a relative drop of sea-level and as sea-level rose again both the marine sediments at Yeroskipos and the fluvial sediments in Kouklia were cut to form the present 50-60m terrace and cliff sequence. The evolution of this portion of the F2 terrace is summarised in Fig.2.19.

#### **2.4.9 Karst.**

Formation of karst depends on the interaction between temperature, lithology, groundwater and biological effects (Estaban & Klappa, 1983). The climate required usually involves rainfall in the order of 1000mm per annum; rainfall of this order, in

Cyprus, is only present on the peaks of the Troodos Massif today (Fig.2.24). However, karst has been identified in the Kyrenia Range, where it is thought to have formed during the Quaternary pluvial phases, i.e. interglacial periods.

The karst of southern Cyprus commonly takes the form of expanded joints (rillenkarren), solution pits, sponge-like karst and the local development of travertine deposits. Karst is poorly developed and is found mainly on the lower two marine terraces within 11m of the present day sea-level. However, travertine deposits are located at 340m ASL (location 2-63a).

The lack of karst complements the presence of caliche on the island, these together support an argument for the existence of a semi-arid climate, with limited rainfall throughout much of the Quaternary. The karstic features, formed on the lower terraces, today lie within metres of the present day sea-level and the water table, i.e. the freshwater-meteoric zone.

## **2.5 COLLUVIUM.**

Colluvium, i.e. any loose heterogeneous and incoherent mass of soil and/or rock fragments deposited by rainwash, sheetwash, or slow continuous downslope creep, usually collecting at the base of a slope (Bates & Jackson, 1980), crops out throughout southern Cyprus. Extensive colluvial sequences are exposed in southern Cyprus, e.g. the Vasilikos Valley (B. Gomez, *pers. comm.*, 1989). The colluvial sequences usually consist of angular, poorly sorted clasts that are derived from local sources. The colluvial units are generally grain-supported, structureless and have a fine grained matrix. Detailed studies of colluvium were not undertaken during the course of this project, but may distinguish between sequences that have formed as a result of faulting, land slipping of clays and hill slope wasting. Studies correlating the colluvial units with the sediments of the Faglomerate Group may also enable the timing of Quaternary fault movement to be deduced, in areas of neotectonic activity, e.g. the Polis-Paphos graben (Chapter 4).

## **2.6 INTERPRETATION, DISCUSSION AND CONCLUSIONS.**

### **2.6.1 Drainage patterns.**

The overall drainage pattern in southern Cyprus comprises a radial pattern, feeding from the Troodos Massif. In south Cyprus a sub-dendritic pattern on the Troodos Massif passes into a broadly parallel drainage along the coast. The classification of Howard (1967) can be applied to this as follows:

- i) the radial drainage pattern of a dome, feeds in all directions from its centre. In Cyprus, the Troodos Massif, and more specifically Mount Olympus, provides a centre for the radial pattern,
- ii) the presence of a dendritic to sub-dendritic drainage pattern suggests that the drainage cuts through a uniformly resistant rock type and that the regional slope was gentle at the time of drainage inception. There may also be some structural control on the drainage. In southern Cyprus the dendritic component of the drainage pattern (Fig.2.3) indicates a uniform resistance by the units of the Troodos ophiolite to erosion,
- iii) the parallel drainage indicates a moderate to steep slope, but could also be related to elongate landforms.

Pre-existing tectonic structures influenced the drainage pattern by providing relief and/or lines of weakness, e.g. the Vasilikos River exploiting the Arakapas Fault Belt. The tectonic influence is hard to distinguish as an independent control from uplift of the Troodos and Kyrenia terranes. The pattern of drainage development is largely independent of lithology with the location of early Quaternary channels having a greater influence on the preserved pattern.

Merritts & Vincent (1989) have postulated that upland streams accumulate the effects of uplift, i.e. base level fall, whereas lowland rivers adjust rapidly to change. The steep sided valleys of the Troodos Massif reflect this argument, especially when they are compared to the broad, low gradient valleys on the Mesaoria Plain and the coastal areas of southern Cyprus. The development of gorges, hanging valleys and rejuvenation features within the drainage pattern of the Quaternary period in southern Cyprus supports the proposition of base-level changes, related to uplift, sea-level and/or climatic changes.

De Vaumas (1959, 1961, 1962) postulated, on geomorphological grounds, that the centre of uplift has shifted through time, from an area to the east of Mount Olympus, west to Mount Olympus itself. The evidence from the drainage pattern throughout southern Cyprus does not support De Vaumas's view, although if the initial uplift of southern Cyprus was not focussed on a single area, i.e. prior to the protrusion of the serpentinite diapir, then the ocean floor topography, which is preserved on Cyprus today (Allerton & Gomez, 1989) will have controlled the location of continental and marine areas. Rapid, focussed uplift (i.e. underthrusting of the African plate and diapiric protrusion) would have brought about more abrupt changes and the difference between this and possible earlier steady "uniform" uplift may account for arguments put forward by De Vaumas (1959, 1961, 1962).

### **2.6.2 Erosion surfaces.**

Most erosion surfaces of southern Cyprus can be correlated with those seen on the north margin of the Troodos Massif (Gomez, 1987). However the erosion surfaces are not always present leading to some confusion in terminology. The coalescence of erosion surfaces and fluvial terraces at distal locations on the Mesaoria Plain and to the south of the Troodos Massif indicates that uplift has been differential, centred on Mount Olympus (Section 2.3; Fig.2.12). Eustatic sea-level changes have influenced the pattern of terrace development in areas of southern Cyprus other than the Mesaoria Plain. This has not always been recognised, e.g. Bagnall (1960), as both an F3 erosion surface and the underlying F3 fluvial sequence have been cut to form a marine cliffline during the F4, e.g. south of Maroni (location 1-162).

Pediment and depositional areas developed with the Fanglomerate Group erosion surfaces and associated terraces on the north Troodos margin. In proximal localities, both strath, where bedrock lithologies rather than alluvium is present beneath the terrace (Leopold *et al.*, 1964), and alluvial fans cut into the Troodos ophiolite and the sedimentary cover sequence, in addition to earlier Fanglomerate Group fluvial sediments. Provenance studies from clasts in the Fanglomerate Group (Section 5.5) illustrated the progressive introduction of new lithologies indicating that backcutting into the source area, i.e. southwards, took place. Predominantly marine Pliocene units beneath the Fanglomerate Group (McCallum, 1989) are terraced as a consequence of absolute uplift of the island during the Pleistocene (e.g. locations 1-28 and 1-83). The lack of Pleistocene marine sediments on the area of the Mesaoria Plain also supports the view that sea-level effects are negligible and did not have a role in the formation of these terraces and erosion surfaces, in a similar fashion to the continental terraces of Oman (Abrams *et al.*, 1988). Similar strath terraces have developed in the Cherwell River valley in New Zealand (Bull, 1990).

The paired terraces throughout the Mesaoria Plain indicate a cyclic erosional history and pulsed environmental change, whilst unpaired terraces provide evidence for slow, continuous environmental change (Morisawa, 1985). Paired terraces and their resulting landforms arise from an increase in energy level allowing downcutting of channels to take place. The paired terraces and associated erosion surfaces that developed during the F3 and F4 phases have formed in valleys that have cut down into previous valleys, resulting in the development of valley fan systems (Muto, 1987). These systems form as a result of changes in base level, i.e. either uplift or sea-level change, with incision down through the previously deposited sediments and underlying basement units. This results in sediment reworking (Chapter 5) and the development of paired terraces

with associated erosion surfaces. Bull (1978) has classified landforms that result from uplift of the San Gabriel mountains in California. Class 1 landforms result from uplift rates in the order of 1-5m/ka. (Hooke, 1972; Smith, 1976) and result in the entrenchment of consolidated and unconsolidated lithologies. Entrenchment, similar to that recorded by Bull (1978) has taken place on Cyprus between the formation of the F1 and F2 times and the development of the channel fan systems. Class 5 uplift (Bull, 1978) occurs when uplift rates are 5cm/ka. and result in the preservation of pedimented terraces and U-shaped valleys, similar to that seen in Cyprus at present. The high rates of uplift that probably occurred in Cyprus during the lower and middle Pleistocene, i.e. class 1 (Bull, 1978), resulted in the rapid erosion of much of the F1 terrace during this period.

Maizels (1987) proposed that Quaternary terraces seen in Oman did not form as a result of uplift, but from Quaternary climatic changes, with flash floods causing rapid downcutting and subsequent deposition. The climate on Cyprus today is typically semi-arid with 5% of the annual precipitation occurring in the summer months, through thunderstorms, and 60% taking place between December and February. Relief (Fig.2.12) has a great effect on the rainfall pattern with a marked windward and lee slope variation (Fig.2.24). The relief also affects temperature with a drop of 5°C/1000m elevation. The mean temperatures throughout the year are shown below (Meteorological survey of Cyprus, 1986):

| Location   | January |      | April |      | July |      | October |      | Average |
|------------|---------|------|-------|------|------|------|---------|------|---------|
|            | Max.    | Min. | Max.  | Min. | Max. | Min. | Max.    | Min. |         |
| Nicosia    | 15      | 5    | 24    | 10   | 37   | 21   | 28      | 15   | 19.3    |
| Larnaca    | 16      | 7    | 23    | 10   | 34   | 21   | 28      | 16   | 19.3    |
| Limassol   | 17      | 8    | 22    | 11   | 32   | 21   | 27      | 16   | 19.2    |
| Paphos     | 17      | 9    | 21    | 13   | 30   | 22   | 26      | 17   | 19.3    |
| Prodhromos | 6       | 1    | 15    | 6    | 27   | 18   | 19      | 11   | 16.8    |

(Temperature in °C.)

Examples of Quaternary climate change on Cyprus do exist (*vid.* Chapters 5 and 7) and it is very likely that the change from cold, dry glacial times to warmer and wetter interglacial periods played a part in the erosion and the formation of the Quaternary terraces. Sancetta *et al.* (1973) suggested that the sea surface temperature during the last interglacial was higher than that seen today (Fig.2.25). Dreghorn (1978) stated that the slope development of northern Cyprus, with deep valleys and smooth slopes reflected a pluvial palaeoclimate during the Pleistocene; the later arid Holocene climate resulting in the landscape losing its vigour. The interpretation made by Dreghorn (1978) supports that made by Vita-Finzi (1969) who suggested that the Mediterranean was undergoing climatic fluctuations during the latest Pleistocene and Holocene which had a direct and



Fig.2.24. A rainfall distribution map of Cyprus (annual average precipitation 1951-1980 in millimetres, Cyprus Meteorological Survey, 1988), demonstrating the controlling influence of topography on the pattern of precipitation.

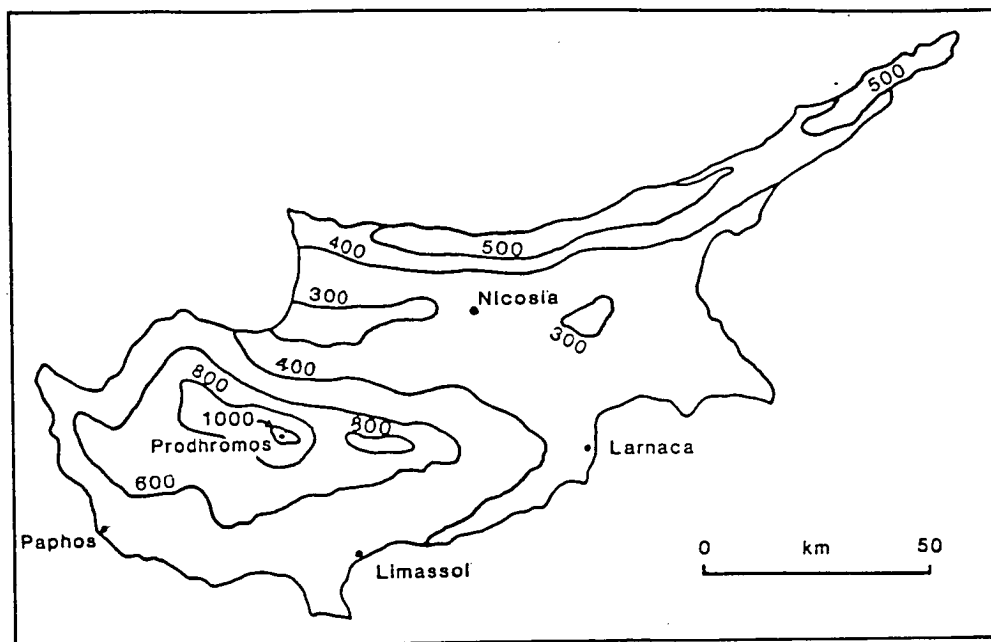
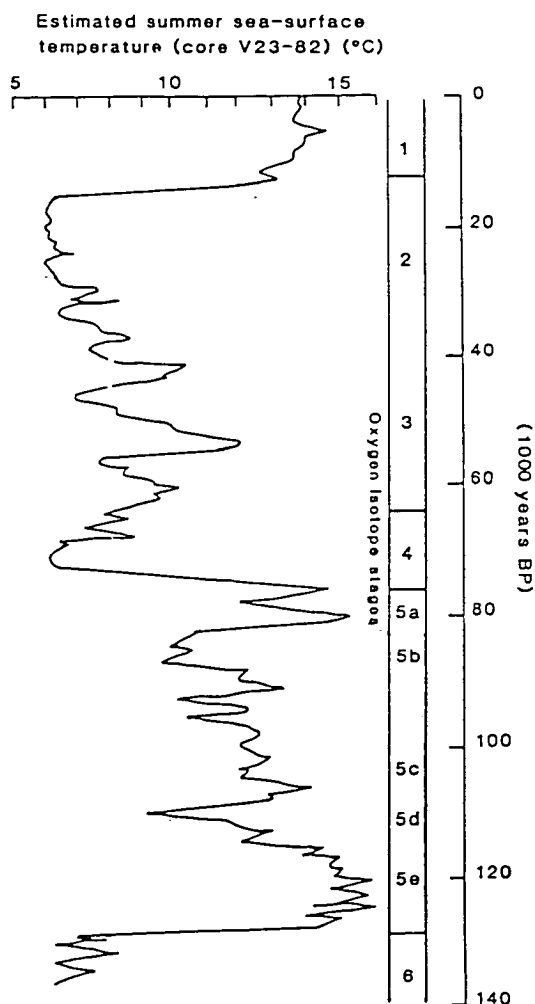


Fig.2.25. A plot of time against estimated summer sea surface temperatures, demonstrating that temperatures were 1-2° warmer during the last interglacial than they are at present (after Sancetta *et al.*, 1973).



indirect, i.e. through vegetation, effect on landscape development. There is no direct evidence to support changes in rainfall (Dreghorn, 1978) between the Pleistocene interglacials and the Holocene. This study interprets the landscape development to reflect rates of base-level and climatic change. The nature of climate change should also be considered, as periodic, e.g. flash flood, events may have a greater influence on landscape development, than steady state changes resulting from higher annual rainfall, as envisaged by Dreghorn (1978) during the Pleistocene. Anthropogenic influences on the formation of the most recent, stable, vegetated alluvium should not be discounted, as deforestation during the Holocene will also have contributed to the formation of Recent terrace sequences (B. Gomez, *pers. comm.*, 1989).

### **2.6.3 Coastal geomorphology.**

The four marine terraces and clifflines exposed in south-west Cyprus can be correlated with equivalent features in the south and south-east of the island, despite the height variation. This agrees with observations from other tectonically active areas of the Mediterranean (Hey, 1978), where large areas have undergone equivalent amounts of uplift with little evidence of local differential movement. The variable heights of the erosion surfaces in southern Cyprus may reflect some or all of the following:

- i) the distance of various areas from the centre of uplift, i.e. the Troodos Massif,
- ii) a variable position on the erosion surface, e.g. that seen at Ayios Yeoryios (location 2-27; Section 2.4.2),
- iii) neotectonic processes have caused the same erosion surface, in different areas to crop out at varying heights.

Points i) and ii) are favoured as:

- a) different locations on a dipping marine erosion surface will be at different heights,
  - b) there is minimal evidence of Quaternary neotectonic activity (Chapter 4),
  - c) absolute dating methods (Chapter 3) have correlated the lower two terraces at the same heights throughout the island,
- and d) if rates of uplift are reduced in the Late Pleistocene (Table 1.10; Chapter 3), then sea-level changes will have had a greater control over the height of these more recent marine erosion surfaces, in relation to the present-day sea-level. Therefore their distance from the Troodos Massif is unimportant, unlike the earlier marine erosion surfaces, that are thought to have formed during a period of rapid uplift (this chapter, Chapter 3; Table 1.10).

The two lowest terraces can be correlated with a high degree of confidence as they are present around much of the coast. In comparison, the correlation of the higher

terraces is more difficult, as they have undergone greater dissection and erosion, especially along the south and south-east coast where unconsolidated fluvial sediments have suffered extensive erosion. The formation of aeolianites has also affected the topography and this is likely to account for some of the anomalies that exist in the sequence of terraces established by Turner (1971) along the west coast of the island. Dune formation is generally restricted to the F2 terrace sequences (Chapters 7 and 8), against and/or over the F3 cliffs and the F3 and F4 erosion surfaces. Hence aeolianites have only had a minor modifying affect on the F1 terrace. The limited development of karst on the F1, F2 and F3 terraces indicates that the zone of karst formation moved away from the terraces. The only well developed karst is seen on the F4 surface suggesting retention of these units in the zone of active karst formation.

The following three factors all suggest that the rate of uplift was decreasing through the Quaternary:

- i) the sole development of gorges (Section 2.2.7) above the F1 terraces,
- ii) the decrease in vertical distance between the early and later Quaternary terraces,
- and iii) evidence for limited tectonic uplift between the formation the F4 terrace and the present day.

The continuity of terraces and terrace heights around the c.340kms of coast from Kato Pyrgos to Famagusta also suggests that, on this scale, the coastal terraces of the island were uplifted as a single entity, with little differential movement. The low angle of dip of the coastal terraces represents depositional dip which does not steepen with older terraces, indicating that very little rotation of these terraces has taken place in contrast to those on the Kyrenia Range (Dreghorn, 1978).

The evidence from the coastal geomorphology corroborates other geomorphological evidence concerning the uplift of Cyprus described elsewhere in this chapter. The studies here do not agree with the findings of Turner (1971) who identified the development of seven Quaternary marine terraces, which resulted from a continuing fall in sea-level, from the Pliocene to date. It has been shown here (Section 2.4.7) that aeolian development has masked the land surface in a number of areas around the southern coast of the island and it is believed that Turner (1971) mistook aeolian dune surfaces as additional terraces.

#### **2.6.4 Discussion.**

De Vaumas (1959, 1961, 1962) identified three and possibly four periods of erosion during the Quaternary. These data agree with Ducloz (1965) and this study which

satisfactorily correlate the mature erosion surfaces, channel fan sequences, paired terraces and related marine landforms, i.e. palaeoclifflines and marine erosion surfaces (Table 1.10), throughout Cyprus.

Carson & Kirkby (1972) state that the rate of emergence of landmasses, resulting from tectonic uplift, is rapid when compared with the rate of denudation. There is therefore little synchronous modification of the geomorphology during periods of uplift. This was probably the case during the early and middle Quaternary, i.e. F1 and F2 (Tables 1.9 and 1.10), with geomorphological modifications lagging behind the uplift (Penck, 1953; Merritts & Vincent, 1989). Merritts & Vincent (1989) have identified incision and channel steepening as the primary response to uplift which then results in the isolation of surfaces, entrenchment (Bull, 1978) and the development of channel fans (Muto, 1987). However, mature erosion surfaces are now present on the north Troodos margin suggesting that the period of rapid uplift was succeeded by more stable conditions, during which time denudation occurred. The period necessary for erosion surfaces and mesa hills to reach maturity is controlled by climate, i.e. the amount and intensity of rainfall, and the erodability of the bedrock and vegetation (Bull, 1978). If it is assumed that a semi-arid climate existed in Cyprus, and especially on the north Troodos margin, during the lower and middle Pleistocene then the time taken for the formation of these mature erosion surfaces and mesas, i.e. pediments and inselbergs (Bull, 1978), will have been in the order of 700-1300ka.. The exact time is dependent on the bedrock (Fig.2.26). This suggests that the formation of mature erosion surfaces above the soft Pliocene sediments began approximately 700ka. B.P., i.e. the early to middle Pleistocene, following a period of rapid uplift (Section 2.3.5) and entrenchment. This is in line with evidence from the north Troodos margin and coastal landforms of southern Cyprus (Section 2.4).

Sea-level changes have undoubtedly played a role in the development of the geomorphology in the coastal zone of southern Cyprus (Muto, 1987). This has probably contributed to the apparently untilted nature of the marine terraces. It is unlikely however, that eustatic sea-level changes had a major effect on the north Troodos margin as the change in gradient resulting from a eustatic fall, or rise, in sea-level would be minimal and similar to that recorded in Oman (Abrams *et al.*, 1988). The evidence presented in this chapter indicates that the whole island has been uplifted and although this appears to have been differential, the distance from the point of greatest uplift, i.e. Mount Olympus, and the presence of concave erosion surface (Section 2.3) has resulted in near horizontal erosion surfaces today. This is in line with evidence from other Mediterranean areas (Hey, 1978) but unlike that seen in the Kyrenia Range (Dreghorn, 1978). Climatic changes have probably played a role in the dissection and entrenchment

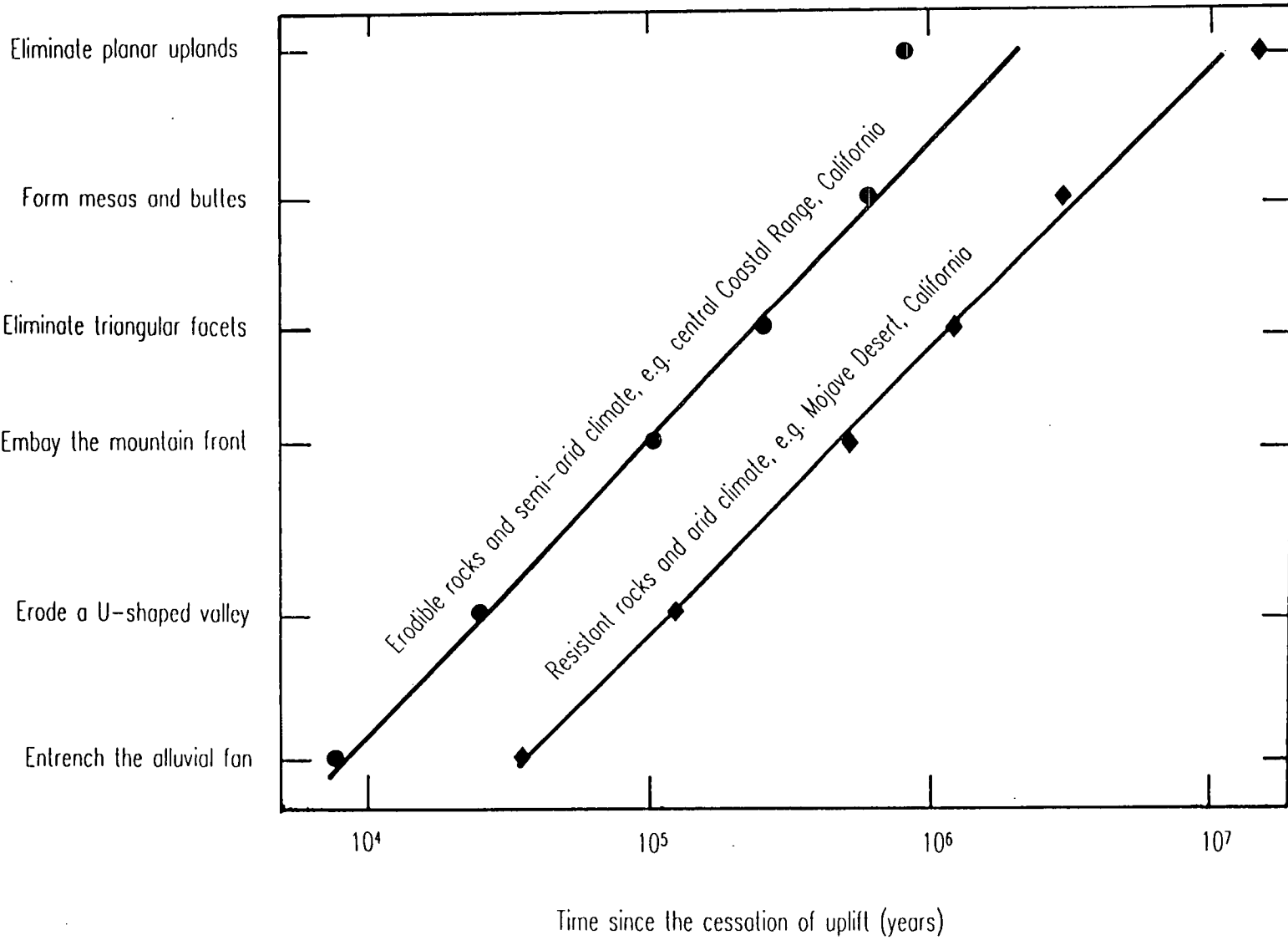


Fig. 2.26. Diagram comparing the estimated times needed for changes in landforms after cessation of active uplift for drainage basins of about 10km<sup>2</sup> and a given climate and rock type (after Bull, 1978).

Note: rates for a semi-arid climate will lie between the lines representing the two extremes.

of the fluvial systems throughout southern Cyprus and it is likely that the river systems "partially reflect Quaternary climate fluctuations within a spatial framework determined by tectonic activity" (Harvey & Wells, 1987), as has been suggested for fluvial systems in semi-arid and arid conditions in south-east Spain (Harvey & Wells, 1987), Oman (Maizels, 1987) and Israel (Frostick & Reid, 1989).

The data presented in this chapter indicates that the island of Cyprus experienced absolute uplift during the Quaternary period (Chapter 3). The presence of a suite of near horizontal marine terraces and associated gorges and palaeocliffines (Sections 2.4 and 2.6.3), indicate that uplift of the whole of southern Cyprus took place. The data from the coastal landforms (Section 2.4), the drainage pattern (Sections 2.2) and the fluvial features (Section 2.3) indicate that uplift was rapid during the lower and middle Quaternary and slowed during the Late Pleistocene, with evidence of submergence during the Holocene (Flemming, 1978).

### **2.6.5 Conclusions.**

In summary, it can be concluded that:

- i) the geomorphological features can be correlated throughout southern Cyprus,
- ii) evidence indicates that four major erosion surface and terrace levels exist in areas of both marine and non-marine influence,
- iii) that eustatic sea-level changes, uplift and climate all played a role in the formation of the preserved geomorphological features,
- iv) the drainage pattern remained broadly constant for the duration of the Quaternary period,
- v) the geomorphology reflects absolute uplift of the whole of southern Cyprus,
- vi) the differential Quaternary uplift was focussed on Mount Olympus,
- vii) the available geomorphological evidence supports rapid uplift during the lower and middle Pleistocene with relative quiescence and possible submergence in the Late Pleistocene and Holocene (Table 1.10).

## Chapter Three: Quaternary biostratigraphy and geochronology.

### 3.1 INTRODUCTION.

This chapter will examine the evidence for biostratigraphic and geochronological correlations of the Quaternary from Cyprus. Evidence that confirms that the F1-F4 stages can be correlated throughout the island will be presented. Palaeontological data, i.e. vertebrate, invertebrate and microfaunal, relating to the correlations, climate change and mammalian evolution will be described and discussed. Absolute and relative geochronologic dates were obtained from coral and mollusc samples during this study using the uranium series disequilibrium, amino-acid epimerization/racemization and  $^{14}\text{C}$  methods (Bowen, 1978; Lowe & Walker, 1984; Mahaney, 1984). The results obtained from these techniques aid the correlation and interpretation of time of formation and uplift of the coastal terraces.

Biostratigraphy can be applied to Quaternary sequences, although this form of relative dating can be problematic. Faunal range zones are of little use as the Quaternary period is short and therefore faunal variations are small. Pliocene molluscan fauna are very similar to many of those seen throughout the Quaternary (Appendix D; Henson *et al.*, 1949; Moshkovitz, 1968). However there are exceptions, notably the introduction of a warm fauna (the "Senegalesse" fauna), which includes the gastropod *Strombus bubonius*. This fauna is believed to be diagnostic of the Tyrrhenian Stage (Pantazis 1966; Moshkovitz, 1968). Assemblage zones, i.e. groups of fauna reflecting ecology and environment (Richards, 1982), are of greater use as they are likely to reflect Quaternary environmental change, e.g. climate variation (Issar, 1979). Hearty (1987) states that diverse marine palaeohabitats and, more importantly, very variable wave energy, resulting in varying coastal geomorphology in Mallorca makes faunal comparisons sensitive to local changes, therefore limiting the value of biostratigraphy. The same variety of coastal geomorphology is seen in Cyprus (Chapter 2) with the "high energy coast" in south-east Cyprus around Larnaca contrasting with wide low-lying beaches and terraces in the south and west of Cyprus represented by the west coast between Paphos and the Akamas Peninsula (Fig.3.1). A stratigraphy based on faunal variations from progressively higher coastal terraces would not necessarily solve chronological problems, as higher terraces are not necessarily older, due to the interaction between tectonic and isostatic uplift and frequent, high amplitude, Quaternary eustatic sea-level changes (Fig.3.2).

Fig. 3.1. The location of sites from which samples for amino-acid racemization, the uranium series disequilibrium and the  $^{14}\text{C}$  methods were collected.

Note: locations recorded in the text of this chapter are also located on this map.

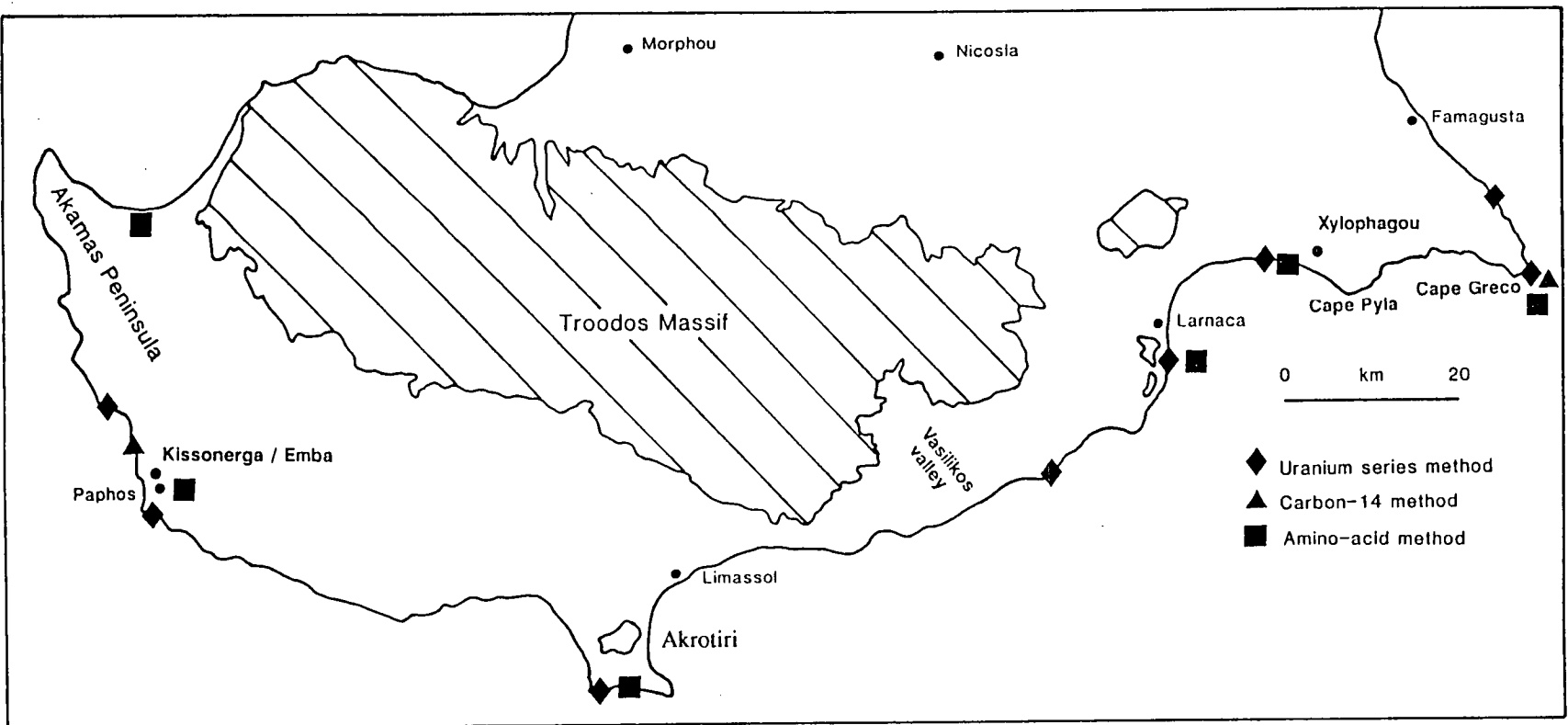




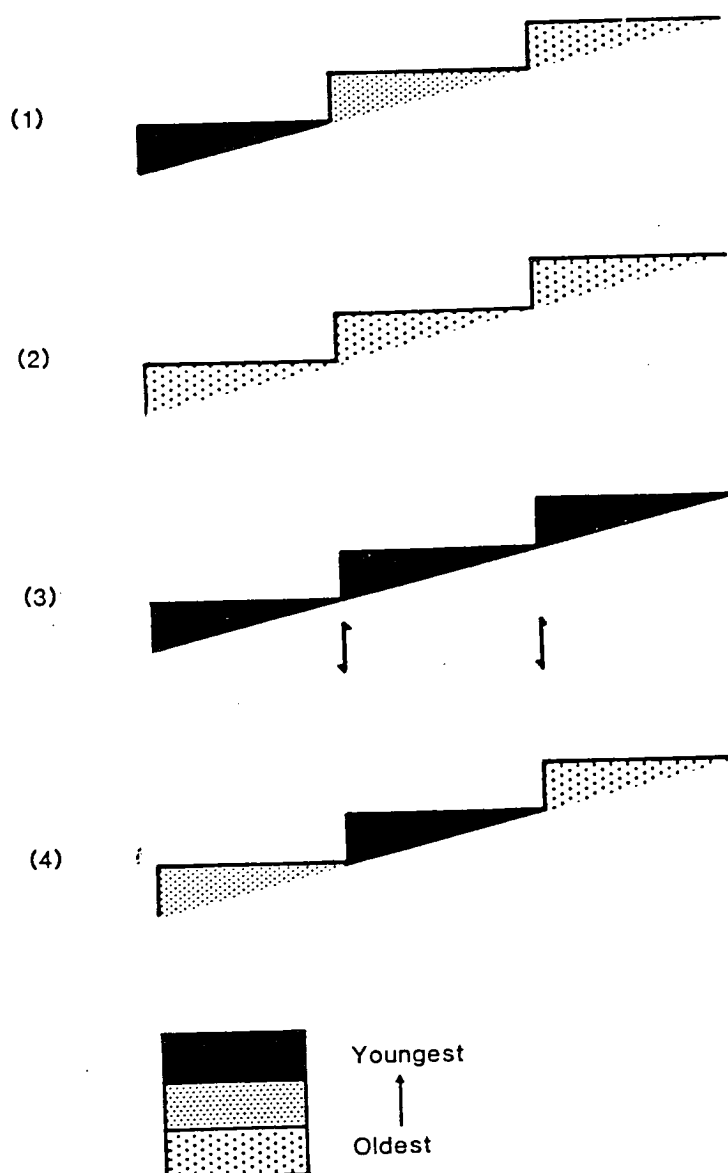
Fig.3.2. The possible combinations of terrace development indicating the importance of absolute age determination and the limited value of altimetric correlations through the view that older terraces are located at higher elevations.

Note: (1) a fall in relative sea-level (i.e. a fall in sea-level, and/or a rising landmass) results in the oldest terraces being preserved at the highest elevations.

(2) uplift at different rates in different areas results in the formation of terraces of the same age at different heights.

(3) faulting of a terrace can result in the development of stepped terraces, which apparently reflect a relative drop in sea-level, i.e. a drop in sea-level and/or uplift, but in actual fact represent terraces of the same age.

(4) the oldest terrace develops, a fall in relative sea-level then results in the formation of the intermediate age terrace, a subsequent rise in the relative sea-level can result in the development of the third, and youngest, terrace in an intermediate location.



Altimetric correlations between different parts of the Mediterranean coastline have also been attempted in the past (Deperet, 1918; Zeuner, 1959). In Cyprus, Pantazis (1966) correlated the F3 (in this study) terrace at Larnaca with a 12m high cliff in Crete, attributing this to the Tyrrhenian II, or Main Monastirian Stage (Table 3.1). Uplift and submergence of terraces as a result of tectonics illustrate that these correlations have a limited value (Fig.3.2).

Table 3.1. Mediterranean marine stage names and height ASL (after Zeuner, 1959).

| Stage name       | Type locality                                | Height (m ASL) |
|------------------|----------------------------------------------|----------------|
| Late Monastirian | Monastir, Tunisia                            | 7-8            |
| Main Monastirian | Monastir, Tunisia                            | 18-20          |
| Tyrrhenian       | Tyrrhenian Sea area                          | 28-32          |
| Milizzian        | Milazzo promontory,<br>north coast of Sicily | 53-60          |
| Sicilian         | Sicily                                       | 80-100         |

In summary, a desirable stratigraphy can best be achieved by the use of a combination of *absolute* and *relative* age data, as discussed below.

### **3.2 PALAEOLOGY.**

#### **3.2.1 Micropalaeontology.**

Micropalaeontological studies of ostracods and foraminifera from the Kakkaristra and Athalassa Formations of the Mesaoria Plain have yielded an ?Upper Pliocene to Lower Pleistocene age (McCallum, 1989). Nannofossil and foraminiferal assemblages from submarine channels at Amathus and Khirokitia, along the southern coast of the island (Fig.2.6), are of latest Pliocene age (Houghton *et al.*, 1990). Grey-green marls found cropping out beneath marine terraces along the southern coast of the island (Chapter 7) have been examined for calcareous nannofossils and foraminifera by Dr. A. Lord and Dr. L. Gallagher (University College London). Reworking, as a result of erosion, has complicated dating, limiting the study to the identification of the youngest species, these are as follows:

i) Cape Greco (location 1-125) and Coral Bay (location 2-25).

*Sphenolithus abies*, Deflandre

*Dicoaster brouweri*, Tan

ii) Polis (location 3-150)

*Dicoaster pentaradaitus*, Tan

*Dicoaster surculus*, Martini and Bramlette

*Dicoaster tamalis*, Kamptner

*Gephyrocapsa*

*Pseudoemiliana*

The foraminifera recorded from the marls are:

i) Cape Greco (location 1-125)

*Globigerinoides quadrilobatus*, d'Orbigny

*G. trilobus*

*G. ruber*

*Globirotalia* sp.

*Orbulina saturalii*

Many of the tests were broken and no there was no evidence for the presence of benthic foraminifera.

ii) Maa Peninsula (location 2-22)

*Globigernoides ruber*

*Nodosaria radricula*, Linne

*Nodosaria rapharia*

*Melonis sodanii*, d'Orbigny

*Perigrina dirupta*, Todd

*Lenticulina* sp.

*Globorotalia margaritae*, Bolli and Bermudez

These fauna suggest a Pliocene age for the marls cropping out at Cape Greco, Coral Bay and Polis, correlating with marls of the Nicosia Formation.

### **3.2.2 Invertebrate palaeontology.**

Studies of the Late Pliocene and Quaternary molluscan populations have previously been made (Moshkovitz, 1968). The molluscan populations of Cyprus are summarised in Appendix D and show two major groups: those with species that are found throughout the Quaternary in the Mediterranean (the "*fanés banales*" of the French) and immigrant faunas. The introduction of immigrant faunas, from latest Pliocene to the present day, allows three climatically controlled faunal assemblages to be recognised

(Issar, 1979; Table 3.2). Warm water molluscs (the "Senegalesse" fauna) are present in the marine terrace sequences at Larnaca indicating the Tyrrhenian Stage (Pantazis, 1966; Moshkovitz, 1968; Table 1.9). This warm "Senegalesse" fauna is thought to have entered the Mediterranean from the Atlantic during the Tyrrhenian Stage, this indicates the onset of warmer water conditions following cooler conditions during the Early and Middle Pleistocene (Issar, 1979). The correlation of Quaternary sequences using the classical stage names has proved to be very misleading (Hey, 1975), as the faunas are longer ranging than suggested by Deperet (1918). Their arrival and departure is not synchronous and faunal facies vary from area to area throughout the Mediterranean region (Hey, 1971; Butzer, 1975).

Table 3.2. Mediterranean Quaternary palaeoclimates (after Issar, 1979).

|                  |                                                                                                                                                                                            |
|------------------|--------------------------------------------------------------------------------------------------------------------------------------------------------------------------------------------|
| Post Tyrrhenian  | - present day faunal assemblage                                                                                                                                                            |
| Tyrrhenian       | - appearance of warm Senegalesse fauna<br>- i.e. <i>Strombus bubonious</i> , <i>Marginopora</i><br>- the warm water fauna exist between 220ka. and 100ka.<br>(Butzer, 1975; Nilsson, 1983) |
| Calabro-Sicilian | - cooling of warm Pliocene climate<br>- appearance of cold marine fauna<br>- i.e. <i>Arctica islandica</i> , <i>Hyalinea baltica</i> .                                                     |

Solitary corals, i.e. *Trochocyathus sp.* and *Flabellum avicula*, are located in the grey-green marl sequences at Maa and Coral Bay (location 2-22). These were not seen elsewhere. Colonies of the cosmopolitan, hermatypic, Mediterranean scleractinian coral, *Cladocora caespitosa*, are found cropping out in the two lower marine terrace levels, the F3 and F4, within 11m and 3m ASL throughout southern Cyprus (Chapter 7), as well as within the F2 terrace (c.50-60m ASL) in the Paphos area. *C. caespitosa* corals are also present within the Pliocene sediments of the Mesaoria Plain (Moore, 1960; Gass, 1960; McCallum 1989). The corals typically form colonies 1-2m in diameter (Plate 3.1) and are found throughout the Mediterranean today, e.g. off the coast of Israel and Morocco (Zibrowius, 1980). However, colonies of the coral are apparently absent from the F1 marine terraces throughout southern Cyprus. The sedimentary environments of all the documented marine carbonate terraces of southern Cyprus, i.e. F1-F4, are very similar (Chapter 7), with rhodolithic coralline algae, rather than coral, dominating during the F1 and F2 (Chapter 7).

PLATE 3.1.

D - Elephant and hippopotami bones set in a matrix of fine green sand, south-east of Xylophagou (location 2-75).

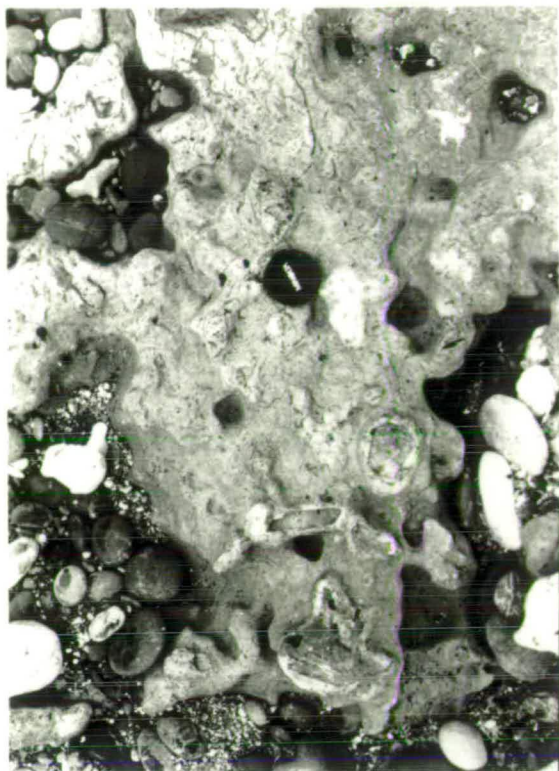
E - A dwarf elephant tusk (ca.60cm long), south-east of Xylophagou (location 2-75).

F - A colony of the coral *Cladocora caespitosa* from the F4 (Late Pleistocene) terrace at Dhekelia (location 2-84).

Note: scale is 50cm long.

Plate 3.1

D



E



F



### **3.2.3 Vertebrate palaeontology.**

#### **3.2.3.1 Introduction.**

Dwarf vertebrate fossil fauna are present on Cyprus for much of the Quaternary period. Interest in this fauna has recently increased with the suggestion that the human occupation of Cyprus pre-dates, and may have contributed to, the extinction of these fauna (Simmons, 1988).

The vertebrate fauna in Cyprus was first studied and described by Bate during the early part of the 20<sup>th</sup> century (Bate, 1903; 1904). The bones are distinct from those found on other Mediterranean islands, especially Sicily and Malta, suggesting that the fauna was endemic (Boekschoten & Sondaar, 1972). The occurrence of different, although closely related, elephants and hippopotami on widely separated islands of the Mediterranean, supports the argument for comparable but independent evolution of the fauna (Bate, 1903). Geological and geophysical evidence indicate that the Troodos Massif was not a submerged landmass during the Quaternary (Gass, 1968) and that deep water will have surrounded the island even during Quaternary eustatic sea-level lows (Fig.2.23). One-way migration to Cyprus is thought to have occurred during the Pleistocene ("Sweepstake" migration; Sondaar, 1986). Elephants and hippopotami are thought to have "island-hopped", swum, or used natural rafts to reach Cyprus (and other Mediterranean islands; Reese, 1989). The migration gave rise to an isolated population, a tendency to dwarfism of the population then followed. Potential advantages of dwarfism were (after Sondaar, 1986):

- i) a lack of predators meant that the fauna did not need to be large for defence,
- ii) a smaller size meant that a larger population could survive in a given area,
- iii) dwarfism allowed for greater mobility in hilly terrains, and therefore greater access to food resources;
- iv) a smaller size allowed the vertebrates to remain cooler, and therefore remain active in hotter climates for longer periods.

The presence of large bone sites on Cyprus suggests that the endemic fauna suffered a dramatic demise as a consequence of social stresses, e.g. over-population and starvation (Sondaar, 1986), climatic and environmental changes, e.g. small temperature fluctuations affecting food availability (Davis, 1981), or man as a predator (Simmons, 1988).

### 3.2.3.2 Occurrence.

Elephants and hippopotami bones have been found in sites in both northern and southern Cyprus. The sites are predominantly cave deposits sited along the flanks of the Kyrenia Mountains and along the southern coast, e.g. Akrotiri, Cape Pyla and Kissonerga (Held, 1990; Fig.3.1). The author was shown two sites, one near Emba village in the south-west of the island (by Dr. Costas Xenophonos) and the other to the west of Xylophagou in the south-east (by a quarry worker) (Fig.3.1). Neither was a cave site, instead the bones were deposited by fluvial processes (Chapter 5). Mammal fossils are also present in Fanglomerate Group and Pleistocene beach and dune sediments on both the southern and northern flanks of the Kyrenia Range (Boekschoten & Sondaar, 1972). Bone localities on the southern slope of the Kyrenia Range have been identified as being Villafranchian (Upper Pliocene-Lower Pleistocene; Ducloz, 1968).

### 3.2.3.3 Fauna.

The dwarf elephant species, *Elephas cypriotes* (Bate, 1903) differs from the Sicilian and Maltese species, *E. melintensis*, by being slightly smaller, with a more simple tooth construction and laterally compressed tusks. The pygmy hippopotamus *Hippopotamus minutus* (Bate, 1903) was subsequently renamed *Phanouris minutus* (Boekschoten & Sondaar, 1972) because of the differences between this and the Maltese and Sicilian hippos. A gazetteer of the known mammal bone sites and the fauna found at each one has been prepared by Held (1990).

A bone site in Fanglomerate Group sediments at Athna, in south-east Cyprus, has produced elephant teeth (molars), but no hippopotamus or elephant bones (D. Reese & S. Held, *pers. comm.*, 1988). The teeth are larger than those associated with *E. cypriotes*. The bones collected from the site at location 2-75 are currently being examined by Dr. David Reese (of the Field Museum of Natural History, Chicago). Studies of the bones collected, and that remain *in situ*, at the bone site to the south-west of Xylophagou (location 2-75) have revealed the following (D. Reese, *pers. comm.*, 1990):

- i) elephant bones - including a tusk 120mm long with a maximum diameter of 52mm, an unfused femur from a young individual, a scapula, fragments of pelvis and molars and incisors,
- ii) hippopotamus bones - including a femur (Plate 3.1).

The hippopotamus bones from location 2-75 and those collected at Akrotiri are of similar size, the elephants bones from location 2-75 are larger than the samples of *E. cypriotes* collected from Akrotiri. Many of the samples from location 2-75 are from sub-



adult elephants. The site at location 2-75 has produced the largest collection of older dwarf elephant remains in Cyprus. Molar tooth samples that have been collected from location 2-75 can be correlated with those from the Kyrenia Range and the Athna tooth collection, as can an elephant tusk found in the Xylophagou area (Held, 1990). The Athna tooth collection and Xylophagou tusk were found in fluvial sediments of the Fanglomerate Group. Location 2-75 is within 2m ASL. A detailed description of the Fanglomerate Group sediments in which these bones were situated, can be found in Chapter 5.

### **3.3 GEOCHRONOLOGICAL DATING METHODS.**

#### **3.3.1 Uranium series disequilibrium method.**

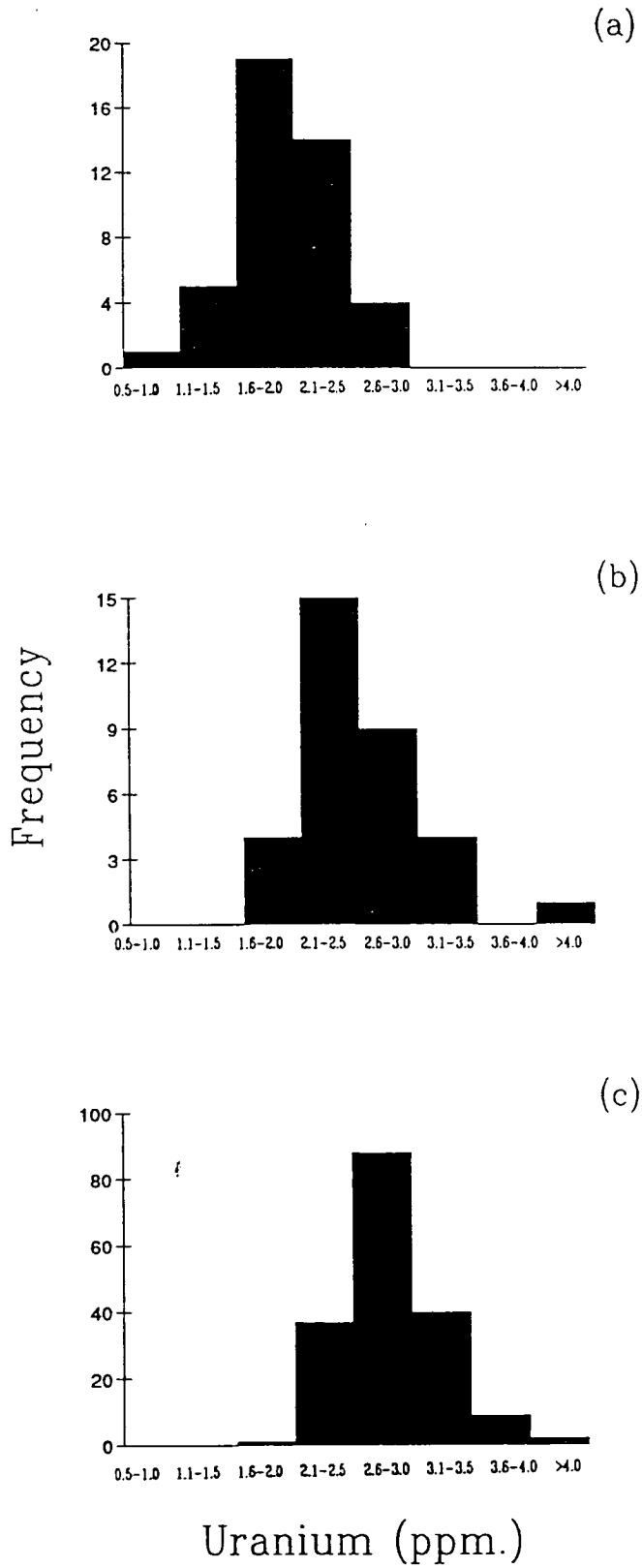
##### **3.3.1.1 Introduction.**

The uranium series disequilibrium method utilises the  $^{234}\text{U}$  and  $^{238}\text{U}$  isotopes and their daughter products, i.e.  $^{230}\text{Th}$ ,  $^{226}\text{Ra}$ . This method is based on the virtual absence of  $^{234}\text{U}$  daughter products in the near-surface marine waters. Corals form a closed system incorporating uranium in to their exoskeleton during life (Ku, 1976) and as such should not contain any  $^{230}\text{Th}$  when living. On death, radioactive decay of  $^{234}\text{U}$  results in the production of its daughter  $^{230}\text{Th}$ ; the ratio of  $^{230}\text{Th}/^{234}\text{U}$  being proportional to the age of the sample. Accurate dates rely on the following assumptions and controls:

- i) that original aragonite is sampled, as dissolution and recrystallization to calcite could result in leaching and scavenging thus giving an incorrect apparent age for the sample,
- ii) the original uranium content should be similar to a modern coral (approximately 3ppm; Fig.3.3),
- iii) the initial  $^{234}\text{U}/^{238}\text{U}$  ratio =  $1.15 \pm 0.015$ , which reflects the disequilibrium found in living coral and present day oceanic waters (Turekian & Chen, 1971; Bender *et al.*, 1979, Chen *et al.*, 1986; Edwards *et al.*, 1986-87). It has been shown that the  $^{234}\text{U}/^{238}\text{U}$  ratio has not varied over the last 200ka. (Ivanovich & Harmon, 1982), which is in keeping with the known long oceanic residence time of uranium, i.e. 400ka. (Turekian & Chen, 1971),
- iv) that the  $^{226}\text{Ra}/^{230}\text{Th}$  ratio agrees with  $^{230}\text{Th}/^{234}\text{U}$  age,
- v) that little or no  $^{232}\text{Th}$  is present in the sample,
- vi) that the  $^{230}\text{Th}/^{234}\text{U}$  age is consistent with stratigraphic and other assessments.

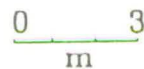
The method has yielded internally consistent and well constrained dates for samples as old as c.350ka., e.g. in New Guinea (Bloom *et al.*, 1974; Chappell & Veeh,

Fig.3.3. A plot of uranium content (ppm) of the coral samples from: a) these uranium series disequilibrium studies; b) other Recent corals; and c) fossils corals from around the world (additional data after Ivanovich & Harmon, 1982).

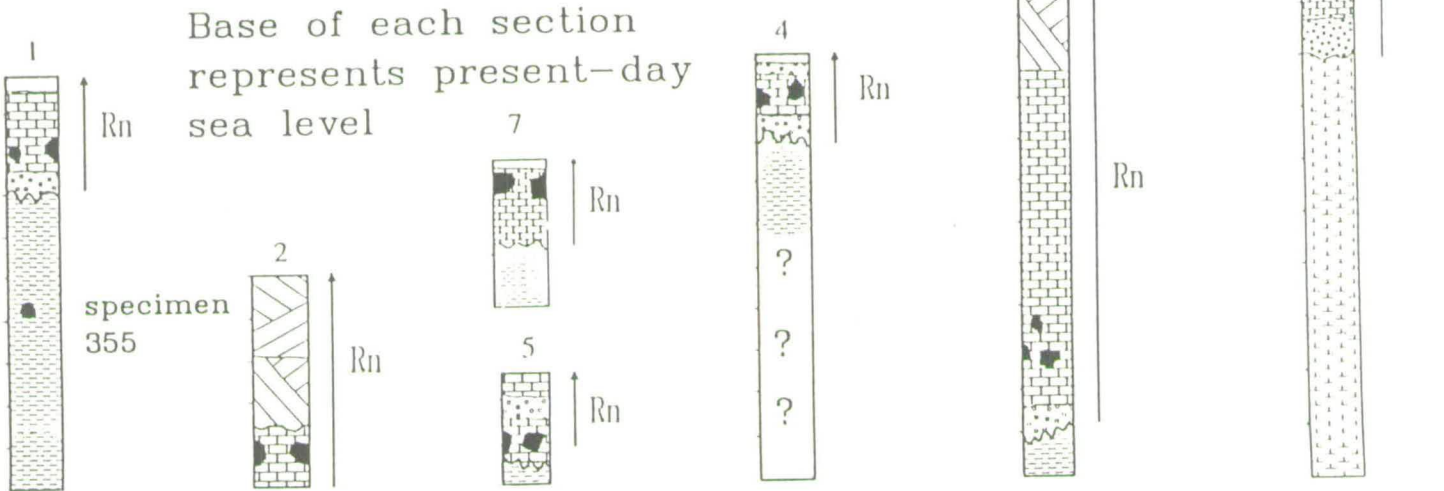
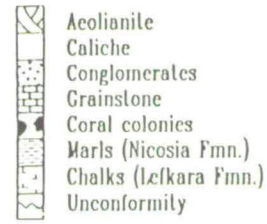




1. Coral Bay (location 2-22)
2. Paphos (location 2-11)
3. Petounda Point (location 3-11)
4. Larnaca (location 1-130)
5. Dhekelia (location 2-76)
6. Cape Greco (location 1-125)
7. Paralimni (location 3-211)



Rn - regression



Base of each section represents present-day sea level

specimen 355

Fig. 3.4. A sketch map and sedimentary logs showing the location and height above present day sea-level of the samples used during uranium series disequilibrium studies.

Table 3.3. Details of the U and Th isotopic and mineralogical compositions, plus age data, for the Late Quaternary Cyprus corals.

| Sample | Locality       | Terrace height (m) | $^{234}\text{U}/^{238}\text{U}$ | $^{230}\text{Th}/^{232}\text{Th}$ | $^{230}\text{Th}/^{234}\text{U}$ | $^{232}\text{Th}$ (dpm/g) | U (ppm) | Arag. (%) | Age (ka) |
|--------|----------------|--------------------|---------------------------------|-----------------------------------|----------------------------------|---------------------------|---------|-----------|----------|
| 021    | Larnaca        | 8-11               | 1.10 ±0.02                      | 68.67 ±8.15                       | 0.84 ±0.01                       | 0.03                      | 2.99    | 90        | 183 ±2   |
| 617a   | Larnaca        | 8-11               | 1.16 ±0.01                      | 63.33 ±4.38                       | 1.01 ±0.01                       | 0.03                      | 2.19    | 99        | > 300    |
| 617b   | Larnaca        | 8-11               | 1.13 ±0.02                      | 85.50 ±7.33                       | 1.03 ±0.01                       | 0.02                      | 1.97    | 99        | > 300    |
| 617c   | Larnaca        | 8-11               | 1.13 ±0.02                      | 41.75 ±2.51                       | 0.88 ±0.01                       | 0.04                      | 2.25    | 97        | 209 ±7   |
| 617d   | Larnaca        | 8-11               | 1.06 ±0.02                      | 84.00 ±6.18                       | 1.11 ±0.02                       | 0.02                      | 1.90    | 98        | > 300    |
| 617e   | Larnaca        | 8-11               | 1.14 ±0.02                      | 43.00 ±4.85                       | 0.86 ±0.02                       | 0.03                      | 1.76    | 98        | 197 ±16  |
| 617f   | Larnaca        | 8-11               | 1.07 ±0.02                      | 154.0 ±19.79                      | 0.97 ±0.01                       | 0.01                      | 1.98    | 98        | > 300    |
| 617g   | Larnaca        | 8-11               | 1.09 ±0.01                      | 41.67 ±3.49                       | 0.77 ±0.01                       | 0.03                      | 2.00    | 85        | *        |
| 617ed  | Larnaca        | 8-11               | 1.07 ±0.03                      | 39.33 ±2.86                       | 0.84 ±0.02                       | 0.03                      | 1.76    | 92        | 183 ±12  |
| 358a   | Coral Bay      | 8-11               | 1.11 ±0.02                      | 163.0 ±41.98                      | 0.82 ±0.02                       | 0.01                      | 2.39    | 91        | 176 ±10  |
| 358b   | Coral Bay      | 8-11               | 1.11 ±0.02                      | 146.0 ±32.38                      | 0.86 ±0.02                       | 0.01                      | 2.05    | 94        | 196 ±12  |
| 358c   | Coral Bay      | 8-11               | 1.11 ±0.03                      | 176.0 ±41.97                      | 0.90 ±0.02                       | 0.01                      | 2.34    | 93        | 226 ±17  |
| 358d   | Coral Bay      | 8-11               | 1.08 ±0.02                      | 111.0 ±22.66                      | 0.72 ±0.01                       | 0.01                      | 1.92    | 70        | *        |
| 358e   | Coral Bay      | 8-11               | 1.03 ±0.03                      | N.a.                              | 0.86 ±0.02                       | 0.00                      | 2.11    | 92        | 196 ±12  |
| 68a/89 | Akrotiri       | 8-11               | 1.11 ±0.03                      | 247.2 ±12.48                      | 1.00 ±0.03                       | 0.01                      | 1.45    | 99        | #        |
| 68b/89 | Akrotiri       | 8-11               | 1.11 ±0.04                      | 206.9 ±4.58                       | 1.12 ±0.04                       | 0.01                      | 1.56    | 97        | #        |
| 68c/89 | Akrotiri       | 8-11               | 1.11 ±0.04                      | 704.0 ±352.1                      | 1.13 ±0.03                       | 0.00                      | 1.50    | 97        | #        |
| 68d/89 | Akrotiri       | 8-11               | 1.10 ±0.02                      | 51.13 ±9.25                       | 1.03 ±0.02                       | 0.02                      | 1.45    | 91        | #        |
| 40a/89 | Petounda Point | 8-11               | 1.11 ±0.02                      | 87.38 ±11.45                      | 0.87 ±0.01                       | 0.01                      | 1.58    | 94        | 203 ±7   |
| 40d/89 | Petounda Point | 8-11               | 1.11 ±0.02                      | 114.6 ±20.68                      | 0.88 ±0.02                       | 0.01                      | 1.42    | 96        | 209 ±15  |
| 200a   | Cape Greco     | 8-11               | 1.11 ±0.02                      | 41.67 ±3.25                       | 0.91 ±0.02                       | 0.03                      | 1.67    | 91        | 229 ±16  |
| 527a   | Cape Greco     | 8-11               | 1.14 ±0.02                      | 39.33 ±3.46                       | 0.74 ±0.01                       | 0.03                      | 1.87    | 91        | 141 ±4   |
| 527b   | Cape Greco     | 8-11               | 1.00 ±0.02                      | 32.25 ±2.89                       | 1.09 ±0.02                       | 0.04                      | 1.58    | 81        | *        |
| 529    | Cape Greco     | 8-11               | 1.11 ±0.03                      | 61.00 ±5.18                       | 0.88 ±0.02                       | 0.02                      | 1.67    | 95        | 209 ±16  |
| 336a   | Paphos         | < 3                | 1.09 ±0.02                      | 66.50 ±8.30                       | 0.66 ±0.01                       | 0.02                      | 2.49    | 96        | 113 ±3   |
| 336b   | Paphos         | < 3                | 1.09 ±0.03                      | 126.0 ±20.23                      | 0.66 ±0.02                       | 0.01                      | 2.36    | 100       | 112 ±6   |
| 336c   | Paphos         | < 3                | 1.17 ±0.03                      | 57.50 ±8.01                       | 0.64 ±0.02                       | 0.02                      | 2.06    | 96        | 108 ±6   |
| 336d   | Paphos         | < 3                | 1.08 ±0.02                      | 72.00 ±10.17                      | 0.67 ±0.01                       | 0.02                      | 2.65    | 98        | 117 ±4   |
| 336e   | Paphos         | < 3                | 1.09 ±0.02                      | 151.0 ±30.85                      | 0.70 ±0.01                       | 0.01                      | 2.65    | 100       | 125 ±4   |
| 598a   | Dhekelia       | < 3                | 1.10 ±0.01                      | 42.33 ±2.96                       | 0.73 ±0.01                       | 0.03                      | 2.10    | 95        | 138 ±4   |
| 598d   | Dhekelia       | < 3                | 1.09 ±0.01                      | 64.50 ±4.27                       | 0.69 ±0.02                       | 0.02                      | 2.30    | 99        | 122 ±3   |
| 598e   | Dhekelia       | < 3                | 1.10 ±0.02                      | 63.50 ±4.34                       | 0.73 ±0.01                       | 0.02                      | 2.13    | 97        | 135 ±4   |
| 598f   | Dhekelia       | < 3                | 1.12 ±0.01                      | 68.00 ±4.00                       | 0.69 ±0.01                       | 0.02                      | 2.35    | 98        | 123 ±3   |
| 598g   | Dhekelia       | < 3                | 1.15 ±0.03                      | 62.00 ±11.09                      | 0.72 ±0.02                       | 0.02                      | 2.01    | 99        | 132 ±7   |
| 598ee  | Dhekelia       | < 3                | 1.14 ±0.02                      | 55.71 ±15.65                      | 0.66 ±0.01                       | 0.01                      | 1.39    | 97        | 113 ±3   |
| P2/89  | Paralimni      | < 3                | 1.11 ±0.02                      | 102.5 ±28.74                      | 0.76 ±0.02                       | 0.01                      | 2.27    | 81        | *        |
| P3/89  | Paralimni      | < 3                | 1.11 ±0.02                      | 113.0 ±11.37                      | 0.73 ±0.01                       | 0.01                      | 1.87    | 91        | 138 ±4   |
| P4/89  | Paralimni      | < 3                | 1.11 ±0.03                      | 42.74 ±3.89                       | 0.71 ±0.01                       | 0.03                      | 1.97    | 96        | 129 ±4   |
| P5/89  | Paralimni      | < 3                | 1.10 ±0.02                      | 33.84 ±3.54                       | 0.78 ±0.01                       | 0.03                      | 1.65    | 82        | *        |
| 355    | Coral Bay      | N.a.               | 0.91 ±0.02                      | 255.0 ±37.83                      | 1.40 ±0.02                       | 0.01                      | 2.68    | 91        | > 300    |
| P1     | Barbados       | N.a.               | 1.15 ±0.02                      | N.a.                              | 0.01 ±0.00                       | 0.01                      | 1.93    | 93        | Recent   |
| P2     | Barbados       | N.a.               | 1.16 ±0.02                      | N.a.                              | 0.01 ±0.00                       | 0.00                      | 2.04    | 100       | Recent   |
| P3     | Barbados       | N.a.               | 1.15 ±0.02                      | N.a.                              | 0.01 ±0.00                       | 0.00                      | 0.74    | 96        | Recent   |

Note: N.a. = not applicable.

\* = age invalid as the sample contains < 90% aragonite.

# =  $^{230}\text{Th}/^{234}\text{U} > 1.0$  (see text for explanation).

Table 3.4. The location and type of sample used for uranium series disequilibrium studies, plus chemical yields and concentrations of uranium in each sample.

| Location number | Sample number | Coral species          | Uranium concentration (ppm) | Th yield (%) | U yield (%) |
|-----------------|---------------|------------------------|-----------------------------|--------------|-------------|
| 1-130           | 021           | <i>C.caespitosa</i>    | 2.99                        | 80           | 76          |
| "               | 617a          | <i>C.caespitosa</i>    | 2.19                        | 77           | 82          |
| "               | 617b          | <i>C.caespitosa</i>    | 1.97                        | 70           | 86          |
| "               | 617c          | <i>C.caespitosa</i>    | 2.25                        | 72           | 75          |
| "               | 617d          | <i>C.caespitosa</i>    | 1.90                        | 78           | 48          |
| "               | 617e          | <i>C.caespitosa</i>    | 1.76                        | 89           | 95          |
| "               | 617f          | <i>C.caespitosa</i>    | 1.98                        | 83           | 57          |
| "               | 617g          | <i>C.caespitosa</i>    | 2.00                        | 94           | 71          |
| "               | 617ed         | <i>C.caespitosa</i>    | 1.76                        | 100          | 92          |
| 2-22            | 358a          | <i>C.caespitosa</i>    | 2.39                        | 58           | 76          |
| "               | 358b          | <i>C.caespitosa</i>    | 2.05                        | 63           | 93          |
| "               | 358c          | <i>C.caespitosa</i>    | 2.34                        | 57           | 69          |
| "               | 358d          | <i>C.caespitosa</i>    | 1.92                        | 73           | 74          |
| "               | 358e          | <i>C.caespitosa</i>    | 2.11                        | 64           | 34          |
| 3-96            | C68a/89       | <i>C.caespitosa</i>    | 1.45                        | 97           | 100         |
| "               | C68b/89       | <i>C.caespitosa</i>    | 1.56                        | 97           | 86          |
| "               | C68c/89       | <i>C.caespitosa</i>    | 1.50                        | 96           | 70          |
| "               | C68d/89       | <i>C.caespitosa</i>    | 1.45                        | 96           | 57          |
| 3-11            | 40a/89        | <i>C.caespitosa</i>    | 1.58                        | 95           | 100         |
| "               | 40d/89        | <i>C.caespitosa</i>    | 1.42                        | 90           | 77          |
| 1-125           | 200a          | <i>C.caespitosa</i>    | 1.67                        | 95           | 71          |
| "               | 527a          | <i>C.caespitosa</i>    | 1.87                        | 83           | 58          |
| "               | 527b          | <i>C.caespitosa</i>    | 1.58                        | 93           | 78          |
| "               | 529           | <i>C.caespitosa</i>    | 1.67                        | 99           | 83          |
| 2-11            | 336a          | <i>C.caespitosa</i>    | 2.49                        | 98           | 85          |
| "               | 336b          | <i>C.caespitosa</i>    | 2.36                        | 89           | 88          |
| "               | 336c          | <i>C.caespitosa</i>    | 2.06                        | 96           | 83          |
| "               | 336d          | <i>C.caespitosa</i>    | 2.65                        | 78           | 42          |
| "               | 336e          | <i>C.caespitosa</i>    | 2.65                        | 72           | 51          |
| 2-84            | 598a          | <i>C.caespitosa</i>    | 2.10                        | 92           | 95          |
| "               | 598d          | <i>C.caespitosa</i>    | 2.30                        | 85           | 88          |
| "               | 598e          | <i>C.caespitosa</i>    | 2.13                        | 94           | 70          |
| "               | 598f          | <i>C.caespitosa</i>    | 2.35                        | 99           | 98          |
| "               | 598g          | <i>C.caespitosa</i>    | 2.01                        | 65           | 74          |
| "               | 598ee         | <i>C.caespitosa</i>    | 1.39                        | 99           | 81          |
| 3-50            | P2/89         | <i>C.caespitosa</i>    | 2.27                        | 66           | 42          |
| "               | P3/89         | <i>C.caespitosa</i>    | 1.87                        | 70           | 65          |
| "               | P4/89         | <i>C.caespitosa</i>    | 1.97                        | 69           | 29          |
| "               | P5/89         | <i>C.caespitosa</i>    | 1.65                        | 72           | 38          |
| 2-22            | 355           | <i>Flabellum sp.</i>   | 2.68                        | 83           | 54          |
| N/A             | P1            | <i>Porites porites</i> | 1.93                        | 22           | 79          |
| "               | P2            | <i>Porites porites</i> | 2.04                        | 29           | 73          |
| "               | P3            | <i>Porites porites</i> | 0.74                        | 65           | 87          |

1978; Chappell, 1983) and Barbados (Mesolella *et al.*, 1969), the upper age limit for the method (Broecker, 1963).

The U-series disequilibrium method has been used extensively on mollusc shells, but these contain only 20% of the uranium found in corals and they form an open rather than closed system. An open system allows uranium to be incorporated into the molluscan shell during diagenesis, i.e. both  $^{238}\text{U}$  and  $^{234}\text{U}$  relative to  $^{238}\text{U}$ , resulting in inaccurate dates. Very few reliable dates have been produced using the U-series method on molluscs samples, dates being variable and inconsistent when checked against independent methods, e.g.  $^{231}\text{Pa}/^{235}\text{U}$  ratio (Kaufman *et al.*, 1971). However, molluscs found in Pleistocene beachrock deposits from the Mediterranean have been successfully dated, yielding consistent results that conform to independently derived data (Stearns & Thurber, 1965). Broecker & Bender (1972) argue that consistent dates can be attained from molluscs found in a carbonate beachrock as a closed system forms rapidly as a result of diagenesis, permitting only minimal changes in the uranium content.

### 3.3.1.2 Sampling and analytical techniques.

The availability of corals in the F3 and F4 marine terraces in Cyprus meant that a recourse to molluscan samples was not necessary during this study. Samples of the coral *Cladocora caespitosa* were collected from the F3 terrace between 11 and 8m ASL (at 5 localities: Cape Greco, Larnaca, Petounda Point, Akrotiri and Coral Bay), and from lower (F4) terraces at less than 3m ASL (at 3 localities: Paralimni, Dhekelia and Paphos; Fig.3.4; Tables 3.3, 3.4 and 3.5). The majority of the corals were sampled from colonies that indicated a life position, e.g. attached to and growing from the substrate, unbroken and growing upwards (Chapter 7; Plate 3.2).

Samples of unaltered aragonitic coral (Plate 3.2), showing no evidence of calcite replacement (Husseini & Matthews, 1972), were selected for isotopic analysis, based on optical microscopic examination, X-ray diffraction and scanning electron microscope studies (Plate 3.2; Table 3.3).

A detailed account of the experimental procedures, age model and  $^{234}\text{U}/^{238}\text{U}$  decay curve data are described in Appendix C. Uranium and thorium isotopes were analysed by  $\alpha$ -spectrometry using silicon surface barrier detectors following the method of Kaufman & Broecker (1965), Thurber *et al.* (1965), Veeh (1966) and Thompson (1973). Complete dissolution of 4.5-6.0g of sample, standard ion exchange separation and electrolysis, prepared the separate U and Th sources. A mixed spike of  $^{232}\text{U}$  and  $^{228}\text{Th}$  was used to determine the isotopic activities of the  $^{232}\text{Th}$ ,  $^{230}\text{Th}$ ,  $^{238}\text{U}$  and  $^{234}\text{U}$

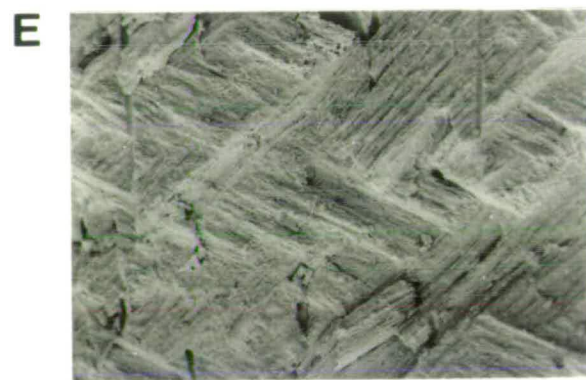
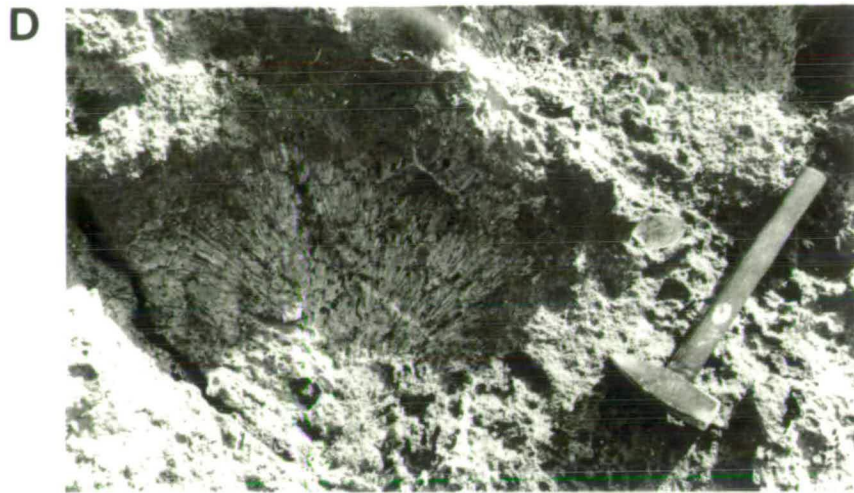
PLATE 3.2.

D - A colony of *Cladocora caespitosa* revealing a life position from the F4 (Late Pleistocene) terrace to the east of Paralimni, south-east Cyprus.

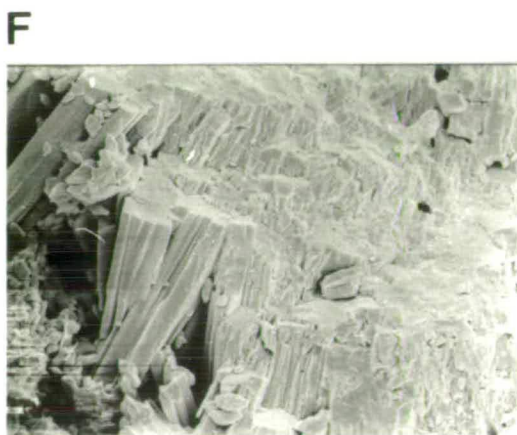
E - A scanning electron microscope image of the original aragonite cross-lamellae structures from the valve of *Glycymeris glycymeris*.

F & G - Scanning electron microscope images of the needle structure of primary aragonite in a specimen of the coral *Cladocora caespitosa*.

# Plate 3.2



40  $\mu\text{m}$



8  $\mu\text{m}$



20  $\mu\text{m}$



isotopes. The samples were counted for two to three days to obtain the requisite counting statistics. Exclusive U and Th isotope detectors were used to minimise the a-recoil contamination. Background counts using identical conditions were routinely determined prior to the counting of each sample. Three samples of recent Barbados coral (P1, P2, P3) were analysed as a control (Table 3.3) The errors quoted here (Tables 3.4 and 3.5) are calculated as one standard deviation ( $1\sigma$ ) of the counting statistics.

### 3.3.1.3 Results of analysis.

The  $^{232}\text{Th}$  activity is consistently very low (less than 0.04 dpm/g; Table 3.3), indicating an absence of contamination, hence non-radiogenic  $^{230}\text{Th}$  is not present as a contaminate, and little or no thorium was introduced after death of the coral. In addition, the initial  $^{230}\text{Th}$  of the control samples (P1, P2, P3) is extremely low, consistent with a recent age of formation; this also rules out possible analytical contamination during analysis.

The  $^{234}\text{U}/^{238}\text{U}$  ratio of the Barbados samples ( $1.15 \pm 0.03$ ) and younger Cyprus corals correspond to the expected initial ratio of modern seawater (Turekian & Chen, 1971; Bender *et al.*, 1979; Chen *et al.*, 1986; Edwards *et al.*, 1986-87) following decay correction (Fig.3.5). Contrasting results were, however, obtained from older samples collected from Larnaca, Akrotiri and Coral Bay, with initial activity  $^{234}\text{U}/^{238}\text{U}$  ratios greater than  $1.15 \pm 0.03$  following decay correction (displayed as the solid line in Fig.3.5).

Some other results appear to be anomalous. Specimen 355 from Coral Bay is considered to be unreliable for the following reasons:

- i) the  $^{234}\text{U}/^{238}\text{U}$  activity ratios, compared with the theoretical curve (Fig.3.5), suggest an age greater than the upper limit of the method, c.350ka. (Broecker, 1963),
- ii) sedimentological and nannofossil evidence (A. Lord & L. Gallagher, *pers. comm.*, 1989) suggest that the terrace containing the coral can be correlated with Pliocene marine successions found elsewhere on Cyprus.

Of the coral samples collected from Larnaca, four yield results consistent with the geological and stratigraphical data, while three other samples give anomalous results. All the samples collected from Akrotiri (samples C68a/89-C68d/89) show anomalous results similar to that seen at Larnaca. These anomalous results (samples 617a,b,d and C68a/89-C68d/89; Table 3.3) have  $^{230}\text{Th}/^{234}\text{U}$  ratios greater than 1.01. It is likely that  $^{230}\text{Th}$  has been added to the system, for the following reasons:

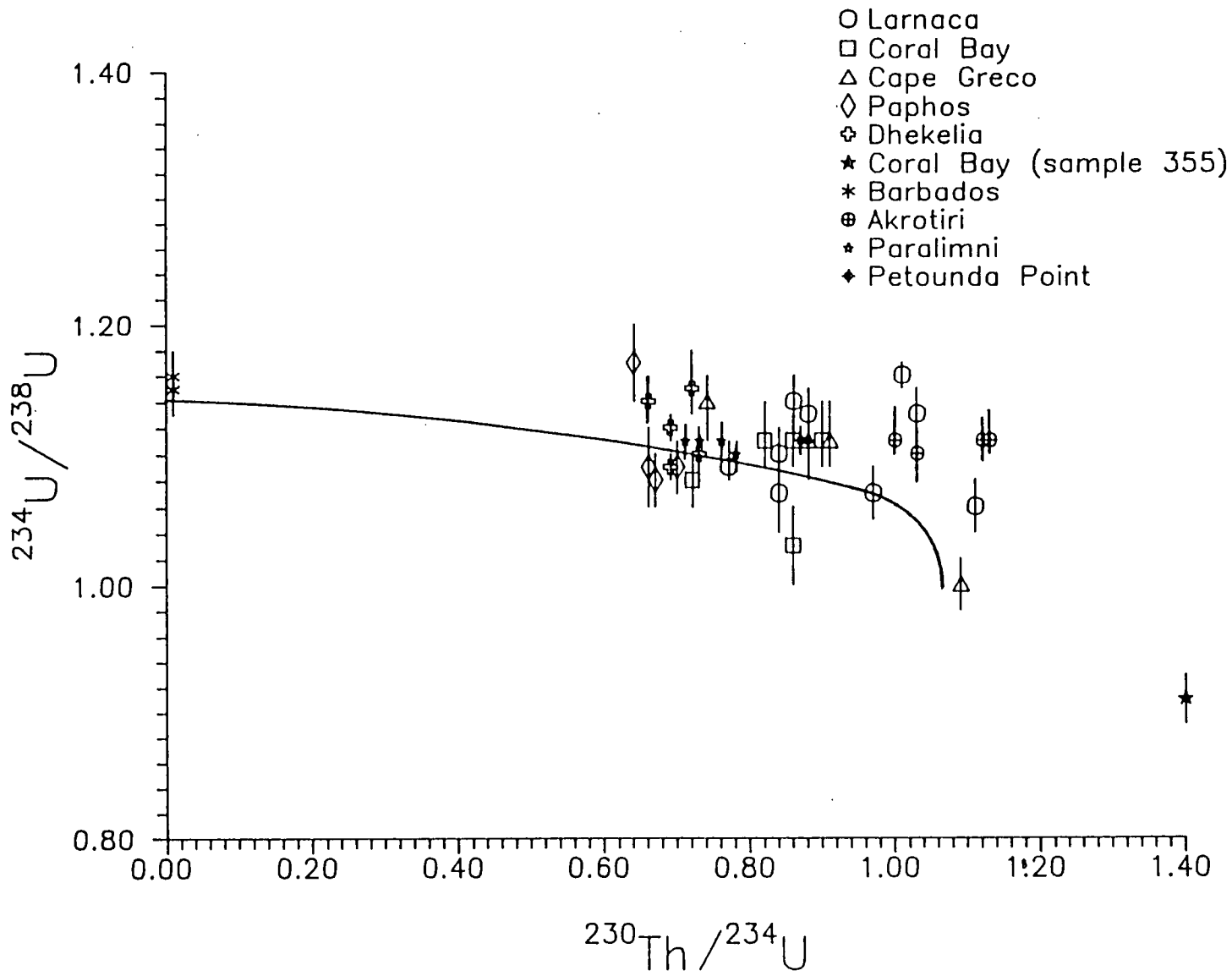


Fig.3.5. Theoretical decay curve of  $^{234}\text{U}/^{238}\text{U}$  versus  $^{230}\text{Th}/^{234}\text{U}$ , and the location of all the data points derived during the course of these uranium series disequilibrium studies.

- i) results from the control samples P1, P2 and P3 militate against contamination of the analytical equipment,
- ii) the  $^{230}\text{Th}/^{232}\text{Th}$  ratios are high, indicating the presence of a closed system,
- iii) high initial  $^{234}\text{U}/^{238}\text{U}$  ratios suggest that  $^{234}\text{U}$  has not been lost from the samples.

Bender *et al.* (1979) showed that  $^{230}\text{Th}$  enrichment has taken place in corals older than 150ka. from Barbados, with  $^{230}\text{Th}$  possibly being released into groundwater from dissolving mollusc shells. This excess  $^{230}\text{Th}$  has then been scavenged by the coral, increasing the initial  $^{230}\text{Th}/^{234}\text{U}$  ratio as a consequence. The anomalous spread of ages obtained for the Cape Greco terrace (Fig.3.4; Table 3.3) could reflect the fact that this is a death assemblage, i.e. reworked, or actually represents two phases of terrace development (see Chapter 7 for details).

Weighted mean average ages of the Cyprus coral samples from each location, excluding those data that are believed to be unreliable, are shown in Table 3.5.

Table 3.5. Weighted mean Uranium series ages for Cyprus coral data.

| Location       | Terrace height<br>ASL (m) | Number of<br>samples | Age (ka.) |
|----------------|---------------------------|----------------------|-----------|
| Petounda Point | 8-11                      | 2                    | 204 ± 6   |
| Coral Bay      | 8-11                      | 3                    | 192 ± 6   |
| Larnaca        | 8-11                      | 4                    | 185 ± 2   |
| Cape Greco *   | 8-11                      | 1                    | 141 ± 4   |
| Cape Greco #   | 8-11                      | 2                    | 219 ± 16  |
| Paralimni      | < 3                       | 2                    | 134 ± 4   |
| Paphos         | < 3                       | 5                    | 130 ± 4   |
| Dhekelia       | < 3                       | 6                    | 116 ± 2   |

Note: # - younger coral from Cape Greco

\* - older corals from Cape Greco

weighted mean - composite results which reflect the relative accuracy of the results from each site.

### 3.3.2 Amino-acid racemization / epimerization.

#### 3.3.2.1 Introduction.

The amino-acid epimerization method employs the chemical reactions that occur during the degradation of proteins, which release abundant and variable amino-acids

(Abelson, 1955). The method investigates the amino-acid glycine, recording the ratio between the D- (dextro-) and L- (levo-) isomers (D-alloisoleucine and L-isoleucine). An isomer results from the epimerization of stereoisomers, one of two plus substances that have the same elementary composition but different structure, and hence different properties. During life the amino-acid takes the form of the L-isoleucine; death will result in epimerization and D-alloisoleucine will develop. The D/L (alle/Ile) ratio will increase after death, from 0.0 to  $1.3 \pm 0.05$  (Miller & Mangerud, 1985); a higher ratio signifying a greater relative elapsed time and hence an older sample. Two forms of amino-acids, bound and free, are found in fossil samples. The free amino-acids are released by natural diagenetic hydrolysis and are therefore absent in living samples. However, these rapidly become an important component after death of the sample, and comprise 30-60% of the total amino-acids over a period of 1-100ka. (Wehmiller, 1988). The bound amino-acid remains in the polypeptide form, changing little after death. The rates of epimerization of free amino-acids are not constant during the diagenetic history. Bound amino-acids also racemize at different rates depending on whether the amino-acid is terminal, i.e. at the end of the structure, or in an interior position. The rates are such that:

terminal > interior = free (Mitterer & Kriasuakul, 1984).

Taxa whose proteins hydrolyse rapidly produce a large number of terminal amino-acids, and therefore racemize more quickly (Wehmiller, 1988). This contrasts with bivalve taxa that contain a large proportion of aspartic acid which hydrolyses more slowly and therefore does not produce fast racemizing terminal amino-acids as quickly (Wehmiller, 1980; Muller, 1984). Reaction rates depend on:

- i) the permeability of the shells,
- ii) the original amino-acid composition,
- iii) the type of protein structure.

Thus, the reaction rates vary and are dependent on the bivalve genus and species that is being analysed (Lajoie *et al.*, 1980; Miller & Hare, 1980). The rate of breakdown of L- to D-isomers is also sensitive to temperature and pH variations. General reviews of the technique include Miller (1987) and Wehmiller (1988).

The amino-acid epimerization technique was used to study the ratio of amino-acids from molluscan shells during the course of this project. The amino-acid ratios obtained are proportional to the age of the samples allowing an amino-acid stratigraphy to be derived. An amino-acid stratigraphy divided into four aminozones has been established in the western and central Mediterranean (Hearty *et al.*, 1986; Hearty, 1987). Hearty *et al.* (1986) define an aminogroup as " representing a collection of equal-age

deposits that due to dissimilar thermal histories, yield alle/Ile ratios that vary relative to the long term regional thermal gradient" (Fig.3.6). Uranium series dating is used to calibrate the amino-acid data across climate boundaries. The relative aminostratigraphy is constrained using absolute dating techniques, e.g. the U-series (Harmon *et al.*, 1983; Hearty, 1987) and  $^{14}\text{C}$  methods (Schroeder & Bada, 1976).

### 3.3.2.2 Analytical methods.

Amino-acid epimerization analysis using high performance liquid chromatography (HPLC) was undertaken by Professor D.Q. Bowen and Dr. G. Sykes, in the laboratories of Royal Holloway and Bedford New College (RHBNC; see Bowen *et al.*, 1985 for details), and by Dr. P. Hearty in the laboratories of Duke University, North Carolina. The analytical methods used for amino-acid epimerization are described in Hare *et al.* (1985) and Engel & Hare (1985). The samples were collected from coastal sites throughout southern Cyprus (Fig.3.1). The samples used during the course of this study consisted solely of the genera *Arca*, *Callista* and *Glycymeris*. These genera were used because:

- i) they have a well defined shell structure (Plate 3.2),
- ii) occur frequently,
- iii) inter- and intra-deposition of the amino-acids is consistent, i.e. the deposition does not vary between shells and from each sampling site on any one shell (Hearty *et al.*, 1986),
- iv) there is no evidence for species variation in the epimerization rate (Hearty *et al.*, 1986),
- v) they have been sampled from the western and central Mediterranean previously, therefore the variation in rates of epimerization related to temperature and pH are known (Hearty *et al.*, 1986),
- vi) a relative amino-stratigraphy constrained by U-series dates has already been constructed for the western and central Mediterranean (Hearty *et al.*, 1986),
- vii) by correlating the results obtained here with the U-series dates (Section 3.3.1), the known contour map for *Glycymeris* alle/Ile ratio, for the last interglacial (5e sea-level maxima), of the western and central Mediterranean (Hearty *et al.*, 1986; Figs.3.6 and 3.7) can be extended into the eastern Mediterranean.

### 3.3.2.3 Results.

The data presented in Table 3.6 represents the peak height alle/Ile ratios of the total "free" fraction released by hydrolysis and peptide bound amino-acids, obtained from the samples run at RHBNC. Two or three samples were taken from each shell, the

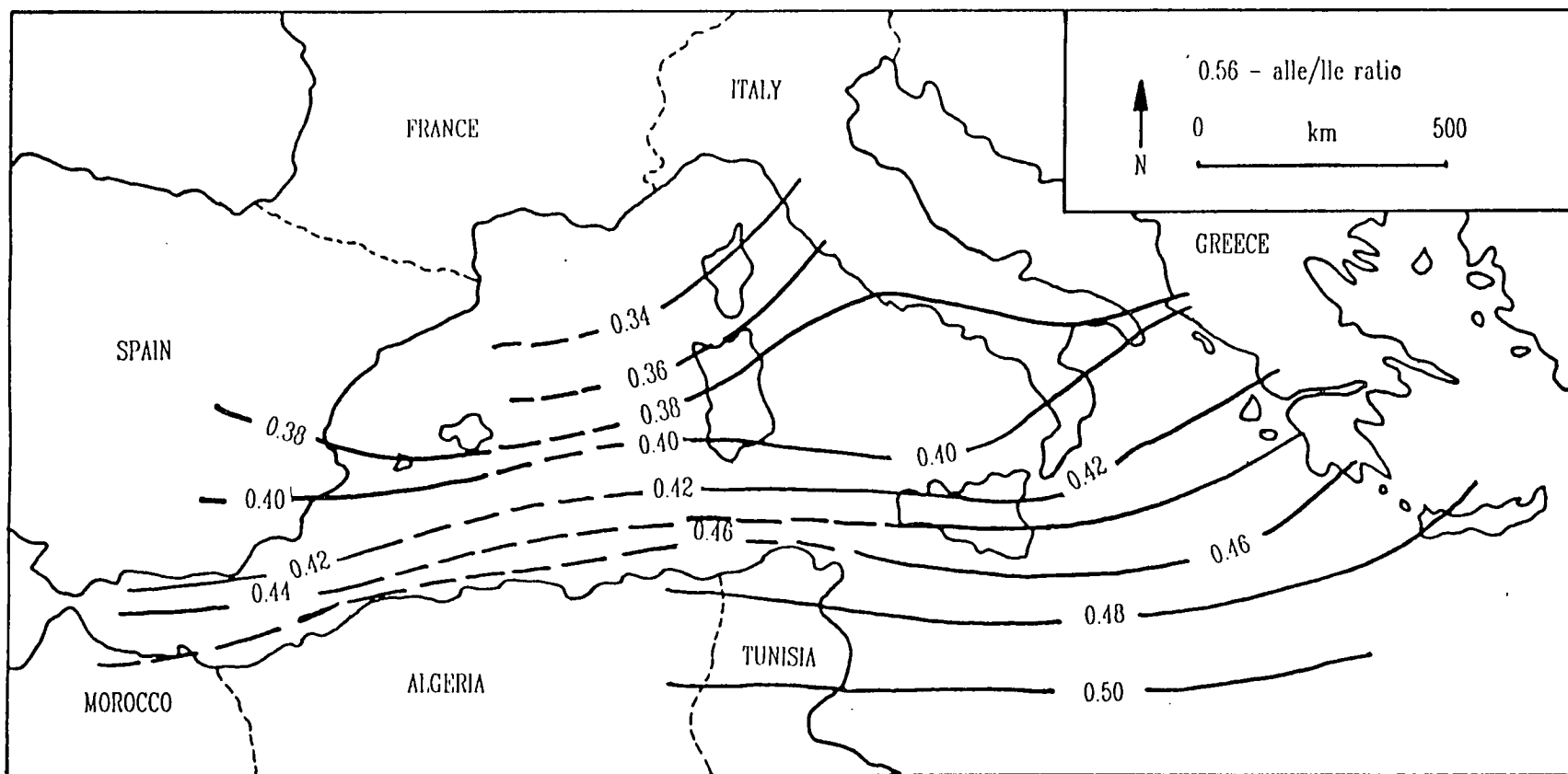


Fig. 3.6. Map of contoured *Glycymeris* alle/lle ratios from the last interglacial deposits of the western and central Mediterranean (after Harty *et al.*, 1986).

Table 3.6. Detailing the location, samples and results obtained with the amino-acid racemization technique.

| Sample                      | Location number              | Height m (ASL) | Species name                                                           | Amino-acid alle/Ile ratio  |
|-----------------------------|------------------------------|----------------|------------------------------------------------------------------------|----------------------------|
| a) LOND 496                 | 1-130 Lamaca                 | 8-11           | <i>Callista chione</i> <sup>+</sup>                                    | 0.521 ± 0.018 (3)          |
| b) LOND 497                 | 1-125 Cape Greco             | 8-11           | <i>Glycymeris bimaculata</i>                                           | 0.231 ± 0.050 (2)          |
| c) LOND 498                 | 1-125 Cape Greco             | 8-11           | <i>Arca noae</i>                                                       | 0.461 ± 0.074 (2)          |
| d) LOND 504                 | 1-125 Cape Greco             | 8-11           | <i>Arca noae</i> <sup>#</sup>                                          | 0.604 ± 0.097 <sup>#</sup> |
| e) LOND 499a                | 1-129 Ormidhia               | 8-11           | <i>G. bimaculata</i>                                                   | 0.544 ± 0.076 (3)          |
| f) LOND 499b                | 1-129 Ormidhia               | < 10           | <i>G. bimaculata</i>                                                   | 0.560 ± 0.170 (2)          |
| g) LOND 505a                | 1-129 Ormidhia               | < 10           | <i>G. bimaculata</i>                                                   | 0.324 ± 0.005 (2)          |
| h) LOND 505b                | 1-129 Ormidhia               | < 10           | <i>G. bimaculata</i>                                                   | 0.683 ± 0.029 (2)          |
| i) LOND 500                 | 1-166 Polis                  | < 10           | <i>G. bimaculata</i>                                                   | 0.390 ± 0.010 (2)          |
| j) LOND 506                 | 1-166 Polis                  | 10             | <i>G. bimaculata</i>                                                   | 0.301 ± 0.109 (3)          |
| Sp258<br>3/303/89<br>C72/89 | 1-166 Polis<br>3-97 Akrotiri | 10<br>< 3      | <i>G. glycymeris</i> <sup>*</sup><br><i>G. glycymeris</i> <sup>*</sup> |                            |
| C230/89                     | 2-5 Paphos                   | 50             | <i>G. glycymeris</i> <sup>*</sup>                                      |                            |
| C229/89                     | 2-3 Paphos                   | 110            | <i>G. glycymeris</i> <sup>*</sup>                                      |                            |
| sp196<br>sp156<br>C78/89    | 1-125 Cape Greco             | 8-11           | <i>G. glycymeris</i> <sup>*</sup>                                      |                            |

LOND - Analysis carried out by Prof. D.Q. Bowen and Dr. Sykes at Royal Holloway and New Bedford College, University of London.

Results are reported as - Mean value ± the standard deviation between the samples (number of samples).

\* - Presently being analysed by Dr. P. Hearty, Duke University, North Carolina, U.S.A.

+ - *Callista chione* has a similar rate of racemization to that of *Glycymeris*.

# - *Arca noae* has slower racemization rate, such that Gly/Arca = 1.31 (Hearty *et al.*, 1987), the ratio is a *Glycymeris* equivalent age.

resultant alle/Ile ratios for each shell were then averaged to give the ratios in Table 3.6, with standard deviation and number of samples per shell being quoted. The letters referred to in the text, correspond with the letters in left hand column of Table 3.6.

The terrace at Larnaca (location 1-130) has been successfully dated, using the U-series method (Section 3.3.1), as being equivalent to the oxygen isotope stage 7 (Shackleton, 1975), the penultimate sea-level high. The Polis terrace (location 1-166) at 10m ASL has been correlated with the Larnaca terrace (Chapter 2). The mean amino-acid results obtained from individual shells in the Larnaca and Polis terrace are 0.521 and 0.504 respectively; a lower mean ratio of 0.301 was also recorded from a shell in the Polis terrace (Table 3.6a, i and j).

The results from Larnaca (location 1-130; Table 3.6a) and the indexed *Arca* and *Glycymeris* values (see Table 3.6 for explanation) at Cape Greco (location 1-125; Table 3.6c and d) suggest an oxygen isotope stage 7 age, in line with the U-series age data collected from Larnaca. Two of the samples from Ormidhia (location 1-129; Table 3.6e and g) have a alle/Ile ratio greater than 0.500, correlatable with the aminogroups F and G, i.e. oxygen isotope stages 7-11 (Hearty *et al.*, 1986). Two other samples from Ormidhia (Table 3.6f and h) have alle/Ile ratios that imply a date younger than oxygen isotope substage 5e. Anomalously low ratios were recorded for one sample at Cape Greco (location 1-125; Table 3.6b), where U-series dates give average ages of  $141 \pm 4$ ka. and  $219 \pm 16$ , but the alle/Ile ratio implies a date younger than oxygen isotope substage 5a.

A limited data base makes any interpretation of the amino-acid data speculative, although the data is broadly correlatable with Hearty *et al.* (1986) and that obtained using the U-series method (Section 3.3.1).

The low alle/Ile ratios from Polis, Ormidhia and Cape Greco (Table 3.6b, f, h and i) appear to contradict the U-series, geomorphological and stratigraphic data. The samples collected from Polis and Ormidhia were taken from detrital sands and gravels in beach and deltaic environments (Chapter 6). These locations are susceptible to groundwater flow and therefore to leaching and contamination because of the high porosity and permeability of the lithologies. This leaching and contamination may have resulted in lower ratios than expected at these localities (P. Hearty, *pers. comm.*, 1990). The low ratio at Cape Greco indicates an age postdating the aminogroup C (Fig.3.7), which is not consistent with the U-series (Table 3.5), geomorphological, or stratigraphic data, suggesting that some alteration during diagenesis (Chapter 7) affected the resultant alle/Ile ratio.



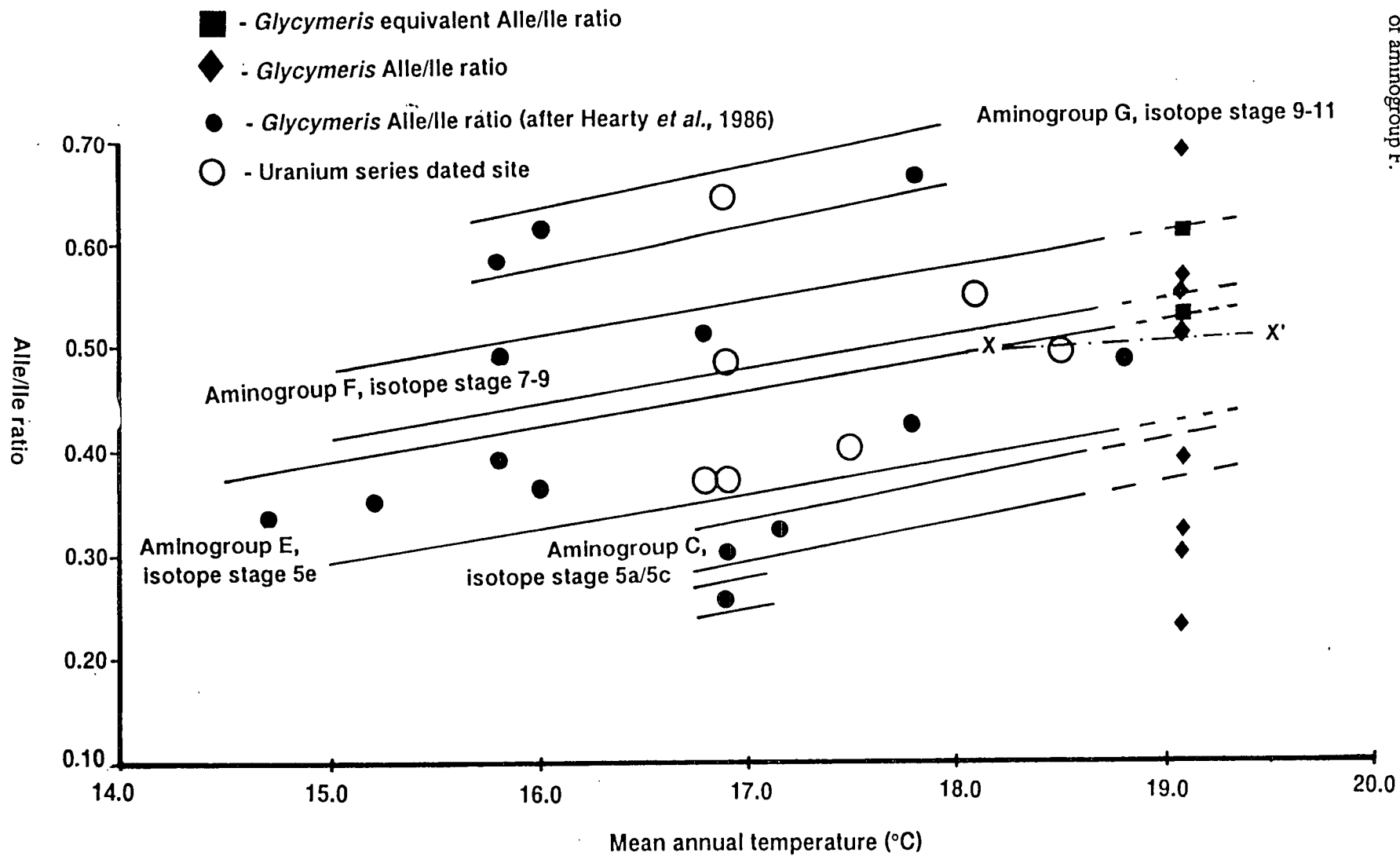


Fig. 3.7. A plot of *Glycymeris* alle/Ile ratios versus mean annual temperature for the whole of the Mediterranean (data from this study and Hearty *et al.*, 1986).  
 Note: line X-X' which is described in the text and represents a lower gradient for the base of aminogroup F.

If it is assumed that the thermal gradient, i.e. variation in temperature from area to area, across the Mediterranean basin today is similar to that seen during the Pleistocene and that the present day annual mean temperature for Cyprus is 19.1°C (for Nicosia during 1970; Boucher, 1975), then aminogroups of Hearty *et al.* (1986) can be extended to include the data collected from Cyprus during this study (Fig.3.7). The mollusc specimens from Cape Greco plot in aminogroup F, i.e. oxygen isotope stage 7 (Shackleton, 1975), whereas the data from Larnaca plot in an extension of aminogroup E (oxygen isotope substage 5e; Fig.3.7). This suggests that:

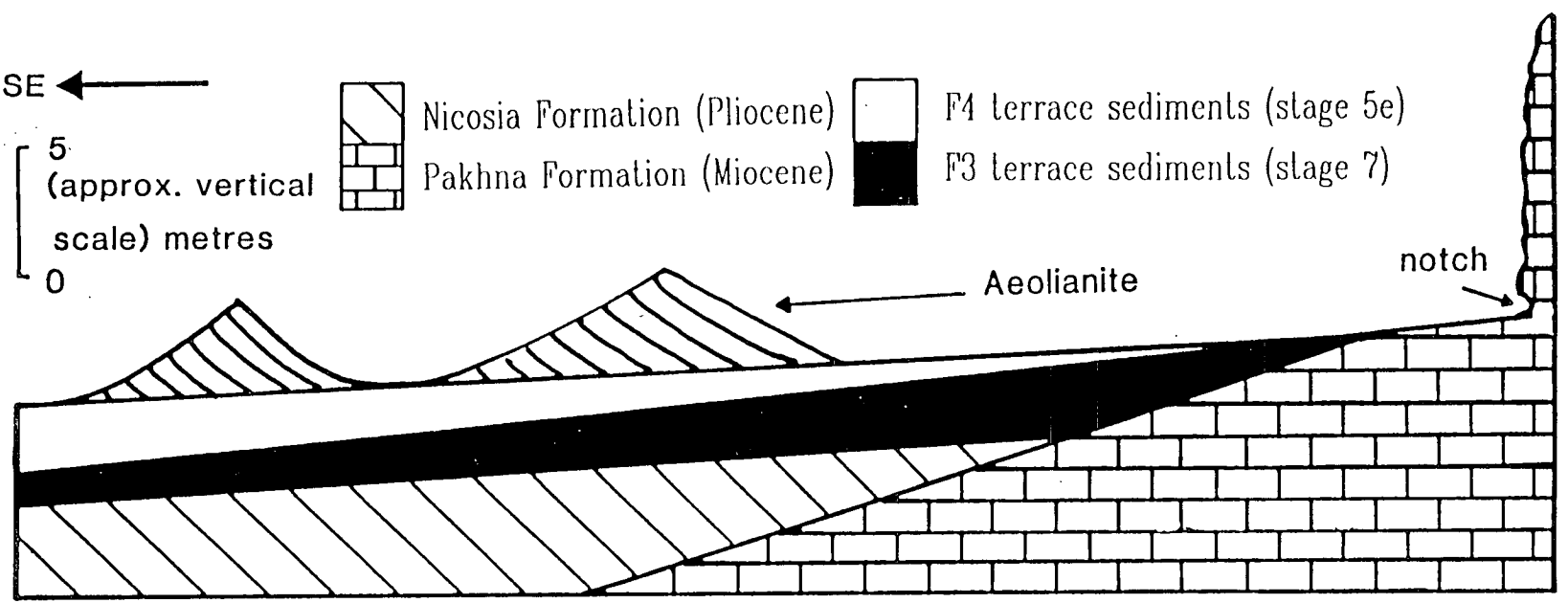
- i) the samples from Cape Greco confirm the ambiguities realised by the U-series data (Section 3.3.1) and imply that the samples were: a) either reworked from the F3 terrace sequences during the substage 5e sea-level high, i.e. F4, as suggested previously (Section 3.3.1), or b) that the Cape Greco terrace may actually represent development during F3 and F4 times, i.e. stage 7 and substage 5e (Chapter 7; Fig.3.8),
- ii a) as the Larnaca terrace, i.e. F3, has been successfully dated using the U-series technique as being equivalent to the oxygen isotope stage 7 sea-level high, then the average mean temperature at Nicosia cannot be used as this is too high, or b) a continuation of the baseline drawn to indicate the base of aminogroup F is too high (Fig.3.7), or c) that diagenetic and/or temperature effects have produced an erroneous result.

If it is assumed that the base of the aminogroup F is lower or the gradient less (indicated by line x-x' on Fig.3.7), which would satisfy U-series and stratigraphic data, then it can be concluded that the previously undated Ormidhia specimens (Table 3.6e and g) are of oxygen isotope stage 7 and older, and that the correlation of the Polis terrace (Chapter 2) with oxygen isotope stage 7, i.e. F3, and the Larnaca terrace is correct.

The difference in alle/Ile ratios between aminogroup E to F is minimal, so extremely well constrained amino-acid and modern annual mean temperature data is necessary if amino-acid ratios are to be used in an area that can not be constrained by U-series dates. Finally, there is a broad correlation between the results obtained during this study and those of Hearty *et al.* (1986) but more samples need to be analysed so that multiple technique analysis of a terrace is achieved, as was the case during this study with the corals and U-series dating. This is needed before high levels of confidence can be placed in the data obtained here, as the method is influenced by many variables. Analysis of a number of specimens of *Glycymeris* and *Arca* from the U-series dated terraces, i.e. Larnaca, Coral Bay, Petounda Point, Paralimni and Paphos, combined with other data (Hearty *et al.*, 1986; Hearty, 1987) would then allow Mediterranean-wide aminogroups to

Fig. 3.8. A sketch showing the relationship between the sedimentary units at Cape Greco.

Note: the unconformable contact between the Miocene and Pliocene successions, the Pliocene and F3 Quaternary sequences, and the F3 and F4 Quaternary units.



be distinguished, provided that the variation in mean annual temperature seen today reflects that seen during the Pleistocene.

### **3.3.3 Radiocarbon method.**

#### **3.3.3.1 Introduction.**

Carbon-14 is an unstable radioisotope which is produced in the upper atmosphere (Libby, 1952). The  $^{14}\text{C}$  mixes with oxygen to form  $\text{CO}_2$  that is in global equilibrium, as a result of mixing. The  $^{14}\text{C}$  is taken up by a subsystem, e.g. mollusc shells, either aragonite or calcite. When the subsystem is isolated, the uptake of  $^{14}\text{C}$  ceases, and radioactive decay and disintegration to nitrogen by  $\beta$ -transformation takes place and an elapsed time since isolation can be calculated. This simple model relies on the following basic assumptions:

- i) constant carbon production has taken place over the last 50-100ka.,
- ii) rapid and uniform mixing, uptake and exchange of the radiocarbon takes place in the global system, i.e. atmosphere, biosphere, hydrosphere,
- iii) the radiocarbon decay rate is constant,
- iv) total isolation of the subsystem takes place, so that "young" or "old" carbon cannot be added,
- v) no isotopic fractionation has occurred to change the standard  $^{14}\text{C}:^{13}\text{C}:^{12}\text{C}$  ratios.

A comparison with modern standards, a knowledge of the half life of the  $^{14}\text{C}$  ( $5730 \pm 40$  years; Godwin, 1962) and the assumption that the  $^{14}\text{C}$  production rate is constant over time, allows a sample to be dated. The  $^{14}\text{C}$  timescale has limitations due to probable variation in the cosmogenic nuclide production, as have been shown by comparisons between  $^{14}\text{C}$  and the U-series dating method (Bard *et al.*, 1990). Detailed reviews of the  $^{14}\text{C}$  method can be found in Bowen (1978) and Terasmae (1984).

The  $^{14}\text{C}$  method has been applied to archaeological samples from Cyprus (Peltenburg, 1982, 1985, Gomez, 1987; Todd, 1987) and more recently to the question of uplift of the island (Vita-Finzi, 1990; this work).

#### **3.3.3.2 Methodology.**

Mollusc shells from the gastropod *Astraea rugosa* and the bivalve *Glycymeris glycymeris* were sampled during this study. One sample from each shell was taken for analysis. The *Astraea rugosa* was collected from the lower marine terrace, i.e. F4, within 3m ASL, west of Kissonerga, on the coast north of Paphos (location 1-31a; Fig.3.1). The

sample of *Glycymeris glycymeris* came from Cape Greco, south-east Cyprus (location 1-125; Fig.3.1).

Table 3.7.  $^{14}\text{C}$  results obtained during previous studies on Cyprus (after Gomez, 1987 and Vita-Finzi, 1990).

| Location                        | Height<br>ASL (m) | Type of sample/<br>species             | $^{14}\text{C}$ age   |
|---------------------------------|-------------------|----------------------------------------|-----------------------|
| Vasilikos Valley <sup>#</sup>   | N.a.              | <i>In situ</i> fire pits               | 6,330 ± 100 BP        |
| Vasilikos Valley <sup>#</sup>   | N.a.              | Carbon fragments                       | 470 ± 80 BP           |
| Yeroskipos <sup>*</sup>         | 30                | <i>Astraea rugosa</i>                  | >43,900 BP            |
| Coral Bay <sup>*</sup>          | 10.6              | <i>Astraea rugosa</i>                  | 32,940 +740/-680 BP   |
| Kato Pyrgos <sup>*</sup>        | 12                | <i>Monodonta turbinata</i>             | 31,900 +710/-650 BP   |
| Ayia Marina <sup>*</sup>        | 13                | <i>Glycymeris violasecens</i>          | >44,240 BP            |
| Ayia Marina <sup>*</sup>        | 12                | <i>Glycymeris violasecens</i>          | 30,710 +400/-380 BP   |
| Baths of Aphrodite <sup>*</sup> | 7                 | <i>Glycymeris violasecens</i>          | 39,330 +1140/-1000 BP |
| West of Kissonerga <sup>*</sup> | 10                | <i>Glycymeris violasecens</i>          | 32,750 +620/-580 BP   |
| West of Kissonerga <sup>*</sup> | 3.6               | <i>Glycymeris sp.</i>                  | 30,270 +310/-300 BP   |
| West of Kissonerga <sup>*</sup> | 5.5               | <i>Spondylus sp.</i>                   | 31,110 +600/-560 BP   |
| West of Kissonerga <sup>*</sup> | 4.0               | <i>M. turbinata</i> + <i>A. rugosa</i> | 30,340 +580/-500 BP   |

Note: # = after Gomez (1987)  
\* = after Vita-Finzi (1990).

The method used here employed the scintillation facility in the laboratory of Professor C. Vita-Finzi, in the Department of Geological Sciences at University College London (UCL). The details of this method are outlined in Vita-Finzi (1983) and form part of Appendix C. The liquid scintillation method employs sealed vials and photomultipliers that detect light caused by scintillation of  $\beta$ -particles. The technique yields first order  $^{14}\text{C}$  dates. The upper limit on ages obtainable using this method, at UCL, is approximately 9.5ka. (Vita-Finzi, 1983).

### 3.3.3.3 Results.

The expected energy spectrum was obtained for both samples UCL118 and UCL120 but the resultant dates obtained from this method were non-finite, i.e. >9.5ka.. Other  $^{14}\text{C}$  dates that are relevant to this work (Table 3.7) have been obtained from ashes within the fluvial sequences in the Vasilikos Valley (Fig.3.1; Gomez, 1987); and from

mollusc samples collected from the lower marine terraces in the Paphos and Polis areas of western Cyprus (Vita-Finzi, 1990).

### **3.4 DISCUSSION AND CONCLUSIONS.**

#### **3.4.1 Discussion.**

The palaeontological data presented in Section 3.2 indicate that the broad Quaternary climatic changes, that is described from Israel (Issar, 1979) are also reflected in the molluscan fauna of Cyprus (Moshkovitz, 1968). The present study also identifies changes in the presence of coral between the latest Pliocene and Recent. The apparent presence or absence of corals during the Quaternary in Cyprus could indicate:

- i) that the highest marine terrace, i.e. the F1 terrace, was formed during sea-level low stand, in a cold glacial period, and that the appearance of red coralline algae rather than coral in this terrace resulted from a drop in water temperature, or a rise in the salinity and nutrient levels (Thunell & Williams, 1989), during these periods,
- ii) that the change in climate identified in other areas of the Mediterranean, e.g. Israel and Mallorca (Issar 1979; Butzer 1975) resulted in the introduction of a "cool water" molluscan fauna during the Calabro-Sicilian stage, followed by a "warm water" fauna during the Tyrrhenian stage. The F3 terrace at Larnaca, identified as Tyrrhenian Stage (Pantazis 1966; Moshkovitz 1968) on the presence of the gastropod *Strombus bubonius* actually corresponds to oxygen isotope stage 7 (Section 3.3.1) so agreeing with the proposal that the "warm" water Tyrrhenian fauna were present in the Mediterranean from c.200ka. to 120ka. (Butzer, 1975; Nilsson, 1983). The occurrence of the "cool water" molluscan fauna corresponds to the dominance of red coralline algae in the sedimentary sequences, as seen in the F1 terrace, while the colonies of *C. caespitosa* relate to warmer periods, e.g. the Upper Pliocene and Tyrrhenian.

The increase in salinity in the eastern Mediterranean during the last glacial period was in the order of 2‰ (Thunell & Williams, 1989) and is likely to have been similar to this during the previous glacial periods, i.e. a maximum of c.41.5‰. The increased salinity would have reduced the bottom-water oxygen concentration and then could have induced density stratification of the eastern Mediterranean. Circulation reversals and the stratification of the water is thought to have caused the eastern Mediterranean to become a nutrient trap during the last deglaciation at c.8ka. B.P. (Thunell & Williams, 1989). The nutrient levels remained apparently constant during the last glacial period, only changing during deglaciation. The <sup>CSF</sup> data presented by Thunell & Williams (1989) indicate that

nutrient levels are likely to have been similar during each of the Quaternary inter-glacial periods.

Three skeletal assemblages have been identified in modern shelf carbonate sediments between 60°N and 60°S (Lees & Buller, 1972; Lees, 1975):

- i) foramol ("temperate water"), where forams, molluscs and calcareous red algae are the dominant grain type,
- ii) chlorozoan ("warm water"), where hermatypic corals and/or calcareous green algae are also present,
- iii) chloralgal ("warm and high salinity"), where calcareous green algae are seen, but coral is absent because of excessive salinity (Fig.3.9)

The predicted skeletal distribution within the eastern Mediterranean today indicates a chloralgal to extended-chlorozoan skeletal population (Fig.3.10; Lees, 1975), which is capable of coping with maximum salinities of c.45‰ (Fig.3.9). Limited glacial salinity levels falling within the range of the chlorozoan and extended-chlorozoan group, suggest that temperature change was the dominant control on the occurrence of foramol and chlorozoan groups. Available evidence concerning the time of formation of the F1 and F2 terraces suggests regressive conditions, indicative of:

- i) a drop in sea-level,
- and/or ii) tectonic uplift,
- and/or iii) progradation of the shoreline sediments out into the marine environment (Chapter 7).

Molluscan faunal changes reflecting climate adjustments, throughout the eastern Mediterranean (Moshkovitz, 1968; Issar, 1979), the presence of coral in Pliocene sediments of the Mesaoria Plain (Gass, 1960; McCallum, 1989), but not in the F1 terraces in Cyprus and the fact that a temperature dependent foramol and chlorozoan relationship does exist, suggests that the coral/red algal relationship relates to changes in temperature in the Mediterranean Sea during the Quaternary. Teichert (1958) has also shown that hermatypic corals only exist in "warm water" but *C. caespitosa* colonies flourish in the cool winter waters, i.e. down to 10°C, of Adriatic Sea at present (Zibrowius, 1980). Thus, the present evidence suggests that Quaternary coral and calcareous red algal populations in Cyprus may reflect climatic changes that were previously only recorded in molluscan populations. Overall, "cooler waters" existed in the lower-middle Pleistocene with warmer conditions in the latest Pliocene and middle-late Pleistocene.

Absolute age data, to corroborate the above arguments, has not been obtained from the corals in the F2 terrace in the Paphos area.

**Fig.3.9. S.T.A.R. (Salinity Temperature Annual Ranges) diagram pair for skeletal grain associations in modern shelf carbonate sediments (after Lees, 1975).**

Note: the dotted lines indicate the approximate limits of near-surface salinity/temperature combinations existing in the modern shelf seas and lagoons.

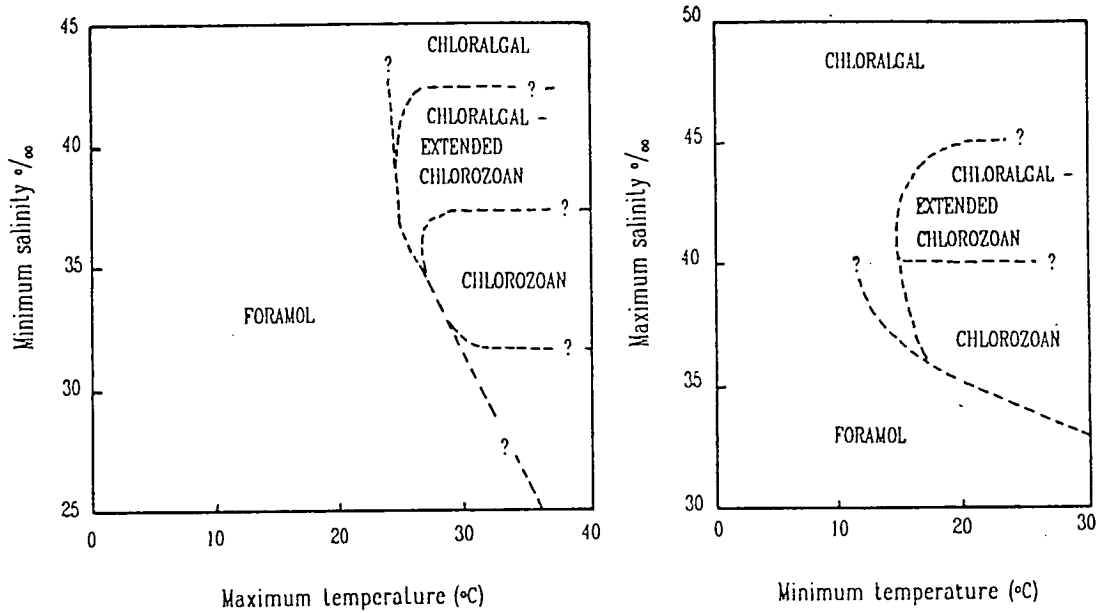
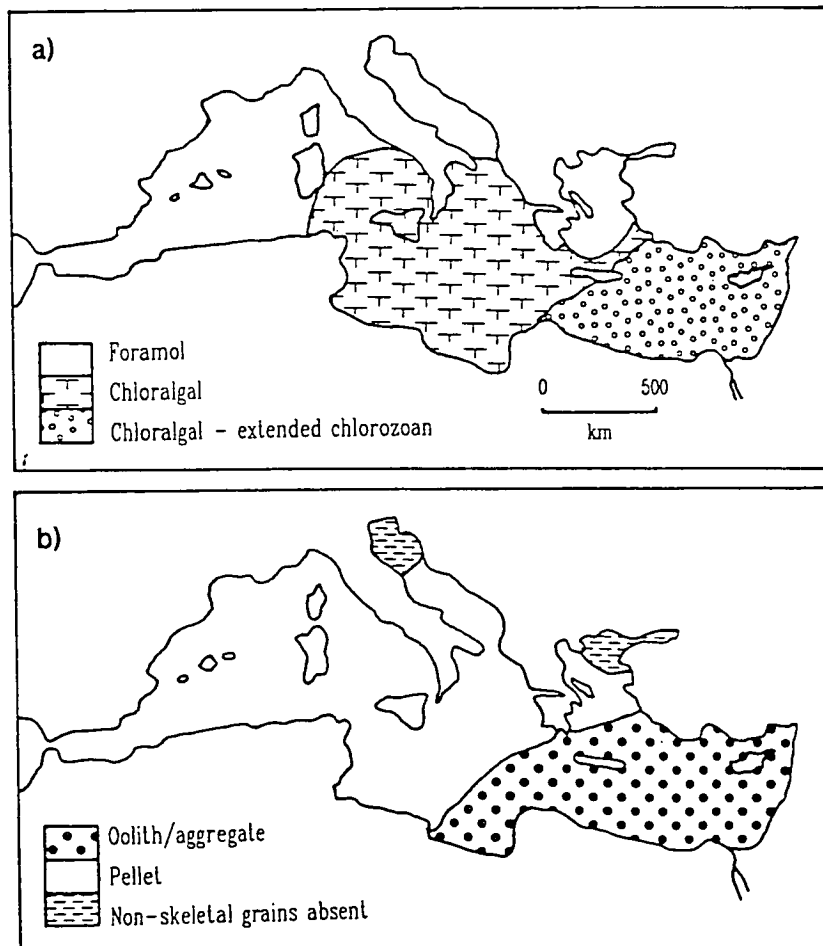


**Fig.3.10. Predicted potential distribution of (a) skeletal and (b) non-skeletal grain associations in the Mediterranean Sea (after Lees, 1975).**





The micropalaeontological evidence from the marl sequences cropping out beneath the F3 terrace, e.g. Cape Greco and Coral Bay, and in the Polis-Paphos graben (location 3-150) indicate a Pliocene age. The marls formed in water depths of c.100-200m (based on sedimentological features, A.H.F. Robertson, *pers. comm.*, 1989; and ostracod data, after A. Lord) and are found within 20-30m ASL, e.g. in the Polis-Paphos graben. This indicates that 130-230m of relative uplift has taken place along the coast since the Pliocene. Micropalaeontological data (Houghton *et al.*, 1990) also indicate that at least some of the Quaternary fluvial channels along the south coast of Cyprus were active as submarine channels in the Pliocene, e.g. the Maroni River (Fig.2.6).

The mammal fauna found in cave and fluvial sediments in southern Cyprus do show a progressive dwarfism through the later part of the Pleistocene. It should be possible, if more samples are collected, to date some of the elephant and hippopotamus teeth and bone using the amino-acid epimerization and  $^{14}\text{C}$  techniques (Simmons, 1988; Belluomini & Bada, 1985), and so allow the fluvial and cave sequences to be dated.

The relative biostratigraphy available from Cyprus gives some indication of the environmental changes that took place during the Quaternary which can be used for broad correlation purposes. In an area where active neotectonic faulting has been occurring throughout the Quaternary (Chapter 4) absolute dating is necessary to correlate different areas of Cyprus. Absolute dates allow geomorphological correlations, determined in Chapter 2, to be confirmed. This work provides the first detailed study of islandwide Quaternary correlations, and the first major use of Quaternary dating methods, outwith those used for archaeological purposes.

The necessity for absolute dates, and redefinition of much of the Mediterranean marine stratigraphy (Section 1.8) arises from the assumption that Quaternary terraces of similar age crop out at the same height, throughout the Mediterranean basin (Zeuner, 1959; Table 3.1). The correlation based on altimetry and then supported by faunal evidence, e.g. the use of the Tyrrhenian "Senegalesse" fauna which ranges over a time greater than one inter-glacial period (Butzer, 1975; Nilsson, 1983), has resulted in a confused stratigraphy. It has been shown that the "Senegalesse" fauna and the oxygen isotope stage 7 "Tyrrhenian" terrace, in Cyprus (Section 3.3.1), and in other areas of the Mediterranean basin (Bonifay & Mars, 1959), crops out 10-12m ASL and is not restricted to 28-32m ASL, contrary to the previous data from Cyprus (Pantazis, 1966; Table 3.1). The Mediterranean shorelines studied by Hey (1978) have been displaced vertically making nonsense of the altimetric correlations of Zeuner (1959), whilst the work of Flemming (1978; Fig.3.11) and Pirazzoli *et al.* (1991), from different Mediterranean

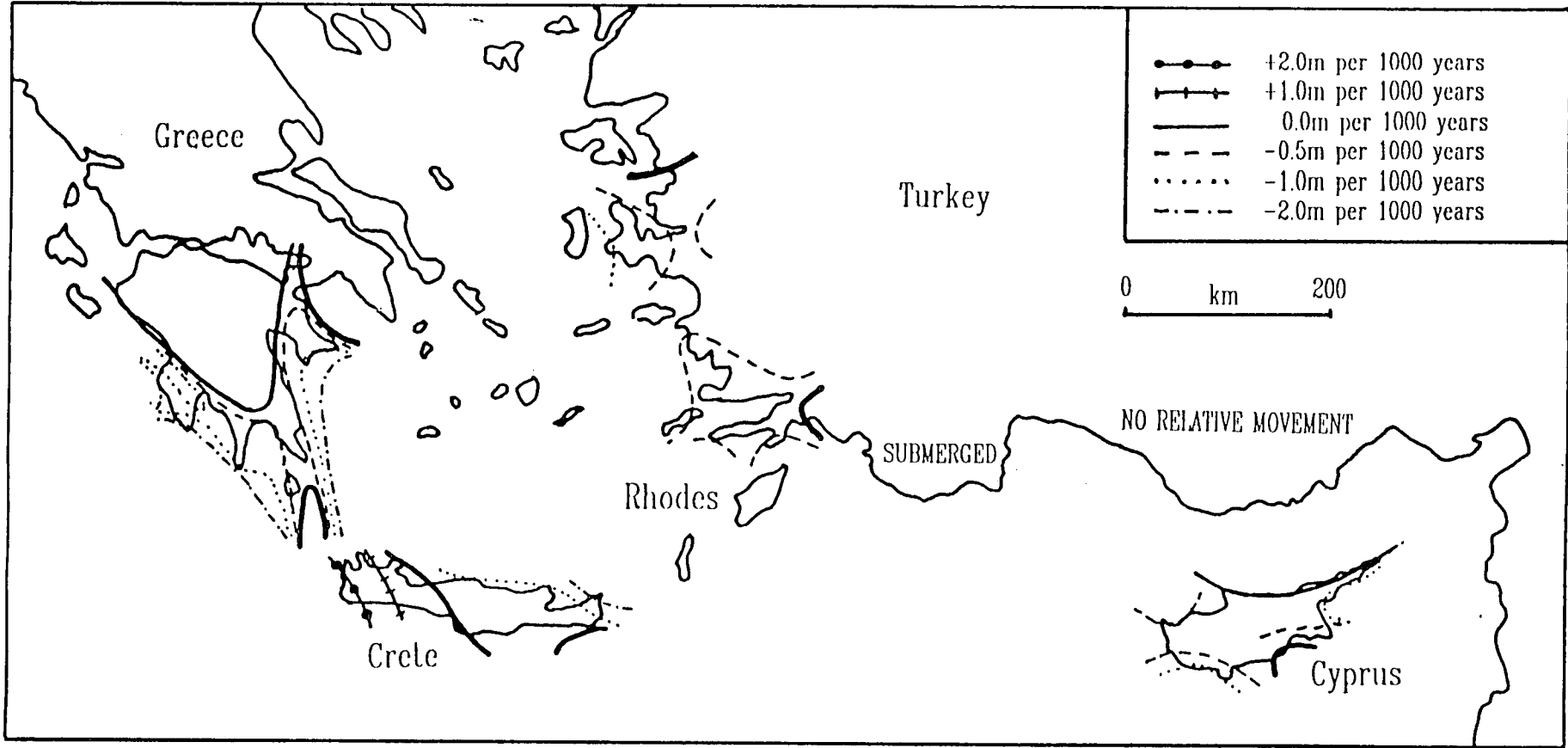


Fig.3.11. Synthesis of regional contours of rate of vertical displacement in metres per millennium relative to present sea-level (after Flemming, 1978).

regions, supports the argument for terraces at a similar elevation forming at different times.

Confirmation of the geomorphological correlations of the coastal terraces throughout southern Cyprus, i.e. F1-F4, based on altimetry, was made using the Quaternary dating methods. Interpretations concerning sea-level changes and rates of change of uplift can also be made.

Any interpretation involving tectonic uplift of Cyprus must take Quaternary eustatic sea-level changes into account. Thus, the U-series age data can be considered in the light of the known chronostratigraphic ages of Quaternary global oxygen isotope stages (Shackleton, 1987; Shackleton & Opdyke, 1973, 1976, Chappell & Shackleton, 1986). On this basis, the 185-219ka. age of the marine terraces suggests a correlation with global oxygen isotope stage 7 and this, in turn, supports the view that no more than 18m of uplift has taken place since this time, assuming that the corals formed at water depths of 10m (based on geomorphological and sedimentological evidence; Chapters 2 and 7). Similarly, the lower marine terrace, less than 3m ASL, can be correlated with the sea-level maximum recorded by oxygen isotope substage 5e, 5-8m higher than the present day maximum (Stearns & Thurber, 1965; Broecker *et al.*, 1968; Mesolella *et al.*, 1969; Bloom *et al.*, 1974; Chappell, 1974; Ku *et al.*, 1974; Stearns, 1976). If correct, the marine terraces less than 3m ASL have undergone little or no uplift, and may even have subsided, in agreement with field observations, Moshkovitz (1968) and Flemming (1978), but contrary to the views of Giangrande *et al.* (1987) and Vita-Finzi (1990; Table 3.7). Giangrande *et al.* (1987) suggested that local differential neotectonic uplift and tilting has taken place in south-west Cyprus during the late Quaternary. However, terraces correlated by these authors, i.e. at Coral Bay and Kato Paphos, have proved to be of different ages in this study (Table 3.5). The U-series isotopic age data show that terraces at similar heights over widely spaced areas of coastal Cyprus (less than 11m and less than 3m ASL) are of similar age (219-185ka. and 141-116ka.). The presence of the F3 terrace 8-11m ASL, compared to 28-32m ASL in other areas of the Mediterranean (Zeuner, 1959) supports the argument for relative stability since c.200ka., in line with the views of Bonifay & Mars (1959), for stage 7 terraces throughout the Mediterranean basin. The apparent absence of a substage 5a (c.75-90ka.; Stearns & Thurber, 1965; Lalou *et al.*, 1971) terrace in Cyprus, which is indicative of a slightly lower sea-level than the substage 5e terrace, e.g. Cerveteri, Italy (Bonadonna & Bigazzi, 1970; Ambrosetti *et al.*, 1972; Hearty *et al.*, 1986), also supports the argument for the relative stability, limited tectonic uplift and local subsidence (Fig.3.11) of Cyprus in the Late Pleistocene and Holocene. Recent amino-acid and U-series data have indicated that two substage 5e sea-level highs may have occurred (Kaufman, 1986; Hearty, 1986; Hollin & Hearty,

1990), although the data here do not necessarily support this argument. More amino-acid analyses and more precise U-series data using isotope dilution mass spectrometry techniques (Edwards *et al.*, 1986-87) may elucidate such subtle changes in sea-level. Split terraces are seen associated with the F1 marine sequences in the Paphos area (location 2-2). These terraces do not appear to be fault controlled and may represent a lower-middle Pleistocene twin sea-level high, preserved as a result of uplift of the island during this period.

Average rates of uplift can be inferred, assuming that the coral colonies developed at depth of 10m below sea level (see Chapter 7 for details). A maximum of 6m of uplift would then have occurred over the past 116ka., assuming that the sea-level maxima during substage 5e was 5-8m higher than the present-day sea-level (Mesolella *et al.*, 1969; Bloom *et al.*, 1974; Chappell, 1974; Stearns, 1976). This would give an average rate of uplift of c.5cm/ka. It should be noted that partial submergence may have taken place during this period (see above). A maximum of 13m of uplift took place between 141ka. and 185ka., at an average rate of c.29cm/ka. The U-series data implies that there is a reduction in rates of uplift over the last 219ka.

### **3.4.2 Conclusions.**

The following conclusions can be drawn from this Chapter:

- i) U-series disequilibrium dates from *C. caespitosa* corals from raised marine terraces in southern Cyprus confirm that the F3 terraces (8-11m ASL), correlated by means of geomorphology, are of similar age, 219-185ka.; as are the F4 terraces (< 3m ASL) from different parts of the island, 141-116ka.,
- ii) the older terraces (8-11m ASL) record maximum uplift at average rates of c.29cm/ka. between 141-185ka. The younger terraces (< 3m ASL) indicate average uplift rates of c.5cm/ka. for 116ka., with the exception of Cape Greco, which suggests a rate of c.12cm/ka.,
- iii) correlation with the Quaternary global isotopic stages confirms that maximum uplift has been limited to 18m during the past 185-219ka., and also suggests that relative subsidence has taken place in some coastal areas over the past 116ka.,
- iv) Quaternary eustatic sea-level changes, rather than tectonic uplift, have controlled the deposition of the exposed littoral sequences during the Late Pleistocene,
- v) broad Quaternary climatic variations indicated by the changes in the Mediterranean molluscan population have also contributed to the presence, or absence of corals in the Quaternary carbonate sequences,
- vi) nannofossil evidence from the Pliocene marl sequence indicates that a minimum of 130m of relative uplift has taken place in coastal areas since this time,

- vii) the amino-acid, U-series,  $^{14}\text{C}$  and faunal evidence are consistent with each other and the geomorphological correlations,
- viii) block uplift of the island has apparently taken place during the Quaternary, with evidence for more recent subsidence (Flemming, 1978; this study). The rate of uplift has varied preventing accurate altimetric correlations between Cyprus and other areas of the Mediterranean, in line with the views of Hey (1978).

## **Chapter Four: Neotectonics.**

### **4.1 INTRODUCTION.**

This chapter will review the existing published data for Quaternary neotectonic activity in Cyprus. Original data obtained during this study will be presented, with the aim of assessing the relationship between the nature of Plio-Quaternary and Quaternary tectonic activity on Cyprus. Data will also be collated to establish whether there is a broad agreement between fault, joint and other kinematic indicators, similar to that recorded in both compressive and extensional regimes elsewhere, e.g. the Qaraden segment of the Arabian graben and trough system (Hancock & Al Kadhi, 1982) and in the Jaca thrust-sheet top basin of the Spanish Pyrenees (Turner & Hancock, 1990).

The neotectonic extensional grabens and basins of southern Cyprus, e.g. Pissouri basin (Fig.4.1), were active until the Late Pliocene-Quaternary (Dupoux 1983; Elion 1983; Table 4.1). The Polis-Paphos graben, in south-west Cyprus, proves to be an exception to the general pattern, as neotectonic faulting continued into the Quaternary (Ward & Robertson, 1987), and now forms the basis of a separate study by Ann Payne at Edinburgh University. The neotectonic basins and grabens are thought to have been initiated in the Miocene as a result of crustal extension related to an active margin, the Cyprus Arc (Robertson *et al.*, 1991). Active Quaternary neotectonic faulting outwith the confines of the extensional basins is limited (Pantazis, 1966; Kluyver, 1969; Gomez, 1987; Giangrande *et al.*, 1987). The tectonic activity in Cyprus today is less intense than active neotectonics seen in the Aegean region, or other areas of the eastern Mediterranean (Peters *et al.*, 1985; Flemming, 1978; Flemming & Woodworth, 1983).

### **4.2. SEISMIC STUDIES.**

Seismic studies of offshore southern Cyprus show evidence for extensive faulting and folding until the Pliocene, related to underthrusting and correlatable with known WNW-ESE lineaments in southern Cyprus (McCallum, 1989; McCallum *et al.*, 1992). Cessation of major deformation in the Plio-Pleistocene is suggested to have been as a consequence of roll-back of the Cyprus trench, during this time, to a position approximately 30km further south (Stride *et al.*, 1977; Riad *et al.*, 1981; McCallum, 1989; McCallum *et al.*, 1992). Reverse faulting is reported off south-west and southern Cyprus, the trend being parallel to the coast (Catani *et al.*, 1983). Seismic data show that the Pleistocene sediments on the southern Cyprus shelf and slope form a discontinuous series of undeformed, uniformly bedded sediments draped over the underlying deformed pre-Pleistocene sedimentary sequence (Fig.4.2). This evidence agrees with seismic data

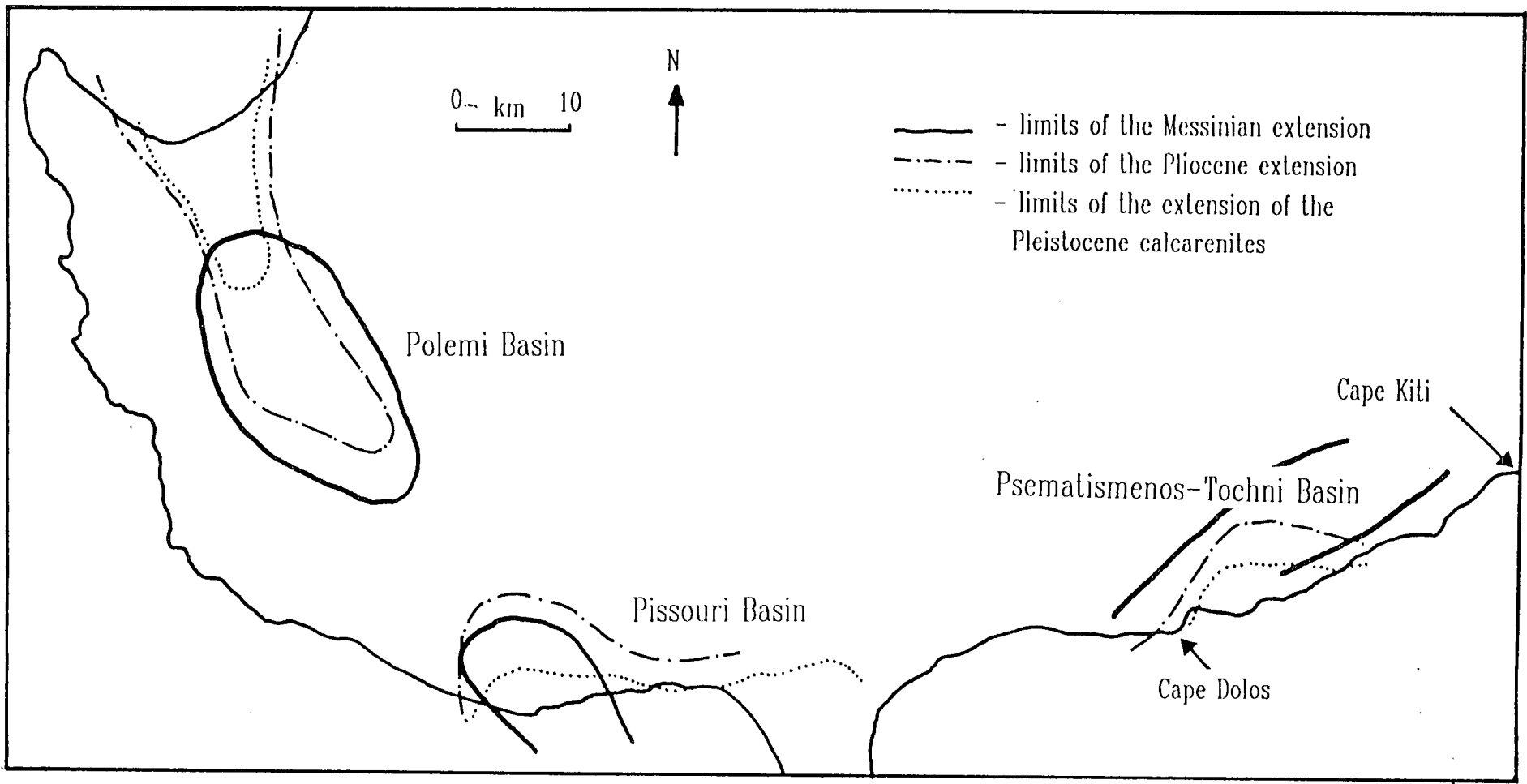


Fig.4.1. The location of the neotectonic grabens and basins of southern Cyprus (after Eilon, 1983).

Table 4.1. Details concerning the extent, timing and nature of Neogene and Quaternary faulting in the grabens and basins of southern Cyprus (after authors recorded at the top of each column).

|                                      | Polis-Paphos graben<br>western Cyprus<br>(Ward & Robertson, 1987)                               | Pissouri Basin<br>southern Cyprus<br>(Elion, 1983)                     | Polemi Basin<br>western Cyprus<br>(Dupoux, 1983)                                                                | Psematismenos-Tochni<br>Basin southern Cyprus<br>(Dupoux, 1983)                                 |
|--------------------------------------|-------------------------------------------------------------------------------------------------|------------------------------------------------------------------------|-----------------------------------------------------------------------------------------------------------------|-------------------------------------------------------------------------------------------------|
| Type and direction<br>of deformation | Extension<br>NNW-SSE                                                                            | Extension<br>WNW-ESE                                                   | Extension<br>NNE-SSW                                                                                            | Extension<br>NNW-SSE                                                                            |
| Other fault sets                     | Transverse faults<br>NW-SE, orthogonal<br>to graben trend                                       | Messinian extension<br>is E-W<br>Middle Pliocene<br>extension is NE-SW | Secondary faults<br>extension WNW-ESE<br>Messinian extension<br>is E-W<br>Middle Pliocene<br>extension is NE-SW | Messinian extension is<br>NW-SE and NNW-SSE<br>Middle Pliocene-<br>Recent extension<br>is NE-SW |
| Time of fault<br>movement            | Upper Miocene<br>(Messinian)-Recent<br><br>Reactivated Lower<br>Cretaceous-Tertiary<br>basement | Messinian-Recent                                                       | Messinian-<br>Quaternary                                                                                        | Messinian-Recent                                                                                |
| Notes                                | Asymmetrical faults                                                                             | Numerous faults<br>during Calabrian<br>extension                       | Normal sub-vertical<br>faults                                                                                   |                                                                                                 |

Note: see Fig.4.1. for the location of the various basins and grabens.



collected from the slope and shelf areas off south and south-east Cyprus that reflect well stratified sedimentary sequences (Catani *et al.*, 1983).

#### **4.3 EARTHQUAKE DATA AND BOREHOLE STRESS STUDIES.**

Small earthquakes, with both onshore and offshore epicentres, occur at regular intervals in the Cyprus region. The earthquakes generally have a magnitude of 2-4.5 on the Richter scale. There were between 326 and 390 earthquakes per annum in the period 1984 to 1986 (Constantiou 1985, 1986, 1987). Larger, deeper earthquakes also occur, with notable examples in 370 A.D., 1189 A.D. and 1953 A.D. (Soren & Lane, 1981). Fault plane solutions from earthquakes off the southern coast of Cyprus indicate compression orientated WNW-ESE (Rotstein & Kafka, 1982). The Cyprus Arc has less associated seismicity than the Hellenic Arc to the west (Stride *et al.*, 1977).

Stress studies and fracture logging of the deep borehole CY-4 situated on the Troodos ophiolite south of the village of Palaekhori, in the dyke complex to the east of Mount Olympus (Haimson *et al.*, 1990) indicate that the maximum ( $S_H$ ) and minimum ( $S_h$ ) horizontal stress directions are  $N70^\circ E \pm 10^\circ$  and  $N20^\circ W \pm 15^\circ$  respectively, in agreement with Rotstein & Kafka (1982). The vertical stress value  $S_v \cong S_H > S_h$  indicates normal and/or strike-slip conditions. There is no evidence of subduction related compression. Breakouts and hydrofracturing were predominantly vertical, strike-slip left lateral. The stress regime is compatible with extension across and normal to an inclined ENE plane, left lateral strike-slip motion is approximately E-W, in line with movement along the Anatolian Fault. The joints trend towards the NE and the principal extension regime is NNW-SSE (Haimson *et al.*, 1990; Fig.4.3).

#### **4.4 FIELD EVIDENCE FOR QUATERNARY FAULTING IN SOUTHERN CYPRUS.**

Active faulting has continued from the Pliocene into the Quaternary in the Neogene basins of southern Cyprus (e.g. Dupoux, 1983; Elion, 1983). Minimal evidence for Quaternary faulting has been identified outwith these basins (Pantazis, 1966; Kluyver, 1969; Gomez, 1987; Giangrande *et al.*, 1987 and this study). Terraces that crop out at different heights in south-west Cyprus have previously been interpreted as having been faulted (Kluyver, 1969; Giangrande *et al.*, 1987), but these have been misinterpreted as the terraces are not of the same age, having formed a different times (Chapters 3 and 7). The only certain piece of evidence for active faulting, outwith the extensional basins, during the Quaternary period, prior to this study, is found in the Vasilikos Valley (Gomez, 1987).

Fig.4.2. Sketch sections of the two seismic lines shot off the southern coast Cyprus between Cape Kiti and Cape Dolos (after McCallum, 1989; McCallum *et al.*, 1992).

Note: location of the capes are shown on Fig.4.1).  
 Correlation of units: A - Lefkara and Pahkna Formation; B - Raised beach deposits; C - Nicosia Formation; D - Recent sediments.

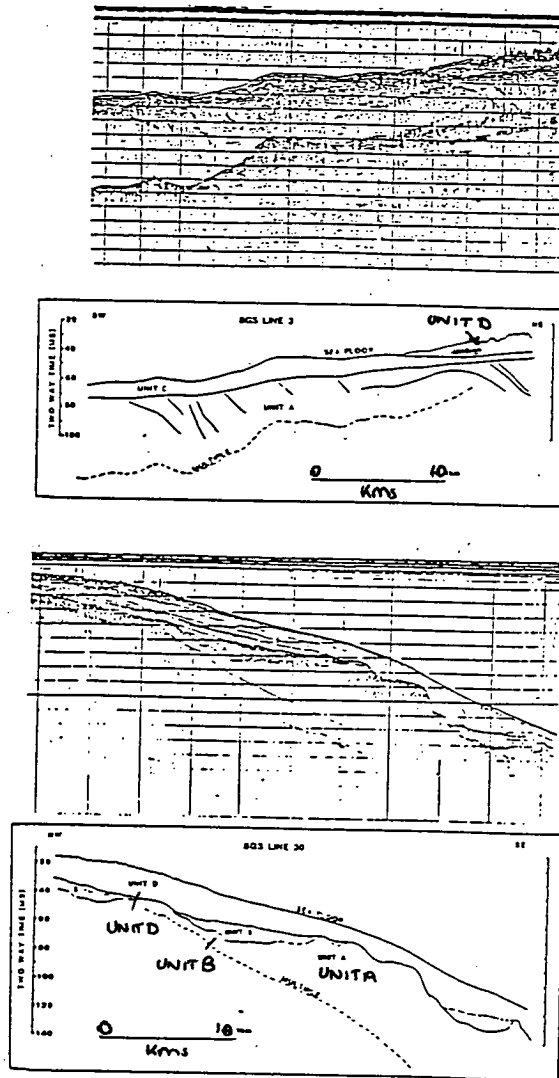
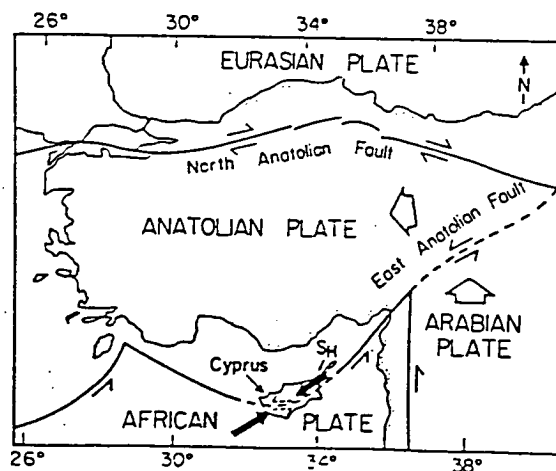


Fig.4.3. Sketch of Cyprus showing the determined  $S_H$  direction and sense of shear predicted (after Haimson *et al.*, 1990).



Two forms of data were collected and examined during this study:

- i) fault data from exposed faulted Quaternary sequences throughout southern Cyprus,
- ii) joint and meso-and micro-scale fractures associated with joints.

The following definitions are used here:

- i) a joint is "a fracture that traverses an outcrop and is not accompanied by any discernible displacement of one face of the fracture relative to the other" (after Hodgson, 1961),
- ii) a fracture is a break in a rock that may or may not have associated displacement (Bates & Jackson, 1980),
- iii) a mesofault has a displacement of between 1mm and 5m and a fault plane area of less than 1000m<sup>2</sup>.

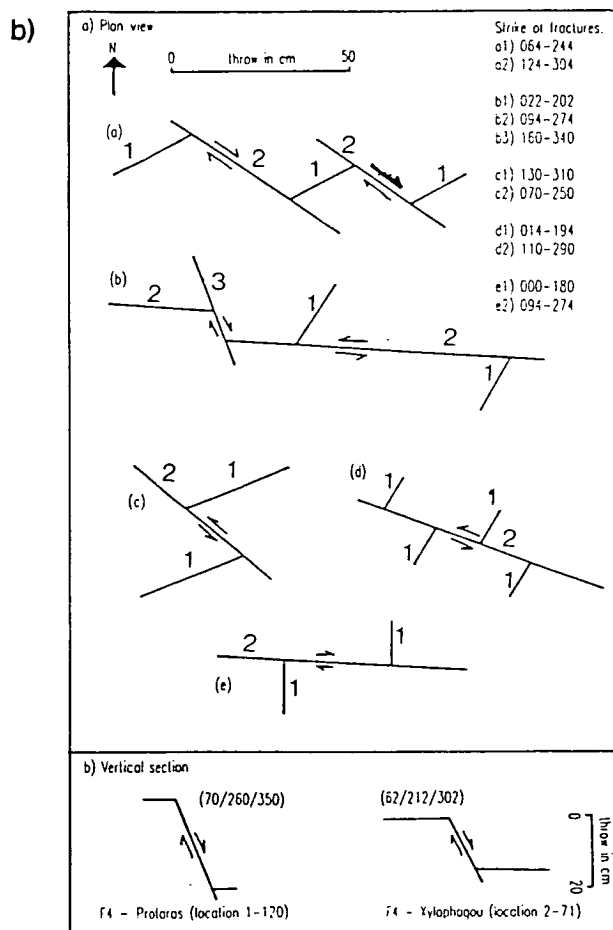
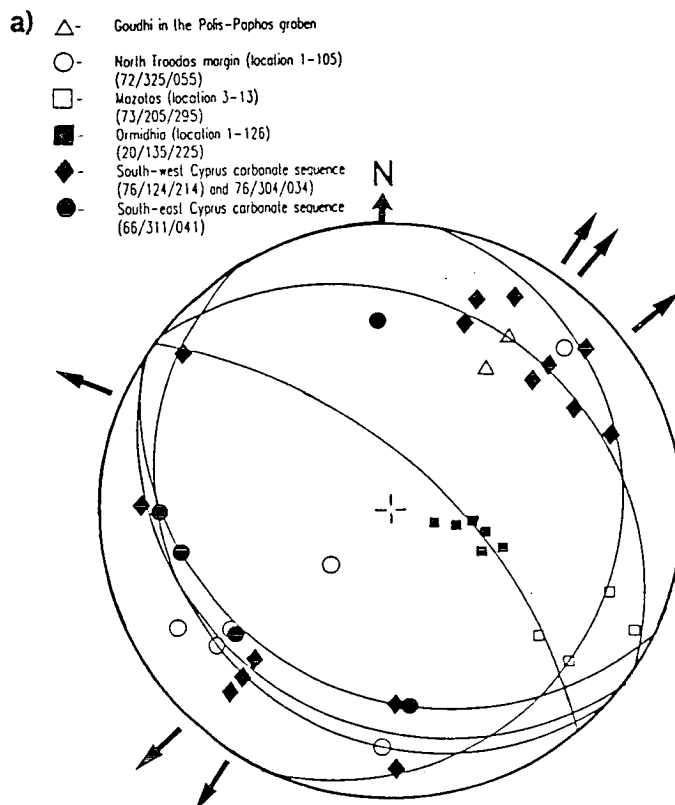
Joint related data was collected from lithified Quaternary and pre-Quaternary terraces in south-west and south-east Cyprus. No evidence of folding was recorded during the course of this study.

The number of faults present in the Quaternary sequences is limited, but examples of normal faults were recorded in the F2 Fanglomerate unit in the western part of the Mesaoria Plain (location 1-105), the F2 deltaic and Fanglomerate units in the Larnaca area (location 3-13; Plates 4.1 and 4.3), the F1, F2 and F4 carbonate sequences in the Paphos area (location 3-31; Plate 4.2) and cutting the F1 Fanglomerate unit sequences in the Polis-Paphos graben near Nata (Plate 4.2) and Goudhi (Plate 5.12). All the faults seen, with one exception in the Miocene chalks at Ayios Yeoryios (location 2-27) were normal, with a high angle of dip and throw varying between 10cm and 4-5m (location 1-126 and 3-13 respectively; Plates 4.1, 4.2 and 4.3). Both sinistral and dextral fault movement was noted.

Field data indicates that fault movement has occurred throughout the Quaternary but that this has not been extensive, although preservation of fault structures in unconsolidated sediments can be poor. Much of the fault movement was undoubtedly caused by regional tectonics and does not reflect local dewatering and overpressuring structures, the plotted data indicating a high degree of uniformity of dip and strike (Fig.4.4a), the strike varies from the WNW to NNW and ESE to SSE. Some evidence of overpressuring and dewatering of sediment was noted at Akrotiri (location 3-96a), where a series of erosion surfaces and associated steeply dipping foresets, related to intra-Pliocene submarine movements, are seen. The structures become more densely packed directly beneath the erosion surfaces. There is no evidence of grain disruption, indicative of faulting. Two sets of near vertical structures are seen, a poorly cemented E-W set and a

**Fig.4.4. a) Lower hemisphere stereographic projection of poles to planes, with average great circles, indicating the dip, strike and trend of the Quaternary fault planes from southern Cyprus; b) sketches showing the cross cutting relationship and therefore relative ages of fractures cutting Quaternary and Neogene sediments of southern Cyprus.**

Note: dip/strike/trend references.



- (a) Paphos coast - F4
- (b) Paphos coast - F4
- (c) Ayios Yeoryios (location 2-21) - pre-Quaternary chalk
- (d) Xylophagou (location 2-71) - F4
- (e) Xylophagou (location 2-71) - F4

PLATE 4.1.

A - Normal faults cutting the deltaic and Fanglomerate Group sequences in southern Cyprus to the west of Larnaca (location 3-13).

Note: 50cm scale to the right of centre of photograph which is taken looking north-east.

B - Normal faults cutting the deltaic sequences but not the overlying Fanglomerate Group sequences (location 3-13). The faults dip at  $70^{\circ}$  and strike at  $200^{\circ}$ .

C - Normal faults with throws in the order of 2-3m cutting both the deltaic and the Fanglomerate Group sediments (location 3-13). The fault dips at  $80^{\circ}$  and strikes  $220^{\circ}$ .

# Plate 4.1

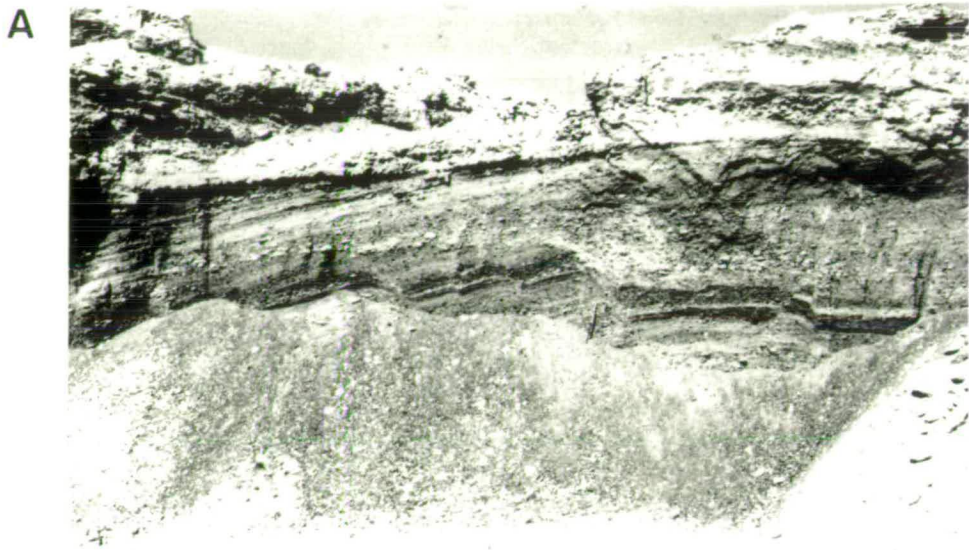


**PLATE 4.2.**

A - Vertical normal fault cutting the F4 marine terrace to the south of Lara (location 2-31). The fault has a throw of c.50cm and strikes north-west to south-east.

Note: the 25cm scale to the left of the fault.

B - A series of normal faults cutting the Fanglomerate Group and younger sediments near the village of Nata at the southern end of the Polis-Paphos graben.

# Plate 4.2

A



B

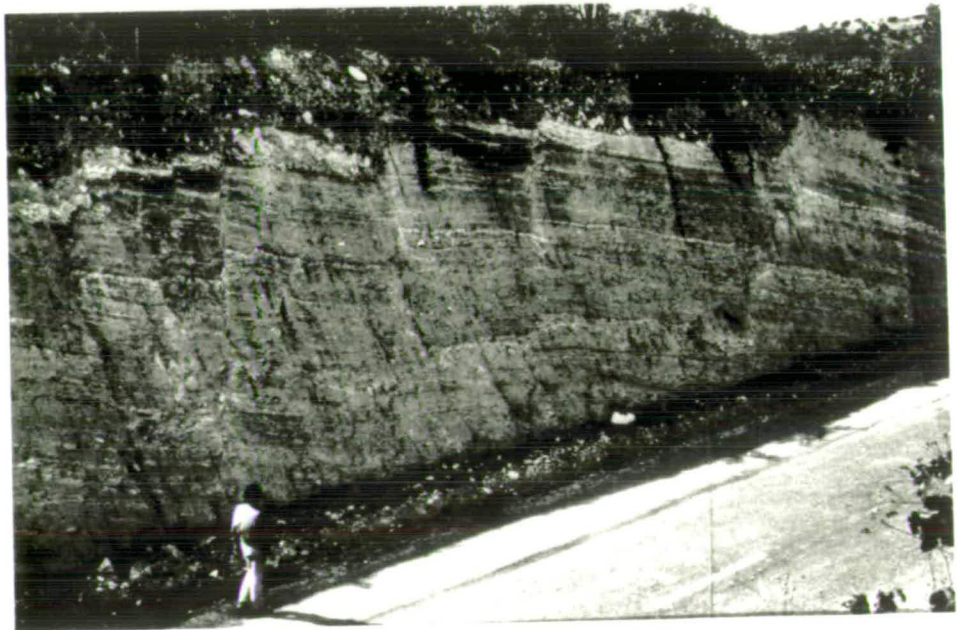
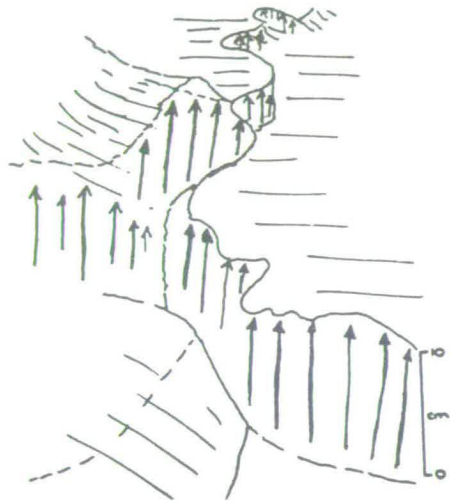




**PLATE 4.3.**

- A - Small scale normal faults cutting shallow marine sequences in a quarry near Ormidhia, south-east Cyprus, viewed looking north.
- B - Displacement fractures covering the F4 marine terrace at Paphos, south-west Cyprus (*cf* Fig.4.4).



- C - Plan view of cross-cutting joints in the F4 (Late Pleistocene) marine terrace at Paphos, south-west Cyprus.

# Plate 4.3

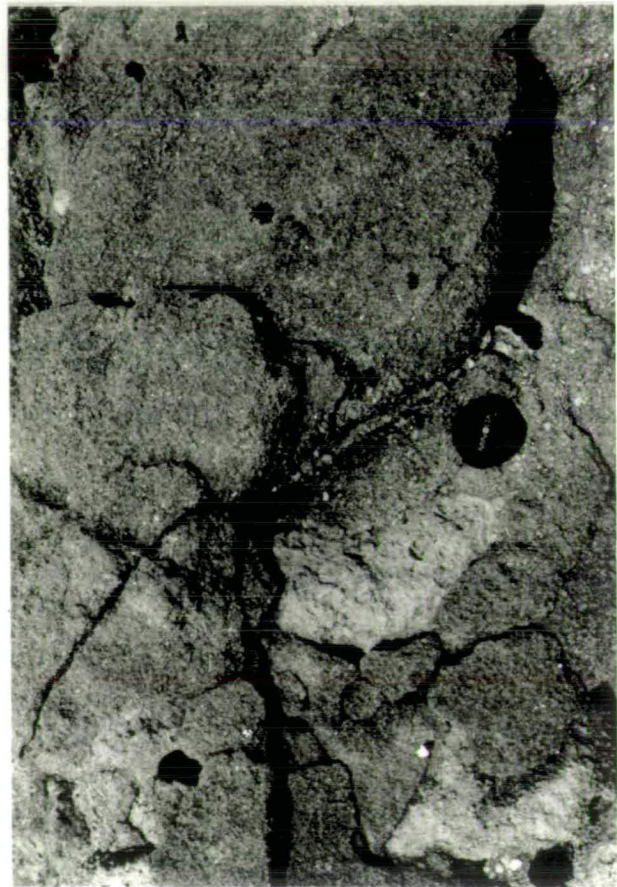
**A**



**B**



**C**



well cemented N-S set, a conjugate set orientated NNW-SSE is also present. The structures recorded here are similar to structures seen in an accretionary complex when hydraulic de-watering is taking place (A.H.F. Robertson, *pers. comm.*, 1989).

The joint and fracture data were collected in order to increase the data base; as there was a paucity of preserved fault planes. The resulting data were used to test the hypothesis that this data source can be used as a kinematic indicator which reflects the uplift of the island and the regional tectonic stresses that were active during the early Quaternary.

The joint data collected during this study are plotted in the form of rose diagrams (Fig.4.5), with fault data being plotted on a lower hemisphere stereographic Wulff net (Fig.4.4a) and shown in sketches (Fig.4.4b and Plate 4.3). The relative age of the joints and fractures is discernible by means of cross-cutting relationships with earlier fractures and joints being displaced by later fractures (Fig.4.4b). This study has been restricted to outcrops in the south-east and south-west of the island because:

- i) lithified Quaternary sequences crop out extensively in these areas,
- ii) a comparison between the early and late Quaternary and pre-Quaternary joint and fracture patterns, i.e. Miocenc limestone outcrops, can be made within each of the two areas,
- iii) the two regions can be compared.

The joint and fracture data collected from south-east and south-west Cyprus dip between  $70^{\circ}$  and  $90^{\circ}$ , i.e. vertical. The joint and fracture data collected from the F4 coastal terrace in the Paphos area and to the north, along the west coast of the island, suggest that three or possibly four major joint and fracture sets are present. These strike between:

- i)  $0^{\circ}$ - $022^{\circ}$ ,
- ii)  $094^{\circ}$ - $110^{\circ}$ ,
- iii)  $140^{\circ}$ - $160^{\circ}$ ,
- iv)  $050^{\circ}$ - $060^{\circ}$  (Fig.4.5).

The  $094^{\circ}$ - $110^{\circ}$  striking joint traces dominate in the Paphos area with very continuous, wide joints compared to the other sets. Cross-cutting relationships, where the fractures are actually meso-scale faults rather than joints *sensu stricto*, differ from site to site but show the following age relationship on the F4 terrace in the Paphos area: the  $0^{\circ}$ - $022^{\circ}$  set (1st) is cut by the  $094^{\circ}$ - $110^{\circ}$  set (2nd), which in turn is cut by the  $140^{\circ}$ - $160^{\circ}$  set (3rd) (Fig.4.4b). The cross cutting relationship is not systematic and varies from west to east across the island (see below). The fractures from the F4 coastal terrace in south-west

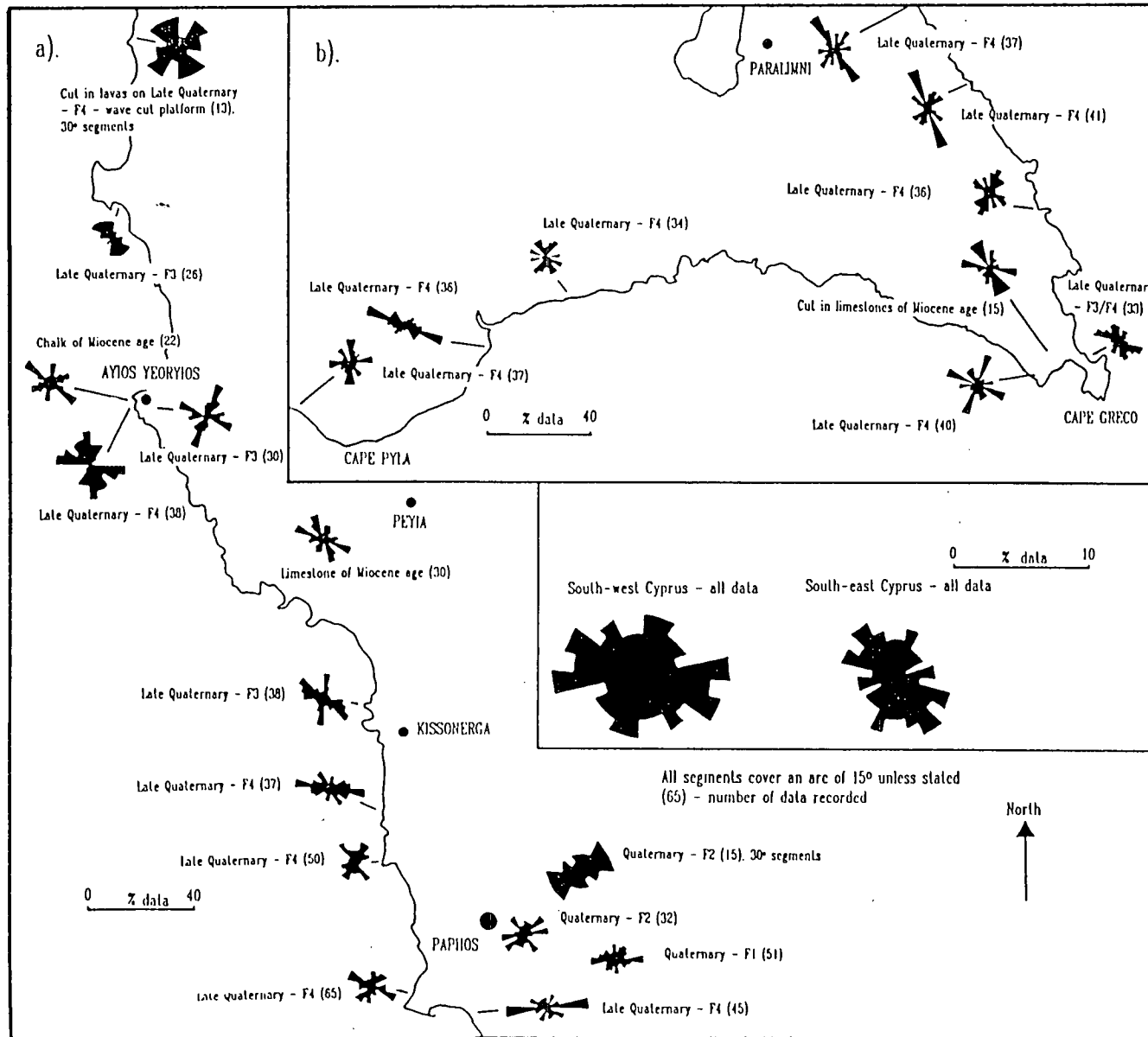


Fig.4.5. Rose diagrams of data collected from joints and fractures that cut the Quaternary and Neogene sediments in southern Cyprus.

Cyprus show both sinistral and dextral lateral movement. Little evidence for vertical movement on fault plane was seen in the F4 terrace of south-west Cyprus, throws being in the order of 10-20cm, although a maximum of 60cm was observed.

The  $0^{\circ}$ - $10^{\circ}$  striking joint set recorded in the Ayios Yeoryios area (location 2-27; Fig.4.5) dominates locally with the  $090^{\circ}$ - $110^{\circ}$  striking joints forming a secondary set of many small, laterally impersistent joints. Fractures indicate that the  $090^{\circ}$ - $110^{\circ}$  joint set pre-dates the  $0^{\circ}$ - $10^{\circ}$  striking set, displacement is lateral, both dextral and sinistral, and generally limited to a maximum horizontal movement of 15cm.

The joints associated with the Miocene limestones from in the F1 terrace to the west of Peyia (Fig.4.5) show evidence of caliche formation along the joints. The formation of caliche (Chapter 9) in joints is not limited to the Miocene limestone but is most pervasive in these units, with an apparent continuation of the horizontal caliche formation down the walls of the joint. This calichification usually caps the majority of the joint walls on the older, Miocene, limestones. Data collected from the F1 and F2 terraces above Paphos show clearer evidence of faulting (Fig.4.4a). The joint and fracture evidence from the F1 and F2 terraces cropping out to the east of Paphos show four sets that run approximately N-S, E-W, NE-SW and NW-SE (Fig.4.5).

The rose diagram of combined joint and fracture data collected from the south-west of Cyprus shows a variable pattern with segments striking between ENE-WSW and NW-SE dominating over NNE-SSW data (Fig.4.5).

The combined joint and fracture data collected from south-east Cyprus indicates that three dominant sets are present; these run NNW-SSE, NW-SE and NNE-SSW.

The  $270^{\circ}$ - $310^{\circ}$  joint set is most pervasive in the F4 terrace in the area of Cape Pyla (locations 2-71 and 1-136; Fig.4.5). The set striking  $320^{\circ}$ - $340^{\circ}$  dominates along the F4 terrace in the Paralimni and Cape Greco areas. Fractures in the Paralimni and Cape Greco area show both vertical and horizontal displacement on planes dipping at between  $70^{\circ}$  and  $90^{\circ}$ . Displacement is limited to 20cm here. The cross-cutting relationship here indicates that the joints striking  $070^{\circ}$ - $090^{\circ}$  predate those striking at  $320^{\circ}$ - $340^{\circ}$  (Fig.4.4b).

The F1 terrace in the Cape Greco area, cut into Miocene limestone, is generally poorly jointed but shows a joint pattern similar in strike to the neptunian dykes and fissured Miocene limestones present, i.e. E-W, ESE-WNW, N-S, NW-SE. These are aligned with the Famagusta graben that has been identified using Bouguer anomaly data (Follows, 1990).

The pattern of joints and fractures seen in Cyprus (Fig.4.5) can be classified in accordance with fracture architecture described by Hancock (1985). Between two and four patterns are seen in the fractures and joints observed, those prescribing the shapes **K** and **I** are certainly present in data collected from sites located on both Miocene and Quaternary outcrops (Fig.4.5). **X** and **A** may also occur. The **I** and **K** pattern appear to occur together almost exclusively with only two examples of a pure **I** pattern observed, e.g. in the F4 terrace to the south of Paphos and at location 1-136 on the east side of Cape Pyla (Fig.4.5). The presence of cross-cutting fractures that displace previous joints and fractures suggests that true **X** and **A** patterns may not be present as they relate to conjugate sets of joints that show no relative displacement. However, two **X** patterns offset from each other are present at a number of locations, e.g. near Ayia Napa and on the west side of Cape Greco (Fig.4.5).

The fracture analysis undertaken during this study agrees with other kinematic indicators, e.g. Plio-Quaternary fault and earthquake data (Rotstein & Kafka, 1982; Table 4.1), indicating WNW-ESE compression and faults striking between WNW-ESE and NNW-SSE (Fig.4.4a), in line with the down borehole data described in Section 4.3. The joint and fracture data (Fig.4.5) also agree in broad terms with the regional stress pattern, although a great deal of noise is present in this data. Hancock (1985) states that vertical joints in sedimentary rocks are indicative of extension, or hybrid structures, and that the **I** shape joint, or fracture pattern, indicates unidirectional extension. The **K** shaped pattern is indicative of extension in a nearly hydrostatic stress field (Engelder, 1982A, B). Closer examination of the dihedral angle ( $2\theta$ ) of joints, along with a consideration of the rheological properties of the rock types present, would be necessary to distinguish between hybrid and conjugate shear joints represented by the **X** shaped pattern.

These joint and fractures are therefore considered useful kinematic indicators where a paucity of other data sources exists. There is a general consistency in the earthquake, down borehole, fault and joint and fracture data, in agreement with that recorded in extensional areas elsewhere, e.g. in the Qaraden segment of the Arabian graben and trough system (Hancock & Al Kadhi, 1982).

A lack of positive fault slip data, i.e. slickensides, and fault plane solutions (Haimson *et al.*, 1990) did not allow palaeo-stress tensors to be determined for the faults and fractures in southern Cyprus (cf. Angelier, 1984).

#### **4.5 DISCUSSION AND CONCLUSIONS.**

The data presented here support the argument that neotectonics have been active on a small scale in southern Cyprus during the Quaternary period. The rarity of large scale faulting, the flat bedded, well stratified nature of the Pleistocene sequences in the seismic sections (Catini *et al.*, 1983; McCallum, 1989; McCallum *et al.*, 1992) and the ability to accurately correlate coastal terraces from west to east around the island (Chapter 3) testifies to this, and indicates that southern Cyprus has acted as a single tectonic unit during the Quaternary. The limited and uniform southern Cyprus Quaternary activity follows the brutal reorganisation in the Lower Pliocene, in line with the view of Dupoux (1983) who suggested that tectonic activity since the Villafranchian (Upper Pliocene-Lower Quaternary) has been minimal. The tectonic activity that has taken place resulted in extensional structures evidenced by micro-fractures, faults, joints and earthquake data, which have resulted in tectonic lineaments striking between WNW-ESE and NNW-SSE. Therefore, these data back up the arguments presented in Chapter 3 for en masse, islandwide, tectonic uplift, similar to that seen in other Mediterranean areas (Hey, 1978). The Polis-Paphos graben, in south-west Cyprus, may prove to be the exception to this uniformity, although available data suggest an alignment of Quaternary structures that are in accord with that found throughout the southern portion of the island (Ward & Robertson, 1987).

The conclusions concerning the Quaternary neotectonics of Cyprus that can be made are:

- i) tectonic activity since the early Quaternary has been minimal, with relative movement being taken up by meso-scale faults and fractures. The evidence from earthquakes shows that tectonic activity is still taking place. However, seismic data, showing the stratified undisturbed nature of the Quaternary sediments, suggest that this has had a minimal effect on the Quaternary sequence,
- ii) seismic sections, earthquake foci, down borehole and fault data show a consistent alignment of structures, striking between WNW-ESE and NNW-SSE,
- iii) joint and fracture data are generally aligned perpendicular to principal axes of extension,
- iv) there is no evidence of Quaternary folding,
- v) there is very little evidence for subduction related processes, as the compression component of the borehole data (Haimson *et al.*, 1990) appears to be taken up by strike-slip motion,
- and vi) all the data are consistent with uniform uplift of the coastal areas throughout the Quaternary period, in line with the evidence presented in Chapter 3.

## **Chapter Five: The Fanglomerate Group.**

### **5.1 INTRODUCTION.**

This chapter will examine the extent, nature and characteristics of the Fanglomerate Group sediments that crop out throughout southern Cyprus. The spatial distribution of the Fanglomerate Group sediments will be described followed by a geographical review of the pattern of sedimentation. Islandwide palaeocurrent data will be presented and compared to the geomorphological data recorded in Chapter 2. The provenance of the Fanglomerate Group will be deduced from borehole data and clast analysis. Discussion and models of possible sedimentological settings will be presented. The geomorphology of the drainage pattern, erosion surfaces and terraces associated with the Fanglomerate Group has been described in Chapter 2.

#### **5.1.1 Nomenclature.**

The Fanglomerate Series has been renamed the Fanglomerate Group here in line with modern standard stratigraphic usage, e.g. Schnek & Muller (1941) and Whittaker *et al.* (1991). The gravels of Ducloz (1965) make up the units of this group on the north Troodos margin. The units of Ducloz (1965) can be correlated with the F1-F4 sequences, that are identified from this work (Tables 1.9 and 1.10) and used elsewhere in this thesis.

#### **5.1.2 Previous work.**

The Fanglomerate Group, a Quaternary continental, fluvial sequence, forms a series of extensive conglomeratic terraces and sheets. Bellamy & Jukes-Browne (1905) and Cowper-Reed (1930) described the "alluvium" on the Mesaoria Plain. Henson *et al.* (1949) state that the Fanglomerate Group is seen in the foothills of the Troodos and Kyrenia Mountains and caps isolated mesa hills on the Mesaoria Plain (Figs.2.7; Plate 2.6). The Memoirs of the Geological Survey Department (Bear, 1960; Gass, 1960; Carr & Bear, 1960) map the extent of the Fanglomerate Group on the north flanks of the Troodos Massif and within the Mesaoria Plain. A detailed map of the Plio-Pleistocene formations, including the Fanglomerate Group, of the central and eastern Mesaoria Plain was produced by Ducloz (1965; Fig.5.1); this differentiated between the various stages of the Fanglomerate Group for the first time. Ducloz (1965) also correlated the Fanglomerate terraces with the Quaternary glacial chronology and the Mediterranean marine stages (Table 1.4). McCallum (1989) examined the Plio-Pleistocene sediments of the north Troodos margin in detail and concluded that this sequence indicated pulsed uplift of the Troodos Massif.



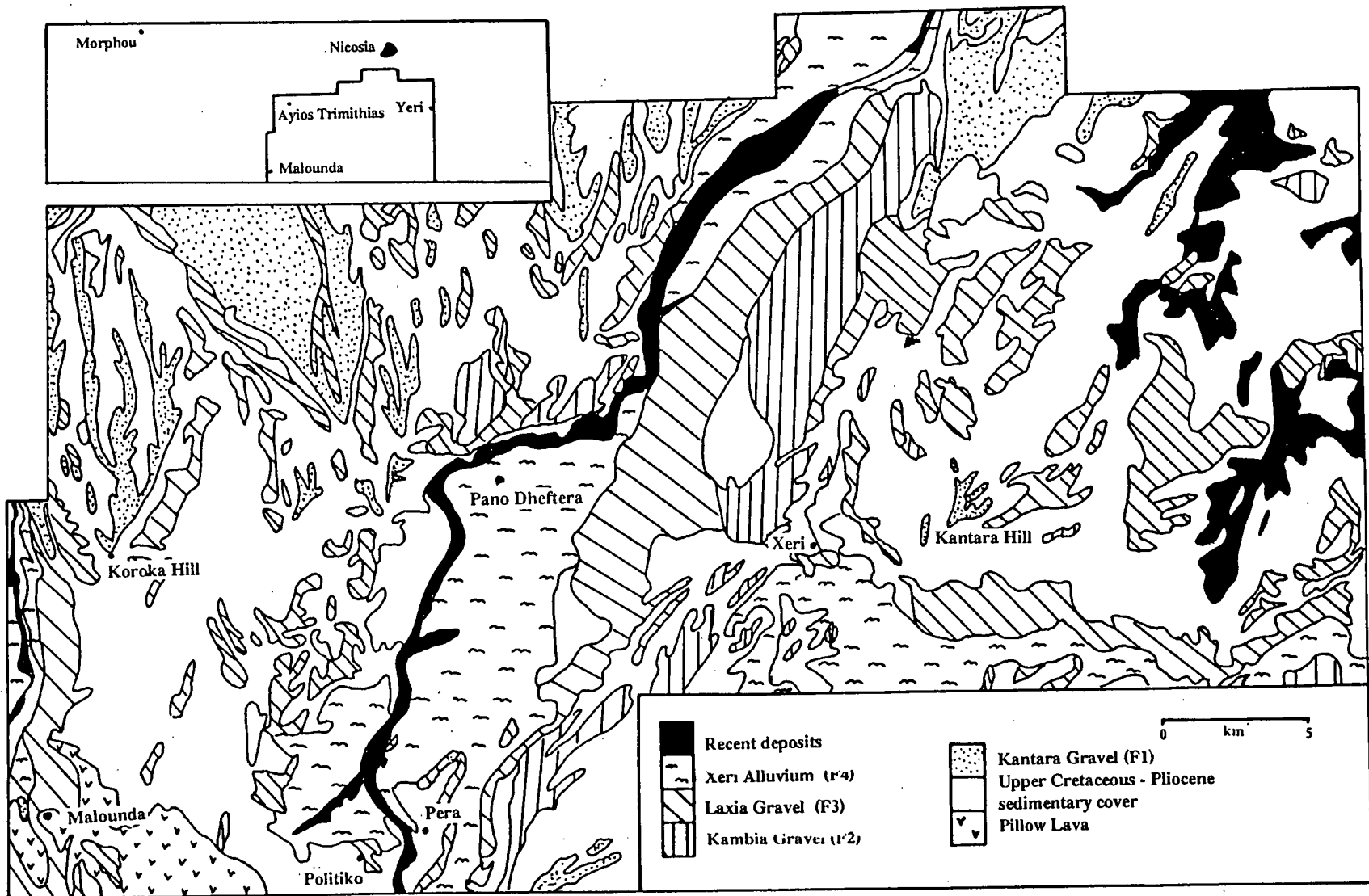


Fig. 5.1. Mapped units of the Fonglomerate Group in the central and eastern Mesaoria Plain (after Ducloz, 1965).

Sedimentary sequences similar to those seen on the north Troodos margin and southern Cyprus are also seen flanking the Kyrenia Mountains. The Fanglomerate Group and the Karka Formation have been identified on both the northern and southern side of the Kyrenia Mountain chain and on the north-west portion of the Mesaoria Plain as series of intermontane lacustrine, fanglomerates, scree and breccias (Moore, 1960; Ducloz, 1968, 1972; Dreghorn, 1978; Baroz, 1979).

## **5.2. GEOGRAPHICAL DISTRIBUTION AND THICKNESS VARIATION.**

The Fanglomerate Group will be discussed as a single unit here, rather than be divided into time slices, for the following reasons:

- i) borehole data do not allow distinction of units between the separate phases, i.e. F1-F4, of Fanglomerate Group deposition,
- ii) the different units of Fanglomerate Group coalesce in areas of coastal southern Cyprus and much deposition took place beyond the present coastline (Chapter 2),
- iii) distal areas on the north Troodos margin fall in areas inaccessible to fieldwork (the buffer zone between the Turkish and Greek controlled portions of the island), preventing data collection. The distribution of the Fanglomerate Group is more extensive (Fig.2.7) than outlined by the Cyprus Geological Map (Pantazis, 1979).

The surface distribution of the Fanglomerate Group sediments gives little indication of the true thickness of these deposits. In south-east Cyprus, for example, the Fanglomerate Group is commonly only a few metres thick. The Fanglomerate Group on the north Troodos margin was recorded at less than 90m thick (Zomenis, 1977) and between 3-5m, and locally 12m, thick (McCallum, 1989). Borehole data, however, show that the thickness of the Fanglomerate Group varies greatly over the north Troodos margin (Fig.5.2). Fanglomerate Group exposures south of Morphou are reported to be 6-7m thick and are thought to be underlain by the Athalassa Formation, although the underlying strata are not seen (Moore, 1960).

Outcrops of the Fanglomerate Group to the south of the Troodos Massif also show a substantial variation in thickness. Borehole data (Fig.5.3) indicate that the conglomerate sequences can be up to 86m thick, although shallow marine environments may also be included in these figures (Chapter 6).

The exposure and borehole data in south-east Cyprus show that the Fanglomerate Group consists of a thin capping unit in the area to the north of Xylophagou, while thicker more extensive exposures are seen to the east, in the Dhekelia area.

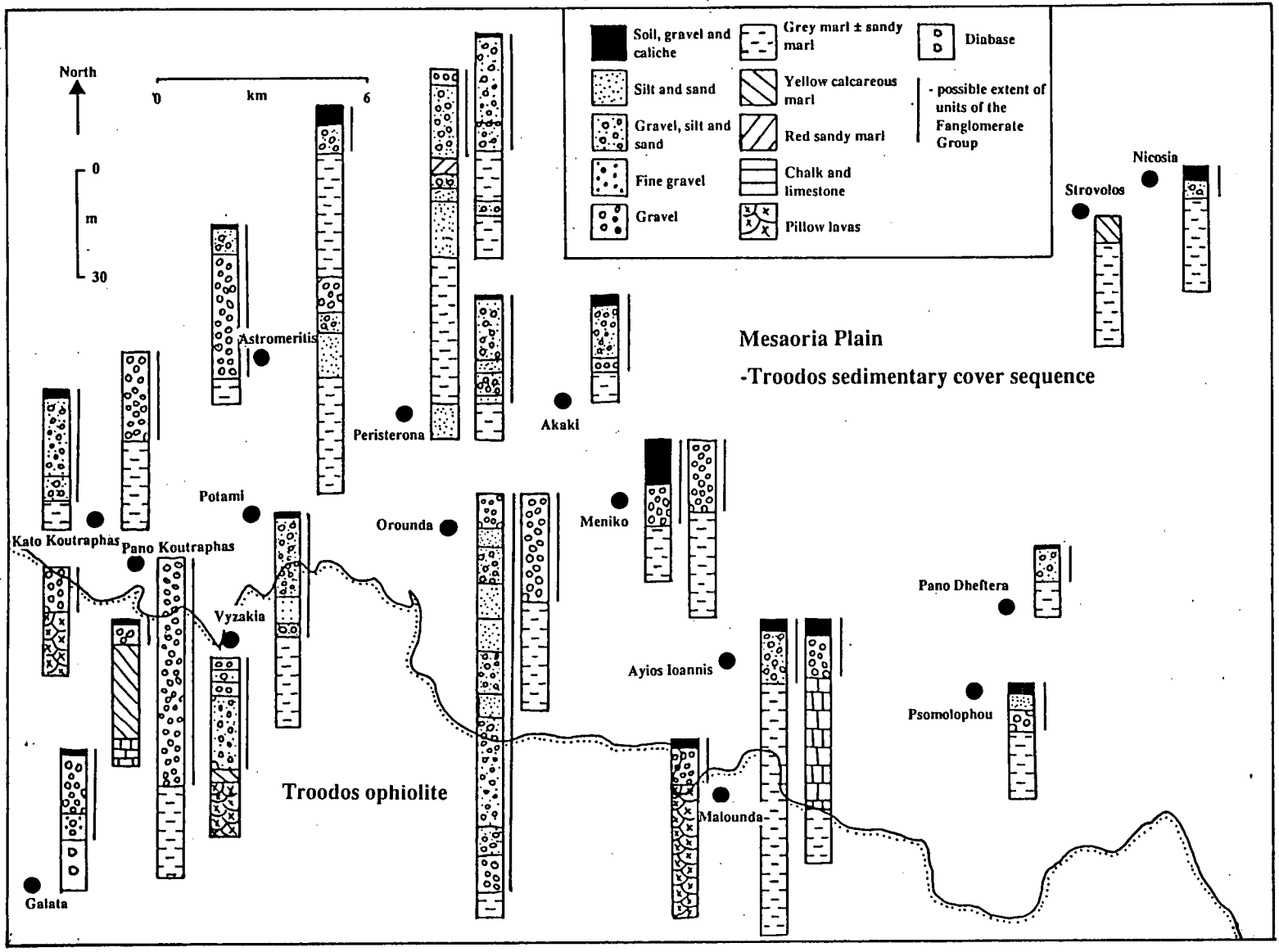
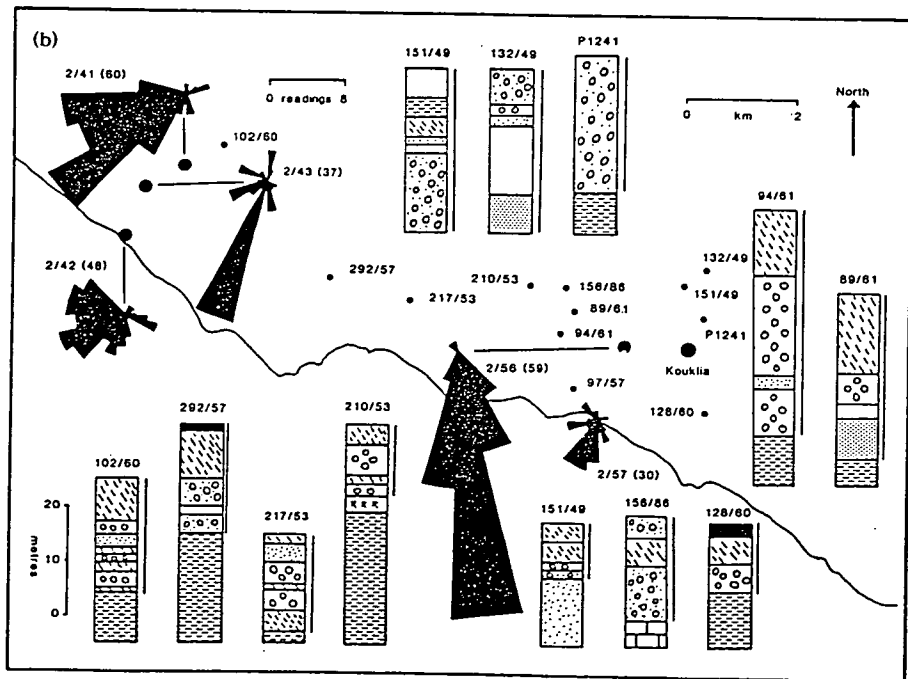
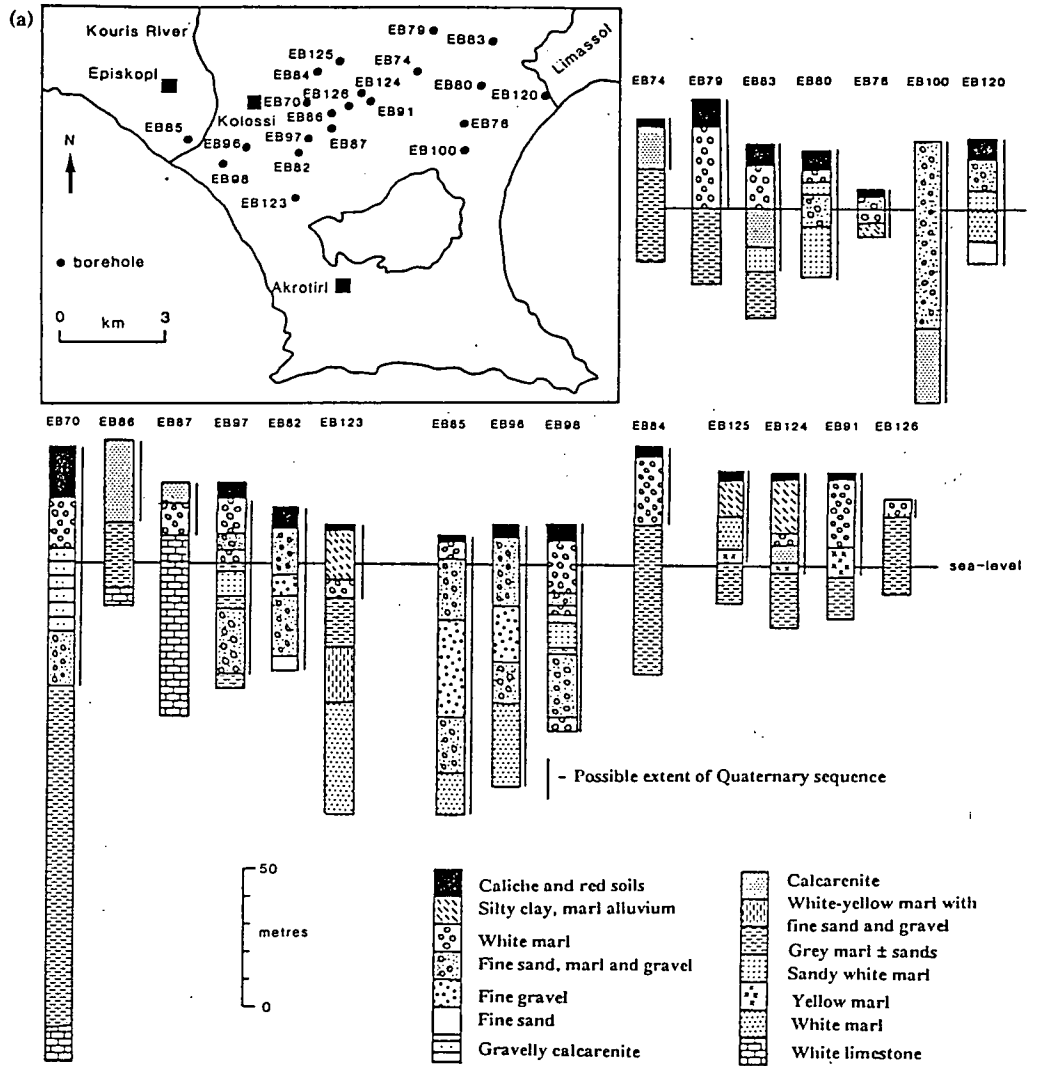


Fig.5.2. Borehole data from the north Troodos margin.

Fig.5.3. a). Borehole data from the Akrotiri Peninsula; b). borehole and palaeocurrent data from south-west Cyprus.



In the south-west of the island the outcrop pattern of the Fanglomerate Group is patchy; sequences less than 5m thick are common. Extensive exposures of the Fanglomerate Group are seen in the Polis-Paphos graben, but they rarely exceed an exposed thickness of 10-15m.

### **5.3 SEDIMENTARY FACIES.**

The facies of the Fanglomerate Group sediments will now be described for each of the following regions in turn:

- i) the north Troodos margin,
- ii) south-east Cyprus,
- iii) the southern portion of the island, from Larnaca to Episkopi,
- iv) the western area, west of Episkopi to Paphos,
- v) the Polis-Paphos graben area, and east to Kato Pyrgos,
- vi) the Kyrenia Range.

The Fanglomerate Group facies in each of these areas will be described in ascending stratigraphic order.

#### **5.3.1 The north Troodos margin.**

##### **5.3.1.1 Introduction.**

Four units of the Fanglomerate Group on the north Troodos margin (Tables 1.9 and 1.10) can be distinguished from each other on the basis of altimetric studies (Ducloz, 1965; Chapter 2). McCallum (1989) did not subdivide the Fanglomerate Group into units but did describe some of the sedimentary facies that exist in the eastern and central areas of the Mesaoria Plain (Table 5.1).

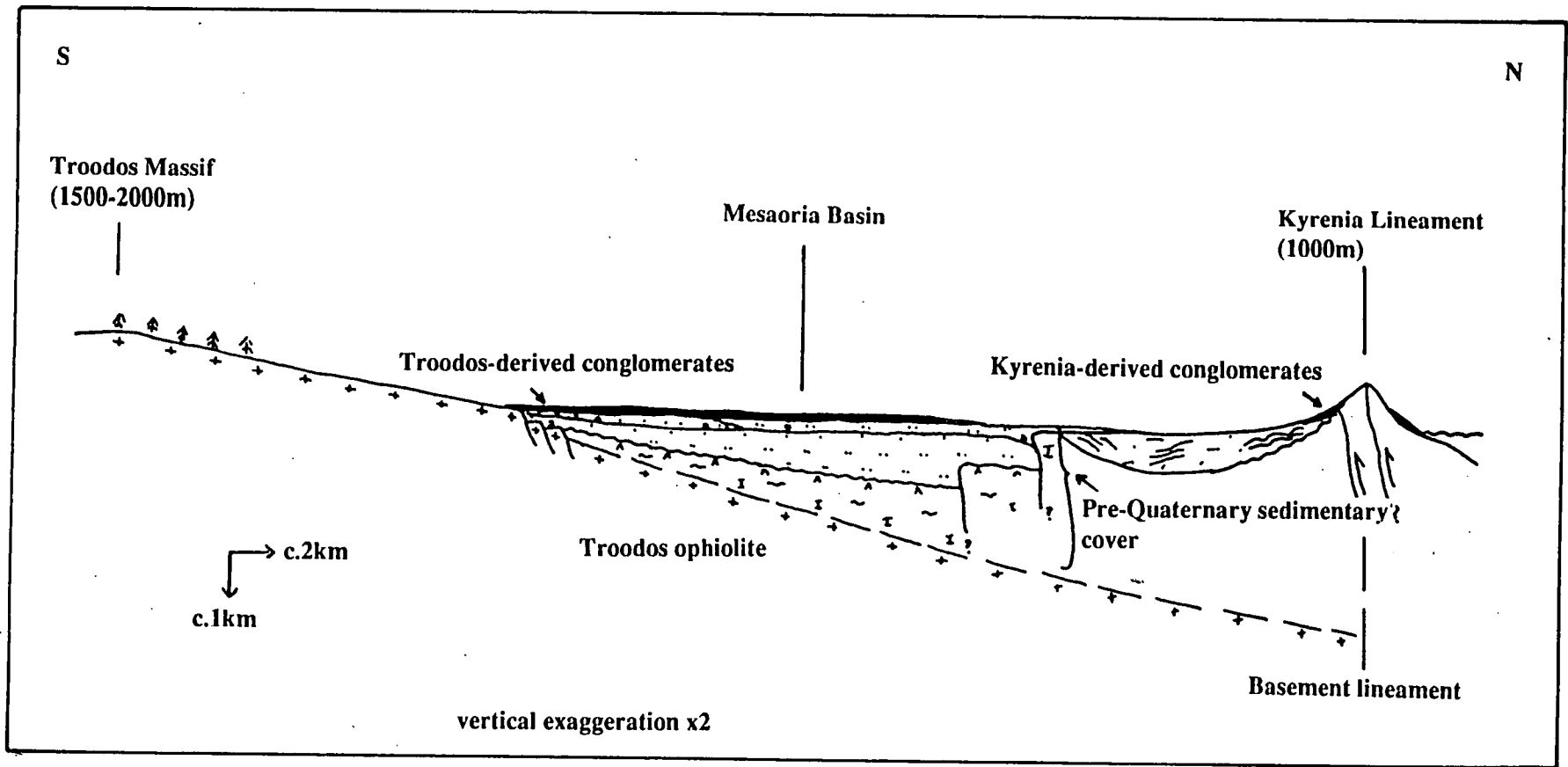
The Fanglomerate Group onlaps onto the younger, i.e. Pliocene, portion of the Troodos cover sequence in the axis of the Mesaoria Plain, overstepping and cutting down into progressively older units of the Troodos sedimentary cover sequence and eventually the Troodos ophiolite basement at the southern and western extent of the Fanglomerate Group exposure (Fig.5.4).

##### **5.3.1.2 The F1 and F2 Fanglomerate units (lower-middle Pleistocene).**

The F1 and F2 Fanglomerate Group units, i.e. the Kantara and Kambia Gravels of Ducloz (1965), are described together in view of their similar sedimentary facies and

Table 5.1. Facies of the Fanglomerate Group (after McCallum, 1989).

| Facies                                                          | Description                                                                                                                                                                                                                                                                                                                                                                                                               | Interpretation                                                                                                                                                                                                                                                                                                                                                                                  |
|-----------------------------------------------------------------|---------------------------------------------------------------------------------------------------------------------------------------------------------------------------------------------------------------------------------------------------------------------------------------------------------------------------------------------------------------------------------------------------------------------------|-------------------------------------------------------------------------------------------------------------------------------------------------------------------------------------------------------------------------------------------------------------------------------------------------------------------------------------------------------------------------------------------------|
| <p>A1<br/>Massive<br/>conglomerates</p>                         | <p>Coarse, poorly sorted pebble-cobble conglomerates, boulders &lt; 55cm diameter, clasts generally 1-10cm diameter. Clasts are angular to sub-rounded. Crude but rare horizontal bedding, Grading is uncommon, coarsening up seen; clast fabric is matrix- to clast-support. Matrix is silty sand. Imbrication weakly developed. Single beds are 1-3m thick, with planar or minor erosive contacts. Unfossiliferous.</p> | <p>Low and high concentration, coarse proximal sheet-flow, as either: i) proximal, waterlain conglomerates; ii) subaerial cohesionless, mass flow; or iii) an intermediate environment between mass flow and waterlain.<br/>Proximal, alluvial fan setting.</p>                                                                                                                                 |
| <p>A2<br/>Cross-bedded<br/>conglomerates</p>                    | <p>Coarse, poorly sorted, pebble-cobble and finer better sorted conglomerates. 2m thick, crude cross-bedded sets. Mainly tabular cross-bedding, with non-erosive bases; cross-bed directions are in line with clast imbrication orientations of facies A1. Clast-supported with a brown, poorly to moderately sorted, sandy matrix. This facies is not common. Unfossiliferous.</p>                                       | <p>Similar to facies Gp (Miall, 1977), developed as crude longitudinal braid bars migrated on an alluvial fan surface. These bars probably developed during periods of more stable flow than facies A1.</p>                                                                                                                                                                                     |
| <p>B1<br/>Interbedded<br/>sands and minor<br/>conglomerates</p> | <p>Brown, fine grained sands interbedded with conglomerate. Poorly to moderately sorted, largely structureless with some horizontal laminations. The thin conglomeratic layers are 10-20cm thick, grain-supported, more mature and better sorted than facies A1 and A2; they are occasionally imbricated.</p>                                                                                                             | <p>These conglomerates reflect initial reworking of the Troodos Massif and, possibly, the Pliocene sediments, prior to the introduction of newly-derived ophiolitic detritus. Sediment laden currents reaching the Troodos foothills decelerated and deposited their load. A lack of evidence for channel and bar development suggest that deposition mainly involved sheetflood processes.</p> |



Note: thickness of the sedimentary sequence is exaggerated.

Fig. 5.4. Sketch section across the north margin of the Troodos Massif and the Mesaoria Plain (after McCallum, 1989).

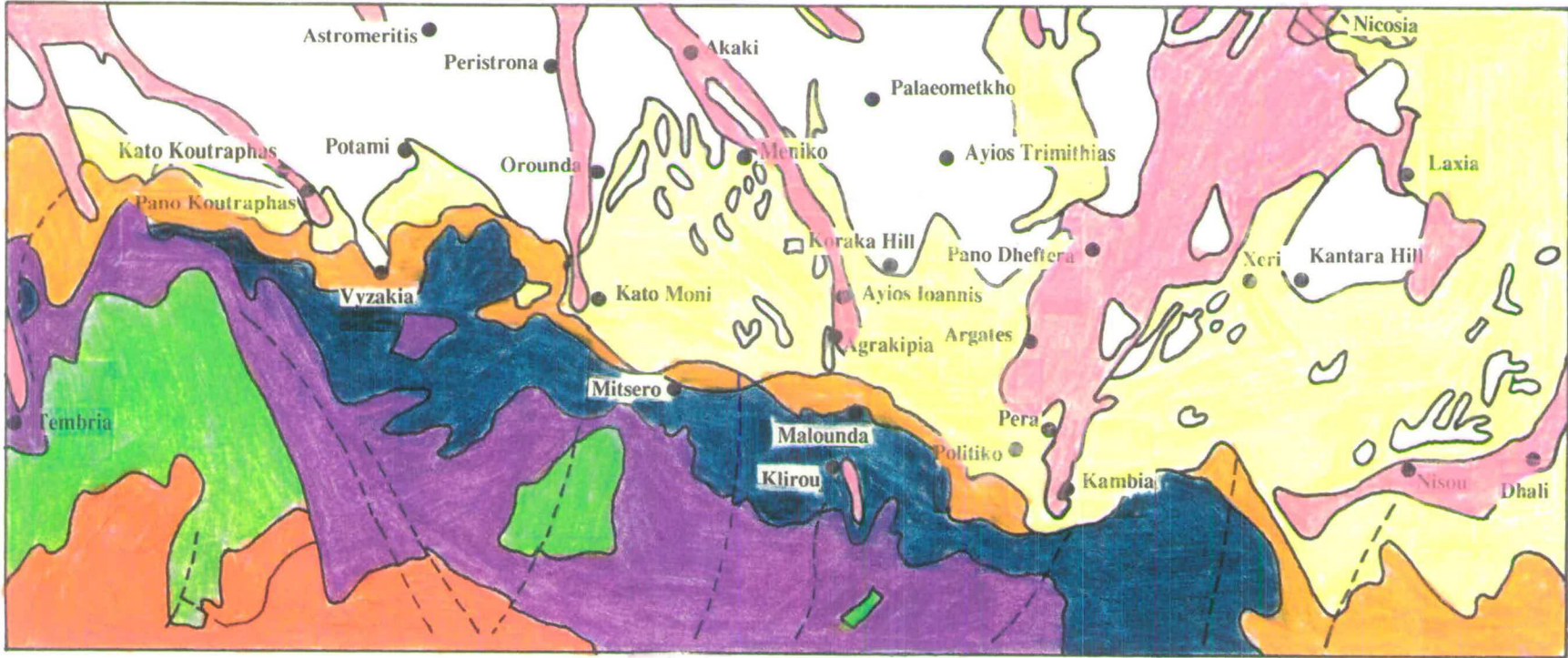
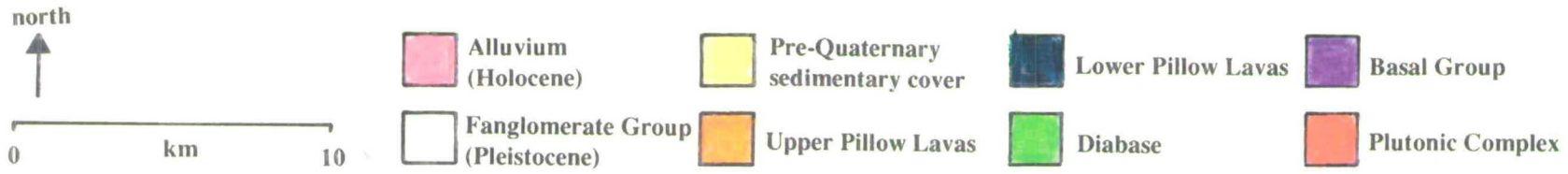


Fig.5.5. Map displaying the geology of the north Troodos margin.  
Note: the location of places mentioned in the text.



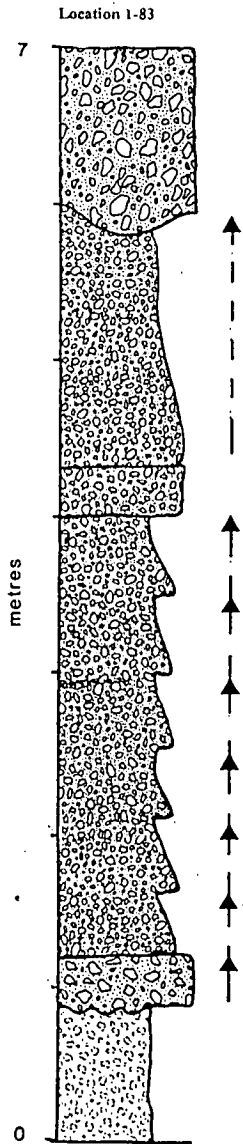
geomorphological characteristics (Chapter 2). The F1 Fanglomerate unit is heavily dissected throughout the Mesaoria Plain (Chapter 2). The F2 Fanglomerate unit is widely exposed in the western portion of the Mesaoria Plain (Fig.5.5; Plates 2.5 and 2.6) and, like the F1 Fanglomerate unit, has been heavily dissected on the eastern portion of the plain. The peneplaned F2 terrace is incised by F3 channels and smaller distributary streams - see Chapter 2 (Potami, location 1-109; Fig.5.5). The F1 and F2 Fanglomerate units are overlain by red terra rossa-type palaeosols and caliche horizons (Potami, Astromeritis and Koraka Hill; locations 1-109, 1-15 and 1-92; Fig.5.5) - see Chapter 9 for details of caliche and palaeosol development.

*i) Proximal development:*

The proximal facies of the F1 and F2 Fanglomerate sequences crop out within 1km of the margin of the Troodos Massif, they overlie Neogene sediments in the Mesaoria Basin and lithologies of the Troodos ophiolite further south. The proximal F1 Fanglomerate unit has been largely eroded (Chapter 2), so this description of proximal lithologies is based on exposures of the F2 Fanglomerate unit.

Proximal conglomerates (Fig.5.6) of the F2 Fanglomerate unit unconformably overlie the Troodos basement at a number of locations along the central north Troodos margin (Vyzakia, Kato Moni and Malounda, locations 1-19, 1-109, 1-83, 1-86, 1-7 and 1-8, respectively; Fig.5.5). The F2 Fanglomerate sediments unconformably cover Neogene sediments to the east and west away from the central Mesaoria Plain, e.g. Kato Koutraphas and Pera (locations 1-20 and 1-97). Sections are generally less than 15m thick, e.g. Vyzakia (location 1-109). Troodos basement lavas that crop out beneath the F2 Fanglomerate unit in the central portion of the north Troodos margin are weathered, commonly capped by a thin caliche horizon and form an unconformable contact with the overlying F2 Fanglomerate unit sediments (Fig.5.6; Plate 5.1). Weathered lavas make up a basal portion of the sedimentary sequence at Kato Moni and Malounda (locations 1-7 and 1-83; Figs.5.5 and 5.6). These weathered lavas form a white to orange silt and sand grade unit, with an irregular contact into the "fresh" lavas beneath and the conglomerates above. The weathered horizons are generally less than 1m thick.

The proximal units at Vyzakia are made up of red, unconsolidated, massive, structureless and poorly sorted conglomerates. The basal contact with the lavas shows extensive relief, 3-4m, and is very uneven. Clasts within the proximal conglomerates are generally less than 80cm in diameter and angular, occasional outsized clasts are present. A large proportion of locally derived lava clasts are found within the proximal conglomerates.



Very coarse, unsorted, grey grain to matrix supported, angular conglomerate. Angular to sub - rounded, Troodos - derived igneous clasts are commonly > 50cm along the "A" axis. The unit is poorly consolidated with a fine conglomerate to sandy matrix. Imbrication of clasts is rare. Some clasts display a coating of caliche.

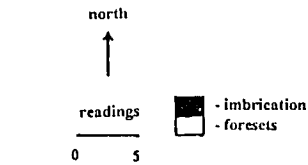
Scoured, erosional contact.

Fining upward sequences of unconsolidated grain to matrix supported conglomerate. An overall fining up sequence is also seen from the base to the top of the unit. This unit is generally planar but infrequent channels are seen towards the top of the unit. These channels are well sorted having a coarse conglomeratic core and finer sediments on the periphery.

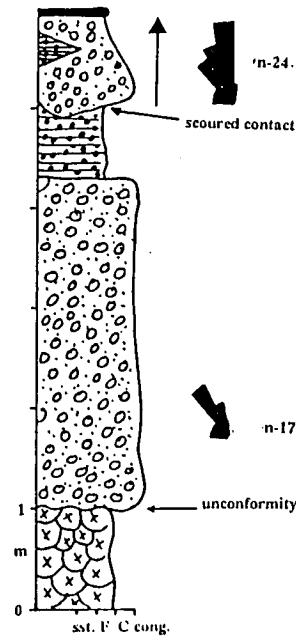
Massive, unsorted, immature, unconsolidated conglomerate. Clasts vary from  $cm^2$  -  $1m^2$  and are angular to sub - rounded and derived from the Troodos Massif.

Erosional contact.

Fine white to orange, silty sand resulting from the weathering of Pillow Lavas. The silty sand passes down into *in situ* Upper Pillow Lavas.



Location 1-86



Location 1-109

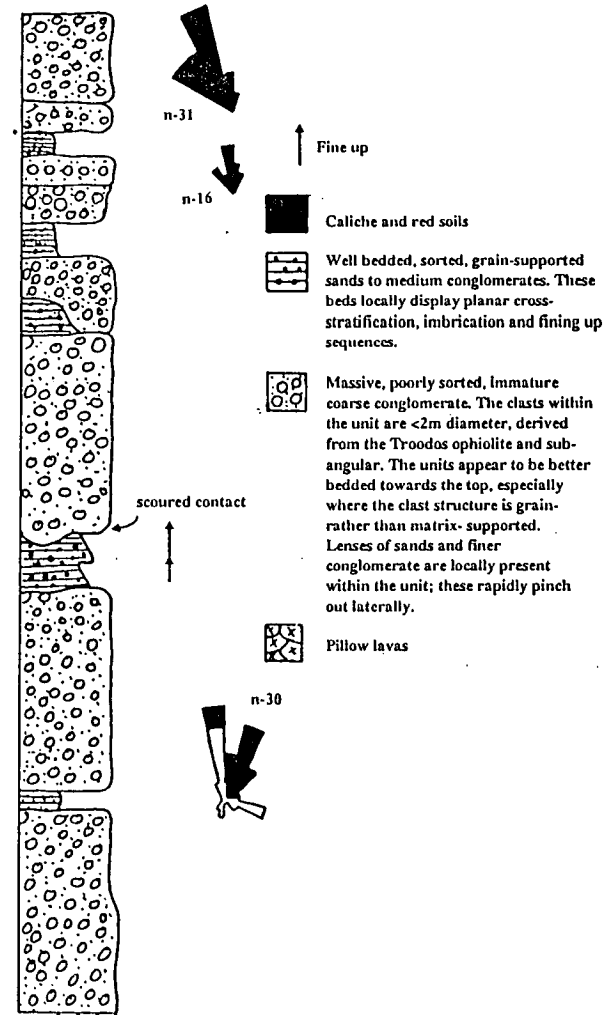


Fig. 5.6. Proximal sections of the Famlglomerate Group from sections on the north Troodos margin.

Fig.5.7. Sketch sections of intermediate units of the Fanglomerate Group on the north Troodos margin.

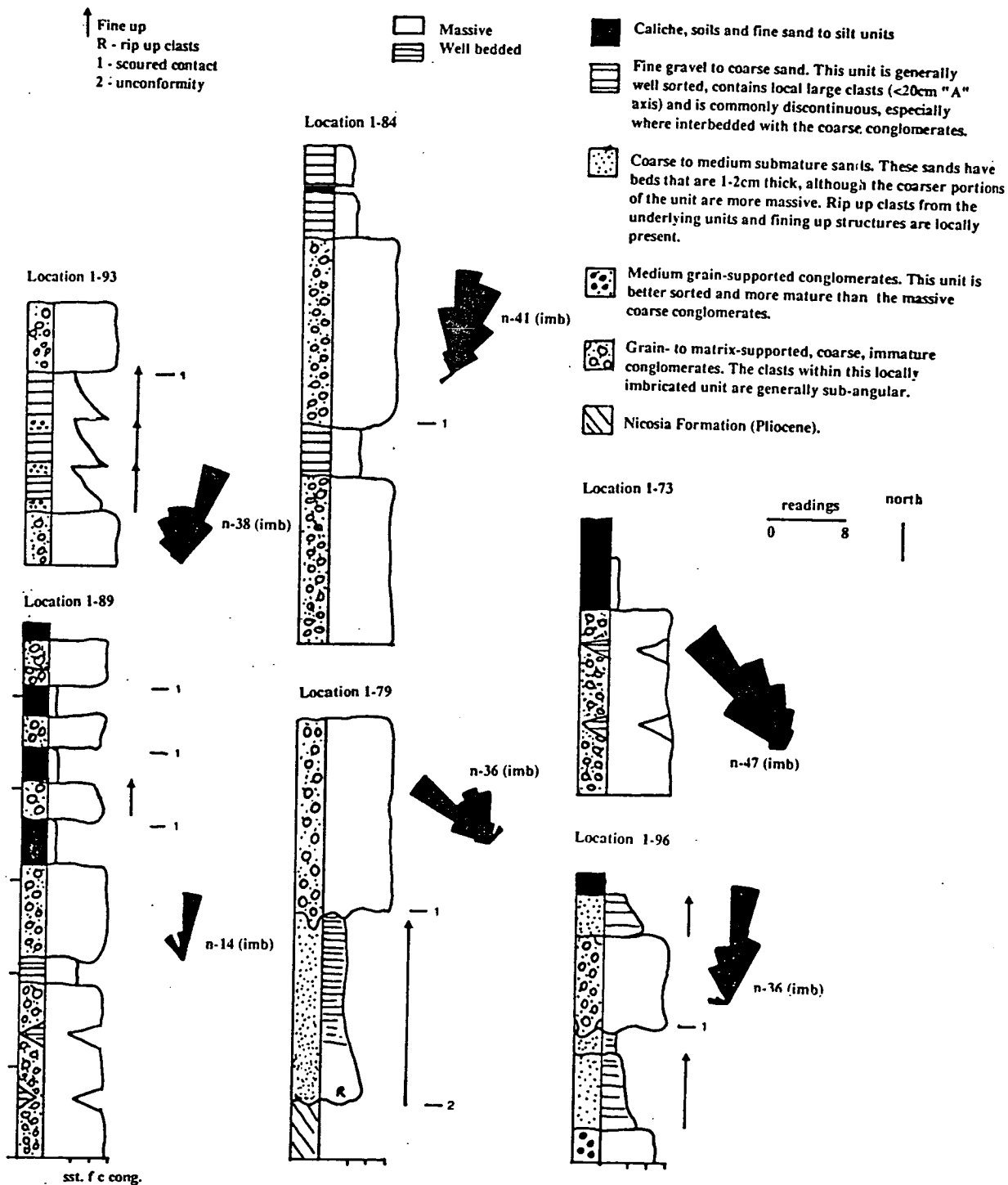


PLATE 5.1.

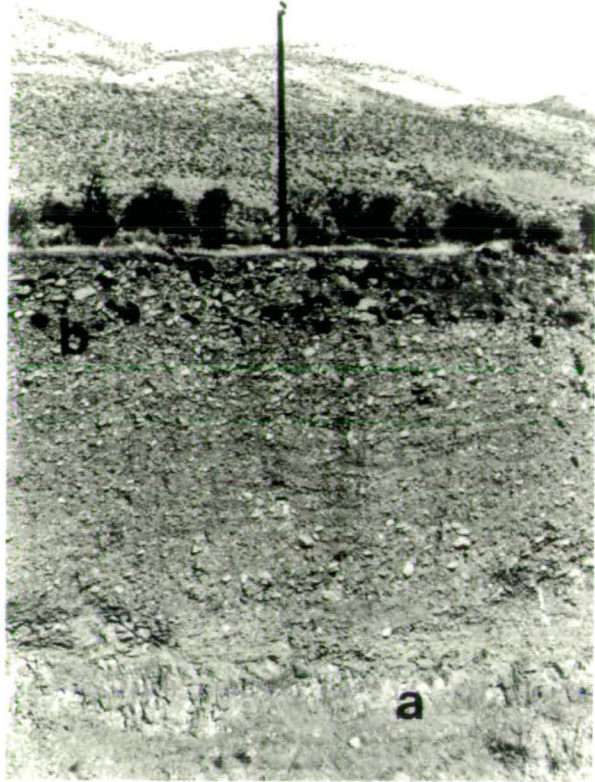
E - coarse conglomerates of the Fanglomerate Group lying unconformably above pillow lavas (a) at Kato Moni (location 1-87) on the north Troodos margin.

Note: chalk and limestones of the Miocene age crop out topographically above the Fanglomerate Group,  
the large number of pulses of coarse conglomerate within the sequence.

1a F - F2 age conglomerates of the Fanglomerate Group (b) cropping out unconformably above pillow lavas (a) at Malounda (location 1-7) on the north Troodos margin.

Plate 5.1

E



F



Inferred proximal sequences are dominated by coarse, massive, structureless, unconsolidated, matrix- to grain-supported conglomerates (Plate 5.2), with a dominantly sand and silt matrix; fine conglomerates locally constitute the matrix. Clasts within the proximal F1 and F2 units are generally angular to sub-angular. These conglomerates are very similar to F1 Fanglomerate units at Koraka Hill and correspond to the A1 facies of McCallum (1989; Table 5.1). Few sedimentary structures exist within proximal sequences of the F2 Fanglomerate unit. There are two phases of development of the coarse conglomerate facies, A1, at Malounda and in the area of Kato Moni (locations 1-7, 1-8 and 1-86; Figs.5.5 and 5.6; Plate 5.2). The conglomerate phases at each of the previously mentioned localities are coarse-grained and clasts up to 2m in diameter crop out at location 1-86; the units are angular to sub-angular and poorly sorted; the imbrication data indicate a local shift in the palaeocurrent direction from the lower to the upper conglomeratic units (Fig.5.6). The basal conglomerate is more commonly orange, whilst the upper conglomerate tends to be grey. A scoured contact is seen between the two conglomeratic units, with the development of caliche and finer-grained sediments, i.e. sands, at Kato Moni and Vyzakia (locations 1-86, 1-19 and 1-119). The basal conglomerates south of Kato Moni (location 1-86) are coarser-grained than the upper units, while the opposite pattern is seen at other exposures west of Kato Moni and at Malounda (locations 1-83 and 1-7 respectively), with the coarser conglomerates being present in the upper conglomeratic units. The basal units tend to have a greater proportion of locally derived lava clasts and fewer diabase and gabbro clasts than the upper unit; also fewer reworked clasts are present.

*ii) Intermediate development:*

Intermediate areas, between proximal and distal locations, are found between 1km and 5km away from the north margin of the Troodos Massif. The coarse conglomerates seen in exposures, on the road west of Akaki (locations 1-67 to 1-70; Figs.5.7 and 5.8); in the area around Orounda (locations 1-90, 1-84 and 1-89; Fig.5.7); and north of Malounda (locations 1-79, 1-81 and 1-91; Fig.5.7) are similar to the conglomerates that crop out at the base and top of the exposed sections in proximal locations (Kato Moni, location 1-86). The coarse conglomerates resemble facies A1 (McCallum, 1989; Table 5.1), with igneous and minor sedimentary clasts, i.e. gypsum and chalk, ranging from 10 to 50cm in diameter. The clasts are commonly polished brown and locally show a caliche crust. The conglomerates, although roughly bedded, are locally graded with fine conglomerates seen towards the top of some units (location 1-89; Fig.5.7). Lateral variation, with pods of fine conglomerate and sand, as well as the appearance of shallow channels distinguish (Plates 5.3-5.6) this unit from the coarse structureless conglomerates that crop out in proximal locations. The interbedded units that crop out between the coarse conglomeratic pulses

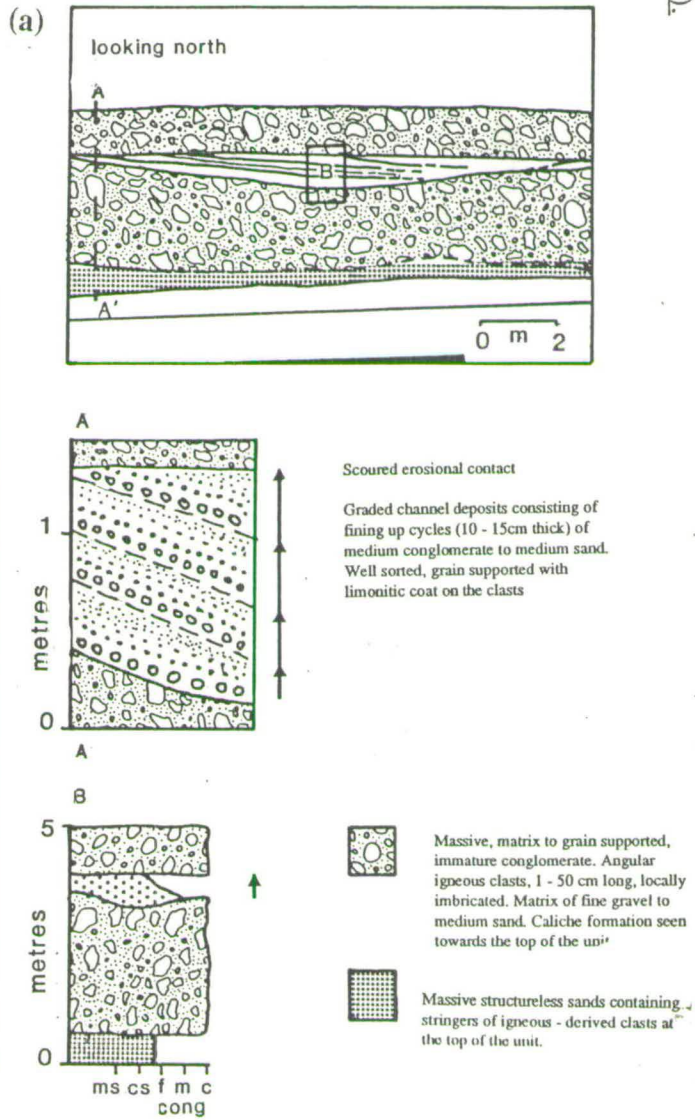
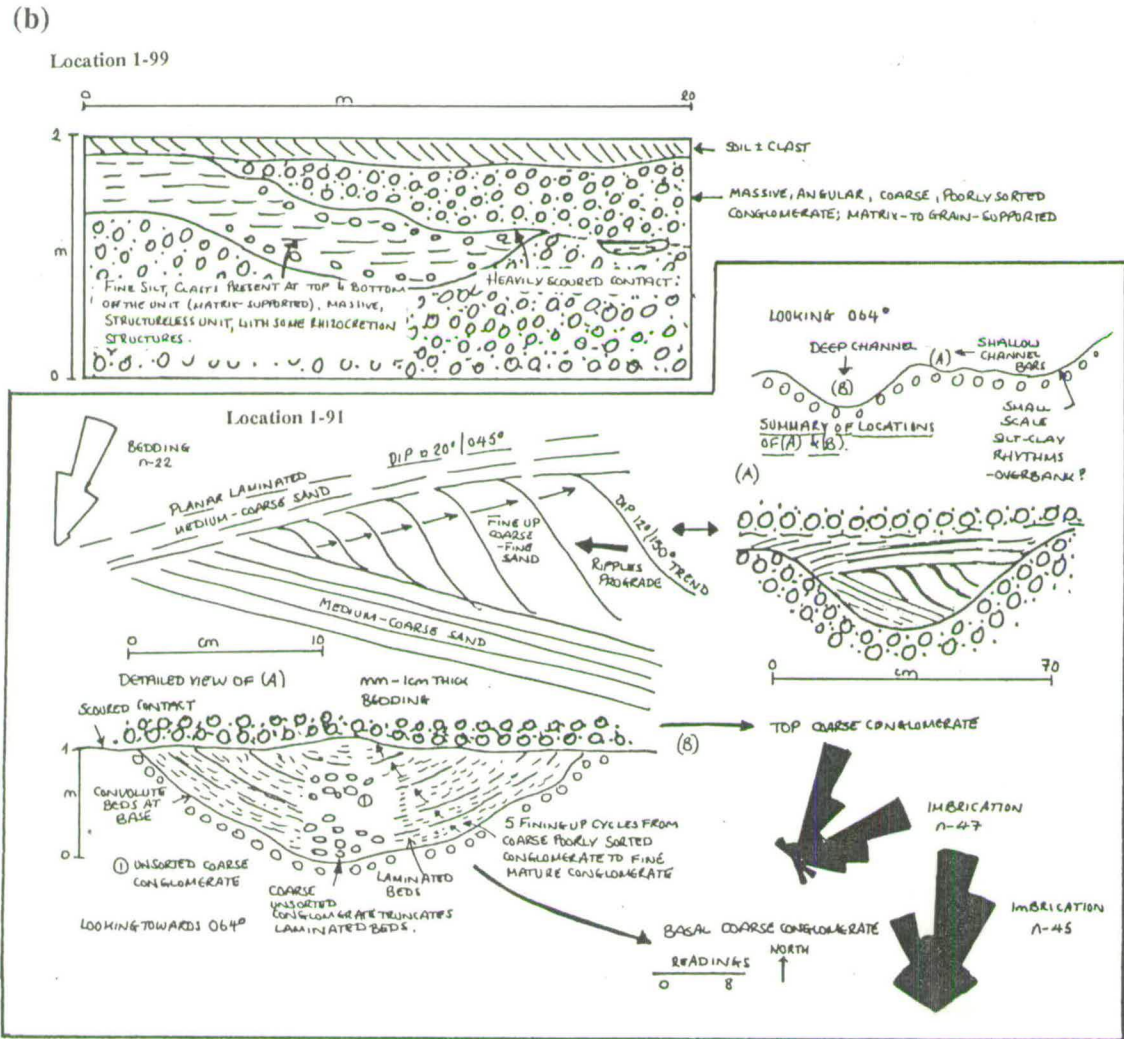
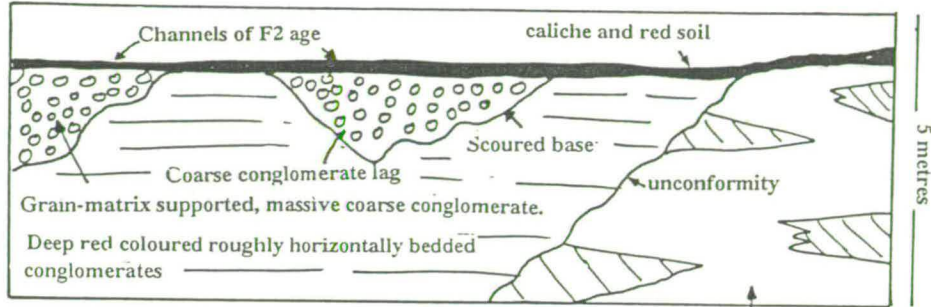


Fig. 5.8. a). Sketch sections of the intermediate units of the Fangelomate Group cropping out at Akaki (location 1-68) and (b). sketches of the structures and sections of the intermediate units at Peratis Hill (location 1-99) and Ayios Ioannis (location 1-91).

Fig.5.9. Sketch sections of the distal sequences of the Fanglerate Group on the north Troodos margin.

Location 1-72



Apalos Formation - Rapidly alternating grey sands, silts and gravels.

Location 1-58

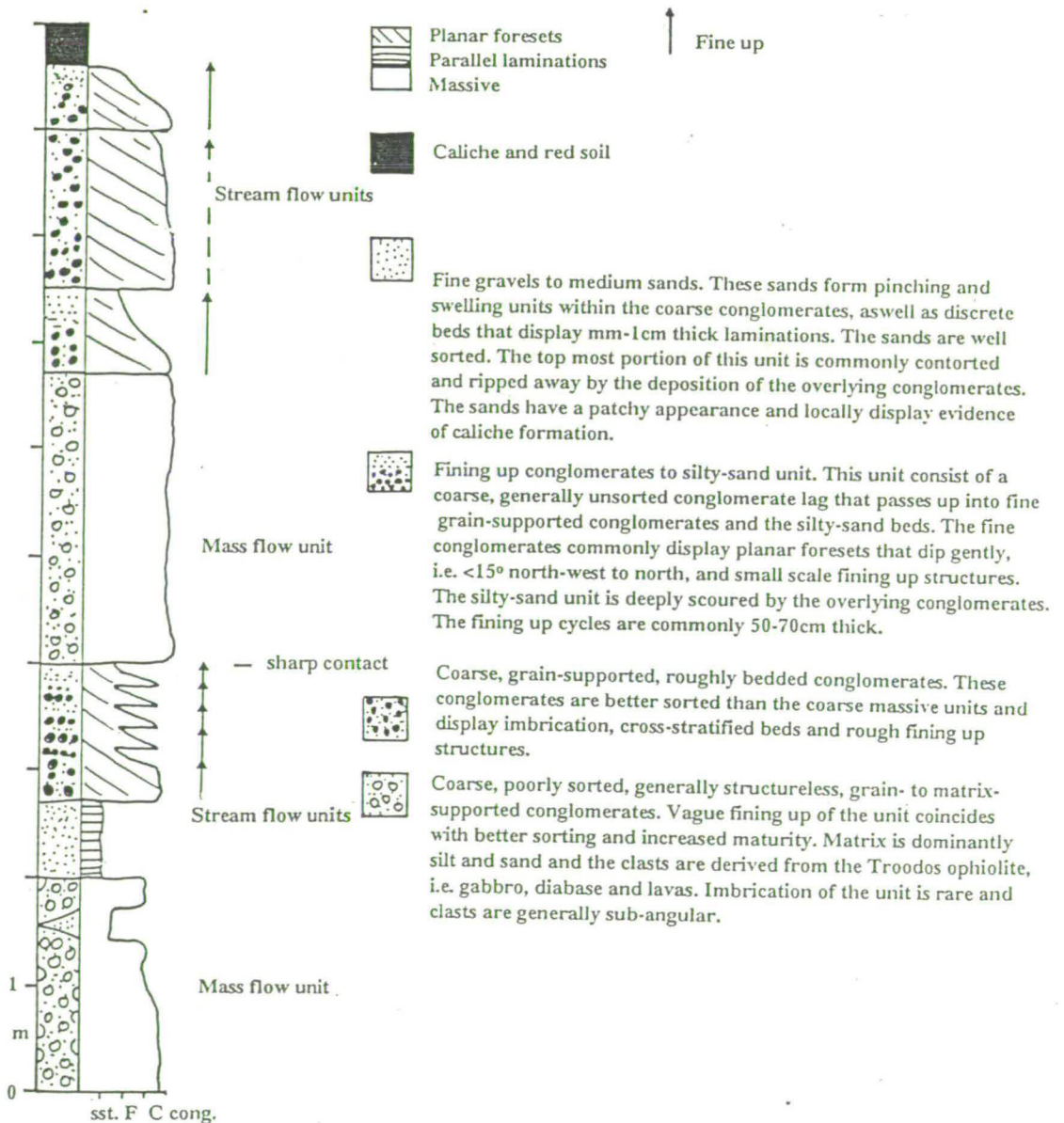
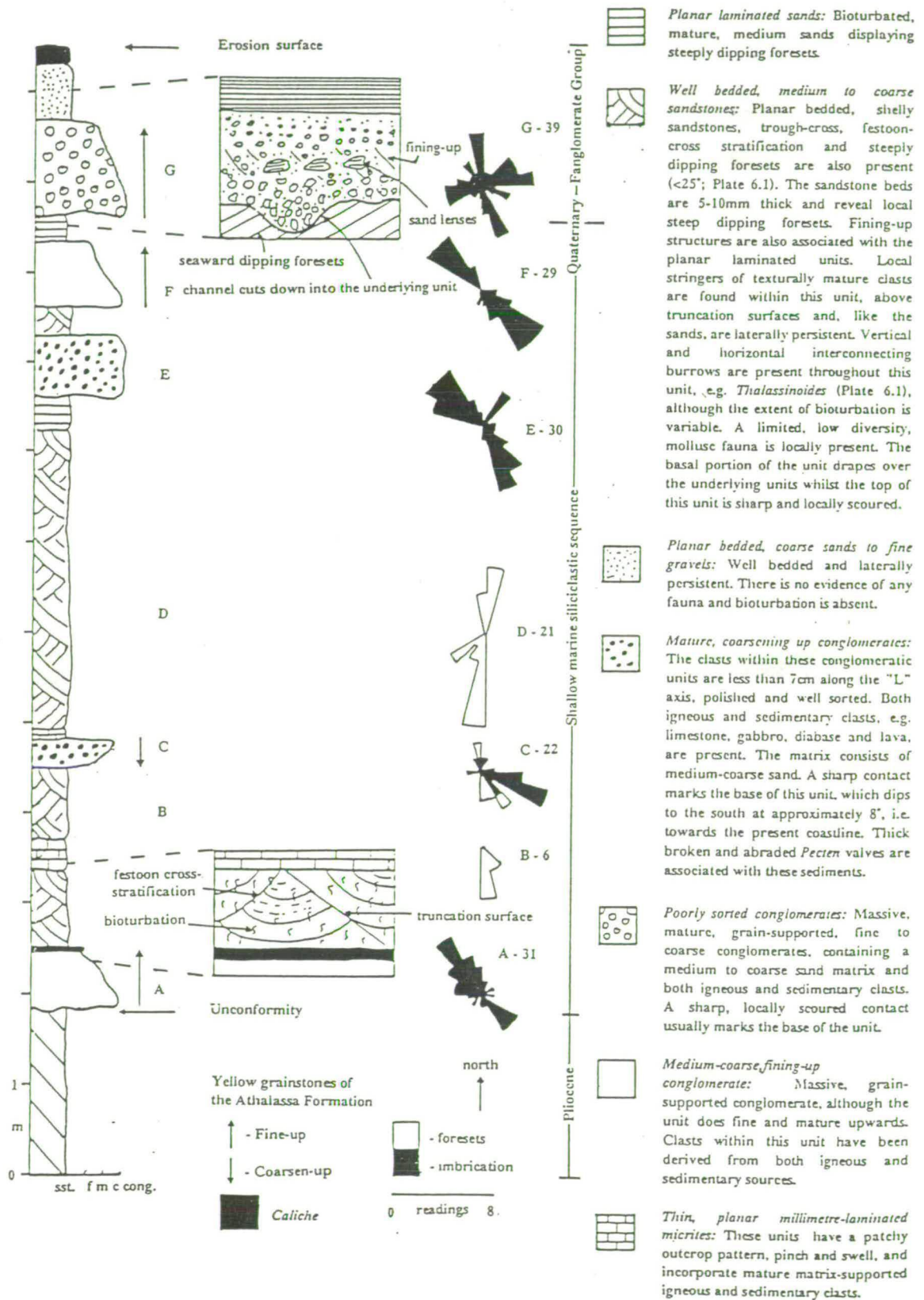




Fig.5.10. Logged section of the Fanglomerate Group units from Dhekelia (location 2-83), south-east Cyprus.

Note: the number next to the rose diagrams refer to the number of measurements taken.



## PLATE 5.2.

E - Illustrating the development of a second coarse pulse of conglomerates capping the F2 sequence at Malounda (location 1-7).

Note: see Fig.5.6 for details.

2b F - Very coarse and imbricated basal conglomerate units of the F2 age sequence at Vyzakia (location 1-19).

Note: the large boulder in the centre of the picture is approximately 1.5m long, the photograph is taken looking towards 030°, the imbrication direction is towards c.300°.

1b G - The contact between the F1 age Fanglomerate unit and the underlying pillow lava sequence at Politiko (location 1-94), an intermediate location on the northern margin of the Troodos Massif.

# Plate 5.2

E



F



G



consist of well sorted, mature conglomerates and sands; these are laterally persistent, graded units. Sedimentary structures other than imbrication are present at intermediate locations (locations 1-89 and 1-91; Fig.5.7). The pattern of sedimentation in the Potami area (locations 1-28 and 1-104; Plates 5.3-5.6) mirrors other intermediate locations that crop out on the north Troodos margin (Fig.5.7), although large channel sequences appear to have cut through the Potami sequences at a later date. The coarse conglomerate at Potami is readily identifiable with the proximal locations seen to the south (location 1-19), as large misfit clasts, up to 1.5m in diameter, are present. Two major conglomeratic phases are present in the Potami sections, separated by soil and caliche horizons (Plates 5.3 and 5.5). The second coarse phase of conglomerate is cut by a large channel and bar sequence. The channel and bar sequence is approximately 200-300m wide, only 3-4m thick, and lateral sediment changes mark the transition from a very coarse conglomeratic channel fill, displaying prograding foresets, to the deposition of fine sediment and the formation of caliche horizons.

Koraka Hill (location 1-92) in the central portion of the Mesaoria Plain provides a typical exposure of the intermediate F1 Fanglomerate unit. The unit lies unconformably above the Pliocene Apalos Formation. The fluvial sediments of the Apalos Formation mark the continuation of the Plio-Quaternary regression in the Mesaoria Basin (Chapter 1). The Apalos Formation consists of a grey, fine grained, fluvial sequence; subordinate conglomerates are also present (McCallum, 1989). The contact between the Apalos Formation and the F1 Fanglomerate unit shows 1-2m of relief, locally, with associated reworking of the Apalos Formation and its caliche and palaeosols. The F1 Fanglomerate unit at Koraka Hill is less than 4m thick and consists of massive, red matrix- to grain-supported conglomerates, with a subordinate silty matrix. The clasts within the conglomerates are angular to sub-rounded and generally less than 60cm in diameter. Caliche development and reddening is prevalent towards the top of the conglomerate sequence. The F1 Fanglomerate unit differs from the underlying Apalos Formation by:

- i) being red rather than grey and buff in colour,
- ii) being coarser grained, with coarse conglomerates and a silt matrix, rather than silts, sands and conglomerates with a chalky matrix,
- iii) having a greater variety of clast types, with a high proportion of gabbro and diabase clasts, rather than the predominance of lava clasts, that are found within the Apalos Formation (Section 5.5.1.1),
- iv) the clasts are generally more angular in the Fanglomerate unit. Other intermediate F1 Fanglomerate units differ from the sequence at Koraka Hill as pulses of massive conglomerate are separated by units of sand and silt (in the area of Peratis Hill, locations 1-93, 1-96 and 1-99; Fig.5.7).

PLATE 5.3.

E - A view of the conglomerate sequence cropping out at proximal-intermediate location of the F2 age Fanglomerate unit at Kato Moni (location 1-101), displaying massive conglomerates, passing up into well bedded units and then massive conglomerates once again.

Note: telegraph pole for scale

F - The preserved F2 age Fanglomerate unit at Potami (location 1-104) displaying a general alternation between coarse conglomerates and sand and caliche development.

Note: see Fig.5.7 for scale and details of the sequence.

G - The F2 age intermediate-distal sequence preserved at Astromeritis (location 1-68), on the north Troodos margin.

Note: the hammer for scale,  
see Fig.5.8. for the details of the preserved sequence.

# Plate 5.3

E



F



G

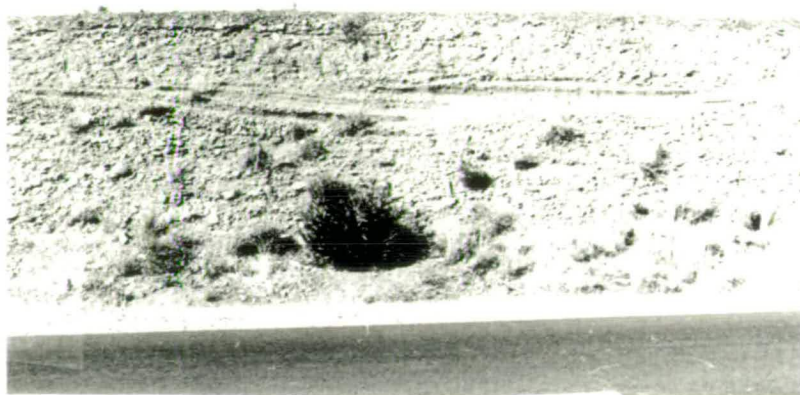


## PLATE 5.4.

D - A view looking towards 092° of the detailed cross-stratified structures of the intermediate F2 age Fanglomerate unit exposed at Ayios Ioannis (location 1-91).

Note: see Fig.5.8. for details and scale.

2c  
E - A flat but locally scoured contact between the sands and conglomerates of the F2 age Fanglomerate unit at Ayios Ioannis (location 1-79).

Note: pen for scale.

F - The develop of a thin lens of sand, less than 20cm thick, overlain by a coarse conglomerate unit at an intermediate location of the F2 Fanglomerate unit at Ayios Ioannis (location 2-91) on the north Troodos margin.

G - The development of a 50cm thick, intermediate, sand unit at Potami (location 1-104) displaying shallow and steeply dipping planar laminated, well sorted, coarse sands.

Plate 5.4

D



E



F



G





## PLATE 5.5.

J - Illustrating the development of sands and silts capped by nodular and powder caliche sandwiched between coarse conglomerate units at Potami (location 1-104) - an intermediate setting.

2d K - A view of the distinct imbrication seen in the conglomerates of the Fanglomerate Group; this example is taken from the intermediate units of F2 age at Potami (location 1-109).

Note: the development of thin sands and the variation in degree of matrix- and grain-support within the unit.

2d L - The intermediate development of two complete cycles of conglomerate deposition at Orounda (location 1-84). The first coarse, immature, poorly sorted conglomerate is capped by powdery caliche; this in turn is overlain by a second coarse conglomerate (c.1m thick) which is once again overlain by caliche.

Note: see Fig.5.7 for details.

Plate 5.5

J



K



L



## PLATE 5.6.

D - The development of alternating units of sub-rounded medium conglomerates with fine well sorted conglomerates seen at Orounda, an intermediate location on the north Troodos margin.

Note: see Fig.5.7. for details.

E - The F1 Fanglomerate unit cropping out at Peratis Hill (location 1-93); this section reveals coarse, poorly sorted conglomerates fining-up into a better sorted, medium conglomerate unit characteristic of an intermediate location.

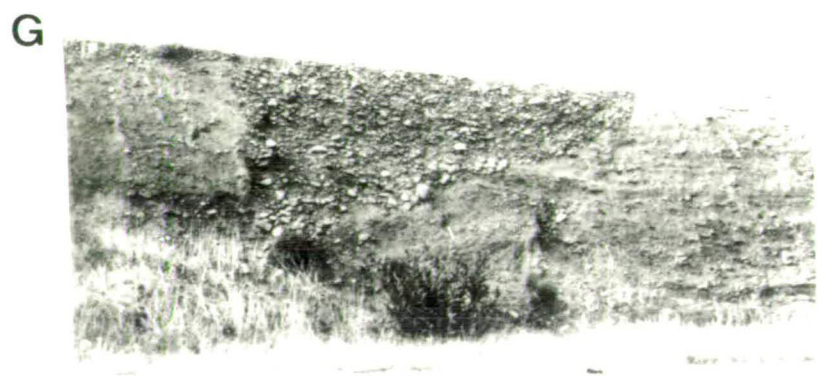
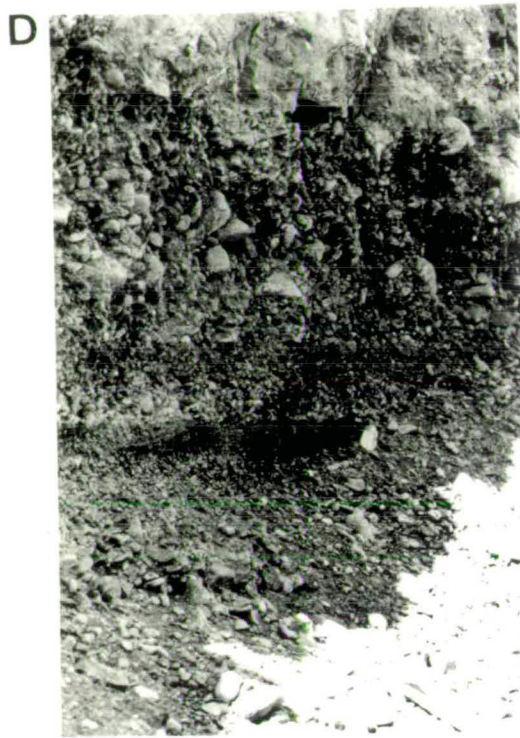
Note: see Fig.5.7 for details.

F - The F1 Fanglomerate unit (dark) cutting down into the Apalos Formation (a) at Kato Koutraphas (location 1-72).

G - F2 age channel cutting into the F1 Fanglomerate unit at Kato Koutraphas (location 1-72) on the north Troodos margin.

2a

Plate 5.6



*iii) Distal development:*

F2 Fanglomerate unit sediments crop out in distal localities, generally more than 5km away from the north Troodos margin (on the main Troodos road between Akaki and Astromeritis, locations 1-12 and 1-27). The F1 Fanglomerate unit is not found in distal location on the north Troodos margin (Chapter 2).

The F2 Fanglomerate, in distal locations, forms well bedded, poorly cemented, channellised deposits, revealing cross-stratification and small fining-up sequences. These distal units unconformably overlie the Troodos lavas and its sedimentary cover sequence (Plate 5.7). Silts and caliche horizons (Chapter 9) are associated with sand and gravels in distal localities. Sections cropping out 10kms north of the proximal F2 Fanglomerate unit exposures reveal a cyclic nature of deposition, with prograding fore-sets overlying massive, structureless conglomerate; caliche and silts cap individual cycles (Fig.5.9; Plate 5.7).

Channels cut down into the preserved F1 and F2 Fanglomerate unit sequences. The best example of this is seen at Kato Koutraphas (location 1-72; Plate 5.6), where Apalos Formation sediments have initially been cut by the F1 Fanglomerate unit, with an unconformable contact. Distal sequences of the red coloured F1 Fanglomerate unit have then been deposited and subsequently incised by channels of the F2 Fanglomerate, which are grey-red in colour. Erosion of the F2 Fanglomerate unit has subsequently lead to the formation of the F2 erosion surface. The F2 Fanglomerate channels are filled with a coarse, immature, grain-supported lag, that passes up into fine grain- to matrix-supported conglomerates. An uneven, scoured contact marks the introduction of immature, massive, poorly bedded, coarse conglomerates, representing the second coarse sediment pulse, that caps many of the exposed F2 sedimentary sequences on the north Troodos margin.

### **5.3.1.3 The F3 Fanglomerate unit (early Late Pleistocene).**

The F3 Fanglomerate unit equates to the Laxia Gravels of Ducloz (1965) and represents a channel fan system which has cut into the mature F2 erosion surfaces (Plate 2.6; Chapter 2). The proximal to distal relationship, associated with the F2 Fanglomerate unit is also incidental here, with examples of the proximal development of the unit cropping out at Vyzakia and Tembria (locations 1-110, 1-113 and 3-66) on the west of the Mesaoria Plain.

In proximal areas the F3 Fanglomerate unit comprises coarse conglomerates similar to those cropping out at proximal locations in F2 Fanglomerate unit (Section

PLATE 5.7.

J - Units of the Kakkaristra Formation (b) unconformably overlain by units of the F2 Fanglomerate unit (a) near Akaki (location 1-12).

K - A section of the distal channel sequences preserved at Astromeritis (location 1-27) on the north Troodos margin.

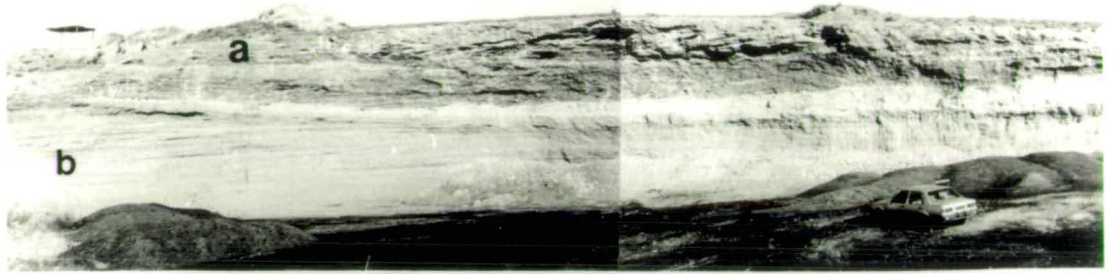
Note: the section is 4m high.  
see Fig.5.9. for details.

L - Sands cropping out between conglomerate units at Astromeritis (location 1-27).  
The sands are not graded, pinch and swell and dip at c.20°.

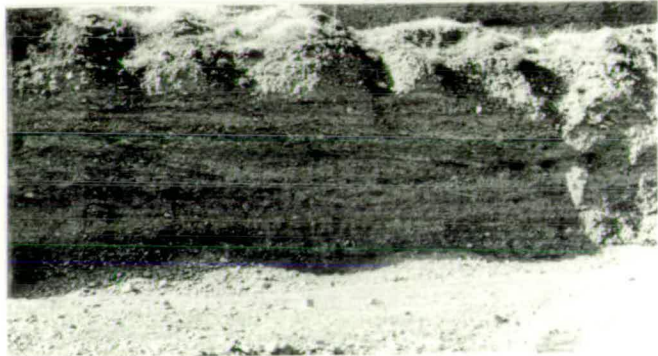
Note: pencil for scale.

Plate 5.7

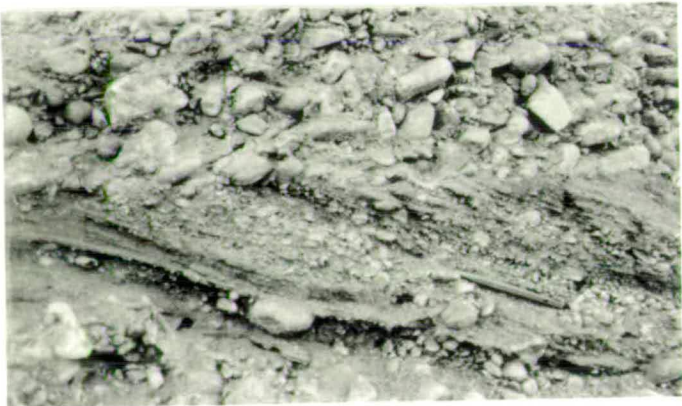
J



K



L



5.3.1.2). The sequences at Vyzakia (location 1-110) crop out at topographically lower levels than the F2 Fanglomerate unit and are c.4-5m thick. A similar pattern is seen to the north of Vyzakia (location 1-113) where the F3 Fanglomerate unit is at a topographically lower level than the F2 Fanglomerate unit but here the F3 unit is in the order of 10m thick. Although the unit is dominated by massive, unsorted, matrix- to grain-supported conglomerates, pockets of well sorted, grain-supported, medium grade conglomerates with associated pebble clusters are also present, although these units are discontinuous. The dominant characteristic of the proximal sequences is their chaotic nature as they have massive bedding and are ungraded. Some large pods of lava, greater than 1m in diameter appear to have been ripped up and incorporated into the unit; these are seen towards the base of the sequence.

The F3 proximal units (e.g. location 1-113) and the bowl-shaped erosion surfaces on the western side of the Mesaoria Plain are commonly capped by caliche, as well as silts and gravels, eroded from the F2 Fanglomerate unit. These sediments appear to form a colluvial deposit that cap the coarse conglomerates of the F3 Fanglomerate unit north of Vyzakia (location 1-113). The colluvial sediments are composed of mixed sands and fine to medium grain-supported gravels. Discontinuous "massive" silty bands are also associated with the sands and gravels. Some of the silt bands may have been derived from the Pliocene silts that crop out beneath the F2 Fanglomerate unit (location 1-115), as these have been eroded to form the bowl-shaped F3 erosion surface (Fig.2.15). The clasts present within the proximal F3 Fanglomerate units in the area to the north and west of Vyzakia (locations 1-113 and 1-114) are dominated by diabase, with subordinate numbers of lava, gabbro and plagiogranite clasts. Many of the lava clasts are angular, reflecting derivation from local sources (Section 5.5).

#### **5.3.1.4 The F4 Fanglomerate unit (late Late Pleistocene).**

The F4 Fanglomerate unit, equating to the Xeri Alluvium of Ducloz (1965), crops out in incised valleys. The F4 Fanglomerate unit, previously described, has been from the central Mesaoria Plain, south of Nicosia (Ducloz, 1965); this study has concentrated on exposures on the western portion of the Mesaoria Plain.

The F4 Fanglomerate unit that crops out on the western Mesaoria Plain forms distinct, commonly vegetated, units lying within 3m of the present river channels. The sediments are predominantly coarse, poorly sorted, grain-supported conglomerates very similar to the facies A1 of McCallum (1989) and to the coarse conglomerates of the F2 and F3 Fanglomerate unit, although the F4 units have a greater proportion of grain to grain contacts. The clasts are predominantly spheroidal and sub-angular. Misfit, oversize



Fig.5.11. Sketch section of the proximal Fanglomerate Group sequences from the sections along the south coast of Cyprus.

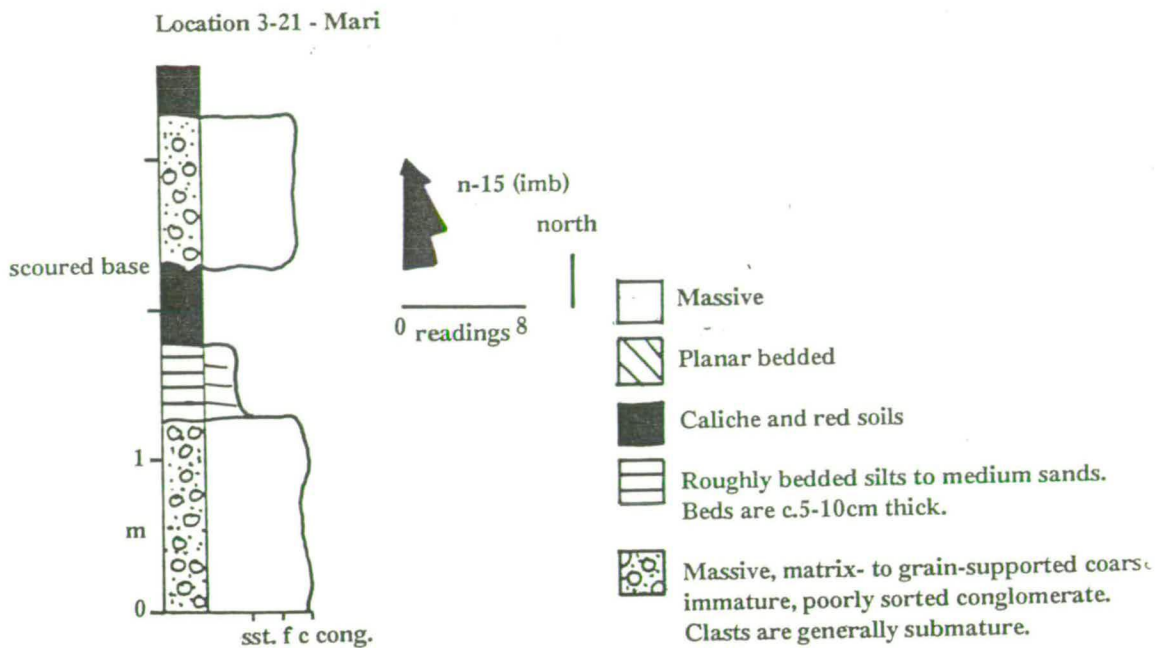
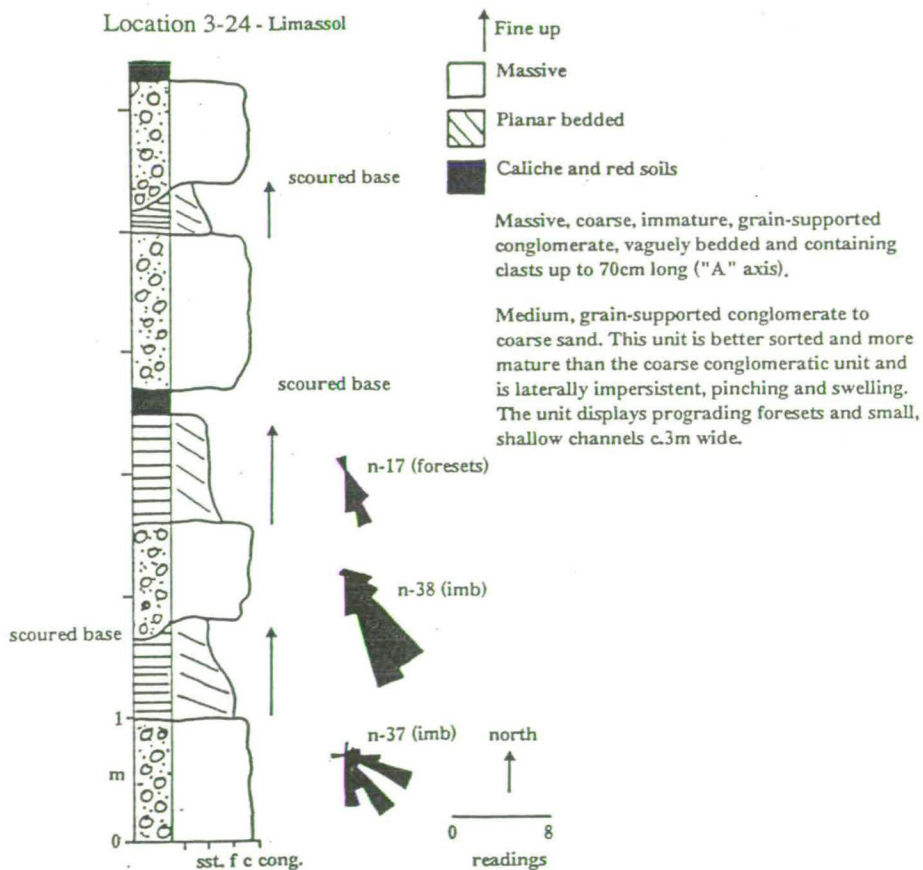


Fig.5.12. Sketch section from distal sequences of the Fanglomerate Group in southern Cyprus.

Note: very rapid lateral changes in the sedimentary sequence are seen (Plate 5.10).



clasts up to 1m in diameter crop out in sections close to Ayios Ioannis (location 1-79); similar sediments are also found further west, e.g. at Kato Moni, in the Kato Koutraphas area and Potami (locations 1-59, 1-83, 1-87 and 1-102, respectively).

The sediments of the F4 Fanglomerate unit on the western Mesaoria Plain are not as variable as those associated with the F2 and F3 Fanglomerate units, a similar pattern is seen on the central Mesaoria Plain (Ducloz, 1965). Ducloz (1965) assigned extensive silt and sand units to the Xeri Alluvium, although these fine-grained sediments are not always present within the F4 Fanglomerate unit of the western Mesaoria Plain.

The F4 Fanglomerate unit on the western part of the Mesaoria Plain crops out within metres of the present day valley floor, however, Ducloz (1965) also described the Xeri Alluvium as being present at heights greater than 20m above the valleys floors.

### **5.3.2 South-eastern Cyprus.**

Units of the Fanglomerate Group in south-east Cyprus represent the easterly extension of the Mesaoria Plain. An extensive erosion surface, commonly capped by red soils and caliche, dominates while associated exposure is restricted. The units of the Fanglomerate Group form a thin cap over much of this area (Section 5.2). A typical exposure is seen in the area to the north of Dhekelia (Fig.2.7) where the Fanglomerate Group unconformably overlies the Pliocene Athalassa Formation and Quaternary shallow marine siliciclastic sequences (Chapter 6). The section resembles that seen at distal locations on the north Troodos margin with channelled sections of poorly sorted, massive, immature, coarse conglomerates being interbedded with mature sands and conglomerates (Fig.5.10). Both igneous and sedimentary clasts are present within the unit, e.g. lava, diabase, gabbro, chalk and chert (Section 5.5.1.2). Imbrication data indicate a variable palaeocurrent (Fig.5.10). The Fanglomerate unit is capped by caliche and red terra rossa-type soils. The presence of Quaternary shallow marine siliciclastic sediments interbedded with this sequence indicates the proximity of this unit to the shoreline during its deposition.

The bone bed cropping out to the south-west of Xylophagou (location 2-75) consists of a well cemented, mature, green sandstone. The bone bed unit is overlain by coarse, poorly sorted unfossiliferous, red conglomerates. The presence of igneous and sedimentary clasts, e.g. grainstones, limestones, diabase, gabbro and lava, within the conglomerate unit indicates a derivation from a number of sources, for example the Troodos ophiolite and the local sedimentary cover sequence. The conglomerates are

unconformably overlain by a sequence of calcarenites, which, in turn are overlain by red silts, sands and poorly sorted, grain-supported conglomerates; these sequences suggest that the bone bed unit may be correlatable with the F3 Fanglomerate unit.

The matrix encasing the mammal bones consists of a well sorted, sub-mature fine to medium sand. Thin section analysis shows that the major components are ophiolitic-derived clasts and minerals, derived sedimentary clasts and abraded fossils and a calcitic cement (Plate 5.9). Ophiolite-derived units consist of lava, diabase lithoclasts and feldspar and pyroxene mineral clasts. The ophiolite-derived clasts are generally less than 0.5mm long and sub-angular; occasional more rounded clasts no greater than 2mm long are also present. The derived fossil fauna are dominated by benthic and planktonic foraminifera. Staining indicates that the  $\text{CaCO}_3$  is dominantly non-ferroan calcite, although some of the fauna stain mauve and blue, indicative of Fe-calcite. Minor abraded mollusc fragments are also present. Delicate ostracod shells are locally concentrated within the matrix. These do not appear to be abraded, or broken, suggesting that they may be primary and *in situ*.

The pore filling cement is dominated by sparry calcite (Plate 5.9). This spar is variably present throughout the unit (Plate 5.9). Circumgranular equant cements surround grains locally. Calcitization has also taken place, relict shell structures are poorly preserved in some clasts and absent in others as if dissolution has occurred. No moldic porosity is seen (Plate 5.9).

### **5.3.3 The south coast between Larnaca and the Akrotiri Peninsula.**

#### **5.3.3.1 Introduction.**

Studies of the Fanglomerate Group on the southern margin of the Troodos Massif have been limited, as the Fanglomerate Group outcrop is very variable. The memoirs of the Geological Survey Department (Bagnall, 1960; Bear & Morel, 1960; Pantazis, 1967) briefly describe the Fanglomerate Group as a series of patchy outcrops of conglomerates, silts and sands. These sediments unconformably overlie, and consist of debris derived from, the Troodos sedimentary cover sequence, the Troodos ophiolite and reworked Fanglomerate Group sediments.

Bagnall (1960) recognised three river terraces in the Larnaca area and correlated these with the marine terraces on the coast. The three terraces recognised by Bagnall (1960) at 80-100 feet, 25-35 feet and 10-20 feet above the valley floor are correlatable with the F2, F3 and F4 Fanglomerate units, respectively, of this study (Table 1.7).

PLATE 5.8.

- J - The development of two distinct fining-up sequences of medium conglomerate to medium sand preserved between two coarse wedges of conglomerate in the Fanglomerate unit at Nikitari (location 1-118) on the north Troodos margin. The higher of the two coarse conglomerate units is capped by soil and caliche.
- K - Sands and conglomerates of the Vasilikos Formation (b) capping the lighter coloured marls of the Nicosia Formation (a) at Vasilikos (location 3-23).
- L - Coarse poorly sorted and immature units of the F2 age Fanglomerate unit (b) cropping out unconformably above the Athalassa Formation (Pliocene) at Episkopi (location 3-28).

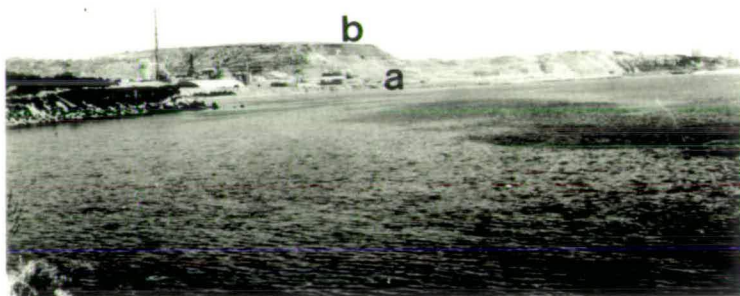
1

Plate 5.8

J



K



L



**PLATE 5.9.**

A - Thin section micrograph of the matrix taken from the bone bed to the south-west of Xylophagou (location 2-75).

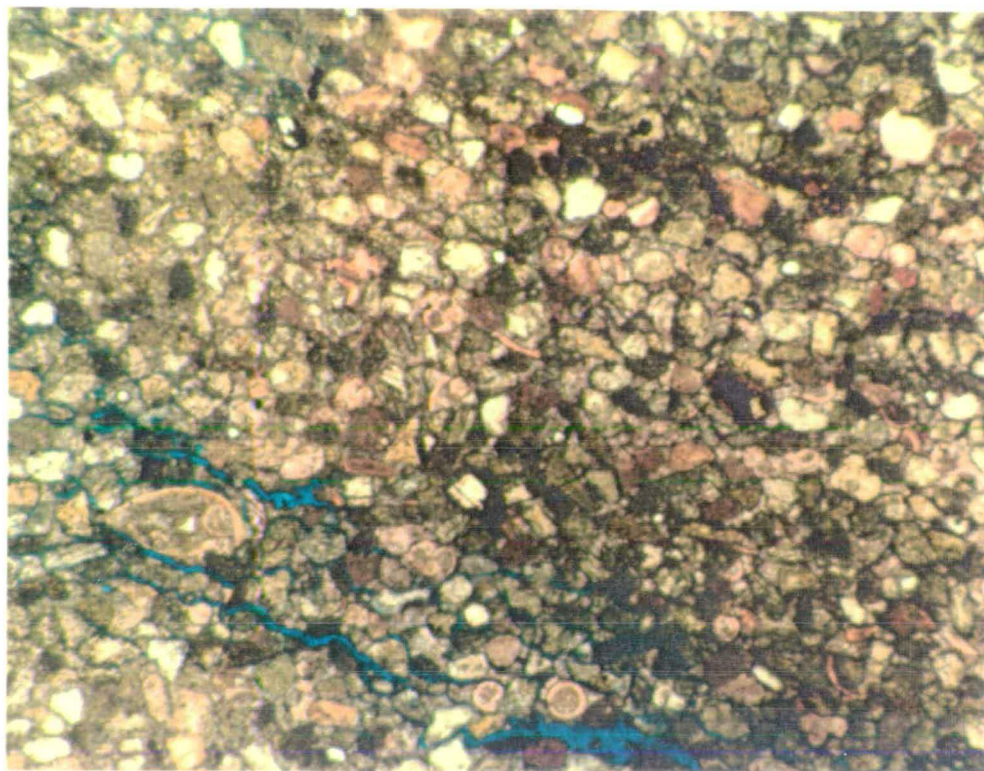
Note: the ostracod tests, planktonic foraminifera, porosity (blue) and the pore filling calcite cement,  
the plate represents a field of view 3mm long.

B - Thin section micrograph of bone and the matrix that encases it. The matrix consists of predominantly sub-angular, reasonably well sorted diabase and lava clasts.

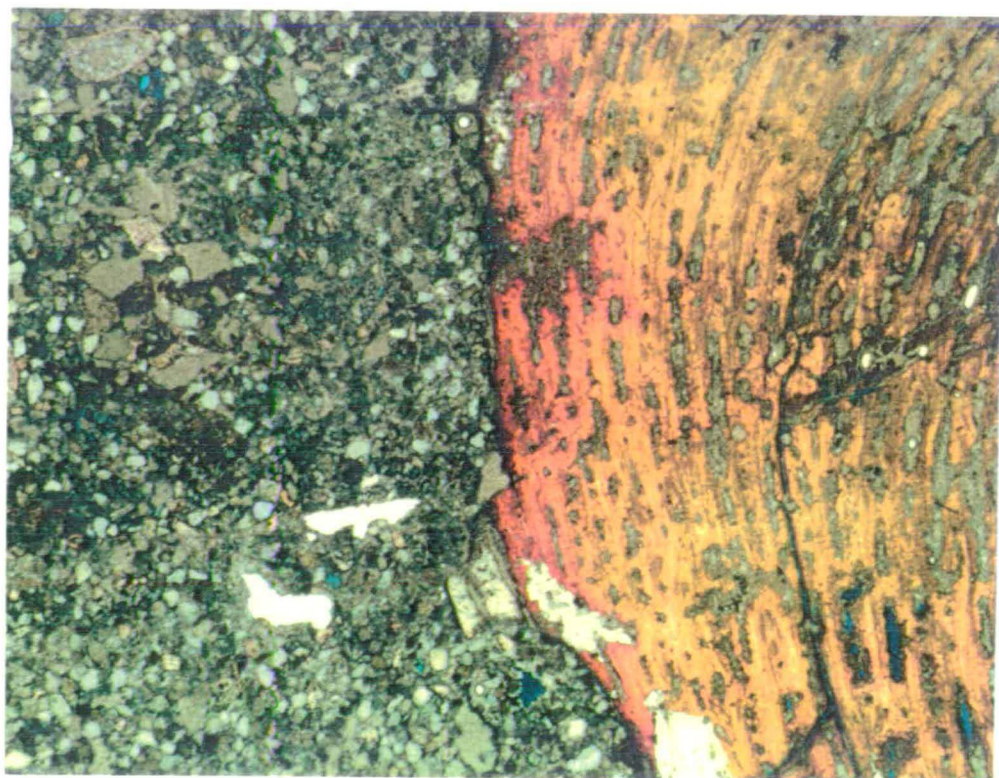
Note: the ostracod test in the top left of the plate,  
the plate represents a field of view 6mm long.

# Plate 5.9

A



B



Pantazis (1967) identified a Higher River Terrace and Alluvium which correlate with the F3 and F4 Fanglomerate units respectively (Table 1.7). Correlations between the lower Vasilikos Valley and other areas of Cyprus were made by Gomez (1987; Table 1.8), who identified four phases of Fanglomerate Group deposition correlatable with the F1 to F4 Fanglomerate units here.

The patchy development of the Fanglomerate units inland, away from the coast, makes correlation difficult. Correlation of the Fanglomerate Group, on the southern Troodos margin was, however, made by means of relative altimetry and correlation with depositional terraces and erosion surfaces (Chapter 2). Correlation at coastal sites was eased by the association of marine terraces and the fluvial sediments of the Fanglomerate Group (Chapter 2).

### 5.3.3.2 The F1 and F2 Fanglomerate units (lower-middle Pleistocene).

The F1 Fanglomerate unit in coastal southern Cyprus is manifested by small, thin, patchy outcrops, for example to the north-west of Tersephanou (north-west of location 3-16), and by the development of terraces within 80m of the basement units in the lower Vasilikos Valley (Gomez, 1987). The outcrops in the Limassol area form isolated exposures and cap hills. It is sometimes difficult to distinguish between the F1 and F2 Fanglomerate units, hence their description together here. Where distinct F1 units are seen, they commonly consist of clasts derived from the Troodos ophiolite and its sedimentary cover, for example north-west of Tersephanou (north-west of location 3-16) where the F1 unit unconformably overlies the chalks of the Lefkara Formation. Gomez (1987) has distinguished between the F1 and F2 Fanglomerate units in the lower Vasilikos Valley, *viz.* the Phalarkros and Mitsinjites terraces (Table 1.8).

The F1 and F2 Fanglomerate units that crop out in proximal-intermediate locations along the southern margin of the Troodos Massif form remnant, isolated outcrops capping hills. The sedimentary sequences are commonly 3-4m thick and resemble those cropping out on the north Troodos margin (Section 5.3.1). Coarse immature, poorly sorted conglomerates dominate the sequence, while subordinate quantities of finer grained sediments, red palaeosols and caliche horizons are also present (Fig.5.11). The coarse conglomerates tend to be matrix- to grain-supported and mirror the A1 facies of McCallum (1989). Two distinct units of coarse conglomerate separated by finer sediments, caliche and palaeosols are seen at a number of localities - north-east of Zyyi (locations 1-163 and 3-20) and south of Mari (location 3-21; Fig.5.11). Derived lava, diabase and chalk clasts constitute the largest proportion of the clasts seen within these units although chert, limestone, gabbro and ultramafic clasts are also present



locally. The presence of clasts is related to the location of the outcrop *vis-a-vis* the drainage pattern (Fig.2.1; Chapter 2). The clasts are generally sub-angular and usually less than 70cm along the "L" axis. The igneous-derived clasts are commonly more mature than those derived from the Troodos sedimentary cover sequence.

The Vasilikos Formation (McCallum, 1989) is correlated with the F1 Fanglomerate unit as it unconformably overlies marls of Pliocene age at Vasilikos (location 3-23; Plate 5.8), crops out within 80m of sea-level and can be correlated with exposures cropping out at Pissouri and in the Larnaca area. The distal sediments of the F1 and F2 Fanglomerate units in the area between Larnaca and the Akrotiri Peninsula resemble the Fanglomerate exposures from the Dhekelia area, south-east Cyprus (Section 5.3.4), as well as distal outcrops on the north Troodos margin. The distal sequences show a variety of sediments, including coarse conglomerates, well bedded fine and medium conglomerates, sands, palaeosols and caliche horizons (Fig.5.12). The coarse conglomerates resemble those seen in proximal localities (see above). These are poorly sorted, immature and massive although some crude bedding is locally present, e.g. the Limassol area (location 3-26). The clasts within the conglomerates are generally 30-40cm along the "L" axis, sub-angular and quite immature, e.g. a roundness value of 0.5-0.6, on the visual roundness scale of Krumbein (1941). Outsize clasts less than 70cm long are also present within the conglomerate units. In the area north of Limassol (location 3-26) where the Garyllis River runs through its enclosed valley, coarse conglomerates of facies A1 (after McCallum, 1989) dominate while a mixed sedimentary sequence is seen 100m south of location 3-26. The mixed sedimentary sequence is more mature, better bedded and contains a greater proportion of sand and silt than associated with the coarse conglomerate unit.

### **5.3.3.3 The F3 Fanglomerate unit (early Late Pleistocene).**

The F3 Fanglomerate unit crops out in many of the large river valleys along the south coast of Cyprus, e.g. Kouris and Pendaskinos Rivers (Fig.2.1). The F3 sections generally occur within 15m of the present day channels. The pattern of sedimentation in many of the valleys is similar. Massive, structureless, grain- to matrix-supported coarse conglomerates are overlain by more mature, generally well bedded and sorted conglomerates, sands and silts (Plate 5.10). The well bedded units are locally graded and commonly interbedded with palaeosol and caliche horizons (Plate 9.2). The top of the well bedded unit is commonly scoured. This marks the onset of the third unit; a coarse, structureless conglomerate, which is analogous to the basal unit. Examples of this sequence are seen at Alaminos, near Kophinou (locations 1-157, 1-155 and 1-162; Fig.5.13). These sequences mirror those F3 successions that crop out on the coast

Fig.5.13. Sketch sections of the F3 Fanglomerate units from the south coast of Cyprus.

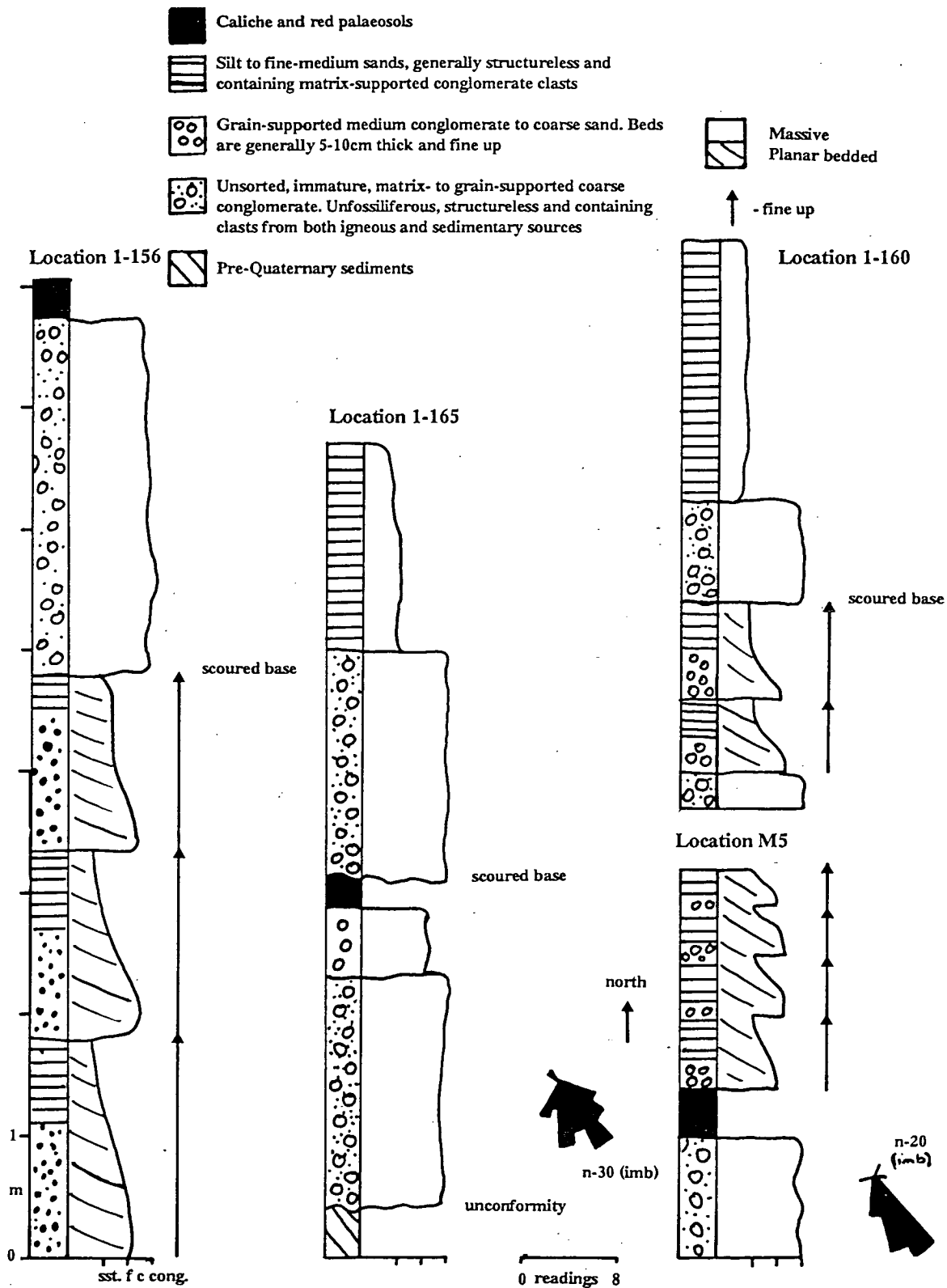


PLATE 5.10.

**J - Distal exposures of the F2 age Fanglomerate unit cropping out at Yermasoya (location 3-24), on the southern margin of the Troodos Massif, displaying a series of small channels and bars picked out by the alternation between the conglomerate and sand units.**

**Note: see Fig.5.12 for details.**

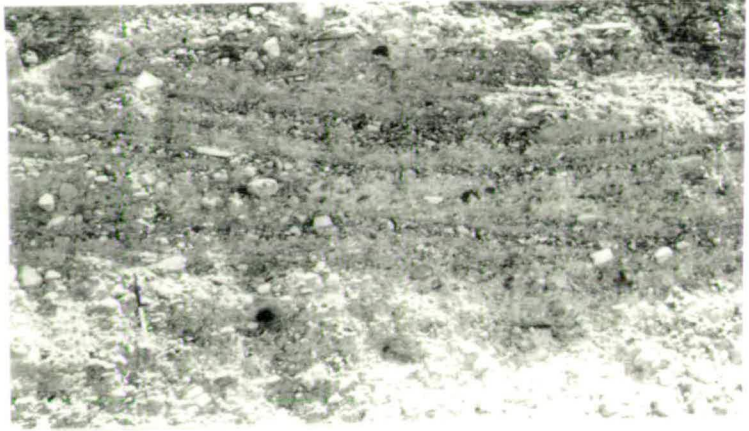
**K - A view, looking east-north-east, of the structures present in the distal channel sequences of the F2 age Fanglomerate unit at Yermasoya (location 3-24).**

**Note: planar bedded units at the top of the plate overlying a series of prograding foresets (dipping to the right; south) to the right of the scale.**

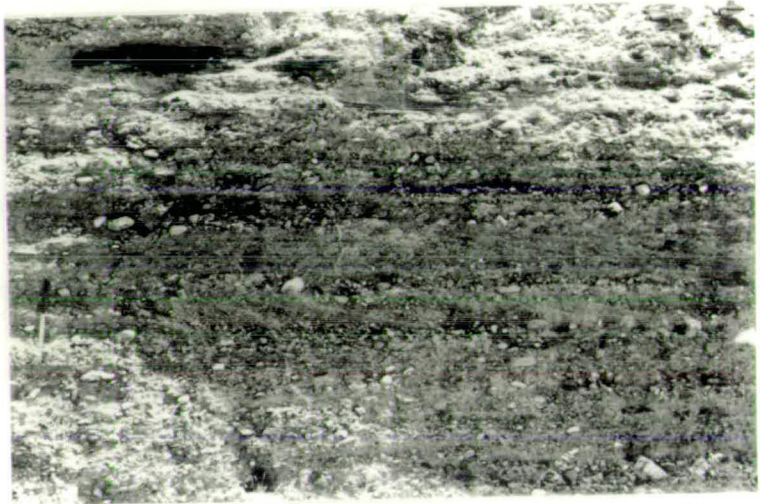
**L - A large channel (b) of F1 age, running 080°-260°, cutting through the Miocene chalks (a) at Kouklia (location 2-54).**

Plate 5.10

J



K



L



between Larnaca and Limassol and were previously interpreted as marine sediments (Bagnall, 1960). It is proposed that the sequences Bagnall (1960) described are actually fluvial sequences.

The typical sequence (Fig.5.13) does not always occur and the following are locally present:

- i) a lack of the well bedded units, e.g. at Khirokitia and north of Maroni (locations M1 and 1-165, respectively; Fig.5.13),
- ii) extensive areas of fine sand and silt which are capped by a unit of coarse, immature, conglomerate, 50-60cm thick (location 1-155),
- iii) the presence of well developed palaeosol and caliche horizons between the basal, massive conglomerate and the well bedded units, e.g. south of Maroni (location M5; Fig.5.13).

#### **5.3.3.4 The F4 Fanglomerate unit and Recent fluvial sediments (late Late Pleistocene-Recent).**

The F4 Fanglomerate unit is best exposed in the major river valleys that issue from the Troodos Massif and in coastal exposures. Exposures in the valleys are at lower topographic levels than the F3 Fanglomerate unit, as seen on the north Troodos margin and recorded by Gomez (1987) for the lower Vasilikos Valley. Excavation pits in the lower Vasilikos Valley (Gomez, 1987) show that 3 to 5 units of silts were deposited at this time, comprising centimetre-sized rhythmic cycles, intercalated with calcareous horizons. The outcrops on the secondary road between Larnaca and Limassol (locations 1-155, 1-156 and 1-165) are generally fine grained, i.e. sand and silt grade, in contrast to the earlier phases of the Fanglomerate Group deposition in this area. The sands and silts cover much of the valley floor but massive, poorly sorted, immature conglomerates are also present. The conglomerates are generally grain-supported and incorporate clasts less than 60cm in diameter. Igneous clasts dominate the units, i.e. lava and diabase, although immature chalk clasts are also present. Local caliche formation has taken place above the conglomerate units resulting in the formation of caliche crusts on clasts of the conglomeratic unit (location 1-162).

The floor of the Vasilikos Valley shows evidence of downcutting by 6m. This was followed by a period of aggradation and alluviation between 5540 to 5010 B.C. (Gomez, 1987). The aggradation preceded a phase of fine-grained overbank sedimentation and subsequent downcutting to form an alluvial terrace within 2m of the present floodplain, as seen in the Tremithios Valley (Gifford, 1978). Incision into this terrace has occurred since Byzantine (c.330-1190 A.D.) times (Gifford, 1978). The conglomerate units cap

Fig.5.14. Sections of the F4 Fanglomerate unit sequences cropping out in southern Cyprus.

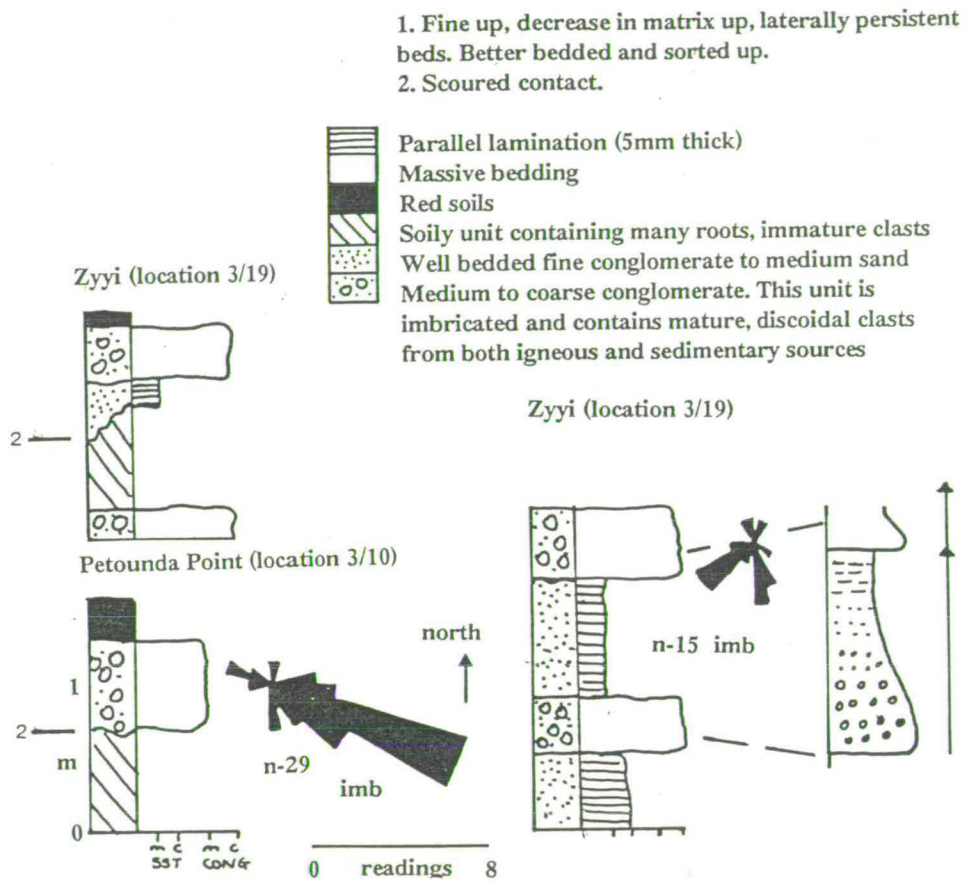
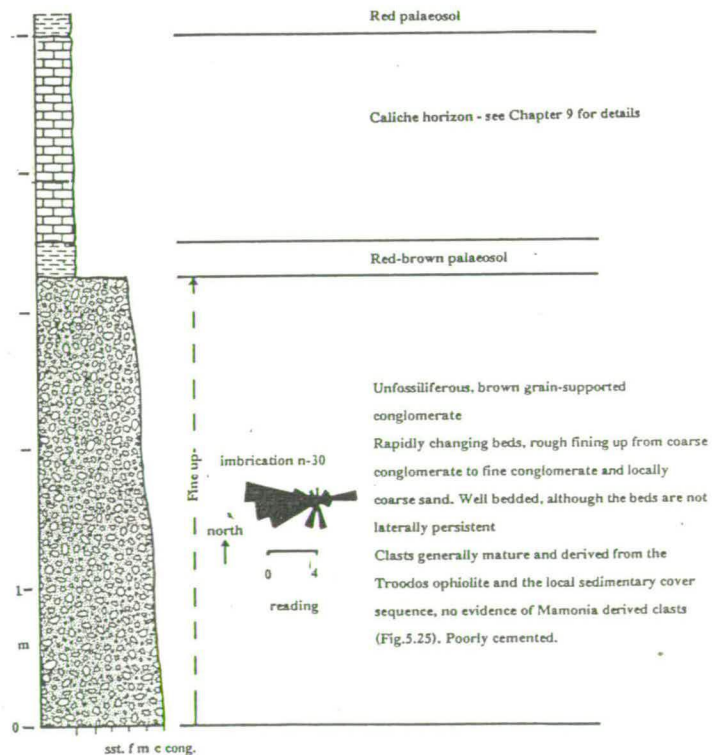


Fig.5.15. Section of the F1 distal sequence preserved at Pissouri (location 3-30).



silty and sandy alluvium in many places (location 1-162). Muddy, poorly sorted alluvium was deposited in the Tremithios River in the Larnaca lowlands (Gifford, 1978) during the latest Pleistocene and early Holocene.

The F4 units have cut down into the underlying Troodos sedimentary cover sequence, for example in the Maroni River valley (locations 1-156 and 1-165), showing that formation of the F4 unit was not purely aggradational. The valleys of the south Troodos margin, e.g. the Pendaskinos River valley (Fig.2.1), are presently c. 300-400m wide and commonly are covered in alluvium; many of these valleys contain misfit streams today.

Seismic surfaces offshore along the south coast, cut by inferred channels of F4 age, can be correlated with fluvial channels onshore, e.g. Zyyi (McCallum, 1989). These shallow conglomerate-filled channels are incised into floodplain conglomerates similar to those associated with the F4 Fanglomerate unit along the southern margin of the Troodos Massif.

Coastal exposures of the F4 Fanglomerate unit are best exposed in Zyyi and Petounda Point (locations 3-19 and 3-10) where sections are presently being eroded by marine action. The sections are generally less than 2m thick and are dominated by massive, poorly consolidated, coarse conglomerates, well bedded sandstones, fine gravels and palaeosol horizons (Fig.5.14). The dominant clasts within the conglomerate units are chalk, lava and diabase.

### **5.3.4 South-western Cyprus.**

#### **5.3.4.1 Introduction.**

There have been no previous studies of the Fanglomerate Group sediments in south-west Cyprus. The Fanglomerate Group is generally poorly exposed in the Paphos area. Outcrops are restricted to quarries, road cuts, river sections and palaeo-clifflines. Five areas of exposure will be described here, in chronological order:

- i) the outcrops of the F1 Fanglomerate unit in the Pissouri area,
- ii) the F1 channel sequences recorded in the road cuts north of Kouklia, at approximately 120m ASL,
- iii) the F2 and F3 fluvial sequences preserved in the area to the north and east of Paphos cropping out in agricultural terraces in the Ezousa River valley (Fig.2.1) and in the palaeo-cliffline in the region of Kouklia and Akhelia,
- iv) limited F4 exposures on the lower coastal plain between Paphos and Kouklia,

v) the floodplain deposits that crop out in the area of Kissonerga, north of Paphos.

#### **5.3.4.2 The F1 Fanglomerate unit (lower Pleistocene).**

The F1 Fanglomerate unit crops out in cliffline exposures, c.100m ASL, at Pissouri (location 3-30) unconformably overlying ?Pliocene conglomeratic fan-delta and marl sequences. The conglomerate unit is covered by a mature erosion surface. The sequence (Fig.5.15) consists of rapidly changing, poorly cemented, broadly fining-up, channelled, conglomerates. The sequences are presently in the order of 5m thick and are overlain by red terra rossa-type palaeosols and thick caliche horizons (Chapter 9). The clasts within the conglomeratic units have been derived from the Troodos ophiolite, i.e. gabbro, diabase and lava and the local sedimentary sequence, i.e. chalks and marls. Ultramafic and Mamonia-derived clasts are not present within this sequence (see Section 5.5 for a more detailed description and discussion of clast provenance). The palaeocurrent data (Fig.5.15) reveal a dominant flow from the east to the west, some evidence for southward flow is also present.








#### **5.3.4.3 Channelled F1 Fanglomerate unit sequences.**

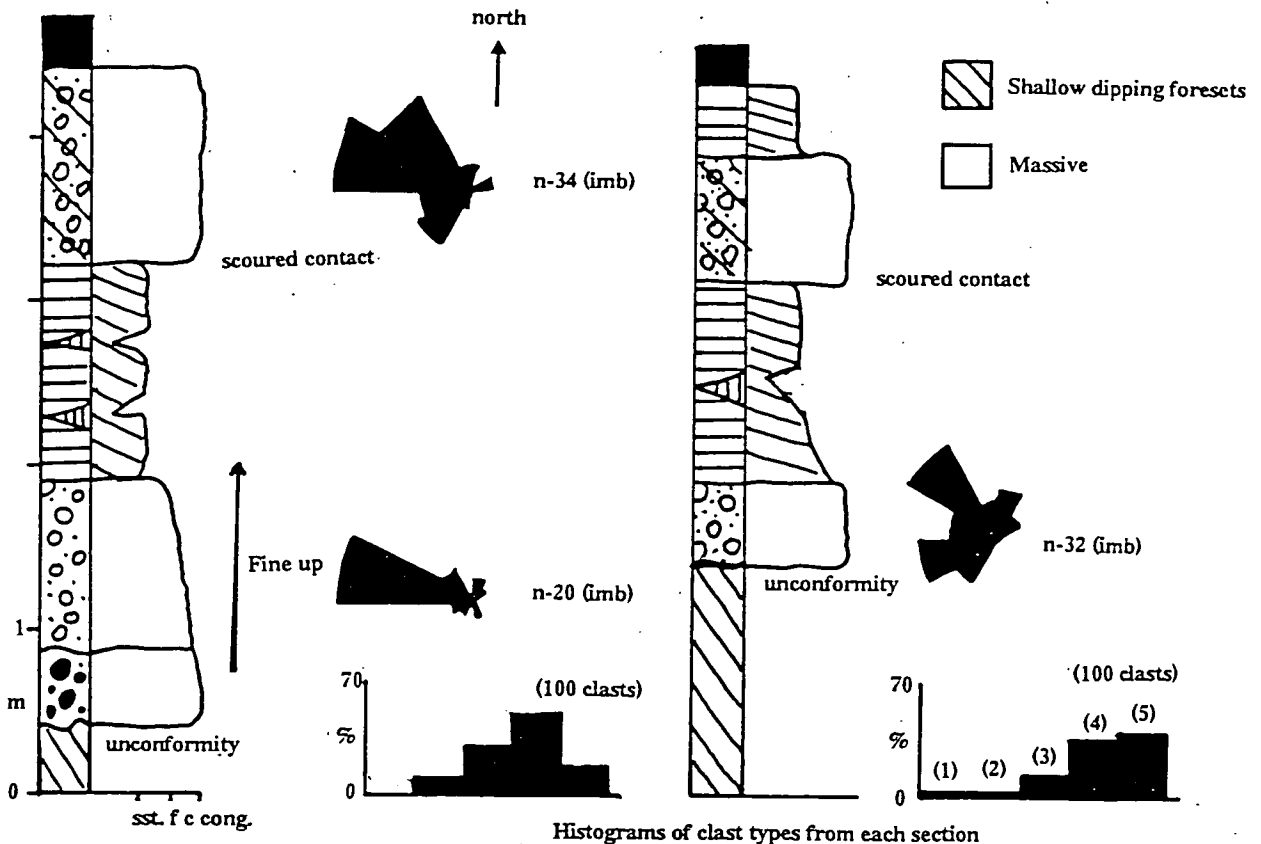
The channelled fluvial sequences lie 70-80m beneath an exposure of earlier fluvio-deltaic sediments (Chapter 6). The channelled sequence is probably correlatable with the F1 depositional phase as the top of the exposure has been eroded to form part of the F1 erosional surface in this area and the F2 cliffline lies topographically beneath this exposure, to the south, in the area around Kouklia (Fig.5.16). The Fanglomerate Group sequence is preserved in single large channels between 40 and 50m wide with a maximum depth of 3.5m (location 2-54). These channels (Plates 5.10 and 5.11) have cut down into the underlying marls of the Pakhna Formation. The channel fill sediments are capped by terra rossa-type soils. A cyclic sedimentary sequence is seen in the mid-point of the channels; a basal unit of coarse conglomerate is succeeded by a vague fining-up unit (fining up to fine gravels) and the cycle is completed with the deposition of a second coarse conglomerate unit which scours into the finer sediments beneath. The second coarse conglomerate unit caps the sequence (Fig.5.16). The pattern of sedimentation within the channel is similar to the intermediate and distal localities on the north Troodos margin (Section 5.3.1).

A second channel sequence unconformably overlies the Pakhna Formation to the west of location 2-54. Units B, C, D, E and F are all present within this second sequence, although there is no major basal lag (Fig.5.16 - log B). The clast composition data from the conglomerates at both localities are very similar (Figs.5.16) although the second



Fig.5.16. Sketch section of the early Quaternary channel sequences that crop out at Koukليا (location 2-54), illustrating palaeocurrent and clast composition data.

-  Unit F: Caliche and red soil
-  Unit E: Coarse conglomerate; this unit has similar characteristics to unit B. The clasts, which show Troodos Massif and Mamonia Complex affinities, are generally not as mature, nor as well rounded as those seen in unit B.
-  Unit D: Fine to medium sands lenses within unit C
-  Unit C: Well bedded (5-10cm thick), grain-supported, fine and medium conglomerates. The clasts within this unit are well sorted, mature and dominated by Troodos-derived lithologies (mainly diabase and lava). The clasts are generally less than 5cm along the "L" axis and spheroidal. The unit is generally well sorted, but rare pockets of fine sand and silt are present. These sands and silts are well bedded forming planar units approximately 1cm thick. This unit is poorly cemented. The unit grades laterally, the proportion of the fine gravels and sand increasing towards the edge of the channel, whilst the proportion of the coarse conglomerates increases towards the centre.
-  Unit B: A grain-supported coarse conglomerate. Locally, fine gravels and coarse sands form the basal unit of this sequence. The contact with the underlying sediments is very irregular. The clasts within the conglomerate unit are generally mature and poorly sorted. Derived igneous clasts dominate and the matrix is mainly derived from the local pre-Quaternary sedimentary sequence being chalky and fine-grained. Some fine gravel is also present within the matrix. A vague fining-up sequence is seen, with better sorted, smaller clasts being present towards the top of the unit. This unit varies laterally, with finer conglomerates at the edges of the channel and very coarse conglomerates in the centre. The unit is poorly cemented throughout.
-  Unit A: Very coarse conglomerate which scours down into the underlying marls
-  Marls - Pakhna Formation



(A)

(1) Serpentinite, (2) Gabbro  
(3) Diabase, (4) Lava, (5) Sediment

(B)

Fig.5.17. Sketch section of the F2 Fanglomerate units that crop out in the Akhelia area, east of Paphos.

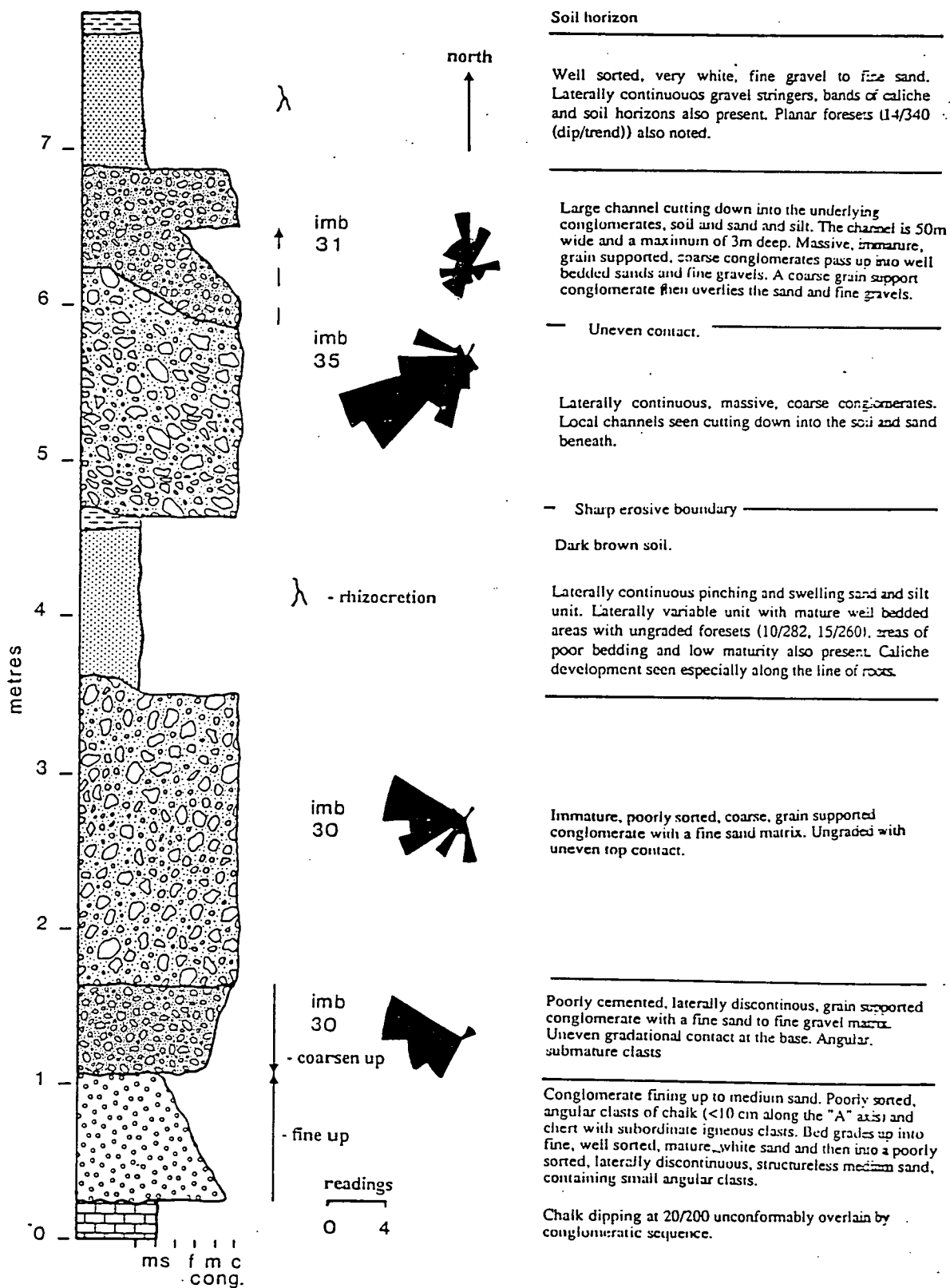


PLATE 5.11.

J - A detailed view of the F1 age channel sequence exposed at Kouklia (location 2-54).

Note: see Fig.5.16 for details.

K - A overview of the F2 age distal braid sequences (b) cropping out above chalks of Miocene age east of Akhelia (location 2-45).

L - A detailed view of the F2 age distal braid sequences cropping out in the quarries at Akhelia, to the east of Paphos (location 2-45).

Note: see Fig.5.17 for details.

Plate 5.11

J



K



L



sequence contains a higher proportion of locally derived sedimentary clasts. The palaeocurrent data from imbrication data collected from both section indicates a flow towards the west to north-west (Fig.5.16).

#### **5.3.4.4 The F1 and F2 Fanglomerate units cropping out in the Paphos area (lower-middle Pleistocene).**

A series of multi-channelled, fluvial Fanglomerate Group sediments of both F1 and F2 age crop out in the area between Yeroskipos and Kouklia (locations 2-44, 2-45, 2-46, 2-48 and 2-63; Plate 5.11). These exposures all have similar characteristics, seaward dipping imbrication, lenticular beds and a general alternation between the deposition of conglomerate and fine silt and sand (Fig.5.17). The units are generally poorly sorted and immature. The fine fractions show evidence for the formation of caliche and soil horizons. One palaeosol horizon is seen forming along the basal contact between the pre-Quaternary marls and chalks, and the Pleistocene sediments, e.g. Koloni (location 2-59). This in turn, is overlain by a sequence of channelled conglomerates. The channels are generally either wide and shallow (1.3m wide by 20-30cm deep), or deeper and narrower (1m by 50-60cm).

#### **5.3.4.5 The F3 and F4 Fanglomerate units in south-west Cyprus (Late Pleistocene).**

The F3 and F4 Fanglomerate units are best exposed to the south-east of Paphos. The fluvial sequences crop out as either river (locations 2-41 and 2-43), or coastal sections (locations 2-42 and 2-57). The F3 and F4 Fanglomerate unit sequences crop out topographically beneath the F2 cliffline and form part of a coastal plain that probably formed during the Late Pleistocene, i.e. F3 and F4 times. The preserved fluvial sequences are probably F4 in age, post-dating the formation of the F4 littoral sequence seen in Paphos (location 2-4) and at Paphos International Airport (location 2-50).

The coastal sections are generally less than 2m thick and show two facies coarse, grain-supported, massive conglomerates (which lie above the present day storm beach and act as a source of sediment to the marine environment, through active present day erosion of these outcrops) and brown, fine sands and silts (Fig.5.18). There is a broad alternation of deposition between the conglomerate and sandy-silt units (locations 2-42 and 2-57; Fig.5.18). The sedimentary sequences within the river sections consist of well bedded alternating conglomerates, sands and silts (location 2-41; Fig.5.18). The beds are laterally impersistent but are cyclic, similar to that found in the coastal sequences (see above; Fig.5.18).

Grain-supported, immature, imbricated coarse conglomerate. This unit is generally poorly sorted though some rough fining up from coarse to medium-fine conglomerate is seen. Clasts are derived from local sediments and both the Troodos Massif and the Maonia Complex. The clasts are generally spherical though some discoidal clasts are present. The unit has a matrix of fine sand to fine gravel, with little cement. Small lenses (<10cm thick) of sand are seen towards the top of the unit.



Well bedded (2 - 3cm thick), laterally continuous, coarse sand, truncated by small channels containing coarse sands and fine gravels. The unit has an uneven contact at the base and is scoured at the top.



Soil and caliche with minor matrix supported clasts



Brown silt to medium sand. This unit is generally structureless, laterally continuous and mature. The basal contact is uneven and the overlying contact with the conglomerates is scoured. Some globules (<1cm diameter) of soft caliche are seen and rhizcretion structures are present.

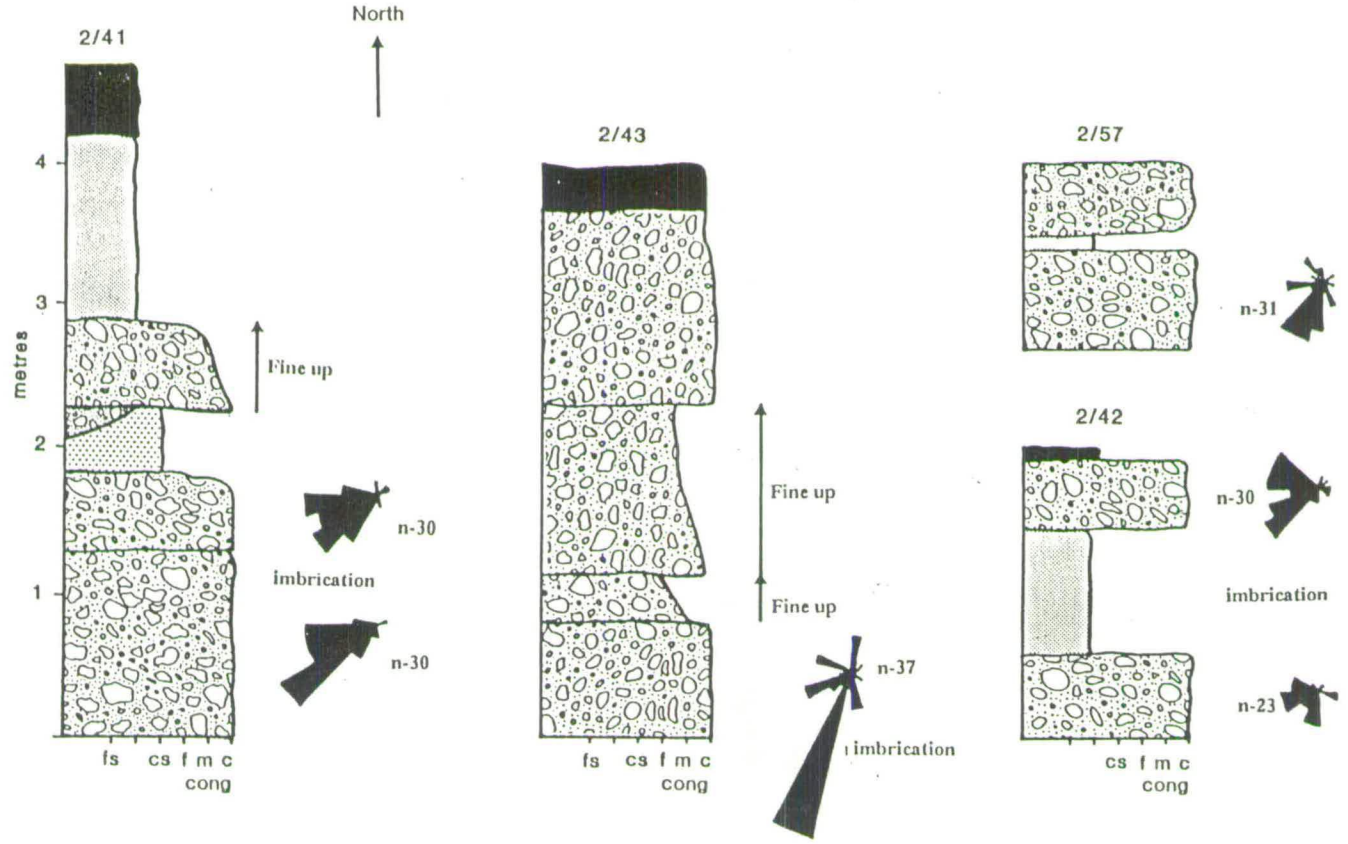


Fig.5.18. Sketch sections of the F4 Funglomerate unit in the Paphos area.

### **5.3.4.6 Floodplain sequences of south-west Cyprus.**

Extensive fine-grained sedimentary sequences that have not previously been described, or included, in the Fanglomerate Group, form part of the fluvial sequence that crops out near Kissonerga village, north of Paphos (location 2-20).

The sedimentary sequence consists of white to buff-brown, and locally red, medium sands and silts (Fig.5.19), interbedded with minor conglomerates. The conglomerates form a minor proportion of the unit. These are occasionally imbricated, poorly sorted and immature and are made up of a range of angular to rounded clasts. The clasts within the conglomeratic units are dominantly, although not exclusively, chalks, cherts and marls. Some gabbro and serpentinite clasts are also present. The conglomerates form grain-supported units in channels, and grain- to matrix-supported deposits where interbedded with the fine sands and silts. Clasts are generally less than 10cm along the "L" axis, although occasional clasts up to 25cm long are present. The sections reveal a series of fining-up sequences (Fig.5.19). The units are generally structureless although distinct bedding, with occasional parallel lamination, is locally present. The beds are laterally persistent, i.e. continuity of bedding over distances of 30-100m. Channels cutting these laterally persistent beds are less than 3m wide and 50-60cm deep and are impersistent (Fig.5.19).

### **5.3.5 The Fanglomerate units of the Polis-Paphos graben.**

Sediments of the Fanglomerate Group crop out throughout the Polis-Paphos graben. The Fanglomerate Group sediments in the southern portion of the graben, as well as those on the limbs of the graben, i.e. east and west, generally rest unconformably over Troodos ophiolite and pre-Quaternary sequences (Plate 5.12). In the central areas, towards the north of the graben, the Fanglomerate Group sediments unconformably overlie deltaic sediments, e.g. in the Limni area (location 2-94), as seen along the south coast in the Mazotos area of south Cyprus (locations 3-13 and 3-18; Chapter 6).

The outcrop pattern of the F1 Fanglomerate unit has been disrupted by neotectonic faulting (Chapter 4), which has resulted in some dissection of the Fanglomerate unit, e.g. at Nata (Plate 4.2). The F2-F4 Fanglomerate units, unlike the F1 unit, have not been as extensively dissected by faulting and, therefore, still crop out at successively lower topographical levels, like that seen elsewhere in southern Cyprus.

The extensive sediments in the F1 and F2 Fanglomerate units resemble exposures in the Akhelia area, e.g. east of Paphos, and distal locations on the north Troodos margin.

Fig.5.19. Logged sections of the floodplain sequences cropping out at Kissonerga to the north of Paphos (location 2-20).

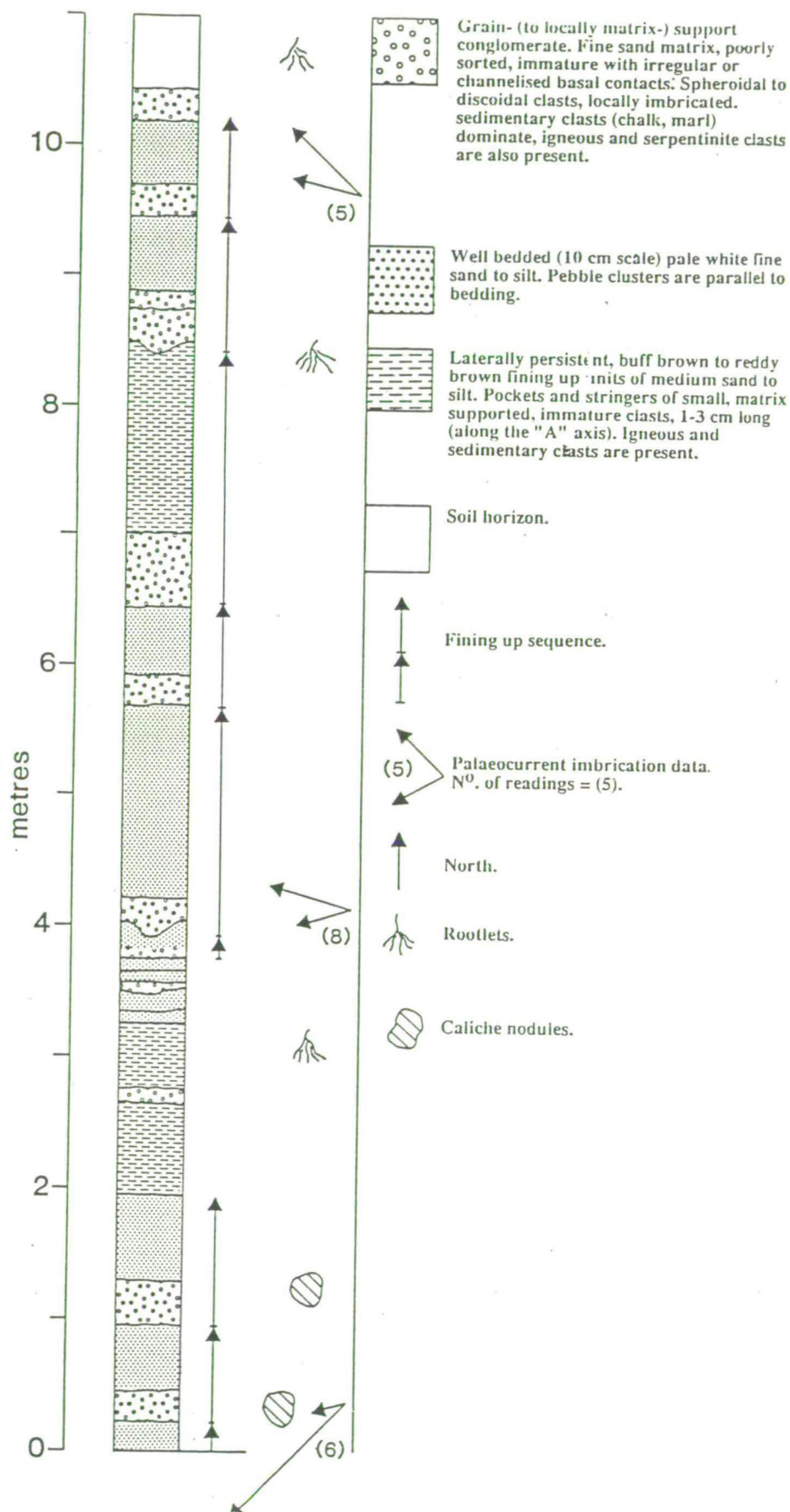


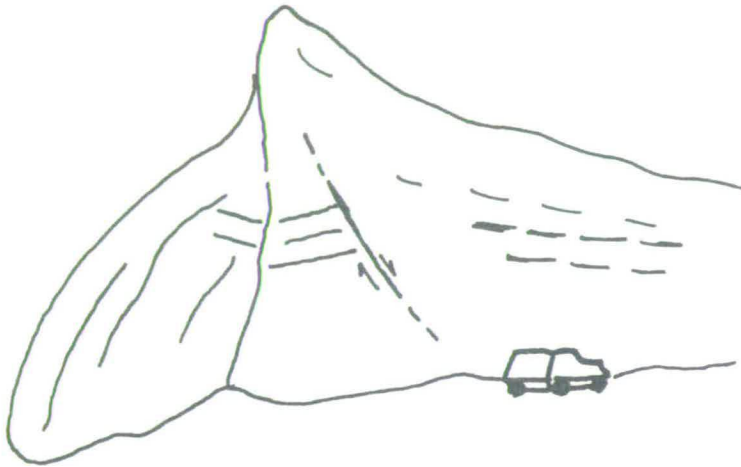


**PLATE 5.12.**

D - Displaying the texture of the coarse conglomerate exposed in the basal unit of the F2 age Fanglomerate sequence at Akhelia (location 2-45), south-west Cyprus.

E - A view of the F1 Fanglomerate unit sequence exposed in a quarry on the western limb of the Polis-Paphos graben above Goudhi.

Note: the normal fault cutting the Fanglomerate unit sequence.



F - Displaying the quadrant used for clast analysis.

# Plate 5.12

D



E



F



The F3 Fanglomerate unit has limited exposures and is generally restricted to areas close to the present river courses, whilst the F4 Fanglomerate units form outcrops within metres of the present day channels.

The F1-F3 Fanglomerate unit sequences consist of coarse, massive, unsorted, channellised, conglomerates, passing up into sands and silt, capped by caliche and palaeosol horizons. The sequences are generally red or grey in colour. The channel sequences commonly cut down into the underlying sediments, cutting through earlier conglomerates and silts, as well as soils, e.g. Prodhomi (location 2-93; Fig.5.20), similar to that seen at Kato Koutraphas, on the north Troodos margin (Plate 5.6). The channels are generally 3-5m wide and shallow - less than 70cm deep, e.g. Prodhomi (location 2-93; Fig.5.20).

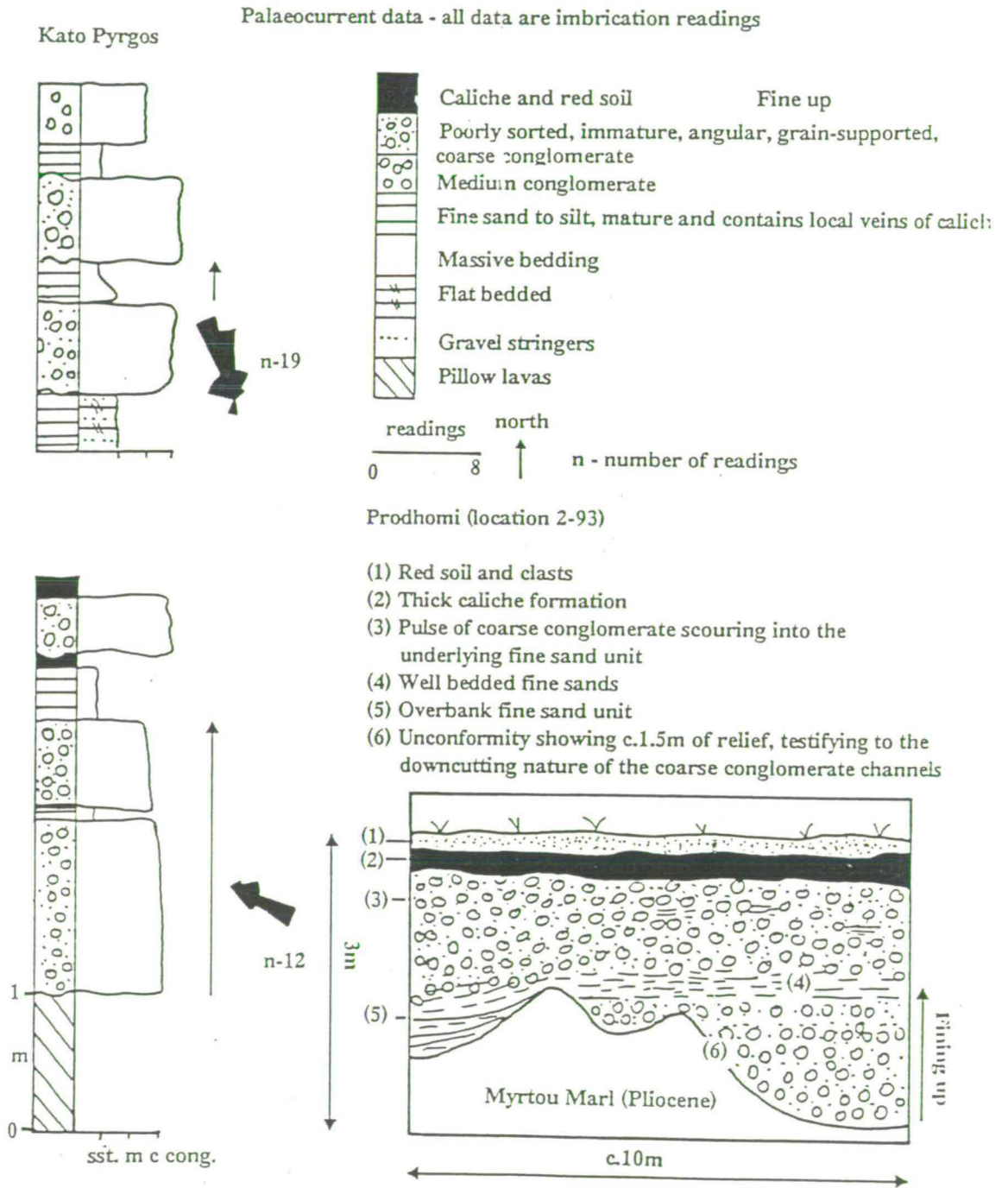
The sediments of the F4 Fanglomerate unit are finer grained than the preceding Fanglomerate units. The clasts within the F4 unit are also generally more mature than those found within the F3 Fanglomerate units, which they cut through, indicative of clast reworking similar to that seen on the south coast of the island (Section 5.3.3.4).

There has been extensive dissection of the Nicosia Marls that crop out on the graben floor beneath the Fanglomerate units. This erosion suggests that much of the original Fanglomerate Group sediment, within the graben axis, may have now been eroded.

### **5.3.6 The Fanglomerate units in the Kato Pyrgos area.**

Kato Pyrgos, abutting the north-west flank of the Troodos ophiolite, is an area where sediments of the Fanglomerate Group can be studied in isolation to ascertain whether any major provenance changes have occurred during the Quaternary. Borehole data show that 57.9m of conglomerates, sands and silts are locally preserved beneath the Pyrgos River valley, unconformably overlying lava and diabase of the Troodos ophiolite. The exposed sections in Kato Pyrgos are correlated by means of local geomorphological features, e.g. palaeo-cliff lines. Exposed sequences of the F2 and F3 Fanglomerate units are similar to those seen on the north Troodos margin and in other areas of southern Cyprus, i.e. a coarse conglomerate lag overlain by well bedded sands and silts, with evidence of caliche horizons, which, in turn, is overlain by another coarse pulse of conglomerate (Fig.5.20). The matrix within the Fanglomerate units consists of fine brown silts and sands. The clasts of the conglomeratic units are solely Troodos-derived, i.e. lava and diabase. The diabase clasts tend to be more mature than the lava clasts which are derived from local sources.

Fig.5.20. Sketch section from the the Polis-Paphos graben and the Kato Pyrgos area of north-west Cyprus.



### **5.3.7 The Fanglomerate units of the Kyrenia Range.**

Although this area has not been studied a brief description, based on the literature (Moore, 1960; Ducloz, 1972) is included for comparison with the Fanglomerate Group in southern Cyprus. Sediments of the Fanglomerate Group crop out both to the north and south of the Kyrenia Range. Coarse gravels, boulder beds and immature conglomerates made up of angular to sub-angular, poorly sorted clasts dominate. Well bedded silts are also present. The units have a chalky matrix and are capped by chalky white soils differing from those seen on the north Troodos margin.

## **5.4 PALAEOCURRENT STUDIES.**

### **5.4.1 Introduction.**

The majority of the palaeocurrent data presented here is derived from clast imbrication, although foreset readings were collected where possible, to enhance this data set.

### **5.4.2 Palaeocurrent data from the north Troodos margin.**

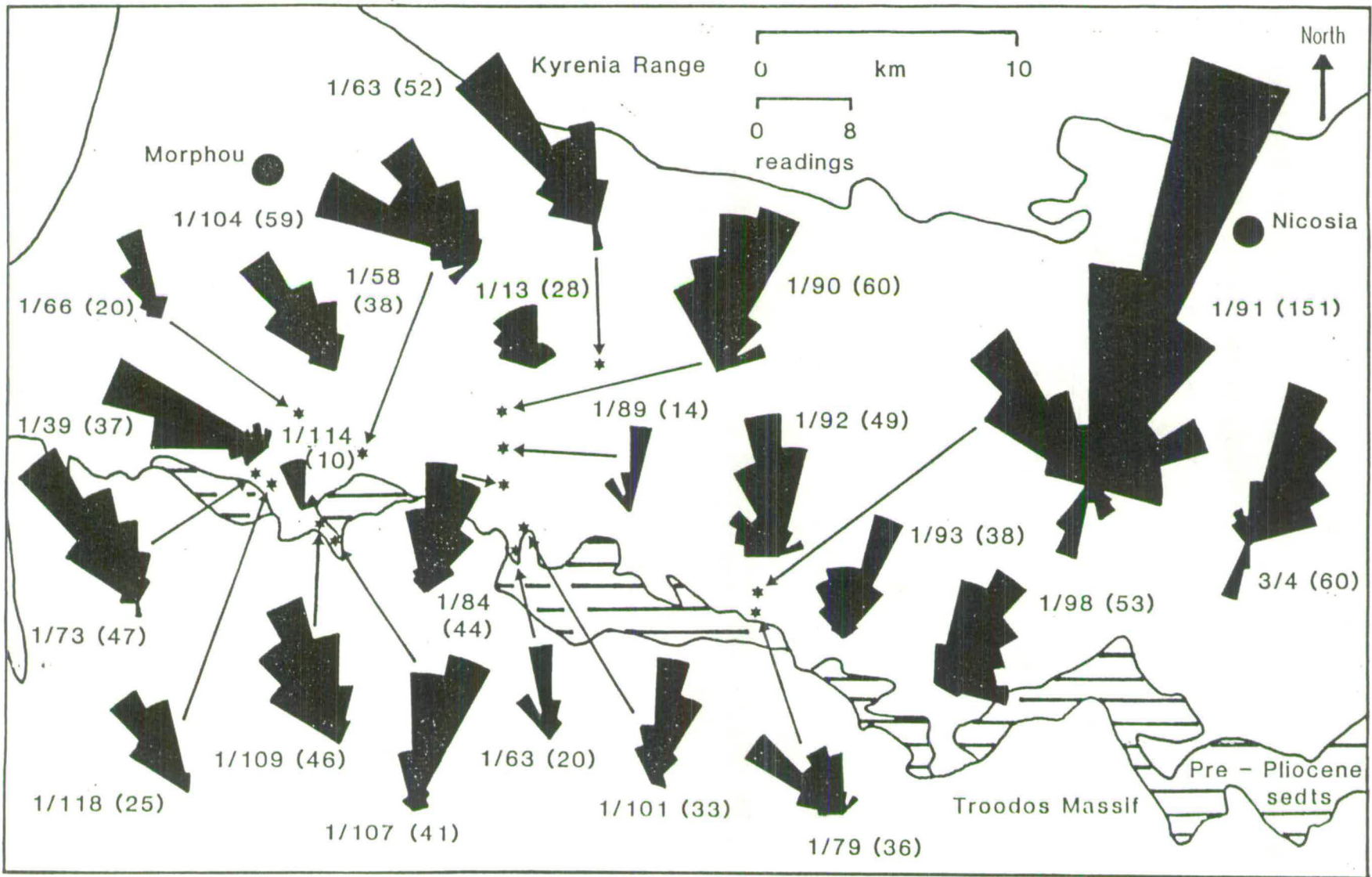
Palaeocurrent data from the north Troodos margin show a swing in flow direction from the north-west, in the west, to the north-east, further east (Fig.5.21). The data also show that a change in palaeocurrent direction is quite common between two pulses of juxtaposed coarse conglomerate units. A shift from the north-west towards the north and east on the north-western flanks of Troodos, and towards the north from the north-east, further east, is generally present (Fig.5.21).

Data collected from the north Troodos margin agree with those collected by McCallum (1989) and complement trends identified from aerial photographs and satellite images (Chapter 2).

### **5.4.3 Coastal southern Cyprus.**

The majority of the palaeocurrent data collected for the coastal areas of southern Cyprus (Figs.5.22) reflect the radial drainage pattern described in Chapter 2. A southward directed pattern dominates in the area between Larnaca and Paphos (Figs.5.3 and 5.22) but does vary between east-south-east and west-south-west. The variation in palaeocurrent direction between the deposition of the F1 and F4 Fanglomerate units is minimal, with a consistent flow in an arc between the east-south-east and west-south-

Fig.5.21. Palaeocurrent data collected from clasts within the units of the Funglomerate Group on the north Troodos margin.



Note: the number next the individual rose diagrams refer to the location and number of clast imbrications recorded.

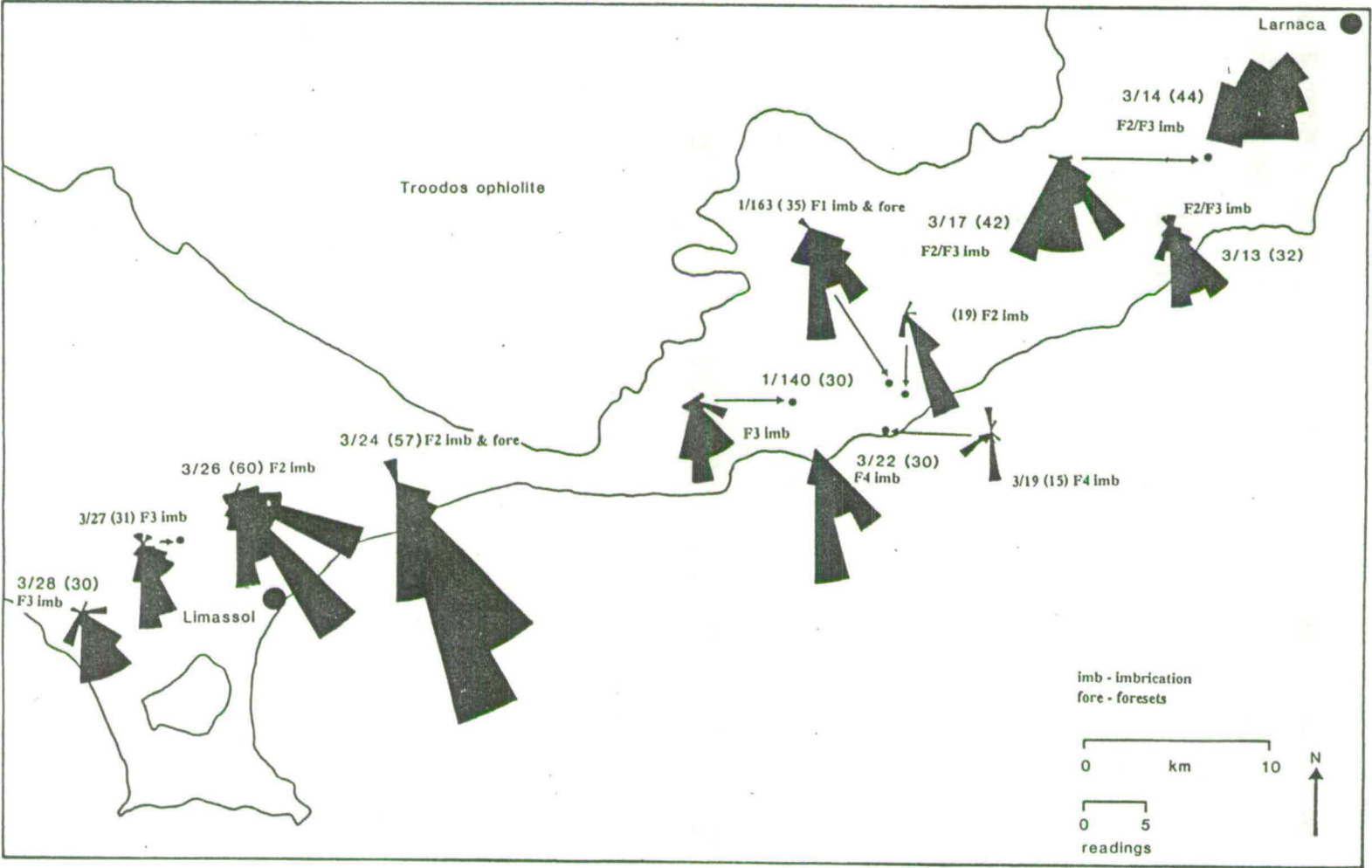


Fig. 5.22. Palaeocurrent data collected from the units of the Fonglomerate Group cropping out along the south coast of Cyprus.

Note: the number next the individual rose diagrams refer to the location and number of clast imbrications recorded.

west. Some minor changes are seen; for example the change from a dominantly east-south-east to a south-south-east flow during the deposition of the F2 and F3 Fanglomerate units, respectively (Fig.5.22). Deviations from a radial palaeocurrent pattern, centred on the Troodos Massif, are locally seen; for example, the Fanglomerate units that crop out at Dhekelia (location 2-83; Fig.5.10), the Fanglomerate units that unconformably overlie braid-delta sequences east of Larnaca (location 3-14; Fig.5.22), the F1 Fanglomerate units that crop out in Pissouri and Kouklia areas (locations 3-30 and 2-54 respectively; Fig.5.23) and those rivers that drain off the southern and western edges of the Polis-Paphos graben (e.g. locations 2-63 and 2-21; Fig.5.22).

#### **5.4.4 The north coast.**

Limited, i.e. clast imbrication, data collected from Kato Pyrgos and the Polis-Paphos graben show a south to north palaeocurrent direction (Fig.5.22).

### **5.5 PROVENANCE STUDIES.**

Provenance studies were carried out in the field and on clay and silt fractions from boreholes at Meniko and Astromeritis (Fig.5.5). The borehole samples were studied using X-ray diffraction and X-ray fluorescence.

#### **5.5.1 Clast analysis within the Fanglomerate Group.**

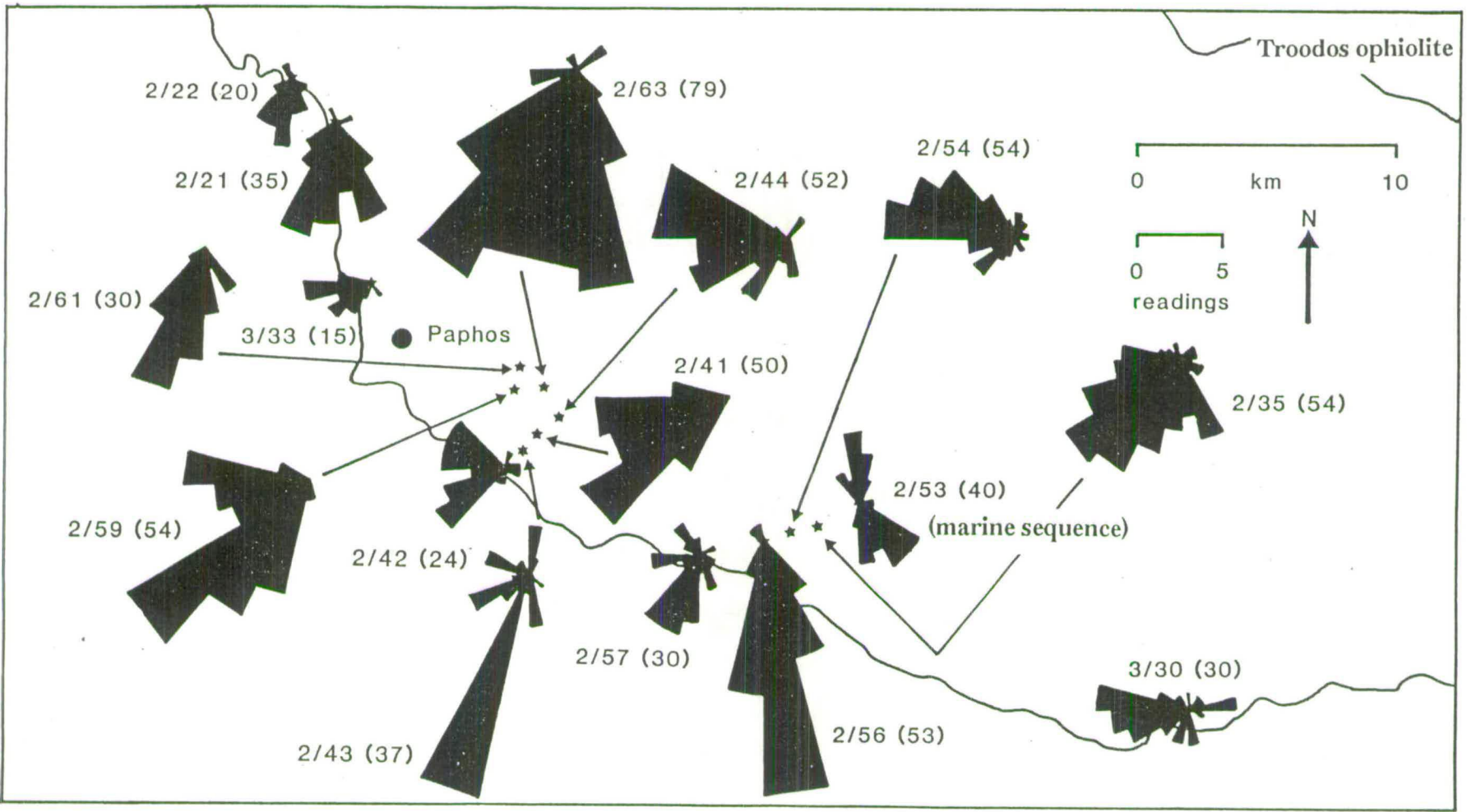
Clast analysis of the conglomerates of the Fanglomerate Group was undertaken using randomly positioned quadrants (Plate 5.12). 50 clasts taken at random from within each quadrant were then identified according to published methods (Boggs, 1969; Pettijohn, 1980; Collinson & Thomson, 1982; Tucker, 1988). Five classes of lithology were identified: ultramafic, gabbro, diabase, lava and sediments. Sedimentary lithologies were identified where diverse sedimentary clasts were present. Provenance studies of clasts were also undertaken within units of the Pliocene Kakkaristra and Apalos Formations on the north Troodos margin; this study allowed a comparison of provenance between the Pliocene and the Quaternary sequences to be made.

##### **5.5.1.1 North Troodos margin.**

In the western and central Mesaoria Plain there are a greater proportion of diabase and gabbroic clasts in the Fanglomerate Group conglomerates than found in the underlying Pliocene lithologies, which are dominated by clasts of lava (Fig.5.24). By contrast, in the eastern portion of the Mesaoria Plain, the provenance in the Fanglomerate



Fig. 5.23. Palaeocurrent from the Fanglomerate Group sequences of south-west Cyprus.

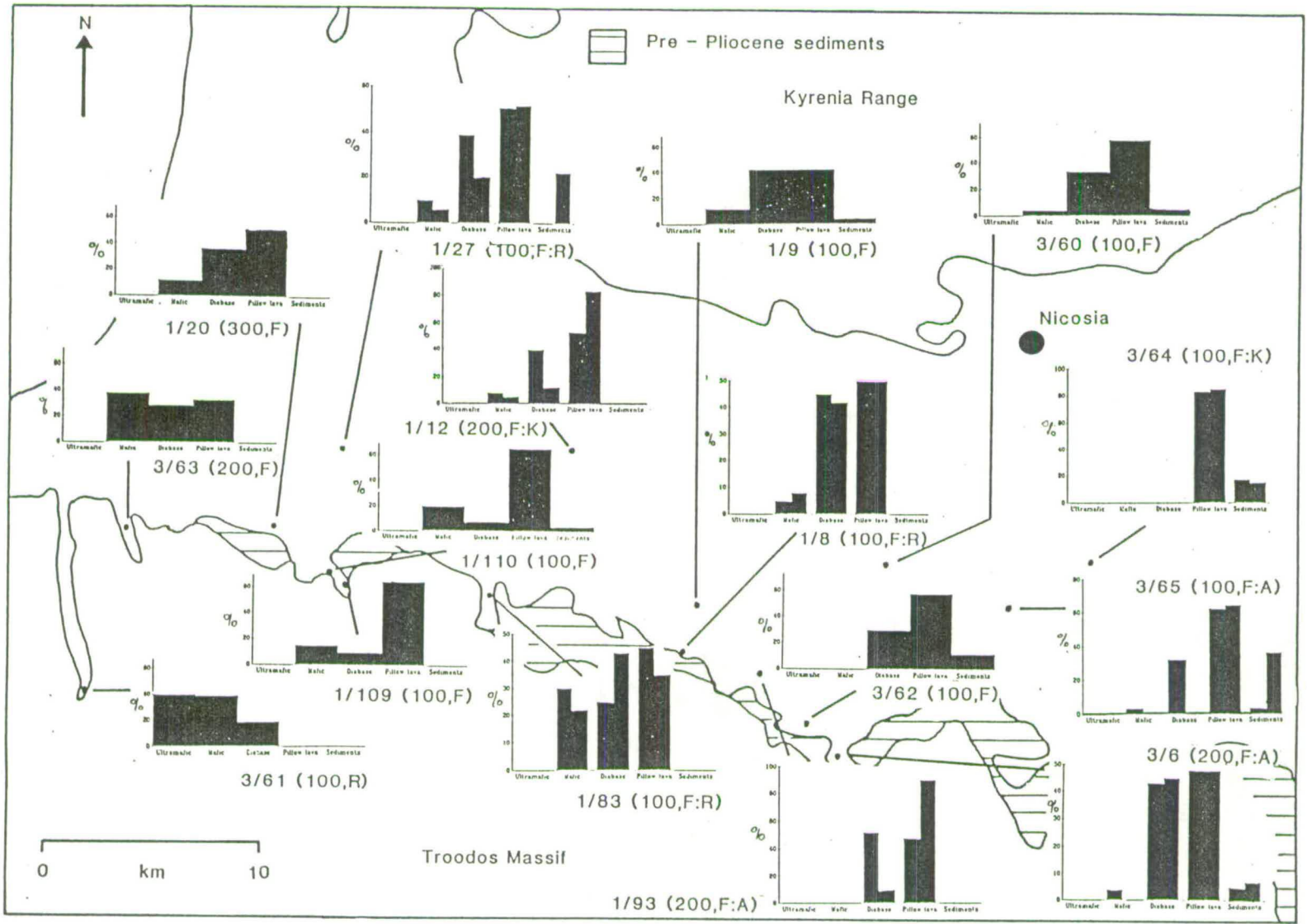


Note: the number next to the individual rose diagrams refer to the location and number of clast imbrications recorded.

Fig. 5.24. Clast analysis data collected from the Fanglomerate Group units on the Mesaoria Plain.

Note: the categories are ultramafics, mafics, diabase, pillow lavas and sediments,

the numbers next to the individual histograms refer to the numbers of clasts counted and the location number, the "F" number refers to the Fanglomerate unit from which the clasts were sampled.



Group is very similar to that seen in the underlying Apalos Formation (Fig.5.24). The variation in clast type between the F1 and F2 Fanglomerate unit conglomerates is negligible. Ultramafic clasts are generally absent from the Fanglomerate Group sediments. The exception occurs in areas close to the Karyotis River valley, e.g. Tembria (location 3-61; Fig.5.24). Ultramafic clasts are also found in exposures of the Fanglomerate Group in the Morphou area (Wilson, 1957; Moore, 1960), where Moore (1960) also reports the presence of gabbro and diabase clasts.

The F4 Fanglomerate unit and Recent sediments that are associated with river courses on the west side of the Mesaoria Plain contain sedimentary clasts, e.g. limestones of Miocene age. The igneous clasts are also generally more mature, in contrast to those associated with the earlier Fanglomerate units, i.e. F1-F3. The proportions of different igneous clasts varies locally (Fig.5.24). The presence of sedimentary clasts, which indicate erosion of older sedimentary units, suggests that erosion of the Fanglomerate Group must have been taking place allowing the exposure and erosion of the sedimentary sequences. This erosion of the sedimentary sequence, coupled with the local variation in igneous clasts present, plus the increased maturity of the igneous clasts in the F4 Fanglomerate unit, suggests that reworking of clasts from older, earlier, Fanglomerate units into the F4 and Recent sequences, has taken place.

#### **5.5.1.2 Clast analysis in south-east Cyprus.**

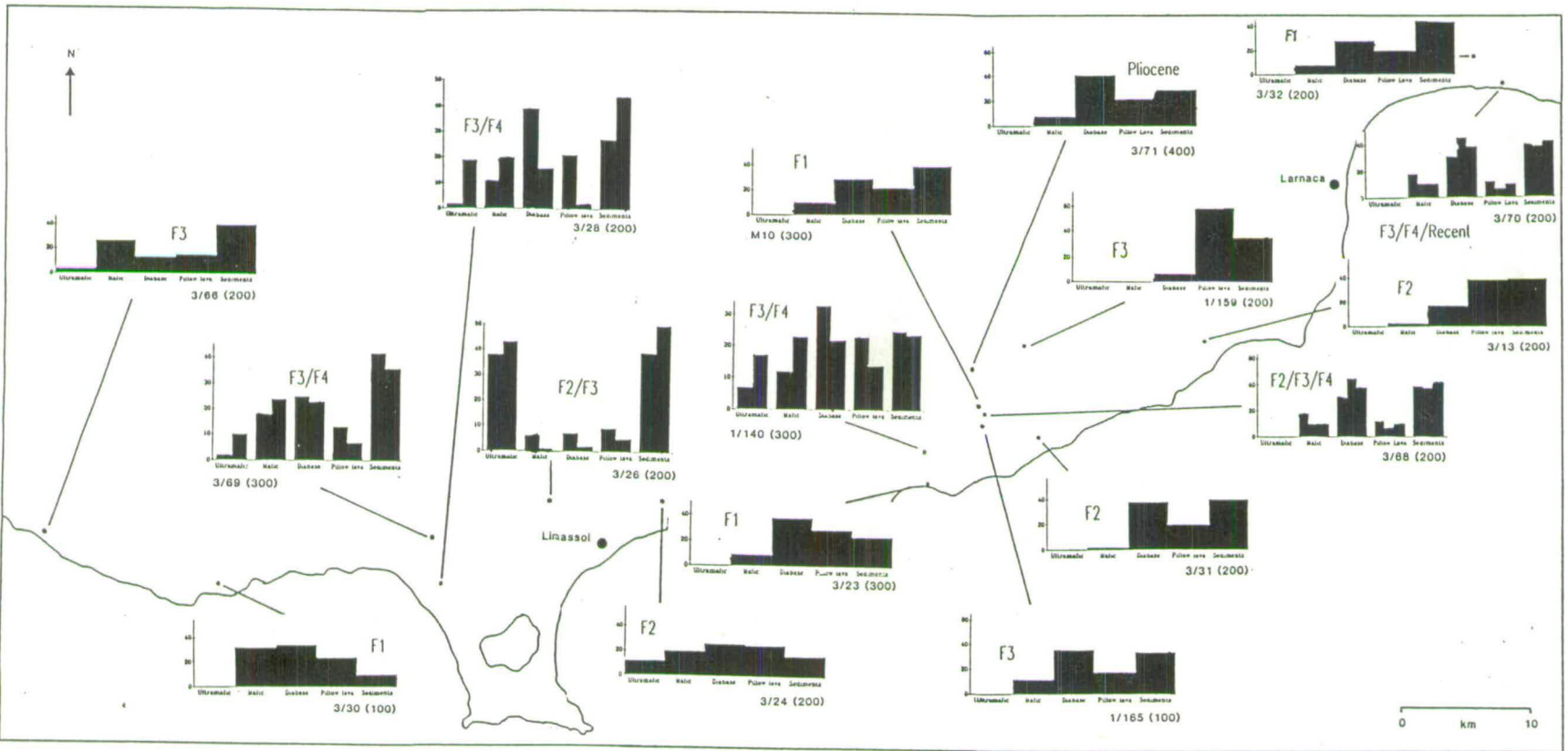
In south-east Cyprus provenance studies of the Fanglomerate Group show the presence of Troodos-derived clasts, as seen on the north Troodos margin, as well as clasts derived from the Troodos sedimentary cover sequence (Fig.5.25). The sedimentary clasts are dominated by chalks and limestones of Palaeogene and Neogene age. A proportion of the lava clasts found within units of the Fanglomerate Group at Dhekelia (location 2-83) differ from the Troodos lava units. This pattern reflects derivation from both the Troulli Inlier and the Troodos Massif (Fig.1.3 and 2.9).

#### **5.5.1.3 The south coast region: Larnaca to Limassol.**

The pre-Quaternary channel sequences preserved in the Khirokitia and Maroni area (Fig.2.6) contain many large blocks, i.e. up to 3-4m long, of reef limestones of Miocene age. Diabase, lava, chalk and gypsum clasts are also present within the channel sequences. The stratigraphically lower portions of these Pliocene channels are dominated by chalk clasts; greater proportions of diabase are seen higher in the sequence. Eaton (1987) correlated the channels with the Miocene succession. However, it is now recognised that these channel sequences are of Upper Pliocene age (Houghton *et al.*,

Fig. 5.25. Clast analysis data collected from the Fonglomerate Group units cropping out along the south coast of Cyprus.

Note: the categories are ultramafics, mafics, diabase, pillow lavas and sediments, the numbers next to the individual histograms refer to the numbers of clasts counted and the location number, the "F" number refers to the Fonglomerate unit from which the clasts were sampled.



1990). The clast composition in the Pliocene channels contrast with that seen in the F3 and F4 Fanglomerate units and with the Recent channel sediments in the Maroni River valley (e.g. locations 1-159 and 1-165; Fig.5.25). The F3 and F4 Fanglomerate units are dominated by gabbro, diabase, lavas and chalk, and contain few reef limestone clasts. Ultramafic clasts are absent from both the Pliocene and Fanglomerate channel sequences. Minor proportions of locally derived, ripped-up, marl clasts, of ?Pliocene age are found within the F1 Fanglomerate unit south of Maroni (location 1-163; Fig.5.25).

The clasts within the F3 and F4 Fanglomerate units are similar throughout this region in areas away from the Maroni River valley. Igneous clasts are generally more mature than locally derived sedimentary clasts in the F3 Fanglomerate exposures (location 1-160). The proportion of igneous to chalk clasts is generally higher in the F3 Fanglomerate unit than in the F4 Fanglomerate unit, where locally derived chalk clasts dominate, e.g. west of Kophinou (location 1-155). Gabbro clasts from the Fanglomerate units in the Maroni River valley have probably been derived from the small, isolated outcrops of the plutonic core and the sheeted dyke complex that crops out in the vicinity of the upper reaches of the Maroni River, as this river does not cut through the main plutonic complex of the Troodos ophiolite (Fig.2.1).

The clast data from the Limassol area show a progressive increase in the proportion of ultramafic clasts through time, i.e. Recent > F4 > F3, as seen in the Kouris River (locations 3-28 and 3-69; Fig.5.25). This increase in the proportion of ultramafic clasts is matched by a decrease in the numbers of the diabase and lava clasts (Fig.5.25). Ultramafic clasts are present in the F2, F3 and F4 Fanglomerate units, as far east as Vasilikos (location 1-140; Fig.5.25). However, ultramafic clasts are absent from the Vasilikos Formation (location 3-23; Fig.5.25), which is equivalent to the F1 Fanglomerate unit. The proportion of mafic clasts in the units to the north and east of Limassol, as far as Vasilikos, varies locally (locations 3-26 and 1-140; Fig.5.25) and the proportion of sedimentary clasts remains reasonably consistent throughout the Quaternary (location 1-140; Fig.5.25).

#### **5.5.1.4 South-west Cyprus, the Polis-Paphos graben and the Kato Pyrgos area.**

The F1 Fanglomerate unit unconformably overlies the ?Pliocene fan-delta sequences in cliffline exposures in the area of Pissouri Bay in south-west Cyprus. The clasts within the Fanglomerate Group unit are derived from both the Troodos Massif and the Miocene Pakhna Formation (Fig.5.15); these data support evidence for river capture in this area (Section 2.2.6).

Studies in the Paphos area (Fig.5.26) reveal an apparently constant clast source during the Quaternary period, contrasting that recorded from the Fanglomerate Group units exposed along the south coast of Cyprus. It is, however, likely that some clast reworking, from earlier into later Fanglomerate units, has taken place. The variety of clasts present within the Fanglomerate units in the Paphos area appears to reflect, directly, the local geology and drainage system (Figs.1.4, 2.1 and 2.4), with clasts derived from the Troodos ophiolite, the Mamonia Complex and the Troodos cover sediments.

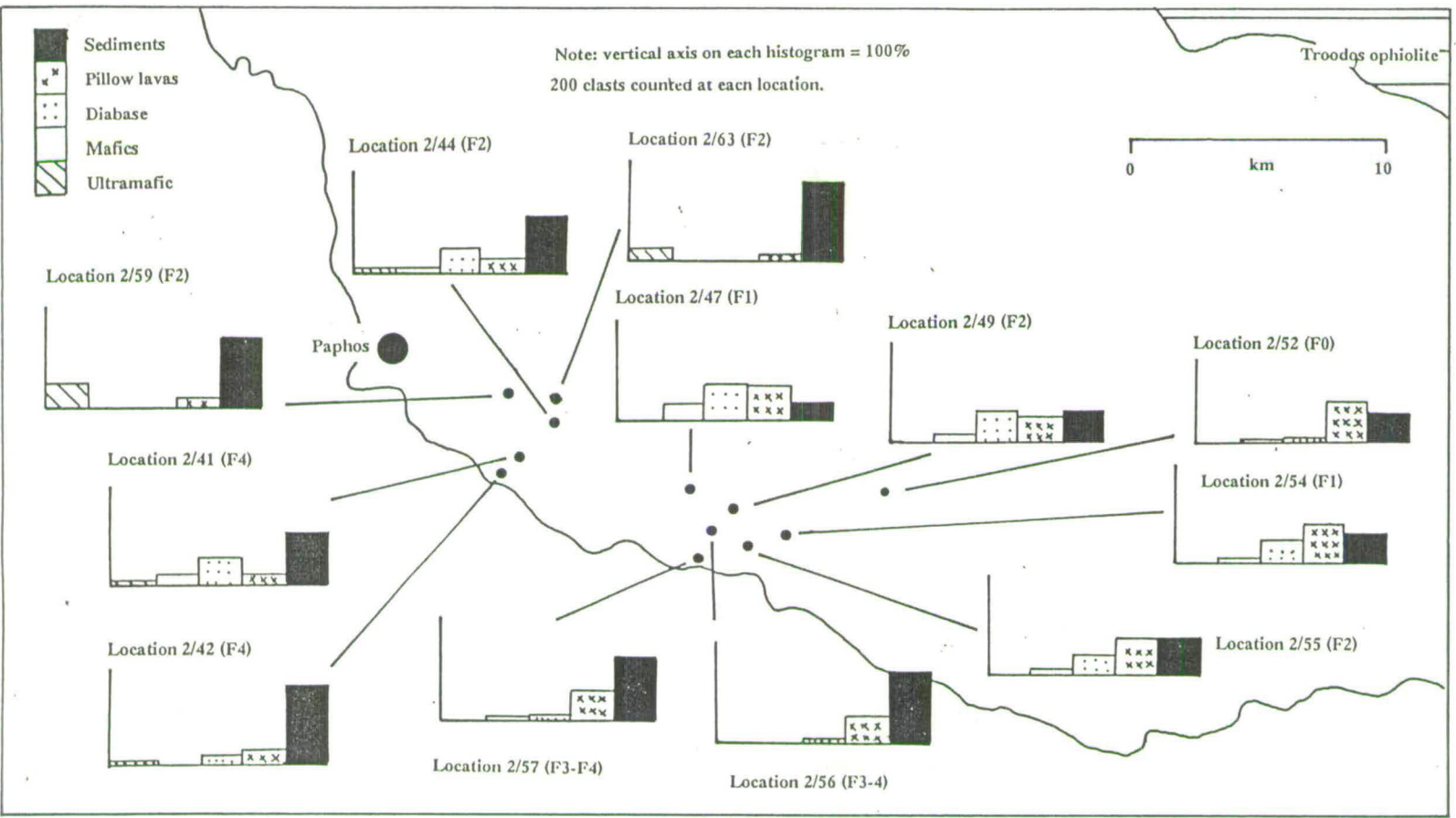
Mamonia-derived clasts are present in many of the units to the north and east of Paphos, in the Kissonerga area. The presence of ultramafic clasts reflects a Mamonia rather than Troodos-derived source. Diabase clasts are present in large quantities in areas where major source rivers have risen in the Troodos Massif, e.g. the Ezousa, Yerapotomos and Dhiarizos Rivers (Fig.2.1), although diabase clasts are not solely derived from the Troodos Massif as slivers of both diabase and gabbro are associated with the Mamonia Complex and crop out to the south of Marathounda, in south-west Cyprus. Gabbroic clasts present within the Fanglomerate units are associated with the Mamonia complex, as the source rivers do not cut the core of the Troodos ophiolite. A rich variety of sedimentary clasts, e.g. chalks, chert, quartzite, marl, limestones, sandstone, siltstone and mudstone, are found within the Fanglomerate units. These are derived, locally, from the Mamonia Complex and the pre-Quaternary Troodos sedimentary cover sequence.

A large proportion of the clasts within the conglomerate sequences of the F1 and F2 Fanglomerate units, in the Polis-Paphos graben, are derived from the Troodos ophiolite. Sedimentary clasts, derived from both the Mamonia complex and the Troodos sedimentary cover sequence (Fig.1.4), are also present within the units of the Fanglomerate Group (Fig.5.26). The F3 Fanglomerate unit contains a greater proportion of locally derived chalks than is the case with the F1 and F2 Fanglomerate units. The chalk clasts within the F3 Fanglomerate unit are commonly large and immature, e.g. at Skouli (location 2-96), contrasting with those derived from the Troodos ophiolite, which are generally more mature. The igneous clasts present within the F1 and F2 Fanglomerate units are generally less mature than those found within the F3 Fanglomerate unit.

#### **5.5.1.5 Fanglomerate units of the Kyrenia Range.**

Clasts exposed in the Fanglomerate Group on the flanks of the Kyrenia Range consist of units of the Hilarion, Lapithos and Kythrea Formations, e.g. limestones, chalks, rhyolites, sandstones, greywackes and conglomerates (Moore, 1960). These lithologies are all restricted to the Kyrenia Range and do not crop out elsewhere on the island.

Fig. 5.26. Clast analysis data from units of the Fanglomerate Group cropping out in south-west Cyprus.



Note: the categories are ultramafics, mafics, diabase, pillow lavas and sediments, the numbers next to the individual histograms refer to the numbers of clasts counted and the location number, the "F" number refers to the Fanglomerate unit from which the clasts were sampled.

### **5.5.2 X-ray diffraction studies.**

X-ray diffraction was utilised to study the composition of the silt and, more specifically, the clay fraction of samples collected from two boreholes on the north Troodos margin, and other related sites.

#### **5.5.2.1 Borehole samples.**

Clay and silt samples were separated, by suspension settling (Hardy & Tucker, 1988), from specimens collected from two boreholes located at Meniko and Astromeritis (Fig.5.5). Both boreholes cut the Quaternary and the underlying Pliocene sedimentary sequence (Fig.5.27). Samples collected from the boreholes were subjected to four X-ray diffraction runs, i.e. air-dried, glycolated and heated to 375°C and 550°C, facilitating the identification of the clay minerals present. One sample, APM 15 (from the base of the Meniko borehole), was also heated to 1200°C to identify amorphous silica (Fig.5.28). The clay minerals were prepared and identified in accordance with Starkey *et al.* (1984) and Hardy & Tucker (1988).

The results of the X-ray diffraction analysis are shown in Appendix E along with the relative peaks of the mineral phases identified.

The clay mineralogies of the borehole samples, that date from the Pliocene, are very consistent. Smectite-chlorite mixed clays dominate, although kaolinite, montmorillonite and illite are also present (Fig.5.29; other X-ray diffraction plots are given in Appendix E). The clay mineralogies do not appear to vary between the boreholes. Some variation in the peak height values of the clays are seen; this suggests that the proportion of clays may vary between samples, although quantitative measurements were not made.

The mineralogy of the clay samples is similar to that seen in two D.S.D.P. holes (375 and 376) that were drilled 40 km to the west of Cyprus on the Florence Rise (Hsu *et al.*, 1978; Fig.1.1). The D.S.D.P. samples are rich in smectite, illite and contain subordinate proportions of chlorite and kaolinite. The clays in the D.S.D.P. boreholes are considered to have been derived from basic igneous units of the Troodos ophiolite (Melieres *et al.*, 1978). Other studies to the north-west of Cyprus also reveal a high proportion of smectite (Shaw, 1978). McCallum (1989) notes that smectite, small amounts of kaolinite and illite and minor proportions of chlorite are found in the Pliocene sediments cropping out on the Mesaoria Plain and suggests that some of this clay could



Fig.5.27. Sections of the lithological variation down boreholes at Meniko and Astromeritis, from which samples were taken for X-ray diffraction and X-ray fluorescence studies.

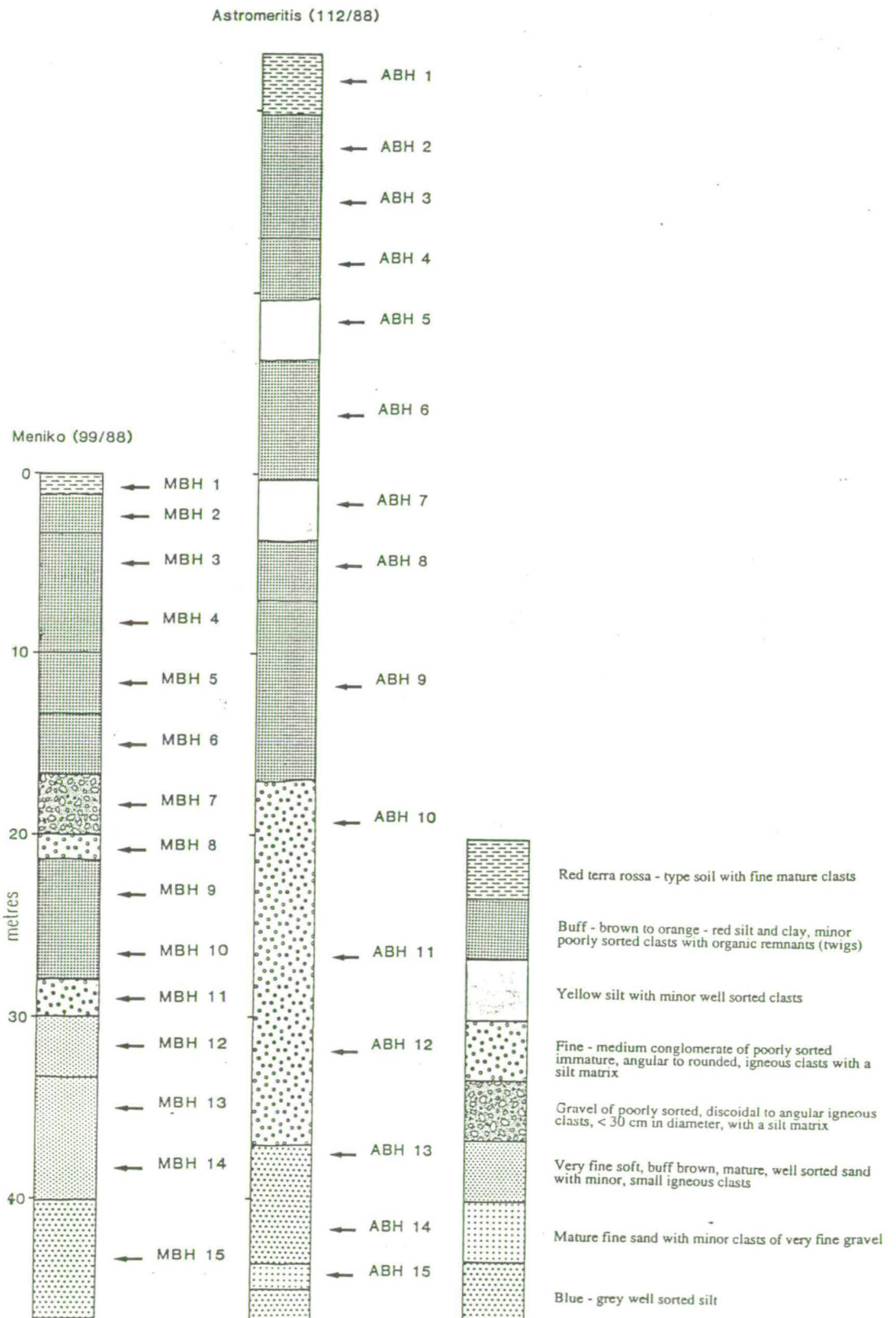


Fig.5.28. Plot of the X-ray diffraction trace of amorphous silica located in the basal sample in the Meniko borehole (APM15) before and after heating at 1200°C.

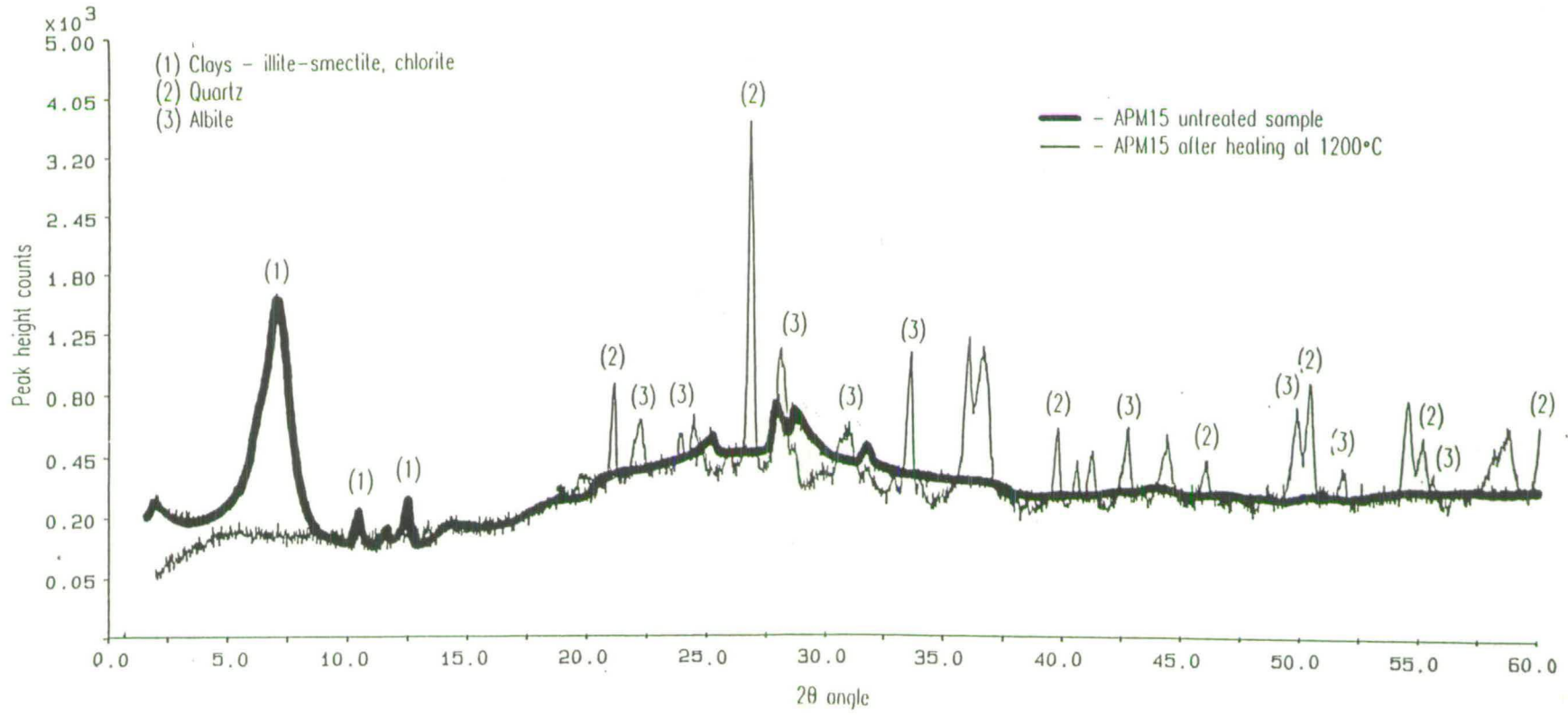


Fig.5.29. Typical X-ray diffraction peaks of clays under different conditions, sampled from the Meniko and Astromeritis boreholes

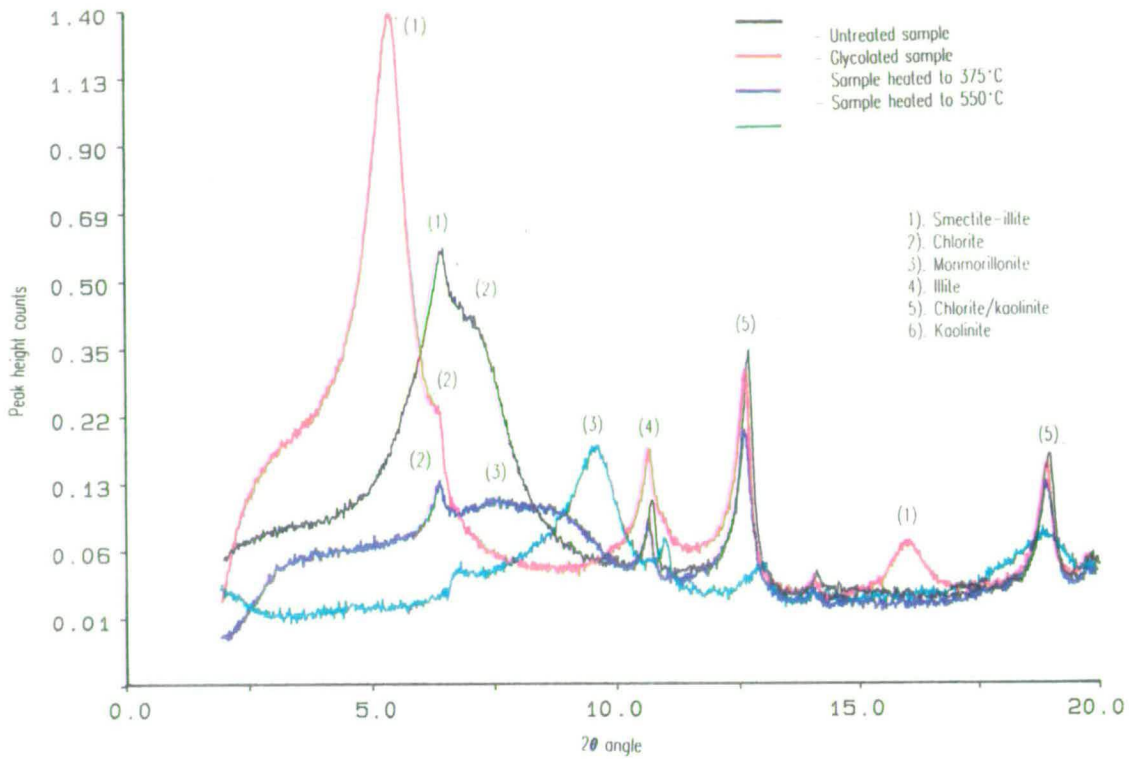
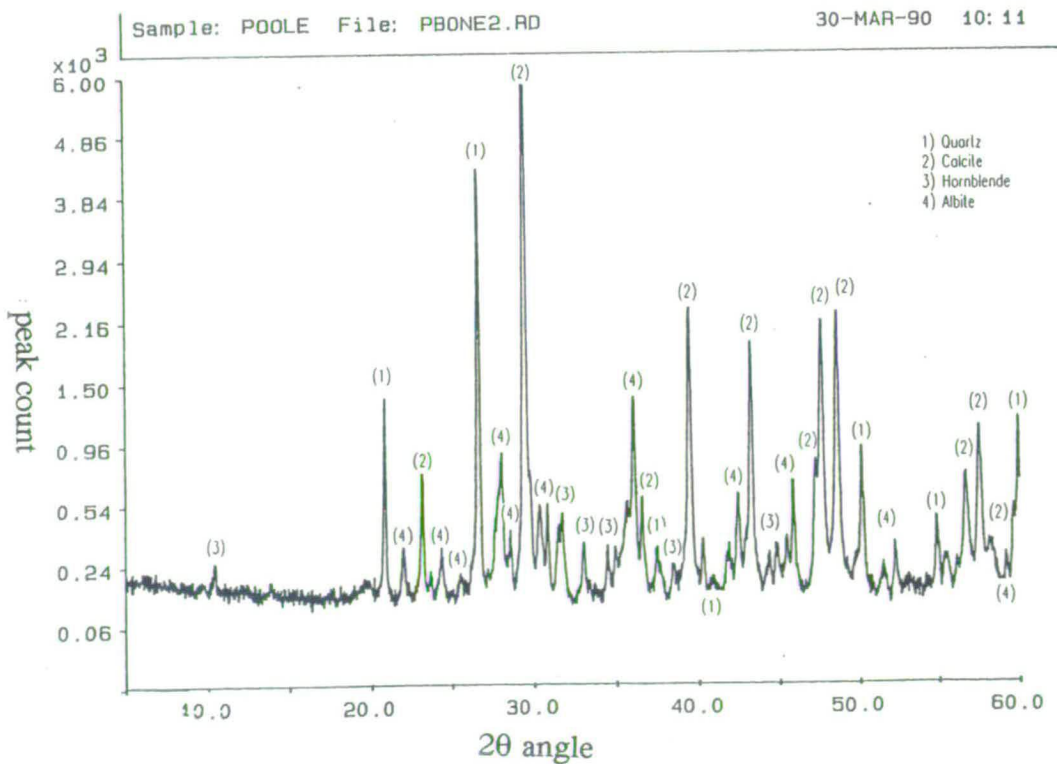


Fig.5.30. X-ray diffraction data from the bone site located to the south-west of Xylophagou (location 2-75).



have been derived from the smectite-rich Kythrea Flysch found in the Kyrenia Range (Baroz, 1979). McCallum (1989) did not discover any vertical, stratigraphical changes in clay mineralogy through the Plio-Pleistocene sedimentary sequence on the Mesaoria Plain. Similarly, this study shows that there is no perceptible change in the clay mineralogy during the Quaternary.

#### **5.5.2.2 X-ray diffraction analysis of bone bed samples from the Fanglomerate Group.**

Samples of matrix collected from the bone bed, which crops out to the south-west of Xylophagou (location 2-75; Section 5.3.2) exhibit a clay mineralogy that is markedly different from that seen in the borehole samples (described above) and contains only traces of illite (Fig.5.30). The absence of clay suggests that the unit was well washed, which supports evidence from the analysis of thin sections (Section 5.3.2). The samples also contain quartz, augite, plagioclase feldspar, hornblende and calcite (Fig.5.30), suggesting a basic igneous, i.e. ophiolite, source for these samples, probably from the Troulli Inlier and/or the Troodos Massif. The calcite present within the samples is probably derived from carbonate cements, the calcareous fauna and derived carbonate clasts (Section 5.3.2).

#### **5.5.3 X-ray fluorescence studies.**

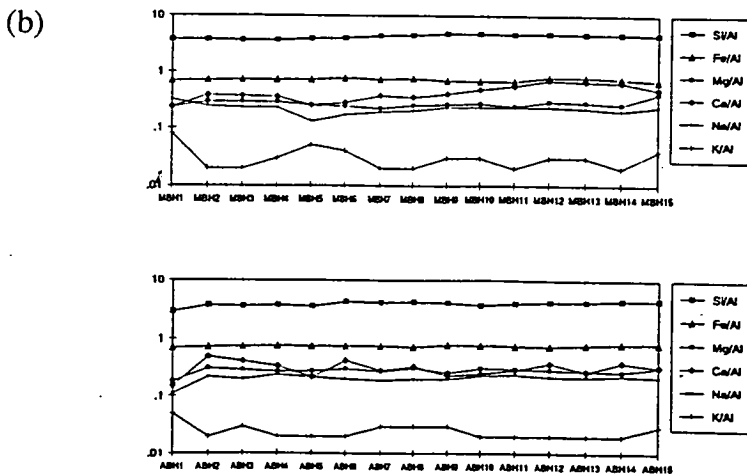
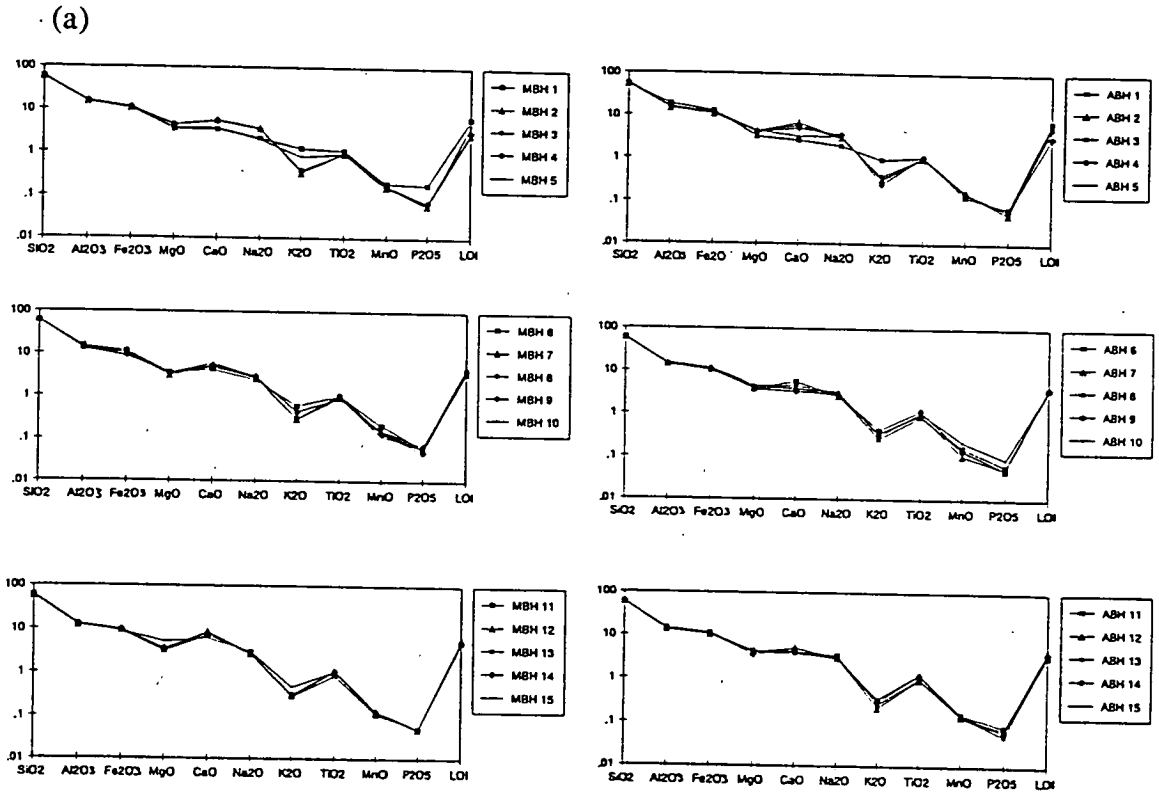
The X-ray fluorescence technique enabled a chemical analysis of the major and minor elements of the silt and clay fractions, collected from Meniko (MBH 1-15) and Astromeritis borehole (ABH 1-15) to be made.

The major element data, obtained from the borehole samples (Fig.5.31 and Appendix E), show minimal variation down the borehole. Results normalised to  $Al_2O_3$ , i.e. each element/ $Al_2O_3$ , are constant for the majority of the borehole samples (Fig.5.31). The exceptions are CaO, which shows some minor variation between samples (Fig.5.31), and  $K_2O$  that peaks in the first sample of each borehole, i.e. the upper soil level.

The absence of any notable change in the major elements present, in either of the boreholes is consistent with the X-ray diffraction results (Section 5.5.2.1). The consistency of the data, down each borehole, suggests that provenance changes are constant throughout the Quaternary. The peak in the  $K_2O$  from the surface samples may reflect potassium added to the soil as a fertilizer, or more likely, soil forming processes. The fluctuations in CaO possibly indicate minor caliche forming processes beneath the soils although the concentrations of CaO are much lower than those seen in the caliche

Fig.5.31. Plots of: a) the major element composition of samples collected from the Meniko and Astromeritis boreholes after X-ray fluorescence analysis; b) spider diagram of major element variations normalised to Al.

Note: MBH - Meniko borehole,  
 ABH - Astromeritis borehole,  
 "Y" axis is percentage plotted on a log scale.



samples (Section 9.4.3). The variation in CaO, like that seen in MgO towards the base of the Meniko borehole, is so small that it may just reflect minor variations in local weathering, provenance, groundwater or sedimentary environment. The overall pattern is one of consistency throughout the length of each borehole.

The trace elements are slightly more variable than the major elements (Fig.5.32). The normalised results (Fig.5.32) show that variations in Ni and Cr, and Zn and Cu are generally in phase, i.e. the trend for Ni matches that for Cr, but the two groups do not corroborate each other, i.e. if a peak is present for Ni and Cr, then a corresponding trough is present for the Zn and Cu.

The down borehole variation in trace element composition is minimal and probably reflects minor, local changes by weathering, groundwater effects and the local presence or absence of mineral phases; although some of the change may reflect the capture of trace elements by clay minerals as kaolinite is commonly enriched in Ni and Cr and Cu is strongly bound by montmorillinite (Rich & Kunze, 1967).

Data collected from D.S.D.P. boreholes on the Florence Rise, to the west of Cyprus (Fig.1.1), show that there is some variation in concentration of trace elements in the Quaternary sequences (Fig.5.33; Coumes & Boltenhagen, 1978). Shaw & Bush (1978) state that the concentrations of trace and major elements in the Morphou sub-province of the Cilia Basin (Fig.1.1) reflect local sedimentary depositional environments and provenance, in line with that seen from the Meniko and Astromeritis borehole samples.

## **5.6 INTERPRETATION, DISCUSSION AND CONCLUSIONS.**

### **5.6.1 Thickness variation.**

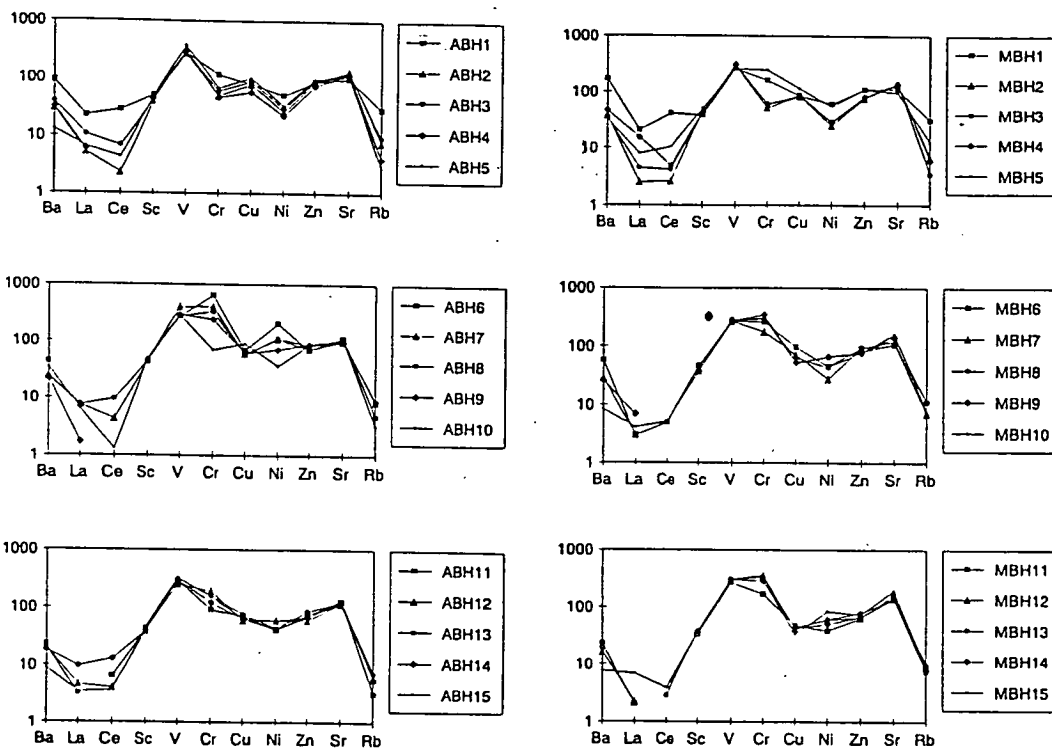
The variation in thickness of the Fanglomerate Group to the north of the Troodos margin reflects:

- i) a proximal, pediment to distal, depositional relationship (Fig.5.34),
- ii) the proximity to valleys supplying sediment from the Troodos Massif (Figs.2.1 and 5.2),
- iii) uplift rates and climate variation (Section 5.6.2.2)
- iv) pre-existing relief prior to the deposition of this group (Section 2.3).

The Fanglomerate Group sediments that unconformably overlie the Pliocene clastic sequences are commonly thicker than those forming capping units on mesa-type

Fig.5.32. Plots of the minor and trace element composition of the samples collected from the Meniko and Astromeritis boreholes after X-ray fluorescence analysis: b) results normalised to Al.

Note: MBH - Meniko borehole,  
 ABH - Astromeritis borehole,  
 "Y" axis is PPM plotted on a log scale.



(b)

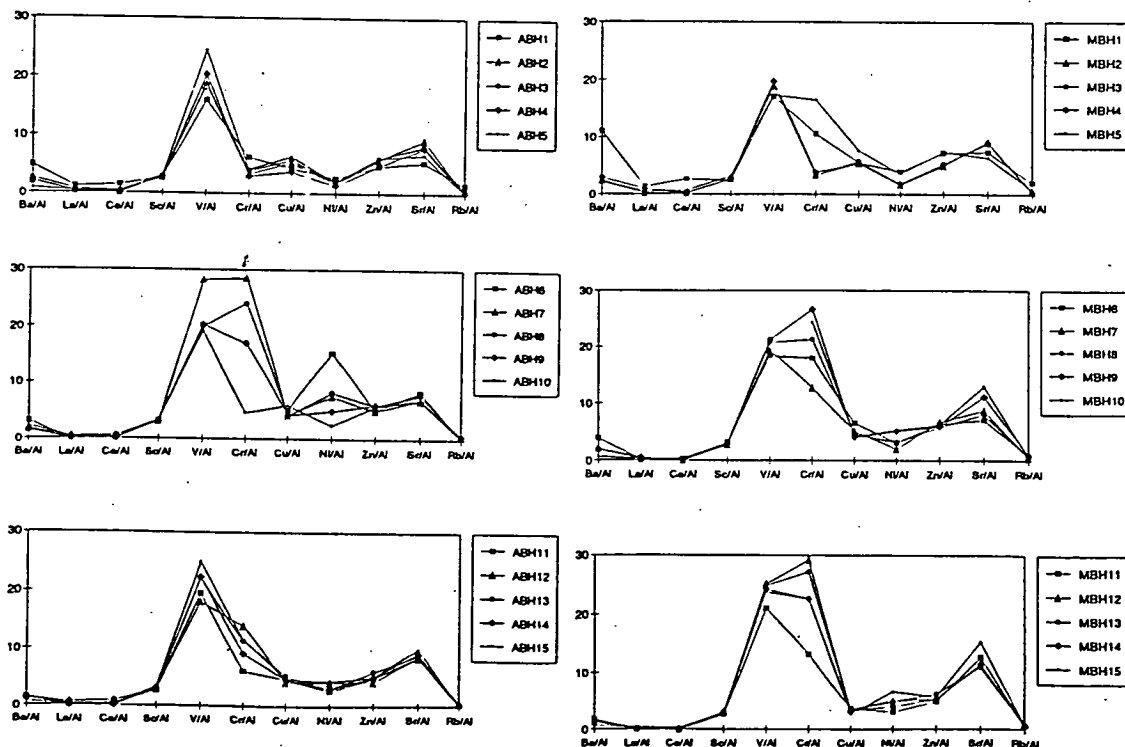


Fig.5.33. Chart showing the results of U.V. quantometer analysis from D.S.D.P. borehole 376 drilled on the Florence Rise (after Coumes & Boltenhagen, 1978).

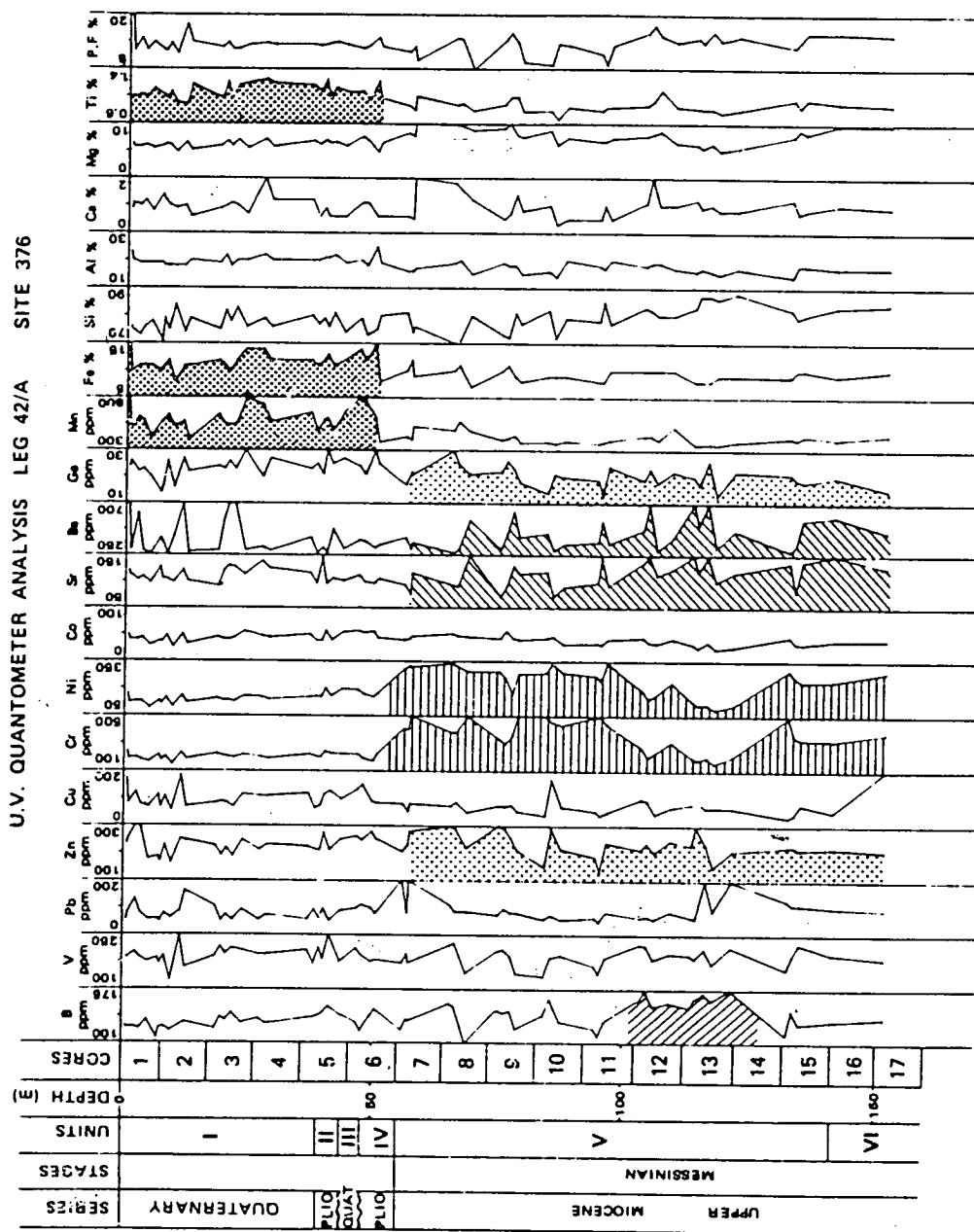
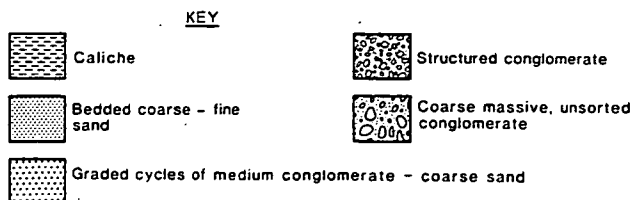
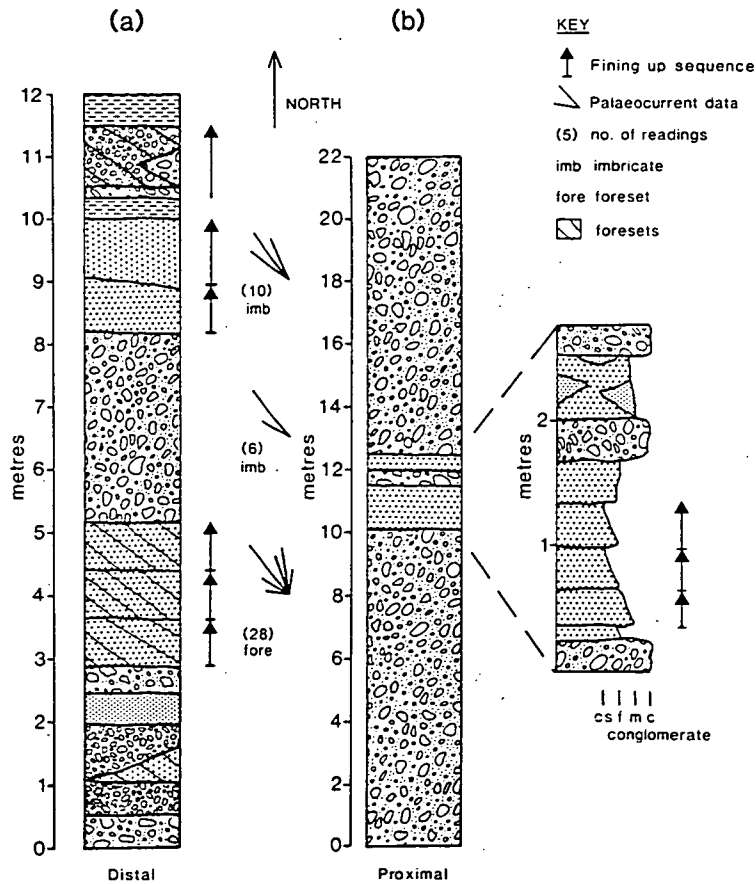
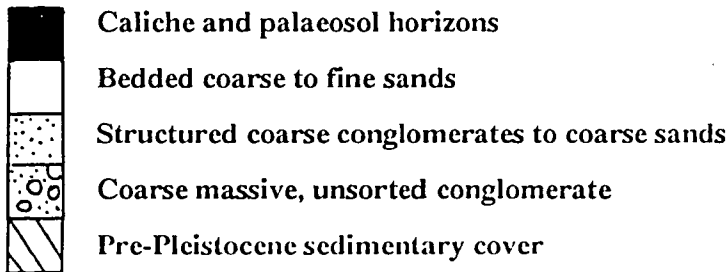
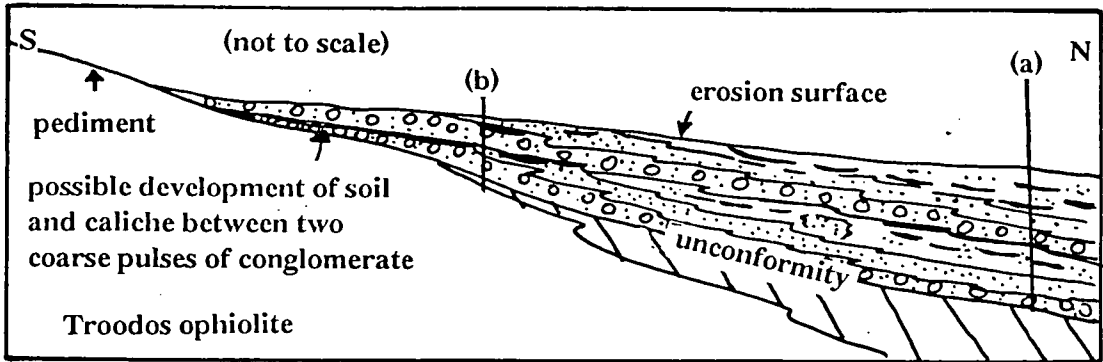




Fig.5.34. Sketch displaying the proximal to distal variation in sedimentation across the north Troodos margin and two sketch sections: a) at a distal location and b) at a proximal location.



hills, e.g. Pera (Section 2.3). The extent of erosion on the peneplaned Quaternary terraces is uncertain.

Details concerning the extent and thickness of the Fanglomerate Group exposures in areas other than the north Troodos margin are more difficult to discern, as much of the sediment appears to have by-passed the southern sub-aerial depositional areas and been deposited directly on to the southern coastal shelf. Estimates of the thickness of the fluvial sequences of the Fanglomerate Group in areas away from the north Troodos margin, cannot be made. The Polis-Paphos graben represents the only area of active large scale, Quaternary, neotectonic faulting (Section 4.4). This faulting has caused the F1 units of the Fanglomerate Group to be dissected and has resulted in exposures 180m ASL at Goudhi (Plate 5.12), on the western flank of the graben, and c.300m ASL in the south, at Nata (Plate 4.2). The thickest Fanglomerate Group sections were recorded at Goudhi and this possibly reflects the influence of tectonics.

## **5.6.2 Sedimentology.**

### **5.6.2.1 Introduction.**

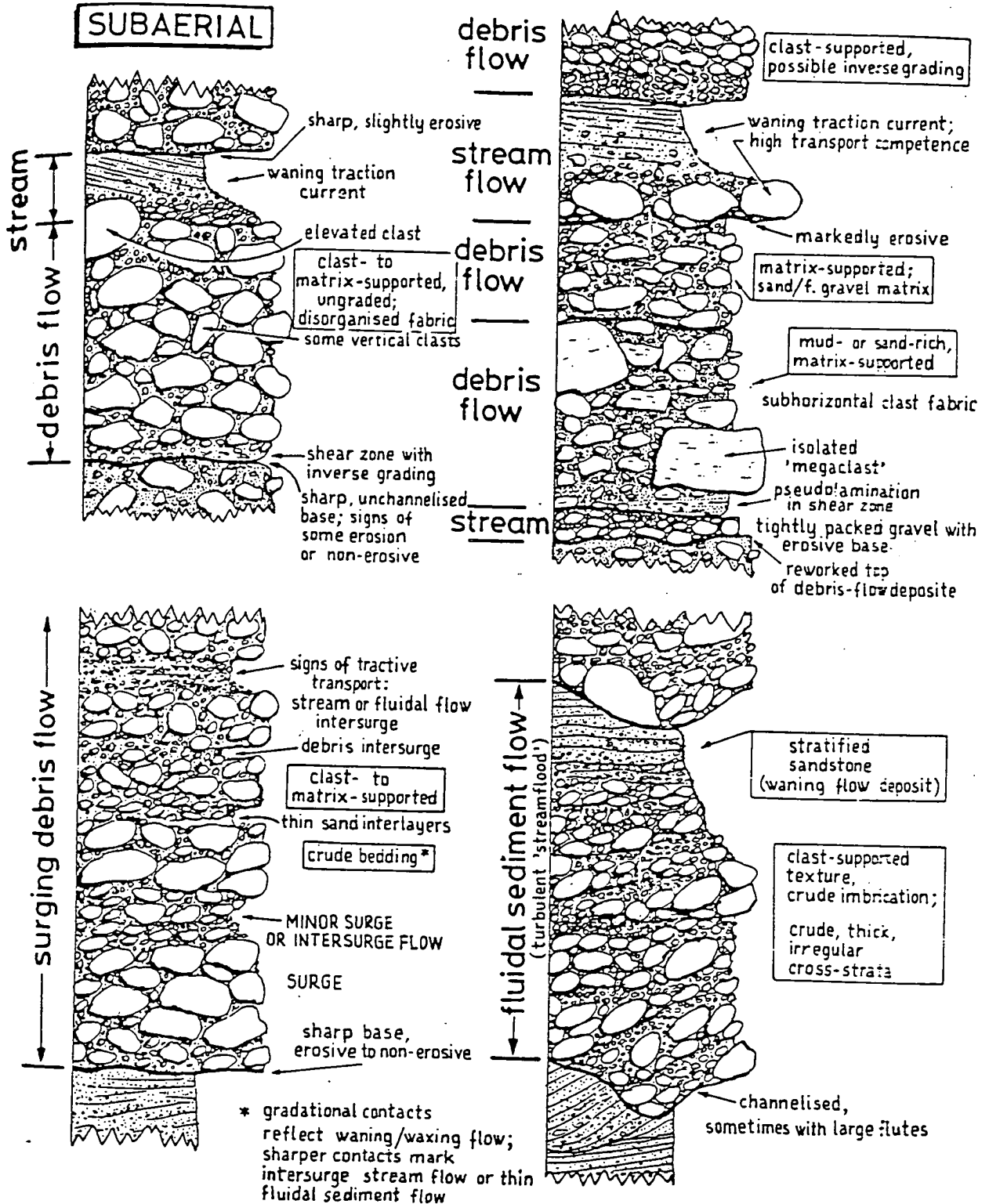
Studies of modern and ancient alluvial fans in semi-arid climatic conditions have been the subject of much research, e.g. modern fans in south-west U.S.A (Blissenbach, 1954; Hooke, 1967; Bull, 1977) and ancient fans in Scotland (Wilson, 1980; Steel, 1974). Blissenbach (1954) concluded that alluvial fan sequences are coarse boulder to clay size detritus, which is angular to rounded and has good to poor stratification, pronounced imbrication, cut and filled channels and four distinct sediment types:

- i) debris flows,
- ii) sheetflood or streamflood sequences,
- iii) braid channel sequences
- iv) floodplain or playa type sequences.

Alluvial conglomerates in semi-arid environments are distinguished from coastal zone conglomeratic sequences by their textural immaturity, the scoured and channellised flow conditions, the variation from vague to distinct stratification and the general absence of well defined beds (Nemec & Steel, 1984).

Gravelly mass flow units are preferentially located on the upper and middle reaches of alluvial fans (Hooke, 1967). These beds are usually sheetlike, ungraded, clast-to matrix-supported and show either no obvious stratification or crude layering, and generally fall into one of four categories (Fig.5.35). The mass flow units are generally

Fig.5.35. Four sections of typical features of mass-flow deposits (after Nemec & Steel, 1984).



sheetlike, slightly to strongly channellised and display normal grading. These flows are intermediate between stream flows and debris flows and have previously been termed streamfloods (Bluck, 1967A; Steel, 1974) and sheetfloods (Wasson, 1977, 1979; Heward, 1978A).

Vertical type-profiles and proximal to distal variations, associated with braided stream sequences, are well documented (e.g. Miall, 1978; Rust, 1978).

Floodplain and playa sequences have been recognised in ancient semi-arid alluvial fan sequences of Scotland, e.g. Devonian age (Steel, 1974), New Red Sandstone (Wilson, 1980). These consist of extensive mudstone and siltstone units, caliche horizons and coarse grained members that commonly scour into the underlying sequence. The sequences are laterally extensive and generally consist of fining-up couplets.

#### **5.6.2.2 North Troodos margin.**

McCallum (1989) proposed the first detailed model for the deposition of the Fanglomerate Group on the north Troodos margin. This model proposed that valley incision occurred, with Fanglomerate Group sediments being deposited within these valleys whilst reworking of the sedimentary cover of the Troodos ophiolite was taking place. These valleys were subsequently flooded with newly-derived conglomerates from the Troodos Massif, resulting in thin sheets of sediment spreading out onto the Mesaoria Plain. Subsequent deep incision resulted in the formation of terraces.

It is suggested from the data presented here, that alluvial fan development took place on the north Troodos margin during the early and middle Pleistocene, i.e. F1 and F2 times (Chapter 2). The fans were fed by rivers feeding off the Troodos Massif (Fig.2.1). The F1 and F2 Fanglomerate units unconformably overlie the basement lithologies on the western and central parts of the Mesaoria Plain but are conformable with the Upper Pliocene sequences in the east. This contrast suggests that either uplift was more intense in the west with some erosion of the underlying Troodos sedimentary cover sequence prior to deposition of the Fanglomerate Group, and/or that the pre-existing topography and drainage system during the Upper Pliocene facilitated steady state fluvial deposition from the Pliocene, i.e. the Apalos Formation (McCallum, 1989), through to the Quaternary, on the eastern portion of the Mesaoria Plain.

Climate changes probably also contributed to the architecture of the fans on the north Troodos margin during the early and middle Pleistocene, as well as the deposition

of the Fonglomerate Group throughout the Quaternary, as the change from generally dry glacial periods to wetter interglacial periods will effect run off, erosion and the style of deposition. A similar interplay of processes, i.e. tectonics versus climate, has been described from the Dead Sea (Frostick & Reid, 1989), Oman (Maizels, 1987) and south-east Spain (Harvey & Wells, 1987).

There is no evidence for the presence of debris flow units in the massive conglomerate sequences that crop out at locations proximal to the north Troodos margin. The lack of debris flow sedimentation probably reflects the proportion of finer-grained sediment available, which in turn results from the general lack of soil cover in semi-arid climates which reduces the amount of fine sediment available (Harvey, 1984). The generally structureless, grain- to matrix-supported, poorly sorted nature of these units, which commonly overlie erosional bases (Section 5.3) resembles rapid deposition by streamflood, or sheetflood, processes, similar to that documented in the Gm conglomerates from the early Tertiary sequences in Wyoming (Kraus, 1984) and the Quaternary sequences in Spain (Harvey, 1984). The variable clast fabric within these sheetflood units reflects the distance that these units have travelled and the relative viscosity of the units. Short travelled units are generally disorganised, whereas sheared laminar flow results in clast orientation as a consequence of clast interaction (Lewis *et al.*, 1980). The development of sheetfloods rather streamfloods is the favoured proposition. Sheetfloods occur as extensive thin sheets of massively bedded conglomerate (Blissenbach, 1954), whilst streamfloods occur when the channels are too deep for sheetflood development. Deposition by sheetflood processes resulted in the deposition of an extensive conglomerate sheet over much of the fan sequence on the north Troodos margin.

Intermediate locations represent median deposition between the proximal and distal extremes. The development of sand units, typically 10-90cm thick, inter-bedded with the conglomerates indicates that shallow, rather than deeper, channels existed (Nemec & Steel, 1984), typical of intermediate locations on semi-arid alluvial fans, *cf.* the Quaternary of Spain (Harvey, 1984). The presence, or absence, of cross-bedding within conglomerate sequences has also been recognised as an indicator of channel depth, with cross-bedding being indicative of deeper channels (Kraus, 1984). Cross-bedding within these intermediate locations is thought to have occurred during the rapid fall in fluid and sediment discharge across a bar, as was suggested by Hein & Walker (1977), supporting an argument for flashy, ephemeral flow across the fans.

Distal locations on the north Troodos margin reflect braided stream flow conditions (Blissenbach, 1954; Miall, 1978) with the development of channel cut and fill, overbank sediments and palaeosols. These sequences also reflect the continuation of a proximal to distal trend, south to north across the Mesaoria Plain. Reworking and downcutting probably resulted in the substantial reworking of mid- and upper-fan sediments to distal locations.

As uplift continued the core of the Troodos Massif is thought to have risen quicker than the Mesaoria Plain (Chapter 2). This resulted in erosion, with fresh Troodos-derived clasts being made available for deposition. The variation in clast types on the north Troodos margin reflects this, with increased numbers of gabbro clasts in the Fanglomerate Group relative to the Pliocene sediments. Studies of tectonic uplift of source areas in Recent alluvial fans (Heward, 1978B) indicate that uplift of the hinterland can result in either deposition on the active fan segment, i.e. the rate of uplift is greater than the rate of stream dissection, or entrenchment and the deposition of a second fan sequence at the toe of the first fan, i.e. the rate of stream dissection is greater than the rate of uplift, and results in isolated hills that are dissected during continued erosion by the rivers. Both of these scenarios have occurred during fan development along the north Troodos margin and have resulted, firstly, in the deposition of the F1 Fanglomerate unit and then the extensive dissection of the F1 Fanglomerate unit during F2 times. A similar process has post-dated the formation of the F2 Fanglomerate unit with downcutting of the drainage along the north Troodos margin resulting in the development of channel fans and mature erosion surfaces (*cf.* Muto, 1987; Chapter 2; Fig.2.2). Distal localities were not uplifted as much, or as rapidly as, the proximal areas of the Mesaoria Plain (Chapter 2). This resulted in the coalescence of the Fanglomerate Group units at distal locations (Figs.2.11 and 5.34).

### **5.6.2.3 Model of deposition in coastal southern Cyprus.**

The model of deposition favoured in areas away from the north Troodos margin is predominantly ephemeral, fluvial sedimentation. Pre-existing topography also influenced the pattern of sedimentation in the west of the island, e.g. the Polis-Paphos graben. Deposition within the southern coastal areas appears to have been controlled by a series of large channels. Some of these channels date back to the Pliocene and possibly the Miocene (Eaton, 1987; Houghton *et al.*, 1990). The initiation of these channels before the Quaternary meant that a series of conduits existed prior to the onset of rapid uplift during the early Pleistocene. This resulted in the formation of channel fans along the south coast of Cyprus, with much of the sediment by-passing the island and being deposited on the

shelf south of Cyprus. A marked proximal to distal change in the pattern of sedimentation occurs along the southern margin of the Troodos Massif which probably reflects the emergence of a fluvial system from an enclosed channel fan (*cf.* Muto, 1987; Heward, 1978B) onto an open plain (Fig.6.12). This change in environment has resulted from a widening of the channels and the development of bars and channels rather than the sheetflood-streamflood deposits that are prevalent in the confined channels closer to the margin of the Troodos Massif. The development of braidplain sequences accounts for the increased sorting of sediments away from the confined channels, with grain- rather than matrix-supported conglomerates. Thin, coarse, matrix- to grain-supported conglomerates of facies A1 overlie the well bedded, mature conglomerate and sand facies. These suggest periodic flood events that have carried their immature, poorly sorted loads on to the plains, beyond the confines of the restricted channels (Fig.6.12). The coarse pulses of facies A1 are thought to be correlatable with the coarse grained capping conglomerates that crop out along the north Troodos margin (Section 5.3.1).

Gravelly flow sediments, i.e. sheetflood and streamflood sequences, make up a minor proportion of the exposed Fonglomerate Group deposits in coastal southern Cyprus, where channellised, braid sequences dominate. The braid sequences commonly unconformably overlie deltaic sequences (Chapter 6) and this relationship suggests that deposition in these areas was dependent on the relative sea-level at that time. McCallum (1989) argues that eustatic sea-level effects are unlikely to have played a major role in the deposition of the Fonglomerate Group on the north Troodos margin, and evidence presented here (this chapter and Chapters 6 and 7) agrees with this. The deposition of Quaternary siliciclastic sediments in areas other than the north Troodos margin has been affected by relative sea-level which has dictated the precise environment of deposition (also see Chapter 6). It should be noted that relative sea-level changes can also include tectonic uplift.

The channellised sequences in south-west Cyprus display rapid changes in bedding, the interbedded nature of the coarse and fine sediments and the presence of palaeosols with root structures, combined with the strong downstream dipping imbrication, suggesting that these sediments were laid down in a fluvial braidplain environment. The channels are small and the conglomerates within them generally grade up into the finer sediments, suggesting an initial high energy pulse followed by a waning flow. The scoured and grain-supported nature of the conglomerates suggest that these were deposited as bedload, or similar, and not as mass flow deposits. The periodic high energy events resulted in the deposition of immature conglomerates, whilst the finer

up stream?  
?

grained, more mature sediments are probably related to a waning flow. The palaeosols and caliche horizons relate to relatively stable periods of non-deposition.

Evidence from the exposures of the Fanglomerate Group sediments in the Polis-Paphos graben suggest that they were deposited as channellised sequences on a braidplain that was initially dissected by faulting, with subsequent dissection resulting from uplift and sea-level changes. The dissection of the graben basement is reflected in the clast maturity and provenance (Section 5.5.1.4). The conglomerates at the northern end of the graben prograde over the deltaic sequence as a result of a relative fall in sea-level, e.g. near Limni (Chapter 6), similar to that seen along the southern coast of Cyprus, e.g. in the area between Larnaca and Limassol. This probably occurred during the deposition of the F3 Fanglomerate unit. The most extensive period of fluvial sedimentation in the graben probably occurred during the deposition of the F1 and F2 Fanglomerate units, when large areas of the graben appear to have been covered by fluvial sediments. The F3 Fanglomerate unit has a more restricted out crop pattern, i.e. the south and central portion of the graben.

The F4 and Holocene Fanglomerate units represent phases of continued alluviation, with the deposition of coarse conglomerate and increasing proportions of fine alluvium. The coarse conglomerates are attributed to a high energy, bedload environment; these pass up into stratified bar deposits. The fine grained alluvium is interpreted as forming in a overbank environment. The finer grained sediments correspond to those seen on the north Troodos margin, i.e. the Xeri Alluvium (Ducloz, 1965). Gomez (1987) correlates the sediments seen in lower Vasilikos Valley with the Older and Younger Fill of Vita-Finzi (1969). The presence of two distinct phases of sedimentation in the Vasilikos Valley, i.e. unstratified conglomerates and channel sediments, and the two coarse pulses of conglomerate found in the coastal exposures at Zyyi and Petounda Point (Fig.5.14), supports the presence of an Older and Younger Fill. These phases of development probably formed as a result of climate change as proposed by Fairbridge (1972), rather than major tectonic uplift. The presence of the Recent coarse conglomerate pulses within the Vasilikos Valley has been attributed to man and the effects of deforestation during Roman times (B. Gomez, *pers. comm.*, 1989), although the size of clasts within these conglomerates suggest flows that are significantly less than those seen along the south margin of the Troodos Massif during the Pleistocene. The floor of the Vasilikos Valley was downcut by 6m in the early Holocene, this was followed by a period of aggradation and alluviation between 5540 to 5010 B.C. (Gomez, 1987); this preceded a phase of fine-grained overbank sedimentation and subsequent downcutting to form an alluvial terrace within 2m of the present floodplain, as seen in the



Tremithios Valley (Gifford, 1978). Incision into this terrace has occurred since Byzantine (c.330-1190 A.D.) times (Gifford, 1978); shards found in this terrace south of Nicosia support this. Muddy, poorly sorted alluvium was deposited in the Tremithios River, in the Larnaca lowlands (Gifford, 1978) during the latest Pleistocene and early Holocene.

The extensive, dominantly fine-grained sediments that crop out in the area to the north of Kissonerga village (Section 5.3.4.6) resemble floodplain sequences that have been described from Recent semi-arid alluvial sequences in south-west U.S.A. (Blissenbach, 1954) and the New Red Sandstone and Devonian of Scotland (Steel, 1974; Wilson, 1980). The presence of shallow but wide conglomerate channels indicates low sinuosity, ephemeral streams (Leopold & Miller, 1956). The deposition of extensive silts is suggestive of deposition as overbank sediments, which were periodically flooded, resulting in the deposition of conglomerate stringers. The presence of roots and caliche horizons within the sedimentary sequence indicates periods of quiescence when flooding was not taking place. The development of thick floodplain sequences has been interpreted as indicating the maintenance of periodic flood activity and a lack of regional channel migration in semi-arid conditions (Wilson, 1980). This supports the geomorphological evidence from south-west Cyprus which indicates a consistent drainage pattern during the Quaternary (Section 2.2.4).

### **5.6.3 Palaeocurrents.**

There is a general swing in palaeocurrent direction from north-west to north-east, from west to east across the Mesaoria Plain, reflecting a radial drainage pattern centred on Mount Olympus. Palaeocurrent data from other areas, away from the North Troodos margin, coincide with the present direction of drainage.

The palaeocurrent data from the Fanglomerate units in southern Cyprus show a pattern which indicates minimal changes in the flow direction throughout the Quaternary, so supporting arguments put forward in Chapter 2. The general southward and radial flow on the south Troodos margin reflects the dominant source area, the Troodos Massif. The exception to this general radial pattern has resulted from the structural control imposed by the development of the Polis-Paphos graben which, locally, has controlled the palaeo-flow.

Data showing deviation from the "normal" southward directed palaeocurrent in southern Cyprus have been collected from fluvial sequences that were deposited outwith the restricted valley fan systems (Section 5.6.2.3; Fig.6.12), in areas of lower river

gradients, e.g. above the deltaic sequence and areas of true braidplain deposition (Section 5.6.2.3; Chapter 6). The drop in gradient and removal of any lateral constraints on sedimentation may have resulted in more sinuous rivers and may explain the diverse palaeocurrent data seen in the Dhekelia and Pissouri area, as well as the variation in palaeocurrent in more distal locations on the Limassol and Paphos coastal plains. The possible example of a large, more sinuous flowing channel is found in the Kouklia area, where a large restricted channel is seen; the palaeocurrent data from this is directly related to the local flow direction of this channel at outcrop and not a radial pattern centred on Mount Olympus (Fig.5.16).

The palaeocurrent data from the south coast of Cyprus replicates that seen on the north Troodos margin, with a general radial pattern. This is more clearly defined in proximal locations, where only minor variations in palaeoflow occur, throughout the Quaternary. The pattern in distal locations is more diverse, reflecting the nature of the coastal plain, with more variable palaeocurrents correlating with isolated rivers, e.g. Kouklia, and braidplain environments on low coastal plains.

#### **5.6.4 Provenance.**

##### **5.6.4.1 North Troodos margin.**

The provenance of the clasts on the north Troodos margin indicate that the major rivers channels that ran off the ultramafic core of the Troodos ophiolite during the Pleistocene also erode the core of the ophiolite today, as ultramafic clasts are only found in the units of the Faglomerate Group that could have been fed by the Karyotis River (Chapter 2). The similarity of clast types seen in both the Pliocene and Pleistocene sequences in the eastern Mesaoria Plain area, south of Nicosia, reflects the drainage pattern in as much as rivers feeding sediment into this area have never cut through the plutonic units of the Troodos ophiolite, i.e. the major source of ultramafic and gabbroic clasts to the Faglomerate Group, although uplift was taking place. The absence of ultramafic clasts and the scarcity of the gabbro clasts reflect directly the lithologies of the ophiolite through which the rivers, that issue out on to the north-east Mesaoria Plain, pass.

The presence of, or increase in, the numbers of sedimentary clasts in the later phases of the Faglomerate Group deposits suggests that the unconformity between the Pleistocene Faglomerate Group and underlying Pliocene sediments:

- i) did not remove a large amount of sediment,

or ii) in subsequent phases of the Fanglomerate deposition, i.e. containing Troodos-derived clasts, eroded much of the previously deposited Fanglomerate sediments, but only minor portions of the sedimentary cover were eroded, until the latter part of the Quaternary,

or iii) much of the soft Pliocene sediment broke down to form a finer fraction, now indistinguishable from the matrix of the Fanglomerate Group.

Arguments i) and ii) are favoured as an unconformity is not seen in the east between the Fanglomerate Group and Pliocene sediments and the topmost Pliocene sediments further east consist of Troodos-derived conglomerates. It is hypothesized that as uplift continued, deeper downcutting into the Pliocene and underlying sedimentary sequence took place (Chapter 2); this resulted in an increased proportion of sedimentary clasts within the later units of the Fanglomerate Group. This suggests that the initial phase of uplift resulted in the deposition of Troodos-derived sediments over the sedimentary cover sequence and that there was minimal downcutting into the Troodos sedimentary cover sequence. There are exceptions to this general pattern, topographically high areas provided sedimentary clasts to the Fanglomerate Group throughout the Quaternary, e.g. Kreatos Hill, near Mitsero, on the north Troodos margin, which generated a limited numbers of limestone clasts throughout the Quaternary period.

The Kyrenia Range did not influence the Fanglomerate Group deposits on the south of the Mesaoria Plain, as clasts derived from the Kyrenia Range are absent from the units of the Fanglomerate Group.

The variation in proportion of Troodos-derived clasts present in the different Fanglomerate units on the north Troodos margin is negligible and could be explained as follows:

- i) the highest source areas of gabbro and diabase were being tapped from the earliest Pleistocene,
- or ii) graben structures in the Troodos Massif exposed lower crustal levels at the same time as diabase.

The second argument may apply locally, as both diabase and minor numbers of gabbroic clasts are present in the Pliocene Kakkaristra Formation but the number of gabbroic clasts in the units of the Fanglomerate Group is much greater than within the units of the Kakkaristra Formation. This increase in the proportion of gabbro clasts suggests that exposure and erosion of most of the gabbro took place later than the exposure and erosion of the diabase. The initial exposure and erosion of the gabbro

source area probably occurred during rapid uplift, i.e. early-middle Quaternary, and the formation of the unconformity postdating the deposition of the Pliocene sequence prior to the deposition of the Faglomerate Group.

#### **5.6.4.2 South-east Cyprus.**

Gabbro clasts found within the fluvial conglomerates of the Faglomerate Group in the Dhekelia area could not have had their source in the Troulli Inlier and must, therefore, been derived from either isolated gabbroic outcrops seen in the eastern portion of the Troodos ophiolite, or from the main gabbroic body in the centre of the Troodos Massif. Derivation from the central body is unlikely as most of the rivers flowing from this area feed north and then west, rather than east. Derivation of the gabbroic clasts from the isolated outcrops in the east of the Troodos Massif is more likely as these rivers flow north and then east. The presence of gabbro clasts also supports an argument for the development of a more extensive drainage system, which flowed through the Dhekelia area and into Larnaca Bay, during the early Quaternary (Section 2.2.3).

#### **5.6.4.3 The south coast.**

The variation in clast provenance between Episkopi and Vasilikos to the south of the Troodos Massif reflects the local drainage pattern and local basement geology, as well as the unroofing of structurally deeper lithologies of the Troodos ophiolite and the Limassol Forest belt. The sedimentary clasts are markedly different from those associated with outcrops in south-east Cyprus. Clasts are predominantly derived from the Miocene Pakhna Formation, rather than the chalks and limestones of Palaeogene and Neogene age, which is the case further east. The Kouris River (Fig.2.1) flows from the core of the Troodos Massif today and can, therefore, transport clasts derived from all parts of the ophiolite. The paucity of ultramafic clasts in the F3 Faglomerate units, and the increased proportion of these in the F4 Faglomerate and Recent units, in the area of the Kouris River suggest that unroofing and erosion of the core of the ophiolite was more marked during the latter part of the Quaternary. By contrast, rivers further east contain large proportions of ultramafic clasts from F2 Faglomerate times onwards. This reflects substantial erosion of a series of sources, i.e. Limassol Forest belt, during the early and middle Pleistocene. The absence of ultramafic clasts in the F1 Faglomerate unit at Vasilikos could reflect:

- i) later local uplift and erosion of the ultramafic units through which the Vasilikos River valley cuts,

or ii) regional unroofing of the Limassol Forest belt, which did not take place until after the deposition of the F1 Fanglomerate unit.

#### **5.6.4.4 South-west Cyprus.**

The proportion of clast types in south-west Cyprus are generally constant throughout the Quaternary, reflecting sources as diverse as units of the Mamonia terrane, the Troodos ophiolite and its sedimentary cover sequence. The presence of mafic and ultramafic units within all Quaternary units of the Fanglomerate Group reflect their presence in the Mamonia terrane. The two exceptions to this pattern of consistency occur at Pissouri and in the Polis-Paphos graben.

In the Pissouri area, channellised Fanglomerate Group deposits have a clast content that was derived from not only the local sedimentary sequence but also from the Troodos Massif. This supports the argument for capture of the Kryos River between the early Quaternary and Recent (Section 2.2.6). The variation in clasts type and maturity in the Polis-Paphos graben between F1 and F3 Fanglomerate times suggests that:

- i) regional erosion occurred before and during the formation of the F1 and F2 Fanglomerate units but that associated downcutting into the local sedimentary "basement" during this time was minimal,
- ii) the increase in the proportion of chalk clasts in the F3 Fanglomerate units reflects a change from regional erosion to more local erosion, resulting in the increased dissection of the local pre-Quaternary sediments,
- iii) reworking of the Troodos-derived clasts was taking place during the formation of the F3 Fanglomerate units
- iv) rapid erosion of the sedimentary clasts was occurring with little evidence of transport prior to deposition.

#### **5.6.5 Summary.**

The sediments of the Fanglomerate Group reflect the uplift and Quaternary climate changes of southern Cyprus. Sea-level changes have also influenced the development of the Fanglomerate Group in coastal areas of southern Cyprus (Fig.6.12). The pattern of sedimentation reveals a proximal to distal relationship, with evidence for the development of alluvial fans, channel fans, braidplain and floodplain environments. The provenance of the Fanglomerate Group sediments reflect local geology and the drainage pattern but the dominant source and control is the Troodos ophiolite. The variation in provenance between the Pliocene-Pleistocene and, locally, the Pleistocene-

Holocene Fanglomerate units, is indicative of progressive unroofing of the Troodos ophiolite and its sedimentary cover sequence. Studies of borehole samples indicate that there has been no major change in provenance during the Quaternary, i.e. there was no introduction from sources other than the Troodos ophiolite and its sedimentary cover sequence. The palaeocurrent pattern is broadly radial, although minor variations resulting from structural controls, e.g. the Polis-Paphos graben, and the development of shallow dipping coastal plains, have facilitated some deviation from this radial pattern. The absence of major changes in the drainage pattern, as indicated by palaeocurrent and provenance studies implies that uplift of the Troodos Massif has been focussed on the same area throughout the Quaternary, i.e. Mount Olympus. Evidence from the sediments of the Fanglomerate Group indicate that there was a waning of activity through the Quaternary, which resulted in less exhaustive erosion and deposition during the Late Pleistocene-Recent, as suggested by the data from the geomorphological and dating studies (Chapters 2 and 3).

## **Chapter Six: Siliciclastic shallow marine sediments.**

### **6.1 INTRODUCTION.**

Previous studies of Plio-Quaternary marine siliciclastic sedimentary sequences have been limited to studies of the Pliocene Kakkaristra Formation, a fan-delta sequence (McCallum, 1989). The Quaternary shallow marine siliciclastic sequences have received scant attention, the only recorded description referring to deltaic outcrops in the Polis-Paphos graben (L. Ward *pers. comm.*, 1987).

This chapter will describe the geographical distribution of the Quaternary deltaic and siliciclastic beach sequences, their sedimentary characteristics, their relationship to the Fanglomerate Group (Chapter 5) and the carbonate littoral sequences (Chapter 7) and interpret their mode of deposition.

### **6.2 GEOGRAPHICAL DISTRIBUTION AND AGE OF SILICICLASTIC SHALLOW MARINE SEQUENCES.**

Marine siliciclastic sediments in southern Cyprus are limited to quarry exposures at the northern end of the Polis-Paphos graben (location 3-106), areas along the southern coastal plain (locations 3-12, 3-13 and 3-18) and exposures between Dhekelia and Xylophagou (locations 2-78 and 2-80; Fig.2.7). The siliciclastic sediments do not form palaeo-cliff lines, unlike the carbonate littoral sediments (Chapter 7). The regressive nature of these marine sediments results in fluvial sequences of the Fanglomerate Group unconformably overlying the shallow marine siliciclastic units. It is therefore likely that these shallow marine siliciclastic sediments make up much of the sub-crop beneath the fluvial sediments of the coastal plain of southern Cyprus (Plate 4.1). A similar pattern of sedimentation is likely to have developed across the Akrotiri Peninsula as borehole data indicate the presence of at least 86m of sands and Troodos-derived conglomerates, the lowest of these being 75m beneath ASL (Fig.5.3). Although the records are poor, it is likely that at least some of the sands and gravels found in the Akrotiri Peninsula boreholes were deposited in a marine environment.

The distribution of the Quaternary deltaic sequences is very similar to that of the Fanglomerate Group, much of the sediment was sourced from the Troodos ophiolite and initially transported by fluvial action (Chapter 5). There are only three areas where carbonate and siliciclastic marine sequences are seen in close proximity: at the north end of the Polis-Paphos graben where carbonate sequences gradually replace siliciclastic marine sequences east of the exposures at Limni (location 3-106), i.e. away from the influence of

the major drainage issuing from the Polis-Paphos graben; in the Lara Bay area of western Cyprus (Chapter 7) and in the area between Dhekelia and Xylophagou where extensive deltaic and beach sequences of F1, F2 and F3 times crop out. These sequences are replaced, in F4 times, by a mixed sequence of carbonate and siliciclastic littoral sediments (Section 7.3.6).

The marine siliciclastic sediments crop out beneath the F3 erosion surface, which forms an extensive plain around much of the south and south-west coast and at the northern end of the Polis-Paphos graben (Figs.2.1 and 2.7). The preserved marine siliciclastic sediments predate the formation of the F3 erosion surface. As an unconformity/discontinuity exists between the F3 fluvial sequences and the underlying deltaic sequences it is difficult to correlate these two depositional events with any great certainty, although the presence of coral heads within the shallow marine siliciclastic sequences may allow them to be dated, in the future, using the U-series method (Chapter 3). It is likely, however, that these sequences are correlatable with the deposition of the F3 carbonate sequences that crop out at Petounda Point (location 3-11) and Larnaca (location 1-130; Chapters 3 and 7). A positive correlation can be made at the northern end of the Polis-Paphos graben, where F3 carbonate sequences which are laterally equivalent, and correlatable, interfinger with the marine siliciclastic sediments, e.g. Argaka (location 3-109; Chapter 7). In south-east Cyprus the marine siliciclastic sequences crop out beneath the F2 erosion surface and are therefore probably related to the F2, and possibly the F1, phase of deposition. No direct evidence for F4 deltaic deposition is seen although some of the sub-crop on the Akrotiri Peninsula (Fig.5.3), and a portion of the sedimentary sequence identified offshore by the use of seismic methods (McCallum, 1989), may have been deposited in a deltaic environment during this period, especially those areas where major rivers continue to feed into the Mediterranean Sea, e.g. the southern coast east of Limassol, Akrotiri Bay, Episkopi Bay and Khrysokhou Bay (Figs.2.7 and 2.17). Much of the direct evidence for the deposition of the F1 deltaic sequence is missing. The absence of F1 exposure may result from erosion, many of the F1 erosion surfaces being today truncated at the coast. The truncation of these surfaces has resulted in the formation of clifflines that presently cut down through the F1 fluvial, rather than marine, sequences. This phenomenon suggests that much of the F1 marine siliciclastic sequence may have been eroded away, e.g. Pissouri (location 3-30).



## **6.3 DESCRIPTION OF THE QUATERNARY DELTAIC SEQUENCES.**

### **6.3.1 South-east Cyprus.**

The most extensive marine siliciclastic sequences in south-east Cyprus crop out between Dhekelia and Xylophagou (Fig.6.1). The sedimentary sequence crop outs in a series of quarries along a 7km east-west stretch of coast. These beds provide some of the thickest and most continuous Quaternary sequences in Cyprus, e.g. the outcrop at location 2-79 is approximately 25m thick and the base of the Quaternary succession is not seen (Plate 6.1). However, most of the exposed sections are less than 10m thick. Although the sediments are laterally persistent, rapid vertical changes occur and a great variety of sediments are seen. Borehole data indicate that the thickest sequence is in the order of 60-65m thick and occurs in the centre of the area (Fig.6.1). The topographic relief associated with the Athalassa and Nicosia Formations (Pliocene) in the east, and limestones of Miocene age cropping out in the west, cause the Quaternary sediments to thin rapidly away from the centre of the area (Fig.6.1). Borehole data record a general coarsening of the Quaternary successions up sequence (Fig.6.1). Thick caliche commonly caps the Quaternary sequences throughout south-east Cyprus.

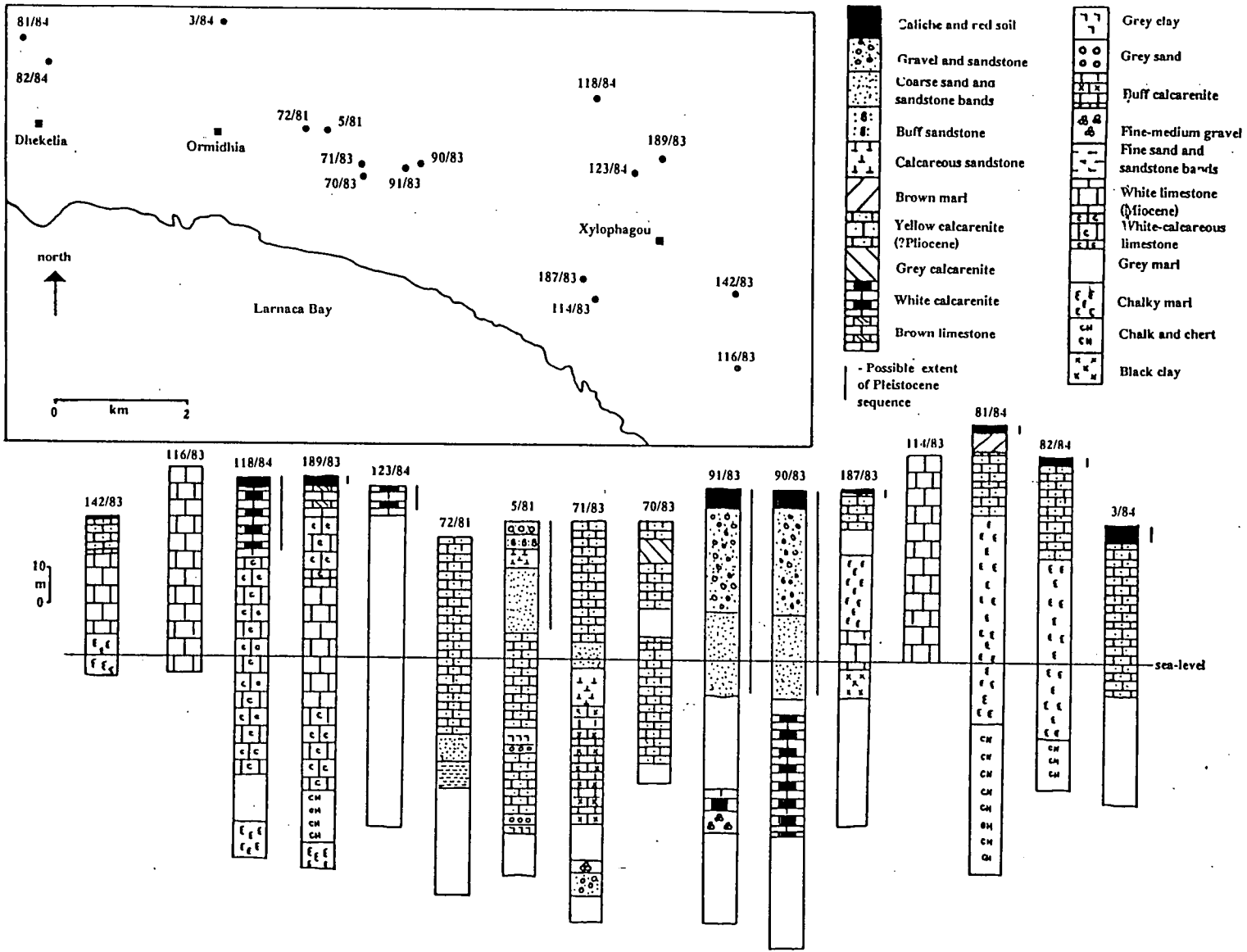
#### **6.3.1.1 The Dhekelia area.**

Outcrops in the Dhekelia area indicate the variation in relief that existed prior to the deposition of the Quaternary sequences (Fig.6.1). Neogene sediments underlie the white grainstones, and sand and gravel sequences of Pleistocene age in the centre of the area. At other locations, i.e. on the periphery of the area, there is a general absence of Pleistocene marine sands and gravels and the Pliocene sediments pass directly into the sediments of the Fanglomerate Group.

The Quaternary sequence in the Dhekelia area is only 10m thick and unconformably overlies calcarenites of the Athalassa Formation. The basal Quaternary unit varies with coarse, poorly sorted, unfossiliferous conglomerates dominating, whilst white grainstones containing a rich fauna, e.g. echinoids, rhodoliths and molluscs, are locally present. Seven sedimentary units, caliche and palaeosols crop out above this basal sequence (Fig.5.10; Plate 6.1).

#### **6.3.1.2 Ormidhia area.**

The sediments in this area are very different from those to the west, i.e. in the Dhekelia area. Here, the effects of the palaeorelief are far less pronounced and the base of



Note: numbers relate to the borehole number and the year that it was drilled.

Fig. 6.1. Borehole data from the Dhekelia to Xylophagou area displaying the variation in thickness of the Quaternary sequences and the pre-existing relief prior to the deposition of the Quaternary sediments.

the Quaternary sedimentary sequence is not seen. The following sedimentary units crop out:

*i) Unit A: well sorted, grained-supported, mature, medium grained conglomerate.*

The unit is commonly bedded and contains mature, discoidal and spheroidal clasts. The matrix of this unit consists of medium to coarse sand. Both sedimentary and igneous clasts are present within the sequence, although the proportions of each vary between localities, as does the maturity of the clasts (Fig.6.2). The beds in this unit are generally between 30 and 50cm thick, dominantly imbricated, but some shallow dipping; prograding foresets are also present. The foresets generally dip towards the south and south-west at  $10^{\circ}$ - $15^{\circ}$  (Fig.6.2). This unit is commonly bioturbated with vertical and horizontal burrows, e.g. *Thalassinoides*. A low diversity, high density molluscan fauna is present, e.g. *Glycymeris*, *Pecten* and *Ostrea*. The mollusc shells are usually abraded and more than 5mm thick. The beds are laterally continuous and not lenticular with beds being traced laterally for more than 5m.

*ii) Unit B: well sorted, fine grained conglomerate.*

This unit consists of mature conglomerates (Fig.6.2). The beds are typically 1-10cm thick and outsized clasts less than 5cm along the "L" axis are present. The larger clasts are commonly discoidal, while the smaller clasts are more spherical. This unit is characteristically unfossiliferous, although a fauna, similar to that found in unit A, is locally present and bioturbation is extensive, e.g. *Thalassinoides* (Plate 6.1). The beds locally display small-scale fining up structures, shallow and steeply dipping foresets, trough-cross-stratification and convoluted beds (Plate 6.2).

*iii) Unit C: mature, well bedded, medium to fine sands.*

This unit is made up of planar bedded medium to fine, very well sorted green and white sand (Fig.6.2; Table 8.1). Shallow dipping foresets ( $<10^{\circ}$ ) and extensive parallel laminations are common, although higher angle foresets ( $<30^{\circ}$ ) are also present. The beds are usually between 5 and 10mm thick and appear to be ungraded. Horizontal and vertical bioturbation is common, e.g. *Thalassinoides*, throughout much of this unit, and particularly pervasive at the base, locally destroying the bedding and sedimentary structures. The predominance of bioturbation results in the massive appearance of this unit. The unit is generally unfossiliferous. Hard white bands of calcium carbonate are locally interbedded with this unit. These bands are generally folded and contorted (Plate 6.2). Some truncation surfaces are present within the unit (location 2-78) and are

Fig.6.2. Sedimentary sections of the shallow marine sequences in the Ormidhia area of south-east Cyprus

Note: see text for description of the units.

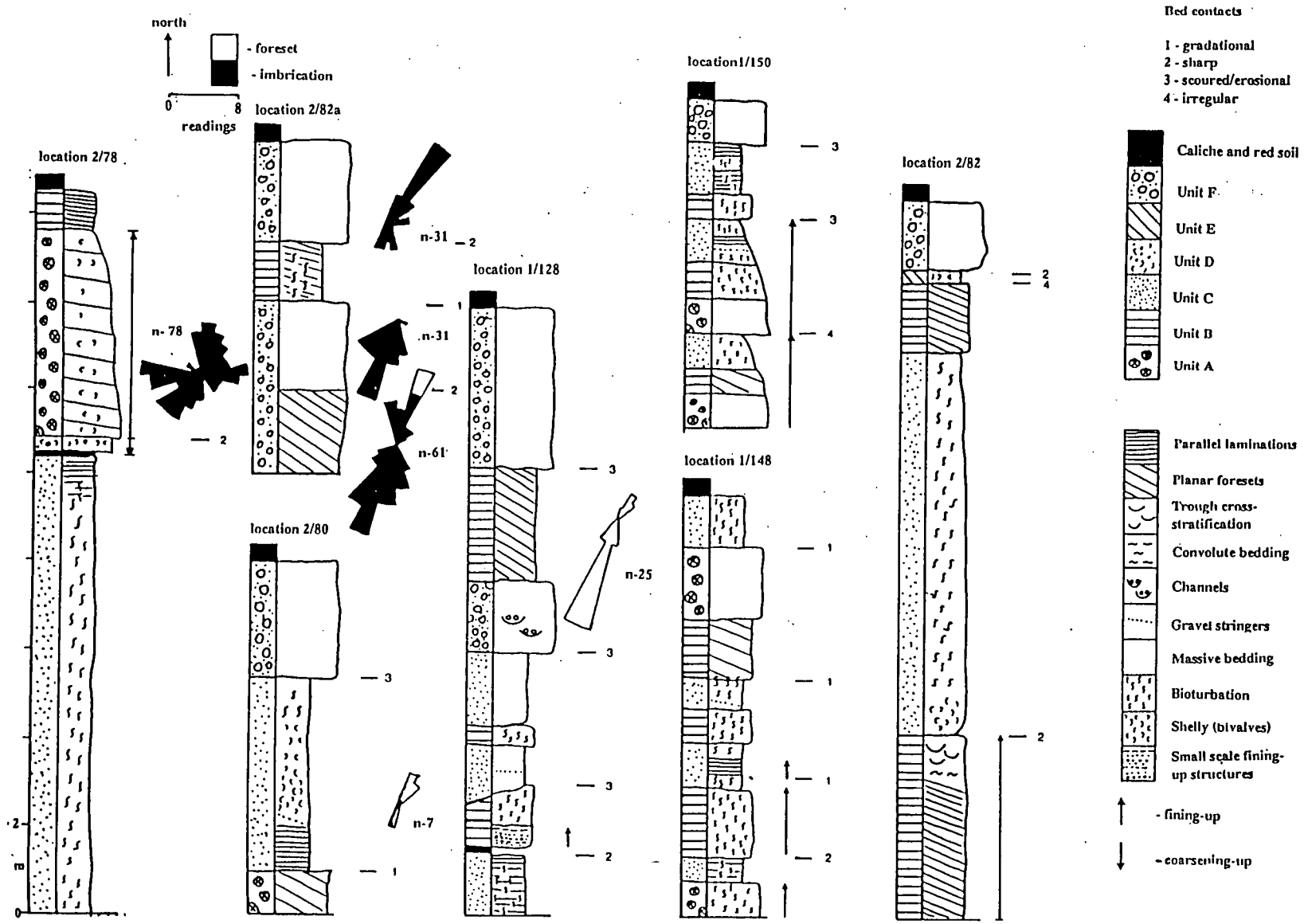


PLATE 6.1

J - Quarry section in the Ormidhia area of south-east Cyprus displaying the lateral continuity of bedding.

Note: the quarry face is c.7m high.

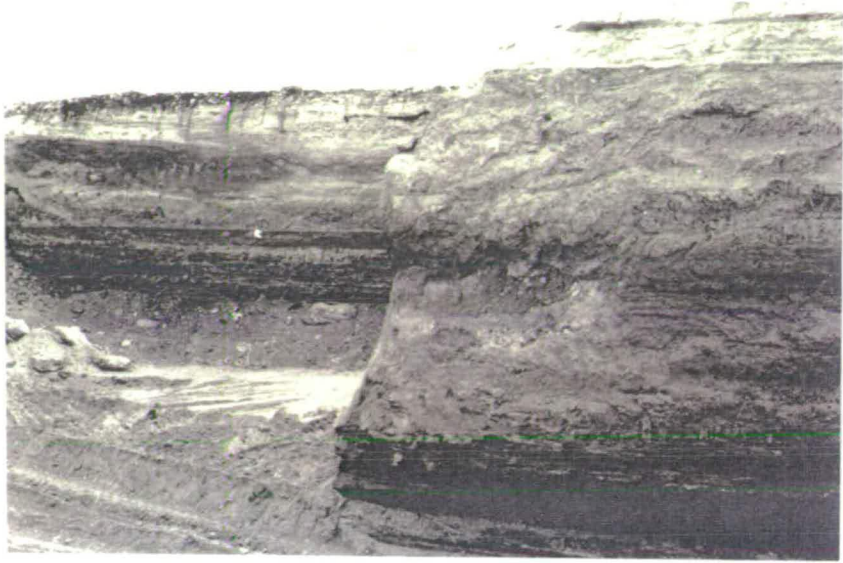
K - Structures preserved in the fine gravel to coarse sand sequences in the sedimentary sequence that crops out at Dhekelia (location 2-83).

Note: see Fig.5.10 for details.

L - *Thalassinoides* burrows cutting across well bedded units of fine gravel and coarse sands at Ormidhia, south-east Cyprus (location 1-148).

# Plate 6.1

J



K



L



**PLATE 6.2.**

J - Convolute, planar and small foresets preserved in the fine gravel and coarse sand sequences cropping out at Ormidhia (location 2-82).

Note: see Fig.6.2 for details.

K - Small fining up cycles from gravel to sand within small prograding foresets of the mature fine gravel to coarse sand units at Ormidhia (location 2-82).

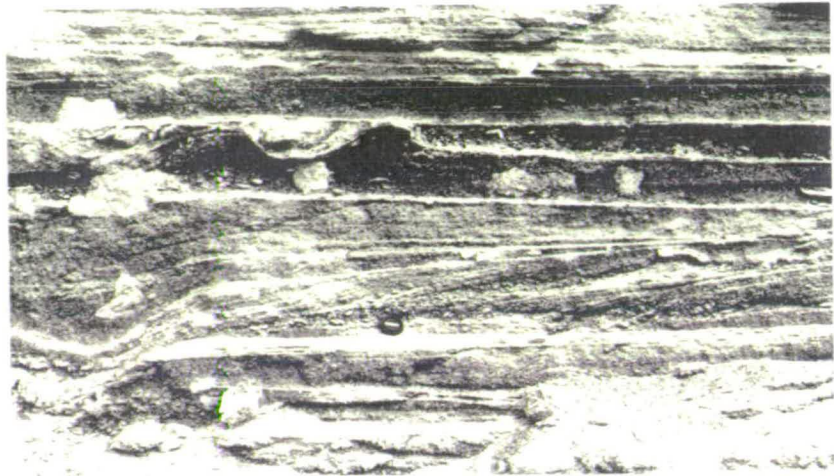
Note: the truncation surface and planar bedded units above the prograding foresets, see Fig.6.2 for details.

L - Convolute bedding preserved within the sands of the sequence cropping out at Ormidhia (location 2-82).

Note: the 25cm scale at the bottom left of the plate.

# Plate 6.2

J



K



L





commonly overlain by a mature lag of mixed igneous and sedimentary clasts, less than 5cm along the "L" axis.

*iv) Unit D: shelly conglomerate.*

This unit is dominated by a low diversity hash of disarticulated, abraded molluscan shells. The fauna mirrors that seen in Unit A. The long axis of the shells are commonly orientated (Fig.6.2). The unit is generally reverse graded from a grey-green sandy base to conglomerates near the top. This unit shows marked lateral changes and is not laterally persistent, unlike units A, B and C. The shelly horizons give way to red fine sands and silts, with subordinate matrix-supported clasts. Palaeosols and caliche horizons cap this unit.

*v) Unit E: white wackestone.*

A thin, planar stratified and centimetre laminated wackestone. The unit dips towards the south. A low diversity bivalve fauna, i.e. *Glycymeris* and *Ostrea*, is present within the unit.

*vi) Unit F: coarse, poorly sorted conglomerate.*

This grain-supported, unfossiliferous coarse conglomerate unit is generally poorly sorted containing clasts commonly less than 10cm ("L" axis). The clasts are spherical to discoidal and have been derived from both igneous and sedimentary sources. The matrix is a fine sand. The unit is unbioturbated and massive, although small channels are locally present.

*v ) The relationship between the sedimentary units.*

The units described above commonly crop out independently of each other, e.g. unit C dominates the succession at location 2-78, but the units are also interbedded. An A-B-C-D succession is commonly seen (location 2-79) with a gradational contact between units A and B, whilst a sharp, conformable contact is seen between units B and C. Unit D can also be present between units A and C (location 2-78; Fig.6.2). The formation of a thin caliche cap above unit C and beneath unit D indicates the presence of local discontinuities in sedimentation (location 2-78; Fig.6.2). Units B and D are commonly missing from the sequence. Unit B is locally indistinguishable from unit A. The contact between unit A and the underlying sediments is usually erosional with the conglomerates scouring down into the underlying units (Plate 6.3).

PLATE 6.3.

J - Shallow dipping planar conglomerates truncating steeply dipping conglomerate units to the south of Ormidhia.

Note: the sequence is c.3m high.

K - Fine planar bedded gravels cropping out within the deltaic sequence above the micrite unit at Mazotos (location 3-13), south Cyprus.

Note: the exposed sequence is c.5m high.

L - The micrite unit within the deltaic sequence at Mazotos (location 3-13) displaying its pinching and swelling nature. The micrite is capped by planar bedded mature fine gravels.

Note: the scale is 50cm long.

# Plate 6.3

J



K



L



Sequences containing all the units, i.e. units in the order A-B-C-D-A, etc., are rare; partial sequences are more common, i.e. units in the order A-B-C-A, etc.; A-B-A-B sequences are the most common. The variation and frequency of detrital input into this area (Chapter 2) has clearly influenced the sedimentary sequence more than those sequences cropping out in the Dhekelia area, to the west (Section 6.3.1.1).

### **6.3.1.3 Outcrops west of Cape Pyla.**

This area is different again from those seen to the west. Limestones and chalks of Miocene age formed a positive erosional topography during the Quaternary and therefore restricted the deposition of Quaternary sediments (Chapter 2). The sediments to the south of Xylophagou (location 2-70) crop out in a coastal section approximately 10m ASL, although the Quaternary sequences are only 3m thick. The basal sediments unconformably overlie chalks of Miocene age and consist of a conglomeratic lag, largely derived from the underlying chalk. The conglomerates are succeeded by a thin sequence of well bedded, fine conglomerates which is capped by caliche. Imbrication data from the conglomerates indicate a bimodal current direction. This sequence passes with a gradational contact, both vertically and laterally, into a 80cm thick shelly grainstone that contains fragmented robust molluscs, e.g. *Glycymeris*. The shells do not appear to be orientated. A small conglomeratic channel has subsequently cut down through the Quaternary and Miocene sediments. These sections are described in more detail in Section 6.4.

### **6.3.2 Southern Cyprus.**

The siliciclastic marine sediments that crop out along the south coast of Cyprus are limited to quarry exposures, the best of which are seen to the north-east of Mazotos (locations 3-12 and 3-13; Plates 4.1 and 6.3).

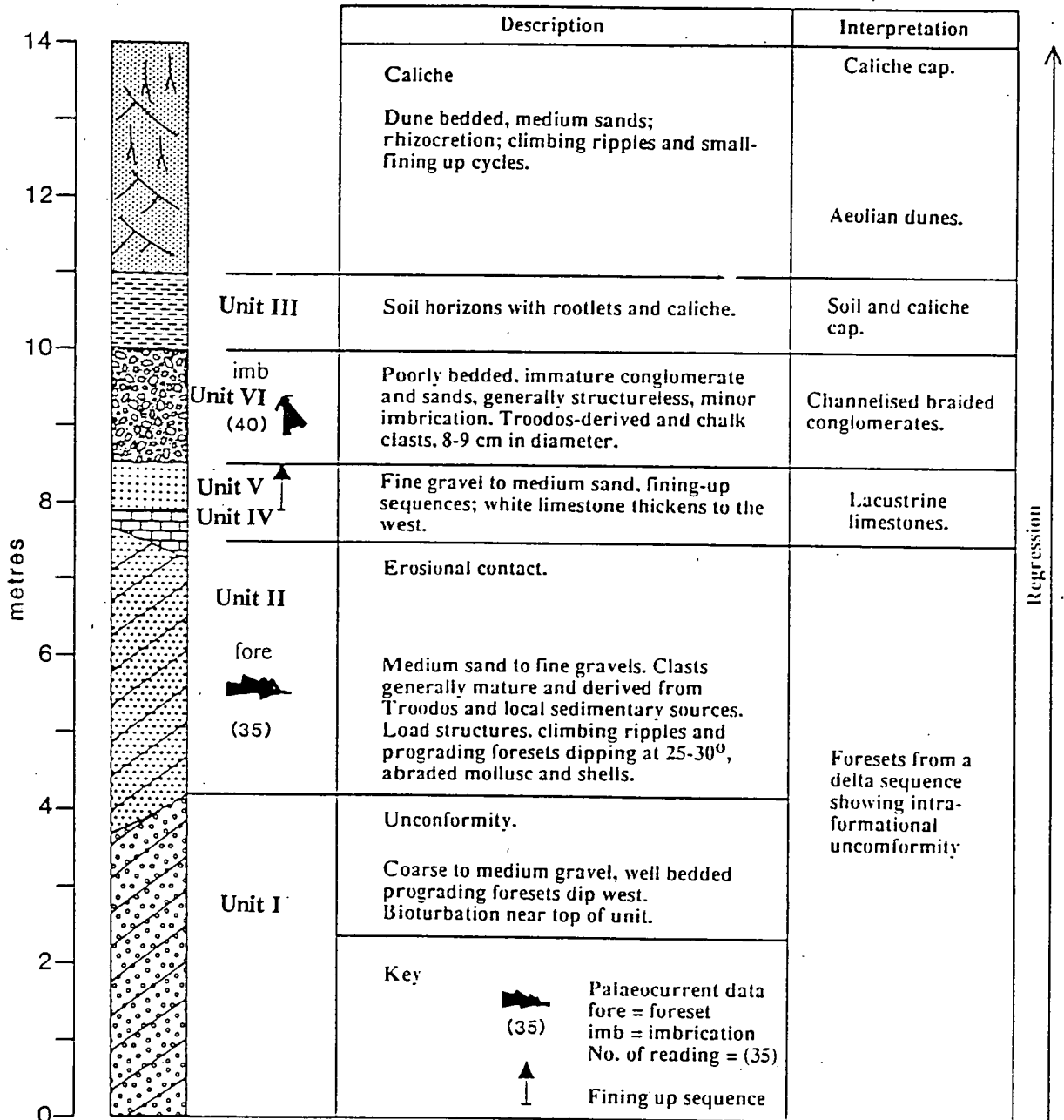
#### **6.3.2.1 Sedimentary units.**

*i) Unit I: prograding shelly, sands and gravels.*

The sequence at location 3-12 fines-up from prograding gravels, containing clasts less than 5cm diameter, into a sequence of interbedded sands and gravels (Fig.6.3). The foresets become steeper where the sands and gravels are interbedded, with a maximum dip of 20°. The unit is locally very shelly, containing many abraded gastropod and bivalve shells, e.g. *Glycymeris* and *Chlamys*.

Fig.6.3. A sketch section from the deltaic sequence that crops out at Mazotos (location 3-13), along the south coast of Cyprus.

Note: the units marked on the figure refer to units described in the text.



ii) *Unit II: well bedded, mature sands and gravels.*

A laterally persistent coarse sand and fine gravel unit crops out above the prograding foresets (Fig.6.3); this well bedded unit fines-up from gravel to sand. Bioturbation causes the sands to have a mixed and massive appearance, locally. The sands contain many small scale structures, e.g. small planar foresets, channels and ripples. The whole sequence is laterally persistent.

iii) *Unit III: soil horizons and associated massive conglomerates.*

The sands and gravels pass up into a thin soil horizon. This, in turn, is overlain with an erosional contact by coarse, immature, massive conglomerates. There is little structure within the conglomerate unit, the exception being the development of minor foresets towards the top of the unit. The unit is poorly to moderately sorted and the largest clasts are 65cm along the "L" axis. This conglomeratic unit is unfossiliferous, unconsolidated and laterally impersistent, as beds cut down through the sequence and mature coarse sands and fine gravels are interbedded with immature medium and coarse grained gravels. Channels that cut down into the poorly sorted conglomerates are more mature and better sorted than the background sediments. Very coarse conglomerates crop out, locally, throughout the unit. Clast imbrication is seen and the more mature, finer-grained units reveal foresets, similar to those seen close Tersephanou (location 3-18).

The pattern of sedimentation at location 3-13 is more complex than that at location 3-12. The base of the section is marked by the presence of medium conglomerates which form a series of prograding foresets, similar to unit I. These conglomerates, like those seen at location 3-12 (see above) are mature and well sorted. The foresets within the medium conglomerate unit dip towards the west at between  $8^{\circ}$  and  $22^{\circ}$  (Fig.6.3). Abraded molluscan shells and fragments of coral are present within the unit. A sharp reactivation surface lies above the beds of medium conglomerates and is succeeded by clast-supported, prograding units of fine gravel to medium sand. A gross fining-up sequence is present within this unit, with coarse to medium sands dominating towards the top of the sequence. Gravel stringers are present although these are not laterally persistent. Small channels containing mature gravels crop out in the lower portion of the succession. Small vertical burrows, less than 1cm diameter, *cf.* the *Thalassinoides* facies, are present within the medium to coarse sand unit, as are a series of sedimentary structures including small scale trough cross-stratification, fining-up laminated sands and ripples. Evidence of soft sediment deformation is also present as are numerous small faults (Chapter 4).

*iv) Unit IV: micrites.*

The white micrites rest conformably, but with an uneven contact, over the prograding gravel units, e.g. unit I (Fig.6.3; Plate 6.3). The micrite reaches an observed maximum thickness of 70cm and pinches out to the west where it is replaced laterally by mature, well sorted sands, similar to those seen in Unit II at location 3-12. This micrite is massive and structureless, and some iron staining is seen in hand specimen. Thin section observations show that micrite dominates but subordinate fragments of allochems are present. The allochems at the base of the unit account for less than 10% of the constituent components of the rock and are dominated by fragments of planktonic foraminifera tests. This part of the micrite unit can therefore be described as a mudstone. An undulose but sharp boundary towards the top of the unit marks the transition to a higher proportion of allochems, again dominated by planktonic foraminifera tests. This portion of the unit can be described as a wackestone. The unit is matrix-supported throughout. The wackestone is truncated by the overlying sands and gravels. The contact between the wackestone and the overlying unit is planar, with little evidence of extensive erosion, or gouging by the overlying clastic sediments, into the underlying micritic sequence.

*v) Unit V: planar bedded gravels and sands.*

The micritic unit is succeeded by three fining up cycles of planar bedded, fine gravel to coarse sand, interbedded with stringers of poorly sorted medium to fine gravel. The beds within this unit are generally structureless and between 20 and 50cm thick. The sands dominate making up approximately two thirds of each cycle. The contact between each cycle is irregular and draped but does not appear to be erosive (Fig.6.3; Plate 6.3).

*vi) Unit VI: coarse immature conglomerates.*

An erosional contact above the planar bedded sands and gravels marks the introduction of coarse, poorly sorted, immature conglomerates. This unit, like the underlying sediments is grain-supported but, unlike the underlying units, contains a higher proportion of matrix and tends to be poorly bedded and locally chaotic. The unit is imbricated and generally better cemented than the underlying mature sediments (Fig.6.3). The unit coarsens away from the contact with coarse sands and fine gravels beneath, passing up into medium to coarse conglomerates, that contain clasts of derived caliche. The clasts are generally less than 8-9cm along the "L" axis and sub-mature, although generally more mature than those clasts associated with units of the Fanglomerate Group (Fig.6.3; Chapter 5). Caliche and soils that overlie the conglomerates are, in turn, overlain by an aeolianite sequence (Fig.6.3; Chapter 8).

### 6.3.2.2 Provenance data.

The provenance data collected from location 3-13 indicate a strong Troodos-derived component. Notably, ultramafic clasts are absent (Fig.6.4). The Troodos-derived clasts are generally more mature than the sedimentary clasts, in both the deltaic and overlying fluvial sequences. The clasts within the deltaic deposits vary in roundness from 0.6 to 0.8 and most are spherical rather than discoidal.

### 6.3.2.3 Palaeocurrent data.

The palaeocurrent data indicate that sediments prograded out from the shoreline in an arc between east and west-north-west (Fig.6.5). The fluvial sediments that overlie the deltaic sequence conform to a similar overall pattern, indicative of a flow off the Troodos Massif (Chapter 5) but having a markedly different pattern at outcrop scale (location 3-13; Figs.6.3 and 6.5).

## 6.3.3 The Polis-Paphos graben.

The Quaternary deltaic sediments from the northern part of the Polis-Paphos graben have previously been described as fan-delta sequences (L. Ward, *pers. comm.*, 1987). The sediments in this area, like those that crop out along the south coast of the island, form limited outcrop to the east of Polis (location 3-106) where active quarrying is taking place. Outcrops also occur where agricultural terraces have been cut in the hillsides to the south-east of Polis (location 1-166).

### 6.3.3.1 Sedimentary units.

The sedimentary sequence in this area shows a gradual facies pattern change, with siliciclastic marine sequences in the Limni area (location 3-106) passing laterally into carbonate littoral sequences further east, e.g. Argaka (location 3-109; Chapter 7). The sequences at Limni (location 3-106; Fig.6.6; Plate 6.4) are similar to those cropping out along the south coast of Cyprus (locations 3-12 and 3-13; Section 6.3.2; Fig.6.3). The base of a deltaic unit is exposed in the Polis area, an unconformity separates the underlying Myrtou Marls, of Pliocene age, from a basal lag. The basal lag is locally succeeded by a thin mixed sand unit, with subordinate gravels, which rapidly grades up into medium to fine sands; thes sands are well bedded and structured, displaying trough-cross stratification, wave laminated ripples and small-scale prograding foresets. The palaeocurrent data collected from this unit (Fig.6.6) indicates a flow towards the south-



Fig.6.4. Provenance data from the clasts within the coarse conglomerate unit of the deltaic sequence cropping out at Mazotos (location 3-13), along the south coast.

Note: the number of clasts measured recorded in brackets

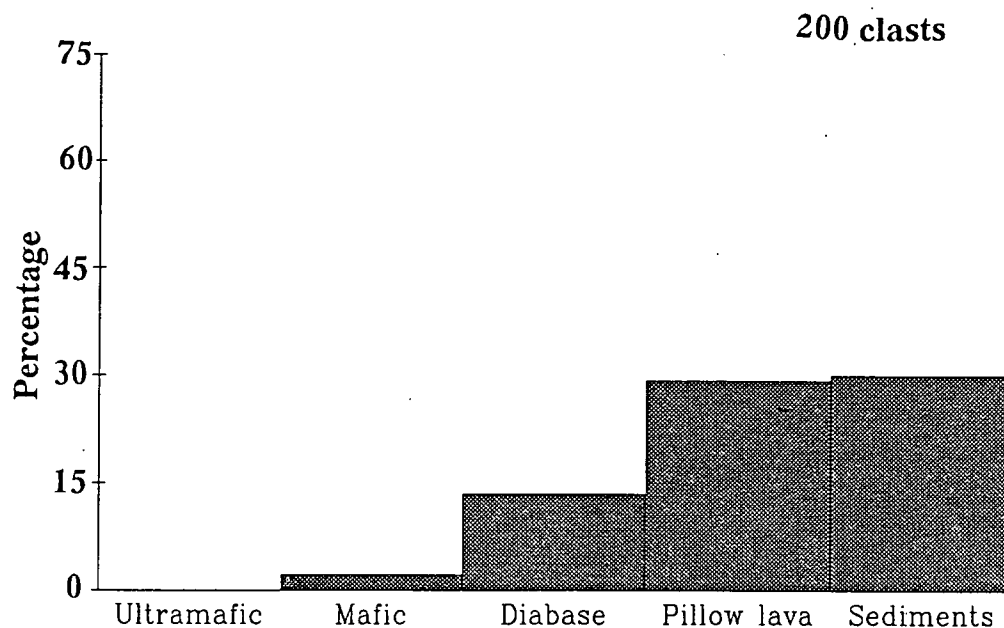
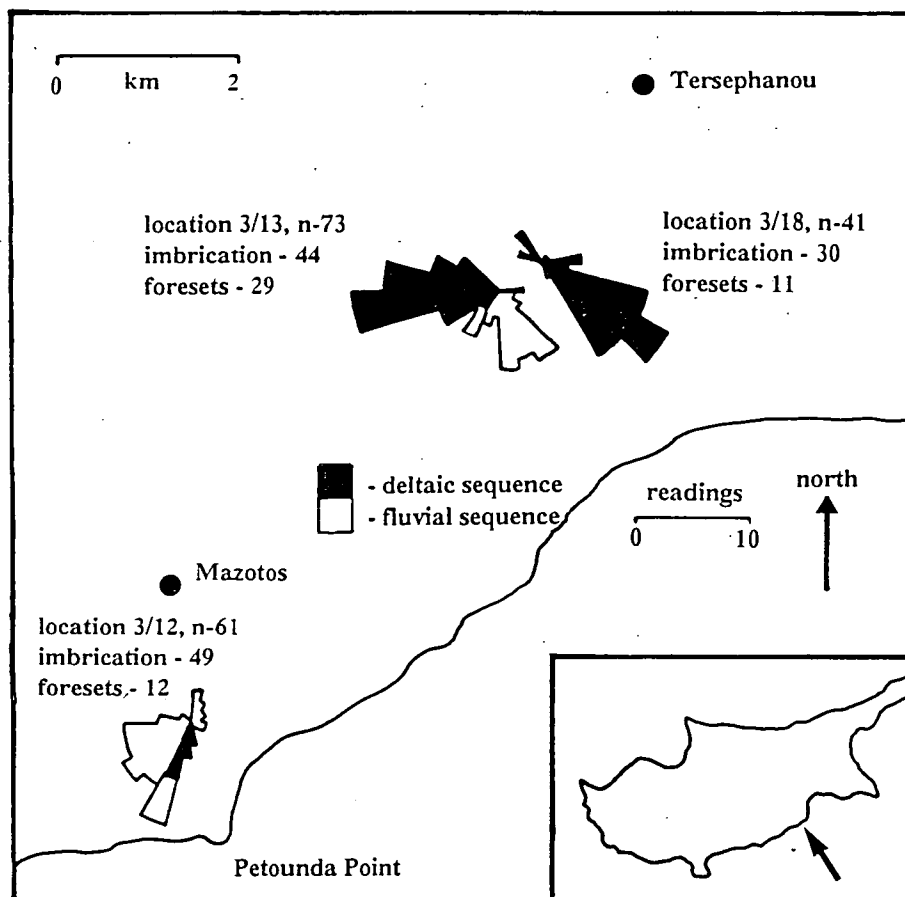
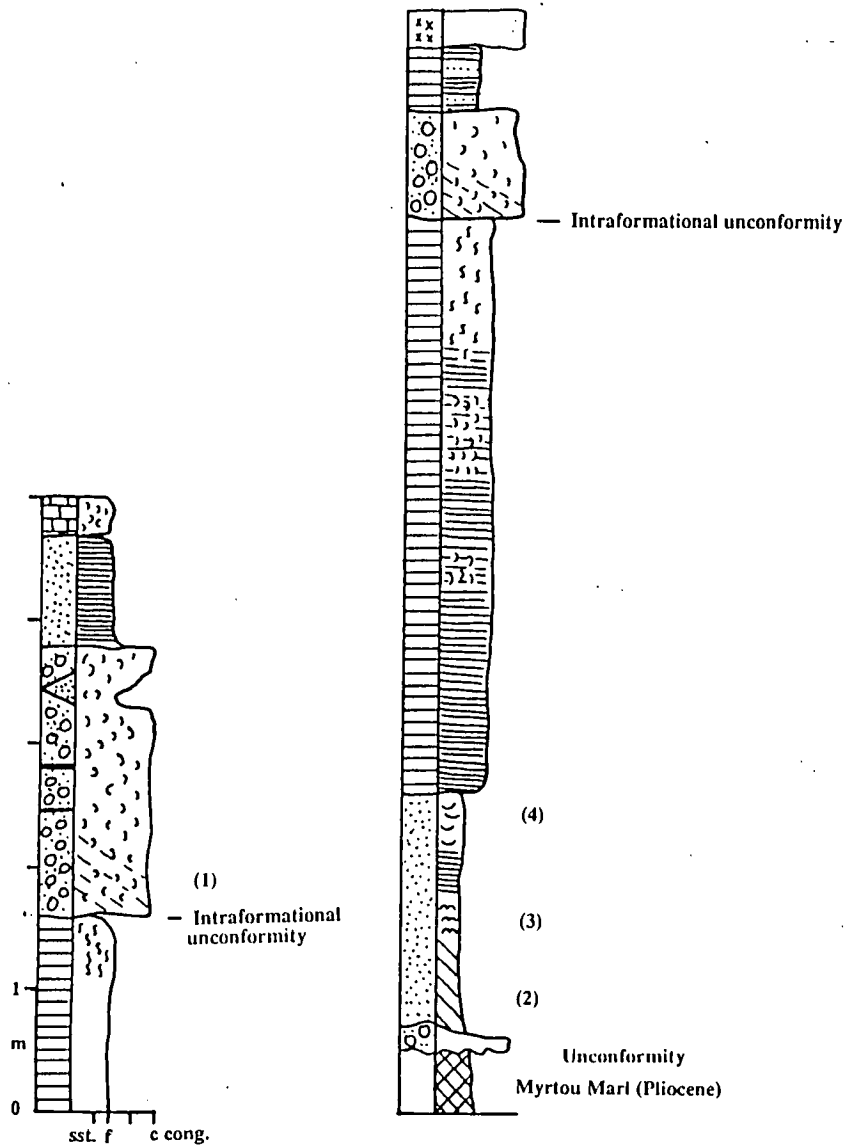
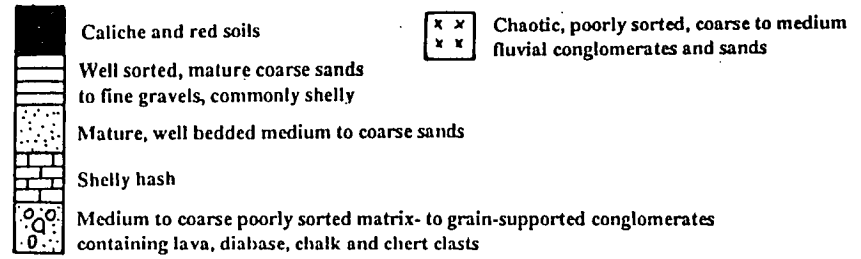


Fig.6.5. Palaeocurrent data from the deltaic, and over lying fluvial, sequences along the south coast of Cyprus.

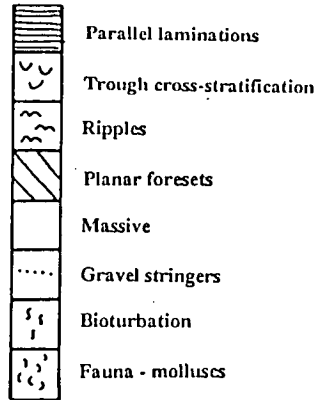




Lithology



Sedimentary structures



Rose diagram

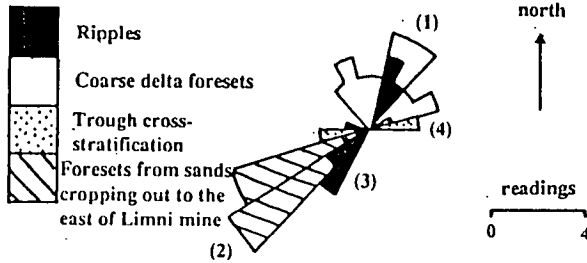


Fig.6.6. Sketch sections of the exposed sedimentary sequences in the area of Limni, at the northern end of the Polis-Paphos graben.

PLATE 6.4.

Panoramic view of the deltaic sequence preserved at Limni (location 3-106) at the northern end of the Polis-Paphos graben.

Note: person for scale,  
the photograph is taken looking east.

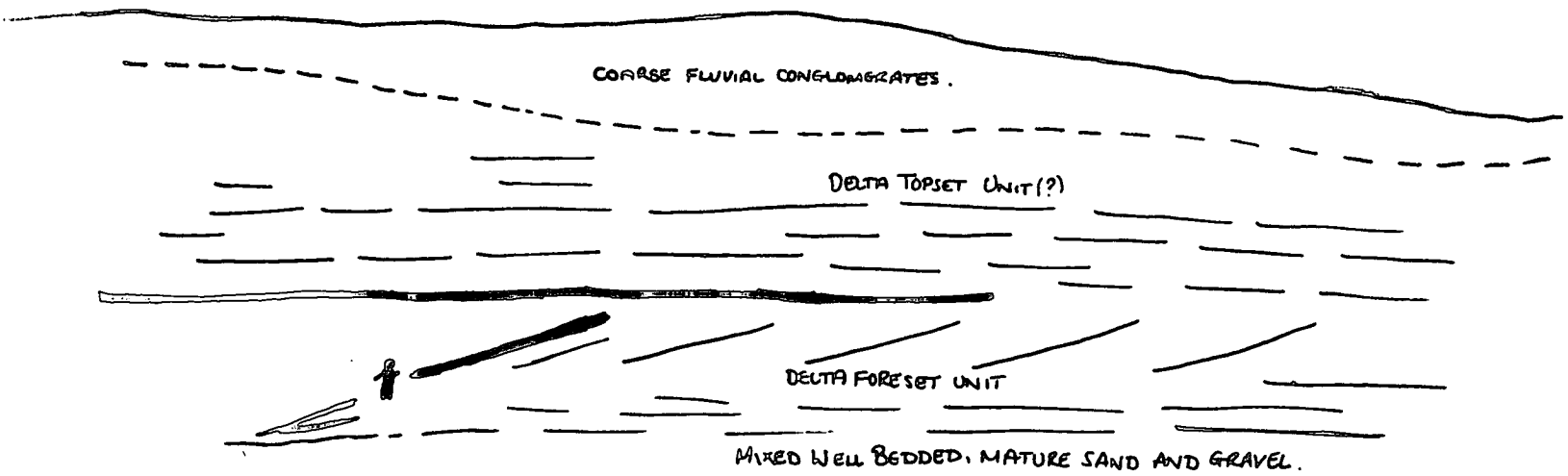




Plate 6.4

west. The laminated sand unit is not present in all parts of the sequence as well bedded gravels are commonly seen lying directly above the basal lag (similar to Unit I; Section 6.3.2.1). The well bedded conglomerate unit has a maximum outcrop thickness of 5m.

The sediments that overlie the well bedded conglomerate unit display rapid vertical changes; intraformational unconformities are also present. At Limni (location 3-106), the intraformational unconformity is overlain by medium to coarse grain-supported conglomerates unlike that seen at location 3-13, near Mazotos (Section 6.3.2). The prograding foresets at this locality dip towards the north-west to north-east (Fig.6.6). The delta front units are overlain by a massive, matrix- to grain-supported, chaotic conglomerate, with evidence of caliche formation, similar to unit VI on the south coast (Section 6.3.2.1). This conglomeratic unit is, in turn, overlain locally by laminated sands, white micritic limestones and fluvial sands and gravels. A hash of mixed gastropod and molluscan shells lying above the whole sequence is also present near Limni (location 3-106).

#### 6.3.4 Deltaic sequences south-west Cyprus.

Limited exposures of mature, well sorted conglomerates exist in south-west Cyprus, the only example being a small quarry to the north-east of Kouklia (location 2-53), which crops out at 220m ASL.

The units in the quarry sequence consist of mature, grain-supported, well bedded and sorted sands and gravels (Fig.6.7). The sequence fines-up from medium gravels to coarse sands, is unfossiliferous, and heavily bioturbated towards the top. Planar laminated beds dipping at  $<7^{\circ}$  are seen, as are a series of prograding forests, that dip up to  $20^{\circ}$ . The beds are laterally persistent (Table 6.1) and the clasts are generally texturally mature, i.e. spheroidal to discoidal, and well sorted (Fig.6.7). A unimodal, north-north-east imbrication direction is locally present within the lower prograding beds, bimodal imbrication is present within the higher units, i.e. both north-north-west and south-south-east (Fig.6.7). The beds dip towards the south-west and south-south-west (Fig.6.7). A distinct truncation surface exists between the steeply dipping foreset unit and the shallow planar bedded units (Plate 6.5).

PLATE 6.5.

J - The preserved sequence of siliciclastic sediments at Kouklia (location 2-53), revealing planar bedded mature gravels truncating the underlying steeply dipping foresets.

Note: scale is 50cm long.

K - Planar bedded beach foresets from the F3 units cropping out in the Dhekelia area.

L - Detailed view of the planar foresets exposed in the fine gravel and coarse sand sequences in the beach sediments at Dhekelia (location 1-129), south-east Cyprus.

Note: scale is 50cm long,  
shelly unit displaying moldic porosity at the top of the white portion of the scale.

M - Displaying the cyclic nature of the gravel and sand sediments in the beach sequences at Dhekelia (location 1-129c).

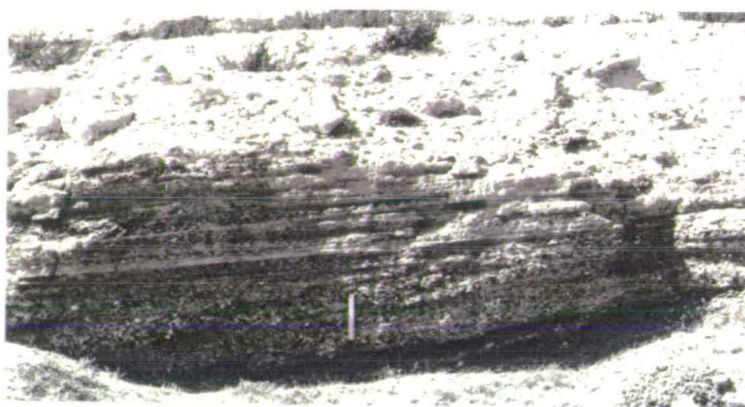
Note: scale is 50cm long.

# Plate 6.5

J



K



L



M



## **6.4 SILICICLASTIC BEACH SEQUENCES.**

### **6.4.1. Introduction.**

Siliciclastic beach sequences are preserved in a series of exposures along the coast between Dhekelia and Xylophagou in south-east Cyprus. These sequences vary from those seen elsewhere on the island as they are not related to the deltaic facies described above, e.g. in the Limni mine area (location 3-106), and are not fluvial sequences that form small coastal cliffs, that have been cut by present, or past, marine erosion, e.g. in the area of Paphos, Zyyi and Vasilikos (Chapter 2 and 5). Low cliffs to the west of Lamaca have been described and interpreted as marine by Bagnall (1960); these are re-interpreted as forming in a fluvial environment.

The discrimination of wave worked conglomerates from fluvial sequences, and therefore the interpretation of coarse grained beach conglomerates has relied on the shape and sorting of clasts, the pebble segregation and relative bed lenticularity and the interpretation of sedimentary successions (Bluck, 1967B; Dobkins & Folk, 1970; Clifton, 1973; Williams & Caldwell, 1988; Gale, 1990; Postma & Nemec, 1990). This study has utilised the criteria previously laid down (Dobkins & Folk, 1970; Clifton, 1973) to aid the interpretation of these sedimentary sequences, although it is understood that a range of variables, including climate, relative base level changes and hydrodynamic conditions, affect the depositional sequences and their preservation potential.

### **6.4.2 F3 and F4 siliciclastic beach sequences of south-east Cyprus.**

A series of siliciclastic beach sequences of F3 and F4 age, crop out in the area of coast between Dhekelia and Xylophagou. These sequences consist of coarse conglomerate units, which are best exposed in the area south of Ormidhia (locations 1-128, 1-129 and 2-77), mixed conglomerate, sand sequences, e.g. south of Xylophagou (locations 1-129a and 2-700), and shelly hash and sub-aerial units. All of the depositional sequences crop out within 10m ASL, i.e. F3 or F4 (Late Pleistocene), with the F4 successions (e.g. location 1-129) commonly lying on the seaward side of a minor F3 cliff, which has been cut into the preceding fluvial and shallow marine deposits. The various sedimentary components of these sequences will now be described.

#### **6.4.2.1 Coarse conglomerate lag.**

These coarse angular, massively bedded conglomerates locally lie unconformably above the underlying pre-Quaternary sedimentary sequence (locations 2-700 and 2-70;



Fig.6.7. Sketch section of the sequences cropping out at Koukليا (location 2-54), south-west Cyprus.

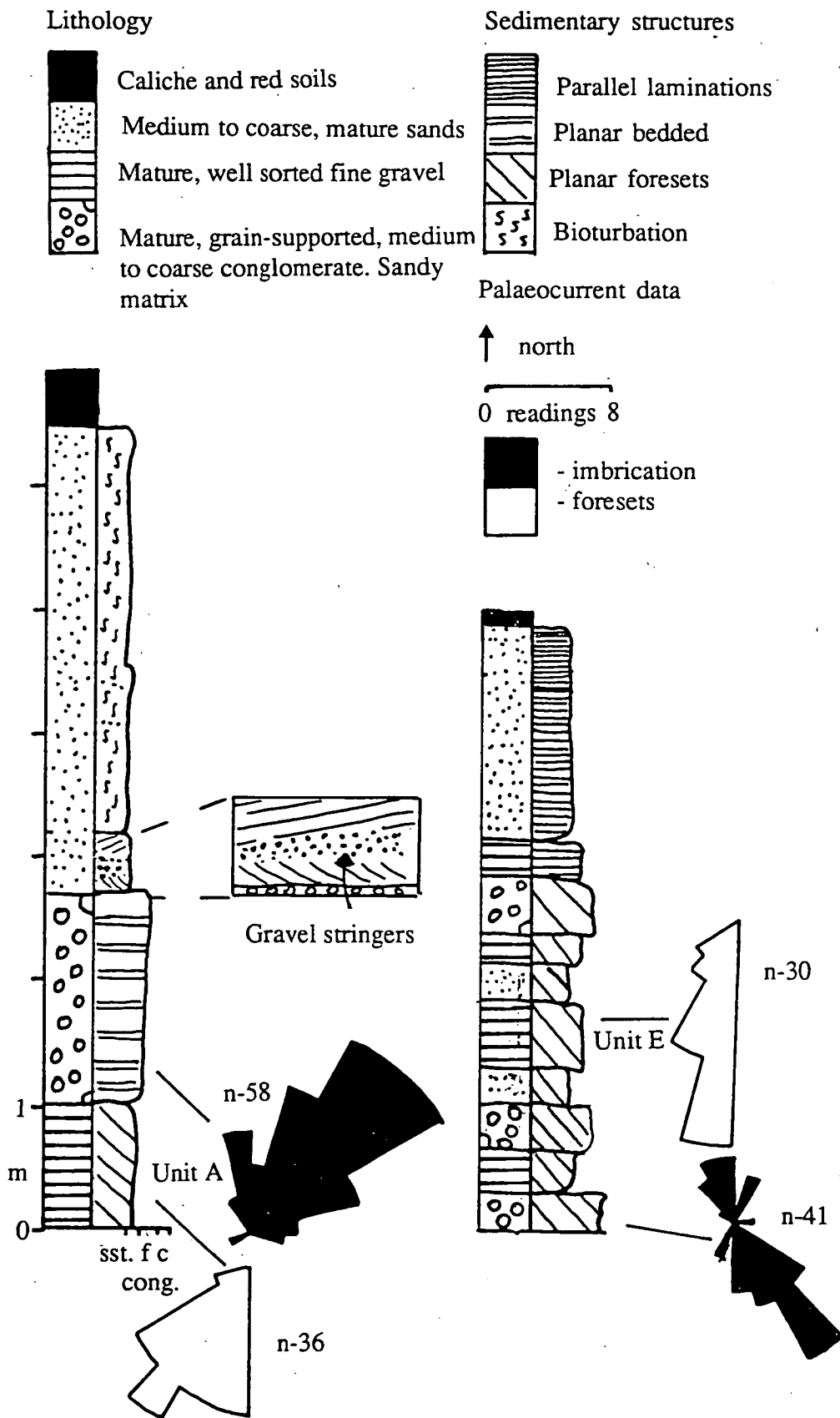


Fig.6.8), where c.1m of associated relief is common. The clasts within this unit are up to 60 cm long ("L" axis) and consist of angular blocks of Miocene limestone and grainstones. Mature igneous clasts are also present. Whole and broken robust shells are found within the unit, e.g. *Glycymeris*, and bioturbation is absent.

Table 6.1. Bed continuity data from the siliciclastic sequence in south-west Cyprus (location 2-53).

Note: see Fig.6.7 for the location of the units within the sequence.

#### UNIT E

| Beds | $\Delta\tau$ | $\gamma$ | $\Lambda$ | C     | P  | Thickness | Notes           |
|------|--------------|----------|-----------|-------|----|-----------|-----------------|
| a    | 21           | 350      | 0.063     | 70-90 | 30 | 21        | Fg, imbn        |
| b    | 40           | 500      | 0.080     | 70-90 | 30 | 60-40     | C - Mg, massive |
| c    | 10           | 400      | 0.025     | 10-30 | 45 | 10        | Csst            |
| d    | 15           | 420      | 0.036     | 50-70 | 10 | 15        | Fg              |
| e    | 10           | 460      | 0.022     | 10-30 | 45 | 10        | Csst            |

#### UNIT A

|   |    |     |       |       |    |       |                    |
|---|----|-----|-------|-------|----|-------|--------------------|
| a | 5  | 500 | 0.010 | 0-10  | 45 | 8-3   | Csst, pl.          |
| b | 8  | 500 | 0.016 | 0-70  | 10 | 11-19 | Fg-Csst, imbn, GS  |
| c | 5  | 500 | 0.010 | 10-30 | 30 | 9-4   | Csst + clasts, pl. |
| d | 3  | 500 | 0.006 | 50-70 | 10 | 27-24 | Fg-Csst, GS, imbn  |
| e | 3  | 220 | 0.016 | 0-10  | 45 | 3     | Fg-Csst            |
| f | 9  | 500 | 0.018 | 70-90 | 30 | 20-11 | Mg                 |
| g | 17 | 500 | 0.034 | 70-90 | 30 | 20-3  | Mg-Fg, GS, imbn    |
| h | 15 | 500 | 0.030 | 0-10  | 45 | 25-10 | Csst + clasts, pl. |

#### Notes:

- i). All measurements are in cms
- ii)  $\Delta\tau$  = Maximum thickness - minimum thickness
- iii)  $\gamma$  = Lateral extent of bed, within 500cms
- iv)  $\Lambda$  = Lenticularity index ( $\Delta\tau/\gamma$ )
- v) C = Estimated percentage class of pebbles  $>4\text{mm}$
- vi) P = Pebble segregation factor (50 - m), where m = the midpoint of the pebble percentage class C
- vii) F - fine, M - medium, C - coarse, g - gravel, sst - sandstone, imbn - imbrication, pl. - parallel laminations

#### 6.4.2.2 Coarse-medium conglomerates.

These coarse-medium conglomerate sequences (Fig.6.8) crop out unconformably above earlier Quaternary and Neogene sediments (location 1-129a), as well as within the sedimentary sequences (Fig.6.8). The conglomerates are commonly grain-supported, imbricated and dip at  $5-10^\circ$  in an arc between south and south-west, or north to north-east (Plate 6.5). Igneous and sedimentary clasts are present as is a high density, low diversity

Fig. 6.8. Sketch sections of the beach sequences cropping out in the F3 and F4 age exposures between Cape Pyla and Dhekelia in south-east Cyprus.

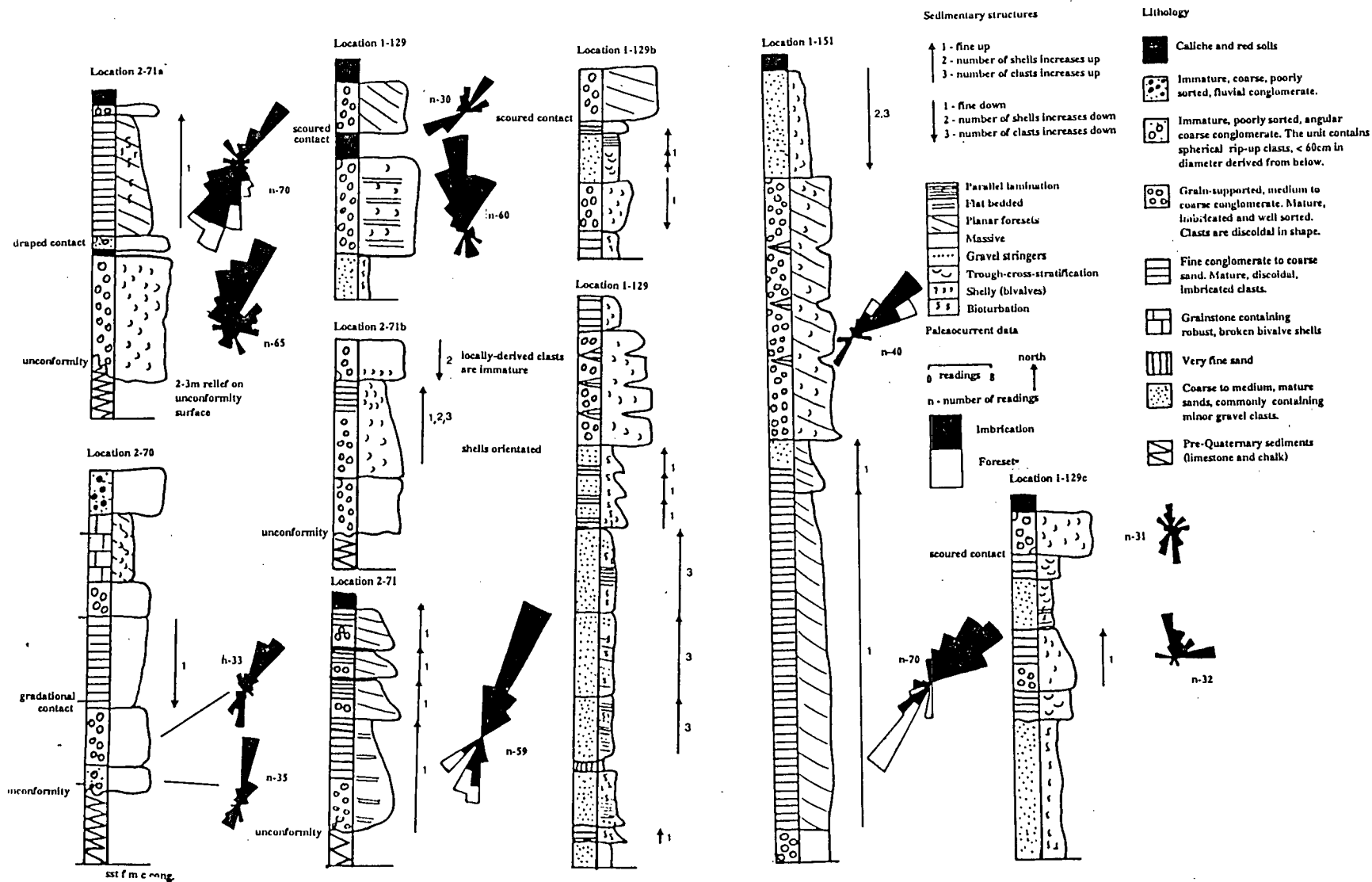


Fig.6.9. Sketch of the structures preserved in the beach sequence near Cape Pyla (location 2-71a), south-east Cyprus.

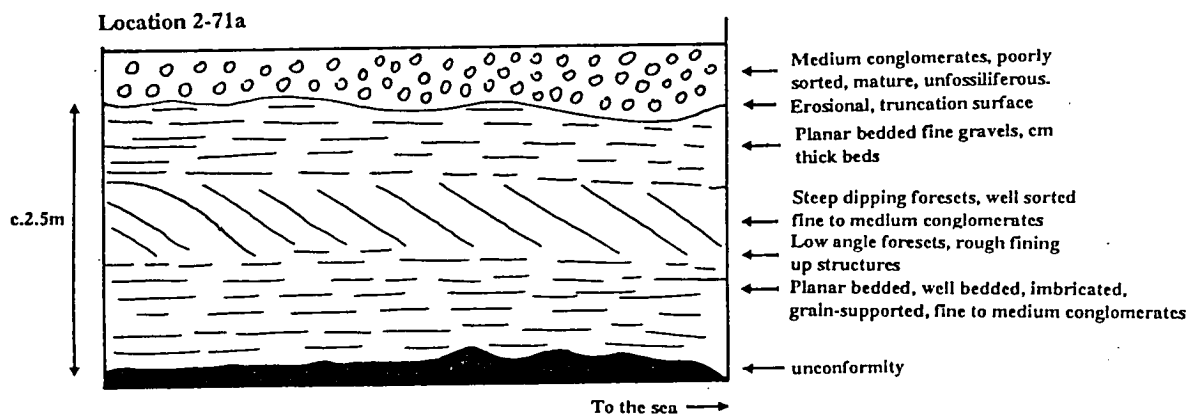
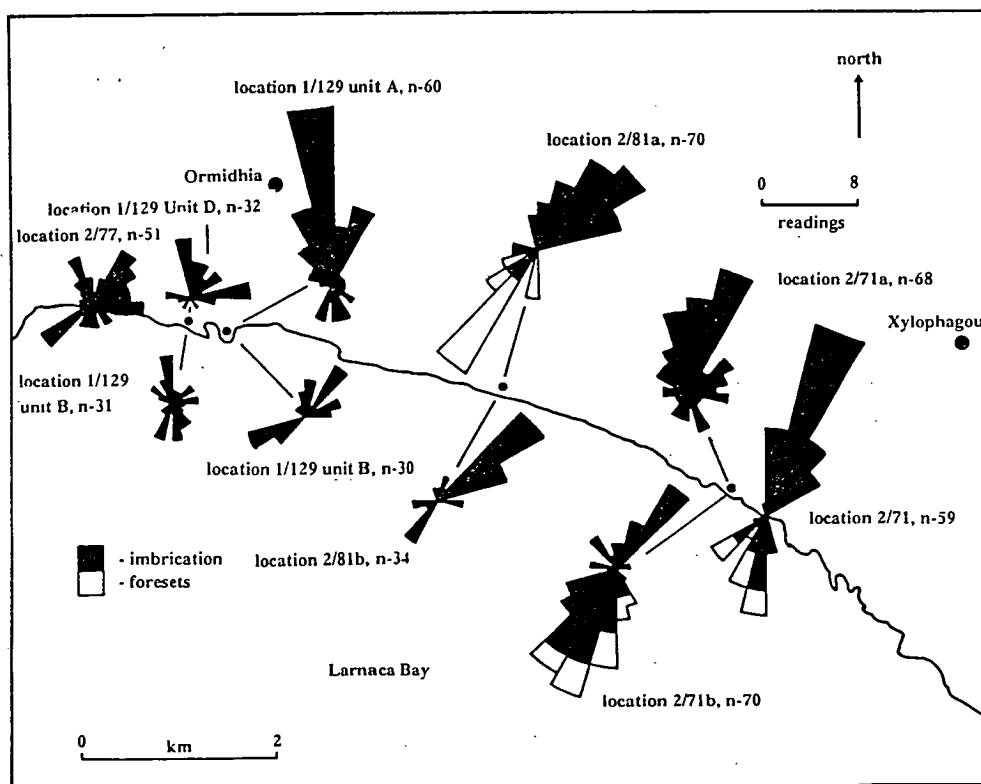


Fig.6.10. Palaeocurrent data from clast imbrication and foresets within the F3 and F4 beach sequences of south-east Cyprus.



mollusc fauna. The valves, locally (location 2-700), lie parallel to bedding at the base of the unit and grade up into a disorganised group towards the top. The beds are laterally persistent and not lenticular. The clasts are generally mature, well sorted becoming better sorted and more mature, as the proportion of the shells increases, up sequence. The clasts at the top of the unit are mostly discoidal and less than 3cm along the "L" axis. This unit is locally interbedded with fining up sequences of gravels and sands, and commonly truncates the underlying beds (Fig.6.9; Plate 6.5).

The coarse-medium conglomerates crop out within the sequences around much of the coast from Ormidhia west towards Dhekelia. Bi- and unimodal imbricated clasts (Figs.6.8 and 6.10) indicate a dominantly north and north-east to south and south-west palaeocurrent.

#### 6.4.2.3 Fine conglomerates and coarse sands.

The fine gravel to coarse sand units are up to 2m thick (location 1-151), well bedded and laterally persistent. The clasts within this unit are generally less than 3cm along the "L" axis and have a discoidal shape. Bioturbated, planar bedded and trough-cross-stratified units (Plate 6.5) and a mollusc fauna, are all locally present. The planar bedded portions of the unit dip at between  $5^{\circ}$ - $10^{\circ}$  offshore, i.e.  $170^{\circ}$ - $190^{\circ}$  (Fig.6.8; Plate 6.5). The trough sets display small fining-up structures from fine gravel to medium sand. A series of truncation surfaces cuts the trough-cross stratification, identified by gravel stringers. The sediments are commonly cyclic, with fine gravels passing up into coarse and medium sand; these sands are capped by a scoured contact and fine gravel. The beds are locally convoluted (*cf.* Plate 6.3); this is generally associated with the influx of rare, large clasts. Imbrication present within these units indicates a dominantly onshore palaeocurrent direction, i.e. towards the north-east (Figs.6.8 and 6.10).

#### 6.4.2.4 Sand units.

Medium to fine, well to very well sorted, shelly sands crop out throughout the beach sequence. The sands occasionally contain fine gravel stringers, usually along the base of the bed, and matrix-supported clasts. The sands are commonly laminated, mm-cm thick, and display planar and trough-cross-stratification. Mollusc valves are commonly orientated parallel to bedding. Bedding is locally absent, although this correlates with the presence of pervasive bioturbation. The unit is poorly cemented and friable.

#### 6.4.2.5 Sub-aerial and shelly hash units.

A shelly hash, similar to that described previously (Section 6.3.3.1) from the Polis area, crops out above the conglomerates at location 2-77 (Fig.6.8). The fauna is dominated by *Glycymeris* and *Ostrea*, these shells not orientated.

Fluvial conglomerates locally cut channels into the beach sequences (location 2-71; Fig.6.8). These conglomerates can be distinguished from the underlying units as they are coarse, immature and poorly sorted, although they do contain mature clasts derived from the underlying units.

Caliche horizon capping the sequence commonly act as a "cement", binding the top unit together. Some red staining of the top most portions of the sequence occurs; this is attributed to the formation of dark red palaeosols that have stained these units.

### 6.5 INTERPRETATION, DISCUSSION AND CONCLUSIONS.

#### 6.5.1 Deltaic sequences of south-east Cyprus.

##### 6.5.1.1 Dhekelia.

The succession at Dhekelia (location 2-83; Fig.5.10) represents a shallow marine sequence. The conglomerates reflect the influence of detritus derived from continental sources, whilst the sands (unit A) represent the steady state background sedimentation. The palaeocurrent data from the conglomeratic unit indicates both an on- and offshore direction (Fig.6.2). The sedimentary structures within the sand units probably represent a variety of shallow marine littoral environments. The truncated and scoured nature of the conglomerates that overlie the well bedded sandstones (unit A) suggest a moderately rapid change in environment which resulted in the transgression of the conglomerates over the sands. Local changes in the relative base level have probably influenced and controlled the timing of deposition of these conglomerates. The absence of evidence of longshore currents, i.e. palaeocurrent direction parallel to the coast, suggests that the change from sand to conglomerate deposition resulted from the introduction of primary clasts into the system. This change suggests either a rise in the base level, i.e. uplift, a drop in sea-level or the possibility of some climatic variation, similar to that described in Chapter 5, which has resulted in increased numbers of clasts being supplied to the marine realm through increased offshore transportation of sediment.

### 6.5.1.2 Ormidhia.

The medium conglomerates, unit A, are interpreted as being deposited in an active, shallow, marine environment. The presence of a fauna - bioturbated horizons - indicates that the environment was not too harsh, however, the thick shelled, low density fauna does suggest a high energy environment (Bourgeois & Leithold, 1984), although this fauna may have been reworked into its current position. The variable maturity of the clasts suggests that they have been introduced from a fluvial source during the formation of this unit and have been subsequently reworked by marine action. The coarse but well sorted nature of the clasts supports an argument for a high energy depositional environment.

The well sorted conglomerates, unit B, probably formed in a high energy shoreface environment. The absence of a fauna and bioturbation suggests either rapid deposition of this part of the sequence in harsh conditions, or continuous erosion and deposition (*cf.* Howard, 1975). The finer grained and generally better sorted, and more mature, nature of this unit over unit A indicates an active environment, actively reworking and sorting these clasts derived from onshore fluvial environments.

The green and grey sands, unit C, are interpreted as forming in an active, high energy shoreface environment. The presence of preserved parallel laminated and cross-bedded sands indicates a high flow regime, possibly associated with a high sediment accumulation rate. The uniform grain size of the sediments supports arguments for a high energy environment. The presence of occasional stringers of gravel indicates that either: lag deposits were reworked by large waves and currents, or that additional clasts were derived from locations closer to the shore. The presence of *Thalassinoides* burrows indicates a neritic-littoral environment (Crimes, 1975). The intensity of the bioturbation varies throughout the unit; the more massive and greatly bioturbated sediments probably formed in slightly deeper conditions, further away from the active wave base, i.e. the lower shoreface. The beds with preserved sedimentary structures probably formed in areas where the physical processes exceeded bioturbation, i.e. in the more active upper shoreface, similar to that seen in the Miocene shoreline deposits of California (Clifton, 1981). The burrows commonly cut straight across bedding surfaces and a horizontal component is frequently absent. This may indicate high rates of sedimentation (*cf.* Howard, 1975). The thickness and uniformity of the sand sequences suggest that they formed in relatively stable conditions, the general change from massive, extensively bioturbated sediments in the lower parts of the sequence, to well bedded, structured and less bioturbated sequences towards the top of the unit may imply progressive shallowing

of the depositional environment, i.e. a general drop in base level and/or possible progradation of the shoreline.

Unit D represents the sub-aerial component of this system. The red colouration of this unit is indicative of oxidation. The shelly "hash", a death assemblage associated with the caliche and soil is probably a storm event deposit which was washed up into the backshore environment. The presence of this unit indicates the continued shore progradation from the shoreface sequences of unit C.

### **6.5.1.3 Cape Pyla.**

The Cape Pyla sequence probably represents a small beach sequence with an initial transgressive basal lag flooding the Miocene erosion surface. The coarse to fine variation in the conglomerates represents a possible storm event, followed by a lower energy waning component. The clasts within the conglomerates may have been subjected to some longshore drift east, as the major fluvial sources in this area during the Quaternary issued into Larnaca Bay in the Ormidhia area further west. Imbrication data may support an argument for longshore drift, as there is a component of the data that trends to the east of the azimuth indicating imbrication orthogonal to the shoreline. The presence of the overlying shelly grainstones implies that the source of detritus may have ceased, and/or this area may have become isolated from the influence of the fluvial sequences to the west, perhaps as a result of a change in the relative base level. The conglomerates that cut down into the Quaternary and Miocene sequences are interpreted as fluvial successions, indicative of a continuing relative regression (Fig.6.8).

### **6.5.1.4 Model of deposition of the deltaic sequence in south-east Cyprus.**

The sedimentary sequences that crop out in south-east Cyprus contrast those Quaternary deltaic sequences that crop out elsewhere on the island, as they are not dominated by conglomeratic deposition (Section 6.3.2 and 6.3.3). The sediments reflect deposition within a shallow marine environment which has been influenced by both marine and fluvial controls. The lateral persistence of beds suggests that similar environmental conditions persisted over a large area. The vertical changes in lithology indicate that changes to the environment were taking place with the switch from a dominantly marine to a fluvial regime resulting in fluvial conglomerates flooding wave dominated marine sediments.

The presence of small faults (outlined in Chapter 4) may have had some control over the variation in the observed sedimentation pattern, but it is more likely that local



environmental changes, e.g. eustatic sea-level changes and changes in the sediment supply resulting from local, or regional tectonic uplift and/or climatic variations, exercised a greater control over the pattern of sedimentation. The shallow water nature of these sediments makes them excellent indicators of subtle changes in the relative sea-level and shoreline progradation.

The pattern of sedimentation in south-east Cyprus reflects the variation in the pre-existing relief of the basin. This changeable pattern also reflects a proximal, e.g. beach, delta top and delta-fluvial interface environments, to distal, e.g. delta front, environment, change in the environment of deposition, which in turn indicates the location of the palaeoshorelines.

### **6.5.2 Deltaic sequences of the south coast and the Polis-Paphos graben.**

#### **6.5.2.1 The south coast.**

The sedimentary sequences cropping out in the Mazotos area (locations 3-12, 3-13 and 3-18; Fig.6.3) represent coarse grained proximal deltaic sequences. Fine grained prodelta and bottom set sediments are absent. The presence of molluscs, although obviously reworked, indicates deposition in a marine rather than lacustrine environment. The clean, well sorted, mature, grain-supported nature of the conglomerate contrasts the overlying fluvial sediments that contain a matrix of silts and sands. The existence of an intra-formational unconformity and soft sediment deformation structures (location 3-13) may be related to fault movement, or disturbance of the area by an earthquake; this may have resulted in the establishment of a submarine erosional surface, similar to that seen in the Crati Basin of Italy (Colella, 1988). The presence of syn-sedimentary faulting within the sequence (Chapter 4) supports this argument. The occurrence of finer grained units above the submarine erosion surface may relate to:

- i) a variable sediment supply to the delta,
- or ii) a change in the relative base level at this time as a result of faulting, which caused distal delta front sediments to be deposited above the coarse proximal sequence. The overlying sequence of horizontally bedded sands and gravels (location 3-12), and mudstones and wackestones (location 3-13) marks the onset of regressive conditions. These sediments represent the delta top succession and were probably deposited in shallow marine conditions. Evidence from the well bedded, horizontal sands and gravels suggest that they were deposited in a high energy environment, with both physical and biological actions determining the nature of the preserved sediments. The micrite-wackestone sequence (location 3-13), by contrast, is likely to have been deposited in quiet, low energy conditions. The lack of detritus and the

massive nature of the bed supports this, indicating that deposition took place away from the influence of marine action during a period of quiescence, although the facies characteristics of this unit are non-diagnostic. The relative regression continued during and after the deposition of the micrites, suggesting that micrite deposition took place in areas away from active deposition of the fluvio-deltaic sediments in a lagoon, or on a shallow, quiet-water platform (Fig.6.11).

The regressive sequence continues with the formation of caliche, later reworked into the fluvial sediments (location 3-13), and the progradation of a fluvial sequence over the delta; this indicates that the relative regression continued (Fig.6.11). The thickness of the preserved fluvial sequence and the nature of the channels suggest that this portion of the sequence formed in shallow channels in a braided river environment, similar to the distal Fanglomerate Group sediments, deposited along the south Troodos margin throughout the Quaternary (Chapter 5).

In summary, the sedimentary sequences described here represent a regressive pattern of sedimentation in which delta front and then delta top sediments are succeeded by a prograding fluvial system. The whole sequence was subsequently subjected to sub-aerial exposure (Fig.6.11). The overall regressive nature of this system is probably related to the relative Quaternary sea-level changes, i.e. uplift and eustasy, although shoreline progradation, resulting from changes in the climate and sediment supply, cannot be discounted. It is likely that the pattern of sedimentation is related to all the variables stated above, i.e. climate, sediment supply, sea-level change and tectonic uplift, similar to that suggested for the deposition of the Fanglomerate Group sediments. Evidence of minor onlap of the delta onshore is present, as identified by the development of the submarine erosion surfaces and the apparent change, up section, from proximal to distal sequences (Fig.6.3). If these features do truly represent a proximal to distal change, then this may represent one of the few transgressive events preserved within the Quaternary sedimentary sequences of Cyprus.

The overall palaeocurrent pattern from the deltaic sequences along the south coast of Cyprus indicates flow in an arc from east to west-north-west (Fig.6.5), which is in broad agreement with the data from the Fanglomerate Group sediments that crop out along the southern Troodos margin, i.e. flow away from the Troodos Massif. The variation in the palaeocurrent data collected from the deltaic sequences at adjoining sites, may result from the size of the deltas, probably indicating a number of small delta systems with individual feeder channels, or a single large delta with a series of lobes, fed from a string of fluvial channels along the coast (Fig.6.12).

Fig.6.11. Summary diagram of the development of the deltaic and overlying fluvial sedimentary sequences in southern Cyprus.

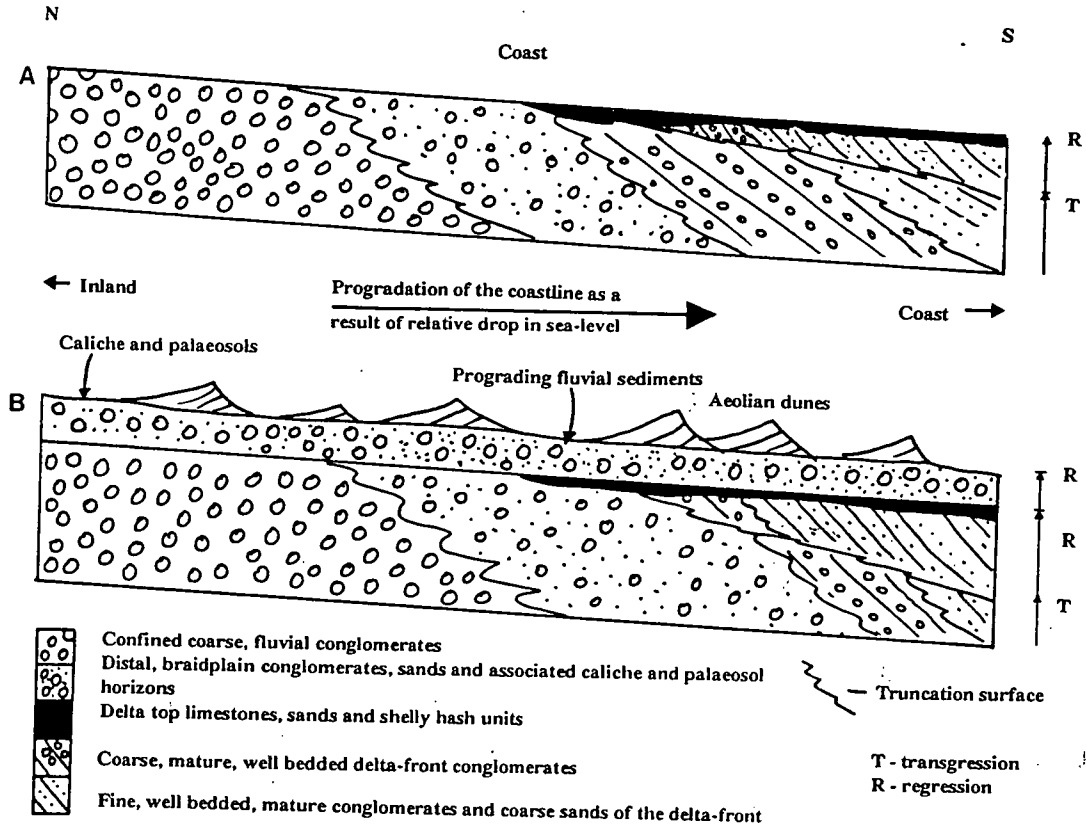
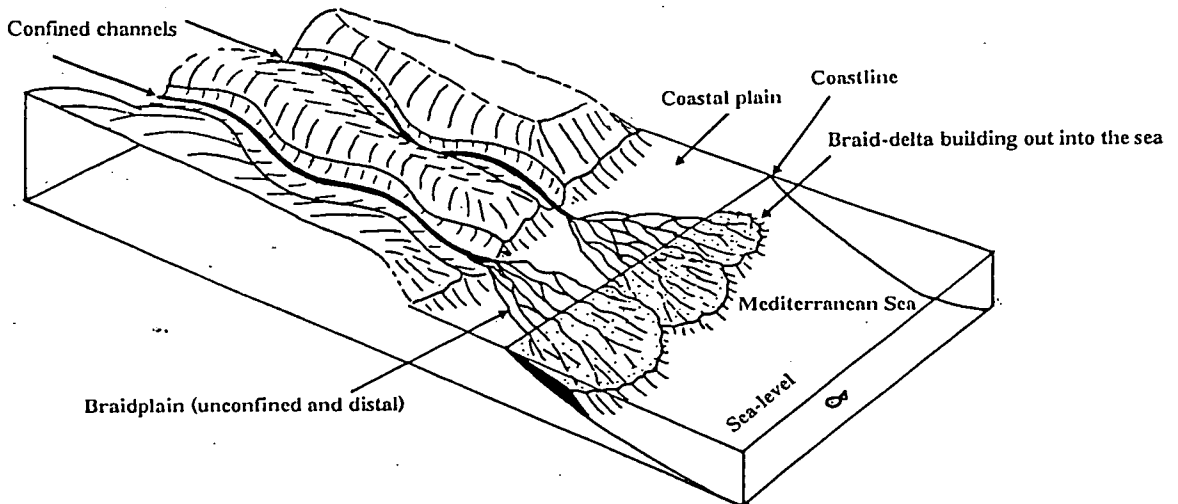


Fig.6.12. Sketch of the perceived development of the deltas along the southern coast of Cyprus.



### 6.5.2.2 The Polis-Paphos graben.

The deltaic sequences in the Polis-Paphos graben represent broadly transgressive and then regressive systems (Fig.6.13). The unconformity over the Myrtou Marls reflects the onset of a transgression, with a marine conglomeratic lag being succeeded by mature, fine grained sediments that have been influenced by marine wave action. The transgressive phase continues with the progradation of a delta out over a shallow shelf. The lack of wave worked sands suggests that the progradation of the delta occurred quite rapidly, and that the deposition of the deltaic sequence was fluviially dominated; the absence of later reworked sediments supports this. Prodelta sediments are absent. Progradation of the delta was probably followed by a period of delta front switching, resulting in the formation of intraformational unconformities which do not reveal a proximal to distal facies change, unlike that seen along the south coast of the island. The lack of available evidence, at present, for local faulting suggests that the intraformational unconformities may have been the product of delta switching, although active faulting in the Polis-Paphos graben was occurring throughout the Pleistocene (Ward & Robertson, 1987; Chapter 4). This faulting may have had a direct influence on delta switching, similar to that suggested for the deltaic sequences along the south coast, e.g. Mazotos (location 3-13). Active tectonics could also have influenced the supply of sediment to the delta from the graben and therefore had an impact on delta switching. The presence of bioturbation towards the top of the delta front sequences may indicate a slight shallowing of conditions, related to a change from delta-front to delta-top sedimentation; this pre-dates the influx of coarse, immature conglomerates that cap much of the delta sequence (Fig.6.6; Plate 6.4). Reworking of the delta front sequence took place during the deposition of the immature conglomerates, resulting in the presence of rip-up clasts, reworked shells and mature clasts within the immature conglomeratic unit. The matrix-supported fabric and chaotic nature of this immature conglomeratic unit suggests that it was deposited as a mass flow deposit in either a fluvial, or shallow marine environment. The presence of caliche horizons identifies periods of sub-aerial exposure. The pattern of sedimentation above this unit varies considerably, some localities revealing a true fluvial signature, with others passing up into well bedded, mature, laminated sands and fine gravels, indicative of an active beach or shallow marine environment. The presence of a white micritic mudstone at Limni (location 3-106), very similar to unit IV at Mazotos (location 3-13; Section 6.3.2), suggests that a low energy lagoon, or shallow platform, existed at this time. Evidence for true sub-aerial conditions are seen towards the top of the sedimentary sequence where mixed aeolian dunes are associated with the fluvial sequence, similar to that seen in the Vasilikos Formation (location 3-23). The shelly hash capping the sequence at Limni (location 3-106; Fig.6.6) was probably deposited in a storm event and resembles that seen above the F3 carbonate sequence at Argaka (location

Fig.6.13. Sketch of the suggested development of the deltaic sequences at the northern end of the Polis-Paphos graben.

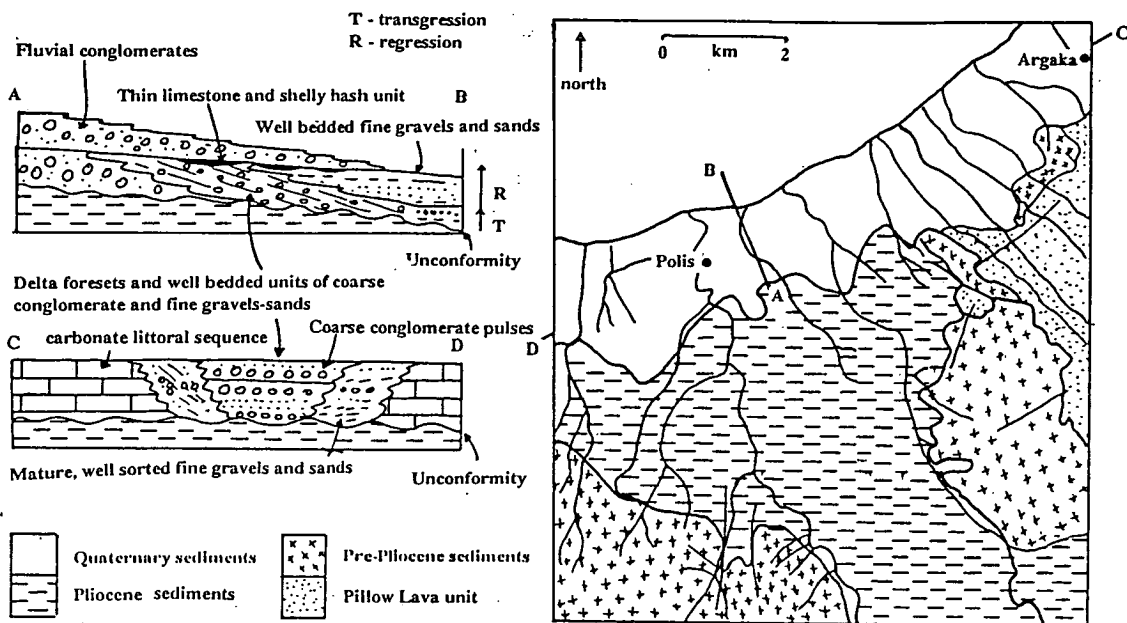
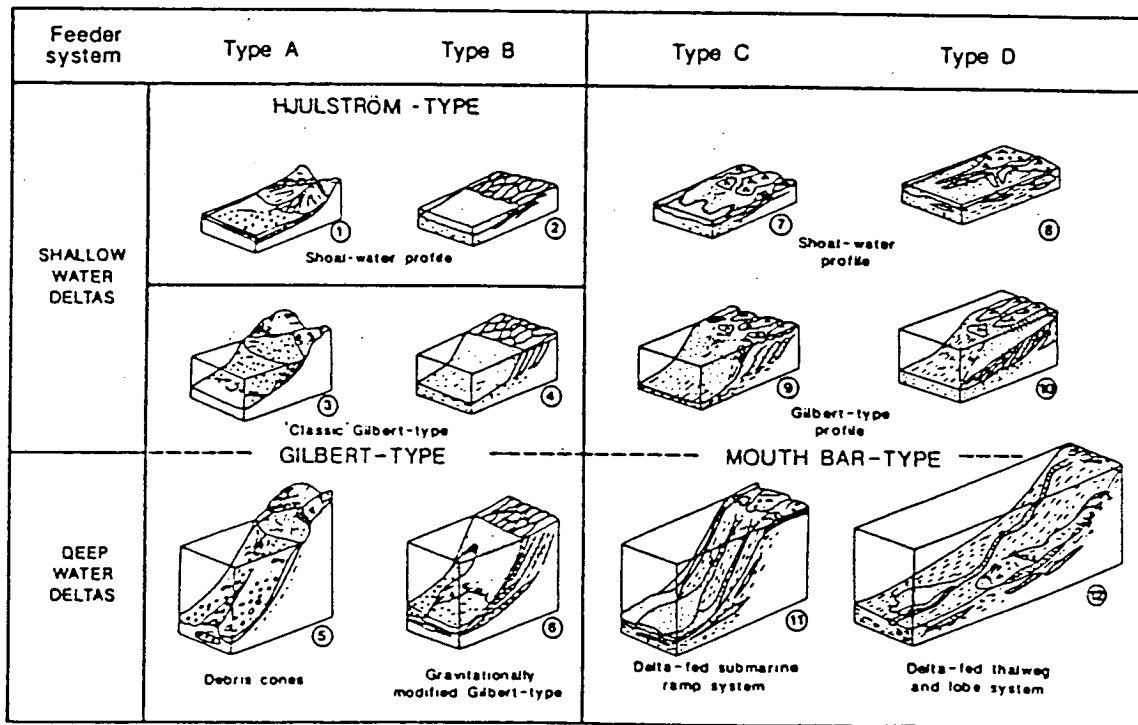


Fig.6.14. Prototypes of deltas dominated by fluvial processes distinguished on the basis of four different feeder/distributary systems and two ranges of basin depth (after Postma, 1989).



3-109) further east. The presence of the hash suggests that the fluvial sediments were deposited in an environment close to sea-level and, therefore, close to the marine environment (Fig.6.6).

The sequences preserved at the northern end of the Polis-Paphos graben formed on a low lying, flat coastal plain under the continuous influence of detritus derived from the graben and surrounding areas (Fig.6.13). Initial development occurred during a transgression prior to later development in a regressive regime (*cf.* Chapter 7). The pattern of sedimentation is likely to have been controlled by fluctuations in sea-level, uplift and climate. The presence of the fluvial conglomerates above the marine sequence probably results from progradation of the shoreline due to a variation in the sediment supply, or climate change. The overall regressive nature of the sequence indicates that even if the coarse pulse of conglomerate does represent some climatic event, it is superimposed on an overall drop in base level (Fig.6.13), similar to that associated with the sediments of the Fonglomerate Group (Chapter 5).

#### 6.5.2.3 Deltaic sequences of south-west Cyprus.

The limited outcrop pattern in the Kouklia area of south-west Cyprus has not facilitated the extensive study of this sequence but the following can be stated.

The presence of well bedded units dipping approximately perpendicular to the palaeoshoreline (Chapter 2) and both onshore and offshore imbrication data supports the view that these sediments have been deposited in a marine environment. The results achieved from the bedding characteristics agree with that found by Clifton (1973) for littoral rather than fluvial sequences. The variation in the pattern of imbrication (Fig.6.7) may have resulted from fluvial source switching and deposition dominated by fluvial processes, and/or reduced marine action during the deposition of these conglomerates at the base of the section (Fig.6.7). The mature nature of the clasts, with discoidal and spheroidal shapes also supports deposition in a marine setting.

The evidence here suggests that deposition of this sequence took place in a shallow marine environment fed by copious fluvial detritus. This detritus has been reworked in active marine conditions and deposited firstly as delta foresets and then as delta topsets. The evidence from clast maturity suggests that marine reworking due to abrasion was limited as most of the clasts have a spherical rather than discoidal shape (Dobkins & Folk, 1970). The pervasive nature of the burrows in the top portion of these sediments suggests high levels of biological activity, possible related to a reduction in the rate of sedimentation and/or a reduction in the detrital input into the area. The change from small scale delta foresets to topsets also indicates deposition in a regressive

regime, and/or an area of channel switching, which has facilitated the deposition of the fine grained sediments as the course channels have switched away. Unfortunately the limited exposure of this sequence does not allow a more detailed description and interpretation of this unit.

The presence of this sequence at c.220m ASL suggests that these deltaic sequences were deposited during the late Pliocene-early Quaternary and are possibly related to the formation of the F1 cliffline, i.e. they form part of the F1 depositional sequence.

#### **6.5.2.4 Models of deposition of the deltaic sediments of the south coast and the Polis-Paphos graben.**

The sequences cropping out along the south coast of the island resemble coarse grained equivalents of Gilbert type deltas, and are either braid- or fan-delta systems. McPherson *et al.* (1988) state that fan-deltas may be indistinguishable from braid-deltas on the basis of subaqueous facies alone but the variation in sorting and maturity of the resulting sediments will distinguish between the two systems. The fluvial dominated systems improve the sorting capacity of the delta, whereas mud-rich debris flows are more likely to occur in association with poorly sorted sediments of fan-deltas. The topsets are not preserved in the deltaic sequences of southern Cyprus; instead the deltaic sediments are overlain by thin limestones, structured sands and a prograding fluvial sequence. The absence of topsets may be attributed, locally, to erosion, as unconformity surfaces are present between in the deltaic and fluvial systems in the Mazotos area (location 3-13). Prograding sub-aerial sediments are unlikely to be present in flow dominated fan- or braid-deltas (Nemec & Steel, 1988); the presence of fluvial channels which have prograded out over the deltas suggest that the systems were stream dominated. As there is no evidence to support the development of alluvial fan sequences along the southern margin of the Troodos Massif (Chapter 5), it would be erroneous to refer to the associated delta sequences as fan-deltas. The deltaic systems in southern Cyprus should probably be described as braid-deltas, or braidplain deltas (Nemec & Steel, 1988) because of the alluvial feeder system which transported the Troodos-derived clasts into the delta environment. The classification of these systems as braidplain deltas is tangible, with much of the evidence concerning the development of the drainage system (Chapter 2) suggesting that major braided rivers in confined channels opened out onto braidplains at distal locations (Fig.6.12). In this way the systems are consistent with the classification of braidplain deltas (Orton, 1988) or braid-deltas (McPherson *et al.*, 1987). Postma (1989) proposed that delta architecture, rather than the alluvial feeder system, or basinal processes, should be used to classify deltas, and that the feeder system should be used as a secondary classification. This would result in the deltas along the

southern coast of the island between Limassol and Lamaca (location 3-13) being classified as shallow water type B4 deltas (Fig.6.14) - classic Gilbert type deltas.

The deltas of the Polis-Paphos graben have been termed fan-delta sequences in the past (L. Ward, *pers. comm.*, 1987). The evidence presented in Section 6.3.3 indicates that the deltas at the northern end of the Polis-Paphos graben are associated with braided river sequences and not the development of alluvial fans. The sequences seen in the northern portion of the Polis-Paphos graben (location 3-106) are therefore interpreted as being shallow water, type B4, braid deltas, similar to those cropping out along the south coast of the island.

### **6.5.3 Siliciclastic beach sequences.**

#### **6.5.3.1 South-east Cyprus**

The F3 and F4 siliciclastic sequences of south-east Cyprus form only a minor portion of this work. However an initial description and interpretation has been given here as a basis for future work. The interpretation given below is intended to indicate how these sediments may fit into the overall picture of Quaternary shallow and littoral siliciclastic marine sedimentation in southern Cyprus.

The preserved sequences in south-east Cyprus can be split into a series of facies, which are interpreted below.

*I) Conglomerate lag:* it is suggested that these coarse, sub- to immature cobbles, boulders and conglomerates, that lie unconformably above the limestones of Miocene age (e.g. location 2-700), represent an initial transgressive lag, similar to that described in Crete (Postma & Nemec, 1990) and from the Quaternary carbonate sequences in southern Cyprus (Chapter 7).

*II) Sands, fine gravels and grainstone sequences:* The sand and fine gravel units form large portions of the beach sequences. Many beds display Type B foresets of Thompson (1937), which are indicative of a foreshore environment. The grainstone sequences reflect littoral deposition (similar to that described in Chapter 7).

*III) Conglomerate units:* These conglomerate units form the main body of the beach sequences and probably represent berms. The generally mature nature of the clasts and the presence of well worn molluscan shells suggests abrasion in an active marine environment (similar to that seen in Tahiti; Dobkins and Folk, 1970). The presence of offshore dipping foresets and predominantly onshore dipping imbricated clasts (Figs.6.8



and 6.10), with some evidence of bimodality and chaotic, imbrication possibly indicates deposition in a storm environment, similar to that seen in Newton (Bluck, 1967), in the infill and imbricate zone (*cf.* Bluck, 1967; Postma & Nemeč, 1990). The orientation of the molluscan shells at the base of the unit, the shallow seaward dipping nature of the beds, the apparent winnowing of the clasts out at the top of the unit to leave a shell lag deposit also supports deposition by storm events.

The shelly nature of these units, the lateral persistence of many of the beds and the imbrication data all support deposition in a storm beach environment. However, the clasts maturity data have been treated with some caution as the clasts vary in maturity. It is suggested that this relates to three controls:

- i) reworking of previously deposited fluvial and marine clasts,
- ii) variation in the length of transport of the clasts,
- iii) the clast lithology, with sediment clasts eroding more easily and in a heterogeneous manner, unlike the igneous clasts derived from the Troodos ophiolite and the Troulli inlier.

The problem of clast maturity has been examined by Dobkins & Folk (1970), who stated that the use of clasts as maturity indicators does produce consistent results for homogeneous lithologies, e.g. basalt and diabase. The lithologies of the Troodos ophiolite, therefore, are likely to give a more accurate indication of the maturity than the overlying sedimentary cover sequence.

It is suggested that the fine gravels and sands form the background, fairweather sediment in many of the sequences, whilst the conglomerates occur as episodic pulses. This has yet to be proved but would explain some of the relationships between unit II and unit III. This interpretation would also support the argument for storm deposition of the conglomerate sequence. Kumar & Sanders (1976) state that the preservation potential of fairweather beach conglomerates is less than storm beaches, as they are more likely to be reworked; this and the presence of red soils between two pulses of conglomerate further support the argument for storm deposits.

The presence of fluvial conglomerates and the formation of palaeosols and caliche suggest that these units, after the initial deposition of the coarse transgressive lag and the deposition of littoral and foreshore sediments, record a period of regression, although this is by no means certain. Studies have recently identified progradational gravel sequences in Italy (Massari & Parea, 1988) and both regressive and transgressive beach sequences in Crete (Postma & Nemeč, 1990), it has been shown that both forms of gravelly beaches have the potential to be preserved.

#### 6.5.4 Summary.

The shallow marine sediments of southern Cyprus have an extensive outcrop and probably equally extensive sub-crop. This pattern mirrors that seen for the deposition of the fluvial sediments of the Fanglomerate Group and is totally unlike the pattern of deposition of the carbonate sequences (Chapter 7), which is not altogether surprising as it has been shown that the major source of sediment is the rising body of southern Cyprus, i.e. the Troodos ophiolite and its sedimentary cover sequence, and that these shallow marine sequences are the identifiable end point of the fluvial system (Chapter 5). The variation in the pattern of siliciclastic shallow marine deposition therefore reflects the fluvial feeder system (Fig.6.14).

The sequences along the south coast of the island and in the Polis-Paphos graben occur in locations where one would expect deltaic sedimentation to be occurring today; however, this does not seem to be the case. This and the change in character of sedimentation in south-east Cyprus, varying from extensive sand and conglomerate sequences in the early and middle Quaternary to what have been interpreted here as coarse limited beach sequences in the Late Quaternary, also supports the argument for a change in the pattern of sedimentation throughout the Quaternary. It is likely that this change results from a decline in the amount of sediment transported from the hinterland to the coast (Chapter 5), and/or switching of the drainage pattern. As drainage pattern switching has largely been ruled out (Chapter 2), except in the Dhekelia and Ormidhia area (Chapter 2), the former argument is preferred, with a reduction in the source sediments affecting the style of shallow marine sedimentation. This reduction in the source of sediment to the shallow marine environment probably reflects short term climate change (similar to that identified in Chapter 5), which has been superimposed on the overall reduction in rate of uplift, of the island, from the early to late Quaternary. The uplift does however facilitate the erosion of pre-existing siliciclastic sequences which may have been the source of some of the clasts for the formation of later beach and shallow marine sequences, i.e. the F3 and F4 beach sequences in south-east Cyprus.

The regressive nature of the shallow marine siliciclastic sediments reflects either uplift and/or a fall in sea-level (similar to that identified for the carbonate sequences; Chapter 7), although the individual components have not been deduced here. The pattern and style of sedimentation, however, probably also reflects the effect of climatic variation and hydrodynamic conditions that prevailed at the time of deposition of these sequences.

## **Chapter Seven: Carbonate littoral and sub-littoral sediments.**

### **7.1 INTRODUCTION.**

Previous studies of the Quaternary marine deposits in Cyprus have been restricted to the following: the well exposed terraces of Late Pleistocene age, i.e. F3 and F4 (Chapter 3), in the coastal area between Larnaca and the Akrotiri Peninsula (Bagnall, 1960; Bear & Morel, 1960; De Vaumas, 1962; Pantazis, 1966, 1967; Moseley, 1976), the terraces of western Cyprus (Turner, 1971) and along the coast to the north of the Kyrenia Range (Moshkovitz, 1966). Palaeontological (Moshkovitz, 1968) and isotopic age determination and correlation studies of the F1-F4 terraces of southern Cyprus have also been undertaken (Vita-Finzi, 1990; Chapters 2 and 3). This chapter will be restricted to a description and interpretation of the Quaternary carbonate littoral and sub-littoral sediments that are associated with the F1-F4 terraces in southern Cyprus. The geomorphology of the terraces, shallow marine siliciclastic, beach and deltaic sediments and related aeolianite sequences are dealt with elsewhere in this thesis (Chapters 2, 6 and 8, respectively).

### **7.2 GEOGRAPHICAL DISTRIBUTION.**

The carbonate littoral and sub-littoral sequences of southern Cyprus have a limited outcrop pattern (Fig.2.7), governed by the drainage pattern (Fig.2.1), which also dictates the arrangement of deposition of shallow marine siliciclastic sediments (Chapter 6). The consistent outcrop pattern of the carbonate sequences, throughout the Quaternary, i.e. F1-F4, adds more weight to the argument that the drainage pattern has undergone minimal changes during this period (Chapter 2).

The carbonate sequences in south-east Cyprus are generally restricted to an area to the east of the Xylophagou "topographic high" (Fig.2.7; Chapter 2). The F1 and F2 terraces that crop out in the Cape Greco area are erosive with limited deposition of Quaternary carbonate sediments. The F3 and F4 terraces form laterally extensive carbonate sequences (Fig.2.7; between Cape Greco and Paralimni, and Cape Greco and Ayia Napa). Limited F3 and F4 carbonate sequences also crop out on the erosional terraces in the area of Cape Pyla, i.e. F3 and F4. Siliciclastic deposition in the Dhekelia area during the early and middle Pleistocene is more restricted during the late Pleistocene (Chapters 2 and 6), permitting the deposition of a carbonate sequence, i.e. F4 (location 2-84).

Quaternary carbonate deposition along the south coast of the island, between Larnaca and the Akrotiri Peninsula, is limited to sequences at Larnaca (location 1-130), Petounda Point (location 3-11) and along the south coast of the Akrotiri Peninsula (location 3-96a; Fig.2.7). These sequences are of F3 age, except for the sediments that crop out along the south coast of the Akrotiri Peninsula, which are of both F3 and F4 age.

Littoral carbonate deposition is most extensive in south-west Cyprus between Paphos and the northern end of the Akamas Peninsula. Carbonate sequences of F1 to F4 age crop out (Fig.2.20) in the Paphos area. Extensive F3 and F4 carbonate terraces occur between Paphos, Coral Bay and Ayios Yeoryios, as well as cropping out on the western side of the Akamas Peninsula.

Limited carbonate sequences of F3 and F4 age crop out at the northern end of the Polis-Paphos graben (Figs.1.3 and 4.1). These sequences are located in areas outwith the influence of the major drainage channels on the extreme eastern edge of the graben, where a continuum from siliciclastic to carbonate sediments is seen (Chapter 6). F3 and F4 carbonate sequences also crop out in areas away from the major rivers west of Kato Pyrgos on the north coast of the island (locations 3-109 and 3-110; Fig.2.7).

### **7.3 SEDIMENTOLOGY OF THE CARBONATE SEQUENCES.**

#### **7.3.1 Introduction.**

Examples of the carbonate littoral and sub-littoral sedimentary sequences will be described in stratigraphic order, i.e. F0-F4, from localities throughout southern Cyprus, from Paralimni in the east to Paphos and Kato Pyrgos in the west.

#### **7.3.2 The F0 carbonate sequences (upper Pliocene-lower Pleistocene).**

The F0 carbonate sequences have a very restricted pattern of exposure, cropping out within the highest terrace in the Paphos area, e.g. Mesoyi (location 2-18), Marathounda (location 2-51), Tremithousa (location 3-35), c.350-360m ASL (Fig.2.20; Chapter 2). The sequences are poorly preserved and are made up of grainstones that lie unconformably above units of the Troodos sedimentary cover, the Mamonia Complex, and very coarse, angular, poorly sorted conglomerates, e.g. Mesoyi (location 2-18; Fig.7.1). The grainstone sequences are less than 5m thick and usually consist of well bedded, planar laminated, mature, medium sands. The grainstone beds at Marathounda (location 2-51) generally dip towards  $097^{\circ}$ - $100^{\circ}$  at between  $10^{\circ}$ - $16^{\circ}$  and are also locally totally disrupted by bioturbation. The grainstones are capped by caliche and soil horizons.

Fig 7.1. Field sketch illustrating the relationship between the pre-Quaternary sediments, the F0 fluvial conglomerates and the F0 grainstone sequence, exposed in an arm of the Koshinas River valley at Mesoyi (location 2-18), south-west Cyprus.

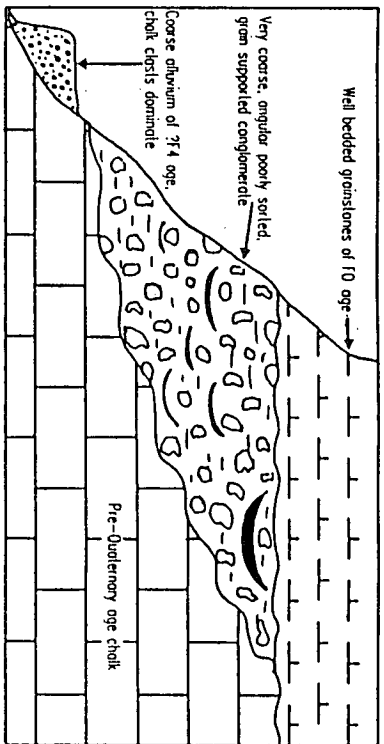
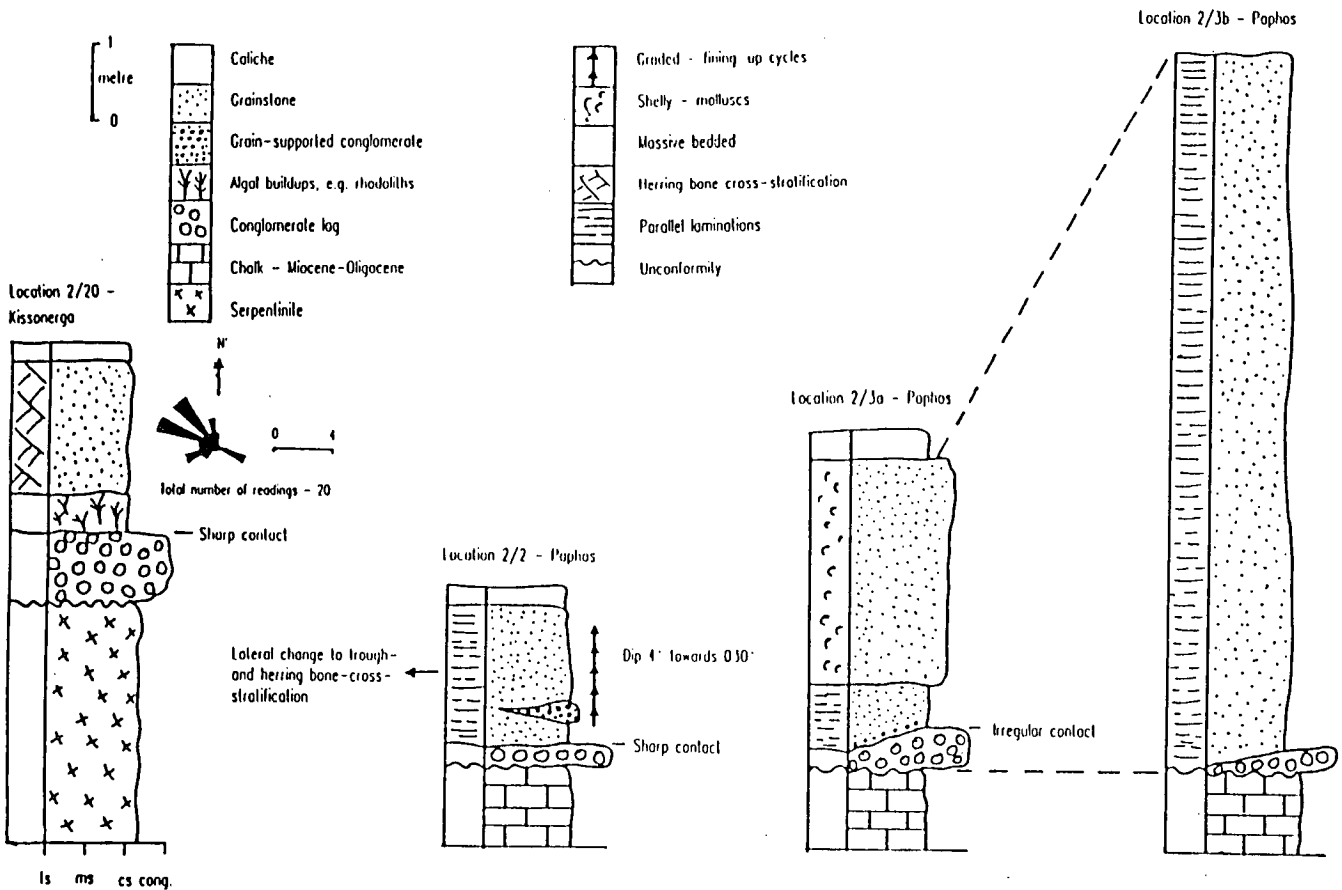


Fig. 7.2. Sketch sections of the sedimentary units of the F1 carbonate sequence that crop out above Paphos (locations 2-2 and 2-3) and Kissonerga (location 2-20).



### **7.3.3 The F1 carbonate sequences (lower-middle Pleistocene).**

#### **7.3.3.1 Introduction.**

The exposed F1 sequence in the Paphos area (location 2-3) unconformably overlies chalks and limestones of Miocene and Oligocene age (Plate 7.1). The overlying F1 sedimentary sequence is generally less than 5m thick, although cliff sections up to 13m thick are present locally, e.g. at the Paphinia Hotel, above Paphos (location 2-3; Fig.7.2). The Quaternary sediments generally make up between 50 and 100% of the exposed vertical sequence. The exposed cliffs are commonly in the order of 10-12m high (location 2-2; Fig.7.2). An unconformity surface at the base of the F1 sedimentary sequence shows extensive relief, up to 2m, and is overlain by a basal lag of locally derived clasts. The lag is succeeded by a branching coralline red algal framework, crustose coralline algae and rhodoliths, which in turn pass up into littoral grainstones, containing abundant molluscs (Fig.7.2). Caliche and soil horizons cap the F1 sequence.

Local variations within the F1 carbonate sequence are also seen, as exemplified by the absence of the conglomerate lag and/or coralline red algal framework (Plate 7.1). Thin stringers of mature conglomerate and isolated clasts are also seen within the grainstone units. Limited exposures of F1 carbonate sequences also crop out in areas to the north of Paphos (locations 2-20 and 2-34; Fig.7.2), where they lie unconformably above serpentinite. These sequences have very similar characteristics to that seen in the localities in the Paphos area.

#### **7.3.3.2 Sedimentary facies.**

*i) Conglomerate lag:* these conglomerate sequences are dominated by locally-derived clasts and a reworked fauna. The lateral and vertical extent of the lag along, and between, sections varies considerably. Clasts derived from sources close to the outcrop, e.g. directly beneath the conglomeratic unit, tend to be immature and contrast with clasts that have been transported into position. At Kissonerga (location 2-20; Fig.7.2) the lag unit is 60-80cm thick containing well rounded igneous clasts and abraded shells, the serpentinite clasts, derived from the unit that lies unconformably beneath the F1 carbonate sequence, are generally angular and less than 1.7m in diameter (Plate 7.1). The lag in the F1 succession east of Lara Point (location 2-34) is very coarse, immature and poorly sorted, with only locally-derived clasts present, e.g. serpentinite. By contrast, the lag at locations in the Paphos area is generally less than 50cm thick and consists of

## PLATE 7.1.

A - F1 carbonate sequence (dark) lying unconformably above chinks of Miocene age (white) exposed in an F2 age cliff above Paphos (location 2-3).

Note: the relief on the unconformity contact.  
the chalk is c.1.5m thick.

B - Sedimentary structures preserved in the F1 grainstone sequences displaying steeply dipping foreset (a), trough-cross-stratification (b) and low angle planar-stratification (c).

Note: scale is 50cm long.

C - Sedimentary structures preserved in the F1 grainstone sequences displaying herring bone-cross-stratification (b) and massively bedded (c) units.

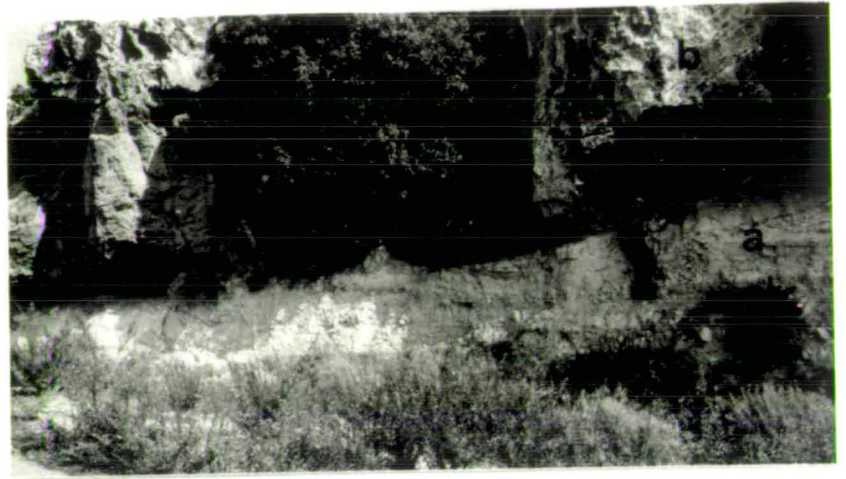
Note: scale is 50cm long.

D - F1 carbonate sequence cropping out above serpentinite (a) north of Paphos (location 2-20). The conglomerate lag (b), dominated by large serpentinite clasts is succeeded by units of grainstone (c).

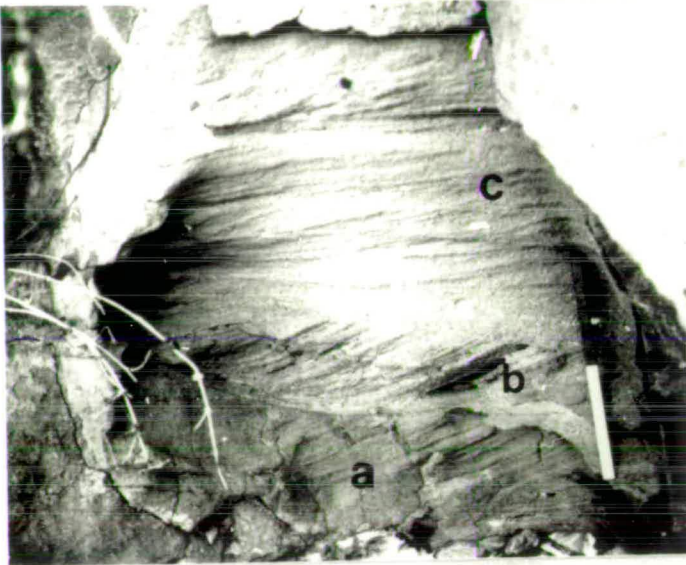
Note: scale is 50cm long.

Plate 7.1

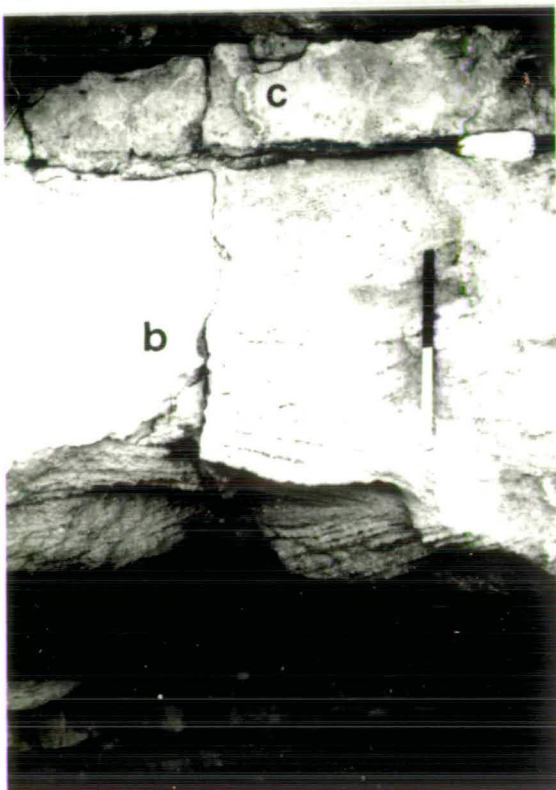
A



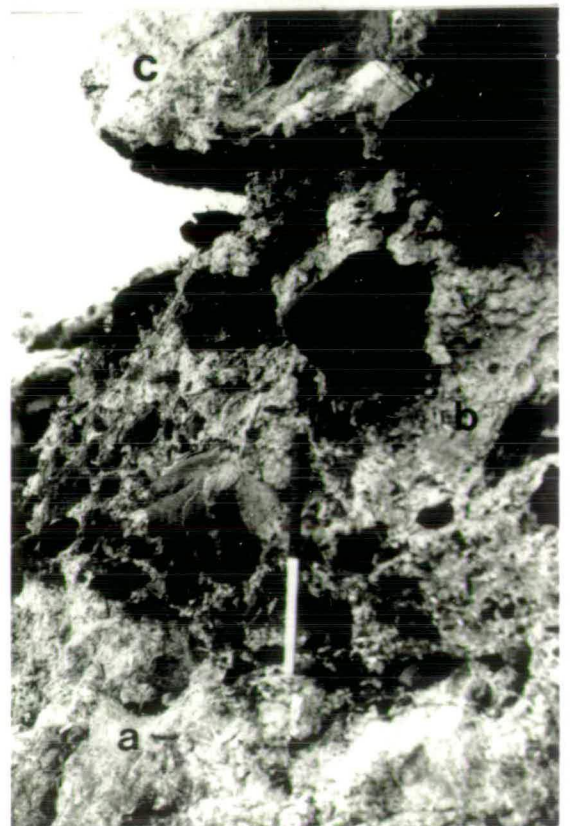
B



C



D





locally-derived clast, i.e. chalks, limestones, which are sub-angular to well rounded, and infrequently discoidal.

ii) *Coralline algal framework and rhodoliths*: small frameworks of delicate branching red coralline algae are present in life position attached to clasts of the lag unit; these are also anchored directly onto the lithologies underlying the unconformity surface, e.g. the serpentinite above Kissonerga (location 2-20). The algal frameworks that have established a hold on the unconformity surface are commonly found in the areas of local high relief, and not in the troughs (Fig.7.3). Encrusting and densely branched, robust, red algal structures, i.e. rhodoliths, are also present. A mixed high diversity and high density fauna is associated with the algal units which have a matrix of medium to coarse bioclastic sand. The succeeding grainstone units appear to swamp the algal structures, preventing further growth of the algae.

iii) *Carbonate grainstones*: grainstones crop out either above the coralline framework unit or directly above the basal lag unit. The basal grainstone contact is usually gradational (locations 2-20 and 2-3; Figs.7.2 and 7.3) and irregular, reflecting the relief of the underlying unconformity surface (Plate 7.1). The grainstones vary extensively, both vertically and laterally (Figs.7.2 and 7.3), with planar laminated beds (dipping at less than 5° seaward), herring bone-, festoon- and trough-cross-stratification, as well as massively bedded units being present. Most of the beds are less than 5cm thick (Plate 7.1). Some grading of the grainstone units is seen, although the majority of the grainstone units are ungraded coarse sands. Grading, where present, ranges from very coarse to medium sand. The grainstones units are generally submature and poorly sorted and are commonly interbedded with coarser, mature, stringers of derived clasts. The unbroken macrofaunal content of the grainstones is commonly low and occupies a death position. Whole thick-shelled molluscs, e.g. *Pecten* and *Ostrea*, are present locally. Bioturbation is generally absent, although vertical tube structures are present in the grainstones in outcrops above Paphos (location 2-2). Bioturbation within the grainstone units is very variable, as a 3-5m thick sequence of coarse grainstone to the east of Lara Bay shows (location 2-34); this is parallel laminated at the base passing up into massive, highly bioturbated grainstones at the top of the unit.

### **7.3.4 The F2 carbonate sequences (Middle Pleistocene).**

#### **7.3.4.1 Introduction.**

The F2 sequences are more extensive than their F1 counterparts, although limited to the west coast between Paphos and Lara (locations 2-5, 2-14 and 2-34). This terrace

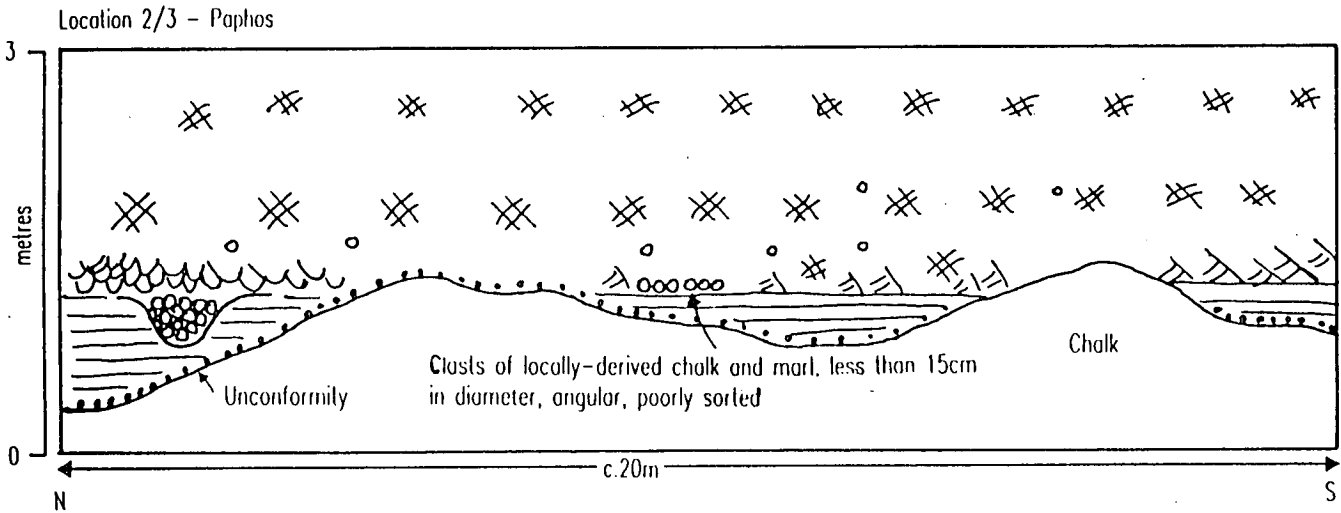
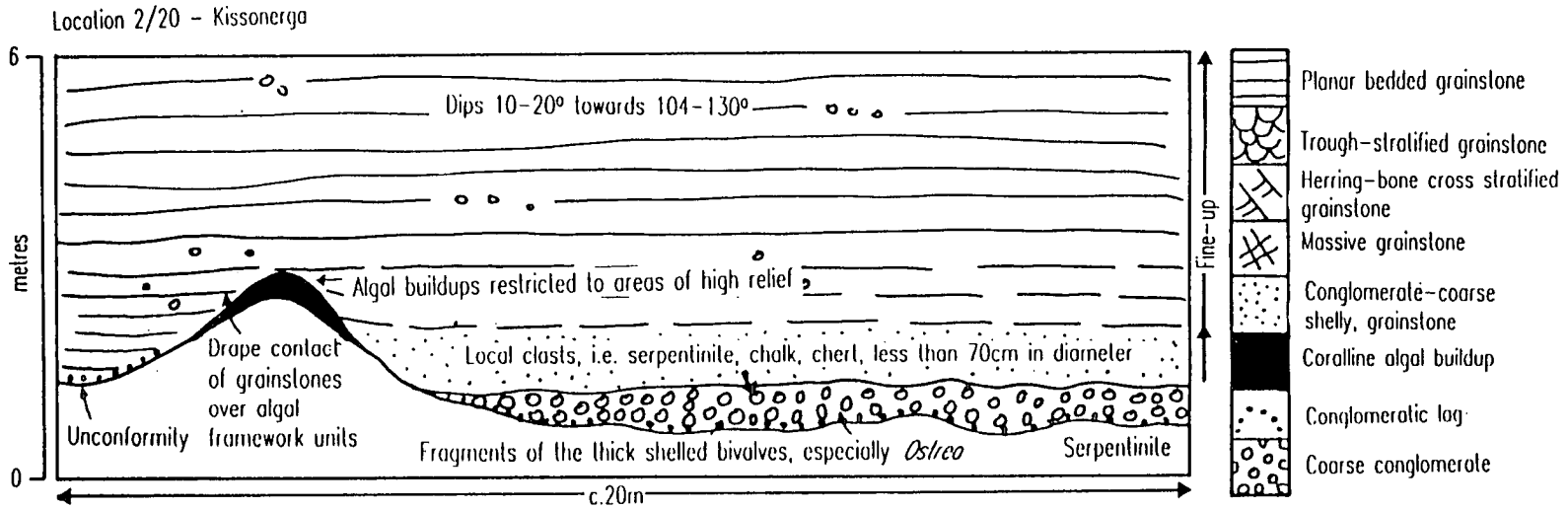


Fig.7.3 Field sketches emphasising the sedimentary relationships in the F1 carbonate sequence in the terrace above Paphos (location 2-3) and at Kissonerga (location 2-20).

lies unconformably above a variety of lithologies, e.g. serpentinite, chalks and limestones of Oligocene and Miocene age, similar to that seen with the F1 carbonate sequences. The variety of sediments seen within the terrace sequence is much greater than that recorded for the F1 sequences, although the three basic components described above and in Chapter 9 are present: i) basal lag above the unconformity, ii) a framework structure of coralline red algae, iii) grainstones. Soils, aeolianites, caliche and mixed detrital-carbonate sequences are also associated with the F2 sequences. The F2 sequences are generally less than 15m thick (Fig.7.4; Plates 7.2 and 7.3).

#### 7.3.4.2 Sedimentary facies.

i) *Basal conglomeratic lag*: The basal lag cropping out in the terrace to the east of Paphos (locations 2-5 and 2-7) consists of locally derived clasts, e.g. limestones and chalks, as well as clasts derived from the Mamonia Complex, e.g. serpentinite and diabase. The clasts are generally mature, less than 10cm along the "L" axis and rounded to discoidal in shape. Broken, abraded and reworked shells of *Glycymeris*, *Ostrea* and *Pecten* are seen. The unit pinches and swells reflecting the irregular contacts seen at both the base and top of the unit (Fig.7.4).

ii) *Coralline red algal frameworks and coral colonies*: The algal framework units are more prominent within the F2 than the F1 sequences (Fig.7.4). The red coralline algal framework present in the basal portions of the F2 sequences is delicate and branching (Plate 7.2), although robust, rolled rhodoliths and crustose algae structures are also present (locations 2-5 and 2-13; Plate 7.2). The height of the red coralline algal framework unit, between 0.5 and 1.5m, appears to have been controlled by two factors; the timing of the influx of coarse grainstones that swamped the algae and the relief on the underlying unconformity surface. Up 2m of relief is seen on the unconformity surface at location 2-5, with algae development being more restricted where the unconformity surface is higher. The algal build-ups nucleated on the small clasts that make up part of the conglomeratic basal lag. Small colonies of the scleractinian coral, *Cladocora caespitosa*, are also found in this unit (location 2-5). These coral colonies are generally less than 40cm in diameter. The majority of the coral colonies are found in an *in situ* life position, indicating growth upwards. The coral colonies are attached to clasts of the basal lag unit, or to the lithified sequences beneath the unconformity surface, e.g. limestones and chalks of Miocene and Oligocene age. Some isolated coral heads, in a death position, are also found locally within this unit (locations 2-12, 2-13 and 2-14). The matrix associated with the framework structures is generally an immature, poorly sorted medium to coarse sand grade grainstone, containing a multitude of tiny shells fragments and rare igneous clasts. A mixed high density, high diversity molluscan fauna including: *Pecten*,

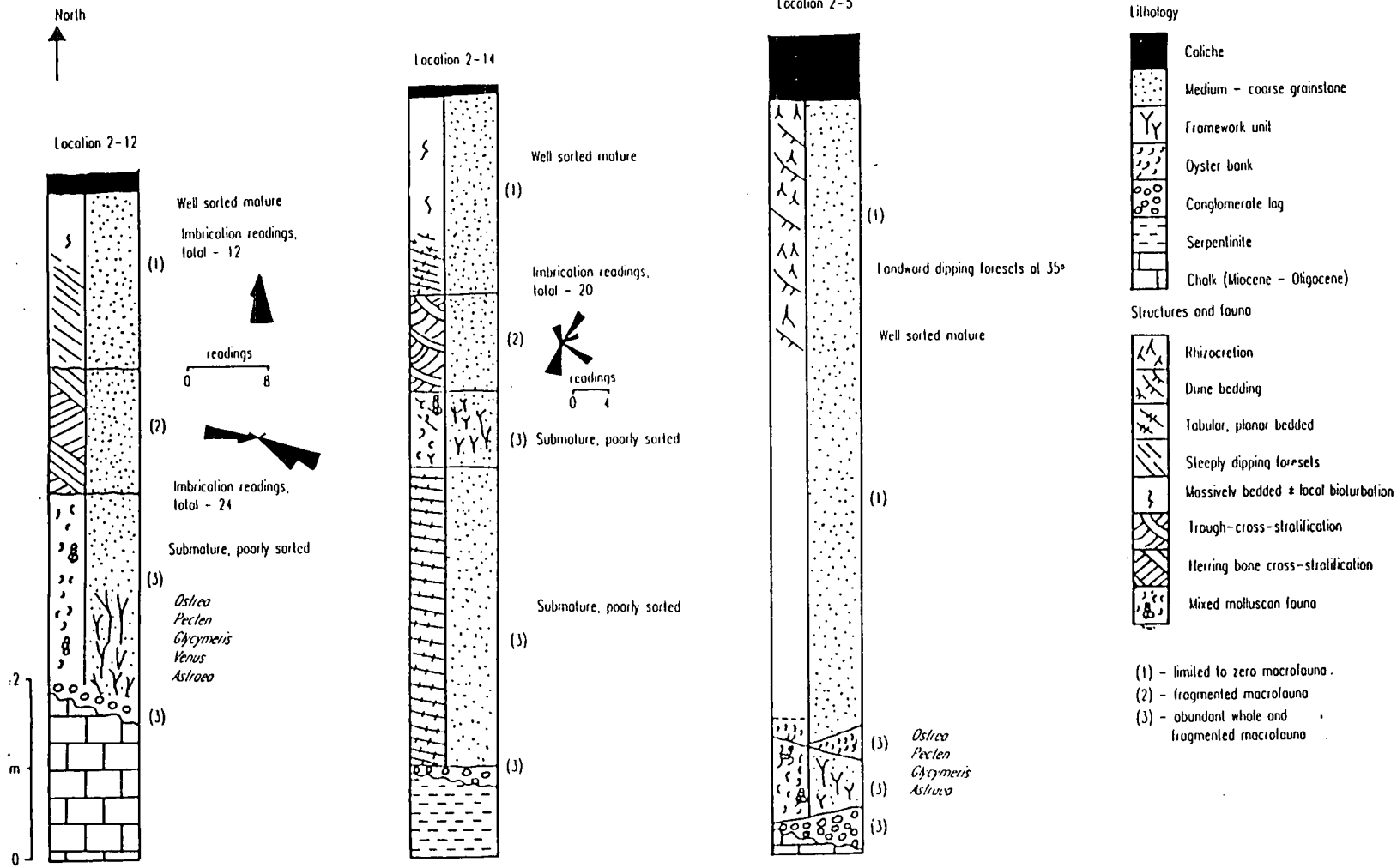


Fig 7.4. Sketch sections of the F2 carbonate sequence that crops out in Paphos (locations 2-5, 2-12, 2-14).

PLATE 7.2.

A - F2 carbonate sequence exposed to the east of Paphos (location 2-5) with Miocene chinks being overlain by a thin conglomerate lag (a), which passes up, and laterally, into a unit of coralline algae (b) which in turn is succeeded by a steeply dipping grainstone sequence (c).

Note: scale is 50cm long.

B - The robust coralline framework unit (a) exposed in the F2 carbonate sequence at location 2-5; this appears to have been swamped by grainstones (b).

Note: scale is 50cm long.

C - Detail of the delicate coralline algal frameworks preserved in the F2 carbonate sequence at location 2-5.

# Plate 7.2

**A**



**B**



**C**

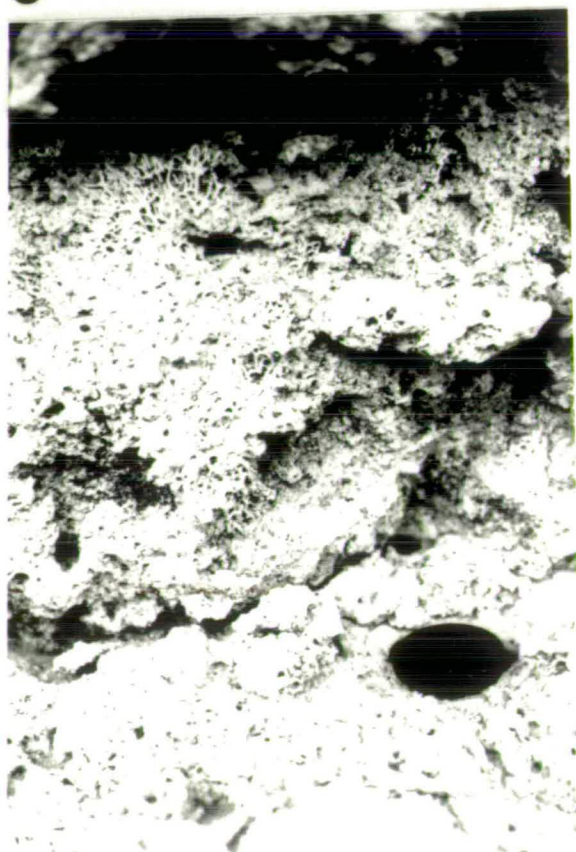


### **PLATE 7.3.**

All the photographs on this plate were taken at the F2 exposure that crops out in Paphos (location 2-14).

A - F2 carbonate sequence consisting of a transgressive lag, algal framework and grainstones.

Note: see Fig.7.4 for details.

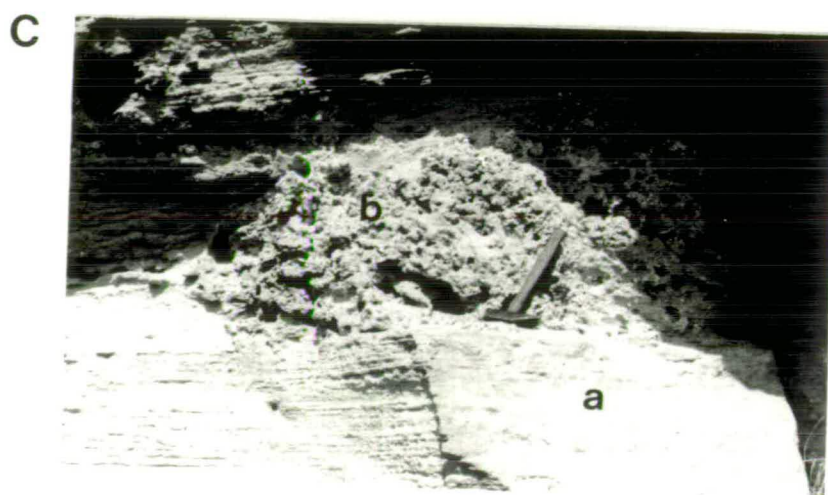
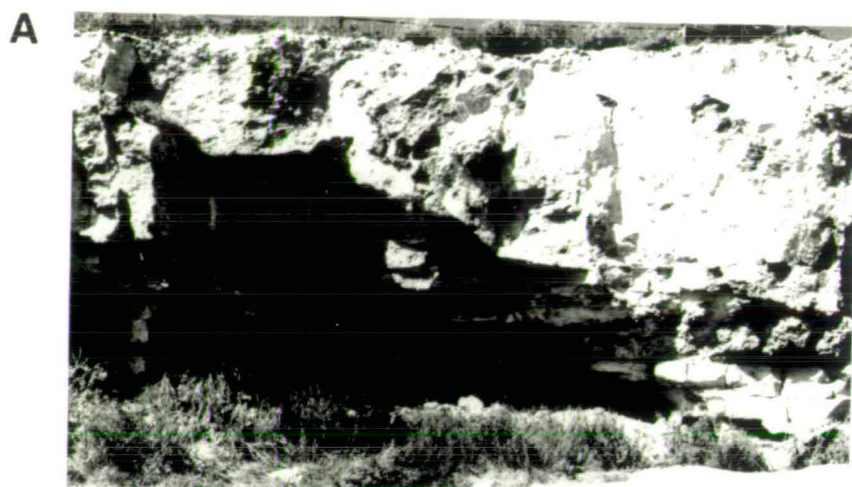
B - Planar stratified and trough-cross stratification structures in the F2 grainstone unit.

Note: scale is 50cm long.

C - Well-laminated low-angle cross-stratified grainstones (a) passing up into a framework unit (b) and then back into the grainstone sequence.

Note: hammer for scale.

# Plate 7.3





*Astraea*, *Venus* and *Glycymeris* is also present within this unit. Oyster banks are seen, locally associated with the framework structures (location 2-5). Grainstones appear to swamp the algal and coral frameworks up section (Fig.7.4; Plate 7.2).

iii) *Grainstones*: the grainstone units locally lie above a very thin lag sequence, e.g. to the north-west of Paphos, location 2-14; Fig.7.4) directly above the unconformity surface. This relationship results in the formation of significant grainstone sequences that pass up, in turn, into the framework unit and then back into the grainstone facies (Fig.7.4; Plate 7.3), although the majority of the F2 grainstone are preceded by basal lag and algal framework structures. The F2 grainstones are commonly medium to coarse sand grade, mature, sorted and poorly cemented. The grainstone sequences exhibit a number of sedimentary structures, i.e. planar-bedded and herring bone- and festoon-cross-stratification (Plates 7.3 and 7.4), yet massive, apparently structureless units are also seen (Fig.7.4). The type of bedding varies both vertically and laterally, with many truncation surfaces being present. Whole macrofossils are generally absent from the grainstone sequences, although abraded broken fragments of molluscs, bryozoan, coral and echinoids are seen. Evidence for bioturbation and subvertical rhizcretion structures is seen locally (location 2-5). Portions of the F2 grainstone sequence in Paphos (locations 2-10 and 2-12) indicate an onshore palaeocurrent direction (Fig.7.4), suggesting aeolian processes (Chapter 8). Field observations (Fig.7.4; Plate 7.4) suggest that littoral sequences may be overlain by aeolianites similar to those seen elsewhere in the F2 sequence in Paphos (location 2-5). By contrast, other F2 grainstones sequences in the Paphos area (e.g. location 2-40) appear to be wholly aeolian (Chapter 8). These onshore palaeocurrent data contrast those data collected from F2 grainstone sequences at other locations in Paphos (locations 2-12 and 2-14), which indicate an offshore, i.e. from south-west to the south-east, and bimodal palaeocurrent direction (Fig.7.4).

iv) *Sub-aerial succession*: the F2 unit in the Paphos area is usually succeeded by the formation of thin caliche and soils. Thick caliche and conglomerates are also locally seen capping the F2 grainstone sequence in the Paphos area, e.g. east of Lara Point (location 2-34) and Yeroskipos (location 2-57a; Fig.7.5).

v) *Mixed sequences*: mixed facies are seen with fluvial sediments (Chapter 5) cropping out in close proximity to the carbonate sequences. The interplay between the two environments results in a sedimentary succession that consists of a coarse basal lag sequence, but this is either overlain by carbonate units and then succeeded by bedded clastic units, or *vice versa*. The proportion of clasts varies throughout the sequence, e.g. in the succession to the north of Paphos (location 2-19; Fig.7.5), with matrix-supported clasts from local and more distant sources appearing in the carbonate sediments. The

**Fig.7.5. Field sketches of: a) the F2 cliff and terrace developed in Paphos (location 2-5); b) the lateral changes seen at location 2-12; c) the swamping of the algal framework unit by grainstones at location 2-5; and d) the sequence of sedimentary structures present at location 2-14.**

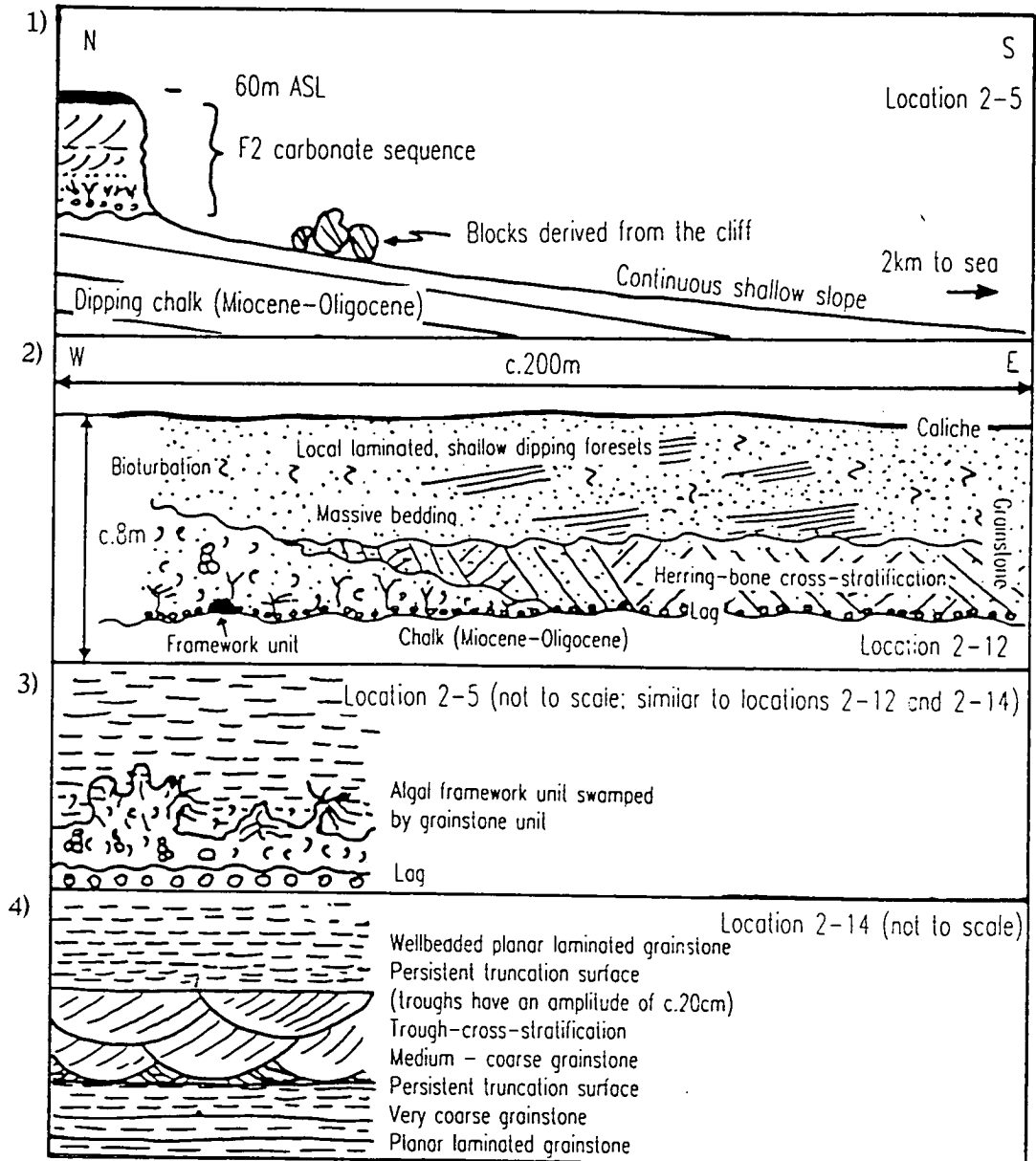


Fig. 7.6. Sketch sections from the F2 carbonate and mixed sedimentary sequences at Yeroskipos (location 2-19 and 2-57a).

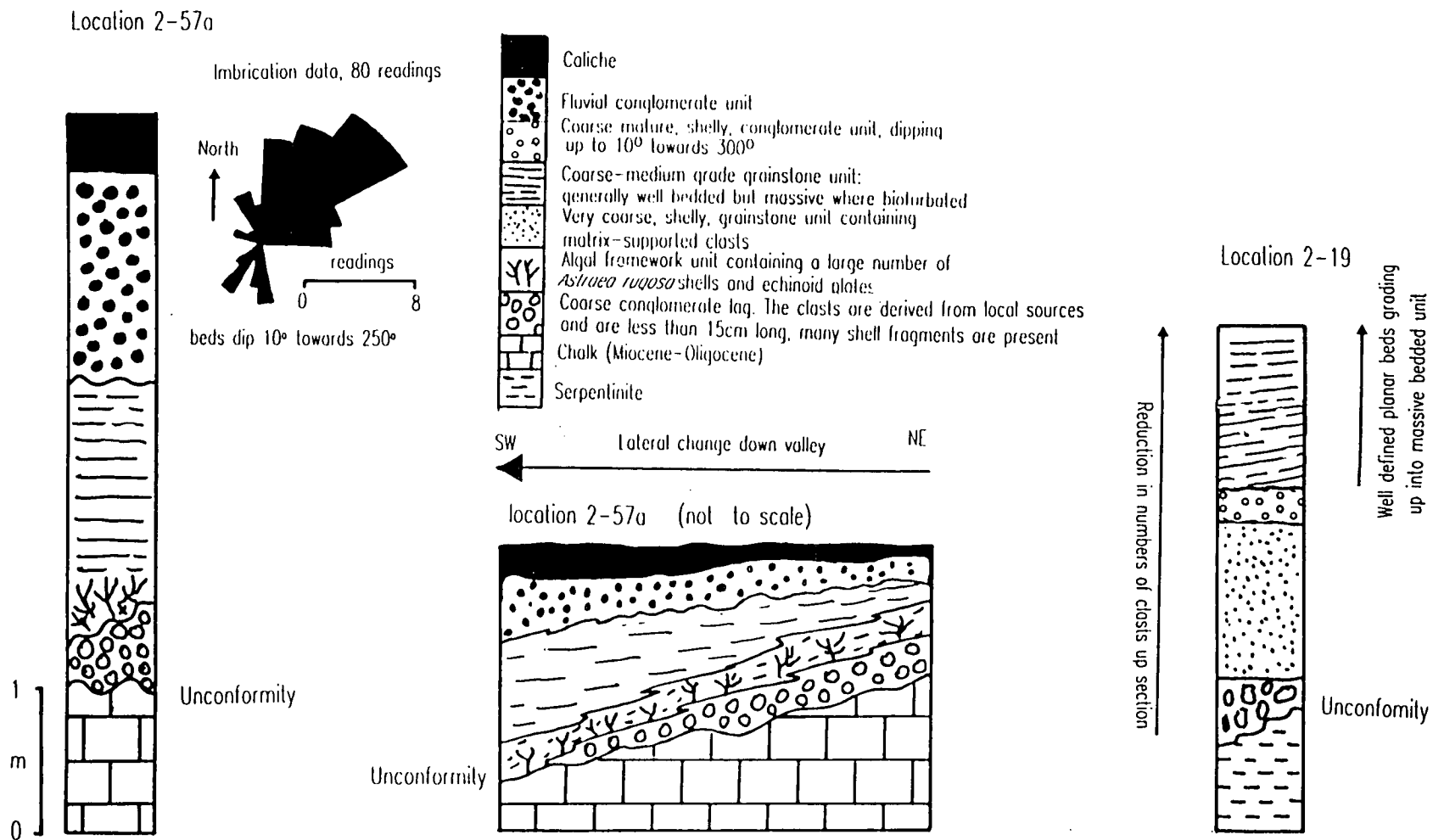


PLATE 7.4.

A - Low angle well-laminated planar stratified grainstones (a) being succeeded by grainstones that dip steeply onshore (b) from the F2 carbonate terrace in Paphos (location 2-10).

Note: the scale is 50cm long.

B - Thick (c.4-5m) unit of planar stratified grainstones preserved in the F2 carbonate terrace sequence in Paphos (location 2-10).

Note: 50cm scale in the hollow in the cliff.

C - Detail of the planar bedded and laminated nature of the coarse grainstone sequences cropping out in the F2 carbonate terraces in the Paphos area.

D - Evidence for small slumps and convolution of the grainstone beds from the F2 grainstone sequence in the Paphos area.

Plate 7.4

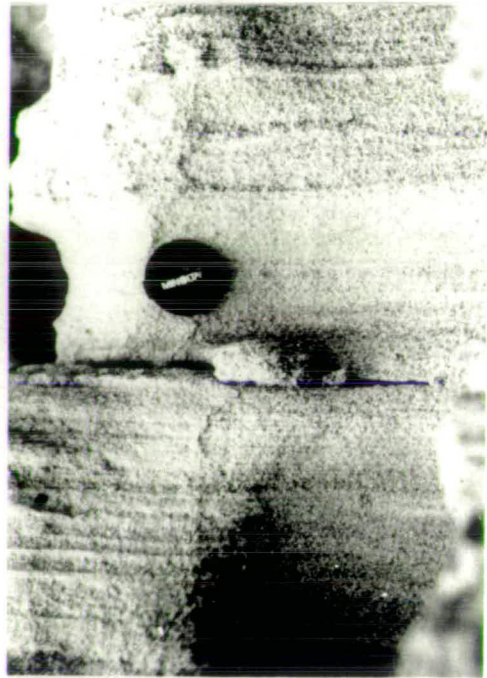
A



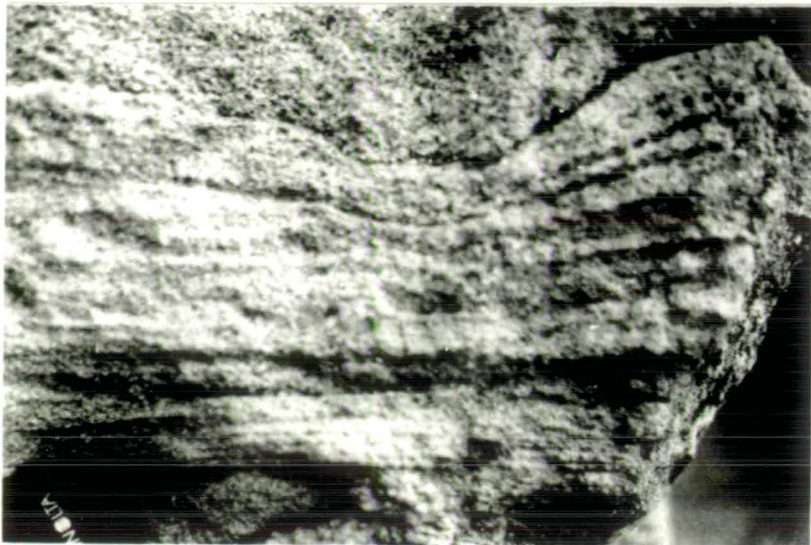
B



C



D



clastic units generally display planar-bedded seaward-dipping units, similar to that seen in the F3 siliciclastic beach sequences in south-east Cyprus (Chapter 6).

### **7.3.5 The F3 carbonate sequences (early Late Pleistocene).**

#### **7.3.5.1 Introduction.**

The F3 successions crop out unconformably above the Pliocene Athalassa and Nicosia Formations at Larnaca, Cape Greco and Coral Bay (locations 1-130, 1-125 and 2-22, respectively; Plate 7.5), deformed Miocene and Oligocene limestones and chalks at Lara Point, Petounda Point and Cape Pyla (locations 2-34, 3-11 and 1-136 respectively; Plate 7.5), and locally above basement units in the south-east of the island, e.g. the Paralimni Melange, on the coast east of Paralimni. The top of the F3 unit crops out within 11m ASL (Figs.3.4 and 3.8; Chapter 2), and associated sedimentary successions are generally less than 5m thick. The F3 terraces have been correlated with the penultimate glacial sea-level high stand (Chapter 3; oxygen isotope stage 7; Shackleton & Opdyke, 1973).

The sedimentary components found in the F1 and F2 terraces are also present within the F3 sequences (Sections 7.3.3 and 7.3.4). Minor lenses of Troodos-derived clasts are present within the carbonate sequences in the Larnaca and Polis areas (location 1-130 and 3-109 respectively). Carbonate aeolianites and caliche formations are also present within the F3 sequences, with extensive preserved dune systems cropping out above the littoral sequences (Fig.3.8; Chapters 2 and 8).

The F3 carbonate sequences from Cape Greco, Larnaca, the Paphos area and in the area to the east of Polis are described in the following sections.

#### **7.3.5.2 Cape Greco.**

The probable F3 carbonate sequence at Cape Greco unconformably overlies marls of the Nicosia Formation (Pliocene) and Terra Limestones (Miocene) and is, in turn, overlain by an F4 carbonate sequence (Figs.3.8 and 7.7).

*i) Conglomeratic lag:* a coarse lag of locally derived marl and limestone clasts lies directly above the unconformity surface (Plate 7.6 and 7.7). Thick worn, molluscan, e.g. *Pecten* and *Glycymeris*, shells form part of the coarse conglomerate lag, which has a matrix of coarse sand. Infilled vertical burrows, less than 2cm in diameter and up to 20cm deep, are seen passing down from the unconformity surface into the marls. These

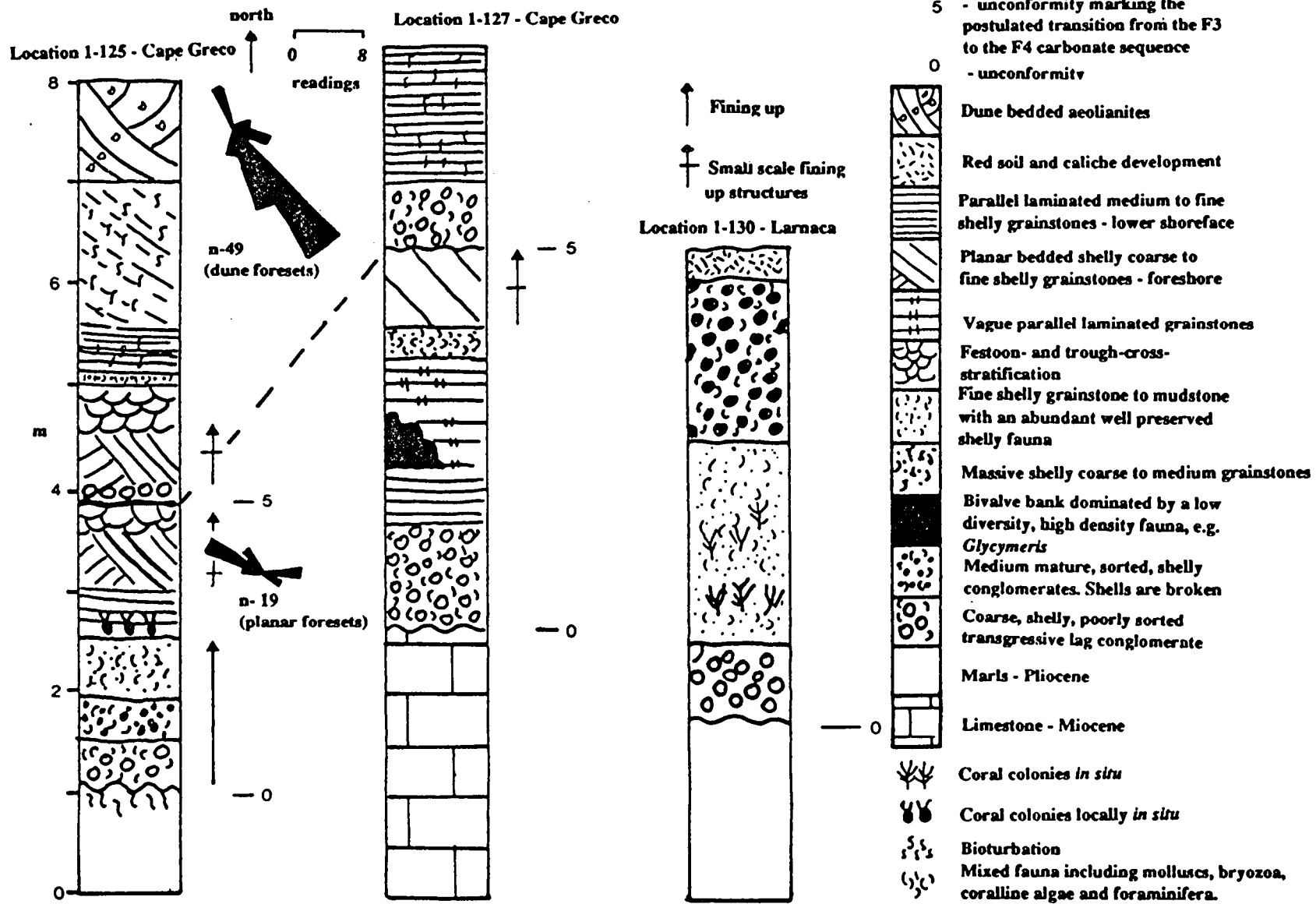


Fig 7.7. Sketch sections of the F3 sedimentary sequences that crop out at Cape Greco (location 1-125 and 1-127) and Larnaca (location 1-130).

PLATE 7.5.

A - The F3 marine terrace lying unconformably above steeply dipping chalks of Miocene age (a) on the coast south of Xylophagou, south-east Cyprus.

Note: the cliff is c.10m high.

B - The F3 marine terrace (b) cropping out unconformably above marls of the Nicosia Formation (a) in Larnaca.

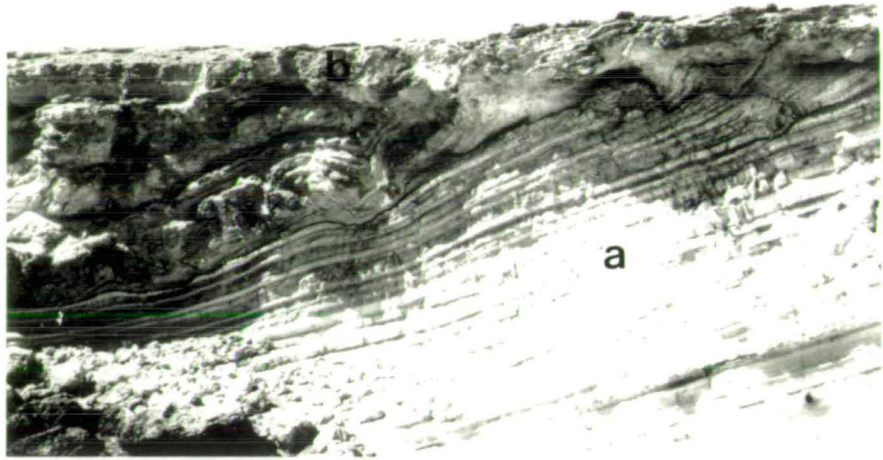
C - A veneer of the F3 marine sequence unconformably overlying the well bedded marls of Pliocene age (a) at Coral Bay, south-west Cyprus.

Note: the sequence is c.8-10m high.

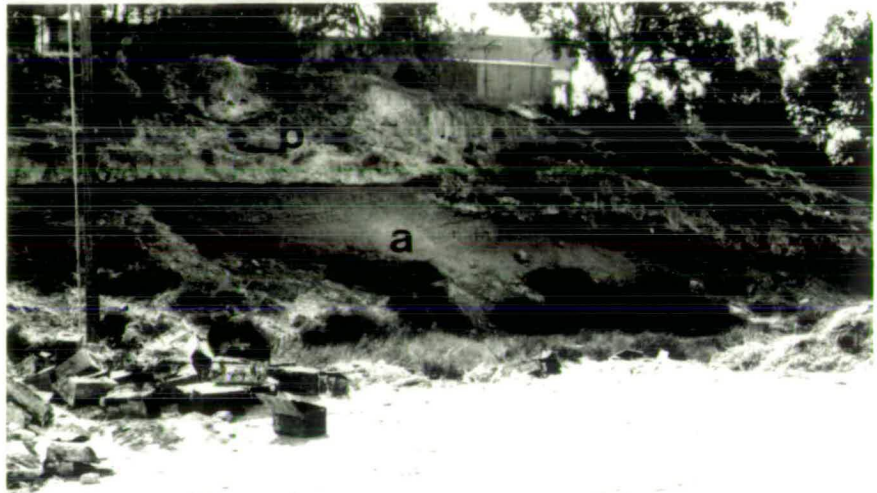


# Plate 7.5

**A**



**B**



**C**

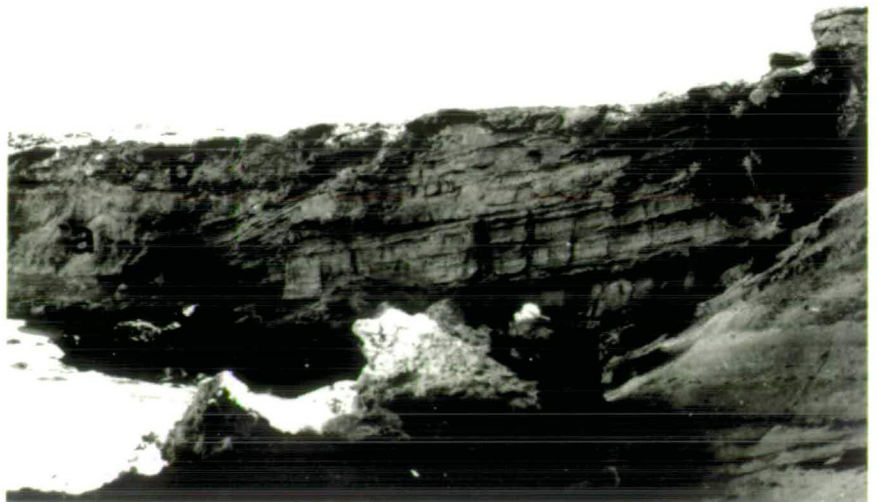


## PLATE 7.6.

All these views come from the F3-F4 carbonate sequence at Cape Greco (location 1-125).

A - A portion of the conglomeratic lag unit unconformably overlying marls of the Nicosia Formation (Pliocene).

B - A portion of the conglomeratic lag unit unconformably overlying the limestones of the Terra Formation (Miocene).

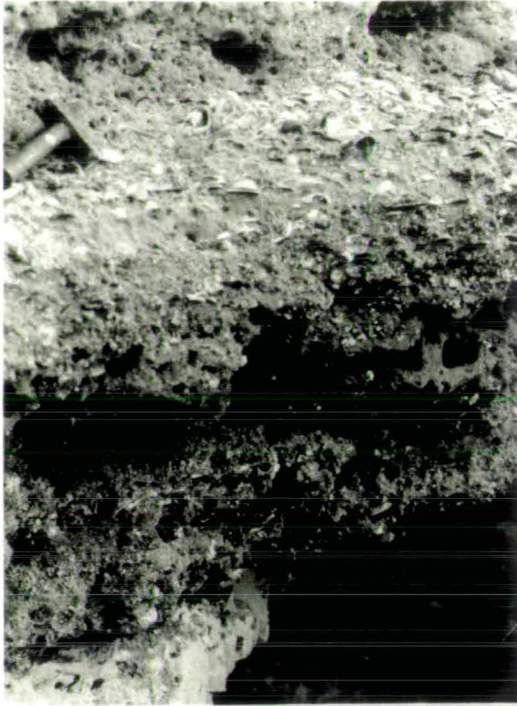
Note: lens cap for scale.

C - A coarse conglomerate lag (a) passes up into a coarse, shelly grainstone unit (b).

D - A portion of the very shelly grainstone unit, found above the conglomeratic lag, revealing whole and broken mollusc shells, heads of the coral *Cladocora caespitosa* and marl and limestone clasts derived from the underlying units of Pliocene and Miocene age.

# Plate 7.6

**A**



**B**



**C**



**D**

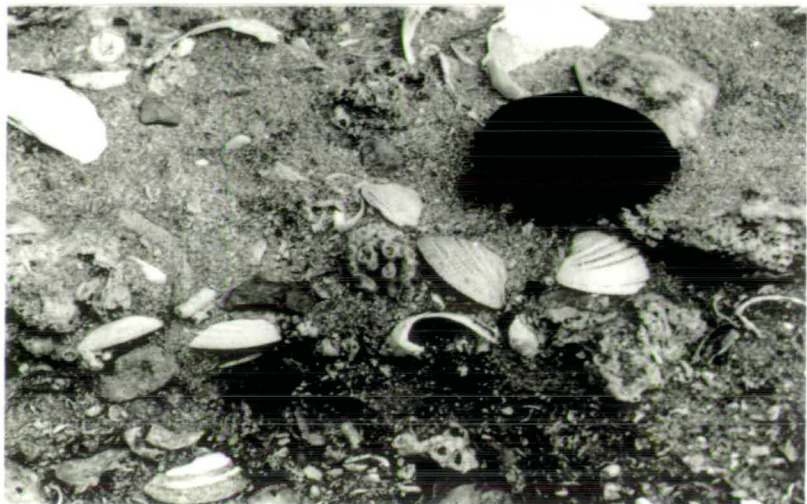


## **PLATE 7.7.**

All these views come from the F3-F4 carbonate sequence at Cape Greco (location 1-125).

A - The whole F3 sequence revealing: the unconformity and basal lag unit (a); the well bedded grainstone units (b); the caliche crust and overlying aeolian dunes (d); and the second conglomerate lag (c) which may be part of the F4 sequence.

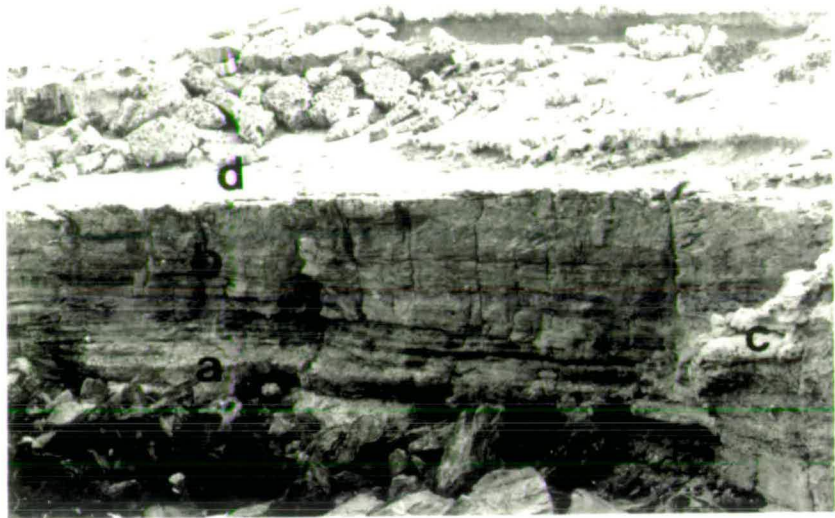
Note: the sequence is c.8m high.

B - A detailed view of a 2m section of the grainstone unit, overlain by a second lag unit (a), displaying festoon- and trough-cross-stratification.

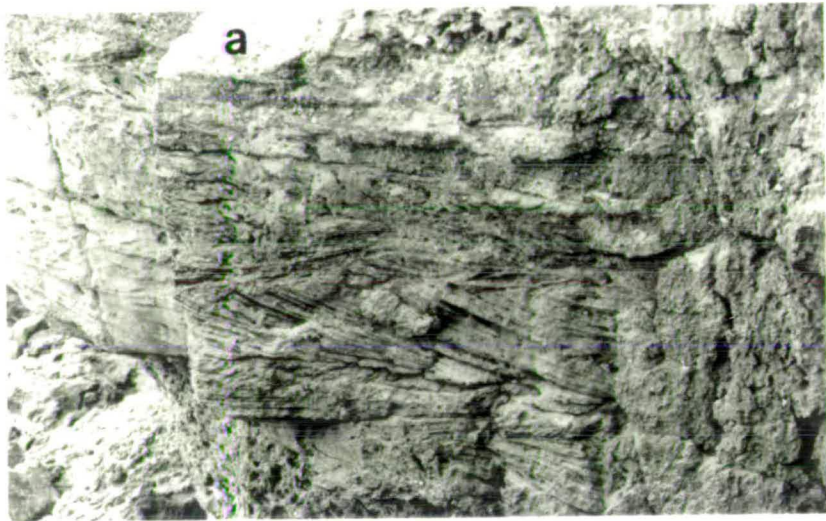
C - A detailed view of the grainstone sequence with: (a) massive coarse, shelly unit; (b) well laminated grainstones; (c) trough-cross-stratified grainstones; and (d) festoon-cross-stratified and vague planar bedded grainstones.

# Plate 7.7

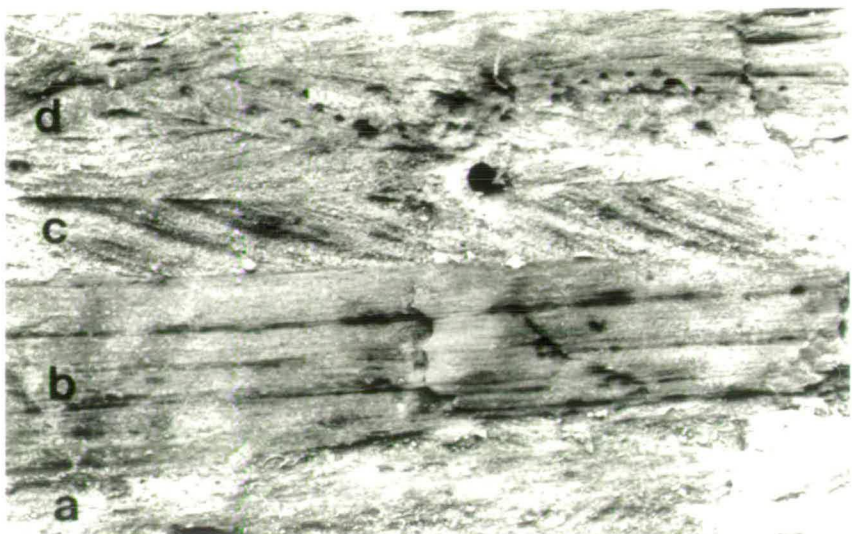
A



B



C



burrows appear to be of the form *Lithophaga sp.* (cf. Lindholm, 1987). A gradational contact marks the appearance of a massive, shelly, coralline unit, which contains a randomly orientated high diversity, high density population of molluscs, bryozoa, echinoid spines, coral and calcareous red algae (Plate 7.6). Local concentrations of bivalves are seen at Cape Greco (location 1-127). This unit is absent locally with the lag unit passing directly up into grainstone units.

ii) *Grainstone units*: these extremely shelly, well bedded, very coarse to medium grained grainstones have a total thickness of less than 5m thick and commonly grade up from the underlying conglomeratic unit (Plate 7.6). The grainstones display a great number of structures including parallel laminations, trough- and festoon-cross-stratification (Plates 7.7 and 7.8; Fig.7.7). Derived clasts are generally absent although whole, broken and abraded bivalve and gastropod shells are present. Small colonies of the coral *Cladocora caespitosa* are also present; these appear to be in death position. The grainstones are generally poorly cemented (Section 7.4.3). Some horizontal bioturbation is seen towards the top of the grainstone succession (Plate 7.8), although the extent of these structures is minimal, well-bedded grainstones are preserved throughout the succession. The grainstone units are locally graded, i.e. from very coarse to medium sands (Plate 7.8), and occasionally truncated, with a scoured contact between very coarse shelly sands and underlying medium grainstones (Plate 7.8). The variety of bedding characteristics probably represents different flow regimes, and in the case of the scoured contacts, possible storm events.

The grainstones locally pass up into a lag of derived clasts, e.g. cemented grainstone and Terra Limestones, and a second grainstone sequence, indicative of deposition of the F4 sedimentary sequence (Plate 7.7).

### 7.3.5.3 Larnaca.

The basic components of the sedimentary sequence at Larnaca are very similar to those seen in the Cape Greco area, with a basal lag passing up into coarse grainstone sequences (Figs.3.4 and 7.7), although packstones are present locally (location 1-130). The grainstones are generally massive, locally bioturbated and contain fragments of molluscs. The packstone, by contrast, contains a well preserved fauna, described previously by Moshkovitz (1968) and Pantazis (1966). Large colonies of the coral *C. caespitosa*, up to 1m in diameter, in life position (Plate 3.2), are present within the packstone units, as are bored and delicate mollusc shells, e.g. *Spondylus* shells with spine still attached, algal plates, echinoid plates and bryozoa. This packstone lies directly above a basal lag of mixed Troodos- and locally-derived clasts, e.g. chert, chalk, diabase, pillow

PLATE 7.8.

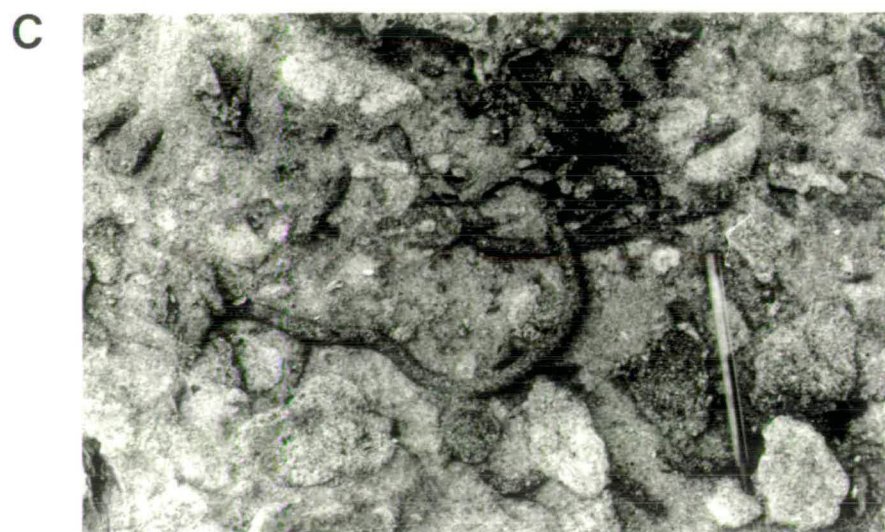
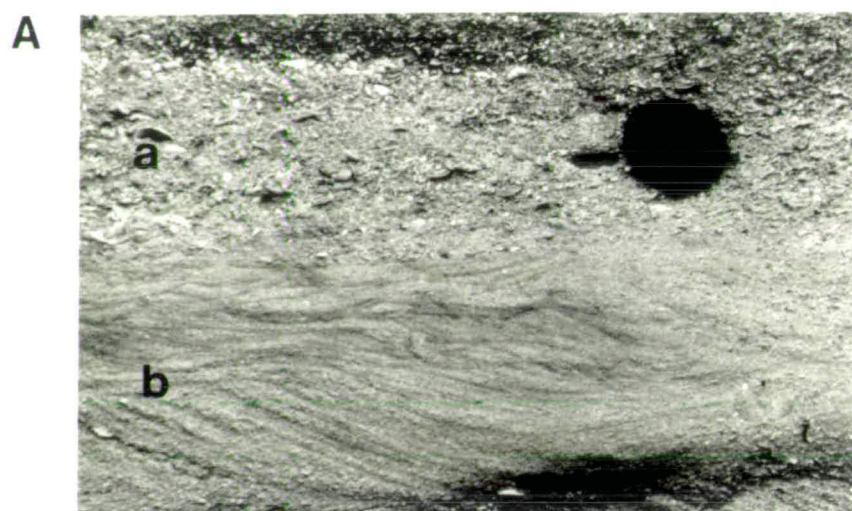
All these views come from the F3-F4 carbonate sequence at Cape Greco (location 1-125).

A - A truncated medium grainstone unit displaying festoon-cross-stratification (b), overlain by a coarse shelly grainstone (a).

B - A well bedded grainstone unit revealing graded-bedding with fining-up from very coarse to medium sands.

C - Horizontal burrows preserved in the grainstone units.

# Plate 7.8





lavas. The clasts within the lag are submature, less than 35cm in diameter and matrix-supported by silt. Thick shelled fossils, e.g. *Ostrea* and *Pecten*, are present within the basal lag unit. Small banks, less than 1m high exist at the base of the lag unit representing relief on the unconformity surface above the Athalassa Formation.

The grainstone and packstone units both pass up into a coarse conglomeratic unit, this unit is in contrast to that forming the basal lag as it better sorted and the clasts are rounded and discoidal in shape. This unit also contains a greater proportion of broken shells than seen lower in the succession and passes up into caliche horizons and massive fine windblown sands (Chapter 8; Gifford, 1978), that cover much of this terrace sequence in the area of the Larnaca Salt Lake.

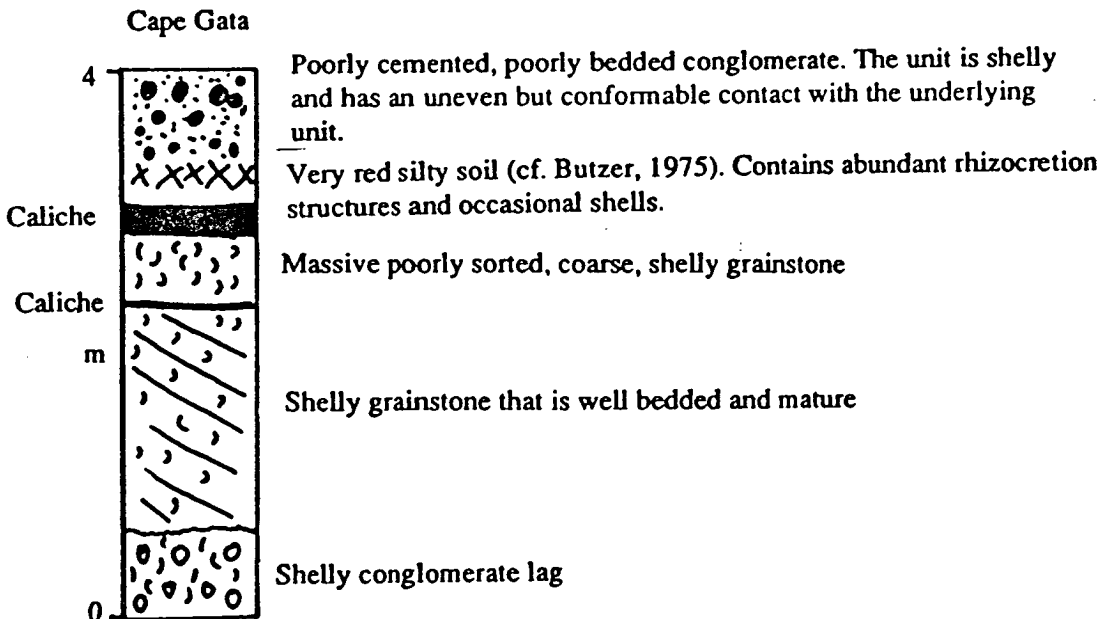
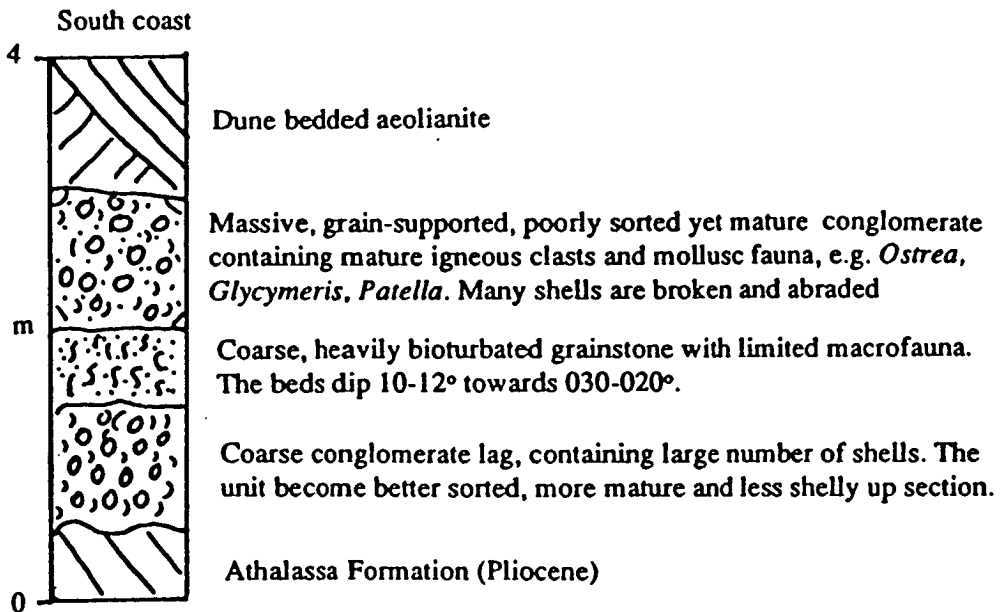
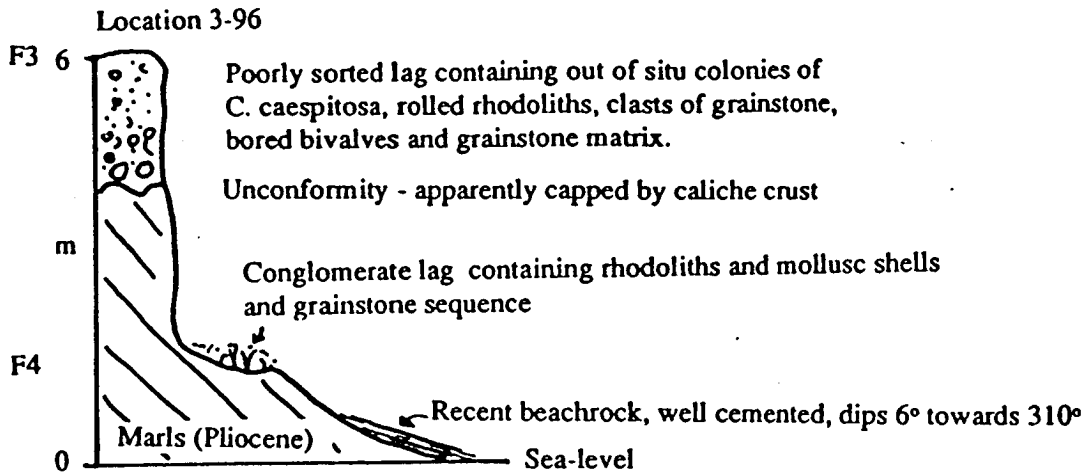
#### **7.3.5.4 Akrotiri Peninsula.**

Limited exposures of the F3 sequences are seen at Cape Gata (location 3-97) and Cape Zevgari (location 3-96) at the east and west end of the Akrotiri Peninsula, respectively. The sequence at Cape Zevgari lies unconformably above Neogene marls and crops out within 8m ASL. The present extent of the exposure is limited to a lag above the unconformity surface, which is capped by caliche. The lag is poorly sorted and contains clasts of marl and a mixed abraded fauna which includes rolled rhodoliths, reworked corals, bored bivalves and specimens of *Patella*. The matrix within the lag consists of a coarse grainstone. The preserved section at Cape Gata (location 3-97) displays three of the four units that are seen at Cape Greco (location 1-125). A conglomeratic lag passes up into a grainstone unit. The grainstone dips gently ( $8^{\circ}$ - $12^{\circ}$ ) seaward ( $350^{\circ}$ - $015^{\circ}$ ) and in turn passes up into caliche. At one site, solution hollows have been cut into the top of the grainstone unit and these have been infilled with grainstones at a later date. The infill has been capped by caliche. At Cape Gata the grainstones pass up into a thin caliche horizon (10cm thick) that, in turn, passes up into a massive, 50cm thick, poorly sorted grainstone (Fig.7.8) which is then capped by a second caliche horizon. A fine grained, red, silty horizon, displaying rhizcretion structures and rare mollusc shells lies above the second caliche horizon. This is overlain in turn, with an uneven contact, by a poorly bedded, coarse sand, containing Troodos- and local sedimentary-derived clasts and mollusc shells (Fig.7.8).

#### **7.3.5.5 West coast of Cyprus.**

The carbonate sequences along the west coast from Coral Bay to Lara Point form the most extensive F3 sequences cropping out around the southern coast of the island. This terrace is also found locally in the area to the north of Kissonerga. The Quaternary

Fig.7.8. Sketch sections and field sketches of the F3 and F4 sedimentary sequences that crop out on southern portion of the Akrotiri Peninsula (locations 3-96, 3-97 and 3-97a).

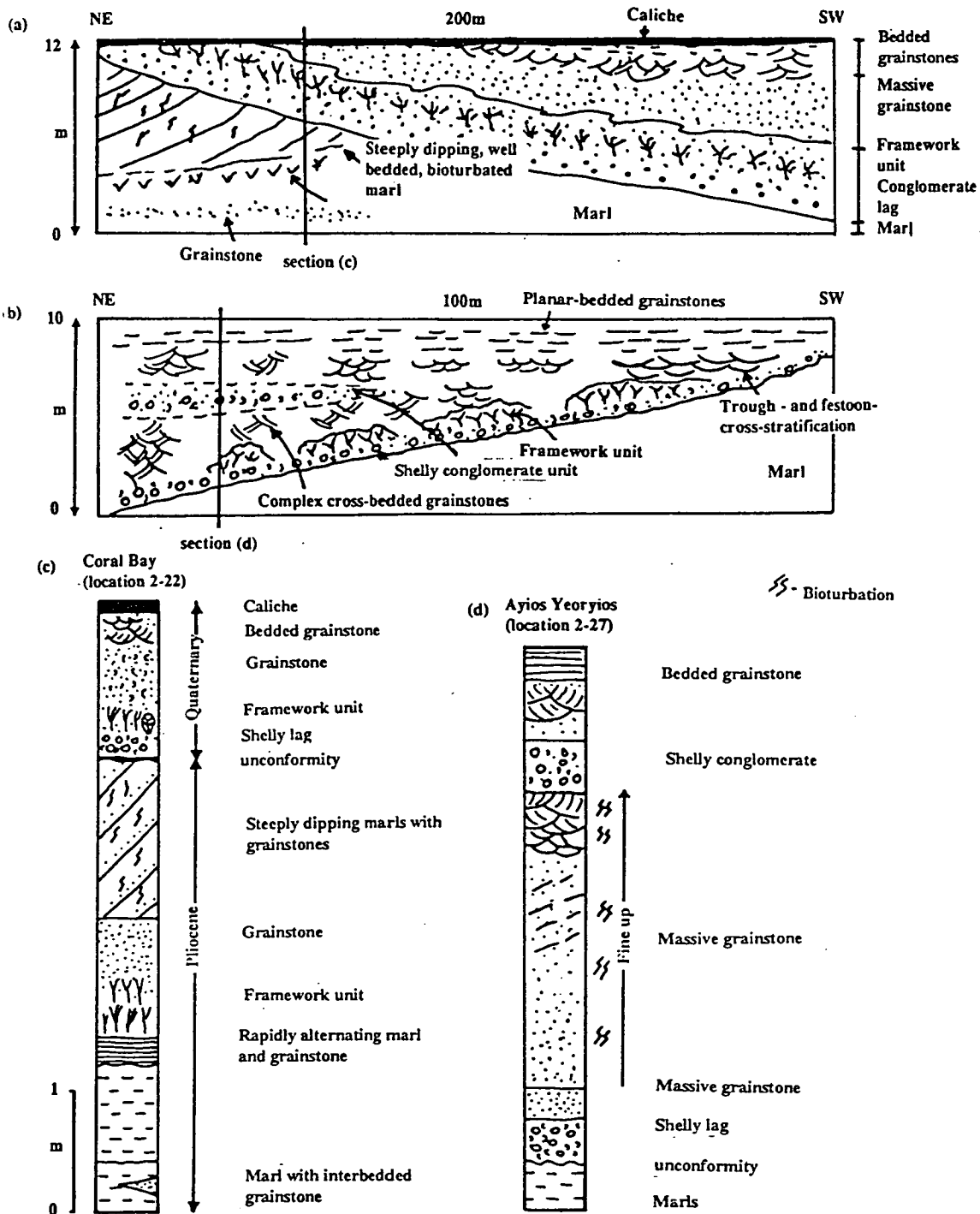


sequences crop out unconformably above marls, chalks and limestones of Pliocene and Miocene age. The marls of Pliocene age that crop out beneath the F3 sequence at Coral Bay (location 2-22; Fig.7.9; Plate 7.5) dip steeply-up to 40° to the north. The marls are occasionally interbedded with heavily bioturbated grainstone units which are preferentially cemented. Solitary corals, i.e. *Flabellum* and *Trochocyathus*, are present within the marl sequence. The sections in the Lara Point area (locations 2-30 and 2-34; Fig.7.10) shows some changes from the marl sequences seen in the Coral Bay area (locations 2-22 and 2-24; Fig.7.9). These marls differ from those seen at Coral Bay (location 2-22) as they are black, white, brown and grey-green in colour. The marls are generally well bedded and extensively bioturbated by 2cm wide vertical burrows, which are especially dense towards the top of the sequence (Fig.7.10); these are similar to those seen at Cape Greco (location 1-125). Conglomeratic clasts within the marl sequence include coarse, less than 20cm diameter, angular intraclasts of marl and mature, well sorted, fine gravels, less than 2cm diameter, containing discoidal clasts of derived serpentinite and Mamonia sediments. The top of the marl sequence is commonly crenulated and disturbed, Ayios Yeoryios (location 2-27; Fig.7.9; Plate 7.9).

The conglomeratic lags that mark the base of the F3 sedimentary sequence are generally mature to sub-mature, consisting of well rounded marl, serpentinite and Mamonia Complex sediment clasts, e.g. chert, sandstone and limestone, generally less than 40cm diameter. The conglomeratic lag lies above an unconformity surface that commonly displays moderate relief of typically 50-70cm. A coralline algal and coral framework is located either directly above the basal lag, or directly on the unconformity surface, similar to that seen in the F2 terrace in the Paphos area (location 2-5). The coral colonies at Coral Bay (location 2-22) are generally less than 60cm diameter and in life position attached to larger clasts of the lag and the underlying marls. The matrix associated with the coral and algal frames is very variable, from coarse to fine sand, massive and very shelly. The grainstone sequences that overlie both the basal lag and the framestones are very shelly with disorientated, thick-shelled molluscs, fragments of bryozoa, coral heads, algal plates and a coarse to very coarse sand matrix (locations 2-22 and 2-27). The massive grainstones pass up into more mature, better sorted, less bioturbated and structured grainstone units up section (Fig.7.9). Structures seen within the grainstone units include trough- and festoon-cross-stratification and seaward dipping, planar-bedded units (Fig.7.9; Plate 7.9). Sections to the south of Lara Point (location 2-30) show a slightly different pattern of sedimentation than is seen at Coral Bay (location 2-22) and Ayios Yeoryios (location 2-27), with mixed clastic and carbonate sequences (Fig.7.10) and the presence of intraformational conglomerates (e.g. location 2-30; Plate 7.10). The same basic components are present with a basal lag, some algal framebuilders,

**Fig.7.9. Section of the ?F3 sequences cropping out at Ayios Yeoryios (location 2-27) and the F3 terrace cropping out at Coral Bay (location 2-22).**

Note: a) is a north-east to south-west section from Coral Bay ,  
 b) is a north-east to south-west section from Ayios Yeoryios.



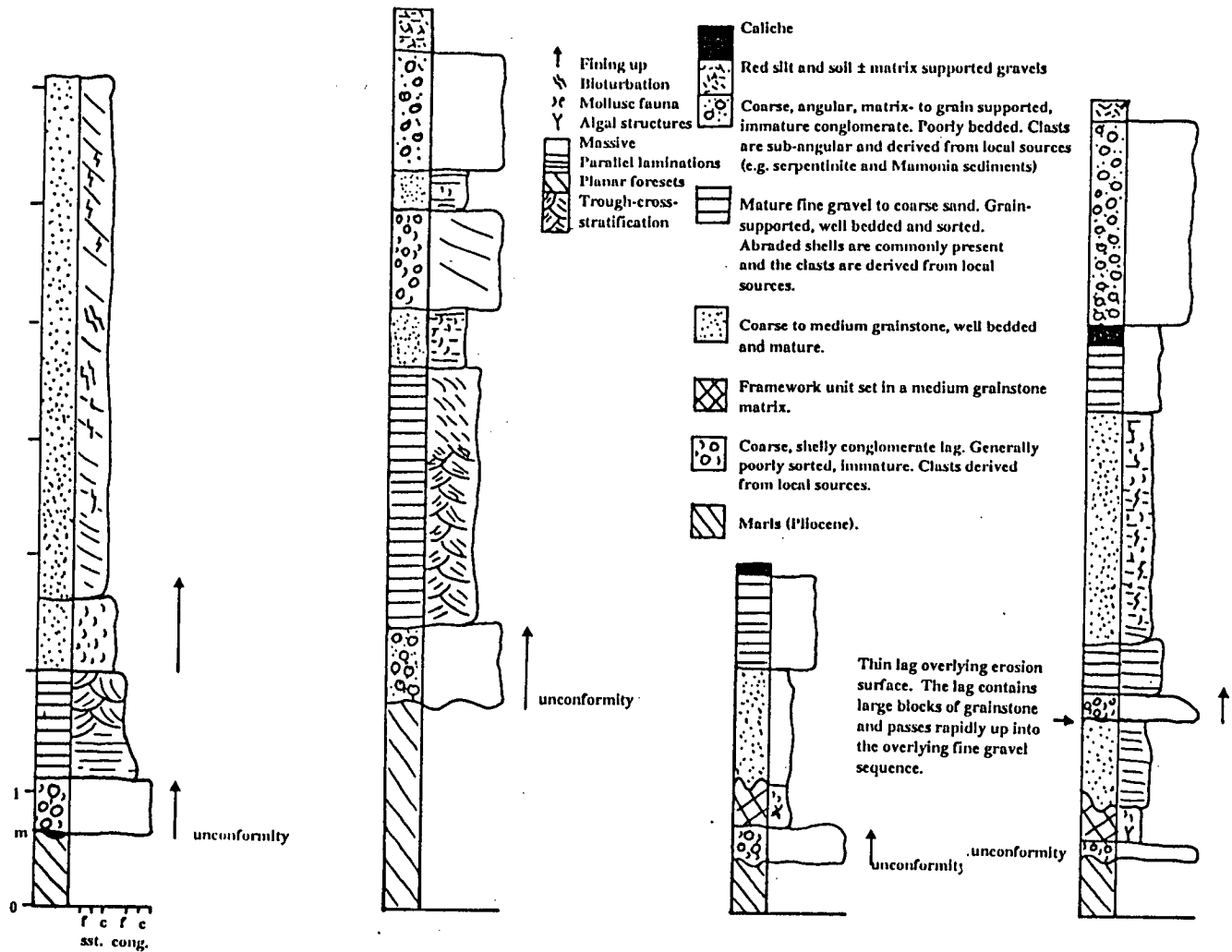


Fig. 7.10. Showing the relationship between the carbonate and siliciclastic F3 sequences that crop out in the area of Lara Point (location 2-30).

PLATE 7.9.

A - A view of the upper most portion of the marl sequence at Ayios Yeoryios (location 2-27) displaying well bedded (a) and then crenulated and disturbed marls as the erosion surface is reached. The marls are overlain, unconformably, by caliche, a thin conglomerate lag and very coarse cap of grainstone.

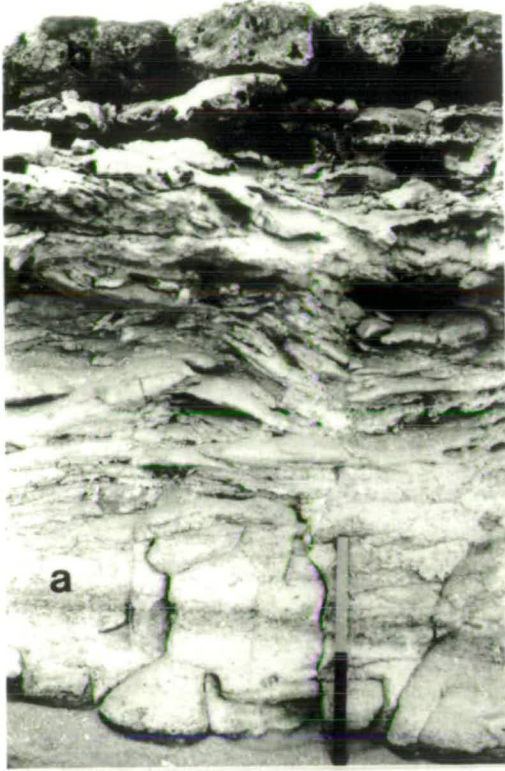
Note: scale is 50cm long.

B - A complex well bedded grainstone unit exposed in the ?F3 sequence at Ayios Yeoryios (location 2-27) displaying shallow and steeply, seaward, dipping cross-stratified and possibly trough-cross-stratified beds. Evidence for rhizocretion structures is present towards the top left of the plate.

C - Festoon-cross-stratification preserved in the ?F3 grainstone sequence at Ayios Yeoryios (location 2-27), viewed towards the east-north-east.

Plate 7.9

**A**



**B**



**C**



well bedded shelly sandstones and grainstones and evidence of bioturbation with deposition of fluvial conglomerates capping the sequence (Plate 7.10).

The probable F3 sequence at Ayios Yeoryios (location 2-27) differs from that seen at other localities, with possible evidence of progradation of the shoreline (Fig.7.9). This progradation has resulted in the deposition of a thicker grainstone unit to the southwest, above the coralline algal framework sequence.

### 7.3.5.6 The north coast between Polis and Kato Pyrgos.

The F3 carbonate sequences along the north coast of the island shows a lateral change to the east, away from the influence of the Polis-Paphos graben, where siliciclastic beach and deltaic sediments dominate (Chapter 6). This change results in the presence of mixed and then carbonate dominated sequences between Argaka and Kato Pyrgos (locations 3-109 and 3-110; Fig.7.11). Pillow lavas of the Troodos ophiolite underlie the F3 terrace throughout much of the area to the west of Polis, the relief on an unconformity surface dictating the extent of F3 deposition. The F3 terrace to the east of Polis, between Argaka and Yialia (location 3-109; Fig.7.11) displays a mixed siliciclastic and carbonate sequence. A coarse, generally immature, basal lag grades up into a mixed detrital and carbonate unit. This unit is well cemented and consists of coarse to fine graded gravels with clasts that are less than 7cm in diameter and carbonate sediments which include fragmented and, locally, whole shells and small *in situ* coral colonies. The conglomerates are sub-mature (0.6-0.7 roundness) and the shells are locally banked up against the unconformity surface. A gradational boundary marks the upward progression into a coarse, shelly grainstone unit. The grainstone contains a high diversity fauna of small whole and large fragmented shells. Detrital clasts are also present within the unit; these are well sorted, mature and less than 2cm diameter. The grainstone shows rough bedding, with locally good parallel lamination, dipping seaward at 10°-15°. Moldic porosity is seen throughout the grainstone unit. The grainstone is capped by caliche.

A cemented bank of well sorted, low diversity, high density bivalves and gastropods, e.g. *Natica* and *Glycymeris* - a shell "hash" - is seen topographically and stratigraphically above the grainstone unit. This unit is found within 50cm of the unconformity surface, towards the back of the palaeo-beach sequence (Fig.7.11).

A second section further east away from the influence of the Polis graben-derived clastic sediments is seen at Kato Pyrgos (location 3-110; Fig.7.11). The outcrop is limited by the extent of the relief on the pillow lava unconformity surface and the outcrop has not been greatly influenced by detritus from the Polis graben. The basal lag that lies



Fig.7.11. Sketch sections of the F3 age sedimentary successions that crop out in the area of: a) Kato Pyrgos (location 3-110); and b) Argaka (location 3-109), on the north coast of Cyprus.

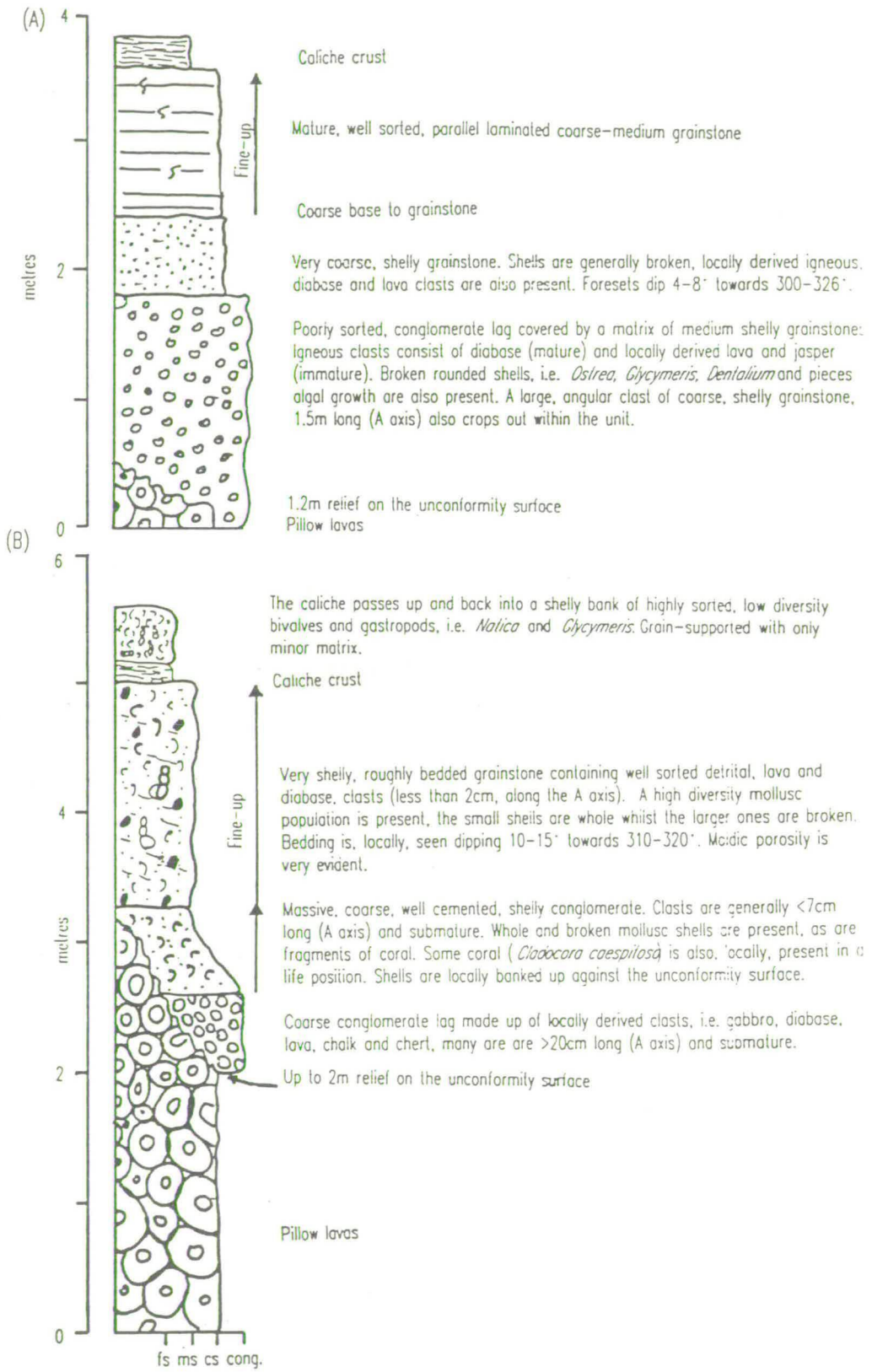


**PLATE 7.10.**

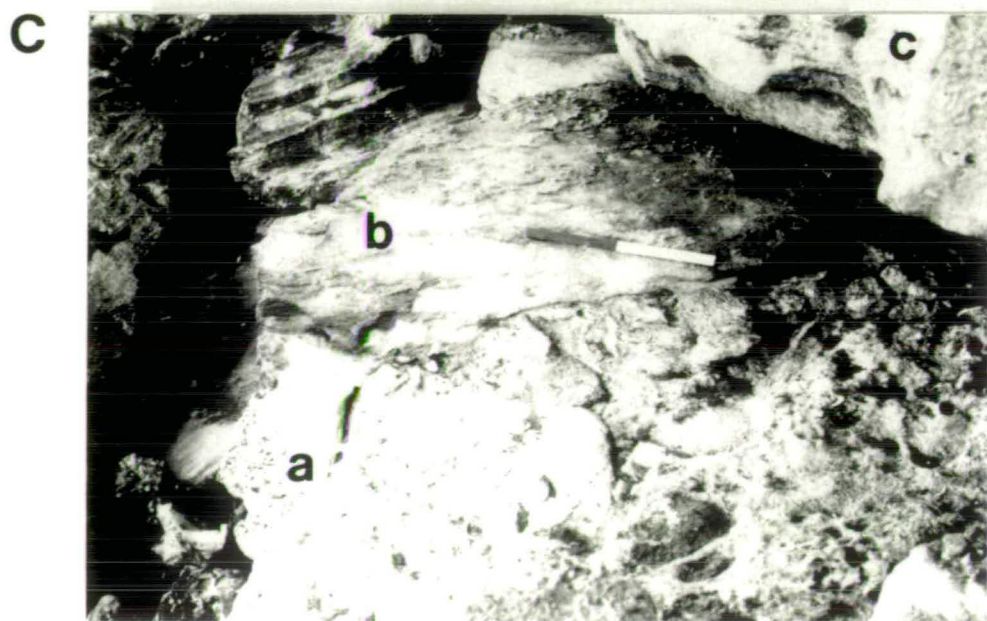
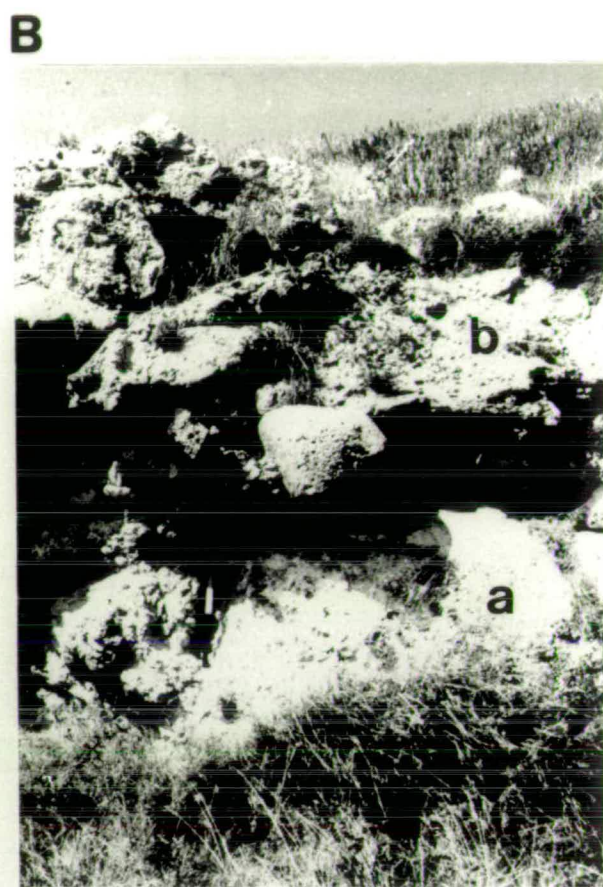
A - A sequence of bioturbated grainstones (a) which are capped by a caliche horizon and palaeosol (b); this in turn is succeeded by aeolianite (c), exposed in the F3 sequence at Lara (location 2-32).

B - An example of a grainstone sequence (a) being capped by coarse fluvial conglomerates (b) from the F4 sequence in Paphos (location 2-19).

C - A portion of the preserved sequence at Lara (location 2-30). The framework unit (a) is overlain by a coarse conglomerate lag, containing large clasts of grainstone (b); this is succeeded by a bedded grainstone sequence.

Note: scale is 50cm long.

# Plate 7.10



unconformably above the pillow lavas consists of well rounded diabase clasts, immature locally-derived pillow lava clasts and rounded and fragmented gastropods, bivalves, dentalium, algae and oysters. The lag is 0.20-1.2m thick and grain-supported. The matrix consists of a coarse shelly grainstone. The lag passes up, with a gradational contact, into coarse grainstone and detrital rich unit, with well sorted, mature clasts. This, in turn, passes up into coarse grainstone containing few whole shells fining-up to a medium grainstone, which is better sorted and bedded towards the top of the unit. Few whole shells are seen in this mature grainstone, which is well laminated, even though local vertical burrows, less than 1cm diameter, are present towards the top of the unit. The laminated unit dips seaward, i.e.  $300^{\circ}$ - $326^{\circ}$ , at  $4^{\circ}$ - $8^{\circ}$ . A thin, less than 30cm thick, caliche cap is seen towards the top of the unit.

The present-day beach sands in the area of Kato Pyrgos (location 3-110) consist of dark, Troodos-derived sands, contrasting those seen during the deposition of the F3 sequence.

#### **7.3.5.7 Deposition of F3 carbonate sediments on wave cut platforms.**

Limited exposures of F3 carbonate sequences are present on the gently seaward dipping wave cut platforms at Cape Pyla (location 1-136) and Lara Point (location 2-33). These exposures have a minimal lateral and vertical extent and are generally restricted to joints and solution hollows formed within the underlying lithologies, i.e. Miocene limestones, chert and chalks. The Quaternary units that crop out at Lara Point are dominated by locally derived angular to rounded chert and chalk clasts, commonly 0.7-1.0m diameter, that are found in association with abundant mollusc shell, a sand matrix and caliche (Plate 7.11). Minor brown-red grainstones associated with colonies of coral (*C. caespitosa*), coralline red algae and molluscan shells are also present. These coarse sands are poorly sorted and well cemented.

### **7.3.6 The F4 carbonate sequences (late Late Pleistocene).**

#### **7.3.6.1 Introduction.**

The base of the F4 sequence is only rarely exposed, as it commonly forms a platform within 3m ASL today. The exception to this is in south-east Cyprus where it lies unconformably above: the Paralimni Melange, limestones of the Terra Member, marls of Nicosia Formation. The F4 sequences also crop out above earlier Quaternary sequences at Cape Greco (location 1-125; Fig.3.8), where the F4 terrace is seen cropping out unconformably above the F3 terrace; and at Dhekelia (locations 2-76 and 2-84), where

**PLATE 7.11.**

**A -** Locally derived, angular to rounded, clasts filling solution hollows in the F3 terrace at Lara Point (location 2-33); this chaotic conglomerate has a sandy matrix and has been calichified.

Note: the length of the plate is equivalent to c.1.5m.

**B -** Coarse mature conglomerates overlain by an aeolianite unit in the F4 sequence at Dhekelia (location 2-76).

Note: the scale is 50cm long.

**C -** A view of the whole of the exposed sequence in the F4 terrace at Dhekelia (location 2-76).

Note: the large mounds in the foreground are coral colonies  
the scale is 50cm long.

Plate 7.11

A



B



C



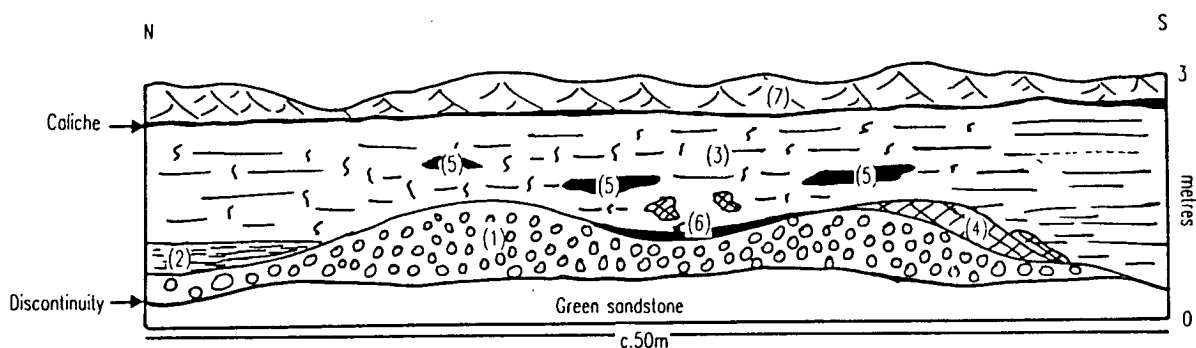
the F4 littoral sequence crops out unconformably above marls of Pliocene age and ?Quaternary mature sands (Chapter 6; Figs.3.4 and 7.12). The exposed sequences are generally less than 2m thick. An exception to this occurs at Cape Greco (location 1-125; Figs.3.4, 3.8 and 7.7) and Paralimni (location 3-50; Fig.3.4). The basic components, outlined previously (Section 7.3.5) for the F3 littoral sequences, are all present in the F4 exposures. F4 sequences in south-east Cyprus at Dhekelia and Cape Greco, Akrotiri and the Paphos area are described below.

### 7.3.6.2 South-east Cyprus.

*i) Cape Greco to the south of Famagusta:* the exposed basal conglomeratic lag at Cape Greco contains solely locally derived clasts, e.g. marls, limestones as well as grainstones derived from the ?F3 terrace. A more diverse clast assemblage, e.g. Troodos-derived and local sediment clasts, is seen further north, to the south of Famagusta for which there are three possible explanations. These are the influence of the drainage system issuing out through Famagusta, at this time (Chapter 2), the presence of Troodos-derived clasts in the Paralimni Melange, the presence of locally exposed basement in this area. The lag passes up into the coral and algae facies and then grainstone units. These are succeeded by caliche, dunes and evidence of later weathering and the formation of solution hollows (Chapters 2, 8 and 9). A thin (5-10cm), cemented, shelly horizon similar to that seen capping the F3 sequence in the Polis area (location 3-109) crops out, locally, at the top of the grainstones towards the base of the palaeo-cliffline of the F4 sequence at Cape Greco (location 1-125).

The F4 sequences within 2-3m ASL to the north of Protaras (location 1-120) have a knobbly appearance, similar to those seen on the coast to the north of Paphos, in the Cape Greco area (location 1-125) and on the south coast of the Akrotiri Peninsula (location 3-96a). These units resemble facies RB3 described by McCallum (1989) from Petounda Point (location 3-11). Fine to medium grainstones that characterise these units are supplemented by the presence of cobbles and pebbles of locally-derived Quaternary lithoclasts and older sedimentary and igneous clasts. Numerous calcitic serpulid worm tubes are also present, as are bored molluscan shells and calcareous algae. These units commonly have a knobbly appearance, some with solution hollows on exposed surfaces (Chapter 2) and local evidence of subsequent infilling by sediment and fossils, especially the gastropod, *Astraea rugosa* (location 1-247; Plate 7.13). McCallum (1989) interpreted the unit at Petounda Point as representing a fossil trottoir, an organically produced calcareous crust that forms in the intertidal and uppermost subtidal zone on rocky shorelines in warm climates (Pérès, 1967). The fauna within trottoirs is dominated by long, uncoiled, vermetid gastropods, calcareous algae and serpulid worms, which

**Fig.7.12. Field sketch of the sediment relations in the F4 carbonate sequence cropping out at Dhekelia (location 2-76).**



(1) Coarse, well cemented, mature conglomerates; these conglomerates are made up of spherical (<16cm long, A axis) lava, diabase, chert and chalk clasts. The unit dips 8-10° towards 160°, clasts are imbricated parallel to 160°. The unit has a sandy matrix. A low diversity, high density mollusc population is present, although there is no evidence of whole shells.

(2) Fine well cemented, very shelly, grain-supported gravel. This unit contains many broken mollusc shells, high density, low diversity population, has a limited lateral extent and dips at between 4-8° towards 207°. The beds are c.5cm thick. The unit coarsens up into a medium conglomerate. Unevenly overlain by grainstone, i.e. unit 3.

(3) Medium, well sorted, mature, planar laminated grainstones. This unit thickens to the south and dips at 10-18° towards 220-230°. The unit appears to have stifled the growth of the coral colonies of unit 4. The unit is locally heavily bioturbated, 70-90% of the unit in some places. Burrows and shells with the unit are finer and more delicate to the north becoming increasingly larger and more robust further south.

(4) Coral colonies in life position. The colonies are up to 2.3m in diameter and nucleated to the underlying conglomerate unit and/or mollusc shells. A high diversity delicate mollusc population is associated with the colonies.

(5) Shelly conglomeratic unit. Mature, well sorted brown and whole shelled, fine-medium conglomerate. There is no apparent discontinuity between this conglomerate unit and the surrounding medium sands.

(6) Fine gravel; this unit is found in the areas of low relief above unit 1 and consists of poorly sorted broken shells, coral fragments, as well as clasts of lava, diabase, chert and chalk. The unit is massive, unbioturbated and grades up into medium sands, i.e. unit 3.

(7) Steeply dipping (<36°) medium and fine aeolian sands; these dip to the north, overlie the caliche and contain abundant rhizcretion structures.



contribute to the formation of cemented carbonate platforms, commonly 20cm thick (Safreil, 1966). It is interesting to note that evidence for three horizons, with characteristics resembling that described above, are present within the ?F3-F4 coastal sequence at Cape Greco (location 1-125). Lithoclasts of bound serpulid burrowed grainstone units are found in the lag sequence above the marls of Pliocene age, i.e. the base of the ?F3 sequence. Similar clasts are also present within the basal lag separating the ?F3 and F4 sequence and a surface similar to that described above is present above the F4 sequence.

*ii) Dhekelia:* the F4 carbonate sequences in the Dhekelia area contrast the shallow water sequences that were deposited in this area during the rest of Quaternary (Chapter 6) with the first development of carbonate-rich facies. The sequences display the four major facies, described previously, i.e. a conglomerate lag, coral framework structures, medium-coarse sand grade grainstones and evidence of sub-aerial sedimentation with fluvial, dune and caliche sequences. Rapid facies changes are seen both vertically and laterally, and extensive relief is associated with the unconformity surface between the marls of Pliocene age, ?Quaternary sands and the F4 Quaternary sequence. The sequence seen on the coast at Dhekelia (locations 2-76 and 2-84; Fig. 7.12; Plate 7.11) contains a mixed, buff-brown coloured grainstone sequence that displays planar laminated beds, passing up into extensively bioturbated units. These are overlain by coarse conglomerates at coastal exposures and a carbonate aeolianite sequence, dipping at 30° towards the north, inland. The carbonate grainstones show less evidence for the presence of detrital sands inland. The F4 grainstones differ from the grainstones of the Athalassa Formation (Pliocene) by being:

- i) generally coarser,
- ii) less mature,
- iii) buff-brown rather than yellow in colour,
- iv) less well cemented and having a reduced moldic porosity.

The corals found in Dhekelia (location 2-76) form the largest colonies seen, i.e. up to 2.3m in diameter (Plate 3.1). The larger coral colonies are attached to the seaward side of the underlying conglomerate, whereas the smaller colonies are found nucleating on shells and individual conglomerate clasts (Plate 7.13). Some of the small colonies (generally less than 40cm diameter) are simply attached to the grainstone substrata.

### **7.3.6.3 Akrotiri.**

The F4 carbonate sequences on the Akrotiri Peninsula are best exposed at Cape Zevgari (location 3-96) and on the south coast of the peninsula (location 3-96a). On the

north side of Cape Zevgari the unconformity surface above the Athalassa Formation passes up into an immature lag that matures upwards with well sorted, 1-2cm size, discoidal clasts being seen towards the top of the unit. The unit is highly fossiliferous at the base with the proportion of macrofossils decreasing up through the unit. The coarse grainstones that lie above the lag deposit are well bedded, dipping between  $10^{\circ}$ - $12^{\circ}$  towards  $020^{\circ}$ - $030^{\circ}$ , i.e. offshore. This unit displays local horizontal bioturbation. Aeolianites lie above the grainstone unit (Fig.7.8). Shelly conglomerates are also seen onlapping unconformably over the F4 carbonate and Athalassa Formation sequences. These shelly conglomerates contrast with the F4 lithologies by having a high clastic input derived from the Troodos ophiolite, i.e. with a high proportion of gabbro clasts. The igneous clasts are mature. Blocks of well laminated grainstones are also present within this unit. The conglomerate is grain-supported, mature but generally poorly sorted; specimens of *Patella* and a large number of abraded, thick mollusc shells, e.g. *Glycymeris* and *Ostrea*, are also present as a high density, low diversity fauna.

Sections of the F4 carbonate sequence along the south coast of the Akrotiri Peninsula (location 3-96a) have a limited vertical extent. These sequences lie unconformably above a variable shelly grainstone and marl sequence (Fig.7.8; Plate 7.12). The basal F4 unit contains blocks of well cemented, derived grainstones, containing corals. Troodos-derived clasts are also found within this unit, contrasting with the lack of Troodos-derived clasts within the Recent beach sequences. Coralline algae and coral frameworks are also present directly on the unconformity surface. A basal unit passes up into a grainstone unit that has a minimal detrital input and a dense, low diversity *Glycymeris* fauna, commonly found as *in situ* nestling patches (Plate 7.12). Extensive coastal dune formation took place after the deposition of the grainstone units (Chapter 8).

#### 7.3.6.4 Paphos.

The F4 carbonate sequence in the Kato Paphos area form a series of exposures within 3m ASL (locations 2-4 and 2-11; Fig.7.13). The four basic facies described previously are present within these units. The lag within the F4 units contains mainly reworked marls derived from the well bedded marls present beneath the unconformity surface and blocks of Quaternary grainstones reworked into position. The clasts are commonly spherical, less than 50cm diameter and submature, although some blocks of derived grainstones up to 1m diameter are present. Coral, rhodoliths, coralline red algae, serpulid worm tube and a high diversity, thick shelled, molluscan population, including *Pecten*, *Ostrea*, *Conus*, *Strombus*, *Barbatia*, *Glycymeris* and *Astraea*, are all present within the basal lag unit. These are all abraded, indicating reworking and a death

Fig. 7.13. Sketch sections of the F4 sequences developed throughout southern Cyprus.

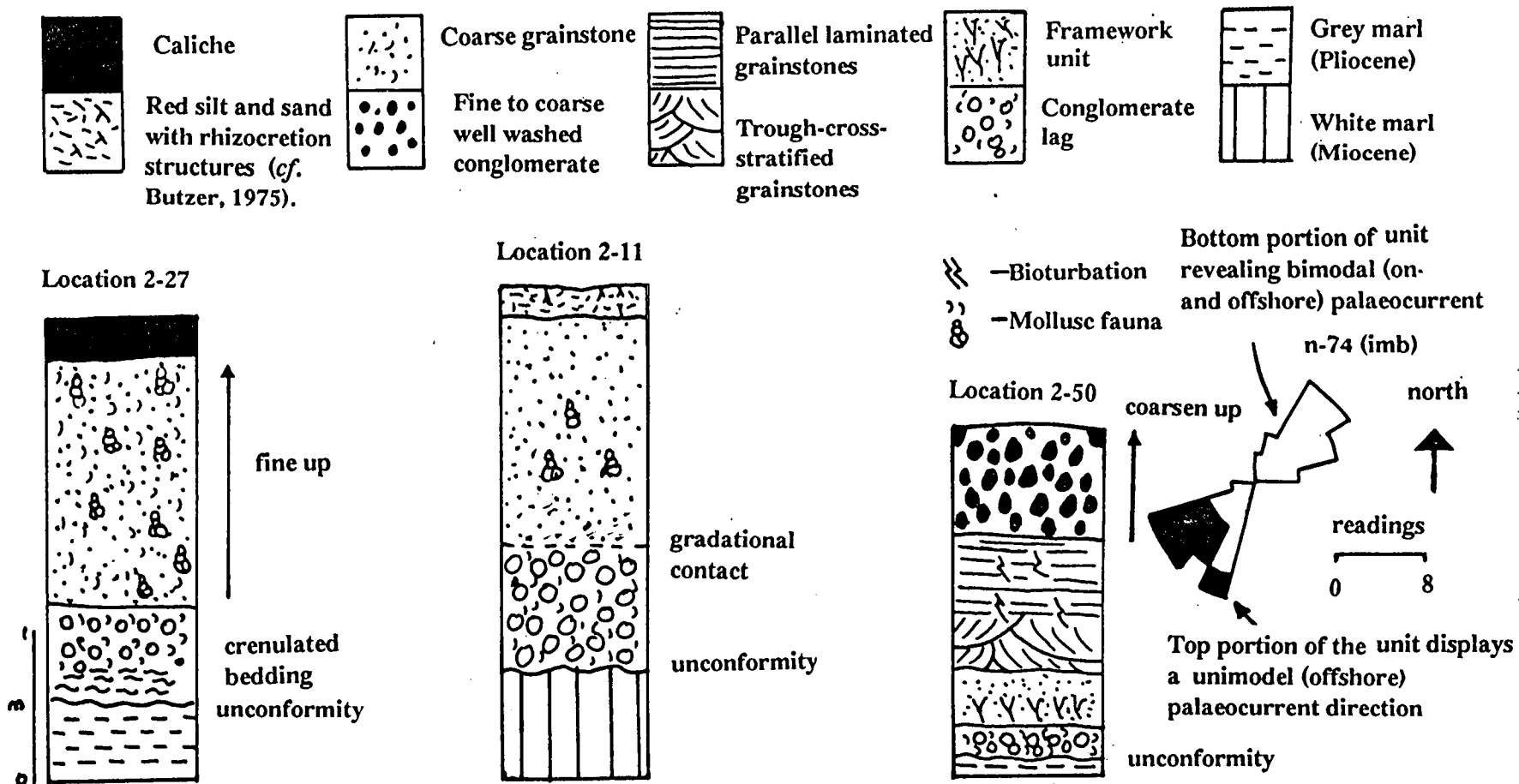


PLATE 7.12.

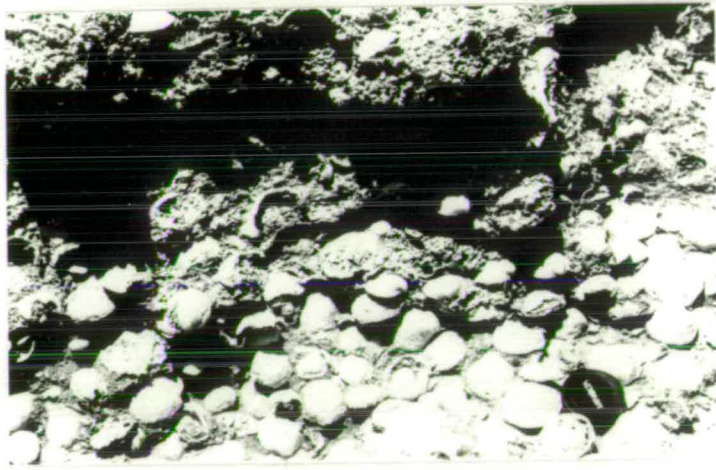
- A - Articulated *Pecten* shells in the top most portion of the Athalassa Formation beneath the F4 terrace on the Akrotiri Peninsula (location 3-97).
- B - A nestling patch of *in situ* high density, low diversity, *Glycymeris* shells in the grainstone unit of the F4 sequence on Akrotiri Peninsula (location 3-97).
- C - Arrow indicating the presence of moldic porosity within the F3/F4 carbonate sequence at Protaras (location 2-100).

# Plate 7.12

A



B



C

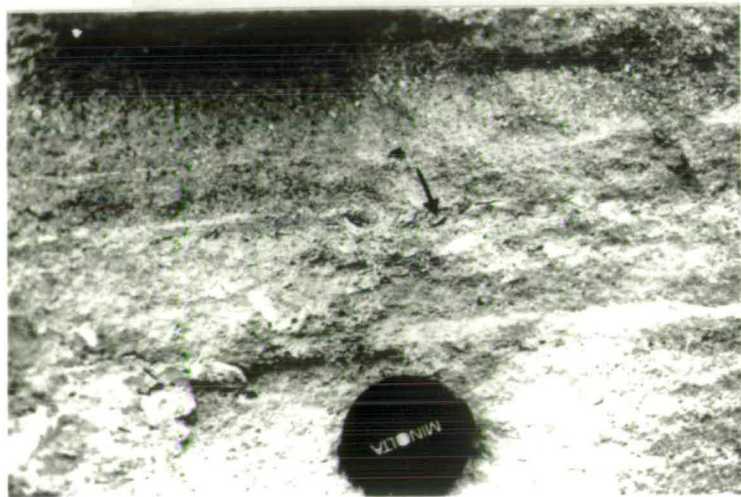


### **PLATE 7.13.**

A - A solution hollow on the F4 terrace at Kissonerga (location 1-247) filled a high density, low diversity fauna dominated by the gastropod *Astraea rugosa*.

B - A small colony of *Cladocora caespitosa* nucleating on a bivalve in the F4 sequence at Dhekelia (location 2-76).

C - A thin section micrograph displaying the development of micrite and pisolitic caliche in the F3/F4 carbonate sequence at Protaras (location 2-100; sample 721).

Note: the field of view is 5mm long.

D - A thin section micrograph of part of the F3 terrace sequence from Larnaca (location 1-130; sample 617) revealing a portion of the coral *Cladocora caespitosa* encrusted by coralline algae (brown).

Note: the field of view is 12mm long.

E - A thin section micrograph of the basal section of the F1 sequence above Paphos (location 2-3) displaying a large number of derived *Lepidocyclina* tests.

Note: the field of view is 8mm.

Plate 7.13

A



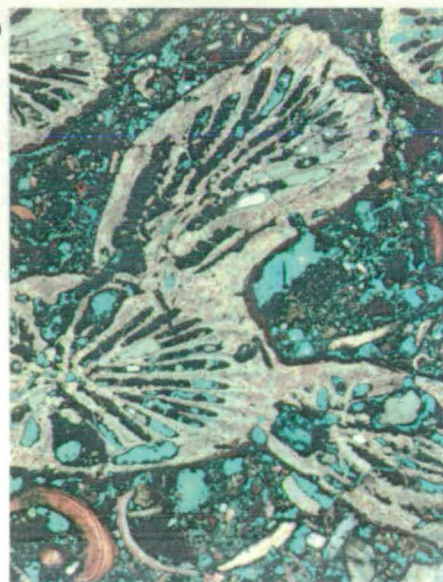
B



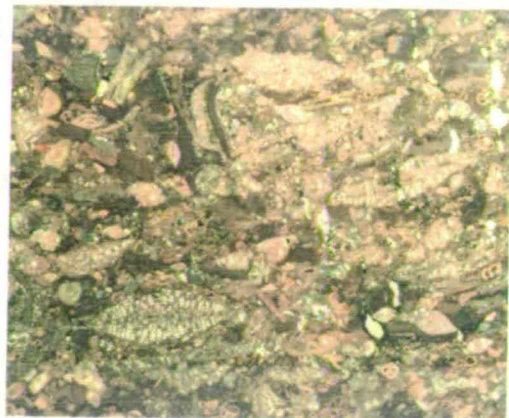
C



D



E



position. The grainstone that succeeds the lag is generally of coarse to medium sand grade, poorly sorted and poorly bedded. Whole and abraded molluscan shells are present within this unit, with local pockets of the gastropod, *Astraea rugosa*. The bivalve *Patella* also occurs locally. A red silty-fine sand unit caps the grainstone; this contains an associated fauna of low diversity gastropod, i.e. *A. rugosa*. Similar sediments are found in solution hollows to the north of Paphos (location 1-247).

Mixed carbonate and siliciclastic sequences are present in the area to the north of Paphos (location 2-19) where a small river channel continues to cut down to the sea today. The F4 carbonate sequence (Fig.7.13) passes up from a coralline red algal framework with an associated robust fauna, dominated by the gastropod *A. rugosa*, into well bedded, parallel laminated, coarse grainstones. This grainstone, in turn, passes up into a mixed unit containing a high proportion of poorly sorted, submature clasts and mixed lithologies, e.g. serpentinite, chalk and calcarenite. A sharp, but irregular, contact marks the introduction of angular, poorly sorted and well cemented conglomeratic beds above the mixed unit. A more recent (post F4) well cemented beachrock lies unconformably above a portion of this F4 sequence, close to the present day sea-level. Mixed carbonate and siliciclastic sequences are also present in the area to the east of Paphos, e.g. near Paphos Airport (location 2-50). The F4 crops out 1.7m ASL with a very shelly coarse lag containing coral, algal and mollusc remains lying unconformably above marls of Neogene age (Fig.7.13). The only coarse conglomerate is seen at the base of the F4 unit where locally derived clasts of marl and further travelled igneous and sedimentary clasts, e.g. diabase, pillow lava, chalk and chert, are present. The shelly, conglomeratic lag unit passes up, conformably, into a mature, well bedded, centimetre thick, coarse grainstone. Shell fragments are present within the grainstone unit and bioturbation is seen towards the top of the sequence. Planar beds dipping at  $12^{\circ}$ - $16^{\circ}$  towards  $200^{\circ}$ - $230^{\circ}$ , i.e. offshore, pass up into trough- and festoon-cross-bedded grainstones. The grainstone unit passes up into a conglomeratic unit that grades up from fine, well sorted conglomerate with dominantly well sorted, discoidal clasts, into a coarser submature, less well sorted conglomerate. The conglomerate unit is grain-supported and well washed throughout. Imbrication data indicate a bimodal palaeocurrent direction for the lower conglomerates, parallel with the trend of the planar-bedded grainstones of this sequence (Fig.7.13), and a unimodal offshore component for the top part of the conglomerate sequence (Fig.7.13). A more recent, well cemented beachrock containing blocks of grainstones derived from the F4 terrace is seen lying unconformably above the F4 terrace. This unit also crops out in solution hollows found within the topmost portion of the underlying F4 terrace, similar to that seen in the more recent beachrock terrace at Cape Zevgari on the Akrotiri Peninsula (location 3-96). The clasts



within this beachrock unit have a similar provenance to that seen in the F4 terrace, e.g. chalk, chert, diabase and lava clasts.

Limited F4 carbonate sequences are also found associated with the wave-cut platform at Cape Pyla (location 1-136). The sediments, restricted to joints in the limestone consist of a coarse well cemented grainstone and a locally-derived, immature, conglomerate unit, similar to that seen in the F3 at Lara Point (location 2-33). Thick oysters, i.e. *Ostrea edulis*, cemented to each other and the underlying limestones are present. The unit is generally red in colour and capped by caliche.

### **7.3.7 Summary of the components of the carbonate sequences.**

In summary, it has been shown in the preceding sections (Sections 7.3.2 to 7.3.6.4) that the F1, F2, F3 and F4 carbonate sequences that crop out throughout southern Cyprus display the same broad characteristics, although the sequences do vary locally. The attributes common to most of the carbonate sequences in southern Cyprus are, from base to top:

- i) an unconformable contact with older sedimentary and igneous sequences,
- ii) a coarse conglomeratic lag made up of predominantly locally-derived clasts and a reworked abraded fauna,
- iii) a framework unit of delicate branching and rhodolithic coralline algae and/or small colonies of the coral *C. caespitosa*. A rich mixed fauna is associated with the framework structures,
- iv) very coarse to medium sand grade grainstone units, displaying a variety of sedimentary structures, e.g. festoon- and trough-cross stratification, bioturbation and local rhizcretion structures,
- v) evidence for sub-aerial exposure, i.e. caliche and palaeosols (Chapter 9) and/or deposition aeolian sequences (Chapter 8).

## **7.4 PETROLOGY AND DIAGENESIS.**

### **7.4.1 Introduction.**

The petrographic study of the carbonate terrace sequences had a fourfold aim:

- i) to study the differences recognised in the field at a microscopic scale,
- ii) to ascertain whether any major petrographic variations exist between the carbonate terraces of different ages, e.g. F0-F4, and at different locations, e.g. Paphos compared to Cape Greco,

- iii) to determine the diagenetic history of the carbonate littoral units and to discern whether the pattern of diagenesis has varied between the lithification of the F0 and F4 terraces,
- iv) to ascertain whether there are any major difference between the carbonate aeolian and littoral grainstone sequences on a petrographic scale (this will be described and discussed in Chapter 8).

#### **7.4.2 Petrographic analysis of the carbonate littoral and sub-littoral sequences.**

Representative suites of samples collected from the F3 and F4 sequences at Cape Greco and Paralimni were sectioned to allow the facies variations recorded in field to be examined in thin section. Point count data from the sections are shown in Tables 7.1 and 7.2.

The suite of specimens from the Protaras area (location 2-100; Fig.7.14) reveals a basal section that coarsens up from a well sorted, submature unit, containing grains less than 1mm in diameter, into a coarse shelly unit. The proportion of detrital clasts, i.e. limestone and marls, decreases up section as the proportion of red algae, shells, pore filling cement, moldic porosity and calcitization increase. This coarse grainstone is succeeded by the development of a fine pisolitic micrite (Plate 7.13). This is, in turn, succeeded by a shelly poorly sorted grainstone that contains a number of lithoclasts from the underlying units, coral heads, red algal fragments, micrite fringes and calcitized shells. Detrital clasts are also present within this unit. These are 5mm in diameter at the base of the section and decrease in size up the unit. The sections at Cape Greco (location 1-125) show a similar pattern with coarse poorly sorted, immature, shelly and detrital grainstone passing up into mature grainstones, with grains generally less than 0.5mm in diameter. These, in turn, are succeeded by coarse, poorly sorted grainstone that contain lithoclasts derived from the underlying units, as well as clasts derived from the local pre-Quaternary sequences, i.e. marls and limestones. This higher unit also contains a combination of well preserved and radically altered shell structures. A mature well sorted grainstone succeeds the formation of the poorly sorted grainstone unit. The mature grainstone is composed of mature carbonate grains less than 0.5mm in diameter. These successions reflect that seen in the field (Section 7.3; Fig.7.7).

The samples collected from the F4 sequence at Dhekelia have a higher proportion of igneous-derived detritus, i.e. derived from the Troodos Massif and the Troulli Inlier, than seen in the sections at Cape Greco and Protaras. The proportion of allochems in the grainstone units (sample 601), but not the lag unit (sample 603), at Dhekelia, e.g. mollusc shells, algal fragments, coral heads, echinoid fragments and benthic and planktonic

**Fig.7.14. Logged section of the small quarry cut into the F3/F4 carbonate sequence at Protoras (location 2-100).**

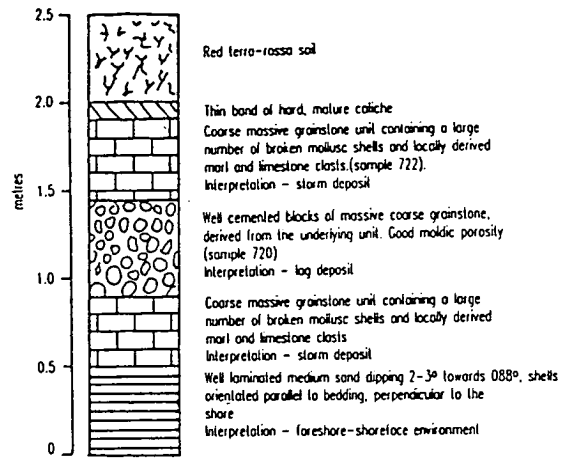


**Fig.7.15. A sketch illustrating the different ways in which an original aragonite skeleton may be altered during meteoric diagenesis (after James & Choquette, 1984).**

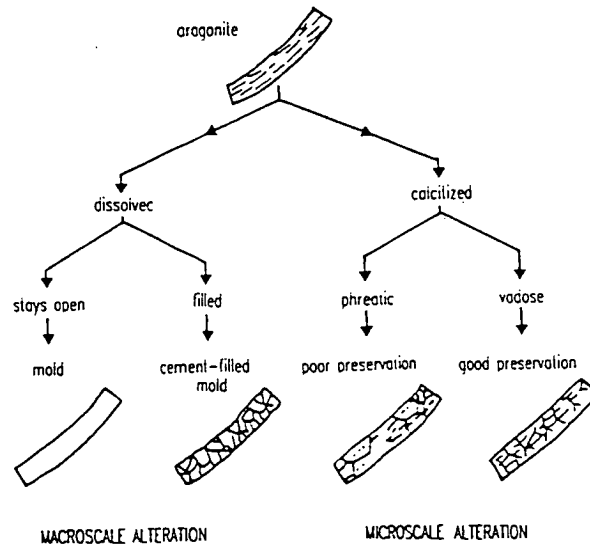


**Fig.7.16. Diagenetic end members of a model for marine and meteoric environments. a) marine diagenesis in a high-energy location, i.e. much cementation as a result of seawater pumping; b) marine diagenesis in stagnant, or low-energy environment, where micritization is dominant; c) meteoric zone with  $\text{CaCO}_3$ -saturated water with cementation and grain replacement; d) meteoric diagenesis in an active zone of much dissolution (after Tucker & Wright, 1990).**

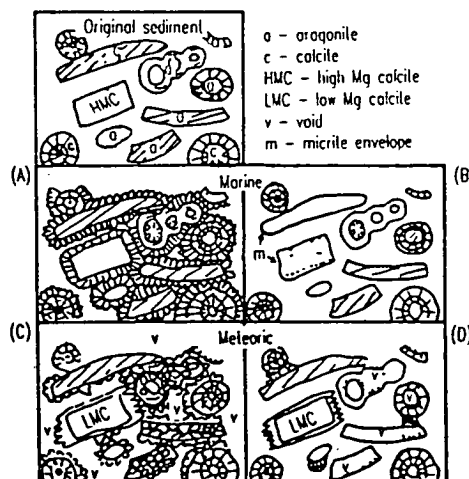


Table 7.1. Point count data from the Quaternary carbonate sequences.

| Location<br>(sample number) | Age                            | Allochems | Derived clasts |          | Porosity | Cement   | Total |
|-----------------------------|--------------------------------|-----------|----------------|----------|----------|----------|-------|
|                             |                                |           | Sedimentary    | Igneous  |          |          |       |
| Pissouri 3-30 (C84/89)      | Pliocene                       | 168 (34)  | 15 (3)         | 94 (19)  | 27 (5)   | 193 (39) | 497   |
| Polis 3-150 (C93/89)        | Pliocene                       | 136 (27)  | 106 (21)       | 115 (23) | 23 (5)   | 120 (24) | 500   |
| Marathounda 2-51 (Mar)      | F <sub>0</sub>                 | 82 (16)   | 215 (43)       | 10 (2)   | 149 (30) | 45 (9)   | 501   |
| Mesoyi 2-18 (Mes)           | F <sub>0</sub>                 | 136 (27)  | 121 (24)       | 52 (10)  | 47 (9)   | 144 (29) | 500   |
| Tremithousa 3-34 (C96/89)   | F <sub>0</sub>                 | 110 (22)  | 128 (26)       | 55 (11)  | 33 (7)   | 174 (35) | 500   |
| Paphos 2-3 (22)             | F <sub>1</sub>                 | 155 (31)  | 126 (25)       | 27 (5)   | 90 (18)  | 102 (20) | 500   |
| Paphos 2-3 (312)            | F <sub>1</sub>                 | 118 (24)  | 203 (39)       | 8 (2)    | 100 (20) | 73 (6)   | 502   |
| Paphos 2-3 (313)            | F <sub>1</sub>                 | 125 (25)  | 208 (42)       | 15 (3)   | 95 (19)  | 58 (12)  | 501   |
| Yeroskipos 2-5 (323)        | F <sub>2</sub>                 | 71 (14)   | 217 (43)       | 0 (0)    | 171 (34) | 44 (9)   | 500   |
| Paphos 2-10 (331)           | F <sub>2</sub>                 | 193 (39)  | 75 (15)        | 8 (2)    | 145 (29) | 80 (16)  | 501   |
| Paphos 2-10 (337)           | F <sub>2</sub>                 | 214 (43)  | 91 (18)        | 12 (2)   | 156 (30) | 31 (6)   | 499   |
| Cape Greco 1-125 (199)      | F <sub>3</sub>                 | 205 (41)  | 125 (25)       | 18 (4)   | 68 (14)  | 85 (17)  | 501   |
| Cape Greco 1-125 (165)      | F <sub>3</sub>                 | 127 (25)  | 95 (19)        | 48 (10)  | 168 (34) | 63 (13)  | 501   |
| Cape Greco 1-125 (168)      | F <sub>3</sub>                 | 185 (37)  | 122 (24)       | 24 (5)   | 116 (23) | 54 (11)  | 501   |
| Cape Greco 1-125 (169)      | F <sub>3</sub>                 | 188 (38)  | 95 (19)        | 107 (21) | 83 (17)  | 27 (5)   | 500   |
| Cape Greco 1-125 (172)      | F <sub>3</sub>                 | 131 (26)  | 117 (23)       | 52 (10)  | 126 (25) | 74 (15)  | 500   |
| Cape Greco 1-125 (173)      | F <sub>4</sub>                 | 243 (48)  | 102 (11)       | 8 (2)    | 100 (20) | 48 (10)  | 501   |
| Larnaca 1-130 (8a)          | F <sub>3</sub>                 | 190 (38)  | 85 (17)        | 30 (6)   | 160 (32) | 35 (7)   | 500   |
| Larnaca 1-130 (618)         | F <sub>3</sub>                 | 196 (39)  | 101 (20)       | 47 (9)   | 117 (23) | 39 (8)   | 500   |
| Coral Bay 2-22 (358)        | F <sub>3</sub>                 | 253 (51)  | 63 (13)        | 4 (1)    | 110 (22) | 70 (14)  | 500   |
| Coral Bay 2-22 (C100/89)    | F <sub>3</sub>                 | 227 (46)  | 87 (17)        | 7 (1)    | 143 (29) | 36 (7)   | 500   |
| Argaka 3-109 (3/301)        | F <sub>3</sub>                 | 107 (21)  | 22 (4)         | 200 (40) | 81 (16)  | 89 (18)  | 499   |
| Argaka 3-109 (3/302)        | F <sub>3</sub>                 | 157 (31)  | 0 (0)          | 25 (5)   | 265 (53) | 54 (11)  | 503   |
| Dhekelia 2-84 (601)         | F <sub>4</sub>                 | 167 (33)  | 50 (10)        | 150 (30) | 50 (10)  | 83 (17)  | 500   |
| Dhekelia 2-84 (603)         | F <sub>4</sub>                 | 98 (20)   | 73 (15)        | 119 (24) | 45 (9)   | 159 (32) | 494   |
| Paphos 2-4 (314)            | F <sub>4</sub>                 | 216 (43)  | 82 (16)        | 49 (10)  | 67 (13)  | 86 (17)  | 500   |
| Paphos 2-4 (316)            | F <sub>4</sub>                 | 250 (50)  | 35 (7)         | 0 (0)    | 145 (29) | 70 (14)  | 500   |
| Paphos 2-4 (318)            | Recent                         | 237 (47)  | 63 (13)        | 13 (3)   | 165 (33) | 22 (4)   | 500   |
| Protaras 2-100 (720)        | F <sub>3</sub> /F <sub>4</sub> | 110 (22)  | 105 (21)       | 61 (12)  | 132 (26) | 91 (18)  | 499   |
| Protaras 2-100 (722)        | F <sub>3</sub> /F <sub>4</sub> | 140 (28)  | 87 (17)        | 35 (7)   | 139 (28) | 99 (20)  | 500   |
| Protaras 2-100 (723)        | F <sub>3</sub> /F <sub>4</sub> | 96 (19)   | 76 (15)        | 106 (21) | 204 (41) | 17 (3)   | 499   |
| Protaras 2-100 (724)        | F <sub>3</sub> /F <sub>4</sub> | 181 (36)  | 85 (17)        | 52 (10)  | 77 (15)  | 106 (21) | 501   |

Note: figures in brackets are percentages.

forams, match that seen throughout the Cape Greco and Protaras sections (Table 7.1). Some of the forams in the sections have been derived from the pre-Quaternary sedimentary sequence, derived sedimentary clasts are also present within the unit (Table 7.1). The derived clasts are mature to sub-mature. The mollusc shells have been bored and also coated with a micrite envelope (see Section 7.4.3 for explanation). The sections from Dhekelia show little variation in the constituent components from the base to the top of the section; the major changes in thin section relate to the variation in the ratio of porosity to cement (Table 7.2).

The suite of specimens taken from the sections at Kato Pyrgos (location 3-110) and Argaka (location 3-109) show a pattern similar to that seen in the coarse, poorly sorted units at Protaras. Some derived igneous clasts, i.e. pillow lava, are present in the Argaka and Kato Pyrgos sections. A shelly hash overlying the section at Argaka (sample 3/302; Table 7.1) differs from the rest of the succession, as it dominated by well preserved molluscan shells that have maintained their original shell mineralogy, i.e. aragonite, are bound by thin meniscus cements (Table 7.1) and contain small igneous clasts within the shell chambers.

The sections from the F3 terrace at Larnaca (location 1-130) are more micritic than those seen in south-east Cyprus. Coral heads have been encrusted by red algae (Plate 7.13), as have the well preserved bivalve. Bryzoan, echinoid, benthic and planktonic forams are also present in this unit. This unit is poorly cemented and has a high primary porosity. There is no evidence for the presence of secondary moldic porosity. This packstone contains a large number of well preserved shells. Small diabase and pillow lava clasts are also present. The packstone is succeeded, up section, by the development of well bedded, mature, sorted grainstone. Clasts derived from both sedimentary and igneous sources are present, as are worn fragments of red algae, molluscs, echinoids and benthic and planktonic forams. Some boring of the shells has taken place and some specimens also showing evidence of calcitization. Some secondary porosity is also present.

Samples were collected from all the terraces in the south-west of the island, i.e. Upper Pliocene, F0-F4, Recent, to test the hypothesis, based on field relations, that there are no discernible changes in the petrology between the Upper Pliocene and Recent. Point count data is shown in Tables 7.1 and 7.2.

The F0 grainstone sequence was sampled at three locations, e.g. Marathounda, Mesoyi and Tremithousa (locations 2-51, 2-18 and 3-34, respectively). Derived sedimentary and igneous clasts are present within all the units. Reworked and abraded

Table 7.2. Ratios of point counted data collected from the carbonate sequences.

| Sample No. and age | All clasts: porosity and cement | Allochems: derived clasts | Porosity: cement | Derived sediment: derived igneous clasts |
|--------------------|---------------------------------|---------------------------|------------------|------------------------------------------|
| 84/89 (Plio.)      | 1:1                             | 2:1                       | 1:8              | 1:6                                      |
| C93/89 (Plio.)     | 2:1                             | 1:2                       | 1:5              | 1:1                                      |
| Mar (F0)           | 2:1                             | 1:3                       | 3:1              | 22:1                                     |
| Mes(F0)            | 2:1                             | 1:1                       | 1:3              | 2:1                                      |
| C96/89 (F0)        | 2:1                             | 1:2                       | 1:5              | 2:1                                      |
| 22 (F1)            | 2:1                             | 1:1                       | 1:1              | 5:1                                      |
| 312 (F1)           | 3:1                             | 1:2                       | 3:1              | 20:1                                     |
| 313 (F1)           | 2:2                             | 1:2                       | 2:1              | 14:1                                     |
| 323 (F2)           | 2:1                             | 1:3                       | 4:1              | ----                                     |
| 331 (F2)           | 2:1                             | 2:1                       | 2:1              | 8:1                                      |
| 337 (F2)           | 2:1                             | 2:1                       | 5:1              | 9:1                                      |
| 199 (F3)           | 3:1                             | 2:1                       | 1:1              | 6:1                                      |
| 165 (F3)           | 1:1                             | 1:1                       | 3:1              | 2:1                                      |
| 168 (F3)           | 2:1                             | 1:1                       | 2:1              | 5:1                                      |
| 169 (F3)           | 3:1                             | 1:1                       | 3:1              | 1:1                                      |
| 172 (F3)           | 2:1                             | 1:2                       | 2:1              | 2:1                                      |
| 173 (F4)           | 2:1                             | 4:1                       | 2:1              | 6:1                                      |
| 8a (F3)            | 2:1                             | 2:1                       | 5:1              | 3:1                                      |
| 618 (F3)           | 2:1                             | 2:1                       | 3:1              | 2:1                                      |
| 358 (F3)           | 2:1                             | 4:1                       | 2:1              | 13:1                                     |
| C100/89 (F3)       | 2:1                             | 3:1                       | 4:1              | 17:1                                     |
| 3/301 (F3)         | 2:1                             | 1:2                       | 1:1              | 1:10                                     |
| 3/302 (F3)         | 1:2                             | 6:1                       | 5:1              | ----                                     |
| 601 (F4)           | 3:1                             | 1:1                       | 1:1              | 1:3                                      |
| 603 (F4)           | 2:1                             | 1:2                       | 1:4              | 1:2                                      |
| 314 (F4)           | 3:1                             | 1:2                       | 1:1              | 2:1                                      |
| 316 (F4)           | 1:1                             | 7:1                       | 2:1              | ----                                     |
| 318 (Recent)       | 2:1                             | 3:1                       | 8:1              | 4:1                                      |
| 720 (F3/F4)        | 1:1                             | 1:2                       | 1:1              | 2:1                                      |
| 722 (F3/F4)        | 1:1                             | 1:1                       | 1:1              | 3:1                                      |
| 723 (F3/F4)        | 1:1                             | 1:2                       | 14:1             | 1:1                                      |
| 724 (F3/F4)        | 2:1                             | 1:1                       | 1:1              | 2:1                                      |

Note: all figures are to 1 significant figure.

planktonic and benthic foraminifera are also present, found as isolated shells and as part of lithoclasts of derived micritic wackestones and packstones. The derived clasts are commonly less than 5mm in diameter. The allochems are dominated by abraded and broken planktonic and benthic forams, red algae fragments, echinoid plates, bryozoa and bivalve and gastropod shells. The grains within all the units are generally subrounded and moderately sorted. The unit at Marathounda is highly porous and poorly cemented, whereas the sections from Tremithousa and Mesoyi are generally well cemented (Tables 7.1 and 7.2). Secondary porosity as a result of dissolution of the fauna is also seen at Mesoyi. Staining indicates that the majority of the sections are made of non-ferroan calcite. These F0 units are very similar to the Pliocene grainstones from the Polis and Pissouri areas (locations 3-150 and 3-30; Tables 7.1 and 7.2). Both Pliocene grainstones have a higher proportion of derived igneous clasts than that present within the F0 sequences. The well cemented grainstones from Pissouri are coarser grained than seen in either the F0, or the Pliocene grainstones from Polis.

The sections from the F1 terrace above Paphos (location 2-3) are dominated by grainstones. The basal section of the F1 terrace, directly above the unconformity, contains a large number of derived *Lepidocyclina* tests from chalks of Miocene age beneath the contact (Plate 7.13). The basal unit is coarse grained and contains a large proportion of red algal, echinoid, molluscan and foraminiferal debris and derived sedimentary clasts (samples 312 and 313; Table 7.1).

The F2 terrace above Paphos (locations 2-5 and 2-10) has a similar appearance to those sections taken from the F1 terrace. Sections taken from the framework facies contain abundant red coralline and encrusting algae (Plate 7.14) and poorly sorted molluscs, echinoids and forams (sample 323; Table 7.1). The grainstone units are more mature and contain many abraded and reworked forams and primary red algae, echinoid plates and molluscan shells. The allochems and derived clasts are generally less than 3mm in diameter, sub-rounded and moderately well sorted (samples 331 and 337; Table 7.1). All the units are poorly cemented (Table 7.1), with a porosity, to cement ratio, ranging between 5:1 and 2:1 (Table 7.2).

The F3 sequences at Coral Bay (location 2-22) were collected from the framework facies above the basal unconformity and grainstone units. The framework facies is dominated by encrusting red algae, similar to that seen in the F3 section at Larnaca (Plate 7.14), and delicate branching red algae of the Corallinaceae family, which probably include the genera *Lithophyllum*, *Neogoniolithon* and *Corallina* (Plate 7.14) as well as heads of the coral *C. caespitosa*. Small (<3mm diameter) subangular detrital clasts, e.g. serpentinite, and derived fragments of planktonic and benthic forams are also

PLATE 7.14.

D - A thin section micrograph of encrusting coralline algal forming a bindstone fabric in the F3 carbonate sequence at Petounda Point (location 3-11; sample C41/89).

Note: The field of view is 6mm long.

E - A thin section micrograph displaying fragments of laminar binding and encrusting coralline algae with evidence of moldic porosity, from the F2 sequence in Paphos (location 2-5b; sample X1).

Note: the field of view is 6mm long.

F - A thin section micrograph of binding coralline algae from the F3 sequence at Cape Greco (location 1-125; sample 199).

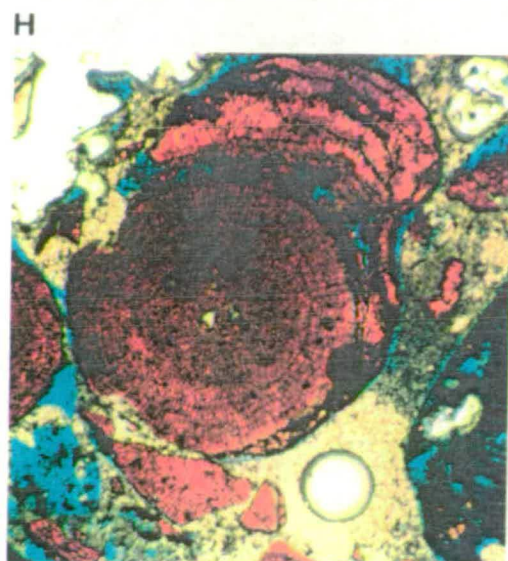
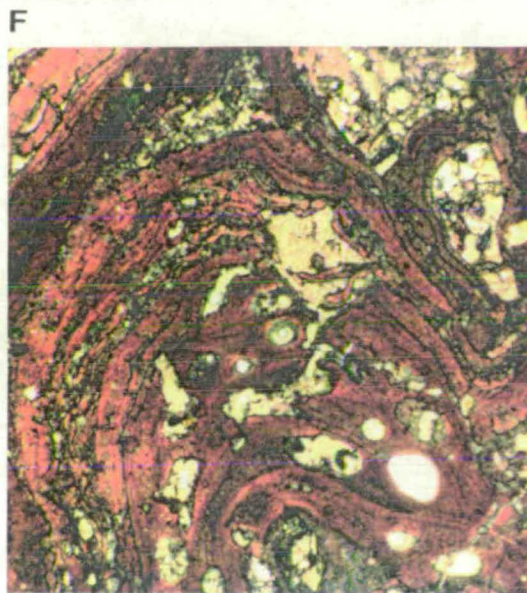
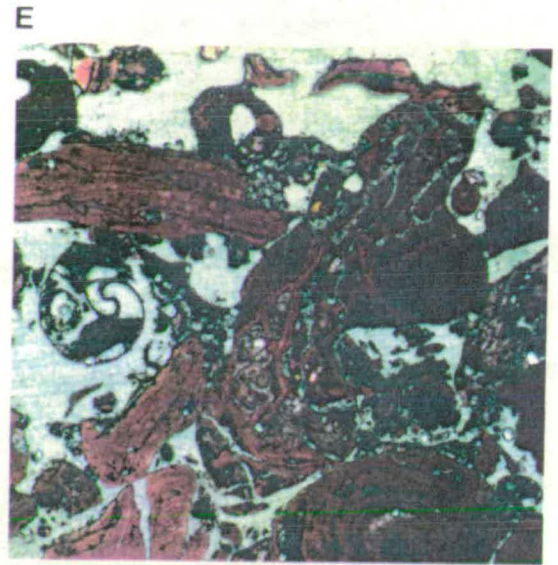
Note: the field of view is 6mm long.

G, H & I - Thin section micrographs of red algae of the Corallinacea family, which probably includes the genera *Lithophyllum*, *Neogoniolithon* and *Corallina*, from Coral Bay (location 2-22; sample C100/89).

Note: the field of views are 4mm, 1.5mm and 2.5mm respectively.



Plate 7.14



present in the section (sample 358; Table 7.1). A section (sample C100/89) taken from the grainstone sequence above the framework facies at Cape Greco contains numerous large fragments of bored, aragonitic bivalves and gastropods, red algae, echinoids, bryozoa, benthic and planktonic forams and derived packstone, wackestone and igneous clasts. This unit, like the framework unit beneath, is poorly cemented and porous, with a porosity to cement ratio of 4:1 (Table 7.2).

The F4 terrace in the Paphos area contains the same fauna as seen in the higher terraces. The grainstones from the F4 terrace have a porosity to cement ratio that varies from 2:1-1:1 (samples 314, 316; Table 7.2). The Recent beachrocks, like the F4 terrace, are generally submature grainstones, that display variable cementation, e.g. sample 318 has a porosity to cement ratio of 8:1 (Table 7.2) which contrasts that seen in the Limassol and Lamaca areas where Recent beachrock cementation is pervasive. The molluscan shells with the Recent beachrocks have been bored, similar to that seen in many of grainstones from the terraces (i.e. F1-F4) in the Paphos area.

#### 7.4.3 Summary.

The data described above and recorded in Tables 7.1 and 7.2 can be summarised as follows:

- i) the variety and proportion of derived clasts in any one location reflects: a) the position within the sedimentary sequences, e.g. lag compared to grainstone, b) the local basement, i.e. whether that is igneous or sedimentary, c) the local influence of siliciclastic deposition, either through reworking, or primary deposition, e.g. the comparison between the Argaka sections which flank the Polis-Paphos graben and the F4 carbonate sequences on the foreshore at Paphos unaffected by derived clasts,
- ii) the data show a general trend that indicates that Pliocene, F0 and F1 sections are better cemented than the latter units but this does vary locally, e.g. the F0 at Marathounda. Local diagenetic controls, as well as the position of the unit in any sedimentary sequences, influence the extent of cementation in the sections,
- iii) the proportion and type of allochems in all the units appears to be reasonably constant, the slightly higher ratios reflecting lag units and the hash seen cropping out at Argaka (samples 173 and 3/302 respectively; Table 7.2),
- iv) the clast to cement and porosity ratio remains quite constant throughout,
- v) there appears to be very little difference between the lithologies that are found associated with the F0 terraces and those seen associated with the F4 and Recent terraces. Those differences that do exist between the F0 and Recent sequences can be explained by the local variations occurring as a result of facies changes and changes in the local environment.

#### **7.4.4 Diagenesis.**

The marine sequences described above (Section 7.4.1) display a series of diagenetic features: micrite envelopes (Plate 7.15); the development of equant, pore filling and fringing, calcite spar (Plate 7.15); the formation of meniscus cements (Plate 7.15); partial and total calcitization and neomorphism of the bivalve, gastropod and coral fauna, with varying degrees of preservation of the original fabric (Plate 7.15); dissolution of aragonitic shells, with a) the subsequent infilling of the voids with calcite (Plate 7.15) or b) the local development of a secondary moldic porosity (Plates 7.12 and 15); the formation of syntaxial overgrowths associated with echinoderm fragments (Plate 7.15) and, finally, the development of micrite networks and caliche crusts (Plate 9.3).

Recent beachrocks in Cyprus, that postdate the last interglacial sea-level maxima, crop out around the coast today. These beachrocks which crop out above and below the present mean sea-level, are generally well cemented. Alexandersson (1969) during a study of beachrocks from the northern Mediterranean coast stated that the lithification of the Recent beachrocks generally decreases landward and can vary from incipient to advanced, with the formation of high-Mg calcite cements. The later appears to be the norm on Cyprus, perhaps indicating that present conditions are more conducive to quick beachrock formation than earlier in the Quaternary, or that these beachrock units have spent a longer period of time in the marine phreatic realm and this has facilitated the development of cohesive beachrock successions.

Previous studies of littoral beachrock horizons in the Mediterranean (e.g. Alexandersson, 1969; El Sayed, 1988) have described two major diagenetic features that are present in Quaternary beachrocks. These are fringe cements and the development of micrite overgrowths. The absence of acicular aragonite associated with the development of micrite overgrowths differs from that recorded in beachrocks in other parts of the world, e.g. in San Salvador Island (Beier, 1985) and Grand Cayman (Moore, 1973), but agrees with that found on Cyprus. The development of micrite overgrowths in the shallow marine environment is now widely attributed to boring, by endolithic algae and fungi (Bathurst, 1966; Kobluk & Risk, 1977), and this appears to be the primary diagenetic feature in the majority of the Quaternary terrace sequences. The non-ferroan calcite cement that succeeds the formation of the micrite envelopes takes the form of an equant and not a fibrous cement in many of the Cyprus sections. This cement is locally porefilling but is more generally restricted to fringing the grains, binding them together. Locally this takes the form of a meniscus fringing cement, indicative of the meteoric rather than marine realm. Alexandersson (1969; 1972) states that the fringing cements from the north Mediterranean are post-depositional additions and that they have the same

PLATE 7.15.

D - A thin section micrograph displaying moldic porosity, micrite envelopes and a coarsening up structure in part of the F3/F4 carbonate sequence exposed at Protaras (location 2-100).

Note: the field of view is 8mm long.

E - A thin section micrograph showing the pore filling cement that developed in the grainstone unit of the F3/F4 sequence at Cape Greco (location 1-125; sample 164).

Note: the field of view is 8mm long.

F - A thin section micrograph displaying meniscus and pendant cements developed in the F3/F4 sequence at Protaras (location 2-100; sample 722).

Note: the field of view is 8mm long.

G - A thin section micrograph showing pore filling calcite cements and the pervasive calcitization, with a ghost of the original structure, of bivalve shells in the ?F0 grainstone sequence at Pissouri (location 3-30; sample C84/89).

Note: the field of view is 3mm long.

H - A thin section micrograph showing complete calcitization of bivalve shells, yet the original fabric is still visible, from the F3/F4 carbonate sequence at Protaras (location 2-100; sample 724).

Note: the field of view is 6mm long.

I - A thin section micrograph showing the development of a syntaxial overgrowth around a echinoid fragment from the F4 carbonate sequence in Paphos (location 2-4; sample 337).

Note: the field of view is 1mm long.

J - A thin section micrograph displaying a partially altered gastropod shell showing both its original mineralogy and fabric (red and white stripes) and an altered fraction (grey and red blobs).

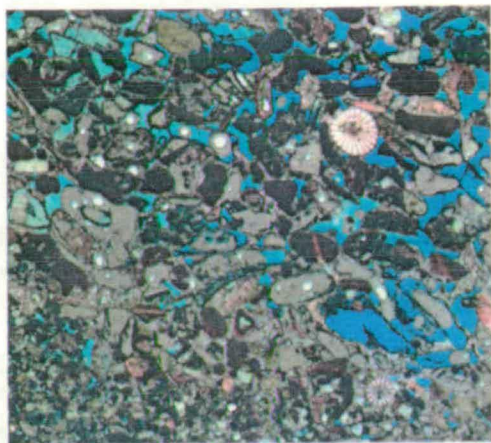
Note: the field of view is 1.5mm long.

K - A thin section micrograph displaying a fragment of a bivalve shell with evidence of boring and the formation of a micrite envelope, from the F4 sequence at Paralimni (location 1-120; sample 124)

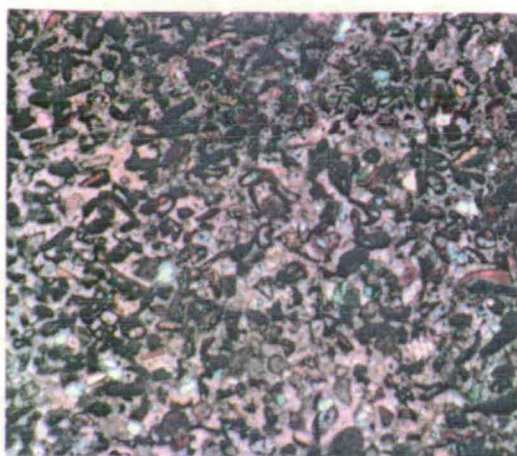
Note: the field of view is 1.3mm long.

Plate 7.15

D



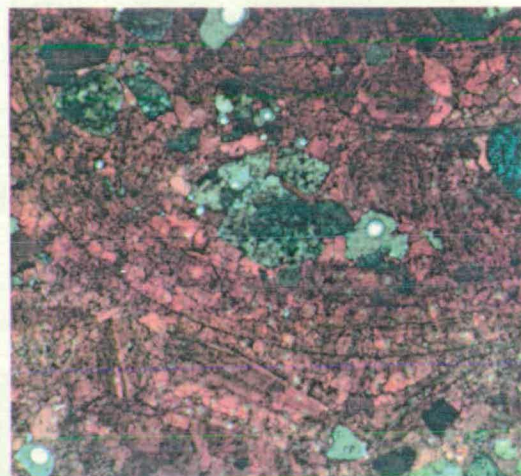
E



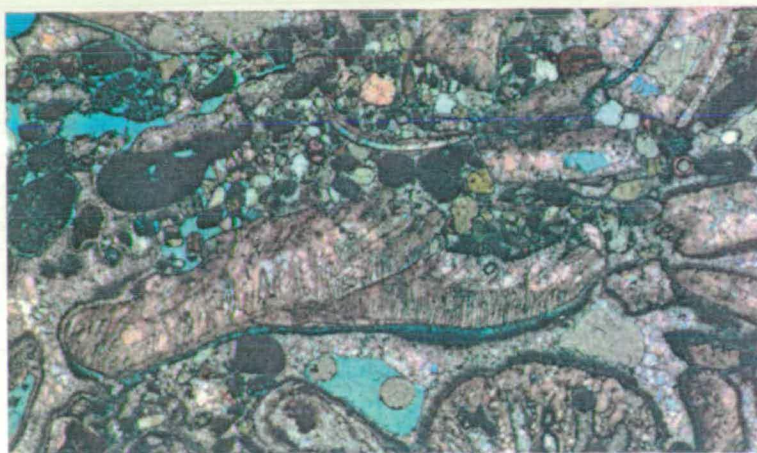
F



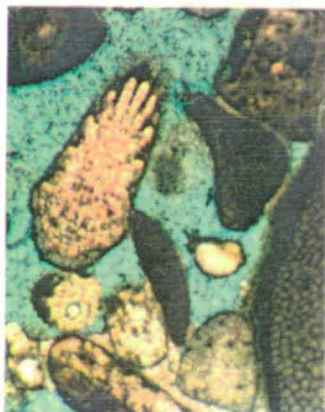
G



H



I



J



K



Mg-content as the micrite. El Sayed (1988) states there is no evidence of vadose cements in the beachrocks from Alexandria, pointing to a phreatic or marine environment for the formation of this fringing cement. The development of fringing cements in either the marine or phreatic realm suggests that the original mineralogy could have been aragonite and that they have been altered to calcite during later diagenetic events, similar to that recorded by Cooper & Flores (1991). Further detailed studies, e.g. isotope, Mg and Sr, of the cements from the Cyprus Quaternary sequences, would determine whether the spar formed in marine or meteoric conditions.

Monocrystalline syntaxial overgrowths on echinoderm fragments are a common diagenetic feature of the meteoric phreatic zone (Longman, 1980). The formation of equant calcite cements and the macroscale dissolution of aragonite, e.g. coral and molluscs, is also a common feature in the meteoric phreatic zone. The dissolution of aragonite can result in either the formation of secondary, i.e. moldic, porosity, or calcitization with the molds filled with a calcitic cement at a later date (Fig.7.15). Microscale calcitization can also take place in the meteoric phreatic realm; this results in the poor preservation of the original shell structure and contrasts with neomorphism in the meteoric vadose zone which results in good preservation of the original shell structure (Fig.7.15; Plate 7.15). Microscale neomorphism of shells is believed to occur when a nanometre-thick water skin, about which the alteration of metastable aragonite to calcite takes place, moves through a rock unit (Wardlaw *et al.*, 1978). The process of neomorphism allows the original structure of the specimen to be retained, due to the presence of insoluble organics and other matter (James, 1974). Sandberg *et al.* (1973) and James & Choquette (1984) have shown that neomorphism may be localised and not complete with, for example, the partial preservation of aragonite and its original structure in a gastropod shell, whilst the rest of the shell has been altered (Plate 7.15). James & Choquette (1984) also note that poorly lithified Pleistocene carbonates with a predominantly metastable fauna are found in the meteoric vadose zone, with rapid alteration being common in the meteoric phreatic zone. The formation of meniscus cements of fine equant crystals is restricted to the meteoric vadose zone.

The diagenetic history of the Quaternary carbonate units within the marine and meteoric zones has been influenced by the presence, or absence, of water. The availability of fresh rainwater is dependent on the climate; the development of extensive caliche horizons within the Quaternary sequences on Cyprus indicates dry semi-arid conditions which allow both aragonite and calcite to be preserved in the meteoric vadose zone. Arid conditions contrast those found in humid environments where extensive dissolution will occur in the meteoric vadose zone (James & Choquette, 1984). James & Choquette (1984) suggest that extensive dissolution and calcitization of aragonite will

occur in the meteoric phreatic zone in areas of semi-arid climate, whilst neomorphism will occur in the meteoric vadose zones. Active precipitation of cements does occur in the meteoric vadose zones in the Quaternary carbonate of Cyprus, e.g. the precipitation of meniscus cements, but this is scarce. The presence of a semi-arid to arid climate in Cyprus during the Quaternary would not promote active cementation in the meteoric vadose zone.

The sedimentological and geochronological data presented earlier (Section 7.3 and Chapter 3 respectively) indicate that the preserved Quaternary carbonate marine sequences have been deposited during relative regressive phases. The diagenetic evidence from the carbonate sequences supports this view, with the features described above indicating a transition from the marine (with the formation of micrite rims and some calcite spar) to the meteoric phreatic realm, and then to the meteoric vadose zone (with the development of syntaxial overgrowths, calcitization and the development of filled and moldic dissolved original aragonite shells). The formation of micrite networks and caliche is indicative of meteoric environments (see Chapter 9 for a detailed description of caliche development). The pattern of cementation, like the pattern of sedimentation (Section 7.3), appears to be constant with the F0-F4 terraces sequences having the same characteristics, although cementation is generally more pervasive in the late Pliocene and F0 grainstones than the F1-F4 sequences in the Paphos area, e.g. samples C84/89, C93/89, C96/89, Mar, Mcs (Tables 7.1 and 7.2). The variation in diagenetic features between different terraces, and even between sample sites on any one terrace, is more likely to reflect local variations in the meteoric realm as uplift of the island coupled with a eustatic fall in sea-level will, possibly, result in the terrace being removed from the meteoric phreatic, i.e. where it is permanently saturated with water, into the meteoric vadose zone, where saturation is sporadic.

The variety of diagenetic features within the same unit, for example both totally replaced and fresh aragonite shells, suggests that some reworking has taken place. This is particularly evident in the Cape Greco area where the F4 terrace lies unconformably over the probable F3. The variation in intrashell mineralogy indicates local alteration as a result of a minimal period of time in the meteoric phreatic zone. The general lack of pervasive cements indicates that these units have only spent a short period of time in the marine, or meteoric, phreatic zone and have rapidly moved into the meteoric vadose zone where minimal alteration will occur, as a result of the semi-arid climate that Cyprus experiences. This argument supports the view that the carbonate sediments formed in a regressive regime, as continued uplift of the island, relative to sea-level, removed these sequences from the phreatic zone and secondly, Recent beachrocks are generally better cemented as they have remained within the meteoric phreatic realm. X-ray diffraction

data collected during the course of the U-series studies, to test whether coral had undergone any dissolution (Chapter 3), show how localised the dissolution changes are, with older terraces, e.g. Petounda Point (location 3-11), just as likely to have original unaltered aragonite as the lower, younger terrace at Paralimni (location 3-50), whereas corals in the terrace at Akrotiri (location 3-96) have undergone extensive dissolution from aragonite to calcite.

It can be concluded that environment, climate and proximity to sea-level and the watertable are the major controls on the development of the observed cements and that these are largely independent of time controls. However, two broad diagenetic pathways are present within the Quaternary carbonate sequences (Fig.7.16).

## **7.5 INTERPRETATION, DISCUSSION AND CONCLUSIONS.**

### **7.5.1 Introduction.**

Carbonate and clastic beach and coastal environments have been the subject of much study (Thompson, 1937; Reineck & Singh, 1975; Harms *et al.*, 1975; Howard & Reineck, 1981; Inden & Moore, 1983; Davis, 1985) and a wide variety of transgressive and retrogressive facies models have been proposed. Inden & Moore (1983) distinguish between transgressive and regressive conditions stating that sediments are rarely preserved in transgressive regimes, but where these are seen a coarse lag of intra-clasts forming a scoured surface is subsequently overlain by a fining-up sequence of burrowed and/or laminated and cross-bedded grainstones, or packstones. In regressive sequences, where preservation of the depositional sedimentary sequence is more common, poorly sorted, cross-bedded grainstones will be succeeded by laminated grainstone and eventually sub-aerial deposits, e.g. aeolian dunes and caliche.

Studies of modern and Quaternary siliciclastic shoreline and shallow marine sequences are quite extensive, e.g. California (Thompson, 1937; Howard & Reineck, 1981), the Gulf of Gaeta, Tyrrhenian Sea (Reineck & Singh, 1975). Studies comparing modern and ancient high energy shorelines and fluvial sequences have also been made (Clifton *et al.*, 1971; Clifton, 1973). The fewer studies of modern high energy carbonate shoreline and shallow marine environments include Bernard *et al.* (1962), Inden & Moore (1983). Studies of Quaternary high energy carbonate, littoral environments have been made (Ward & Brady, 1979; Ward *et al.*, 1985).



## **7.5.2 Interpretation.**

The Quaternary carbonate sediments from Cyprus, i.e. F0 to F4 age, are believed to have been deposited in similar environments as a consequence of the interaction throughout the Quaternary of eustatic sea-level fluctuations and the tectonic uplift of the island. The sedimentary facies recognised during the course of this study will now be interpreted in turn (Fig.7.17).

### **7.5.2.1 The basal unconformity surface and conglomeratic lag sequence.**

The conglomerate lags, or ravinements (Swift, 1968) are interpreted as forming in a transgressive regime with reworked, earlier, locally derived clasts, worn shells and lithoclasts being incorporated into the lag sequence, e.g. as occurs in Southern California (DeCelles, 1987). Transgressive lag sequences are common components of carbonate shoreline successions, cropping out above eroded, bored and burrowed "basement" units beneath an unconformity surface (Ward & Brady, 1979; Inden & Moore, 1983; Ward *et al.*, 1985). The presence of a lag deposit indicates the onset of onlap and transgression of the shoreline over a previously exposed and eroding surface.

### **7.5.2.2 Coral and coralline algal framebuilders.**

There is no evidence of Quaternary shelf sediments preserved onshore in southern Cyprus today. The sediments that formed in the deepest marine waters in the Quaternary carbonate sequences are probably the coral and red algal framework units, which are restricted to the shallow marine photic zone. The framebuilders, in life position, are attached to clasts within the transgressive lag facies, or to the basement lithologies beneath the unconformity surface, and commonly crop out above lag unit, or on areas of positive relief associated with the unconformity surface.

Presently the coral *C. caespitosa* is found in the Mediterranean in the circa littoral zone, commonly down to a depth of 50m (Zibrowius, 1980). Hearty (1986) reports that *C. caespitosa* is typically found in shallow, coastal waters.

The red coralline algae forms delicate branching frameworks, or robust rhodoliths, and is the dominant framework structure in the F1 and F2 carbonate sequences. *Lithophyllum*, *Neogoniolithon* and *Corallina*, all member of the Corallinaceae family, are three of the genera present within the carbonate sequences. The Corallinaceae family occupy niches throughout the marine environment (Wray, 1977), but the three genera cited above are primarily found in shallow, i.e. down to 40m (Fig.7.18), warm

**Fig.7.17. Summary diagram of the components of the F0-F4 carbonate sedimentary sequences (outlined in the text).**

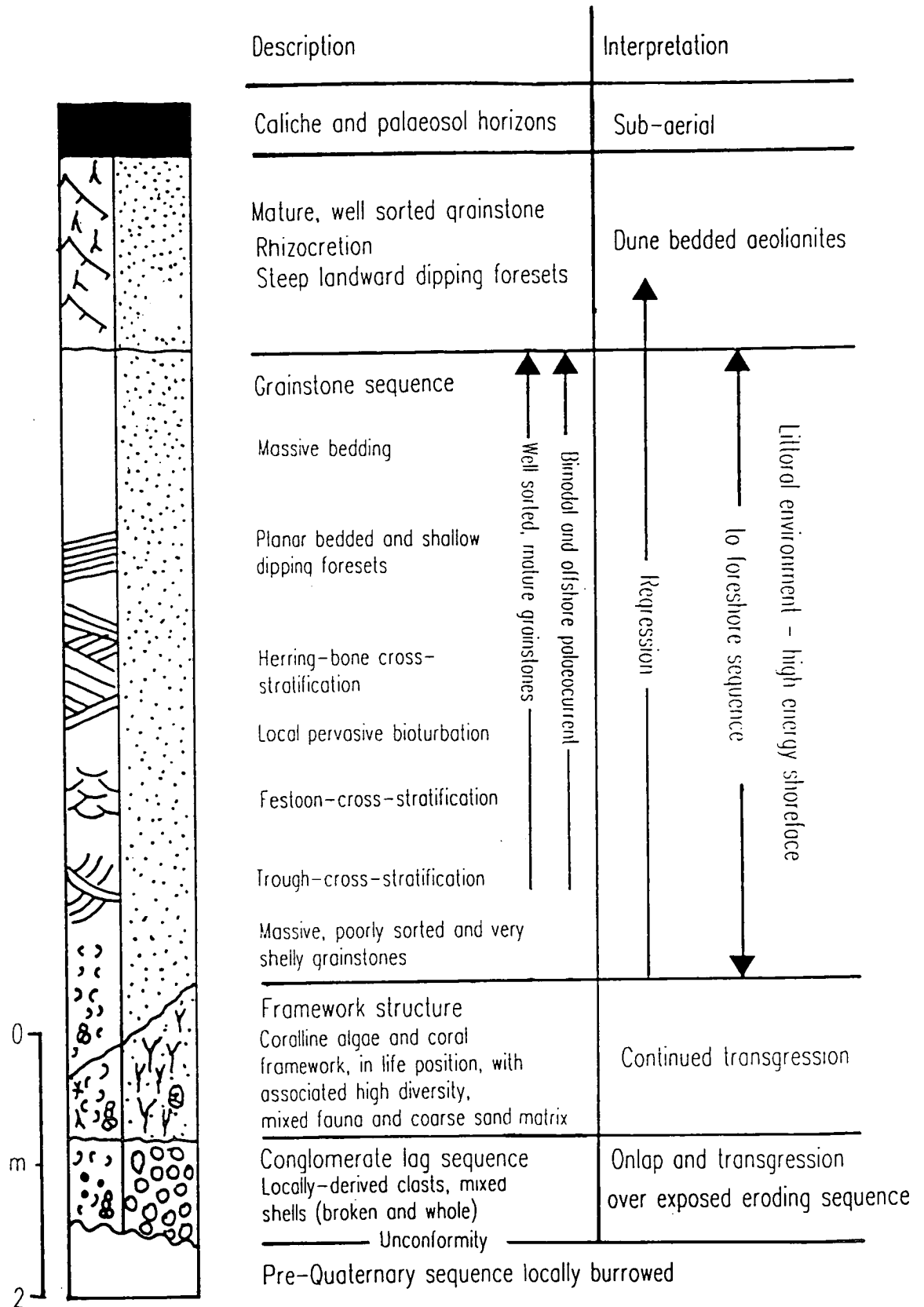


Fig.7.18. Depth distribution and percentage of crustose coralline algae genera in the Hawaiian Archipelago (after Adey et al., 1982).

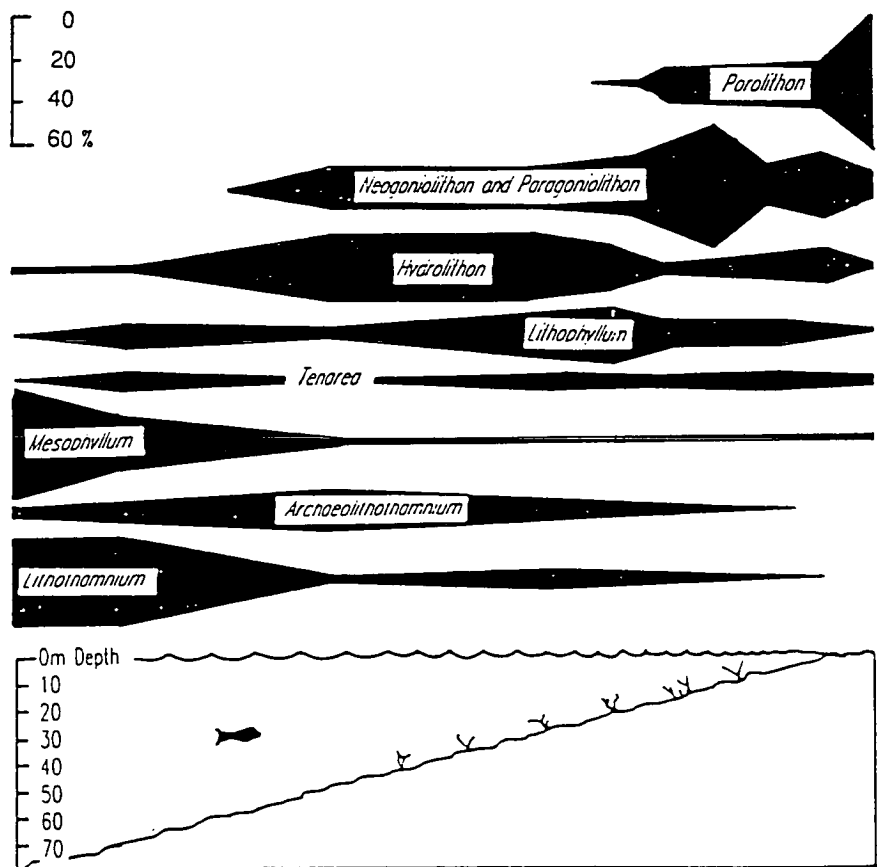
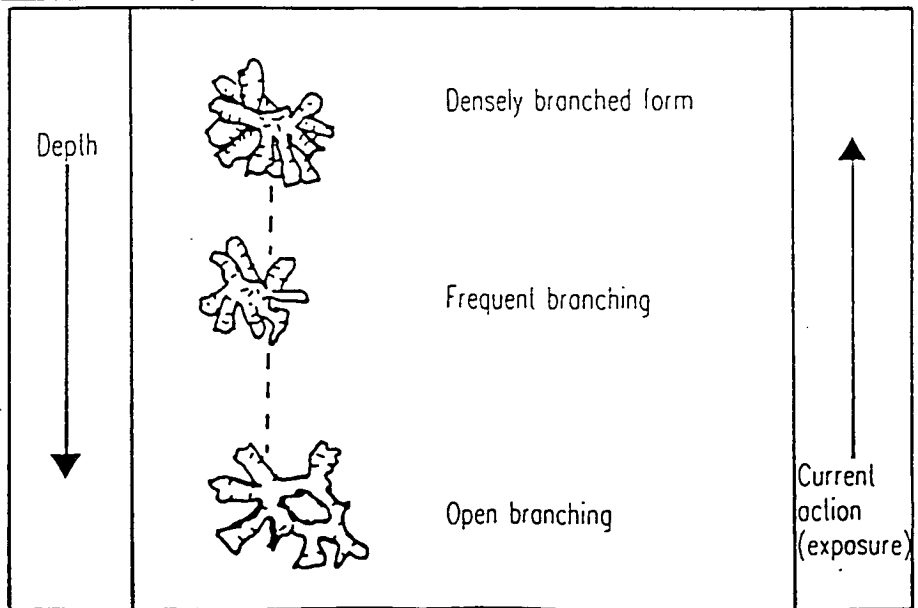


Fig.7.19. Growth-form continuum within the same species of free-living coralline as a function of depth (suggested by Wray, 1971) and current action (observed by Bosence, 1976) (after Wray, 1977).



marine waters that are subject to intermediate to strong light (Adey & Macintyre, 1973; Adey & Burke, 1976). *Lithophyllum* and *Neogoniolithon* are members of the subfamily Melobesoideae, i.e. crustose coralline algae, whereas *Corallina* is a member of the Corallinoideae subfamily, i.e. articulated coralline algae. Studies of the coralline algae from the Hawaiian Archipelago indicate that *Neogoniolithon* and *Lithophyllum* are present in water depths of <10m and 10-40m respectively (Adey *et al.*, 1982). Turbulent waters are favoured as these prevent the algae becoming choked by sediment although excessive currents will cause the algae to break up. However, crustose algae and the more robust rhodoliths can occupy an active environment close to sea-level (Adey & Burke, 1976; Bosellini & Ginsburg, 1970). The variable location of branching coralline algae in the Paphos area (locations 2-5, 2-20 and 2-27) probably reflects the prevalent marine conditions at the time of formation. The growth of branching coralline algae on high ground, associated with the unconformity surface (Fig.7.3), may have been associated with slightly lower energy conditions and a high sediment accumulation rate in contrast to branching algal frameworks that formed in troughs, or flatter areas, elsewhere on the unconformity surface. A high energy environment with its reduced threat of extensive sediment input, possibly permitted conditions that allowed the growth of extensive branching algal frameworks in the trough, or flat areas, created by the unconformity surface (Figs.7.4 and 7.9; locations 2-5 and 2-27). The general upward progression from branching to crustose and free-living, densely branched rhodoliths suggests an increase in the energy of the system up sequence (location 2-5), probably related to a shallowing environment at this time. The same pattern of open branching to densely branched free-living rhodoliths was recorded in Recent forms in western Ireland (Bosence, 1976) and interpreted to indicate the variation in current action and depth (Fig.7.19; Wray, 1971; Bosence, 1976). The correlation of coralline branch density and depth and current action does not always exist, as articulated coralline algae is resilient and frameworks are found in high energy environments, e.g. associated with pounding surf (Wray, 1977). The close relationship between encrusting coralline algae and coral development and the formation of algal crusts around the coral heads, e.g. the F3 terrace at Larnaca (location 1-130; Plate 7.13), compares with that seen presently in the fringing reefs of Hawaii, with coralline algae constituting 40% of the reef surface, through binding and encrusting of the reef surface (Littler, 1973). The algal and coral growths and local frimestones are interpreted as forming small frameworks in active shallow marine environments representing deposition and growth during a sea-level maxima. Age data from the F3 and F4 terrace supports this (Chapter 3).

The massive grainstones with an associated high density and high diversity fauna found in close association with the framework units were also probably deposited in an active, shallow marine environment. Data from the ecology of the molluscs present

within the framework and grainstone units (see below) indicate a shallow marine to intertidal habitat, in keeping with the shallow marine environments interpreted here (Moore, 1969; Richards, 1982).

The molluscan fauna present within the carbonate sequences does not show any major variations throughout the Quaternary; the presence, or absence of coral and the warm water Senegalesse fauna being the exception. The habitat of bivalves found in the Quaternary carbonate sediments is shown in Table 7.3.

The genera mentioned in Table 7.3 are not present commonly in a life position and are found more generally as single, detached, reworked valves. The faunal group indicates shallow littoral, sub-littoral and intertidal environments, with good light and energetic conditions, which agrees with the interpretation that the molluscan fauna of the F3 terrace in Larnaca is indicative of shallow marine waters, i.e. 10-30m (Moshkovitz, 1968). The abraded, broken and locally thickened form of many of the shells, e.g. the Pectenids and Glycymerids at Cape Greco (location 1-125), indicates a high energy shallow marine environment, similar to that recorded by Stanley (1970).

Table 7.3. Habitat of the fossil bivalves commonly found in the Quaternary sequences in Cyprus (habitat related to shell morphology after Moore, 1969).

| Habitat                                                                               | Faunal examples                    |
|---------------------------------------------------------------------------------------|------------------------------------|
| <u>Epifaunal</u> - attached                                                           |                                    |
| Cemented on to the substrata and rocks                                                | <i>Ostrea</i>                      |
| Byssate nestles in active environments,<br>and are commonly found on wave cut benches | <i>Arca</i> and <i>Barbatia</i>    |
| Closely attached byssate                                                              | <i>Mytilus</i> and <i>Modiolus</i> |
| <u>Epifaunal</u> - free living                                                        |                                    |
| Swimmers                                                                              | <i>Pecten</i>                      |
| Non-swimmers                                                                          | <i>Glycymeris</i>                  |
| <u>Semi-infaunal</u>                                                                  |                                    |
| Littoral with very shallow water                                                      | Pinnidae and Mytilidae             |
| <u>Infaunal</u>                                                                       |                                    |
| Shallow infaunal                                                                      | Cardiidae and <i>Nucula</i>        |

### 7.5.2.3 Grainstones

The grainstone sequences that generally range from massive coarse, poorly sorted units at the base of the succession to well bedded, locally bioturbated and then rhizocreted units at the top of the succession. These sequences represent a lower shoreface to upper shoreface, and then foreshore and backshore, succession. This interpretation is supported by the presence of trough cross-stratified, laminated, festoon- and planar-dipping units, as well as generally offshore, or bimodal, palaeocurrent indicators, which are indicative of the shoreface and foreshore zones, similar to those cropping out elsewhere in Recent and Pleistocene beach sequences (Thompson, 1937; Ward & Brady, 1979; Inden & Moore, 1983). The presence or absence of bioturbation within these sequences not only testifies to the precise location of a unit within the littoral environment but also to the relative rates of sedimentation during the deposition of these grainstone sequences, as rapid rates of sedimentation are likely to hinder the development of burrows. The grainstones are generally more mature and better sorted towards the top of the successions, in line with deposition above the upper shoreface. The vast majority of the sediments deposited within the beach sequences have been derived from offshore sources, as few lithoclasts are seen, and the sediments are generally dominated by carbonate grains, and not derived detritus from onshore locations. Nevertheless exceptions are seen, e.g. the area around Polis (location 3-109) and in the Dhekelia area (location 2-84). The local presence of coarse, scoured, worn, shelly horizons with derived coral heads and local gravel clasts interbedded with the littoral sediments, e.g. Cape Greco (location 1-125), may indicate deposition during storms, as strong rip currents which would transport this variety of sediment are commonly associated with stormy conditions (Davis & Fox, 1972, 1975). These coarser, poorer sorted sediments result from the shift of a mass of shallow marine sediment onshore. The opposite effect is seen to the south of Lara Point (location 2-30), where progradation of the fluvial sediments out over the shallow marine sequences caused the seaward transport of sediment to take place, resulting in deposition over the littoral sequence. The grainstones commonly appear to have swamped and choked the framework structures, e.g. the F2 terrace in Paphos (location 2-5). This indicates that either the beach sequences were prograding offshore, or that a relative drop in sea-level was taking place. The latter appears to be more likely as the sedimentary sequence above the framework facies appears to be wholly regressive and the majority of the grainstone sediment came from the sea, so it is unlikely to form a prograding sequence purely as a consequence of sediment supply. The absence of fine grained sediments in this facies, with much of the grainstone being made up of medium to coarse sands, is indicative of high energy shorelines (Folk & Cotera, 1970).

#### **7.5.2.4 Sub-aerial deposits.**

The presence of dune, fluvial, caliche and soil sequences, which lie conformably above the grainstone sequences, indicates the continuation of the regressive sequence up into the sub-aerial environment. The presence, for example, of rhizcretion structures, onland dipping forests and terrestrial gastropods (Chapter 8) supports this argument.

#### **7.5.2.5 Diagenetic data.**

Diagenetic features, such as, the development of micrite envelopes, syntaxial overgrowths, calcitized and neomorphic features and porefilling, meniscus and pendant cements (Section 7.4.3) indicate that diagenesis of the carbonate sequences has occurred in the marine, meteoric phreatic and meteoric vadose zones. The pattern of diagenesis suggests that much of the primary diagenetic alteration occurred in the phreatic zone, with successive changes taking place in the vadose zone. The incomplete cementation of the majority of the Quaternary carbonate sediments indicates that these have undergone an early removal from the zones of active alteration and cementation, i.e. the phreatic zone in semi-arid environments, in line with that suggested by James & Choquette (1984). These authors highlight the residence time as an important factor controlling alteration and diagenesis in any one diagenetic realm. The pattern of diagenetic alteration in the carbonate sequences, therefore, follows the pattern of sedimentation, as deposition and diagenetic alteration associated with successive terraces indicates a transgressive and then regressive regime. Continuing regression and associated tectonic uplift resulted in the removal of many of the carbonate sequences away from the zones of active diagenetic alteration.

#### **7.5.3 Summary.**

Local changes are located within the terrace sequences, for example: the presence of solely algal frameworks, lacking corals, in the F1 terraces, the presence of detritus within the F3 carbonate sequences at Larnaca (location 1-130), Lara Point (location 2-30) and in the Polis area (location 3-109), the presence of grainstone sequences directly above the lag, rather than above framebuilder units (locations 2-3), the presence or lack of aeolianite, or fluvial sequences above the grainstone units (locations 2-34 and 2-50) and the presence of heavily bound bindstones associated with a micritic matrix and better preserved fauna, like those seen at Larnaca (location 1-130). All these factors indicate minor changes to the local pattern of sedimentation but this should not mask the overall pattern, seen throughout the Quaternary, in the carbonate littoral and sub-littoral sediments, which primarily represent a series of transgressive and then regressive,

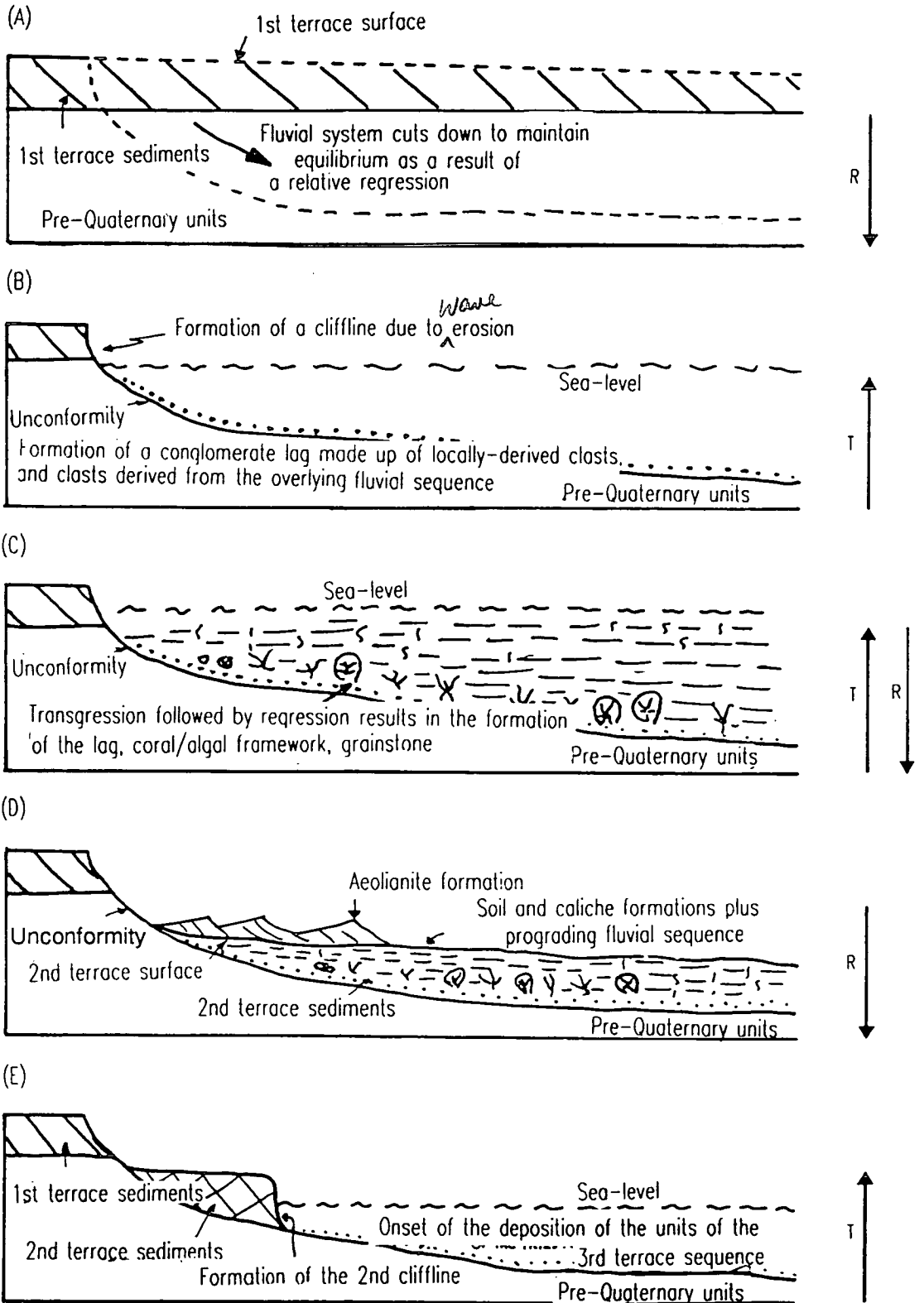
offlapping sequences (Fig.7.20). The carbonate sequences on Cyprus are generally quite thin, lenticular and narrow indicative of regressive beach sequences (Scholle *et al.*, 1983).

The formation of the F3 and F4 coral colonies occurred during eustatic sea-level maxima (Chapter 3). A drop in the eustatic sea-level subsequently occurred and has been represented by the deposition of lower shoreface to foreshore and sub-aerial sequences, i.e. regressive succession. It can be concluded, therefore, that deposition of the F3 and F4 carbonate sediments has been controlled by eustatic sea-level changes. The preservation of regressive carbonate sequences from 360m ASL to <3m ASL suggests that another relative "regressive event", of larger magnitude, has been continuing throughout the Quaternary, i.e. tectonic uplift and isostatic rebound of the island, and it is this that has caused the carbonate sedimentary sequences, the formation of which were controlled by the eustatic sea-level changes, to be preserved (Fig.7.20).



**Fig.7.20. Sketch profiles of the progressive mode of formation of the F0-F4 carbonate sedimentary sequences, the marine clifflines and terraces during the Quaternary period in Cyprus.**

T - transgression  
R - regression



## **Chapter Eight: Aeolianite formation.**

### **8.1 INTRODUCTION.**

Quaternary aeolianites from Cyprus have received little attention in the past. Bagnall (1960), Pantazis (1967), Moseley (1976) and McCallum (1989) described and identified blown sands and dunes in areas along the south coast of Cyprus between Larnaca and the Akrotiri Peninsula. Moore (1960) recorded blown sands in the Kormakitis-Astromeritis area, near Morphou, suggesting that they were of Recent age. The aeolian sediments have all been described as poorly consolidated, mixed sands. These mixed sands on Cyprus are one of two types of Quaternary aeolian sediments, the other being carbonate aeolianites. Carbonate aeolianites have been studied in detail from other parts of the Mediterranean, e.g. Mallorca (Butzer, 1962, 1963, 1975), Israel (Yaalon & Laronne, 1971), Sardinia (Fierro & Ozer, 1974). The Quaternary aeolianites can yield important information concerning environmental conditions, the interaction between tectonic uplift and eustatic sea-level changes and explain the geomorphology resulting after the deposition of these units in southern Cyprus (Plates 2.9 and 2.11; Chapter 2 and Follows, 1990).

### **8.2 GEOGRAPHICAL DISTRIBUTION.**

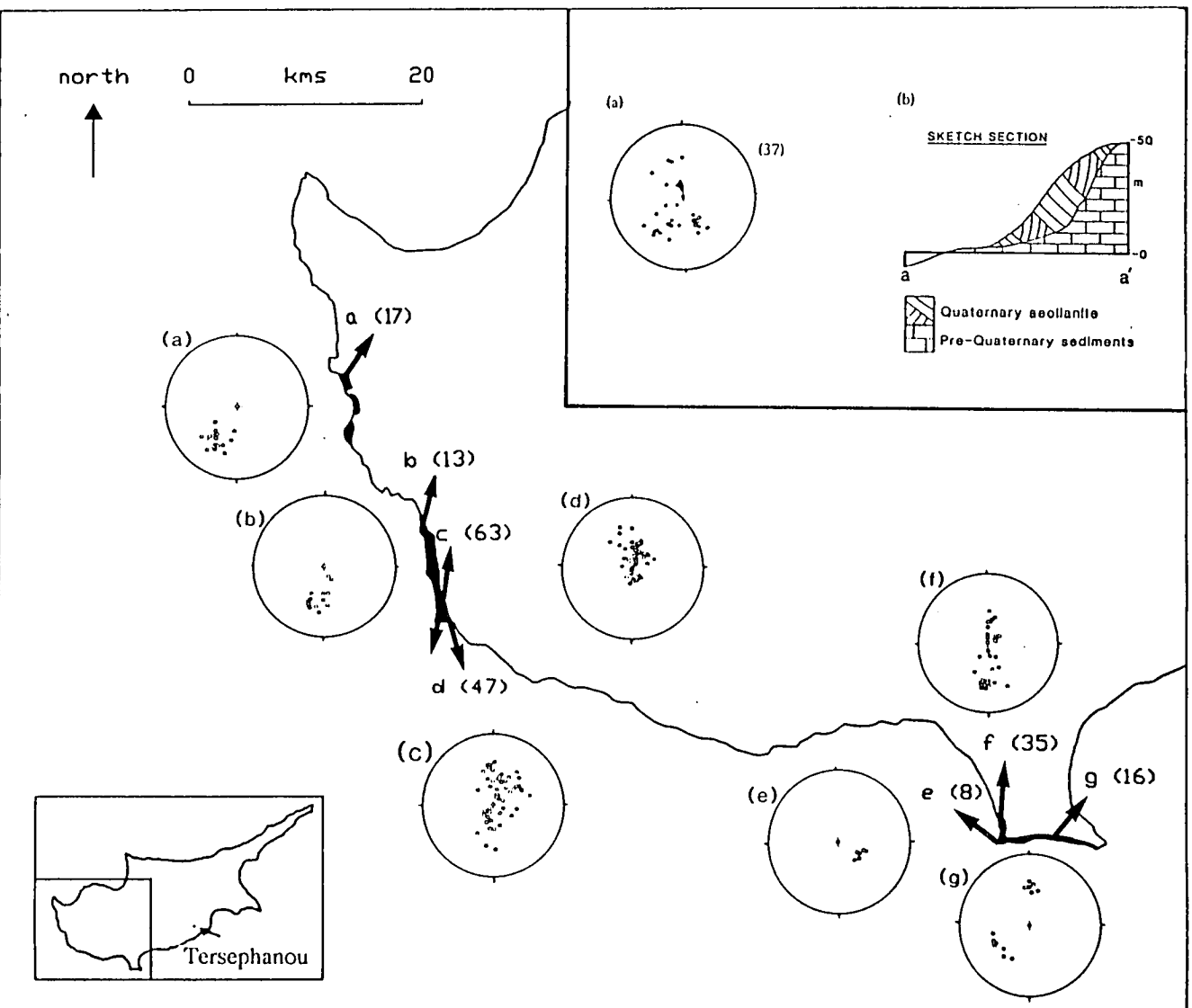
The Quaternary aeolian sequences (as outlined in Chapter 2) are found throughout southern Cyprus. The sequences can be split into two broad categories: those that are dominantly made up of bioclastic sediment and those that comprise mixed clastic detrital and carbonate sediments. Aeolian sediments are not restricted to the lower terraces; they are also preserved away from the present-day coastline and are found associated with the evolution of the F2, F3 and F4 phases of Quaternary development.

The carbonate aeolianites are found in locations away from the influence of major drainage and detrital input, mirroring the locations relating to the formation of the carbonate littoral and sub-littoral sequences (Chapter 7). These sequences crop out along the west coast, north of Paphos, e.g. south of Lara Bay (location 2-30), in Kato Paphos (location 1-57), the south coast of the Akrotiri Peninsula (locations 3-96a and 3-97) and in the far south-east of the island, e.g. Cape Greco (location 1-125) and in the area of Paralimni and Protaras (Follows, 1990).

The mixed aeolian sediments, by contrast, are found in close proximity to the major river courses and associated braid-delta and fluvial sediments, e.g. on the Akrotiri

**Fig. 8.1. Lower hemisphere stereographic plot of poles to planes on foreset dip from aeolianites from southern Cyprus, i.e. palaeocurrent.**

Note: the plot utilized *Wulff* equal angle stereonet, the maximum radius of the circle is equivalent to a dip of 40°. inset (a) a stereographic plot of aeolianites at Tersephanou, (b) a sketch of the outcrop pattern of the aeolianites banking up against the cliff on the south coast of the Akrotiri Peninsula.



Peninsula (location 3-28), south-west of Tersephanou (location 3-18) and above the Vasilikos Valley (McCallum, 1989).

### **8.3 LITHOLOGICAL DESCRIPTION.**

The Quaternary aeolianites crop out either unconformably above Neogene and Quaternary sediments, e.g. Akrotiri (location 3-96a), or form part of a continuous sedimentary sequence, in both fluvial, e.g. the VIb subfacies of the Vasilikos Formation, south of Mari (McCallum, 1989), and regressive littoral environments (Chapter 7). Dunes frequently form isolated topographic highs and also bank up and over palaeocliffs (Fig.8.1; Chapter 2).

The estimated thickness of the aeolianite sequences vary. McCallum (1989) attributed a thickness of 4m for dunes of the Vasilikos Formation, i.e. the possible F1 equivalent at Vasilikos. Moore (1960) stated that dunes in the Kormakitis-Astromeritis area built up by banking against and, locally, over cliffs that are between 20 and 30m high. In the Paphos area (locations 1-57 and 2-40) the dunes form part of the continuous regressive sequence. These are generally less than 15m high and form, low isolated hillocks (Fig.2.20); a similar pattern is seen in the Cape Greco area of south-east Cyprus (location 1-126). The dunes that have formed by banking up against the cliffs along the south and south-west coast of the island, e.g. on the Akrotiri Peninsula (locations 3-28 and 3-96a) and south of Lara Bay (location 2-30), appear to be less than 40m thick. The thickness of these aeolianites reflects the height of the cliff, against which they have formed. The lateral extent of the aeolianites is also dependent on the underlying topography. For example, at Akrotiri the F4 dunes crop out within 100m of the present shoreline, whereas on the west coast and in south-east Cyprus, they bank over the F3 terrace and can be traced inland for hundreds of metres.

The mixed and carbonate aeolianite sequences are both commonly well bedded (cm-thick beds) and laminated. The laminations occasionally show some evidence of fining-up, e.g. in Paphos (location 1-57). The most common structure associated with the aeolianite sediments are planar dune-bedded foresets. Some trough cross-stratification and bedding which dips, "falsely", seaward is also present in the aeolianites that crop out in Paphos and Akrotiri (locations 1-57 and 3-96a respectively; Plate 8.1). The dune-bedded foresets generally dip inland, away from the coast in an arc 45° wide; these foresets generally dip at between 13° and 30°, although beds dipping up to 39° are also seen (Fig.8.1). The "falsely" bedded aeolianites that have banked up against cliffs have steeply dipping foresets, i.e. up to 35°, that dip both landward and seaward, e.g. on the Akrotiri Peninsula (locations 3-28 and 3-96a; Plate 8.1). Truncation structures are also

## PLATE 8.1.

D - Aeolian sands of F4 age banked up against the cliff along the south coast of the Akrotiri Peninsula (location 3-96a); this has resulted in "false" bedding, with foresets dipping steeply towards the south (the right of the plate) away from the cliff, i.e. offshore.

Note: scale is 50cm long.

E - F4 age aeolianites on the south coast of the Akrotiri Peninsula (location 3-96a) dipping both into and away from the cliff, i.e. on and offshore.

F - Steeply dipping foresets of aeolianite, filling a depression in the unconformity surface over the marls and calcarenites of the Athalassa and Nicosia Formation, along the south coast of the Akrotiri Peninsula (location 3-96a); these foresets dip towards the sea, i.e. away from the cliff.

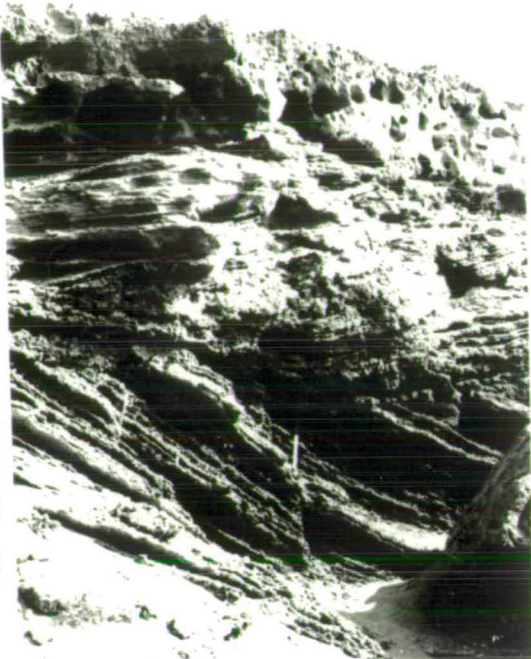
Note: scale is 50cm long.

G - F3/4 aeolianites at Paphos (location 1-57) displaying steeply dipping foresets, truncation surfaces and evidence of extensive rhizocretion structures.

Note: scale is 50cm long.

Plate 8.1

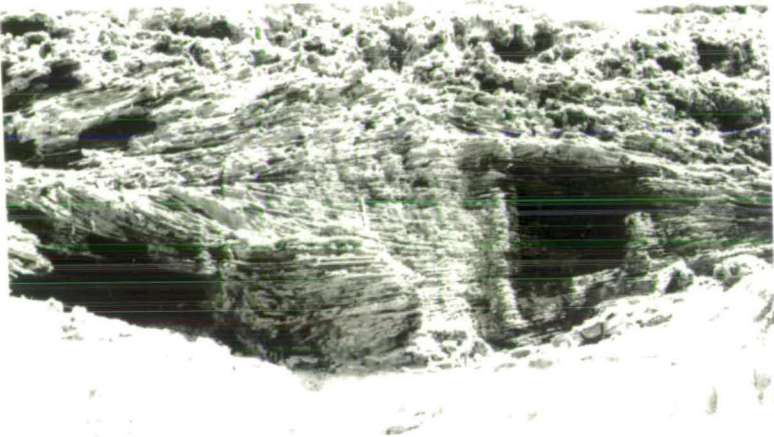
D



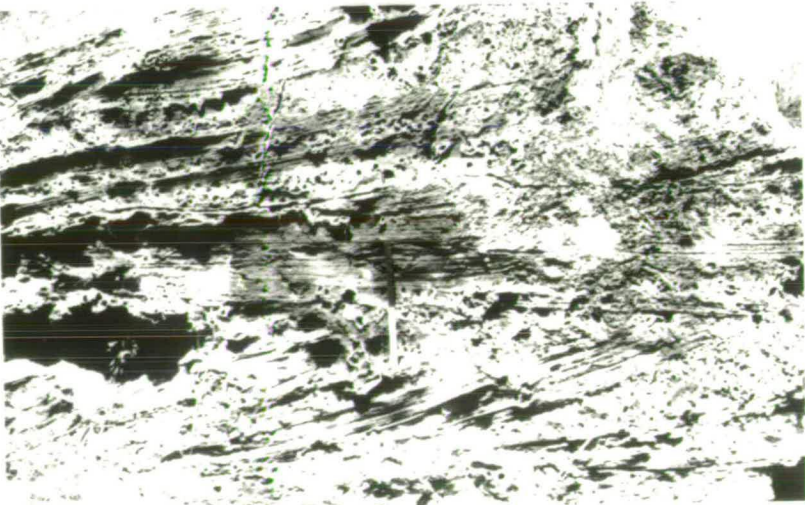
E



F



G



present; these generally dip at less than  $10^\circ$  and are commonly covered by a basal lag of coarse shell fragments and associated climbing ripples, e.g. south-west of Tersephanou (location 3-18) and Paphos (location 2-40; Plate 8.2). Convoluted and distorted dune beds are also present within the aeolianite sequences. These are characteristically located beneath the truncation surfaces, e.g. Paphos (location 2-40; Plate 8.2). Small channels have cut into the dune bedding (location 1-57), causing disruption of the beds. The channel structures are c.20cm wide and have an amplitude of c.10cm.

There is no invertebrate fauna (micro- or macro-) associated with the aeolianites, other than a derived fauna as a result of reworking (Section 8.4). One exception exists: a sample of the terrestrial gastropod *Helix sp.* is found in dunes cropping out at Cape Greco (location 1-125). Carbonate-filled, vertical, tapered, pipe structures, less than 5cm diameter, are present within the carbonate aeolianites. These structures have been calichified and can extend for 2-4m down into the dune sequences, e.g. along the west coast between Lara and Paphos (locations 2-34 and 1-57; Plates 8.2 and 8.3). These pipe structures terminate at truncation surfaces, or the top of the dunes. Similar horizontal pipes cover the truncation surfaces but these, unlike the vertical pipe structure, bifurcate and are clearly tapered (Plate 8.3). These pipes represent rhizocretion, i.e. root, structures. The vertical pipes are probably large taproots, similar to those recorded in Bermuda (Mackenzie, 1964A) and the Yucatan (Harms *et al.*, 1974; Ward, 1975).

The truncation surfaces on the dunes indicate a time of erosion rather than deposition. Rhizocretion structures beneath and parallel to the truncation surfaces suggest that the dunes have been vegetated and bound prior to the continuation of active deposition and dune coalescence. The presence of a coarse shelly lag associated with the truncation surfaces of the aeolianites, e.g. to the south-west of Tersephanou (location 3-18), suggests that dune formation took place in areas proximal to the sediment source and that coarser debris might be rolled across the dune surface, whilst the medium sands, that form the dunes, were being eroded away. The crumpling and contortion of the foresets has been attributed to the degree of sand cohesion, and therefore, the relative moisture of the dunes (Glennie, 1970; McKee & Ward, 1983). The variation in dip of the dune foresets is likely to represent either variation in the rate of cementation of the sediment (Land, 1964) or the presence of vegetation on the dunes, acting as a baffle to prevent migration (Yaalon, 1975). Rapidly cementing dunes are likely to have foresets that dip at a steeper angle and this may explain the variation in dip seen between the mixed dunes and the carbonate dunes, as the carbonate dunes are better cemented. The carbonate dunes also form a hummocky topography (Chapter 2; Plate 2.13) that is not so prevalent within the mixed dunes. The angle of repose of the dunes is also grain size dependent, with a higher angles of dip being associated with coarser sands (Bagnold, 1954). The

PLATE 8.2.

D - F2 age aeolianites in Paphos (location 2-40) displaying a truncation surface above steeply, landward, dipping aeolianites; these are overlain by shallow dipping, highly rhizocreted, well bedded aeolian sands.

Note: scale is 50cm long.

E - Steeply dipping,  $<30^\circ$ , aeolian sands (e) overlain by a truncation surface (f) which in turn is overlain by gently dipping,  $<10^\circ$ , aeolian sands (g). The truncation surface which marks the discontinuity is made up of a stoney lag horizon.

F - Sequence of distorted aeolian foresets (e) beneath a truncation surface and well bedded aeolian sands from F2 aeolianite sequence in Paphos (location 2-40).

Note: lens cap for scale.

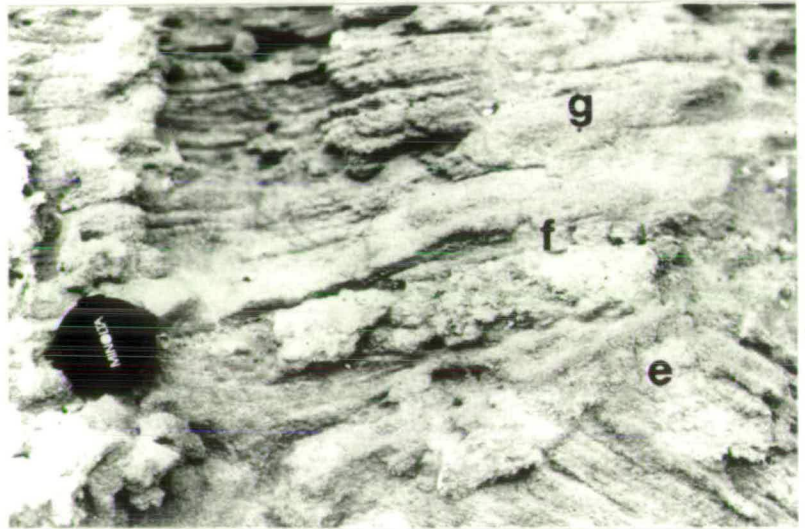


Plate 8.2

D



E



F



**PLATE 8.3.**

D - Horizontal rhizcretion structures preserved on a bedding plane of the F3/F4 aeolianite in Paphos (location 1-57).

Note: the tapered nature of the structures indicated by the arrows.

E - A thin section micrograph of mixed aeolian sands from Tersephanou (location 3-17; sample C48/89). The blue resin indicates the degree of porosity of these sands.

Note: the micrograph represents a field of view 12mm long.

F - A thin section micrograph of the F3/F4 aeolian sands from Cape Greco (location 1-125). The absence of blue resin and the abundance of micrite suggests that the porosity has been reduced as a result of caliche formation.

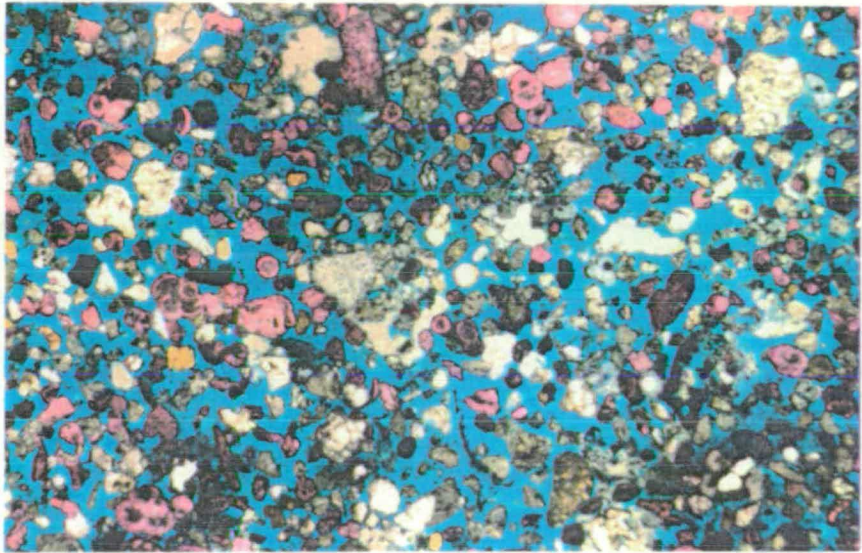
Note: the micrograph represents a field of view 12mm long.

# Plate 8.3

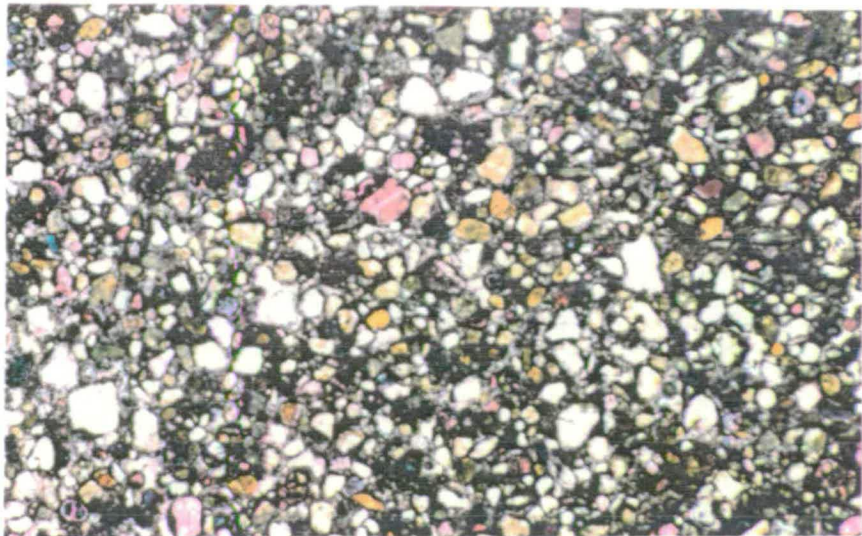
D



E



F



moderately sorted nature of the medium dune sands that crop out in southern Cyprus fit this criteria by displaying generally steeply dipping foresets.

## **8.4 PETROLOGY.**

### **8.4.1 The mixed clastic aeolianites.**

The mixed clastic aeolianites, like the shallow marine siliciclastic sequences (Chapter 6), crop out in areas of extensive fluvial systems. The green and brown coloured sands that form these dunes are made up of mixed Troodos derived grains and grains derived from the local sedimentary sequences. Abraded shell debris is seen; this includes whole foraminiferal tests. McCallum (1989) stated that the sands from the Vasilikos Formation (facies VIb) are fine-grained and well sorted. The results obtained by McCallum (1989) do not conform to those obtained along the south coast of Cyprus for mixed clastic aeolianites during this study. Dry sieving indicates that the mixed clastic aeolianites of southern Cyprus are moderately to moderately-well sorted sands, although well sorted sands are locally present. A mean and median grain size of medium and fine sand respectively, with a symmetrical to very positively skewed distribution, indicates that few fractions finer, and none coarser, than the mean are seen (Table 8.1; Fig.8.2a and b). Dry sieved samples of sand from deltaic and beach environments are generally finer, i.e. fine sand to very fine sand, and commonly better sorted (Table 8.1), with symmetrical, positive and negative skews.

The grainsize analysis, although limited, indicates that the delta and beach sands, which are likely to be one source of sediment for the Quaternary mixed dunes, are generally better sorted and finer-grained than the dune sands (Fig.8.2a and b). Sorting and grainsize varies across a single dune and between two localities less than 1km apart, i.e. Akrotiri (locations 3-96 and 3-96a). These variations arise as a result of local hydrodynamic conditions and the local sediment source. The evidence indicates that the mixed dunes are generally sub-mature, moderately-well sorted and form from fine to medium sands. This evidence also suggests that only limited transport, probably by means of saltation, and sorting of the sediment has taken place, with the sediment being derived from the local fluvial, or exposed beach and deltaic sequences (Chapters 5 and 6).

The Troodos-derived dark coloured portion of the sand is generally sub-mature, with sub-angular to sub-rounded grains. The sedimentary clasts and shell fragments are generally more rounded than the Troodos clasts. The maturity of the Troodos-derived grains increase as successively smaller size fractions were examined, but never exceeded the mature and rounded stage. These results agree with that found in the Kormakiti-

Table 8.1. Grain size analysis of Quaternary mixed clastic aeolianites.

| Location              | Sample | Mean grainsize | Medium grainsize | Sorting    | Skewness    | Environment               |
|-----------------------|--------|----------------|------------------|------------|-------------|---------------------------|
| Akrotiri (3-96)       | c69/89 | 1.68           | 1.59 (MS)        | 0.65 (MWS) | 0.19 (PS)   | Aeolian                   |
| Akrotiri (3-96)       | c68/89 | 2.46           | 2.57 (FS)        | 0.96 (MS)  | -0.08 (S)   | Aeolian                   |
| Tersephanou (3-17)    | c48/89 | 1.85           | 1.43 (MS)        | 0.52 (MWS) | 0.77 (VPS)  | Aeolian                   |
| Petounda Point (3-10) | c36/89 | 1.88           | 1.92 (MS)        | 0.86 (MS)  | -0.06 (S)   | Aeolian                   |
| Mazotos (3-16)        | c46/89 | 2.88           | 2.74 (FS)        | 0.42 (WS)  | 0.24 (PS)   | Aeolian                   |
| Maroni (3-31)         | c85/89 | 2.79           | 2.84 (FS)        | 0.56 (MWS) | -0.03 (S)   | ? Aeolian                 |
| Petounda Point (3-10) | c34/89 | 2.00           | 2.05 (FS)        | 0.68 (MWS) | -0.10 (NS)  | Coastal dune              |
| Xylophagou (2-82)     | sp590  | 3.18           | 3.19 (VFS)       | 0.65 (MWS) | -0.09 (S)   | Delta/beach*              |
| Ormidhia (2-79)       | sp572  | 2.20           | 2.62 (FS)        | 0.89 (MS)  | -0.36 (VNS) | Deltaic laminated sand*   |
| Ormidhia (2-79)       | sp569  | 2.98           | 3.00 (VFS)       | 0.57 (MWS) | -0.01 (S)   | Deltaic mature sand*      |
| Mazotos (3-13)        | c65/89 | 2.89           | 2.57 (FS)        | 0.40 (WS)  | 0.74 (VPS)  | Deltaic mature sandstone* |
| Petounda Point (3-10) | c35/89 | 2.38           | 2.37 (FS)        | 0.44 (WS)  | 0.02 (S)    | Modern beach sand         |

Note: All data are recorded to 2 decimal places.

Phi units are used throughout (where  $\Phi = -\log_2 d$  ( $d$  = diameter of grain in millimetres; after Krumbein, 1934).

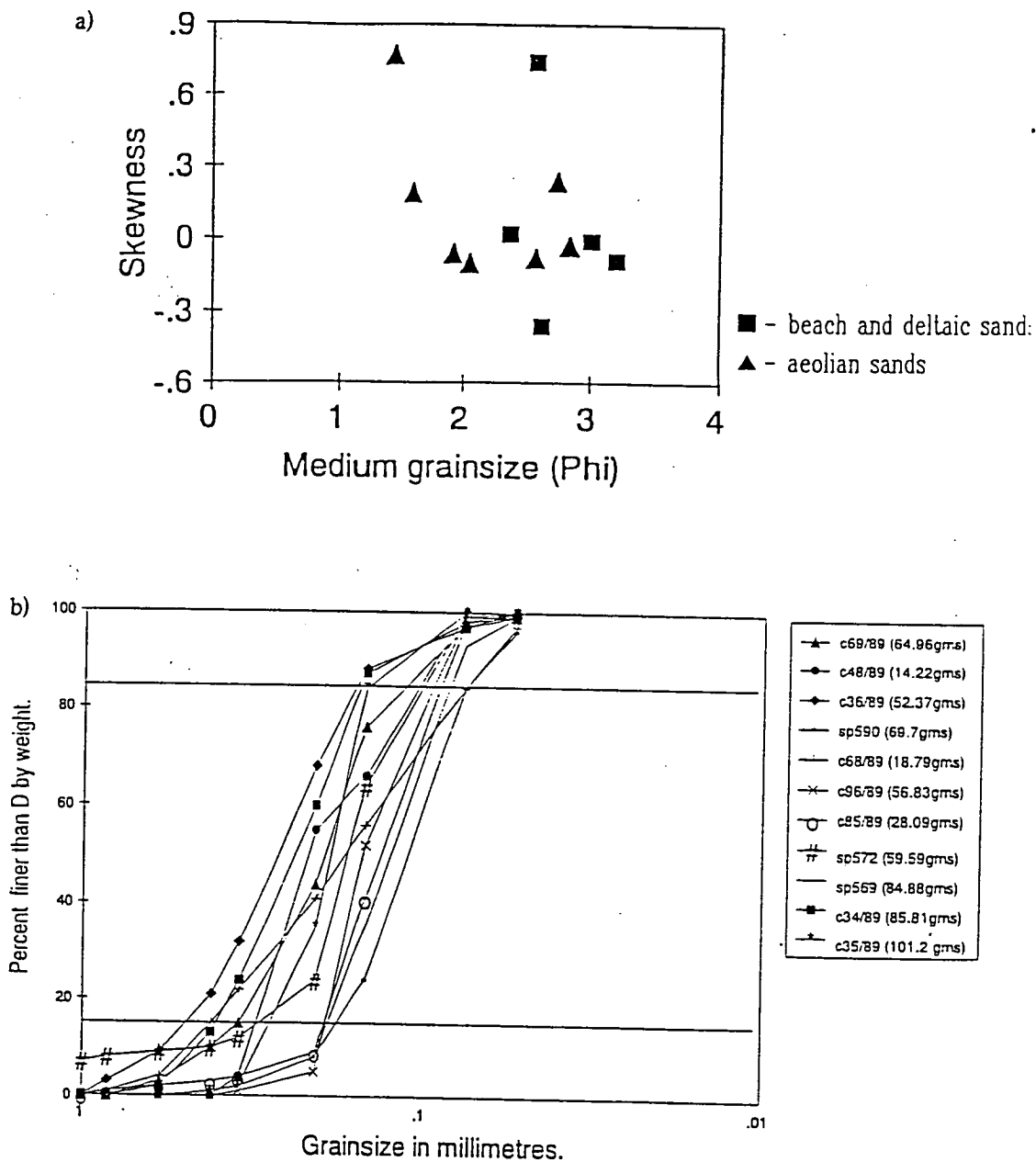
\* - see Chapter 6 for details of sedimentary environment.

Grainsize - MS = medium sand, FS = fine sand, VFS = very fine sand.

Sorting - MS = moderately sorted, MWS = moderately well sorted, WS = well sorted.

Skewness - VPS = very positive skew, PS = positive skew, S = symmetrical, NS = negative skew, VNS = very negative skew.

Fig.8.2. a) Skewness versus medium grainsize plots of beach/delta and mixed clastic aeolianite sediments from outcrops in southern Cyprus; b) plot of grainsize distribution of mixed clast aeolianites from southern Cyprus.



Astromeritis area (Moore 1960), where the sands are yellow, medium grained and poorly sorted.

The mixed aeolian sediments have a submature appearance in thin section. The clasts are dominated by the presence of igneous clasts, derived from the Troodos, e.g. diabase and pillow lava, and locally-derived sediments, e.g. chalk; Table 8.2. The majority of allochems present within the mixed aeolianites, e.g. planktonic and benthic foraminifera, are reworked from pre-Quaternary chalks and limestones although the presence of red algae and abraded and well worn molluscan shells (Plate 8.3) repeats that seen in the Quaternary littoral sequences (Chapter 7), and are therefore likely to be primary, rather than secondary reworked allochems. The mixed clastic aeolianites have a clast to porosity and cement ratio of c.1:1 (Table 8.2). These mixed aeolianites are poorly cemented, with point counting revealing cement to porosity ratios between 1:8 and 1:3 (Table 8.2). Examination of the samples from locations 3-96 and 3-17 suggests that these sediments are bound by the formation of caliche. Ramifying rhizocretion structures preserved in these sediments (Section 8.3) have also been calichified (Plates 8.1 and 8.3).

#### **8.4.2 Carbonate aeolianites.**

Petrographic studies of the carbonate aeolianites show that these units are dominated by the presence of reworked allochem grains of red algae, molluscs, benthic and planktonic foraminifera, coral, echinoid and bryzoan fragments. The grains are usually less than 0.5mm in diameter, broken and abraded, although locally samples are coarser than this, with grains up to 1.5mm in diameter, e.g. sample E1 from the Cape Greco area. Reworked local sedimentary clasts and fossils are present within the sediments, as are igneous clasts, although these are generally a minor component (Table 8.2). The grains commonly have a sub-rounded to sub-angular shape and are moderately to quite-well sorted. The sediments frequently have a corroded appearance in thin section. Point counting of the thin sections shows the variation in components between mixed and carbonate aeolianites (Table 8.2).

The carbonate aeolianite are generally better cemented than the mixed aeolian sediments, although the extent of cementation in the carbonate aeolianites does vary. The ratio of clasts to cement and porosity is frequently 1:1 but the ratio of porosity to cement can vary from c.3:1 to 1:1 (Table 8.2). The type of cement varies considerably between different carbonate aeolianite sequences, for example pendant and meniscus cements of fine spar are present in samples of aeolianite from Paphos (sample 17). Micrite envelopes are generally absent. Calcitization of some shell structures is seen whereas others remain as fresh unaltered aragonite. A secondary moldic porosity has also locally developed

Table 8.2. Point count data from the Quaternary aeolianite sequences of southern Cyprus.

| Location and sample number         | Type of aeolianite | Recent and reworked allochems | Igneous clasts | Porosity | Cement   | Total | Ratio of clasts to porosity | Ratio of porosity to cement |
|------------------------------------|--------------------|-------------------------------|----------------|----------|----------|-------|-----------------------------|-----------------------------|
| Paphos (1-57)<br>sp.28             | C                  | 255 (49)                      | 25 (5)         | 125 (24) | 123 (23) | 528   | 1:1                         | 1:1                         |
| Paphos (1-51)<br>sp.17             | C                  | 246 (49)                      | 3 (1)          | 170 (34) | 82 (16)  | 501   | 1:1                         | 2:1                         |
| Cape Greco<br>sp.B                 | C                  | 252 (50)                      | 6 (1)          | 160 (32) | 82 (16)  | 500   | 1:1                         | 2:1                         |
| Cape Greco<br>sp.                  | C                  | 235 (47)                      | 11 (2)         | 178 (36) | 76 (15)  | 500   | 1:1                         | 2:1                         |
| Cape Greco<br>sp.                  | C                  | 200 (40)                      | 73 (14)        | 113 (23) | 114 (23) | 500   | 1:1                         | 1:1                         |
| Cape Greco<br>sp.                  | C                  | 251 (50)                      | 6 (1)          | 102 (20) | 142 (28) | 500   | 1:1                         | 1:1                         |
| Emba (2-17)<br>sp.350              | C                  | 213 (44)                      | 56 (11)        | 104 (21) | 117 (24) | 500   | 1:1                         | 1:1                         |
| Cape Greco (1-125)<br>sp.163       | C                  | 263 (52)                      | 15 (3)         | 153 (31) | 69 (14)  | 500   | 1:1                         | 2:1                         |
| Petounda Point (3-11)<br>sp.C42/89 | M                  | 162 (32)                      | 136 (27)       | 179 (36) | 23 (5)   | 500   | 1:1                         | 8:1                         |
| Tersephanou (3-17)                 |                    |                               |                |          |          |       |                             |                             |

Note: Sp. - sample number  
M - mixed  
C - carbonate  
Numbers in brackets are percentages.



(Plate 8.3) The same pattern of cementation is seen in the aeolianites from Cape Greco (location 1-126; sample B-E1) and Emba (location 2-17; sample 350), where porosity levels are high. Sample 28, also from Paphos, has a 1:1 porosity to cement ratio (Table 8.2), dissolution and calcitization of the molluscan shell structures is high and secondary porosity is prevalent (Plate 8.3), as is the development of pore-filling spar cement. Some micrite envelopes are present and syntaxial overgrowths are locally seen associated with fragments of echinoids. The pattern of cementation is patchy, with well cemented areas lying alongside areas of higher porosity. The cements from both the carbonate and mixed aeolianite sequences are non-ferroan calcite.

The variation in cementation and preservation of original mineralogy and structure reflects two components of the formation of the dune structures:

- i) the preservation of micrite envelopes, calcitized shells and fringing cements associated with locally derived, reworked allochems characterizes cementation in the marine phreatic zone,
- ii) the fringing and pore-filling spar, as well as the development of secondary, moldic, porosity delineates diagenesis in the meteoric realm. The variability of meteoric diagenesis, both locally and at different points on the island, represents the movement of groundwater through the aeolianites. The development of pore and fringing spar, along with the establishment of a secondary moldic porosity, indicates active diagenesis within the phreatic and vadose meteoric realm.

Poorly cemented sediments, containing allochems, that retain their original shell structure indicate a position in the vadose zone away from the areas of active diagenesis, similar to that recorded in Section 7.4.3. The scant cement reflects either rapid movement of the unit away from the active diagenetic realm or the complete absence of the unit from areas of active diagenesis, similar to that recorded by James & Choquette (1984).

### **8.5 PALAEOCURRENT DATA.**

The palaeocurrent data (Fig.8.1) represents measurements collected from both the mixed and carbonate Quaternary aeolian sequences. The azimuth modal data for locations (Fig.8.1) are shown in Table 8.3.

Additional data were collected by Follows (1990) for Quaternary carbonate aeolianite sequences in south-east Cyprus (Fig.8.3) and from the dunes associated with the Vasilikos Formation, a mixed aeolianite sequence, where a predominantly south-westerly wind has been suggested (McCallum, 1989). The present day surface winds in the area of Cyprus vary throughout the year. A high percentage of northerly and

northeasterly winds, with an average wind speed of 12-17 knots, blow during the winter. Southwesterly winds predominate throughout the rest of the year, with the average wind speeds varying between 5-13 knots (U.S. Navy Report, 1985, Fig.8.4).

Table 8.3. Foreset data collected from the Quaternary aeolianite sequence from southern Cyprus.

| Location | Number of readings | Mean foreset dip | Vector mean (deg) | Magnitude of vector |
|----------|--------------------|------------------|-------------------|---------------------|
| 1-57     | 81                 | 16               | 076               | 17%                 |
| 2-10     | 34                 | 25               | 161*              | 92%                 |
| 2-12     | 35                 | 21               | 169*              | 43%                 |
| 2-27     | 70                 | 17               | 270*              | 31%                 |
| 2-32     | 18                 | 30               | 033               | 93%                 |
| 2-35     | 10                 | 31               | 067               | 92%                 |
| 2-40     | 47                 | 13               | 023               | 33%                 |
| 3-18     | 37                 | 21               | 033               | 34%                 |
| 3-29     | 30                 | 23               | 005               | 38%                 |
| 3-96     | 10                 | 19               | 300               | 98%                 |
| 3-96a    | 19                 | 28               | 299               | 41%                 |
| 3-101    | 13                 | 27               | 004               | 95%                 |
| EF1      | 40                 | --               | 086               | 41%                 |
| EF2      | 15                 | --               | 005               | 61%                 |

Note: EF1 and EF2 - after data taken from Follows (1990) from south-east Cyprus. EF1 is a location close to Protaras and EF2 is a site west of Cape Greco (these data are shown in Fig.8.3). The magnitude of the vector indicates a level of confidence in the result; for example a low magnitude vector may be indicative of bimodal dipping foresets (location 3-96a; Fig.8.1).  
\* - data indicate seaward dip of foresets.

The palaeowind system during the Quaternary is thought to have been zoned into belts similar to that recorded today (Opdyke, 1961); evidence from Bermuda (Mackenzie, 1964B) supports this argument. Data collected from the Gargaresh calcarenite in Libya (Hoque, 1975) and from the Pliocene to Holocene age aeolianites on the Mediterranean coast of Israel (Yaalon & Laronne, 1971) are in general agreement with Opdyke (1961). Hoque (1975) states that anomalies seen in the azimuth modes probably result from changes in the palaeowind that could possibly complement Quaternary climatic changes.

The vector data collected from Cyprus indicate that the wind direction during the latter part of the Quaternary (represented by the data collected from locations 1-57, 2-35,

Fig.8.3. Rose diagrams of palaeocurrent data from the Quaternary carbonate aeolianite sequences in south-east Cyprus (after Follows, 1990).

Note: area of palaeorelief.

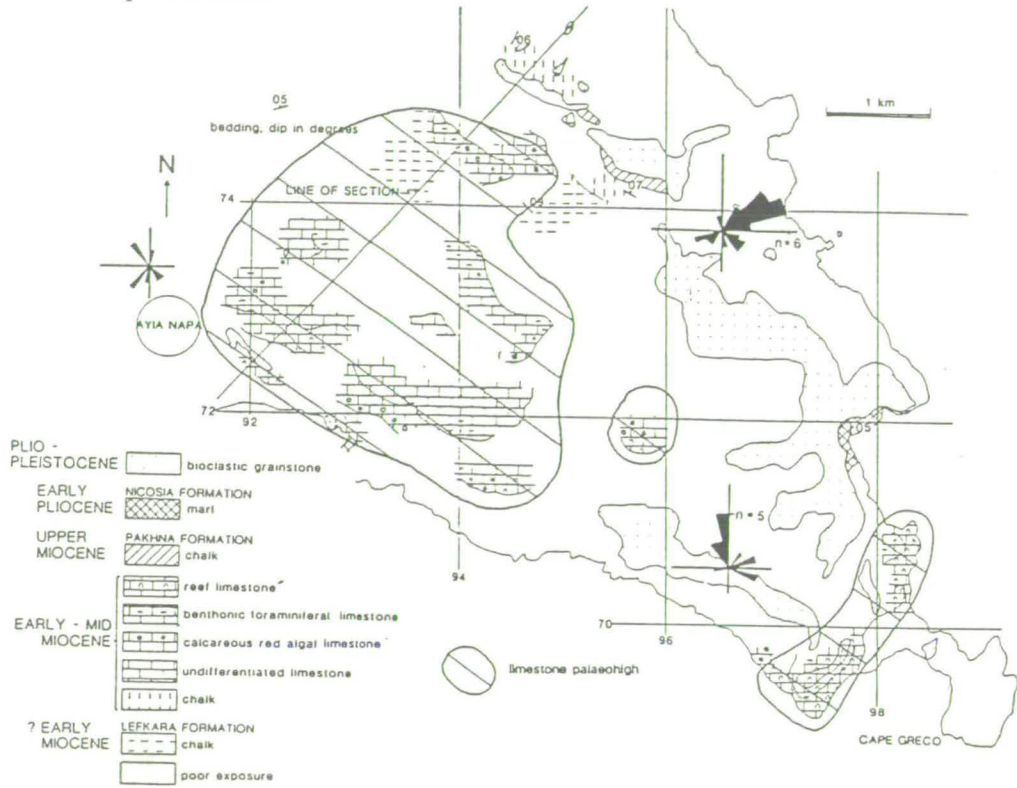
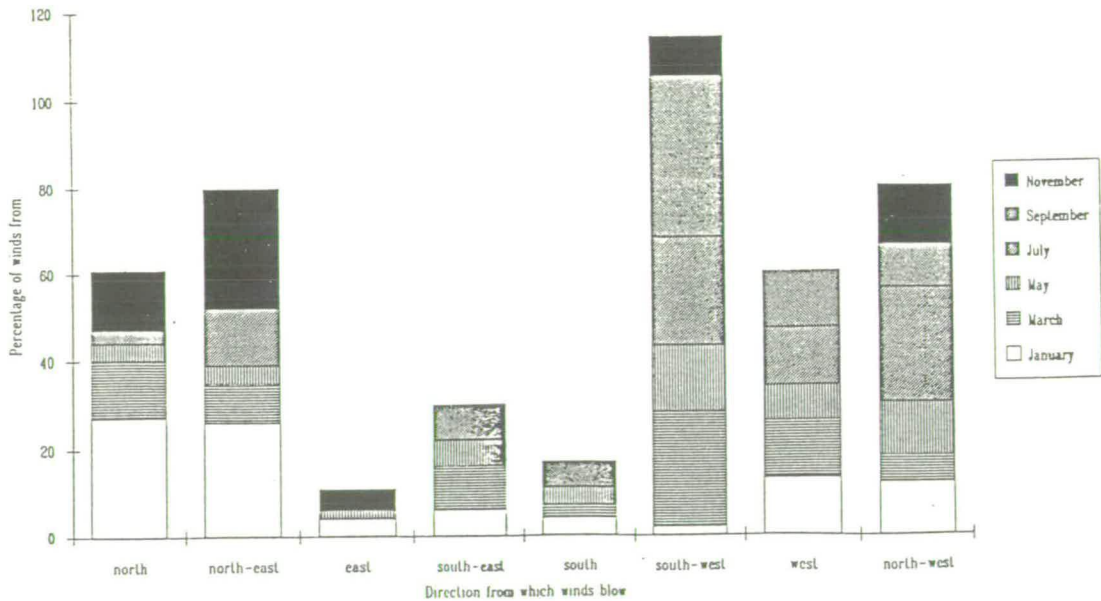


Fig.8.4. Cumulative annual surface winds in the present day eastern Mediterranean (after U.S. Navy Report, 1985).

Note: the chart takes account of winds of force 2-9 on the Beaufort scale, the residue of the winds are made up of calms and those of force 1, or less.



2-40, 3-29, 3-91, 3-96, 3-96a, 3-101, EF1 and EF2) was similar to that seen today, with onshore winds coming from the south and south-west. The data collected from the Tersephanou area (location 3-18) shows the same characteristics, these dunes forming from mixed sediment along the south coast of the island (Fig.8.1). Follows (1990) has suggested that the outcrop pattern and the palaeocurrent data from the aeolianites in the south-east of the island indicate funnelling of the wind through gaps in the relief (Fig.8.3). This is probably correct but the azimuth modes also indicate a prevailing south to south-westerly wind, reflecting that seen elsewhere, during the Quaternary. Relief has also affected the data collected at Akrotiri (locations 3-97, 3-96, 3-96a), where the vector mean value has been influenced by dunes banking up against cliffs and the development seaward dipping foresets (Plate 8.1). The vector means at some localities in the Paphos area (locations 2-10, 2-12 and 2-27) indicate a seaward palaeocurrent direction. The steeply dipping, largely unfossiliferous grainstones that crop out at these locations, which were discussed in Chapter 7, probably represent part of the littoral sequence, rather than the aeolianite sequence, although their character is similar to other carbonate aeolianites cropping out at in the Paphos area (locations 2-40 and 1-57). Aeolianite sequences do crop out above littoral sequences in the F2 terraces in Paphos (location 2-5 and 2-40); field evidence from location 2-10, i.e. steep dipping foresets (Plate 7.4), suggests that a similar relationship may exist at this location, although the high magnitude vector of foresets dipping to the south, may indicate otherwise. The consistency of the palaeocurrent data from Paphos and other areas supports the argument for these sands being deposited in a littoral, rather than aeolian regime. This highlights one of the problems associated with the identification of aeolianites, as many aeolianite sequences may have been misidentified because of the similarity between littoral and dune sands (Scholle *et al.* 1983). Knowledge of the palaeocoastline, from sedimentological and geomorphological studies (Chapter 7 and 2 respectively) and previous studies of the Quaternary palaeowind direction in the eastern Mediterranean basin (Yaalon & Laronne, 1971; Hoque, 1975), aid the interpretation of Quaternary aeolianite sequences in Cyprus.

## **8.6 RECENT DUNE FORMATION.**

Aeolian dune formation has taken place during the Holocene and Recent. Dunes have developed in the area of the Lamaca Salt Lake and engulfed the Hellenistic/Roman aqueduct that fed Kition, ancient Lamaca, during the period between 400-700 A.D. (Bagnall, 1960; Gifford, 1978). Recent dunes have also developed to the east of Morphou Bay (Wilson, 1957; Moore, 1960) where they have blown up against, and locally over, coastal cliffs, which vary from 20 to 30m high. A third area of Recent dunes formation on the west coast of the island, the area of Lara Point, north of Paphos, was observed

during this study. These dunes are less than 20m high and appear to be banked up against Miocene age chalks.

### **8.7 DISCUSSION AND CONCLUSIONS.**

Very few pre-Quaternary aeolianites have been interpreted as such (McKee & Ward, 1983); this situation arises from the difficulty of distinguishing between aeolian and other nearshore sediments, as they have a very similar composition and characteristics (Glennie, 1970; Section 8.4). The Quaternary Gargaresh Limestone in Libya has been attributed to both a marine and continental environment (Hoque, 1975), as the littoral sands are so similar to aeolian deposits. The same situation arose during this study with sands at locations 2-10, 2-12 and 2-27 having the same characteristics as the aeolianites. The following criteria have been used during this study to distinguish aeolian sediments from littoral sequences:

- i) a lack of fauna, except derived marine material,
- ii) rhizcretion structures,
- iii) fine laminated, cross-stratified sands that have steeply dipping foresets that dip predominantly landward, in agreement with palaeo-wind data,
- iv) geomorphological evidence, e.g. banking up against previously formed cliffs, and forming small topographical features.

The characteristics of the mixed clastic aeolianites made their environmental interpretation easier, as they crop out banked up against palaeo-cliffines, e.g. at Akrotiri (location 3-28), or above deltaic and fluvial sequences, e.g. near Tersephanou (location 3-18), in an environment where the sedimentary sequence shows a relative regression.

It was not possible to use the maturity, the sorting, or the fauna (other than the presence of non-marine gastropods) as an indicator of whether a particular outcrop formed in a marine or aeolian environment, as the sediment is characteristically moderately sorted and sub-mature, and very little transport from the source of the sediment has taken place. It is likely that the elapsed time between the deposition of the marine sand and the formation of the dunes was short, allowing minimal time for sorting, or increased maturity. The sand reservoir for dune formation is also the primary sand of the littoral environment, so the composition of one will mirror the other. These factors are common to many Quaternary aeolianite sequences (e.g. Butzer, 1975; Hoque, 1975).

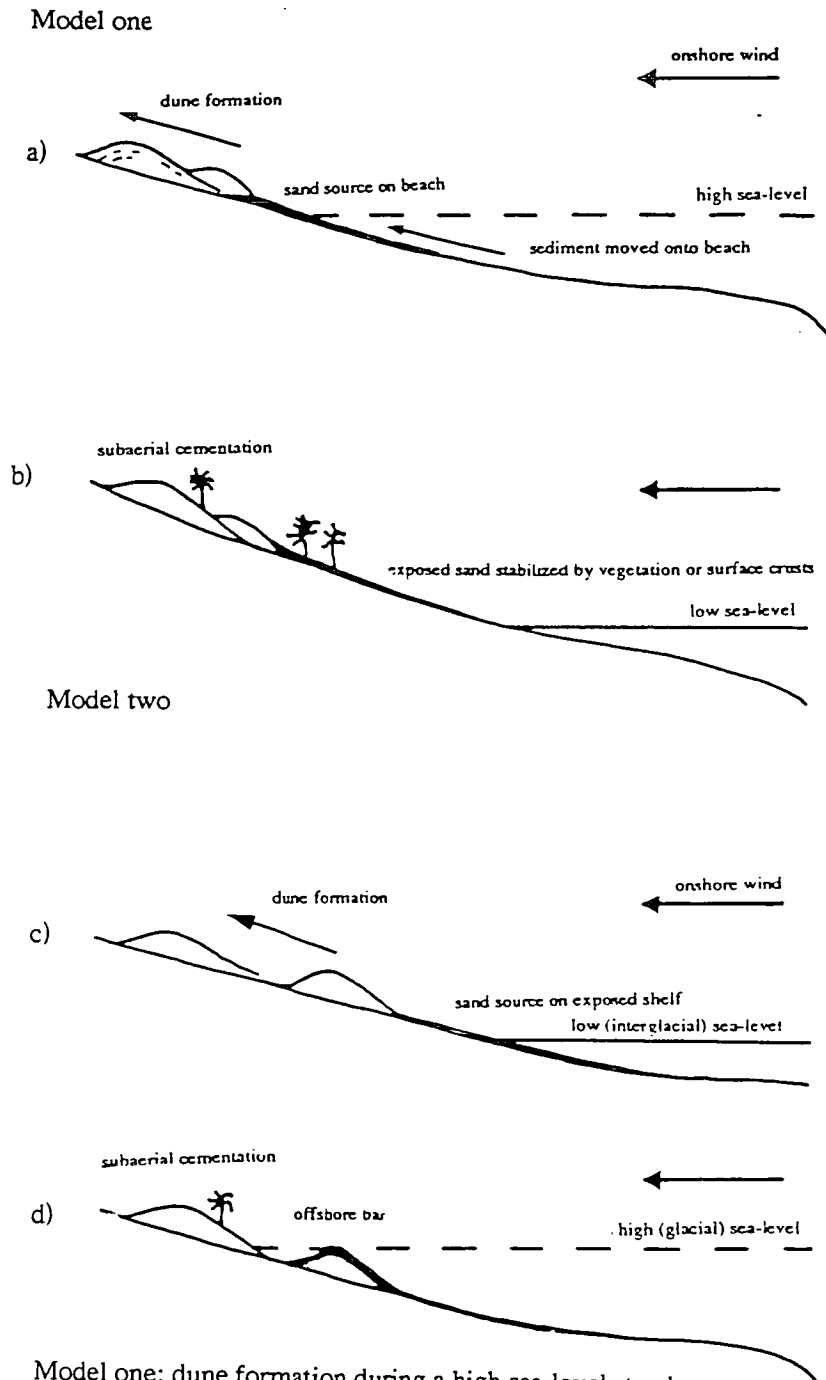
## **8.8 MODEL OF FORMATION OF THE CARBONATE AEOLIANITES.**

The formation of aeolianites in Cyprus is dependent on three factors: wind, sand supply and vegetation. Climate is not an important factor influencing dune formation, as aeolianite formation takes place under very varying climatic regimes: arid (Inman *et al.*, 1966), temperate (Messenger, 1958) and humid with high rainfall (Cooper, 1958). The dense vegetation in the humid tropics generally prevents dune formation and chemical action rapidly weathers the carbonate aeolianites (Jennings, 1964). The presence of vegetation is an important factor in the preservation of aeolianites, as this provides a baffle to the wind, and binds the sediment together (Yaalon, 1975).

The timing of formation of Quaternary coastal aeolian dunes has been the subject of much debate. Two models of dune formation, relative to eustatic sea-level changes, have been suggested (Fig.8.5). Bretz (1960), Land *et al.* (1967) and Vacher (1973) support the concept that dune formation takes place during a eustatic sea-level high (Fig.8.5a and b). Sayles (1931), Fairbridge & Teichert (1953) and Maud (1968) argue that dune formation occurs during a low sea-level stand (Fig.8.5c and d), when a more arid, glacial, climate existed (Rognon & Williams, 1977; Sarnthein, 1978). A third model (Sarbaris *et al.*, 1962; Hey, 1962) suggests that dunes develop between model one and two, following a sea-level maxima as sea-level dropped (Fig.8.5a and c). The third model is favoured for the Quaternary carbonate aeolianite formation in Cyprus; it has also been the preferred interpretation of Quaternary dune formation elsewhere in the Mediterranean (Hey, 1962; Sabaris *et al.*, 1962; Butzer, 1975). The following evidence from the coastal Quaternary aeolianite sequences on Cyprus supports the third model:

- i) rapid cementation of the littoral sequences has taken place in the phreatic and meteoric realms (Section 7.4.3), yet carbonate aeolianites are present, this suggests that dune formation happened soon after the deposition of the littoral sequences,
- ii) the littoral sequences were deposited in a regressive regime (Chapter 7); aeolianite deposition marks the continuation of these regression events,
- iii) the presence of meteoric cements in the carbonate aeolianites shows that cementation occurred in a sub-aerial environment and not in the marine realm, as a result of a rising sea-level, as suggested by the formation of dunes during a sea-level minima (Fig.8.5c and d),
- iv) the U-series dates (Chapter 3) from the littoral sequences indicate that they have formed during a eustatic sea-level maxima. The dunes lie conformably above these sequences, suggestive of a continuous succession to a sea-level low, i.e. regression,
- v) the coastal geomorphology of the west coast (Chapter 2) indicates that the cemented dunes that formed after the isotope 7 sea-level high, i.e. associated with the

Fig.8.5. Models of carbonate dune formation (after Gardiner, 1984).



Model one: dune formation during a high sea-level stand.

- (a) Dunes form during period of high sea-level
- (b) Cementation and weathering takes place during a low sea-level stand

Model two: dune formation occurs during a low sea-level stand.

- (c) Large tracts of sand exposed to wind action during the low sea-level stand, i.e. glacial, periods of greater aridity in low latitudes, results in dune formation
- (d) Sand supply is more restricted during the periods of sea-level maxima, i.e. interglacials; this restricts dunes formation and results in dune stabilization, cementation and weathering.

F3 terrace development, were subsequently cut, to form a cliffline, by the 5e sea-level high, i.e. the development of the F4 terrace. This evidence suggests that aeolian formation and cementation took place between the two eustatic sea-level highs,

vi) the amount of sediment needed for dune formation along the south coast of the Akrotiri Peninsula and along the west coast, north of Paphos, is too great to have been present during a high sea-level. A lower sea-level during glacial periods, down to possibly 120m beneath the present day sea-level (Shackleton *et al.*, 1984), would leave an ample reservoir of sediment available for dune formation,

vii) the presence of derived bioclastic sediment and abraded shells and tests in the coastal carbonate aeolianites, identical to those seen in the underlying littoral sequences, indicates that the carbonate dunes were derived from previously deposited littoral sediments.



## **Chapter Nine: Quaternary caliche and palaeosols: their formation and development.**

### **9.1 INTRODUCTION.**

Caliche and palaeosol development in southern Cyprus was extensive during the Quaternary. These lithologies were overlooked in the past and, though not a major area of research during this study, yield important data concerning both the Quaternary climate and sedimentary environments. This chapter has three aims:

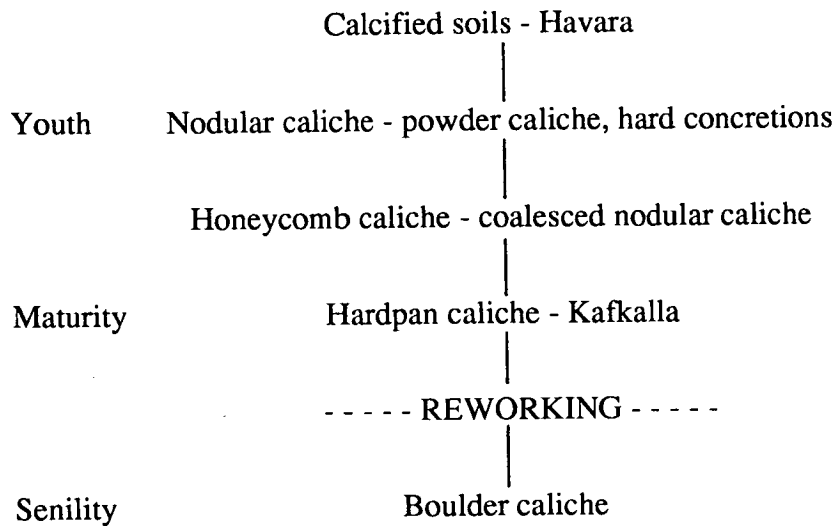
- i) to outline the extent and nature of the caliche deposits found in southern Cyprus, adding to the work of Pantazis (1973), and describe field relationships, mineralogy and chemistry,
- ii) to produce a model of formation of the caliche formations in Cyprus,
- iii) to compare the caliche types, and mode of formation on Cyprus, with ancient and modern examples described in the literature.

A caliche, or calcrete, is a fine grained secondary carbonate (Tucker & Wright, 1990). The caliche deposits of Cyprus have previously been split into two divisions according to the characteristics of these secondary limestones: havara, which is a soft calcareous deposit and kafkalla, which is a hard calcareous crust.

The caliche horizons of Cyprus were described (Wilson, 1957; Gilliland, 1960; Dreghorn, 1978) as forming near the surface. Gass (1960) stated that caliches probably formed beneath soil cover and that their formation was not necessarily dependent on the presence of a carbonate bedrock. Pantazis (1973) studied the formation of caliche in more detail, concluding that the havara was a freshwater limestone and kafkalla formed due to hardening of the havara. Pantazis (1973) also interpreted the thickening of the kafkalla as being related to both microclimatic conditions and the ability of the havara to retain water within a perched water table. Thus the groundwater was oversaturated with respect to  $\text{CaCO}_3$  and precipitated a hard crust on exposure, the kafkalla. Pantazis (1973) suggested that the formation of havara resulted from freshwater deposition of locally-derived carbonate horizons.

Studies of caliche from South Africa (Netterberg, 1967), south-western USA (Machette, 1985), the Kalahari desert (Watts, 1980) and a review of caliche formation (Goudie, 1973; Tucker & Wright, 1990) all suggest that an ideal caliche stratigraphy exists (Figs.9.1 and 9.2).

Fig.9.1 Caliche stratigraphy after Netterberg (1967).



Models of caliche formation stress five criteria that must be satisfied for caliche formation to occur (Goudie, 1973; Watts, 1980; Wright, 1990):

- i) a semi-arid climate with rainfall in the order of 40-60cm, although caliche does form in areas where the annual rainfall is greater than 60cm,
- ii) a source of  $\text{CaCO}_3$ ,
- iii) a relatively stable environment in areas away from active sedimentation,
- iv) the presence of groundwater to allow capillary action to take place,
- v) a period of stability when the accretion rate of the caliche exceeds the rate of sedimentation. If sedimentation rates are greater than caliche accretion rates, then either caliche formation is poorly developed and immature, or does not take place (Fig.9.3).

## 9.2 DISTRIBUTION OF CALICHE IN CYPRUS.

Pantazis (1961) showed the distribution of caliche horizons (Fig.9.4), but this map failed to include caliches capping exposed limestones and many other lithologies, e.g. the extensive calichification of the Mesaoria Plain. However, caliches do not commonly cap units of the Troodos ophiolite. Caliche horizons are also preserved within the sedimentary sequence as in the Messinian sequences (Orszag-Sperber *et al.*, 1989). Younger caliches are found as thin layers between the Pliocene Kakkaristra Formation and the Faglomerate Group units on the north Troodos margin (location 1-9), whilst multiple caliche horizons and associated soil horizons developed near Kolossi, west of Limassol and south of Nicosia (locations 3-28 and 3-4; Fig.9.5a and c). The best preserved

Fig.9.2. The stages of caliche development (after Machette, 1985).

Note: 1- youthful and 6 - senile.

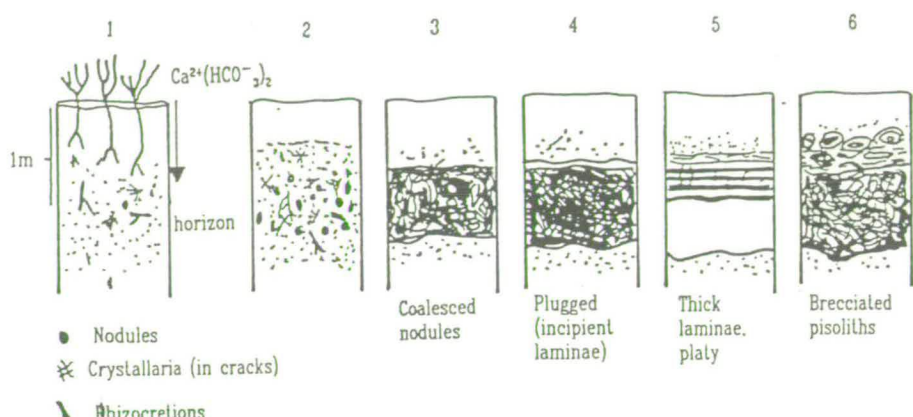


Fig.9.3. The relationship between the rate of caliche formation and the rate of sediment accretion (after Wright, 1990).

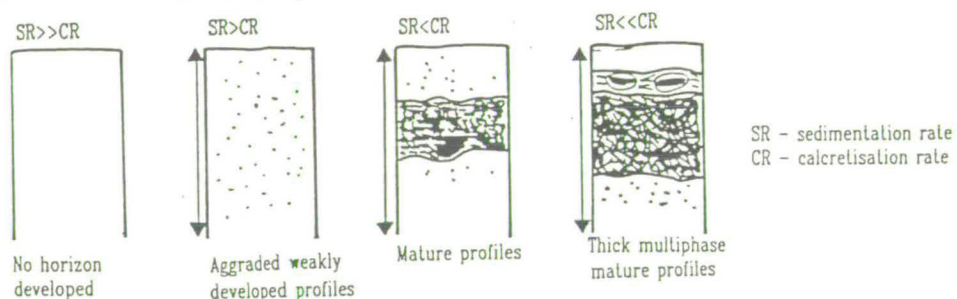


Fig.9.4. The distribution of caliche on Cyprus (after Pantazis, 1961 and this study).

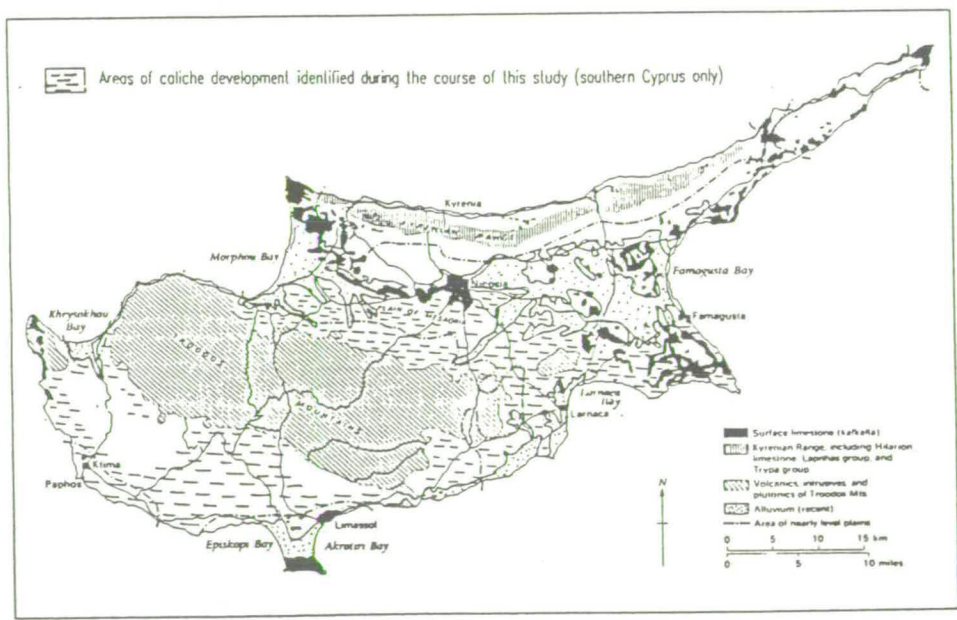
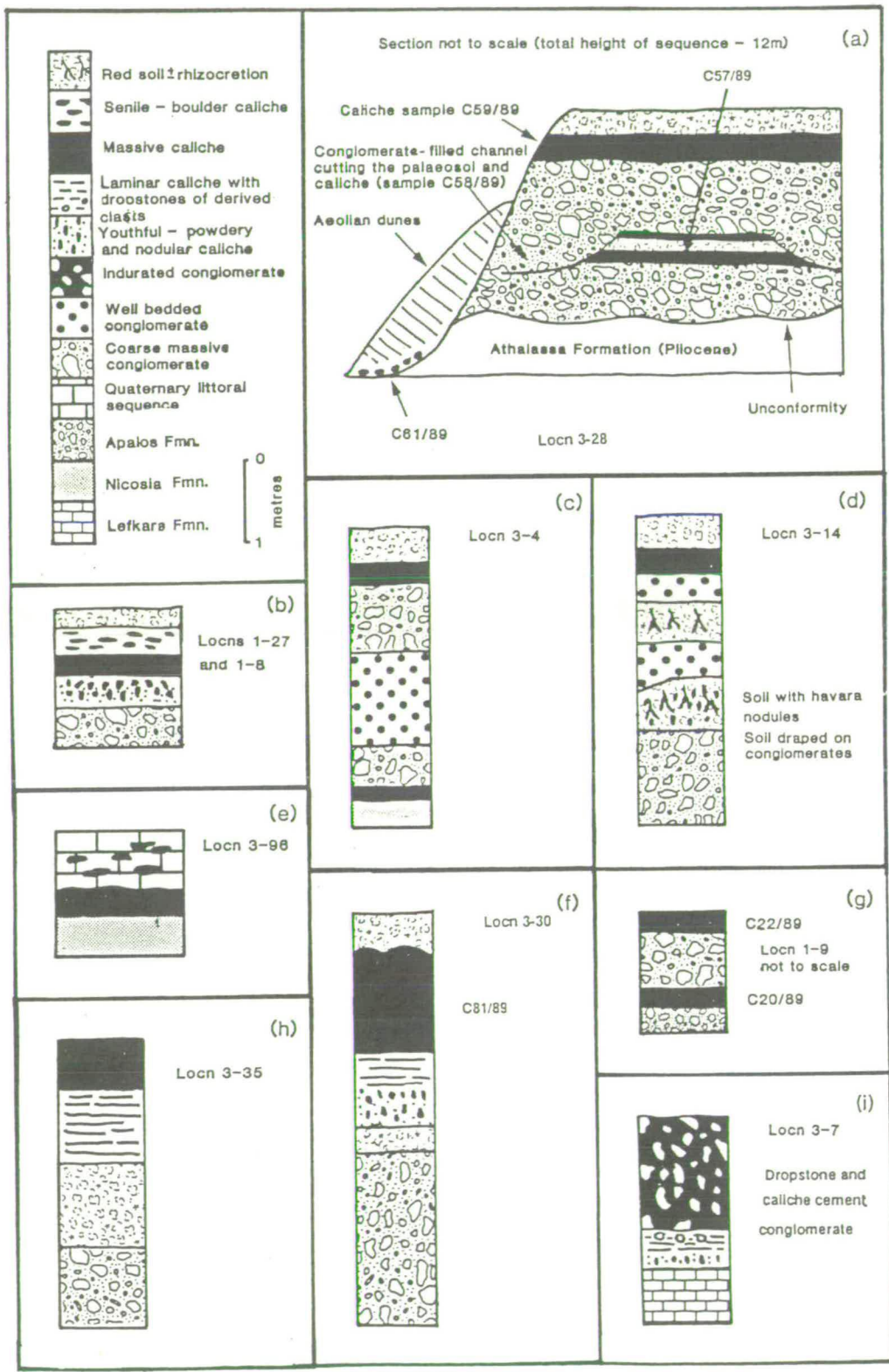


Fig.9.5. Sketch sections of caliche and palaeosol horizons from southern Cyprus.

Note: sample sites are referenced in the text.



examples of caliche are precipitated towards the top of the Pleistocene Faglomerate Group sediments, e.g. Pissouri and Kambia (locations 3-30 and 3-6; Fig.9.5f; Plate 9.1) where the sequences are up to 3m thick and have a stratigraphy similar to the idealised sequence recorded by Machette (1985) in south-west USA (Fig.9.2).

### **9.3 CALICHE DEVELOPMENT ON CYPRUS.**

There were two distinct environments of caliche formation on Cyprus: that associated with Quaternary carbonate sequences and pre-Quaternary lithologies and that associated with Quaternary alluvial sequences. The caliches in both cases are buff-cream to orange in colour.

The caliche horizons associated with the carbonate sequences and pre-Quaternary lithologies tend to form single hardcrusts of caliche, e.g. Petounda Point (location 3-11) and west of Vasilikos (location 1-143; Plate 9.2). Exceptions to this simple crust are noted, e.g. at Akrotiri (location 3-96), where a hard crust of caliche is found lying between the Pliocene Nicosia Formation and the Quaternary littoral sequence (Fig.9.5e and Plate 9.2). The crust at Akrotiri has formed a boulder caliche - the senile stage of Netterberg (1967) - with caliche debris being incorporated within the Quaternary sequence. It is also common to see thin hard crusts of caliche lying between the Pliocene sediments and overlying Quaternary sequence throughout southern Cyprus (location 1-9; Fig.9.5d). Thin caliche crusts are less common between units of the Troodos ophiolite and the overlying Quaternary sequence, e.g. Malounda on the north Troodos margin (location 1-76).

The second environment of caliche formation in Cyprus, is associated with palaeosols and fluvial sedimentary sequences. These caliches commonly form a stratigraphy (Fig.9.1 and 9.2) with soft havara passing up into hard, laminated and massive kafkalla. Examples are found at Pissouri (location 3-30; Fig.9.5f; Plate 9.1) and Kambia (location 3-6; Plate 9.1). Senile caliche is locally developed, e.g. on the north Troodos margin (locations 1-27 and 1-8; Fig.9.5b). Elsewhere, similar caliche deposits, e.g. the Kalahari (Watts, 1980) and the south-west USA (Machette, 1985), have been called pedogenic caliches, a term that will be used here.

Pedogenic caliche is exposed in greatly varying thickness, centimetres to metres, with commonly two, or more, phases of caliche within a single fluvial sequence (locations 3-4 and 3-28; Fig.9.5a and c). Caliche crops out beneath red soils (location 1-27; Fig.9.5b) and also provides, locally, the only cement bonding the clasts of the alluvial Faglomerate Group. The most extensive example of induration occurs west of Larnaca

PLATE 9.1.

D - A complete, juvenile to senile, caliche sequence preserved above the Fanglomerate Group sediments at Kambia on the north Troodos margin (location 3-6). Havara, calcified soil (d), merges up into powder and nodular caliche (e), which in turn passes up into coalesced nodules and honeycomb caliche (f), which is capped by platy, brecciated caliche (g).

Note: scale is 50cm long.

E - Caliche sequence preserved above the F1 Fanglomerate unit at Pissouri (location 3-30) revealing nodular, honeycomb and hardpan caliche.

Note: see Plate 9.1d for details,  
the sequence is c.2m high.

F - An example of a thick hardpan caliche, exposed between two soil units beneath the F1 erosion surface at Trimithousa (location 3-35) in south-west Cyprus.

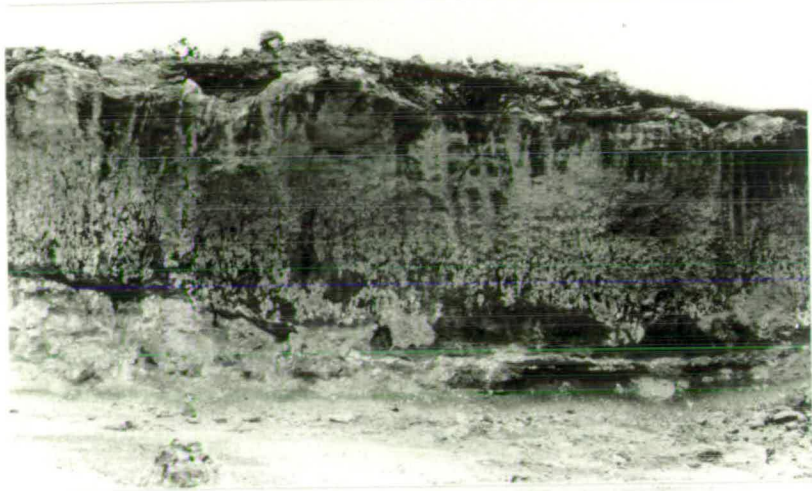
Note: the scale is 50cm long,  
the top of the scale marks the base of the caliche unit and the top of the lower soil horizon.

Plate 9.1

D



E



F

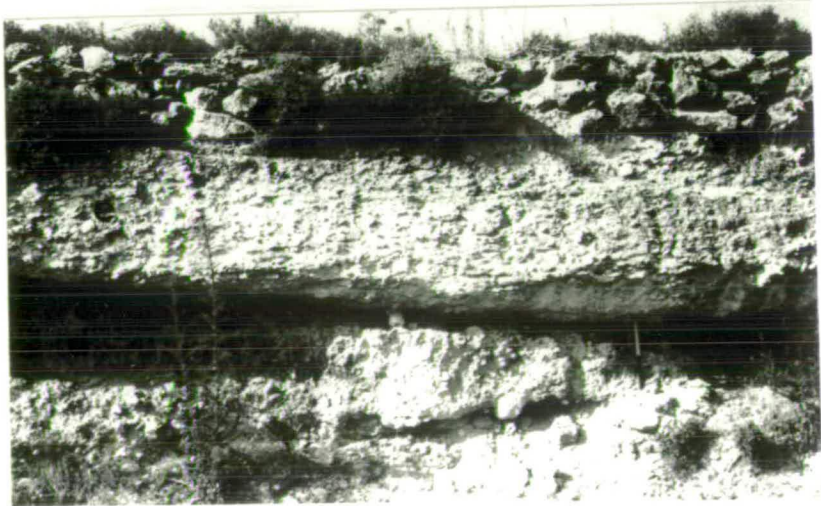


## PLATE 9.2.

D - A series of thin mature caliche crusts and nodules marking the unconformity between the Nicosia Formation and the Quaternary grainstone sequence on the Akrotiri Peninsula (location 3-96).

Note: the sequence is c.70cm high,  
arrows mark the caliche horizons and nodules.

E - Caliche crust capping the F4 terrace at Paralimni (location 1-120).

F - Red palaeosol forming within the Fanglomerate Group sequence (a) on the Akrotiri Peninsula (location 3-28), the palaeosol is capped by a thin caliche horizon (b).

Note: the cliff is c.12m high,  
see Fig.9.5a for details.

G - Multiple palaeosol horizons present within the units of the Fanglomerate Group at Astromeritis (a; location 1-27).

Note: the scale is 50cm long.

H - Red terra-rossa type soils capping the F3/F4 carbonate grainstone sequence at Protaras (location 2-100).

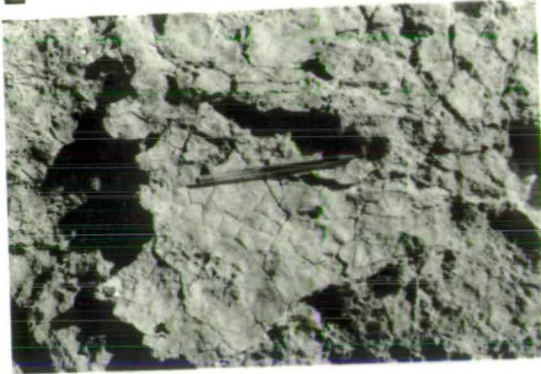


Plate 9.2

D



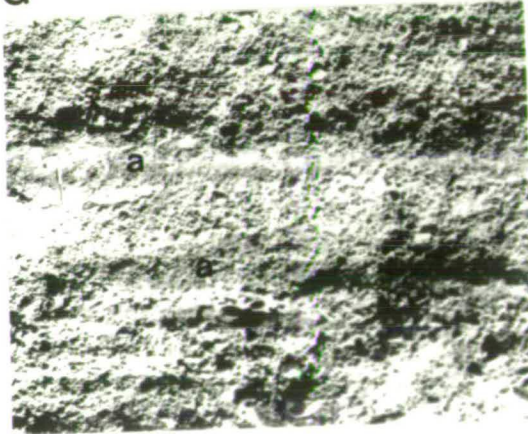
E



F



G



H



(location 3-7, Fig.9.5i), where conglomerates of the Fanglomerate Group were deposited above chalk and subsequent calichification has completely cemented the clasts, locally. A "dropstone" structure developed with conglomerate clasts supported and cemented by caliche.

#### **9.4 PETROLOGY AND GEOCHEMISTRY OF THE CALICHE HORIZONS.**

Samples of caliche were studied on a spectrum of scales, from hand specimen and thin section down to analysis using both X-ray fluorescence and X-ray diffraction.

The samples used in this study are listed below:

| Sample  | Location | Bedrock characteristics |
|---------|----------|-------------------------|
| 1-1     | ---      | Miocene lithology       |
| C20/89  | 1-9      | Apalos Formation        |
| C22/89  | 1-9      | Fanglomerate Group      |
| C28/89  | 3-6      | Fanglomerate Group      |
| C29/89  | 3-6      | Fanglomerate Group      |
| C30/89  | 3-6      | Fanglomerate Group      |
| C33/89  | 3-3      | Fanglomerate Group      |
| C33A/89 | 3-9      | Lefkara Formation       |
| C58/89  | 3-28     | Fanglomerate Group      |
| C59/89  | 3-28     | Fanglomerate Group      |
| C61/89  | 3-28     | Athalassa Formation     |
| C81/89  | 3-30     | Fanglomerate Group      |

##### **9.4.1 Caliche petrology.**

Hand specimens of kafkalla (Pantazis, 1973) illustrated the multitude of clasts incorporated into the lower, less mature, portion of caliche horizons. Kafkalla is documented forming both distinct laminated and massive units, commonly found where a thin conglomerate overlies a carbonate bedrock (location 3-7, see below). In addition, kafkalla forms around various nuclei, commonly in areas away from indurated caliche cements. Caliche rinds found on the lower faces of *in situ* clasts are locally laminated and usually less than 3mm thick, e.g. on the north Troodos Margin (locations 1-82 and 1-89).

Caliche taken from a crust coating Miocene limestone (sample 1-1) is homogeneous micrite, with little porosity. Derived planktonic foraminifera are present

within the sample, though these and small derived clasts (less than 1mm in diameter) make up less than 10% of the section.

Rough laminae and autofracturing, i.e. contemporaneous fracturing during the formation of the caliche, create a fabric in the caliches associated with the Faglomerate Group sediments on the north Troodos margin. The autofracturing and lamination of this unit has resulted in microspar precipitation in voids. Gradational fabrics are created by the gradual reduction in numbers of clasts within the caliche up section (Plate 9.3). Thin sections from the north Troodos margin show clast gradation with clasts less than 1cm in diameter in the lower portion of the unit, fining up, with grains less than 0.1mm in diameter towards the top of the unit.

Caliche cropping out above Quaternary littoral sequences comprises thin structureless micrite, capped by rough laminar crusts (Plate 9.3). The caliche sequence is generally less than 5cm thick. Irregular pisolites, i.e. small, subspherical accretionary bodies of  $\text{CaCO}_3$ , are also present within these caliche exposures; these commonly have a complex nuclei and irregular laminations (Plate 9.3). A gradation of clast types is also present towards the top of the unit, with a smaller proportion of foraminifera tests, algal matter and molluscan shells corresponding to increased numbers of detrital clasts. Some foraminifera tests are micritised (Plate 9.3).

The fabrics within the caliche horizons is apparently dictated by the depositional environment of the sediments on which they have formed (Section 9.3).

#### **9.4.2 X-ray diffraction data.**

X-ray diffraction studies of selected caliche horizons from Cyprus demonstrate a simple mineralogy with calcite, quartz, feldspar (albite to anorthite) and montmorillonite/illite (Appendix E) present (sample 1-1, mainly of calcite; Fig.9.6). There is no evidence to support the presence of aragonite in any of the samples, in keeping with that recorded from caliches studied elsewhere (Watts, 1980). Pantazis (1973) showed that the abundance and presence of other phases, e.g. calcite and feldspar, reflected the local provenance and hence the proximity of the outcrops to lithologies of the Troodos Massif, the Kyrenia Range and the Mamonia Complex (Table 9.1a and b).

The solely calcite mineralogy of the samples taken from the highest horizons of pedogenic caliche (C81/89 and C58/89) reflect the mature nature of these caliche samples (Fig.9.7a). The samples C20/89 and C22/89 exhibit a very similar mineralogy to that seen

Fig.9.6. X-ray diffraction peak height plot of a typical caliche sample capping limestone of Miocene age on the north Troodos margin.

Note: Reference plots of mineral phases 2θ angles are presented in Appendix E.

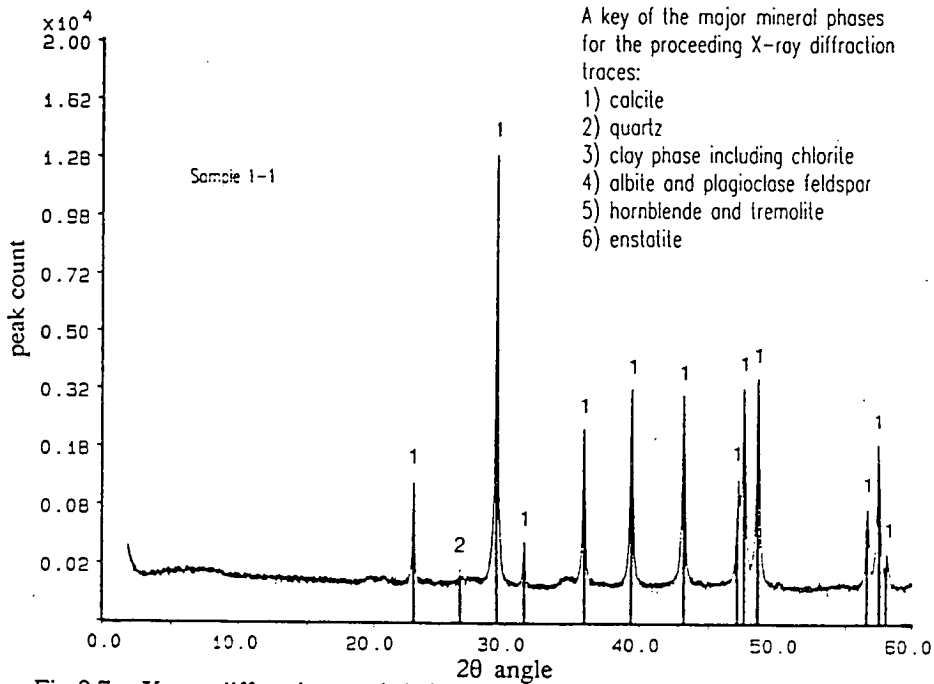


Fig.9.7. X-ray diffraction peak height plots of silt and clay fractions from pedogenic caliche samples.

Note: sample numbers are referenced in the text and reference plots of mineral phases 2θ angles are presented in Appendix E.

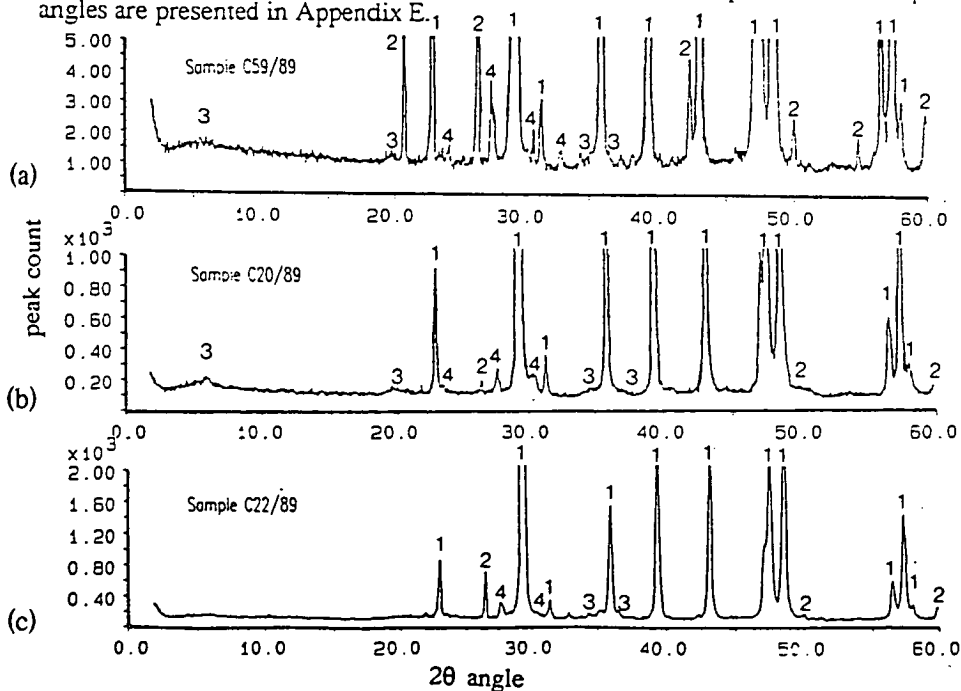


PLATE 9.3.

E - A portion of the pedogenic caliche horizon preserved at Perakhorio (location 3-4; sample C18/89) revealing the rapid reduction in numbers of clasts, up section, between the Fanglomerate Group sediments and the indurated caliche.

Note: the reticulated structure of the mature caliche towards the top of the plate, the micrograph represents a field of view 10mm long.

F - Showing the development of pisolitic and laminated caliche horizons within a mature caliche unit capping the F3/F4 carbonate sequence at Cape Greco (location 1-124; sample 151).

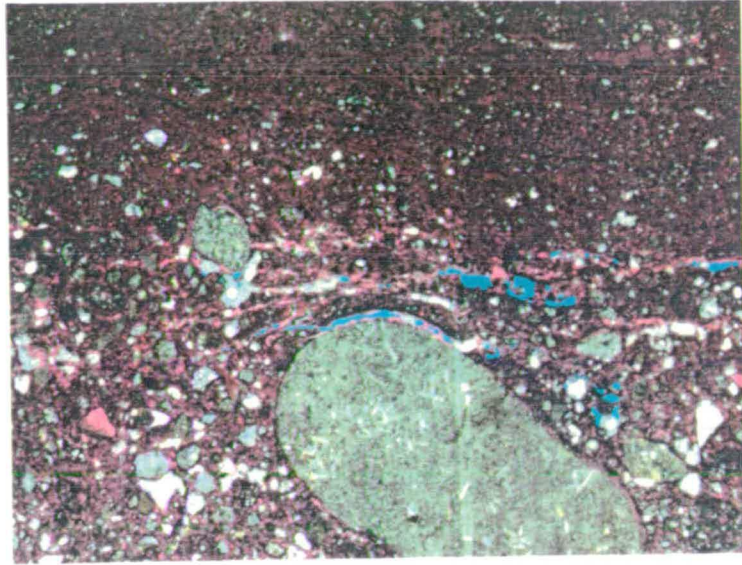
Note: the micrograph represents a field of view 2mm long.

G - Pisoliths developed within the caliche capping the F4 marine terrace at Paralimni (location 1-120; sample 134).

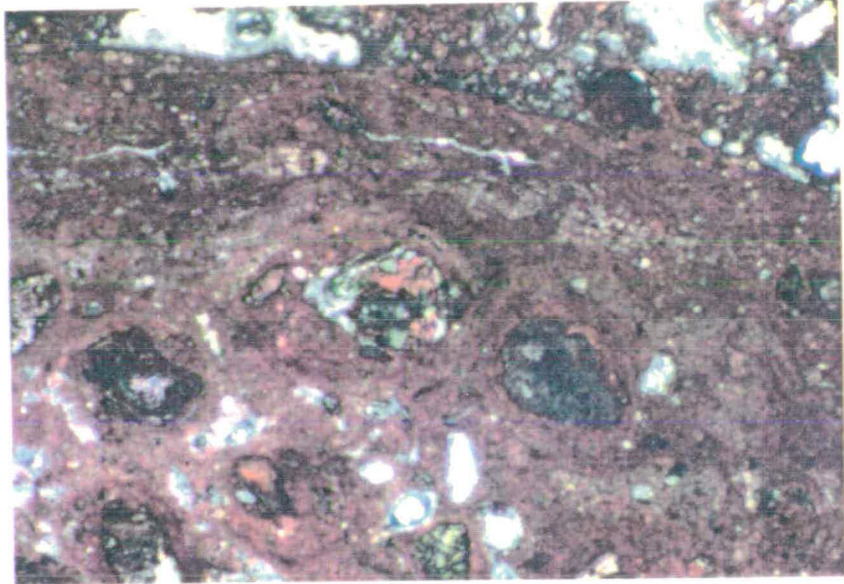
Note: the micrograph represents a field of view 6mm long.

Plate 9.3

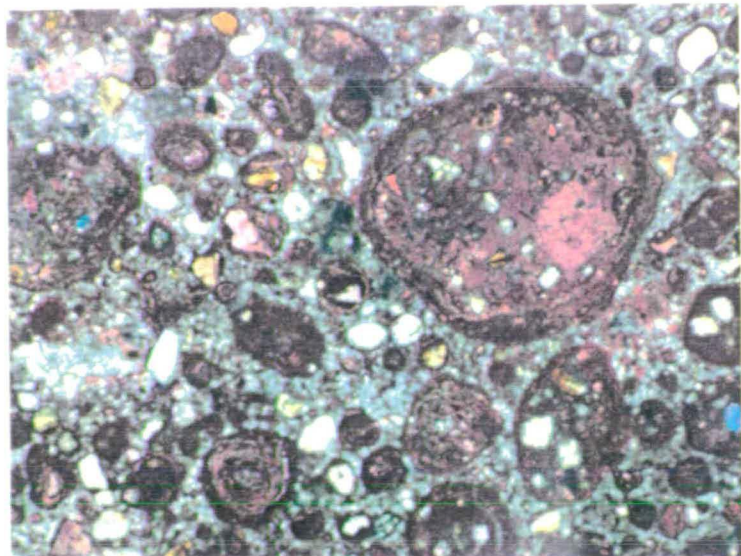
E



F



G



in C58/89 and C81/89 with calcite, feldspar, quartz, montmorillonite and illite present in both (Fig.9.7b and c). Semi-quantative comparisons of peak heights between different sample patterns indicates minor variation in the proportions of clay and quartz present. The high proportion of quartz in C22/89 is also detected in the relatively high weight percentage  $\text{SiO}_2$  in the X-ray fluorescence sample (Fig.9.8; Section 9.4.3). Caliche was also sampled from the base to the top of the exposure (C28/89-C29/89-C30/89) but no change in mineralogy was detected (Fig.9.9).

Caliche samples C33/89 and C33A/89 overlying different bedrock show some variation in the mineralogy present (Fig.9.10a and b). Although both samples contain calcite, feldspar, quartz and montmorillonite/illite, semi-quantative analysis showed less clay to be present in sample C33A/89 (from above the chalks) than C33/89 (from above the Fonglomerate Group); dolomite is also present (Fig.9.10a and b).

In summary, the mineralogy of the caliche samples is generally uniform, dominated by calcite. Subtle variation may relate to either local conditions, such as the influence of the bedrock and local provenance, e.g. the presence of dolomite in sample C33/89 and the mono mineralogical nature of caliche sampled above a Miocene limestone (sample 1-1), or the maturity of the caliche under examination.

#### **9.4.3 X-ray fluorescence data.**

Pantazis (1973) documented the following analysis from kalfkalla samples from southern Cyprus:

- i)  $\text{CaCO}_3 = 75-91\%$ ,
- ii)  $\text{MgCO}_3 = 0.88-7.14\%$ ,
- iii)  $\text{Al}_2\text{O}_3$  and  $\text{Fe}_2\text{O}_3 = 3.25-3.06\%$ ,
- iv)  $\text{CaO} = 42.5-51.4\%$ ,

By comparison X-ray fluorescence analysis of caliche from this study (Fig.9.8) demonstrate marked variation in the geochemistry, e.g. 50% (sample 1-1; Fig.9.8e) to 35%  $\text{CaO}$  (C29/89; Fig.9.5b and e). The weight percentage of  $\text{SiO}_2$  varies in an inverse relationship with the  $\text{CaO}$  (Fig.9.8). The loss on ignition of  $\text{CO}_2$ ,  $\text{H}_2\text{O}$  and other volatiles is high, suggesting that much of the  $\text{CaO}$  is derived from calcite. The following trace-elements: Ce, Cr, Ni and Zn do not show any noticeable change between samples (Fig.9.11). Sample C33/89 is taken from the caliche that caps the Fonglomerate Group sediments above Kandara Hill, on the north Troodos margin, whereas C33A/89 is taken from a caliche capping the chalks of the Lefkara Formation at Mazotos (location 3-9). The X-ray fluorescence data clearly reflects precipitation on different substrata with the

**Fig.9.8. Spider diagram of caliche samples subjected to major X-ray fluorescence elemental determination.**

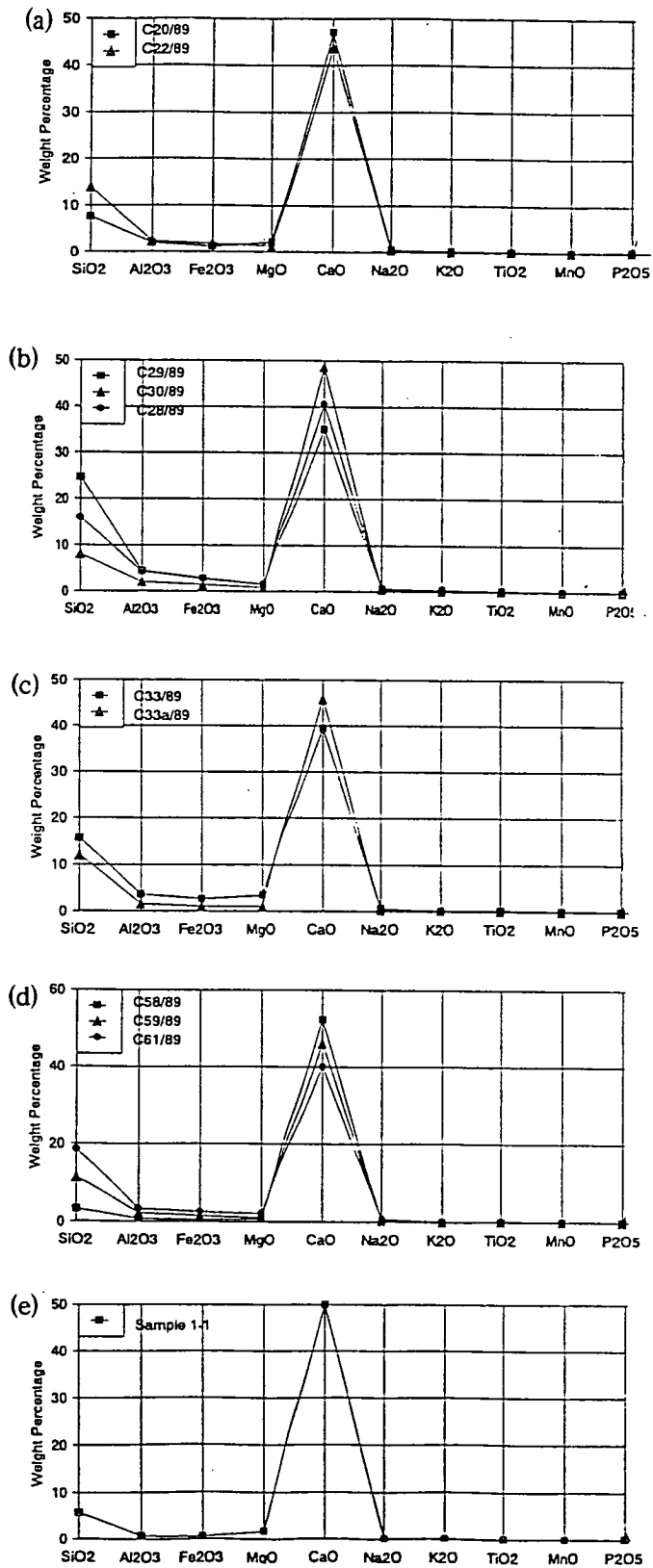




Fig.9.9. X-ray diffraction peaks taken from the base, middle and top of a pedogenic caliche sample from Kambia on the north Troodos margin.

Note: sample C28/89 is taken from the base, C29/89 the middle and C30/89 top, of the section (location 3-6; see Plate 9.1d for details). Reference plots of mineral phases 2θ angles are presented in Appendix E.

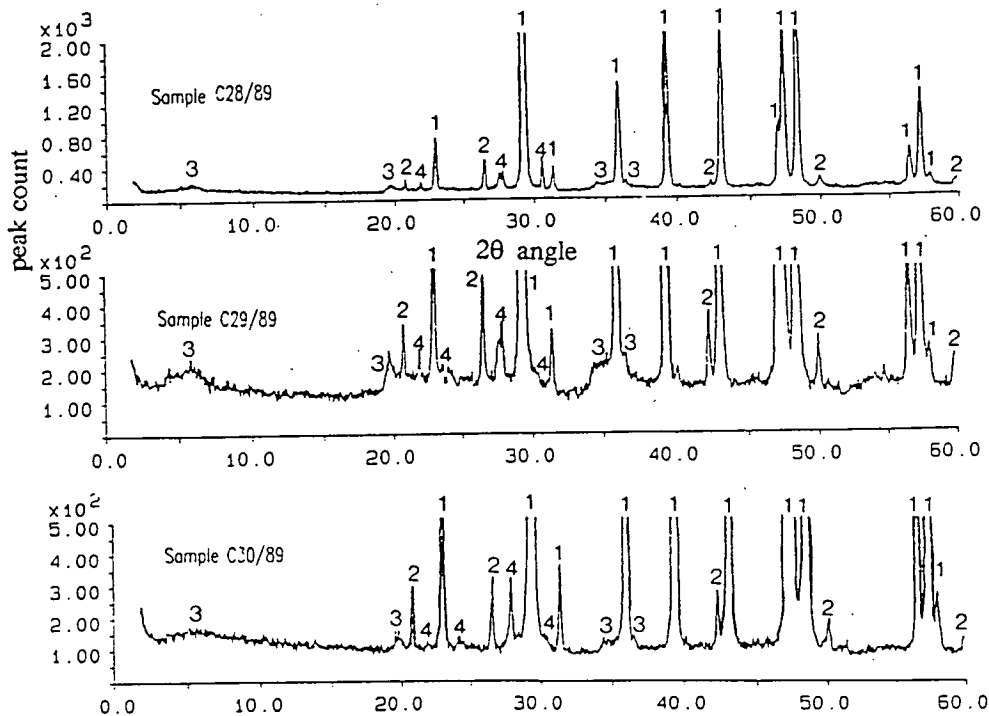


Fig.9.10. X-ray diffraction traces of samples capping a variety of bedrocks without commensurate changes in the constituent mineralogy.

Note: sample numbers are referenced in the text and reference plots of mineral phases 2θ angles are presented in Appendix E.

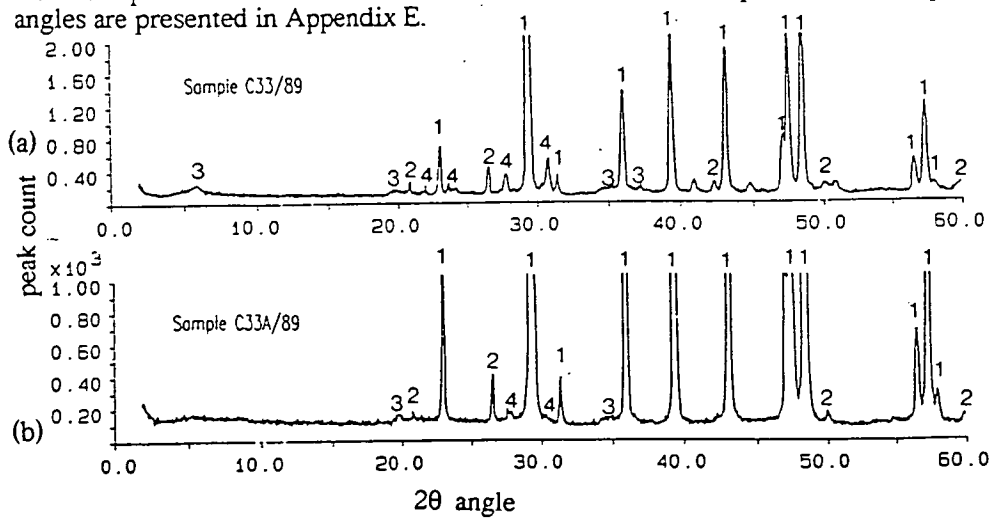
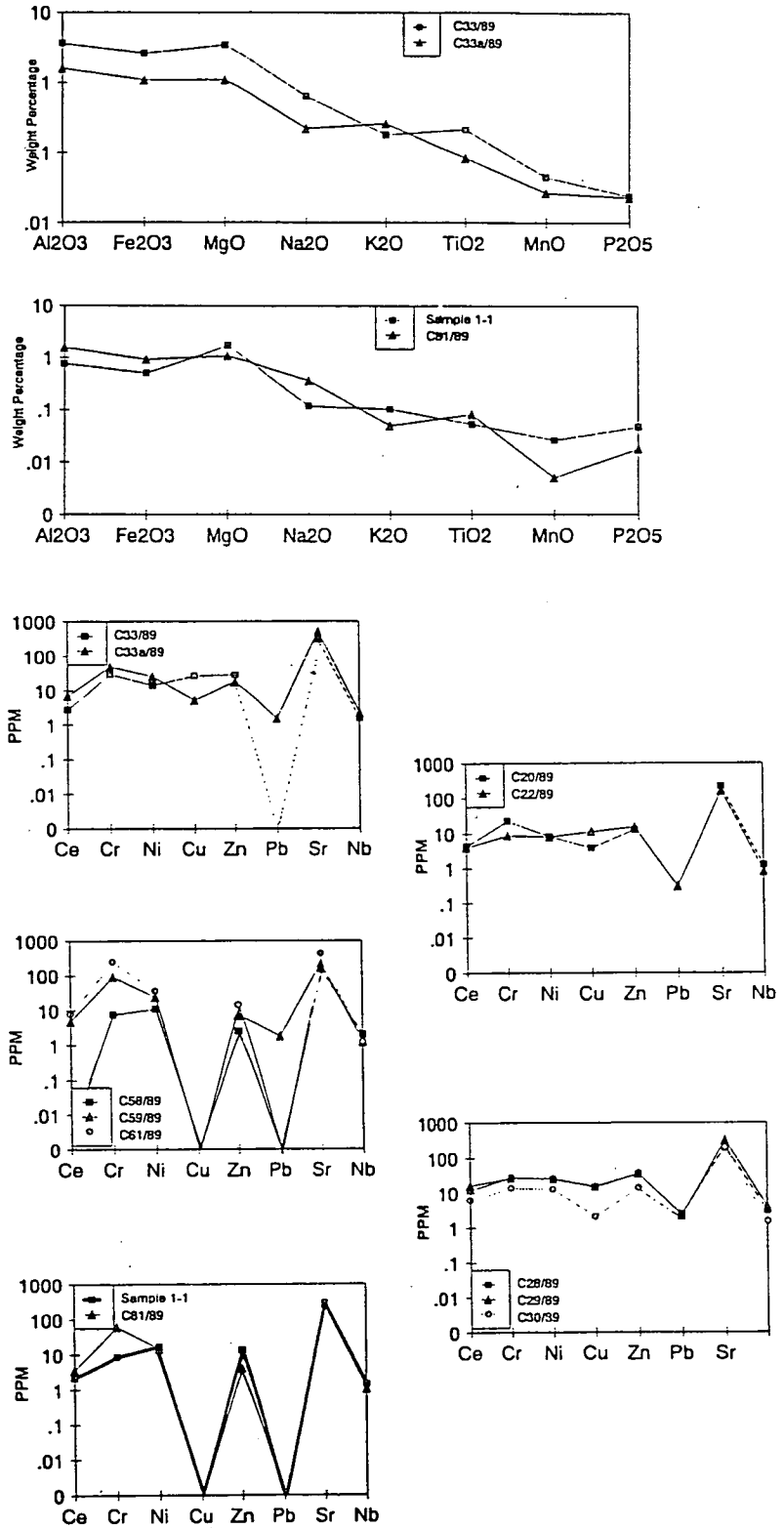


Fig.9.11. X-ray fluorescence trace and minor element variation from caliche samples in southern Cyprus.

Note: locations are recorded in the text.



caliche overlying the chalk having higher values of CaO but lower proportions of  $\text{Al}_2\text{O}_3$ ,  $\text{Fe}_2\text{O}_3$ ,  $\text{SiO}_2$  and MgO as well as lower proportions of Cu and Pb (Fig.9.11). The pattern seen at location 3-9 matches that found for sample 1-1, a caliche overlying Miocene limestones.

Similar variance is registered even in the analysis of samples from the same locality, e.g. the sample series C58/89, C59/89 and C61/89 from Kolossi, west of Limassol (location 3-28; Fig.9.8). Although C58/89 and C59/89 have similar characteristics, C61/89 shows a noticeably higher absolute value of  $\text{SiO}_2$  and Cr, and a lower value of CaO (Figs.9.8 and 9.11).

A caliche horizon cropping out at Pera (location 3-6; samples C28/89, C29/89 and C30/89) exhibited a compositional variation up sequence, as the caliche progressively matures, changing from havara to kafkalla. The changes involve lower  $\text{SiO}_2$ , Cu and Pb values and an increase in CaO up the sequence (Fig.9.8 and 9.11). The caliche at this location overlies conglomerates of the Fanglomerate Group and hence the lowest sample reflects the bedrock (sample C33/89), however, the stratigraphically higher samples, and that seen at Pissouri (location 3-30; sample C81/89; Figs.9.8 and 9.11) also found overlying Fanglomerate Group sediments, reflect the composition seen in the samples taken from units overlying limestone and chalk lithologies (samples C33A/89 and 1-1).

These results suggest that the chemical composition of the caliches, dominated by CaO, varies little in multiple caliche horizons, like those seen at locations 3-28 (samples C58/89 and C59/89) and 3-9 (samples C20/89 and C22/89). Although substrate has an effect on the composition of the caliche, as shown by samples 1-1, C33/89 and C33A/89, the most noticeable variations occur within mature caliches (location 3-6), where increasing maturity towards the top of the unit results in greater compositional changes from caliches found above the Fanglomerate Group sediments than those precipitated above limestones and chinks. The variation in composition between C61/89, and C58/89 and C59/89, could reflect the solution source, from which the caliche is precipitated, with both C58/89 and C59/89 derived from palaeosols, groundwater and the Fanglomerate Group conglomerate. Sample C61/89 has formed on a discontinuity surface and is overlain by aeolianites (Chapter 8), suggesting that caliche composition will have been effected by a derived wind blown component, similar to that suggested for the caliches of Texas and north Mexico (Reeves, 1970).

The X-ray fluorescence results reveal that the subtle changes in caliche chemistry are predominantly linked to substrate type and the caliche maturity.

## **9.5 SPEED AND DEGREE OF FORMATION OF RECENT CALICHE.**

If caliche forms at the surface, then modern day caliche deposits in Cyprus must be limited. Archaeological excavations, however, in the ancient site of Tenta, near Kalavastos (built on Miocene chalks, limestones and marls) cut through a hard caliche crust that exists less than 2m beneath the present day land surface (I. Todd, *pers. comm.*, 1989). This implies either that caliche on Cyprus forms at sub-surface levels, as pedogenic deposits, in line with the views of Watts (1980) or soil development has taken place subsequent to caliche formation and that caliche formation in the Kalavastos area of Cyprus has been very rapid with hard crust forming in a maximum of 10ka.. As noted earlier the pattern of formation of caliche associated with carbonate bedrock contrasts that seen on the north Troodos margin and other areas away from a carbonate bedrock, where the development of Recent caliche associated with the Faglomerate Group sediments is limited. Limited caliche development is documented by other workers studying Recent alluvial sediments in Mediterranean valleys (Daloni, 1951; Vita-Finzi, 1969). The differential formation of caliche in the Recent geological past reflects the importance of an abundant carbonate source.

## **9.6 MODELS OF FORMATION OF THE CALICHE.**

It is proposed that two types of caliche formation took on Cyprus during the late Pliocene and Quaternary.

### **9.6.1 Pedogenic caliche.**

In the alluvial environment caliche formation is associated with soil development, similar to that seen in the Kalahari (Watts, 1980). The close relationship between palaeosols and caliche formation supports this argument (Fig.9.5). The formation of pedogenic caliche can be modelled either with capillary rise (Price, 1933), or groundwater flow (Wanless, 1922). The capillary rise model depends on the minerals being leached from soils and descending to low levels during cool, wet periods and ascending in hot, dry periods resulting in the precipitation of caliche. The groundwater model relies on the flow of groundwater close to the surface, transporting high concentrations of dissolved salts, e.g. Ca, with high rates of evaporation causing precipitation of caliche. The precipitation of the caliche is aided by artesian, hydrostatic pressure and a falling water table (Goudie, 1973). The precise mode of formation depends on local conditions as both the capillary rise of leachates and the availability of groundwater are important factors governing the formation of pedogenic caliche. Soil

horizons can be present above and below pedogenic caliche. The formation of mature caliche horizons occurs when caliche accretion rates exceed sedimentation rates (Netterberg, 1967; Wright, 1990; Fig.9.3). Mature pedogenic caliche horizons are not always present (location 3-4; Fig.9.5c) or totally preserved, due to channel avulsion and subsequent erosion, as occurs on the Akrotiri Peninsula (location 3-28; Fig.9.5a), or due to a lack of time for formation of mature horizons. This suggests that the sedimentary environment played a major role in the formation and preservation of these caliche formations and that residence time in the zone of active caliche formation also governs the development of pedogenic caliche. Additionally, the availability of carbonate, local variation in rainfall (Gile, 1977; McFadden, 1988) and the influence of rhizcretion (Wright *et al.*, 1988) have also caused intra-basinal variation in the formation of pedogenic caliche. Caliche maturity therefore, does not simply relate to time.

Havara is an integral part of the model of caliche development (Figs.9.1 and 9.2) forming the youthful portion of the caliche formation hierarchy (Netterberg, 1967). The proposition that havara is intrinsically related to the formation of mature caliches disagrees with Pantazis (1973) who suggested that it was an unrelated freshwater carbonate.

### **9.6.2 Mature crust.**

The second type of caliche consists solely of a hard mature caliche crust. These units cap the pre-Quaternary carbonate lithologies of the Troodos sedimentary cover sequence. Palaeosols are rarely associated with this type of caliche today. The local source of carbonate suggests that formation of this type of caliche happened quite rapidly, as witnessed at Tenta (see above), probably through rapid dissolution, capillary rise and precipitation of the underlying carbonate. Formation of a caliche crust on carbonate bedrock has been described by Multer & Hoffmeister (1968) from the Florida Keys (Fig.9.12) and James (1972) from Barbados. The crusts of the Florida Keys were seen to be both laminated and massive. Similar crusts cap the exposed carbonate lithologies in Cyprus, where micritisation and the introduction of detrital clasts has taken place, suggesting some alteration in the phreatic zone and the introduction of detrital clasts on exposure (location 2-100). The semi-arid climate aids the rapid formation of this type of caliche. These formations conform to those of Multer & Hoffmeister (1968) who state that formation of these crusts occurs on exposed bedrock which usually borders soil covered areas. Similar formations were recognised in Western Australia where a direct correlation between bedrock type and crust formation was suggested (Woolnough, 1930). This correlation was criticised by Grubb (1963) who stated that the lateral transport of carbonate had been ignored.

Fig.9.12. Schematic illustration of some mechanisms responsible for subaerial caliche crusts (after Multer & Hoffmeister, 1968).

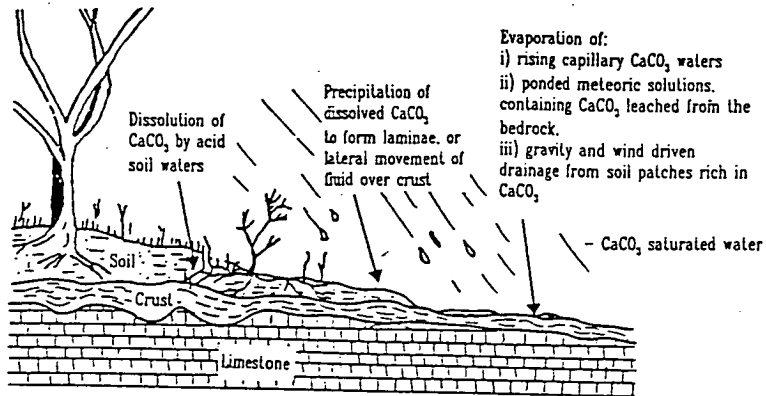


Fig.9.13. X-ray diffraction trace showing the mineralogy of the palaeosol sample C57/89 from within a sequence of the Faglomerate Group on the Akrotiri Peninsula.

Note: see Fig.9.5 for the precise location of the sample within the section. Reference plots of mineral phases 2θ angles are presented in Appendix E

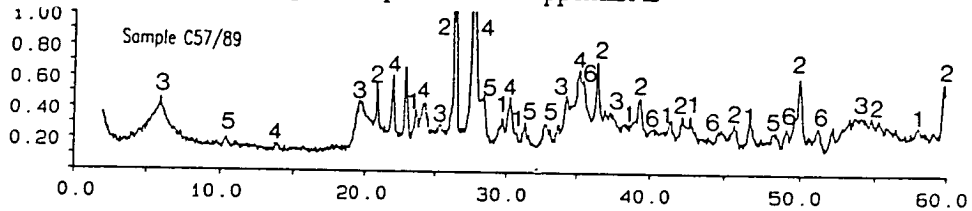
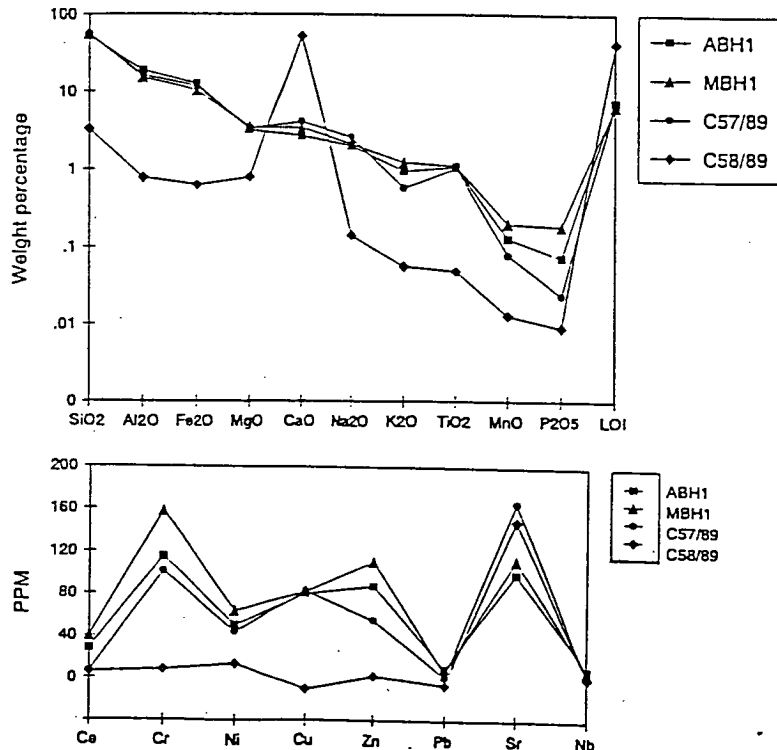


Fig.9.14. X-ray fluorescence trace of the major and minor elements from the palaeosol horizon (sample C57/89) and the caliche beneath it (sample C58/89), from the Faglomerate Group on the Akrotiri Peninsula (location 3-28), and the top of the borehole samples from Meniko (sample MBH1) and Astromeritis (sample ABH1), on the north Troodos margin.

Note: details of the boreholes can be found in Chapter 5.  
LOI - loss on ignition.



It has been shown here that two types of caliche can exist, the type of formation being dependent not only on the climate and groundwater flow but on the sedimentary environment of deposition, if any, and the bedrock on which the caliches have formed.

In summary, the variance in the development of pedogenic caliche and caliche crusts results from:

- i) a semi-arid climate with approximately 40-60cm of rainfall,
- ii) groundwater availability and capillary action,
- iii) the substrata above which the caliche has formed,
- iv) a readily available source of carbonate,
- v) the sedimentary environment of deposition,
- vi) residence time within an environment of caliche formation and hence, the relationship between rate of sedimentation and rate of caliche formation.

These six factors have governed the type and speed of caliche formation and development that has taken place.

## **9.7 PALAEO SOL DEVELOPMENT.**

### **9.7.1 Palaeosol characteristics.**

The palaeosols were not examined in any great detail during this study. The soils form single horizons capping the terraces on the north Troodos margin and carbonate sequences throughout southern Cyprus, e.g. Protaras (location 2-100; Plate 9.2). Multiple soil horizons are seen in more distal locations in southern, south-western and south-eastern Cyprus as well as on the north Troodos margin (locations 3-28, 1-58 and 3-14, Fig.9.5; Plate 9.2).

The soils are generally thin, less than 1m thick, and commonly red in colour; though grey soils are also seen. Rhizocretion fabrics are developed within the soils. A close association exists between soil horizons and that of caliche, with caliche horizons cropping out both above and below the soil horizons (Fig.9.5c, f and h).

The soil samples ABH1 and MBH1 were taken from terrace top soils at different localities on the F2 terrace on the north Troodos margin, whilst C57/89 represents a sample taken from within the exposed sedimentary sequence at location 3-28 (Fig.9.5). The palaeosol horizons associated with the caliches were analysed using X-ray diffraction and X-ray fluorescence. These samples, like those taken from the borehole samples on the north Troodos margin (Chapter 5, samples MBH1 and ABH1), had a mineralogy of

albite, quartz, tremolite, montmorillonite and very minor calcite (Fig.9.13). The clay and silt fractions of the borehole samples (ABH1 and MBH1, Fig.5.27) were examined in detail and revealed that the clays present consist of: smectite, chlorite (ripidolite), kaolinite and montmorillonite. The X-ray fluorescence analysis of the soil horizons showed that the major oxide and trace element chemistry of the soils is very similar but minor variations are recorded in the  $K_2O$ ,  $MnO$  and  $P_2O_5$  components (Fig.9.11a and b).

### **9.7.2 Interpretation.**

The soils from Cyprus have been described as terra-rossa-type (Pantazis, 1973; Dregghorn, 1978). A terra-rossa soil is generally red in colour, with an associated carbonate substratum and karstification (Bates and Jackson, 1980), which hold true in Cyprus, although karstification is generally absent. The presence of the expanding clay smectite, evidence for extensive rhizcretion structures and a close association with pedogenic carbonate suggest that these are possibly vertisols (soils that contain at least 30% expanding clays, e.g. smectite, and display shrink and swell structures resulting from rapid changes between wet to dry conditions) similar to those seen in the Palaeozoic palaeosols of the central and southern Appalachians (Driese *et al.*, 1990). The low CaO content within the soils, especially that seen in specimen C57/89 (location 3-28), may reflect the efficiency of the CaO leaching during caliche formation. This pattern is similar to that detailed in Texas and north Mexico (Reeves 1970) and Barbados (James, 1972) where the soils were a source of  $CaCO_3$  for caliche formation. Reeves (1970) suggests that carbonic acid from rainwater combined with  $CO_2$  from the atmosphere and soils caused the soil carbonate to dissolve and subsequently contribute towards the formation of caliche. The variation in the trace-element and oxide chemical composition in the soils probably reflects local variation in the soil provenance, the overall nature of the soil chemistry and physical characteristics of the soil, all suggesting that the soils studied here are similar. The variation seen, both in trace-elements and oxide composition between the soil sample (C57/89) and caliche sample (C58/89) at location 3-28, could indicate the preferential incorporation of minerals and trace-elements from groundwater during caliche formation, as well as the inclusion of clasts within the caliche from the bedrock and soil horizons. The concentration of Sr seen within caliche samples, e.g. C58/89, is also generally higher than that within juxtaposed soil samples, e.g. C57/89 (Fig.9.6c-g).

Further investigation of the palaeosols in Cyprus is needed to give a better account of their spatial and temporal variation and how they compare to the present day soils throughout the island.



The proximal to distal relationship characterized by a change from single soil horizons to multiple sequences could be interpreted as reflecting two types of changes away from the margins of the Troodos Massif. The first of these changes could illustrate the combination of differential rates of uplift and Quaternary climatic changes (Chapters 2 and 5), where it was suggested that the Troodos Massif was uplifted at a faster rate than the Mesaoria Plain and coastal southern Cyprus. This differential uplift has resulted in terraces with single soils horizons, similar to that recorded in the Charwell River valley, New Zealand, which are identified as resulting from rapid tectonic uplift and Quaternary climatic changes (Bull, 1990). The presence of single soil horizons on lower strath terraces supports an argument for absolute, rather than relative, changes in the base level. The formation of multiple soil horizons is indicative of tectonically stable areas (Bull, 1990), where the soil horizons are buried under subsequent aggradational events. The existence of these multiple soil horizons reflects relative changes in base level, and/or changes in the watershed variables, e.g. stream power. The formation of multiple soil horizons during the Quaternary of Cyprus could also, therefore, reflect the differential uplift of the island. The presence of the multiple soil sequences in distal localities could also be explained by the sedimentary environments of deposition, as multiple soils are more likely to develop within distal braidplain sequences where the pattern of sedimentation was constantly shifting (Chapter 5). Quaternary climate changes, rather than tectonic uplift, can explain the formation of terraces in fluvial environments (Frostick & Reid, 1989; Harvey & Wells, 1987); these climatic changes cause aggradation, avulsion and hence facilitate the development of multiple palaeosol horizons. It is suggested here that the development of the soil horizons associated with the proximal fluvial sequences and terraces on Cyprus, e.g. across the north Troodos margin, reflect the strong tectonic uplift that is taking place. It is suggested that the formation of multiple palaeosol sequences at distal localities on Cyprus does not necessarily signify tectonically stable areas, as suggested by Bull (1990), but a complex inter-relationship between tectonic uplift, climate change and the sedimentary environment of deposition.

## **9.8 CONCLUSIONS.**

The following conclusions can be drawn from the study of Quaternary palaeosols and caliche horizons on Cyprus:

- i) the formation of both the kafkalla and havara horizons on Cyprus reflects calichification,
- ii) the substratum on which calichification has taken place will play a major role in the speed of caliche formation,

- iii) the type of caliche horizon present, whether pedogenic, or caliche crust, is dependent on the presence of palaeosols and substratum,
- iv) the groundwater and capillary models are both applicable to caliche formation in Cyprus,
- v) extensive caliche formation has taken place during the Pleistocene. The apparent lack of caliches forming on non-carbonate substratum, during the Holocene, may reflect climate change during this period, as identified by Vita-Finzi (1969) and Dreghorn (1978),
- vi) palaeosol horizons have developed throughout the Quaternary and the development of single, or multiple horizons reflect a combination of climate change, base level changes and the sedimentary environment of deposition.

## **Chapter Ten: Discussion and conclusions.**

### **10.1 EVOLUTION OF CYPRUS DURING THE QUATERNARY PERIOD.**

#### **10.1.1 Upper Pliocene-lower Pleistocene: early uplift.**

The sediments within the 350-360m terrace in south-western Cyprus are correlated with a terrace on the southern flanks of the Kyrenia Range (Ducloz, 1968; Dreghorn, 1978) from which Upper Pliocene foraminifera were identified (Mantis, 1970). The 350-360m terrace is also correlated with deposition of the Athalassa and Kakkaristra Formations (Table 1.9) in the Mesaoria Plain (Ducloz, 1965; McCallum, 1989) and with submarine channels, exemplified by those at Khirokitia and Amathus (Houghton *et al.*, 1990), which contain latest Pliocene (c.2.2-1.8 Ma.) nannofossils and planktonic foraminifera. The Kakkaristra Formation is dated by ostracods as Upper Pliocene to lower Pleistocene (McCallum, 1989). The 350-360m terrace, therefore was established during the earliest Pleistocene, after an early phase of uplift (Table 1.10).

#### **10.1.2 Lower Pleistocene-middle Pleistocene (F1 and F2): main phase of uplift.**

The main control on the lower to middle Pleistocene F1 and F2 Fan conglomerate units and associated terrace deposition was tectonic. The development of large-scale alluvial fans on the north Troodos margin relate to drastic uplift and downcutting. However, climatic effects probably had considerable control over the architecture of the fans. A similar interplay of processes is described from the Dead Sea, Israel (Frostick & Reid, 1989) and south-east Spain (Harvey & Wells, 1987).

The alluvial fans on the northern margin of the Troodos Massif were deposited as proximal sheetflood deposits, which pass distally into channelised braided systems. Such a depositional setting would account for the thickness variations in the F1 and F2 Fan conglomerate units. A pediment area bordered the Troodos Massif, with a thicker sedimentary succession to the north. Inter-channel areas were subject to less incision and survived as thin conglomeratic deposits lapping onto the Troodos Massif and pre-Quaternary sediments. Large alluvial fans did not develop during the lower-middle Pleistocene to the south of the Troodos Massif. Instead, large incised channels, e.g. Kouris River, carried sediment from the rising Troodos Massif southwards, to areas close to, or beyond the present coast, e.g. Pissouri, while proximal channelised sequences passed out into braidplain environments, e.g. Kolossi. Seismic data suggest that a large proportion of the detritus derived from the Troodos Massif at this time is now located in offshore slope areas (McCallum, 1989). Thus, several of the rivers may have already

existed in the pre-Pleistocene, e.g. Maroni and Kouris Rivers. Continued uplift associated with downcutting of channels on both the north and south margin of the Troodos Massif resulted in back cutting of the drainage towards the Troodos Massif and the development of mature erosion surfaces on the now isolated, dissected F1 fan-sheets and terraces. Further uplift also caused greater dissection of the Troodos ophiolite as deeper structural levels were exposed.

The presence of ultramafic clasts (Wilson, 1958) in the F1 Fanglomerate Group, transported by the Karyotis River (Chapter 5), is evidence of erosion of the ultramafic core of the Troodos Massif in early Pleistocene, yet ultramafic clasts are not found in the F1 Fanglomerate unit deposits away from this area, a similar pattern to that observed today (Chapter 5). The implication is that the drainage pattern of the early Pleistocene was similar to the present (Chapters 2 and 5). Direct evidence of river capture during this period is seen in the Limassol area, where the Kouris River has captured the Kryos River, which can be traced back onto the Troodos Massif. Evidence from the F1 Fanglomerate unit conglomerates at Pissouri, which contain Troodos-derived clasts (Chapter 5), suggests that the Paramali and Evdhimou Rivers, which now do not rise in the Troodos Massif were also modified by river capture. Similarly, the presence of gabbroic clasts in both deltaic and fluvial deposits (Chapters 5 and 6) in south-east Cyprus points to the existence of a major drainage system flowing southwards, off the northern margin of the Troodos Massif during the lower-middle Pleistocene. As no major river channels flow in this area today, the suggestion that river capture has taken place is perhaps demonstrated in the pattern of drainage now seen, with the Pedieos and Yialias Rivers flowing out towards Famagusta Bay, rather than into Larnaca Bay.

The relative uplift during the lower-middle Pleistocene, i.e. F1 and F2, also resulted in the formation of two palaeo-cliffines at 350-360m and 100-110m ASL (Chapter 2), and the deposition of regressive-upwards, sedimentary successions (Chapters 5, 6, 7 and 8). In addition, gorges on the west coast of the island that cut down from the 350-360m terrace to the 100-110m terrace reflect rapid relative uplift, similar to that described from the Kyrenia Range of northern Cyprus (Dreghorn, 1978).

Carbonate aeolian, littoral and sub-littoral sequences also developed during the lower-middle Pleistocene, i.e. F1 and F2. These crop out in areas away from the influence of the Troodos drainage systems, particularly to the west of the Akamas Peninsula which was a pre-existing topographic high (Fig.2.7). The offlapping carbonate sequence are interpreted as forming during a relative sea-level fall, i.e. a combination of a sea-level fall and tectonic uplift (Chapter 7). The siliciclastic quarry sequences that date

from this period in south-east Cyprus also represent an overall regression from deltaic to fluvial sequences (Chapter 6).

Eustatic sea-level fall and tectonic uplift caused the progradation of fluvial channels and down-cutting into the Pleistocene carbonate sequences in the Kouklia area, in south-west Cyprus. A subsequent rise in sea-level, i.e. F3 related, resulted in the formation of the 50-60m terrace, cutting sediments from marine, fluvial and sub-aerial environments (Fig.2.19).

### **10.1.3 Early Late Pleistocene (F3): further uplift.**

Systematically lowered topographic levels of littoral, deltaic and fluvial deposition, plus the presence of extensive erosion surfaces, indicate that uplift continued after F2 times, i.e. Middle Pleistocene. Littoral deposits were preserved due to this subsequent relative uplift. The emergence allowed unconsolidated littoral sands to be blown onshore to form migrating dunes that banked up against and over palaeo-cliffines.

Up to 12m of uplift and incision into the pre-existing alluvial fan system took place on the Mesaoria Plain during this time, resulting in the formation of channel fan systems (cf. Muto, 1987). Islandwide relative uplift was limited, although downcutting into the Pliocene and older sedimentary cover sequence and the lithologies of the Troodos ophiolite gave rise to sediment and Troodos-derived clasts. Reworking of Troodos-derived clasts also continued. Widespread channels tended to be shallow, dominated by sands and gravels. Deltas containing much reworked, mature gravel developed along the axis of the Polis-Paphos graben and around the southern coast of the island. These gravels are interbedded with sands and overlain by a thin limestone (Chapter 6). The deltas are overlain locally by thin, discontinuous sequences of littoral sediments, e.g. Polis. The deltaic sequences are also overlain by poorly sorted fluvial conglomerates, e.g. Larnaca area (Chapter 6), consistent with overall regression, as also indicated by the presence of sub-littoral to sub-aerial carbonate sequences, e.g. Larnaca (Chapter 7). This regression culminated in the formation of an extensive erosional surface (Chapter 2).

By the end of the F3, i.e. early Late Pleistocene, phase an extensive coastal plain had developed, extending out beyond the present coastline, as a result of a eustatic sea-level fall.

#### **10.1.4 Late Late Pleistocene-Holocene (F4): slightly lowered base levels, submergence and anthropogenic influences.**

The coral ages from the late Late Pleistocene, i.e. F4, terraces correlate with the Tyrrhenian sea-level high (oxygen isotope stage 5e; Shackleton, 1975). Widespread littoral deposits in Cyprus apparently relate to this transgressive/regressive event. A maximum uplift in the order of 6m has taken place since this time (Chapter 3), assuming that the Tyrrhenian sea-level high was 5-8m higher than the present day sea-level (Mesolella *et al.*, 1969; Bloom *et al.*, 1974; Chappell, 1974; Stearns, 1976). The high sea-level accounts for the formation of cliffs under which, apparently anomalously wide, low lying beaches are seen today, e.g. below Curium, and the formation and preservation of sea caves 2-3m ASL, e.g. Cape Pyla.

A "transgressive model" for aeolianite formation (Land *et al.*, 1967; Vacher 1973) is not favoured for the Quaternary sequences in Cyprus, as the lithified F3 dunes on the west coast appear to have been cut and/or eroded by the 5e sea-level high and not formed at that time. The F4 dunes overlie the dated littoral sequence which is correlated with the 5e sea-level high. The high-angle of repose, lack of capping soils, dominantly onshore palaeocurrent directions and knowledge that a drier climate (Rognon & Williams, 1977; Sarnthein, 1978) is likely to have existed during a glacial episode, are all consistent with the hypothesis that large-scale onshore migration of aeolianites took place. Thus, the available evidence points to formation of the dunes during a time of falling sea-level, in line with evidence from other Mediterranean aeolianites (Hey, 1962; Sabaris, 1962; Butzer, 1975).

Minimal uplift and incision into the pre-existing channel fan system took place on the Mesaoria Plain during F4 times. Islandwide relative uplift was limited, with little scope for erosion of the Troodos Massif, but reworking of the Troodos-derived clasts continued. Widespread channels tended to be shallow containing sands and gravels. Alluvial deposits of this age are best developed in the south and south-west of the island. In the north Troodos region valleys are floored by alluvial conglomerates and sands with a mixed clastic input. The axis of the Polis-Paphos graben and an embayment near Pissouri are filled with similar deposits. Excavation pits in the lower Vasilikos Valley show that 3 to 5 units of silts were deposited at this time, comprising centimetre-sized rhythmic cycles, intercalated with calcareous horizons (Gomez, 1987). Limited uplift is consistent with the observed minimal downcutting of pre-existing channels and the domination of silt and floodplain deposits to the north and south of the Troodos Massif, in contrast to the older fan sequences.

Limited relative uplift of the island occurred during the period from the last glacial to the present. The sedimentary sequences and geomorphological changes during the latest Pleistocene and Holocene periods reflect anthropogenic, climatic, eustatic and/or continuing minor tectonic effects, in line with the views of Flemming (1978), Gomez (1987) and this study, but contrary to the views of Giangrande *et al.* (1987) and Vita-Finzi (1990), who suggest that rapid uplift and extensive neotectonic faulting took place during this time.

## **10.2 DISCUSSION.**

### **10.2.1 Tectonic uplift versus isostatic effects.**

The processes causing uplift were discussed in Chapter 1. These included northward subduction, serpentinization, possible seamount underthrusting and thickening of the crust beneath Cyprus. Similar processes are reported elsewhere, e.g. the Japan Trench (Cadet *et al.*, 1987), the Mariana forearc (Fryer *et al.*, 1985) and the Coastal Range of California (Carlson, 1984). The effect of isostatic readjustment has been considered in areas of glacial loading and subsequent deglaciation (Mörner, 1976A; Clark, *et al.*, 1978) but have received scant attention in relation to uplift of mountain belts (England & Molnar, 1990). England & Molnar (1990) state that surface uplift, i.e. a motion opposite to the gravity vector, is the crucial component to consider when uplift rates are being discussed as this gives an absolute figure of movement away from a datum, such as the geoid, or mean present day sea-level. Surface uplift is considered important as:

surface uplift = uplift of rock minus exhumation.

In other words, if the exhumation is greater than rock uplift, then surface uplift will be negative as a result of the isostatic readjustment, even though rock uplift is taking place.

It has been shown, during the course of this study (Chapters 5 and 7), that the formation of the Quaternary sedimentary sequence in Cyprus has been influenced by climatic change, similar to that recorded elsewhere (e.g. Lees & Buller, 1972; Maizels, 1987; Harvey & Wells, 1987; Frostick & Reid, 1989). Erosion rates are dependent on the magnitude of the rainfall, rock type, structure and vegetation cover (Bloom, 1978) and it has been documented that dramatic morphologies can occur where there has been no surface uplift, as exhumation exceeds rock uplift (Molnar & England, 1990). Isostatic readjustments take place over a timescale of  $10^4$  years (Cathles, 1978) and become

difficult to distinguish from surface uplift features when longer timescales are being considered, i.e. the Quaternary period. So climatic variations coupled with variable tectonic uplift rates, rock type, structure and vegetation can lead to variable exhumation rates and therefore variable isostatic readjustment.

The data from the regional tectonics suggest that surface uplift has taken place in southern Cyprus; these data are supported by the presence of raised marine terraces and sediments that have been displaced relative to sea-level. The regressive nature of the Tertiary sedimentary sequence (Robertson, 1977; Robertson *et al.*, 1991) and the presence of these marine sediments above the present day sea-level are evidence for surface uplift, although the erosion surfaces on the Troodos Massif and the peneplaned terraces and erosion surfaces on the Mesaoria Plain themselves yield limited information concerning surface uplift, as there is no datum against which to fix these.

Tectonic uplift of southern Cyprus is clearly established and it is probably coupled with a component of isostatic readjustment that has occurred as a result of exhumation and tectonic uplift. The presence of erosion surfaces on the Troodos Massif may lead to an assumed surface uplift rate that is greater than the actual rate, hence uplift rates quoted here refer to the dated coastal terraces, which are well constrained. Numerical estimates of uplift of the Troodos Massif have not been attempted as these are likely to refer to a combination of the isostatic and surface uplift components.

### **10.2.2 Uplift versus sea-level change.**

The Troodos Massif has been uplifted during a period of glacio-eustatic sea-level change. To what extent can the two processes be disentangled in the Quaternary of southern Cyprus ?

During the earliest Pleistocene, both tectonism and sea-level changes influenced erosion and deposition. The highest 350-360m terrace is only preserved in south-west Cyprus, probably because this area was away from the later focus of uplift and thus survived erosion. The dominant control on erosion and sedimentation, during the early to mid-Pleistocene, was drastic uplift centred on Mount Olympus, modified by glacio-eustatic effects observed in coastal areas. The exact timing of the deposition of the dominant F1 sequence remains poorly known owing to the lack of datable material in the localised correlative littoral deposits. A late Lower Pleistocene age, i.e. c.1Ma., for the climax of uplift is probable, if it is assumed that the mature landforms on the Mesaoria Plain took c.700ka. to form (Chapter 2). The correlative littoral deposits, preserved only in areas away from the main focus of uplift and erosion from the Troodos Massif, i.e.



south-west Cyprus, indicate that sea-level was relatively high during part of the F1 depositional phase, i.e. early-middle Pleistocene, thus further emphasising the dominant role of tectonic uplift at this time. Regression followed, indicating sea-level fall and/or continued regional uplift and the period was marked by the deposition of the F2, i.e. middle Pleistocene, sediments. The F2 features mirror those of the F1, with similar fluvial and marine sediments. Channels of F2 age cut down into F1 terraces and the pre-Quaternary sediments suggesting that tectonic uplift, with possible associated isostatic effects (Section 10.2.1), continued during the F2 phase. The evidence from the Kouklia area in south-west Cyprus suggests that this tectonic uplift occurred during a falling, or low eustatic sea-level stand, allowing tectonic uplift and sea-level change to be differentiated in Cyprus for the first time (Fig.2 19).

Dates from corals in the Late Pleistocene, i.e. F3, marine terraces correspond to oxygen isotope 7 (Shackleton, 1975) and suggest that 13m of tectonic uplift took place between 130ka. and 192ka. (Chapter 3). The later stages of uplift were marked by regressive successions of shallow marine sediments, aeolianite and caliche deposits and the development of palaeo-clifflines. Dissection of pre-existing erosion surfaces took place with fluvial channel incision, regressive braid-delta accumulation and the development of erosion surfaces covered with caliche and terra-rossa-type palaeosols.

During the F4 phase, i.e. late Late Pleistocene, since c.130ka., sea-level change, specifically, transgression and regression, associated with the 5e sea-level high was the dominant control on the erosive and sedimentary features in south Cyprus, although limited uplift may have taken place (Chapter 3). A maximum of 6m of uplift has taken place in the past 116ka. (Chapter 3) confirming that eustatic sea-level change and not tectonics has been the dominant control in the latest Pleistocene.

During the Holocene (post-10ka.) glacio-eustatic change has clearly dominated sedimentation, modified by relatively minor tectonic movements - mainly subsidence of some coastal regions (Flemming, 1978). Regression, resulting from an estimated sea-level fall of 110-120m (Shackleton *et al.*, 1984) during the last glacial (40-10ka.; Dansgaard *et al.*, 1982), is widely recognisable in the form of offshore and onshore peneplaned surfaces and shallow conglomerate-filled channels.

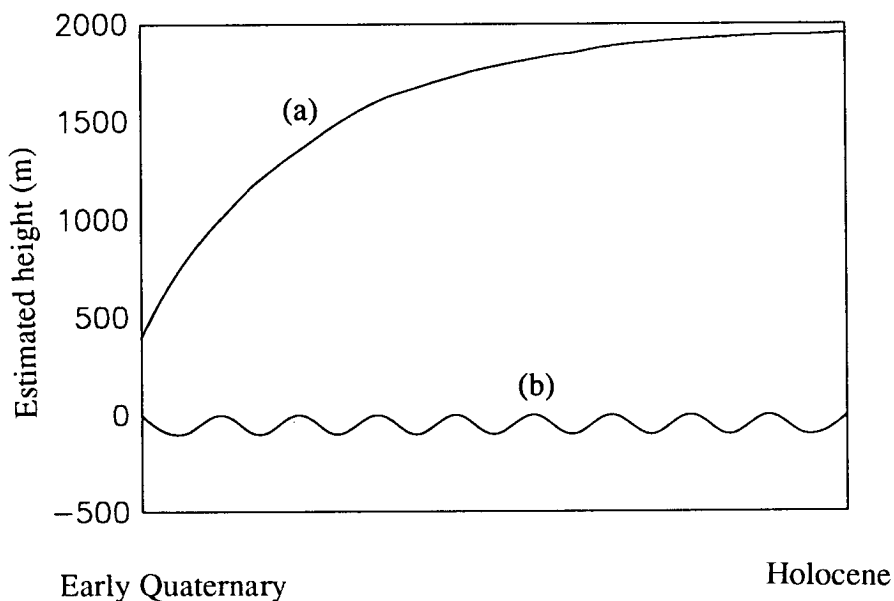
Anthropogenic influences have apparently dominated sedimentation, related to deforestation and agriculture during the Holocene. Gradual tectonic movements may have been taking place, but are not distinguishable. Silting, flooding and further downcutting to the present level occurred between 5540-5010 B.C. Late Holocene alluvial terraces were locally incised between 330-1190 A.D. (Gomez, 1987).

### **10.2.3 Nature of tectonic control.**

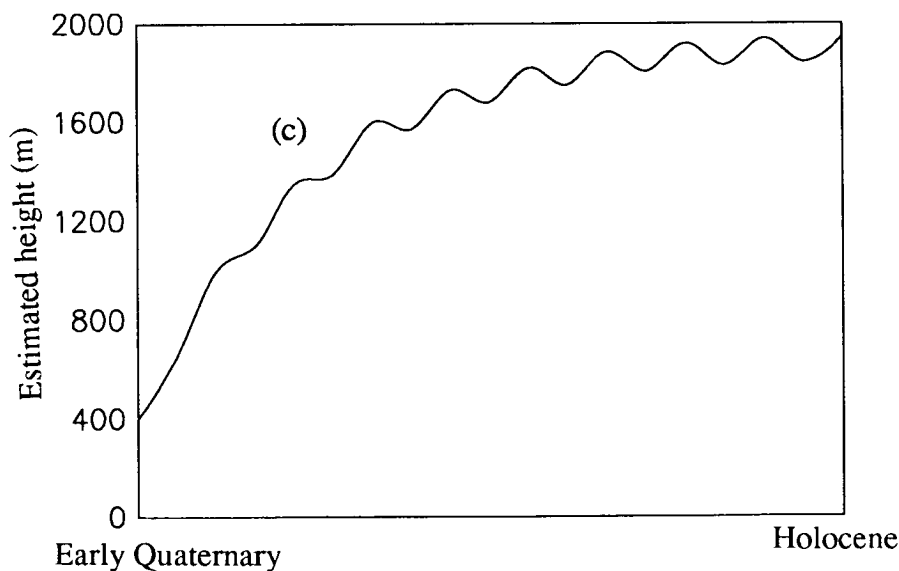
After the inferred initiation of northwards subduction along an active margin south of Cyprus, probably in earliest Miocene, southern Cyprus began to emerge with localised compression in the south, in the Miocene, and extension in the north, i.e. the Mesaoria basin, in the Late Miocene-Early Pliocene (Robertson *et al.*, 1991). Extension in the north was accompanied by uplift of the north Troodos margin areas that flanked the main graben, i.e. Mesaoria basin, with accompanying erosion and marine fan-delta deposition (McCallum, 1989). Focussed uplift of the Troodos Massif first became evident in the Late Pliocene-early Pleistocene with the deposition of the Kakkaristra and Apalos Formations, while marine deposition persisted on the south Kyrenia flank and probably in the Mesaoria basin into the early Quaternary. One alternative to explain the main tectonic uplift in early to mid-Pleistocene is serpentinite-driven diapiric protrusion of the ultramafic core of the Troodos Massif (Gass & Masson-Smith, 1963). Another is underthrusting of a continental fragment, or seamount, northwards beneath Cyprus during the Quaternary. Underthrusting of a seamount, e.g. the Eratosthenes Seamount (Fig.1.1), could have triggered serpentinitization and thus diapiric uplift of the Troodos Massif (Robertson, 1990) combined with regional uplift of the whole of Cyprus (including the Kyrenia Range). Serpentinite diapirism will only occur after ophiolite emplacement has taken place and will only continue as long as the negative buoyancy remains high enough to allow vertical movement to continue (Andrews-Speed & Johns, 1985; Fig.1.2), therefore erosion, and rates of erosion, of the lithologies above the diapir, will control the extent of vertical movement. The rate of erosion, coupled with isostatic effects (Section 10.2.1), are likely to control the vertical extent and speed of protrusion of the diapir. It should be noted that southern Cyprus was uplifted as a single structural entity with little evidence of major differential faulting (chapter 4), other than in the Polis-Paphos graben in south-west Cyprus where extension continued into the Quaternary. This agrees with observations from other tectonically active areas of the Mediterranean (Hey, 1978), where large areas have undergone equivalent amounts of uplift with little evidence of active faulting and local differential movement.

One outstanding problem is to determine whether the documented phases of relative uplift represent truly episodic tectonic pulses of uplift, or were instead the result of superimposition of the glacio-eustatic sea-level changes on a single cycle of accelerating and decelerating tectonic uplift. While initially favouring the first scenario (McCallum & Robertson, 1990), it is now believed that the second possibility is at least likely, especially if the rising serpentinite diapir was the dominant control on uplift (Fig.10.1; Table 1.10). However, it is recognised that earth movements tend to be episodic and irregular over short time scales (Ambraseys, 1971; Flemming &

Fig.10.1. Schematic curves indicating the possible interaction between eustatic sea-level change and tectonic uplift, and any associated isostatic component, in relation to the Quaternary evolution of Cyprus.



- (a) Curve representing the height of southern Cyprus, and specifically Mount Olympus, as a result of uplift.  
 (b) Curve representing a cyclic eustatic sea-level throughout the Quaternary period: assuming a complete cycle every 100ka. and very little variation between the height of the maximum and minimum sea-level throughout the period.



- (c) The sum of curves (a) and (b) displaying periods of constructive and destructive interference between sea-level and uplift. A schematic relative sea-level curve for the Quaternary of Cyprus.

Woodworth, 1988). Resolution of this problem is unlikely without absolute ages of the earlier, crustal uplift phases.

### **10.3 CONCLUSIONS.**

#### **10.3.1 Geomorphology.**

- i) the geomorphological features can be correlated throughout southern Cyprus,
- ii) the geomorphology reflects absolute uplift of the whole of southern Cyprus,
- iii) the available geomorphological evidence supports rapid uplift during the lower and middle Pleistocene, with relative quiescence and possible submergence in the Late Pleistocene and Holocene (Table 1.10),
- iv) nannofossil evidence from the Pliocene marl sequences and the presence of ? Upper Pliocene sediments in the 350-360m marine terrace indicate that a minimum of c.350m absolute uplift has taken place in coastal areas since this time,
- v) the four Quaternary erosion surfaces and terrace levels that crop out on the Mesaoria Plain can be correlated with the marine and non-marine erosion surfaces and terraces that crop out around coastal southern Cyprus,
- vi) U-series coral data from raised marine terraces in southern Cyprus confirm that the F3 terraces (8-11m ASL), correlated by means of geomorphology, are of similar age, 219-185ka., as are the F4 terraces (< 3m ASL) from different parts of the island which date from 141-116ka.,
- vii) the F3 terraces (8-11m ASL) record maximum uplift at an average rate of 29cm/ka. in the period 141-185ka. The younger F4 terraces (< 3m ASL) indicate a maximum uplift at an average rate of 5cm/ka. for the last 116ka., with the exception of Cape Greco which suggests a rate of 12cm/ka.. Correlation with the Quaternary global isotopic stages confirms that maximum uplift has been limited to 18m during the past 185-219ka. and also suggests that relative subsidence has taken place in some coastal areas over the past 116ka.,
- viii) the drainage pattern has remained broadly constant for the duration of the Quaternary period. This is supported by the palaeocurrent data from the sedimentary sequences which is broadly radial and centred on the Troodos Massif, although minor variations resulting from structural controls, e.g. the Polis-Paphos graben, and the development of shallow dipping coastal plains, have facilitated some deviation from this radial pattern,
- ix) the absence of major changes in the drainage pattern suggests that the focus of uplift of the Troodos Massif has remained the same throughout the Quaternary, i.e. Mount Olympus,

- x) the coastal geomorphology of the west coast indicates that the carbonate aeolianites that formed after the isotope 7 sea-level high, i.e. associated with the F3 terrace development, were subsequently cut, to form a cliffline, by the 5e sea-level high, i.e. the development of the F4 terrace, indicating that the dune formation followed the sea-level maxima,
- xi) that eustatic sea-level changes, uplift, isostasy and climate have all played a role in the formation of the preserved geomorphological features,
- xii) the rate of uplift during the Quaternary has varied, thus preventing accurate altimetric correlations with other areas of the Mediterranean, contrary to the views of Turner (1971) but in line with those of Hey (1978).

### **10.3.2 Sedimentology.**

- i) the Quaternary sediments of Cyprus can be split into three broad categories: the siliciclastic sediments, the carbonate sediments and the secondary sediments, i.e. soils and caliche. The siliciclastic fluvial sediments, i.e. the Fanglomerate Group, are the sole components on the north Troodos margin. Siliciclastic fluvial, marine and mixed aeolian sequences are the dominant sediments in areas where drainage feeds from the Troodos Massif along the southern coast of the island. The carbonate sequences by contrast are restricted to sub-littoral and aeolian sequences; these have an intrinsic relationship and are generally located in areas remote from the influence of the Troodos Massif's drainage system. The secondary sediments are found throughout southern Cyprus,
- ii) evidence from the sediments of the Fanglomerate Group indicate that there has been a waning of activity through the Quaternary. This has resulted in less exhaustive erosion and deposition during the Late Pleistocene-Recent,
- iii) the deposition of the Fanglomerate Group sediments on the north Troodos margin reflects uplift and Quaternary climate changes,
- iv) sea-level changes have influenced the development of the Fanglomerate Group in coastal areas of southern Cyprus, as is noted at distal locations where fluvial sediments have prograded over beach and delta successions, indicating a regressive sequence,
- v) the pattern of sedimentation of the Fanglomerate Group reveals a proximal to distal relationship, with evidence for the development of alluvial fans, channel fans, braidplain and floodplain environments,
- vi) the provenance of the Fanglomerate Group and marine siliciclastic sediments reflect local geology and the drainage pattern but the dominant source is the Troodos ophiolite,

- vii) the variation in provenance between the Pliocene and Pleistocene, and locally the Pleistocene to Holocene, Fanlomerate units is indicative of progressive unroofing of the Troodos ophiolite and its sedimentary cover sequence,
- viii) there has been no major change in provenance during the Quaternary, i.e. the absence of any introduction from a source other than the Troodos ophiolite and its sedimentary cover sequence,
- ix) the mixed dunes crop out in both coastal and inshore settings, e.g. those associated with fluvial sequences as exemplified by the Vasilikos Formation (McCallum, 1989), and are commonly associated with the regressive siliciclastic sequences,
- x) the carbonate littoral and sub-littoral sediments represent a series of transgressive, and then regressive, offlapping sequences, culminating in deposition of carbonate aeolianites. The U-series dates show that the F3 and F4 littoral sequences have formed during a eustatic sea-level maxima. The aeolianite sequences lie conformably above the littoral sequences and so formed during a sea-level fall, i.e. regression. The lowered sea-level during a glacial period (c.-120m ASL; Shackleton *et al.*, 1984) provides an ample reservoir of sediment available for dune formation,
- xi) the derived bioclastic sediment and abraded shells and tests in the coastal carbonate aeolianites, identical to those seen in the underlying littoral sequences, indicate that the carbonate dunes were derived from previously deposited littoral sediments,
- xii) the U-series data confirm that the deposition of the F3 and F4 carbonate sediments has been controlled by eustatic sea-level changes rather than a relative sea-level fall, i.e. eustatic and associated uplift,
- xiii) broad Quaternary climatic variations indicated by the changes in the Mediterranean molluscan population may have contributed to the presence, or absence, of corals in the Quaternary carbonate sequences,
- xiv) cementation of the littoral sequences has been variable and indicates diagenetic alteration in both the phreatic and meteoric realms, whereas the aeolian sequences have only undergone meteoric cementation indicating sub-aerial rather than marine processes,
- xv) the formation of both the kafkalla and havara horizons on Cyprus reflects calichification,
- xvi) the substratum on which calichification has taken place will play a major role in both the speed and type of caliche formation,
- xvii) the type of caliche horizon present, whether pedogenic or caliche crust, is dependent on the presence of palaeosols and substratum,
- xviii) the groundwater and capillary models are both applicable to caliche formation in Cyprus,

xix) extensive caliche formation has taken place during the Pleistocene. The apparent lack of caliche forming on non-carbonate substratum, during the Holocene, may reflect climate change during this period, as identified in Cyprus and elsewhere in the Mediterranean region (Vita-Finzi, 1969; Dreghorn, 1978),

xx) palaeosol horizons have developed throughout the Quaternary. The development of single or multiple palaeosol horizons reflect a combination of climate change, base level changes and the sedimentary environment of deposition.

### **10.3.3 Neotectonics.**

i) block uplift of the island has apparently taken place during the Quaternary as geomorphological and radiometric data indicate that terraces can be correlated throughout southern Cyprus,

ii) tectonic activity since the early Quaternary has been minimal, with relative movement being taken up by meso-scale faults and fractures. The evidence from earthquakes shows that tectonic activity is still taking place. However, seismic data showing the stratified and undisturbed nature of the Quaternary sediments indicate that this has had a minimal effect on the Quaternary sequences,

iii) seismic sections, earthquake foci, down borehole and fault data show a consistent alignment of structures, striking between WNW-ESE and NNW-SSE,

iv) joint and fracture data are generally aligned perpendicular to principal axes of extension,

v) there is no evidence of Quaternary folding,

vi) there is very little evidence for present day subduction related processes, as the compression component of the borehole data (Haimson *et al.*, 1990) appears to be taken up by strike-slip motion.

### **10.3.4 General.**

i) the radiometric data, i.e. amino-acid, U-series,  $^{14}\text{C}$ , and faunal evidence are consistent with each other and the geomorphological correlations, which in turn correlate with the sedimentological data,

ii) tectonic uplift has probably been the dominant control during the Lower and Middle Pleistocene, whereas Quaternary eustatic sea-level changes have controlled the deposition of the exposed littoral sequences during the Late Pleistocene,

iii) all the data are consistent with uniform uplift of the coastal areas throughout the Quaternary period,

iv) the uplift has been differential, and probably focussed on Mount Olympus, throughout the Quaternary period,

- v) eustatic sea-level changes, uplift, isostasy and climate have all played a role in the formation and preservation of the Quaternary sedimentological and geomorphological features in southern Cyprus,
- vi) evidence indicates that subsidence has occurred in the latest Pleistocene and Holocene (Flemming, 1978; this study).

### **10.3.5 Summary.**

The potential to correlate geomorphological terrace surfaces, alluvial systems and coastal marine and non-marine settings throughout southern Cyprus provides an ideal opportunity to assess the importance of tectonic uplift versus sea-level change in the Quaternary unroofing of the Troodos ophiolite. Following earlier uplift, the Troodos Massif underwent drastic, focussed uplift in the late-early to middle-Pleistocene (c.1.5-1Ma.), with a further weaker phase of uplift continuing into the late Late Pleistocene (c.130ka.). The uplift corresponded to times of high relative sea-levels, followed by relative regression. The dominant control in the late Quaternary was thus eustatic, particularly the Tyrrenian highstand (c.130ka.). A maximum of 6m of uplift has taken place since 116ka. and there is evidence of Holocene submergence of some coastal areas (Flemming, 1978). The slowing and/or cessation of tectonic uplift could correspond to the absence of present day subduction beneath southern Cyprus. The overall tectonic setting during the Quaternary involved the overriding plate of a northwards-dipping subduction zone, that was punctured by the diapiric protrusion of serpentinite, possibly associated with the collision of a seamount with the Cyprus trench.

### **10.4 FURTHER WORK.**

Further studies that could provide more valuable data concerning the Quaternary evolution of Cyprus are:

- i) radiometric age determination of the *in situ* coral from the F2 terrace sequence; these data would better constrain rates of uplift and deduce whether this F2 terrace formed during a eustatic sea-level maxima, or minima. Radiometric dating of caliche formations may also possibly confirm the correlation of the erosion surfaces on the north Troodos margin,
- ii) more detailed neotectonic studies, especially shallow seismic surveys off south-western coast of Cyprus; these will allow the extent, nature and timing of neotectonic faulting, associated with the continuing formation of the Polis-Paphos graben, during the Quaternary and Recent to be deduced,
- iii) more detailed studies of the palaeosols, and especially pollen, so that more accurate estimates of the Quaternary climate can be made,



- iv) studies of the extensive colluvial sediments may aid future studies of fault movement, as much of the unconsolidated sediment is likely to undergo gravity movement during periods of tectonic activity,
- v) a study similar to this, tying the sedimentology, geomorphology and neotectonics to the south and the north of Kyrenia Range would allow the rate and style of uplift in the Kyrenia Range to be compared and contrasted with the southern portion of the island. This complimentary study would allow conclusions concerning the regional setting during the Quaternary to be made, as well as deductions concerning the processes and nature of uplift in each of these areas.

## References

- ABELSON, P.H., 1955. Organic constituents of fossils. *Carnegie Institution, Washington, Yearbook*, v.54, p.107-109.
- ABRAHAMSEN, N. & SCHONHARTING, G., 1987. Palaeomagnetic timing of the rotation and translation of Cyprus. *Earth and Planetary Science Letters*, v.81, p.409-418.
- ABRAMS, M., CHADWICK, O. & ROTHERY, D., 1988. Quaternary history of the Semail ophiolite along the Butinah coast, Oman. *Abstract for the international discussion meeting; the geology and tectonics of the Oman region, Edinburgh, March 1988*, p.4.
- ADEY, W.H. & MACINTYRE, I.G., 1973. Crustose coralline algae: a re-evaluation in the geological sciences. *Geological Society of America Bulletin*, v.84, p.883-904.
- ADEY, W.H. & BURKE, R., 1976. Holocene bioherms (algal ridges and bank barrier reefs) of the eastern Caribbean. *Geological Society of America Bulletin*, v.87, p.95-109.
- ADEY, W.H., TOWNSEND, R.A. & BOYKINS, W.T., 1982. The crustose coralline algae of the Hawaiian Archipelago. *Smithsonian Institute Contribution, Marine Science*, no.15, p.1-74
- ALEXANDERSSON, T.E., 1969. Recent littoral and sublittoral high Mg-calcite lithification in the Mediterranean. *Sedimentology*, v.12, p.47-61.
- ALEXANDERSSON, T.E., 1972. Mediterranean beachrock cementation: marine precipitation of Mg-calcite. *in: Stanley, D.J. (ed.) The Mediterranean Sea Dowden, Hutchinson and Ross*, p.203-223.
- ALLERTON, S. & GOMEZ, B., 1989. Structural geomorphology of south-east Troodos, in the vicinity of Pano Lefkara, Cyprus. *Geografiska Annaler.*, v.71A, p.221-231.
- ALLERTON, S. & VINE, F.J., 1990. Palaeomagnetic and structural studies in the southeastern part of the Troodos complex. *in: Malpas, J., Moores, E., Panayiotou, A. & Xenophontos, C. (eds.), Ophiolites: oceanic crustal analogues. Proceedings of the Symposium "Troodos 1987", Nicosia, Cyprus*, p.99-112.
- AMBROSEYS, N.N., 1971. Value of historical records of earthquakes. *Nature*, v.232, p.375-379 .
- AMBROSETTI, P., AZZAROLI, A., BONADONNA, F.P. & FOLLIERI, M., 1972. A scheme of Pleistocene chronology for the Tyrrhenian side of central Italy. *Bulletin of the Geological Society of Italy*, v.91, p.169-180.
- ANASTASAKIS, G. & KELLING, G., 1991. Tectonic connection of the Hellenic and Cyprus arcs and related geotectonic elements. *Marine Geology*, v.97, p.261-278.
- ANDREWS-SPEED, C.P. & JOHNS, C.C., 1985. Basement diapirism associated with the emplacement of major ophiolite nappes: some constraints. *Tectonophysics*, v.118, p.43-59.
- ANGELIER, J., 1978. Tectonic evolution of the Hellenic arc since the Late Miocene. *Tectonophysics*, v.49, p.23-36.
- ANGELIER, J., 1984. Tectonic analysis of fault slip data sets. *Journal Geophysical Research*, v.89, p.5835-5848.
- BAGNALL, P.S., 1960. The geology and mineral resources of the Pano Lefkara-Lamaca area. *Geological Survey Department, Cyprus, Memoir 5*, 116pp.
- BAGNOLD, R.A., 1954. The physics of blown sand and desert dunes. *Methuen, London*, 2<sup>nd</sup> edition.

- BARD, E., HAMILTON, B., FAIRBANKS, R.G. & ZINDLER, A., 1990. Calibration of the  $^{14}\text{C}$  timescale over the past 30,000 years using mass spectrometric U-Th ages from Barbados. *Nature*, v.345, p.405-409.
- BAROZ, F., BIZON, G., BIZON, J.-J., HEIMANN, K.O., MALLET, J.-P., MULLER, C., ORSZAG-SPERBER, F., ROUCHY, J.-M. & WEISGERBER, F., 1978. Le Miocène terminal et le Pliocène dans la région de Polemi (Chypre Ouest): milieux de dépôt. *Académie des Sciences, Comptes Rendus Hebdomadaires des Séances, Paris*, v.D286, p.1771-1774.
- BAROZ, F., 1979. Étude géologique dans le Pentadactylos et de la Mésooria (Chypre septentrionale). *Ph.d. thesis University of Nancy*, 365pp.
- BATE, D.M.A., 1903. Preliminary notes on the discovery of a pygmy elephant in the Pleistocene of Cyprus. *Proceedings of the Royal Society of London*, v.71, p.498-500.
- BATE, D.M.A., 1904. Further notes on the remains of *Elephas cypriotes*, Bate, from a cave deposit in Cyprus. *Proceedings of the Royal Society of London*, v.74, p.120-121.
- BATES, P.L. & JACKSON, J.A. (EDS.), 1980. Glossary of geology. *American Geological Institute*, 2<sup>nd</sup> edition, 749pp.
- BATHURST, R.G.C., 1966. Boring algae, micrite envelopes and lithification of molluscan biosparites. *Journal of Geology*, v.5, p.15-32.
- BEAR, L.M., 1960. The geology and mineral resources of the Akaki-Lythrodondha area. *Geological Survey Department, Cyprus, Memoir 3*, 122pp.
- BEAR, L.M. & MOREL, S.W., 1960. The Geology and Mineral Resources of the Agros-Akrotiri area. *Geological Survey Department of Cyprus, Memoir 7*, 88pp.
- BEIER, J.A., 1985. Diagenesis of Quaternary Bahamian beachrock: petrographic and isotopic evidence. *Journal of Sedimentary Petrology*, v.55, p.755-761.
- BELLAMY, C.V. & JUKES-BROWNE, A.J., 1905. The Geology of Cyprus. *W. Brendon and Son, Plymouth, Devon*, 72pp.
- BELLUOMINI, G. & BADA, J.L., 1985. Isoleucine epimerization ages of the dwarf elephants of Sicily. *Geology*, v.13, p.451-452.
- BEN-AVRAHAM, Z. & NUR, A., 1986. Collisional processes in the Eastern Mediterranean. *Geologische Rundschau*, v.75, p.209-217.
- BEN-AVRAHAM, Z., KEMPLER, D. & GINZBURG, A., 1988. Plate convergence in the Cyprian Arc. *Tectonophysics*, v.146, p.231-240.
- BENDER, M.L., FAIRBANKS, R.G., TAYLOR, F.W., MATTHEWS, R.K., GODDARD, J.G. & BROECKER, W.S., 1979. Uranium series dating of Pleistocene reef tracts of Barbados, West Indies. *Geological Society of America Bulletin*, v.90, p.577-594.
- BERGER, A.L., IMBRIE, J., HAYS, G., KUKLA, G. & SALTZMAN, B. (EDS.), 1984. Milankovitch and Climate: understanding the response to astronomical forcing. *Reidal Publishing Company*, p.434 and 532.
- BERNARD, H.E., LEBLANC, R.J. & MAJOR C.F., 1962. Recent and Pleistocene geology of south east Texas, geology of the Gulf Coast and central Texas and guide book of excursion. *Houston Geological Society*, p.175-224.
- BLISSENBACH, E., 1954. Geology of alluvial fans in semi-arid regions. *Geological Society of America Bulletin*, v.65, p.175-190.

- BLOOM, A.L., BROECKER, W.S., CHAPPELL, J.M.A., MATTHEWS, R.K. & MESOLELLA, K.J., 1974. Quaternary sea level fluctuations on a tectonic coast: new  $^{230}\text{Th}/^{234}\text{U}$  dates from the Huon Peninsula, New Guinea. *Quaternary Research*, v.4, p.185-205.
- BLOOM, A.L., 1978. Geomorphology. *Eaglewood Cliffs, New York, Prentice-Hall, 510pp.*
- BLUCK, B.J., 1967A. Deposition of some Upper Old Red Sandstone conglomerates in the Clyde area: a study in the significance of bedding. *Scottish Journal of Geology*, v.3, p.139-167.
- BLUCK, B.J., 1967B. Sedimentation of beach gravels: examples from south Wales. *Journal of Sedimentary Petrology*, v.37, p.128-156.
- BOEKSCHOTEN, G.J. & SONDAAR, P.Y., 1972. On the Fossil Mammalia of Cyprus, I and II. *Proceedings Series B Koninkl. Nederland Akedemie Van Weteneschappen*, v.75, p.306-338.
- BOGGS, S. JNR., 1969. Relationship of size and composition in pebble counts. *Journal of Sedimentary Petrology*, v.39, p.1243-1247.
- BONADONNA, F.P. & BIGAZZI, G., 1970. Studi sul Pleistocene del Lazio. VIII. Datazione di tufi intertirreniani della zona di Cerveteri (Roma) mediante il metodo delle tracce di fissione. *Geological Society of Italy Bulletin*, v.89, p.463-473.
- BONATTI, E., 1976. Serpentinite protrusions in the oceanic crust. *Earth and Planetary Science Letters*, v.32, p.107-113.
- BONHOMMET, N., ROPERCH, P. & CALZA, F., 1988. Palaeomagnetic arguments from block rotations along the Arakapas fault (Cyprus). *Geology*, v.16, p.422-425.
- BONIFAY, E. & MARS, P., 1959. Le Tyrrhenian dans le cadre de la chronologie Quaternaire Mediterranee. *Geological Society of France Bulletin*, v.7, p.62-78.
- BOSELLINI, A. & GINSBURG, R.N., 1970. Form and internal structure of recent algal nodules (rhodolites) from Bermuda. *Journal of Geology*, v.79, p.669-682.
- BOSENCE, D.W.J., 1976. Ecological studies on two unattached coralline algae from western Ireland. *Palaeontology*, v.19, p.365-395.
- BOUCHER, K., 1975. Global climate. *English University Press, p.236-237.*
- BOURGEOIS, J. & LEITHOLD, E.L., 1984. Wave worked conglomerates - depositional processes and criteria for recognition. *in: Koster, E.M. and Steel, R.J. (eds.), Sedimentology of gravels and conglomerates. Special Publication of the Canadian Geological Society, Memoir 10, p.331-343.*
- BOWEN, D.Q., 1978. Quaternary geology: a stratigraphic framework for multidisciplinary work. *Pergamon, Oxford, 235pp.*
- BOWEN, D.Q., SYKES, G.A., REEVES, A., MILLER, G.H., ANDREWS, J.T., BREW, J.S. & HARE, P.E., 1985. Amino-acid geochronology of raised beaches in SW Britain. *Quaternary Science Reviews*, v.4, p.279-318.
- BOYLE, J.F., 1984. The origin and geochemistry of the metalliferous sediments of the Troodos Massif, Cyprus. *Unpublished Ph.d. thesis Edinburgh University, 277pp.*
- BRETZ, J.H., 1960. Bermuda: a partially drowned late marine, Pleistocene karst. *Geological Society of America Bulletin*, v.71, p.1729-1754.

- BROECKER, W.S., 1963. A preliminary evaluation of U-series inequilibrium as a tool for absolute age measurement on marine carbonates. *Journal of Geophysical Research*, v.68, p.2817-2834.
- BROECKER, W.S., THURBER, D.L., GODDARD, J., KU, T.L., MATTHEWS, R.K. & MESOLELLA, K.J., 1968. Milankovitch hypothesis supported by precise dating of coral reefs and deep sea sediments. *Science*, v.159, p.297-300.
- BROECKER, W.S. & BENDER, M.L., 1972. Age determination of marine strandlines. in: Bishop, W.W. & Miller, J.A. (eds.), *Calibration of hominoid evolution*, p.19-38.
- BULL, W.B., 1977. The alluvial fan environment. *Progress in Physical Geography*, v.1, p.222-270.
- BULL, W.B., 1978. Geomorphic tectonic activity classes of the south front of the San Gabriel mountains, California. *United States Geological Survey, Contact Report 14-08-001-G-394; Office of earthquakes, volcanoes and engineering, Menlo Park, California, 59pp.*
- BULL, W.B., 1985. Correlation of flights of global marine terraces. in: Morisawa, M. & Hack, J. (eds.) *Tectonic Geomorphology. Proceedings of the 15th Annual Geomorphology Symposium, State University of New York at Binghamton, Winchester, Massachusetts, George Allen & Unwin*, p.129-152.
- BULL, W.B. & COOPER, A.P., 1986. Uplifted marine terraces along the Alpine fault: New Zealand. *Science*, v.234, p.1225-1228.
- BULL, W.B., 1990. Stream-terrace genesis: implications for soil development. *Geomorphology*, v.3, p.351-367.
- BURST, J.F., 1976. Argillaceous sediments dewatering. *Annual Reviews of Earth and Planetary Science Letters*, v.4, p.293-318.
- BUTZER, K.W. & CUERDA, J., 1962. Coastal stratigraphy of Southern Mallorca and its implications for the Pleistocene chronology of the Mediterranean Sea. *Journal of Geology*, v.70, p.398-416.
- BUTZER, K.W., 1962. Coastal geomorphology of Majorca. *Annals of the Association of American Geographers*, v.52, p.191-212.
- BUTZER, K.W., 1963. Climatic-geomorphologic interpretation of Pleistocene sediments in the Eurafrikan subtropics. *Viking Fund Publications in Anthropology*, v.36, p.1-27.
- BUTZER, K.W., 1975. Pleistocene littoral sedimentology cycles of the Mediterranean basin: A Mallorquin View. in: Butzer, K.W. & Issac, G.L. (eds.), *After the Australopithecines: Stratigraphy, Ecology and Culture Change in the Middle Pleistocene*, Moulton, The Hague, p.25-72.
- CADET, J.-P., KOBAYASHI, K., AUBOUIN, J., BOULEGUE, J., DEPLUS, C., DUBOIS, J., VON HUENE, R., JOLIVET, L., KANAZAWA, T., KASAHARA, J., KOIZUMI, K., LALLEMAND, S., NAKAMURA, Y., PAUTOT, G., SUYEHRO, K., TANI, S., TOKUYAMA, H. & YAMAAZAKI, T., 1987. The Japan Trench and its juncture with the Kuril Trench: cruise results of the Kaiko project, Leg 3. *Earth and Planetary Science Letters*, v.83, p.267-284.
- CARLSON, C., 1984. Stratigraphic and structural significance of foliate serpentine breccias, Wilbur Springs. *Society of Economic Palaeontologists and Mineralogist, Field Trip Guidebook no.3*, p.108-112.
- CARLSON, R.L. & MELIA, P.J., 1984. Subduction hinge migration. *Tectonophysics*, v.102, p.399-411.
- CARR, J.M. & BEAR, L.M., 1960. The geology and mineral resources of the Peristerona-Lagoudhera area. *Geological Survey Department, Cyprus, Memoir 2*, 79pp.

- CARSON, M.A. & KIRKBY, M.J., 1972. Hillslope form and process. *Cambridge University Press, London*, 475pp.
- CATHLES, L.M., III, 1975. The viscosity of the earth's mantle. *Princeton University Press, Princeton, New Jersey*.
- CATINI, G., LENARDON, G., MARCHETTI, A., TUNIS, G. & VINCI, A., 1983. Sedimentological and seismic features in the Cyprian sector of the eastern Mediterranean sea: preliminary results. *Bollettino di Oceanologia Teorica ed Applicata*, v.1N, p.311-317.
- CHAPPELL, J., 1974. Geology of coral terraces, Huon Peninsula, New Guinea. A study of Quaternary movements and sea-level changes. *Geological Society of America Bulletin*, v.85, p.553-570.
- CHAPPELL, J. & VEEH, H.H., 1978. Late Quaternary movements and sea-level changes at Timor and Atauro Island. *Geological Society of America Bulletin*, v.89, p.356-368.
- CHAPPELL, J., 1983. A revised sea-level record for the last 300,000 years on Papua New Guinea. *Search*, v.14, p.99-101.
- CHAPPELL, J. & SHACKLETON, N.J., 1986. Oxygen isotopes and sea-level. *Nature*, v.324, p.137-140.
- CHEN, J.H., EDWARDS, R.L., & WASSERBURG, G.J., 1986.  $^{238}\text{U}$ ,  $^{234}\text{U}$  and  $^{232}\text{Th}$  in seawater. *Earth and Planetary Science Letters*, v.80, p.241-251.
- CLARK, J.A., FARRELL, W.E. & PELTIER, W.R., 1978. Global changes in postglacial sea-level, a numerical calculation. *Quaternary Research*, v.9, p.265-287.
- CLIFTON, H.E., 1973. Pebble segregation and bed lenticularity in wave worked versus alluvial gravels. *Sedimentology*, v.20, p.173-187.
- CLIFTON, H.E., 1981. Progradational sequences in Miocene shoreline deposits south eastern Calierite Range, California. *Journal of Sedimentary Petrology*, v.51, p.165-184.
- CLIFTON, H.E., HUNTER, R.E. & PHILLIPS, R.L., 1971. Depositional structures and processes in the non-barred high energy nearshore. *Journal of Sedimentary Petrology*, v.41, p.651-670.
- CLUBE, T.M.M., 1985. The palaeorotation of the Troodos microplate. *Unpublished Ph.d. thesis, University of Edinburgh*, 277pp.
- CLUBE, T.M.M. & ROBERTSON, A.H.F., 1986. The palaeorotation of the Troodos microplate, Cyprus, in the Lower Mesozoic-Early Cenozoic plate tectonic framework of the Eastern Mediterranean. *Surveys in Geophysics*, no.8, p.375-437.
- COLELLA, A., 1988. Pliocene-Holocene fan deltas and braid deltas in the Crati Basin, southern Italy: a consequence of varying tectonic conditions. in: Nemeč, W. & Steel, R.J. (eds.), Fan deltas: sedimentology and tectonic settings *Blackie*, p.50-74.
- COLEMAN, R.G., 1977. Ophiolites, ancient oceanic lithosphere. *Springer-verlag*, 229pp.
- COLLIER, R.E.LI., 1990. Eustatic and tectonic controls upon Quaternary coastal sedimentation in the Corinth Basin, Greece. *Journal of the Geological Society of London*, v.147, p.301-314.
- COLLINSON, J.D. & THOMPSON, D.B., 1982. Sedimentary structures. *Allen and Unwin, London*, 194pp.
- CONEY, P.J., JONES, D.L. & MONGER, J.W.H., 1980. Cordilleran suspect terranes. *Nature*, v.288, p.329-333.
- CONSTANTINO, G., 1985. Annual report of the Geological Survey department for the year 1984. *Geological Survey Department of Cyprus, Nicosia*.

- CONSTANTINOU, G., 1986. Annual report of the Geological Survey department for the year 1985. *Geological Survey Department of Cyprus, Nicosia*.
- CONSTANTINOU, G., 1987. Annual report of the Geological Survey department for the year 1986. *Geological Survey Department of Cyprus, Nicosia*.
- COOPER, J.A.G. & FLORES, R.M., 1991. Shoreline deposits and diagenesis resulting from two Late Pleistocene highstands near +5 and +6 metres, Durban, south Africa. *Marine Geology*, v.97, p.125-143.
- COOPER, W.S., 1958. Coastal sand dunes of Oregon and Washington. *Geological Society of America Memoir 72, 169pp*.
- COUMES, F. & BOLTENHAGEN, C., 1978. Trace element distribution in D.S.D.P. sites 372, 374, 375 and 376 in the Mediterranean Sea. *in: Hsu, K.J., Mondadert, L., Bernoulli, D., Cita, M.B., Erickson, A., Garrison, R.E., Kidd, R.B., Mélières, F., Müller, C. & Wright, R. Initial Reports of the Deep Sea Drilling Project, 42 Part 1, U.S. Government Printing Office, Washington, p.493-506*.
- COWPER-REED, F.R., 1930. Contributions to the geology of Cyprus. *Geological Magazine*, v.67, p.241-271.
- CRIMES, T.P., 1975. The stratigraphical significance of trace fossils. *in: Frey, R.W. (ed.). A synthesis of principles, problems and procedures in ichnology. Springer-Verlag, New York, p.109-131*.
- CROLL, J., 1875. Climate and time in their Geological Relations, a Theory of secular Change of the Earth's Climate. *Dalby, Ibister Co., London, 577pp*.
- DALONI, M., 1951. Sur la genese et l'age des terrains a Croute, Nords Africains. *Colloques internationaux, centre national de la recherche scientifique, v.35, p.278-285*.
- DANSGAARD, W., CLAUSEN, H.B., GUNDESTRUP, N., HAMMER, C.U., JOHNSEN, S.F., KRISTINSDOTTIR, P.M. & REEH, N., 1982. A new Greenland deep ice core. *Science*, v.218, p.1273-1277.
- DAVIES, J.L. (ED.), 1980. Geographical variation in coastal development. *Longmans, London, 212pp*.
- DAVIS, R.A. (JNR.) & FOX, W.T., 1972. Coastal processes and nearshore sand bars. *Journal of Sedimentary Petrology*, v.42, p.401-412.
- DAVIS, R.A. (JNR.) & FOX, W.T., 1975. Process response patterns in beach and nearshore sedimentation; I, Mustang Island, Texas. *Journal of Sedimentary Petrology*, v.45, p.852-865.
- DAVIS, R.A. (JNR.), 1985. Beach and nearshore zone. *in: Davis, R.A. jnr (ed.) Coastal sedimentary environments, Springer-Verlag, p.379-438*.
- DAVIS, S.J., 1981. The effects of temperature change and domestication on the body size of late Pleistocene to Holocene mammals in Israel. *Palaeobiology*, v.7, p.101-114.
- DE VAUMAS, E., 1959. The Principal geomorphological regions of Cyprus, *in: Ingham, F. (ed.) Annual Report of the Geological Department of Cyprus for 1958, p.38-43*.
- DE VAUMAS, E., 1961. *Further contributions to the geomorphology of Cyprus. in: Ingham, F. (ed.) Annual Report of the Geological Department of Cyprus for 1960, p.23-34*.
- DE VAUMAS, E., 1962. Notes on the geomorphology of Cyprus. *in: Ingham, F. (ed.) Annual Report of the Geological Department of Cyprus for 1961, p.28-34*.

- DECELLES, P.G., 1987. Variable preservation of Middle Tertiary coarse grained nearshore to outer shelf storm deposits in southern California. *Journal of Sedimentary Petrology*, v.57, p.250-264.
- DEPERET, C., 1918. Essai de coordination chronologique generale des temps quaternaire. *Research Paris Academy of Science C.R.*, v.167, p.418-422.
- DERCOURT, J., ZONENSHAIN, L.P., RICOU, L.-E., KAZMIN, V.G., LE PICHON, X., KNIPPER, A.L., GRANDJACQUET, C., SBORTSHIKOV, I.M., GEYSSANT, J., LEPVRIER, C., PECHERSKY, D.H., BOULIN, J., SIBUET, J.-C., SAVOSTIN, L.A., SOROKHTIN, O., WESTHAL, M., BAZHENOV, M.L., LAUER, J.P. & BLJU-DUVAL, B., 1985. Geological evolution of the Tethys Belt from the Atlantic to the Pamirs since the Lias. *Tectonophysics*, v.123, p.241-315.
- DEWEY, J.F. & SENGOR, A.M.C., 1979. Aegean and surrounding regions: complex multiplate and continum tectonics in a convergent zone. *Geological Society America Bulletin*, v.90, p.84-92.
- DEWEY, J.F., 1980. Episodicity, sequence and style at convergent plate boundaries. in: Strangeway, D.F. (ed.). The continental crust and it's mineral deposits. *Geologists Association of Canada Special Publication*, v.20, p.553-573.
- DEWEY, J.F., HEMPTON, M.R., KIDD, W.S.F. SARGLU, F. & SENGOR, A.C.M., 1986. Shortening of continental lithosphere: the neotectonics of Anatolia, a young collision zone. in: Coward, M.P. & Ries, A.C. (eds.), Collision tectonics. *Geological Society Of London Special Publication*, v.19, p.3-36.
- DEWEY, J.F., PITMAN, W.C., RYAN, W.F.R & BONNIN, J., 1973. Plate tectonics and the evolution of the Alpine system. *Geological Society America Bulletin*, v.84, p.3127-3180.
- DICKINSON, W.R., 1966. Table Mountain serpentinite extrusion in California Coastal Ranges. *Geological Society America Bulletin*, v.77, p.451-472.
- DICKSON, J.A.D., 1965. A modified staining technique for carbonates in thin section. *Nature*, v.205, p.587.
- DMITRIEV, L.V., 1975. Serpentinization of oceanic hyperbasites. in: Recent contributions to Geochemistry, translated from Russian. Wiley and Son, New York, p.243-250.
- DOBKINS, J.E. & FOLK, R.L., 1970. Shape development in Tahiti-nui. *Journal of Sedimentary Petrology*, v.40, p.1167-1203.
- DREGHORN, W. 1978. Landforms of the Girne Range, Northern Cyprus. *The Mineral Research and Exploration Institute of Turkey*, no.172, 222pp.
- DRIESE, S.G., FOREMAN, J.L., COTTER, E., NICKELSEN, R.P. & GRAY, M.B., 1990. Depositional, pedogenic and diagenetic controls on palaeovertisol development, Palaeozoic of Central and Southern Appalachians. *Abstracts of the 13th International Sedimentary Congress, Nottingham, U.K., IAS/BGS*, p.141.
- DUCLOZ, C., 1965. Revision of the Pliocene and Quaternary stratigraphy of the central Mesaoria. in: Hadji Stavrinou, Y. (ed.), Annual Report of the Geological Survey Department of Cyprus for 1964, Nicosia, Cyprus, p.31-42.
- DUCLOZ, C., 1968. Les formations quaternaires de la région de Klepini (Chypre) et leur place dans la chronologie du Quaternaire méditerranéen. *Archives des Sciences, Genève*, no.20, 196pp.
- DUCLOZ, C., 1972. The geology of the Bellapais-Kythrea area of the central Kyrenia Range. *Geological Survey Department of Cyprus, Bulletin*, n.6, 75pp.



- DUPOUX, B., 1983. Étude comparée de la tectonique Néogène des bassins du sud de Chypre et du bassin d'Antalya (Turquie). *Thèse Docteur 3em. Cycle (Unpublished), Université de Paris Sud, Centre d'Orsay, France, 116pp.*
- EATON, S. 1987. The sedimentology of Mid to Late Miocene carbonates and evaporites in Southern Cyprus. *Unpublished Ph.d. thesis, Edinburgh University, 259pp.*
- EDWARDS, R.L., CHEN, J.H., & WASSERBURG, G.J., 1986-87.  $^{238}\text{U}$ - $^{234}\text{U}$ - $^{230}\text{Th}$ - $^{232}\text{Th}$  systematics and the precise measurement of time over the past 500,000 years. *Earth and Planetary Science Letters, v.81, p.175-192.*
- EL-SAYAD, M.K.H., 1988. Beachrock cementation in Alexandria, Egypt. *Marine Geology, v.80, p.29-35.*
- ELION, P., 1983. Étude structurale et sédimentologique du bassin Néogène de Pissouri (Chypre). *Thèse Docteur 3em. Cycle (Unpublished), Université de Paris Sud, Centre d'Orsay, France, 235pp.*
- ENGEL, M.H. & HARE, P.E., 1985. Gas liquid chromatographic separation of amino-acids and their derivatives. *in: Barrett, G.C. (ed.), Chemistry and biochemistry of the amino-acids. Chapman and Hall, p.462-479.*
- ENGELDER, T., 1982A. Is there a genetic relationship between selected regional joints and contemporary stress within the lithosphere of North America. *Tectonics, v.1, p.161-177.*
- ENGELDER, T., 1982B. Reply to comment by A.E. Scheidegger on 'Is there a genetic relationship between selected regional joints and contemporary stress within the lithosphere of North America' by T. Engelder. *Tectonics, v.1, p.465-470.*
- ENGLAND, P & MOLNAR, P., 1990. Surface uplift, uplift of rocks, and exhumation of rocks. *Geology, v.18, p.1173-1177.*
- ESTABAN, M. & KLAPPA, C.F., 1983. Subaerial exposure. *in: Scholle, P., Bebout, D.G. & Moore, C.H. (eds.), Carbonate depositional environments. American Association of Petroleum Geologists, Memoir 33, Chapter 3, p.1-54.*
- FAIRBRIDGE, R.W. & TEICHERT, C., 1953. Soil horizons and marine bands in the coastal limestones of Western Australia. *Journal of the Proceedings of the Royal Society of New South Wales, v.86, p.68-86.*
- FAIRBRIDGE, R.W., 1972. Quaternary sedimentation in the Mediterranean region controlled by tectonics, palaeoclimates and sea-level. *in: Stanley, D.J. (ed.), The Mediterranean Sea. Dowden, Hutchinson and Ross, Stroudsburg, Pennsylvania, p.99-113.*
- FIERRO, G. & OZER, A., 1974. Relations entre les depots eoliens Quaternaires et les sediments marins du Golfe de l'Asinara et des Bouches de Bonifacio (Sardaigne). *Memoire dell'Instituto Italiano di Paleontologia Umana, v.II, p.347-355.*
- FINETTI, I., 1976. Mediterranean ridge: a young submerged chain associated with the Hellenic arc. *Bollettino di Geofisica Teorica ed Applicata, Trieste, v.14, p.291-342.*
- FITTON, J.G., JAMES, D.E. & THIRLWALL, M.F., 1984. A users guide to the X.R.F. analysis of rock samples. *Unpublished Report, Grant Institute of Geology, Edinburgh University, 34pp.*
- FLEMMING, N.C. & WOODWORTH, P.L., 1988. Monthly mean sea levels in Greece 1969-1983 compared to relative vertical land movements measured over different time scales. *Tectonophysics, v.148, p.59-72.*

- FLEMMING, N.C., 1978. Holocene eustatic changes and coastal tectonics in the north eastern Mediterranean: implications for models of crustal consumption. *Philosophical Transactions of the Royal Society of London*, v.A289, p.405-458.
- FOLK, R.L. & COTERA, A.S., 1970. Carbonate sand cays of Alacran Reef, Yucatan. *Sediment: Atoll Research Bulletin no.137*, pp.16
- FOLLOWS, E.J., 1990. Sedimentology and tectonic setting of Miocene reef and related sediments in Cyprus. *Unpublished Ph.d. thesis, Edinburgh University*, 379pp.
- FOLLOWS, E.J. & ROBERTSON, A.H.F., 1990. Sedimentology and structural setting of Miocene reefal limestones in Cyprus. in: Malpas, J., Moores, E., Panayiotou, A. & Xenophontos, C. (eds.), Ophiolites: oceanic crustal analogues. *Proceedings of the Symposium "Troodos 1987", Nicosia, Cyprus*, p.207-216.
- FOLLOWS, E.J., 1991. Pattern of sedimentation and diagenesis in reefs of the Miocene of Cyprus. *Sedimentary Geology* (in press).
- FORBES, E., 1846. On the connection between the distribution of the existing fauna and flora of the British Isles. *Geology Survey of Great Britain, Memoir no.1*, p.336-342.
- FROSTICK, L.E. & REID, I., 1989. Climatic versus tectonic controls on fan sequences; lessons from the Dead Sea, Israel. *Journal of the Geological Society of London*, v.146, p.527-539.
- FRYER, P., AMBOS, E.L. & HUSSONG, D.M., 1985. Origin and emplacement of Mariana forearc seamounts. *Geology*, v.13, p.774-777.
- GALE, S.J., 1990. The shape of beach gravels. *Journal of Sedimentary Petrology*, v.60, p.787-789.
- GARDINER, R.A.M., 1984. Aeolianites. in: Goudie, A. & Pye, K. (eds.). Chemical sediments and geomorphology: precipitates and residua in the near surface environment. *Academic Press*, p.265-301.
- GASS, I.G., 1960. The geology and mineral resources of the Dhali area. *Geological survey Department of Cyprus, Memoir 4*, 116pp.
- GASS, I.G. & MASSON-SMITH, D., 1963. The geology and gravity anomalies of the Troodos Massif, Cyprus. *Philosophical Transactions of the Royal Society of London*, v.A255, p.417-467.
- GASS, I.G., 1968. Is the Troodos Massif of Cyprus a fragment of Mesozoic ocean floor? *Nature*, v.220, p.39-42.
- GASS, I.G., 1990. Ophiolites and oceanic lithosphere. in: Malpas, J., Moores, E., Panayiotou, A. & Xenophontos, C. (eds.), Ophiolites: oceanic crustal analogues. *Proceedings of the Symposium "Troodos 1987", Nicosia, Cyprus*, p.1-12.
- GIANGRANDE, C., RICHARDS, G., KENNET, D. & ADAMS, J. 1987. Cyprus underwater survey, 1983-1984. A preliminary report. in: Karageorghis, V. (ed.), *Report of the Department of Antiquities, Cyprus*, p.185-197.
- GIFFORD, J.A. 1978. Palaeogeography of archaeological sites of the Lamaca lowlands, south eastern Cyprus. *Unpublished Ph.d. thesis, University of Minnesota*, 198pp.
- GILE, L.H., 1977. Holocene soils and soil - geomorphic relations in a semiarid region of southern New Mexico. *Quaternary Research*, v.7, p.112-132.
- GILLILAND, J.A., 1960. Progress report. in: Ingham F. (ed.), *Annual Report of the Geological Survey Department of Cyprus for the year 1959, Nicosia*, p.33-36.

- GLENNIE, K.W., 1970. Desert sedimentary environments. *Elsevier*, 222pp.
- GODWIN, H., 1962. Half-life of radiocarbon. *Nature*, v.195, p.984.
- GOLDSMITH, V., 1985. Coastal dunes. in: Davis, R.A., jnr. (ed.), *Coastal Sedimentary Environments*, Springer-Verlag, p.303-378.
- GOMEZ, B., 1987. The alluvial terraces and fills of the Lower Vasilikos Valley, in the vicinity of Kalavassos, Cyprus. *Transactions of the Institute of British Geographers*, v.12, p.345-359.
- GOUDIE, A., 1973. Duricrusts in tropical and sub-tropical landscapes. *Clarendon Press, Oxford*, 174pp.
- GRANT-TAYLOR, T.L., 1972. Conditions for the use of calcium carbonate as a dating material. in: Rafter, T.A. & Grant-Taylor, T.L. (eds.), *International conference on radiocarbon dating*, 8<sup>th</sup> Proceedings: Wellington, New Zealand, Royal Society of New Zealand, p.56-59.
- GRUBB, P.L.C., 1963. Critical factors in the genesis, extent and grade of some residual bauxite deposits. *Economic Geology*, v.58, p.1267-1277.
- HAIMSON, B.C., LEE, M.Y., BAUMGARTNER, J. & RUMMEL, F., 1990. Plate tectonics and structure inferences from *in situ* stress measurements and fracture logging in drillhole CY-4, Troodos ophiolite, Cyprus. in: Malpas, J., Moores, E., Panayiotou, A. & Xenophontos, C. (eds.), *Ophiolites: oceanic crustal analogues. Proceedings of the Symposium "Troodos 1987", Nicosia, Cyprus*, p.131-138.
- HANCOCK, P.L. & AL KADHI, A., 1982. Significance of arcuate joint sets connecting oblique grabens in central Arabia. *Mitteilungen Geologisch Institute, ETH University of Zurich, Neue Folge*, v.239a, 128-131.
- HANCOCK, P.L., 1985. Brittle microtectonics: principles and practice. *Journal of Structural Geology*, v. 7, p.437-457.
- HARDY, R. & TUCKER, M., 1988. X-ray powder diffraction of sediments. in: Tucker, M. (ed.), *Techniques in sedimentology*. Blackwell Scientific Publications, Oxford, p.191-228.
- HARE, P.E., ST. JOHN, P.A. & ENGEL, M.H., 1985. Ion exchange separation of amino-acids. in: Barrett, G.C. (ed.), *Chemistry and biochemistry of the amino-acids*. Chapman & Hall, p.415-425.
- HARLAND, W.B., ARMSTRONG, R.L., COX, A.V., CRAIG, L.E., SMITH, A.G & SMITH, D.G., 1989. A geologic time scale. *Cambridge University Press*. 260pp.
- HARMON, R.S., MITTERER, R.M., KRIAUSAKUL, N., LAND, L.S., SCHWARCZ, H.P., GARRETT, P., LARSON, G.J., VACHER, H.L. & ROWE, M., 1983. U-series and amino acid racemization geochronology of Bermuda: implications for eustatic sea level fluctuations over the past 250,000 years. *Palaeogeography, Palaeoclimatology, Palaeoecology*, v.44, p.41-70.
- HARMS, J.C., CHOQUETTE, P.W. & BRADY, M.J., 1974. Carbonate sand waves, Isla Mujeres, Yucatan. in: Field seminar on water and carbonate rocks of the Yucatan Peninsula, Mexico, northeastern coast. *Annual meeting fieldtrip guidebook, Geological Society of America*, p.122-147.
- HARMS, J.C., SOUTHARD, J.B. & SPEARING, D.R., 1975. Depositional environments as interpreted from primary sedimentary structures and stratification sequence. *Society of Economic Palaeontologists and Mineralogists, Short course no.2*, 161pp.
- HARRISON, J.C., 1955. An interpretation of the gravity anomalies in the eastern Mediterranean. *Philosophical Transactions of the Royal Society of London*, v.A248, p.283-325.

- HARVEY, A.M. & WELLS, S.G., 1987. Response of Quaternary fluvial systems to differential epeirogenic uplift: Aguas and Feos river systems, southeast Spain. *Geology*, v.15, p.689-693.
- HARVEY, A.M., 1984. Debris flows and fluvial deposits in Spanish Quaternary alluvial fans: implications for fan morphology. in: Koster, E.H. & Steel, R.J. (eds.), *Sedimentology of gravels and conglomerates. Canadian Society of Petroleum Geologists. Memoir 10*, p.123-132.
- HEARTY, P.J., 1986. An inventory of last interglacial (sensu lato) age deposits from the Mediterranean basin. *Zeitschrift fur Geomorphologie, Supplementum 62*, p.51-69.
- HEARTY, P.J. & HOLLIN, J.T., 1986. Aminostratigraphy of Quaternary shorelines in Bermuda. *Geological Society of America, Annual meeting, abstracts with programme, 18,6*.
- HEARTY, P.J., MILLER, G.H., STEARNS, C.E. & SZABO, B.J., 1986. Aminostratigraphy of Quaternary shorelines in the Mediterranean Basin. *Geological Society of America Bulletin*, v.97, p.850-858.
- HEARTY, P.J., 1987. New data on the Pleistocene of Mallorca. *Quaternary Science Reviews*, v.6, p.245-259.
- HEIN, F.J. & WALKER, R.G., 1977. Bar evolution and development of stratification in the gravelly braided Kicking Horse River, British Columbia. *Canadian Journal of Earth Sciences*, v.14, p.562-570.
- HELD, S.O., 1990. Contributions to the early prehistoric archaeology of Cyprus. *Unpublished Ph.d. thesis, University of London, 430pp*.
- HENSON, F.R.S., BROWNE, R.V. & MCGINTY, J., 1949. A synopsis of the stratigraphy and geological history of Cyprus. *Quarterly Journal of the Geological Society of London*, v.105, p.1-41.
- HEWARD, A.P., 1978A. Alluvial fan and lacustrine sediments from the Stephanian A and B (La Magdalena, Cinera-Matallina and Sabero) coalfields, northern Spain. *Sedimentology*, v.25, p.451-488.
- HEWARD, A.P., 1978B. Alluvial fan sequence and megasequence models: with examples from westphalian "d"-Stephanian "b" coalfields, northern Spain. in: Miall, A.D. (ed.), *Fluvial sedimentology. Canadian Society of Petroleum Geologists, Memoir 5*, p.669-702.
- HEY, R.W., 1962. The Quaternary and Palaeolithic of northern Libya. *Quaternaria*, v.6, p.435-450.
- HEY, R.W., 1971. Quaternary shorelines of the Mediterranean and Black Seas. *Quaternaria*, v.15, p.271-284.
- HEY, R.W., 1975. Classification of the Mediterranean Quaternary. *Geological Magazine*, v.112, p.201-202.
- HEY, R.W., 1978. Horizontal Quaternary shorelines of the Mediterranean. *Quaternary Research*, v.10, p.197-203.
- HODGSON, R.A., 1961. Regional study of jointing in Comb Ridge-Navajo mountain area, Arizona and Utah. *American Association of Petroleum Geologists Bulletin*, v.45, p.1-38.
- HOLLIN, J.T. & HEARTY, P.J., 1990. South Carolina interglacial sites and stage 5 sea levels. *Quaternary Research*, v.33, p.1-17.
- HOOKE, R. LE B., 1967. Processes on arid region alluvial fans. *Journal of Geology*, v.75, p.609-629.

- HOOKE, R. LE B., 1972. Geomorphic evidence for late-Wisconsin and Holocene deformation, Death Valley, California. *Geological Society of America Bulletin*, v.83, p.2073-2098.
- HOQUE, M., 1975. An analysis of cross-stratification of Gargaresh Calcarene (Tripoli, Libya) and Pleistocene palaeowinds. *Geological Magazine*, v.112, p.393-401.
- HOUGHTON, S.D., JENKINS, D.G., GASS, I.G. & XENOPHONTOS, C., 1990. Microfossil evidence for a latest Pliocene age for the Amathus and Khirokitia channel deposits, southern Cyprus, and thereby the unroofing of the Troodos massif. in: Malpas, J., Moores, E., Panayiotou, A. & Xenophontos, C. (eds.), Ophiolites: oceanic crustal analogues. *Proceedings of the Symposium "Troodos 1987", Nicosia, Cyprus*, p.231-234.
- HOWARD, A.D., 1967. Drainage analysis in geologic interpretation: A summation. *American Association of Petroleum Geologists Bulletin*, v.51, p.2246-2259.
- HOWARD, J.D., 1975. The sedimentological significance of trace fossils. in: Frey, R.W. (ed.). A synthesis of principles, problems and procedures in ichnology. *Spring-Verlag, New York*, p.131-147.
- HOWARD, J.D. & REINECK, H-E., 1981. Depositional facies of high energy beach to offshore sequence: comparison with low energy sequence. *American Association of Petroleum Geologists Bulletin*, v.65, p.807-832.
- HSU, K.J., MONDADERT, L., BERNOULLI, D., CITA, M.B., ERICKSON, A., GARRISON, R.E., KIDD, R.B., MELIERES, F., MÜLLER, C. & WRIGHT, R., 1978. History of the Mediterranean salinity crisis. *Initial Reports of the Deep Sea Drilling Project, 42 Part 1, U.S. Government Printing Office, Washington*, p.1053-1078.
- HUSSEINI, S.I. & MATTHEWS, R.K., 1972. Distribution of high-magnesium calcite in lime muds of the Great Bahama Bank - diagenetic implications. *Journal of Sedimentary Petrology*, v.42, p.179-182.
- INMAN, D.L., EWING, G.C. & CORLISS, J.B., 1966. Coastal sand dunes of Guerrero Negro, Baja California, Mexico. *Geological Society America Bulletin*, v.77, p.787-802.
- INDEN, R.F. & MOORE, C.H., 1983. Beach carbonates. in: Scholle, P.A., Bebout, D.G. & Moore, C.H. (eds.), Carbonate depositional environments. *Association of American Petroleum Geologists, Memoir 33*, p.211-267.
- ISSAR, A., 1979. Stratigraphy and palaeoclimates of the Pleistocene of Central and Northern Israel. *Palaeogeography, Palaeoclimatology, Palaeoecology*, v.20, p.261-280.
- IVANOVICH, M. & HARMON, R.S., 1982. U-series disequilibrium: applications to environmental problems. *Clarendon Press, Oxford*, 571pp.
- JAMES, N.P., 1972. Holocene and Pleistocene calcareous crust (caliche) profiles: criteria for subaerial exposure. *Journal of Sedimentary Petrology*, v.42, p.817-836.
- JAMES, N.P., 1974. Diagenesis of scleractinian corals in the subaerial vadose environment. *Journal of Palaeontology*, v.48, p.785-799.
- JAMES, N.P. & CHOQUETTE, P.W., 1984. Diagenesis of limestones - the meteoric diagenetic environment. *Geoscience Canada*, v.11, p.161-194.
- JENNINGS, J.N., 1964. The question of coastal dunes in tropical humid climates, *Zeitschrift für Geomorphologie, (Mortenson Birthday Volume)*, v.8, p.150-154.

- KAUFMAN, A. & BROECKER, W.S., 1965. Comparison of  $^{230}\text{Th}$  and  $^{14}\text{C}$  ages for carbonate materials from lakes Lahontan and Bonneville. *Journal of Geophysical Research*, v.70, p.4039-4054.
- KAUFMANN, A., BROECKER, W.S., KU, T.L. & THURBER, D.L., 1971. U-series dating of Dead sea basin carbonates. *Geochimica et Cosmochimica Acta.*, v.35, p.1269-1281.
- KAUFMAN, A., 1986. The distribution of  $^{230}\text{Th}/^{234}\text{U}$  ages in corals and the number of last interglacial high sea-stands. *Quaternary Research*, v.25, p.55-62.
- KEMPLER, D & BEN-AVRAHAM, Z. 1987. The tectonic evolution of the Cyprean Arc. *Annales Tectonicae*, v.1, p.58-71.
- KENNETT, J.P., 1986. Marine geology. *Acedemic Press*, p.745-751.
- KERAUDREN, B. & SOREL, D. 1987. The terraces of Corinth (Greece) - a detailed record of eustatic sea-level variations during the last 500,000 years. *Marine Geology*, v.77, p.99-107.
- KIDD, R.B. & BENOULLI, D., 1978. Lithologic findings of D.S.D.P. leg 42a, Mediterranean Sea. in: Hsu, K. et al., *Initial reports of the deep sea drilling project*, v.42, Washington, p.1079-1093.
- KIDSON, C., 1982. Sea-level changes in the Holocene. *Quaternary Science Reviews*, v.1, p.121-151.
- KLUYVER, H.M., 1969. Report on a regional geological mapping in the Paphos District. Y. Hji Stavrinou (ed.), *Geological Survey of Cyprus, Nicosia, Bulletin no.4*, p.21-36.
- KOBLUK, D.R. & RISK, M.J., 1977. Micritization and carbonate-grain binding by endolithic algae. *American Association of Petroleum Geologists, Bulletin*, v.61, p.1069-1082.
- KRAUS, M.J., 1984. Sedimentology and tectonic setting of early Tertiary quartzite conglomerates, north west Wyoming. in: Koster, E.H. & Steel, R.J. (eds.), *Sedimentology of gravels and conglomerates. Canadian Society of Petroleum Geologists Memoir 10*, p.203-216.
- KRUMBEIN, W.C., 1934. Size frequency distributions of sediments. *Journal of Sedimentary Petrology*, v.4, p.65-77.
- KRUMBEIN, W.C., 1941. Measurement and geological significance of shape and roundness of sedimentary particles. *Journal of Sedimentary Petrology*, v.11, p.68.
- KU, T.L., KIMMEL, M.A., EASTON, W.H. & O'NEIL, T.J., 1974. Eustatic sea-level 120,000 years ago on Oahu, Hawaii. *Science*, v.183, p.959-962.
- KU, T.L., 1976. The uranium series methods of age determination. *Annual Review of Earth and Planetary Science*, v.4, p.347-379
- KUKLA, G.J., 1975. Missing link between Milankovitch and climate. *Nature*, v.253, p.600-603.
- KUMAR, N. & SAUNDERS, J.E., 1976. Characteristics of shoreface storm deposits: modern and ancient examples. *Journal of Sedimentary Petrology*, v.46, p.145-162.
- Lajoie, K.R., PEDERSON, E. & GEROW, B.A., 1980. Amino-acid bone dating: a feasibility study, south San Francisco Bay region, California. in: Hare, P.E., Hoering, T.C. & King, K. (eds.), *Biogeochemistry of amino-acids, John Wiley, New York*, p.477-489.
- LALOU, C., DUPLESSY, J.C. & NGUYEN, H.V., 1971. Donnees geochronologiques actuelles sur les niveaux de l'interglaciaire Riss/Wurm. *Revue Geographique, Physical Geology Dynamic.*, v.13, p.447-461.

- LAND, L.S., 1964. Eolian cross-bedding in the beach dune environment, Sapelo Island, Georgia. *Journal of Sedimentary Petrology*, v.32, p.289-394.
- LAND, L.S., 1967. Diagenesis of skeletal carbonate. *Journal of Sedimentary Petrology*, v.37, p.914-930.
- LAND, L.S., MACKENZIE, F.T. & GOULD, S.J., 1967. Pleistocene history of Bermuda. *Geological Society America Bulletin*, v.78, p.993-1006.
- LAPIERRE, H., 1975. Les formations sédimentaires et éruptives des nappes de Mamonia et leurs relations avec le massif de Troodos (Chypre occidentale). *Mémoire de la Société Géologique de France, Paris*, 123, 132pp.
- LAPIERRE, H. & ROCCI, G.G., 1976. Le volcanisme du sud-ouest de Chypre et le problème de l'ouverture des régions Téthysiennes au Trias. *Tectonophysics*, v.30, p.299-313.
- LE PICHON, X. & ANGELIER, J., 1979. The Hellenic arc and trench system: a key to the neotectonic evolution of the eastern Mediterranean. *Tectonophysics*, v.60, p.1-42.
- LE PICHON, X., KOBAYASHI, K., CADET, J.-P., IYAMA, T., NAKAMURA, K., PAUTOT, G., RENARD, Y., & THE KAIKO SCIENTIFIC CREW, 1987. Project Kaiko - Introduction. *Earth and Planet Science Letters*, v.83, p.183-185.
- LEEDER, M.R., SEGER, M.J. & STARK, C., 1990. Sedimentation and tectonic geomorphology adjacent to major active and inactive faults, southern Greece. *Journal of the Geological Society of London*, v.148, p.331-344.
- LEES, A. & BULLER, A.T., 1972. Modern temperate-water and warm-water shelf carbonate sediments contrasted. *Marine Geology*, v.13, p.67-73.
- LEES, A., 1975. Possible influence of salinity and temperature on modern shelf carbonate sedimentation. *Marine Geology*, v.19, p.159-198.
- LEOPOLD, L.B. & MILLER, J.R., 1956. Ephemeral streams-hydraulic factors and their relation to the drainage net. *Professional Paper, United States Geological Survey*, 282-B, p.39-85.
- LEOPOLD, L.B., WOLMAN, M.G. & MILLER, J.P., 1964. Fluvial processes in geomorphology. *Freeman and Co., San Francisco*, 522pp.
- LEWIS, D.W., LAIRD, M.G. & POWELL, R.D., 1980. Debris flow deposits of early Miocene age, Deadman Stream, Marlborough. *Sedimentary Geology*, v.27, p.83-118.
- LIBBY, L.F. 1952. Radiocarbon dating. *University of Chicago Press, Chicago*, 124pp.
- LINDHOLM, R.C., 1987. A practical approach to sedimentology. *Allen & Unwin, London*, 276pp.
- LITTLER, M.M., 1973. The crustose Corallianaceae. *Oceanography, Marine Biology Annual Review*, v.10, p.311-347.
- LONGMAN, M.W., 1980. Carbonate diagenetic textures from nearshore diagenetic environments. *American Association of Petroleum Geologists Bulletin*, v.64, p.461-487.
- LORT, J.M., 1971. The tectonics of the Eastern Mediterranean: a geophysical review. *Reviews of Geophysics and Space Physics*, v.9, p.189-216.
- LOWE, J.J. & WALKER, M.J.C., 1984. Reconstructing Quaternary environments. *Longman, London*, 389pp.
- LYELL, C., 1839. Nouveaux éléments de géologie. *Paris*.

- MACHETTE, M.N., 1985. Calcic soils of the southwestern United States. *in*: Wiede, D.L. (ed.), Soils and Quaternary geology of the southwestern United States. *Geological Society of America Special Paper no.203*, p.1-21.
- MACKENZIE, F.T., 1964A. Bermuda calcareous dune cross-bedding. *Science*, v.144, p.1449-1450.
- MACKENZIE, F.T., 1964B. Bermuda Pleistocene eolianites and palaeowinds. *Sedimentology*, v.3, p.52-64.
- MACLEOD, C.J., 1990. Role of the southern Troodos Transform Fault in the rotation of the Cyprus microplate: evidence from the Eastern Limassol Forest Complex. *in*: Malpas, J., Moores, E., Panayiotou, A. & Xenophontos, C. (eds.), Ophiolites: oceanic crustal analogues. *Proceedings of the Symposium "Troodos 1987", Nicosia, Cyprus*, p.75-86.
- MCCALLUM, J.E., 1989. Sedimentation and tectonics of the Plio-Pleistocene of Cyprus. *Unpublished Ph.d. thesis, Edinburgh University*, 263pp.
- MCCALLUM, J.E. & ROBERTSON, A.H.F. 1990. Pulsed Uplift of the Troodos Massif - evidence from the Plio-Pleistocene Mesaoria Basin. *in*: Malpas, J., Moores, E., Panayiotou, A. & Xenophontos, C. (eds.), Ophiolites: oceanic crustal analogues. *Proceedings of the Symposium "Troodos 1987", Nicosia, Cyprus*, p.217-230.
- MCCALLUM, J.E., SCRUTTON, R.A., ROBERTSON, A.H.F. & FERRARI, W., 1992. Seismostratigraphy and Neogene-Recent depositional history of the south central continental margin of Cyprus. (in prep).
- MCFADDEN, L.D., 1988. Climatic influences on rates and process of soil development in Quaternary deposits of southern California. *in*: Reinhardt, J. & Sigleo, W.R. (eds), Palaeosols and Weathering Through Geologic Time. *Geological Society of America Special Paper no.216*, p.153-177.
- MCKEE, E.D. & WARD, W.C., 1983. Eolian environment. *in*: Scholle, P., Bebout, D.G. & Moore, C.H. (eds), Carbonate depositional environments. *American Association of Petroleum Geologists, Memoir 33, Chapter 3*, p.130-170.
- MCKENZIE, D.P., 1970. Plate tectonics of the Mediterranean Region. *Nature*, v.226, p.239-243.
- MCKENZIE, D.P., 1972. Active tectonics of the Mediterranean region. *Geophysical Journal of the Royal Astronomical Society*, v.30, p.109-185.
- MCKENZIE, D.P., 1976. The east Anatolian fault: a major structure in eastern Turkey. *Earth and Planetary Science Letters*, v.29, p.189-193.
- MCKENZIE, D.P., 1978. Active tectonics of the Alpine-Himalayan belt: the Aegean Sea and surrounding regions (tectonics of Aegean region). *Geophysical Journal of the Royal Astronomical Society*, v.55, p.217-254.
- MCPHERSON, J.G., SHANMUGAM, G. & MOIOLA, R.J., 1987. Fan-deltas and braid-deltas: varieties of coarse grained deltas. *Geological Society of America Bulletin*, v.99, p.331-340.
- MCPHERSON, J.G., SHANMUGAM, G. & MOIOLA, R.J., 1988. Fan deltas and braid deltas: conceptual problems. *in*: Nemeč, W. & Steel, R.J. (eds.). Fan deltas: sedimentology and tectonic settings. *Blackie*, p.14-22 .
- MAHANEY, W.C. (ED.), 1984. Quaternary dating methods. *Developments in palaeontology and stratigraphy*, no.7, Elsevier, 431pp.
- MAIZELS, J.K., 1987. Plio-Pleistocene raised channel systems of western Sharqiya (Wahiba), Oman. *in*: Frostick, L. & Reid, I. (eds.), Desert sediments: ancient and modern. *Geological Society of London Special Publication v.35*, p.31-50.



- MAIZELS, J.K., 1988. Long term, episodic fan growth and palaeochannel evolution on exhumed Cenozoic alluvial fans of interior Oman. *Abstract for the international discussion meeting: the geology and tectonics of the Oman region, Edinburgh, March 1988.*
- MAKRIS, J., BEN-AVRAHAM, Z., BEHLE, A., GINZBURG, A., GIESE, P., STEINMETZ, L., WHITMARSH, R.B. & ELEFThERIOU, S., 1983. Seismic refraction profiles between Cyprus and Israel and their interpretations. *Geophysical Journal of the Royal Astronomical Society*, v.75, p.575-591.
- MANTIS, N. 1970. Upper Cretaceous-Tertiary foraminiferal-zones in Cyprus. *Epithris, Cyprus Research Centre, Nicosia*, v.3, p.227-241.
- MARGARITZ, M. & TAYLOR, H.P. (JNR.), 1974. Oxygen and hydrogen isotope studies of serpentinization in the Troodos ophiolite complex, Cyprus. *Earth and Planetary. Science Letters*, v.23, p.8-14.
- MASSARI, F. & PAREA, G.C., 1988. Progradational gravel beach sequences in a moderate- to high-energy microtidal marine environment. *Sedimentology*, v.35, p.881-890.
- MAUD, R.R., 1968. Quaternary geomorphology and soil development in coastal Natal. *Zeitschrift fur Geomorphologie, Supplementum 7*, p.155-199.
- MELIERES, F., CHAMLEY, H., COUMES, F. & ROUGE, P., 1978. X-ray mineralogy studies. *in: Hsu, K.J., Mondadert, L., Bernoulli, D., Cita, M.B., Erickson, A., Garrison, R.E., Kidd, R.B., Mélières, F., Müller, C. & Wright, R. Initial Reports of the Deep Sea Drilling Project, 42 Part 1, U.S. Government Printing Office, Washington*, p.361-385.
- MERRITTS, D. & VINCENT, K.R., 1989. Geomorphic response of coastal streams to low, intermediate and high rates of uplift, Mendocino triple junction region, northern California. *Geological Society of America Bulletin*, v.101, p.1373-1388.
- MESOLELLA, K.J., MATTHEWS, R.K., BROECKER, W.S. & THURBER, D.L., 1969. The astronomical theory of climatic change: Barbados data. *Journal of Geology*, v.77, p.250-274.
- MESSENGER, C., 1958. A geomorphic study of the dunes of the Provincetown Peninsula, Cape Cod, Massachusetts. *Unpublished MSc. thesis, University of Massachusetts, 198pp.*
- METEOROLOGICAL SURVEY OF CYPRUS, 1986. Meteorological paper series no.7. *Meteorological Survey of Cyprus, Nicosia, Cyprus, 2<sup>nd</sup> edition, 56pp.*
- MIALI, A.D., 1978. Lithofacies types and vertical profile models in braided river deposits: a summary. *in: Miall, A.D. (ed.), Fluvial sedimentology. Canadian Society of Petroleum Geologists, Memoir 5*, p.597-604.
- MILLER, G.H. & HARE, P.E., 1980. Amino-acid geochronology: integrity of the carbonate matrix and potential of molluscan fossils. *in: Hare, P.E., Hoering, T.C. & King, K, jnr. (eds.), Biochemistry of amino-acids, John Wiley, New York*, p.415-443.
- MILLER, G.H. & MANGERUD, J., 1985. Aminostratigraphy of the European marine interglacial deposits. *Quaternary Science Review*, v.4, p.215-278.
- MILLER, G.H., 1987. Amino-acid geochronology: resolution and precision. *International Union for Quaternary Research, xiii<sup>th</sup> International Congress, Canada, July 1987 programme with abstracts.*
- MITTERER, R.M. & KRIAUSAKUL, N., 1984. Comparison of rates and degree of isoleucine epimerization in dipeptides and tripeptides. *Organic Geochemistry*, v.7, p.91-98.

- MOLNAR, P. & ENGLAND, P., 1990. Temperatures, heat flux, and frictional stress near major thrust faults. *Journal of Geophysical Research*, v.95, p.4833-4856.
- MOORE, C.H. (JNR), 1973. Intertidal carbonate cementation, Grand Cayman, West Indies. *Journal of Sedimentary Petrology*, v.43, p.591-602.
- MOORE, R.C., 1969. Treatise of invertebrate palaeontology. Part N, v.1, Mollusca 6, Bivalvia. *Geological Society of America and University of Kansas*, 489pp.
- MOORE, T.A., 1960. The Geology and Mineral resources of the Astromeritis-Kormakiti area. *Cyprus Geological Survey Department, Memoir 6*, 96pp.
- MOORES, E.M. & VINE, F.J., 1971. The Troodos Massif, Cyprus and other ophiolites as oceanic crust: evaluation and implications. *Philosophical Transactions of the Royal Society of London*, v.A268, p.433-466.
- MORISAWA, M., 1985. Rivers: form and process. *Geomorphology Texts no.7*, Longman, London, 222pp.
- MORISAWA, M. & HACK, J. (EDS.), 1985. Tectonic geomorphology. *Proceedings of the 15<sup>th</sup> annual geomorphology symposium, State University of New York at Binghamton: Winchester, Massachusetts. George Allen & Unwin*, 390pp.
- MORNER, N-A, 1976A. Eustasy and geoidal changes. *Journal of Geology*, v.84, p.123-151.
- MORNER, N-A, 1976B. The Pleistocene/Holocene boundary: a proposed boundary stratotype in Gothenburg, Sweden. *Boreas*, v.5, p.193-275.
- MOSELEY, F., 1976. The Neogene and Quaternary of Akrotiri, Cyprus. Determined by means of a rapid ground reconnaissance assisted by stereo-line-overlap photographs. *Mercian Geologist*, v.6, p.49-58.
- MOSHKOVITZ, S., 1966. The age of the Kyrenia Formation in Cyprus. *in: Drooger, C.W. et al., International Union of Geological sciences, Commission on Stratigraphy, Berne*, p.303-308.
- MOSHKOVITZ, S., 1968. The Mollusca in the marine Pliocene and Pleistocene sediments of the South Eastern Mediterranean basin (Cyprus-Israel). *Unpublished Ph.d. thesis, Hebrew University, Jerusalem*, 153pp.
- MUKASA, S.B. & LUDDEN, J.N., 1987. Uranium-lead ages of plagiogranites from the Troodos ophiolite, Cyprus and their tectonic significance. *Geology*, v.15, p.825-828.
- MULLER, P.J., 1984. Isoleucine epimerization in Quaternary planktonic foraminifera: effects of diagenetic hydrolysis and leaching, and Atlantic-Pacific intercore correlations. *Meteor Forschungsergebnisse, Reihe C., Geologie und Geophysik*, v.38, p.25-47.
- MULTER, H.G. & HOFFMEISTER, J.E., 1968. Subaerial laminated crusts of the Florida Keys. *Geological Society of America Bulletin*, v.79, p.183-192.
- MUMPTON, F.A. & THOMPSON, C.S., 1975. Mineralogy and origin of the Coalinga asbestos deposits. *Clays and Clay Mineralogy*, v.23, p.131-144.
- MURTON, B.J., 1986. Anomalous oceanic lithosphere formed in a leaky transform fault: evidence from the Western Limassol Forest Complex, Cyprus. *Journal of the Geological Society of London*, v.143, p.845-854.
- MURTON, B.J. & GASS, I.G., 1986. Western Limassol Forest Complex, Cyprus: part of an Upper Cretaceous leaky transform fault. *Geology*, v.14, p.255-258.

- MURTON, B.J., 1990. Was the Troodos Transform Fault a victim of microplate rotation ? *in*: Malpas, J., Moores, E., Panayiotou, A. & Xenophontos, C. (eds.), *Ophiolites: oceanic crustal analogues. Proceedings of the Symposium "Troodos 1987", Nicosia, Cyprus, p.87-98.*
- MUTO, T., 1987. Coastal Fan processes controlled by sea-level changes: a Quaternary example from the Tenryugawa Fan System, Pacific coast of central Japan. *Journal of Geology, v.95, p.716-724.*
- NEEV, D., 1975. Tectonic evolution of the Middle East and the Levantine basin. *Geology, v.3, p.683-687.*
- NEMEC, G.W. & STEEL, R.J., 1984. Alluvial and coastal conglomerates: their significant features and some comments on gravelly mass-flow deposits. *in*: Koster, E.H. & Steel, R.J. (eds.), *Sedimentology of gravels and conglomerates. Canadian Society of Petroleum Geologists Memoir 10, p.1-31.*
- NEMEC, W. & STEEL, R.J., 1988. What is a fan delta and how do we recognise it ? *in*: Nemeč, W. & Steel, R.J. (eds.). *Fan deltas: sedimentology and tectonic setting, Blackie, p.3-13.*
- NETTERBERG, F., 1967. Calcrete research project. *Progress Report, RS/8/7 C.S.I.R., N.I.R.R., Pretoria, South Africa.*
- NILSSON, T., 1983. The Pleistocene: geology and life in the Quaternary ice age. *Reidal, 651pp.*
- NORRISH, K. & HUTTON, J.T., 1969. An accurate X-ray spectrographic method for the analysis of a wide range of geological samples. *Geochimica et Cosmochimica Acta, v.33, p.431-453.*
- NORTH, R.G., 1974. Seismic slip rates in the Mediterranean and Middle East. *Nature, v.252, p.560-563.*
- NUR, A. & BEN-AVRAHAM, Z., 1978. The eastern Mediterranean and the Levant: tectonics of continental collision. *Tectonophysics, v.46, p.297-311.*
- OPDYKE, N.D., 1961. The palaeoclimatological significance of desert sandstones. *in*: Nairn, A.E.M. (ed.), *Descriptive palaeoclimatology. Interscience, New York, p.45-59.*
- ORSZAG-SPERBER, F., ROUCHY, J.-M., BIZON, G., BIZON, J.-J., CRAVATTE, J. & MULLER, C. 1980. La sédimentation messinienne dans le bassin de Polemi (Chypre). *Géologie Méditerranéenne, v.7, p.91-102.*
- ORSZAG-SPERBER, F., ROUCHY, J.-M. & ELION, P., 1989. The sedimentary expression of regional tectonic events during the Miocene-Pliocene transition in the southern Cyprus basins. *Geological Magazine, v.136, p.291-299.*
- ORTON, G.J., 1988. A spectrum of Middle Ordovician fan deltas and braidplain deltas, north Wales: a consequence of varying fluvial clastic input. *in*: Nemeč, W. & Steel, R.J. (eds.). *Fan deltas: sedimentology and tectonic settings, Blackie, p.23-49.*
- PANTAZIS, T.M., 1961. A study of some havara and kafkalla samples of Cyprus. *Unpublished report, Ministry of Agriculture, Nicosia, Cyprus, p.1-32.*
- PANTAZIS, T.M., 1966. Tyrrhenian terraces of the Larnaca area, south eastern Cyprus. *in*: Ingham, F. (ed.), *Annual report of the Geological Survey Department of Cyprus for 1966, Nicosia, Cyprus, p.29-34.*
- PANTAZIS, T.M., 1967. The geology and mineral resources of the Pharmakas-Kalavastos area. *Geological Survey Department, Cyprus, Memoir 8, 190pp.*
- PANTAZIS, T.M., 1973. A study of secondary limestones (havara and kafkalla) of Cyprus. *Bulletin of the Cyprus Geographical Association - Geographical Chronicles, v.2, p.12-39.*

- PANTAZIS, T.M., 1979. The 1:250,000 geological map of Cyprus. *Geological Survey Department, Nicosia, Cyprus*.
- PEARCE, J.A., LIPPARD, S.J. & ROBERTS, S., 1984. Characteristics and tectonic significance of supra-subduction zone ophiolites. in: Gass, I.G., Lippard, S.J. & Shelton, A.W. (eds.), *Ophiolites and Oceanic lithosphere. Geological Society of London, Special Publication, v.16, p.77-96*.
- PELTENBURG, E.J., 1982. Vrysi: a subterranean settlement in Cyprus, excavations at *prehistoric Ayios Epikititos Vrysi, 1969-1973. Warminster, Aris and Philips Ltd*.
- PELTENBURG, E.J., 1985. Lemba archaeological project v.1: excavations at Lemba Lakkous, 1976-1983. *Studies in Mediterranean archaeology, Goteborg, v.LXX:1, Chap.2, p.16-18*.
- PENCK, W., 1953. Morphological analysis of landforms. *Macmillan, London, 429pp*.
- PERES, J.M., 1967. The Mediterranean benthos. *Oceanography and Marine Biology, Annual Review, v.5, p.449-534*.
- PETERS, J.M., TROELSTRA, S.R. & HARTEN, D. VAN, 1985. Late Neogene and Quaternary vertical movements in eastern Crete and their regional significance. *Journal of the Geological Society of London, v.142, p.501-513*.
- PETTIJOHN, E.J., 1980. Sedimentary Rocks. *Harper & Row, 3rd edition, 628pp*.
- PIAZZOLI, P.A., LABOREL, J. SALIEGE, J.F., EROL, O., KAYAN, I. & PERSON, A., 1991. Holocene raised shorelines on the Hatay coasts (Turkey): Palaeoecological and tectonic implications. *Marine Geology, v.96, p.295-311*.
- PITTMAN, E.D., 1979. Recent advances in sandstone diagenesis. *Annual Reviews of Earth Science Planetary Letters, v.7, p.39-62*.
- POSTMA, G., 1989. An analysis of the variation in delta architecture. *Abstract for the Annual Meeting of the British Sedimentological Research Group, Leeds December 1989*.
- POSTMA, G. & NEMEC, W., 1990. Regressive and transgressive sequences in a raised Holocene gravelly beach, south western Crete. *Sedimentology, v.37, p.907-920*.
- PRICE, W.A., 1933. The Reynosa problem of southern Texas and the origin of caliche. *American Association of Petroleum Geologists Bulletin, v.37, p.1075-1077*.
- REESE, D.S., 1989. Tracking the extinct pygmy hippotamus of Cyprus. *Field museum of natural history (Chicago) Bulletin, 60/2, p.22-29*.
- REEVES, C.C., 1970. Origin, classification and geologic history of caliche of the southern plains, Texas and eastern New Mexico. *Journal of Geology, v.78, p.352-362*.
- REINECK, H-E. & SINGH, I.B., 1975. Depositional sedimentary environments. *Springer-Verlag, 439pp*.
- RIAD, S., REFAI, E. & CHALIB, M., 1981. Bouguer anomalies and crustal structure in the Eastern Mediterranean. *Tectonophysics, v.71, p.253-266*.
- RICH, C.I. & KUNZE, G.W. (EDS.), 1967. Soil clay mineralogy: a symposium and chemistry. *University of North Carolina Press, 330pp*.
- RICHARDS, G.W., 1982. Intertidal molluscs as sea-level indicators: a comparative study of modern and fossil Mediterranean assemblages. *Unpublished Ph. thesis, University of London, 286pp*.

- RITTENHOUSE, G., 1943. A visual method of estimating two dimensional sphericity. *Journal of Sedimentary Petrology*, v.13, p.80-81.
- ROBERTSON, A.H.F., 1977. Tertiary uplift of the Troodos Massif, Cyprus. *Geological Society of America Bulletin*, v.88, p.1763-1772.
- ROBERTSON, A.H.F. & WOODCOCK, N.H., 1979. The Mamonia Complex, southwest Cyprus: the evolution and emplacement of a Mesozoic continental margin. *Geological Society of America Bulletin*, v.90, p.651-665.
- ROBERTSON, A.H.F. & WOODCOCK, N.H., 1980. Tectonic setting of the Troodos Massif in the Eastern Mediterranean. in: Panayiotou, A. (ed.), *Ophiolites. Proceedings of the International ophiolite symposium, Nicosia, Cyprus*, p.36-49.
- ROBERTSON, A.H.F. & DIXON, J.E., 1984. Introduction: aspects of the geological evolution of the Eastern Mediterranean. in: Dixon, J.E. & Robertson, A.H.F. (eds.), *The Geological Evolution of the Eastern Mediterranean. Special Publication Geological Society of London*, v.17, p.1-74.
- ROBERTSON, A.H.F. & WOODCOCK, N.H., 1984A. Sedimentary history of the south-western segment of the Mesozoic-Tertiary Anatolia continental margin, south-western Turkey. *Eclogae Geologicae Helveticae*, v.75, p.517-562.
- ROBERTSON, A.H.F. & WOODCOCK, N.H., 1984B. The south-west segment of the Antalya complex, Turkey, as a Mesozoic-Tertiary Tethyan continental margin. in: Dixon, J.D. & Robertson, A.H.F. (eds.), *The Geological Evolution of the Eastern Mediterranean. Special Publication Geological Society of London*, v.17, p.251-273.
- ROBERTSON, A.H.F. & WOODCOCK, N.H., 1986. The role of the Kyrenia lineament, Cyprus, in the geological evolution of the Eastern Mediterranean area. in: Reading, H.G., Watterson J. & White, S.H. (eds.), *Major crustal lineaments and their influence on the geological history of the continental lithosphere. Philosophical Transactions of the Royal Society of London*, v.A314, p.141-177.
- ROBERTSON, A.H.F., 1990. Tectonic evolution of Cyprus. in: Malpas, J., Moores, E., Panayiotou, A. & Xenophontos, C. (eds.), *Ophiolites: oceanic crustal analogues. Proceedings of the Symposium "Troodos 1987", Nicosia, Cyprus*, p.235-252.
- ROBERTSON, A.H.F., EATON, S., FOLLOWS, E.J. & MCCALLUM, J.E., 1991. Role of tectonics versus sea-level change in the Neogene (Miocene-Pliocene) evolution of the Cyprus active margin. in: MacDonald, D.I.M. (ed.), *Sea-level change at active plate margins. Special Publication of the international Association of Sedimentologists*, v.12, p.331-369.
- ROGNON, P. & WILLIAMS, M.A.J. 1977. Late Quaternary climatic changes in Australia and North Africa: a preliminary interpretation. *Palaeogeography, Palaeoclimatology, Palaeoecology*, v.21, p.285-327.
- ROTSTEIN, Y. & KAFKA, A.L., 1982. Seimotectonics of the southern boundary of Anatolia, Eastern Mediterranean region: subduction, collision and arc jumping. *Journal of Geophysical Research*, v.187, p.7694-7704.
- ROTSTEIN, Y., 1984. Counter clockwise rotation of the Anatolian Block. *Tectonophysics*, v.108, p.71-91.
- RUST, B.R., 1978. Depositional models for braided alluvium. in: Miall, A.D. (ed.), *Fluvial sedimentology. Canadian Association of Petroleum Geologists, Memoir 5*, p.605-625.
- SABARIS, L.S. 1962. Le quaternaire marin des Balears et ses rapports avec les côtes Méditerranéennes de la Peninsule Iberique. *Quaternaria*, v.6, p.309-342.

- SAFRIEL, U., 1966. Recent vermatid formation on the Mediterranean shore of Israel. *Proceedings of the Malacological Society, London*, v.37, p.27-37.
- SANCETTA, C., IMBRIE, J. & KIPP, N.G., 1973. Climatic record of the past 130,000 years in the North Atlantic deep-sea core V23-83: correlation with the terrestrial record. *Quaternary Research*, v.3, p.110-116.
- SANDBERG, P.A., SCHNEIDERMAN, N. & WINDER, S.J., 1973. Aragonite ultrastructure relics in calcite-replaced Pleistocene skeletons. *Nature*, v.245, p.133-134.
- SARNTHEIN, M. 1978. Sand deserts during glacial maximum and climatic optimum. *Nature*, v.272, p.43-46.
- SAYLES, R.W., 1931. Bermuda during the Ice Age. *Proceedings of the American Academy of Arts and Science*, v.66, p.381-468.
- SCHNEK, H.G. & MULLER, S.W., 1941. Stratigraphic terminology. *Geological Society of America Bulletin*, v.52, p.1419-1426.
- SCHOLLE, P.A., 1978. A color illustrated guide to carbonate rock constituents, textures, cements, and porosities. *American Association of Petroleum Geologists, Memoir no.27*, 241pp.
- SCHOLLE, P., BEBOUT, D.G. & MOORE, C.H. (EDS.), 1983. Carbonate depositional environments. *American Association of Petroleum Geologists, Memoir 33*, 708pp.
- SCHROEDER, R.A. & BADA, J.L., 1976. A review of the geochemical applications of the amino-acid racemization reaction. *Earth Science Reviews*, v.12, p.347-391.
- SCHWARCZ, H.P., 1979. Uranium series dating of contaminated travertine: a two component model. *McMaster University technical memo. 79-1*, 14pp.
- SELLI, R., ACCORSI, C.A. & BANDINI, M., 1977. The Urica section (Calabria, Italy). a potential Neogene/Quaternary boundary stratotype. *Giornale di Geologia*, v.42, p.181-204.
- SENGOR, A.M.C., 1979. The north Anatolian transform fault: its' age, offset and tectonic significance. *Journal of the Geological Society of London*, v.136, p.262-282.
- SHACKLETON, J.C., VAN ANDEL, T.H. & RUNNELS, C.N., 1984. Coastal palaeogeography of the Central and Western Mediterranean during the last 125,000 years and it's archaeological implications. *Journal of Field Archaeology*, v.4, p.307-314.
- SHACKLETON, N.J. & OPDYKE, N.D., 1973. Oxygen isotope and palaeomagnetic stratigraphy of equatorial Pacific core V28-238: Oxygen isotope temperatures and ice volumes on a  $10^5$  and  $10^6$  scale. *Quaternary Research*, v.3, p.39-55.
- SHACKLETON, N.J., 1975. The stratigraphic record of deep-sea cores and its implications for the assessment of glacials, interglacials and interstadials in the Mid-Pleistocene. in: Butzer, K.W. & Issac, G.Li. (eds.), *After the Australopithecines: Stratigraphy, Ecology and Culture Change in the Middle Pleistocene*. Moulton, The Hague, p.1-24
- SHACKLETON, N.J. & OPDYKE, N.D., 1976. Oxygen isotope and palaeomagnetic stratigraphy of Pacific core V28-239, Late Pliocene to Latest Pleistocene. *Geological Society of America Memoir 145*, p.449-464.
- SHACKLETON, N.J., 1987. Oxygen isotopes, ice volume and sea level. *Quaternary Science Reviews*, v.6, p.183-190.
- SHAW, H.F., 1978. The clay mineralogy of the Recent surface sediments from the Cilicia Basin, northeast Mediterranean. *Marine Geology*, v.26, p.M51-M58.

- SHAW, H.F. & BUSH, P.R., 1978. The mineralogy and geochemistry of the Recent surface sediments of the Cilicia Basin, northeast Mediterranean. *Marine Geology*, v.27, p.115-136.
- SHEPARD, F.P., 1963. Submarine geology. *Harper & Row, New York, 2<sup>nd</sup> edition, 557pp.*
- SHORT, A.D., 1988. Holocene coastal dune formation in southern Australia: a case study. *Sedimentary Geology*, v.55, p.121-142.
- SIFFET, P., 1966. Contribution a l'etude des detecteurs a rayonnements nucleaire a semi-conducteurs. *Unpublished Ph.d. thesis, University of Strasbourg.*
- SIMMONS, A.H., 1988. Extinct pygmy hippopotamus and early man in Cyprus. *Nature*, v.333, p.554-557.
- SIMONIAN, K.O. & GASS, I.G., 1978. Arakapas fault belt Cyprus: a fossil transform fault. *Geological Society America Bulletin*, v.89, p.1220-1230.
- SMITH, R.S.V., 1976. Late Quaternary pluvial history of Pananut Valley, Inyo and San Bernardino Counties, California. *Unpublished Ph.d thesis, California Institute of Technology, 295pp.*
- SONDAAR, P.Y., 1986. The island sweepstake. *Natural History*, v.95, p.50-57.
- SOREN, D. & LANE, E., 1981. New ideas about the destruction of Paphos. *in: Karageorghis, V. (ed.), Report of the Department of Antiquities, Cyprus, p.178-183.*
- STANLEY, S.M., 1970. Relation of shell form to life habit in the Bivalvia (Mollusca). *Geological Society of America Memoir, no.125, 296pp.*
- STARKEY, H.C., BLACKMON, P.D. & HAUFF, P.L., 1984. The routine mineralogical analysis of clay bearing samples. *United States Geological Survey Bulletin, No.1563.*
- STEARNS, C.E. & THURBER, D.L., 1965. <sup>230</sup>Th-<sup>234</sup>U dates of Late Pleistocene marine fossils from the Mediterranean and Mallorcan littoral. *Quaternaria*, v.7, p.29-42.
- STEARNS, C.E. 1976. Estimates of the position of sea level between 140,000 and 75,000 years ago. *Quaternary Research*, v.6, p.443-449.
- STEEL, R.J., 1974. New Red Sandstone floodplain and piedmont sedimentation in the Hebridean Province, Scotland. *Journal of Sedimentary Petrology*, v.44, p.336-357.
- STRIDE, A.H., BELDERSON, R.H. & KENYON, N.H., 1977. Evolving miogeanticlines of the Eastern Mediterranean (Hellenic, Calabrian and Cyprus outer ridges). *Philosophical Transactions of the Royal Society of London*, v.A284, p.255-285.
- SWARBRICK, R.E., 1979. The sedimentology and structure of S.W. Cyprus and its relationship to the Troodos Complex. *Unpublished Ph.d. thesis, Cambridge University, 342pp.*
- SWARBRICK, R.E., 1980. The Mamonnia Complex of S.W. Cyprus: A Mesozoic continental margin and its relationship with the Troodos Complex. *In: Panayiotou, A. (ed.), Ophiolites. Proceedings of the International Ophiolite Symposium, Nicosia, Cyprus, 1979, p.86-92.*
- SWARBRICK, R.E. & ROBERTSON, A.H.F., 1980. Revised stratigraphy of the Mesozoic rocks of southern Cyprus. *Geological Magazine*, v.117, p.547-563.
- SWIFT, D.J.P., 1968. Coastal erosion and transgressive stratigraphy. *Journal of Geology*, v.76, p.444-456.
- TALVITE, N.A., 1972. Electrodeposition of actinides for alpha spectrometric determination. *Analytical Chemistry*, v.44, p.280-283.

- TANNER, W.F., 1968. Multiple influences on sea-level changes in the Tertiary. *Palaeogeography, Palaeoclimatology, Palaeoecology*, v.5, p.165-171.
- TEICHERT, C., 1958. Cold- and deep-water coral banks. *American Association of Petroleum Geologists Bulletin*, v.42, p.1064-1082.
- TERASMAE, J., 1984. Radiocarbon dating: some problems and potential developments. in: Mahaney, W.C. (ed.), *Quaternary dating methods. Developments in Palaeontology and Stratigraphy 7*, p.1-17.
- THOMPSON, P., 1973. Procedures for extraction and isotopic analysis of uranium and thorium from speleothem. *Department of Geology technical memorandum 73-9, McMaster University, Hamilton*.
- THOMPSON, W.O., 1937. Original structures of beaches, bars and dunes. *Geological Society of America Bulletin*, v.48, p.723-752.
- THUNELL, R.C. & WILLIAMS, D.F., 1989. Glacial-Holocene salinity changes in the Mediterranean Sea: hydrographic and depositional effects. *Nature*, v.338, p.493-496.
- THURBER, D.L., BROECKER, W.S., BLANCHARD, R.L. & POTRATZ, H.A., 1965. Uranium-series ages of Pacific atoll corals. *Science*, v.149, p.55-58.
- TODD, I.A., 1987. Vasilikos valley project 6: excavations at Kalavassos Tenta, v.1. *Studies in Mediterranean archaeology, Goteborg*, v.LXXI:6, Chapter 8, p.173-178.
- TSUBOI, C., 1983. Gravity. *George Allen & Unwin, London*, 254pp.
- TUCKER, M.E. (ED.), 1988. Techniques in sedimentology. *Blackwell Scientific Publications, Oxford*, 394pp.
- TUCKER, M.E. & WRIGHT, V.P., 1990. Carbonate Sedimentology. *Blackwell Scientific Publications, Oxford*, 482pp.
- TUREKIAN, K.K. & CHEN, L.H., 1971. The marine geochemistry of the uranium isotopes,  $^{230}\text{Th}$  and  $^{231}\text{Pa}$ . in: Brunfelt, A.O. & Steinnes, E. (eds.), *Activation analysis in geochemistry and cosmochemistry. Oslo Universitetsforlaget*, p.311-320.
- TURNER, J.P. & HANCOCK, P.L., 1990. Relationships between thrusting and joint systems in the Jaca thrust-top basin, Spanish Pyrenees. *Journal of Structural Geology*, v.12, p.217-226.
- TURNER, W.M., 1971. Quaternary sea-levels of western Cyprus. *Quaternaria*, v.15, p.197-202.
- U.S. NAVY REPORT, 1985. Oceanography of the Mediterranean Basin. *Oceanographic Analysis Division, U.S. Naval Oceanographic Office, Report no.130*, p.27-56.
- VACHER, L. 1973. Coastal dunes of younger Bermuda. in: Coates, D.R. (ed.), *Coastal geomorphology. Publications in Geomorphology, State University of New York*, p.355-391.
- VEEH, H.H., 1966.  $^{230}\text{Th}/^{234}\text{U}$  and  $^{234}\text{U}/^{238}\text{U}$  ages of Pleistocene high sea level stand. *Journal of Geophysical Research*, v.71, p.3379-3386.
- VINE, F.J., POSTER, C.K. & GASS, I.G., 1973. Aeromagnetic survey of the Troodos igneous Massif. *Nature*, v.244, p.34-38.
- VITA-FINZI, C., 1969. The Mediterranean valleys: geological changes in historical times. *Cambridge University Press, Cambridge*, 140pp.



- VITA-FINZI, C. & KING, G.C.P., 1985. The seismicity, geomorphology and structural evolution of the Corinth area of Greece. *Philosophical Transactions of the Royal Society of London*, v.A314, p.379-407.
- VITA-FINZI, C., 1980.  $^{14}\text{C}$  dating of Recent crustal movements in the Persian Gulf and Iranian Makran. *Radiocarbon*, v.22, p.763-773.
- VITA-FINZI, C., 1983. First order  $^{14}\text{C}$  dating of Holocene molluscs. *Earth and Planetary Science Letters*, v.65, p.389-392.
- VITA-FINZI, C., 1990.  $^{14}\text{C}$  dating of Late Quaternary uplift in western Cyprus. *Tectonophysics*, v.172, p.135-140.
- WANLESS, H.R., 1922. Lithology of the White River sediments. *Proceedings of the American Philosophical Society*, v.61, p.184-203.
- WARD, L.C. & ROBERTSON, A.H.F., 1987. Structural and sedimentological development of the Miocene-Recent Polis extensional graben, NW Cyprus. *Abstracts for: Symposium: Troodos 1987, ophiolites and oceanic lithosphere. Geological Survey Department, Nicosia, Cyprus*, p.45.
- WARD, W.C., 1975. Petrology and diagenesis of carbonate eolianites of north western Yucatan Peninsula, Mexico. in: Wantland, K.F. & Pusey, W.C. III (eds.), Belize shelf carbonate sediments, clastic sediments and ecology. *American Association of Petroleum Geologists, studies in geology*, no.2, p.500-571.
- WARD, W.C. & BRADY, M.J., 1979. Strandline sedimentation of carbonate grainstones, Upper Pleistocene, Yucatan Peninsula, Mexico. *American Association of Petroleum Geologists Bulletin*, v.63, p.362-369.
- WARD, W.C., WEIDIE, A.E. & BACK, W., 1985. Geology and hydrology of the Yucatan. *New Orleans Geological Society*, 160pp.
- WARDLAW, N., OLDERSHAW, A. & STOUT, M., 1978. Transformation of aragonite to calcite in a marine gastropod. *Canadian Journal of Earth Sciences*, v.15, p.1861-1866.
- WASSON, R.J., 1977. Last-glacial alluvial fan sedimentation in the Lower Derwent Valley, Tasmania. *Sedimentology*, v.24, p.781-799.
- WASSON, R.J., 1979. Sedimentary history of the Mundi-Mundi alluvial fans, western New South Wales. *Sedimentary Geology*, v.22, p.21-51.
- WATTS, N.L., 1980. Quaternary pedogenic calcretes from the Kalahari (southern Africa): mineralogy, genesis and diagenesis. *Sedimentology*, v.27, p.661-686.
- WEHMILLER, J.F., 1980. Intergeneric differences in apparent racemization kinetics in molluscs and foraminifera: implications for models of diagenetic racemization. in: Hare, P.E., Hoering, T.C. & King, K, jnr. (eds.), Biogeochemistry on amino-acids. *John Wiley, New York*. p.341-355.
- WEHMILLER, J.F., 1988. Amino-acid racemization: applications in chemical taxonomy and chronostratigraphy of Quaternary fossils. *Paper prepared for the 1989 International Geological Congress Workshop on metazoan biomineralization (organizers Carter, J.G. & Bandel, K.)*, 57pp.
- WHITTAKER, A., COPE, J.C.W., COWIE, J.W., GIBBONS, W., HAILWOOD, E.A., HOUSE, M.R., JENKINS, D.G., RAWSON, P.F., RUSHTON, A.W.A., SMITH, D.G., THOMAS, A.T. & WIMBLETON, D.A., 1991. A guide to stratigraphical procedure. *Journal of the Geological Society of London*, v.148, p.813-824.

- WILLIAMS, A.T. & CALDWELL, N.E. 1988. Particle size and shape in pebble-beach sedimentation. *Marine Geology*, v.82, p.199-215.
- WILSON, A.C., 1980. The Devonian sedimentation and tectonism of a rapidly subsiding semi-arid fluvial basin in the Midland Valley of Scotland. *Scottish Journal of Geology*, v.16, p.291-313.
- WILSON, R.A.M., 1957. Progress report. in: Ingham, F. (ed.), Annual Report of the Geological Survey Department for the year 1956, *Nicosia, Cyprus*, p.23-27.
- WILSON, R.A.M., 1958. The Geology of the Xeros-Troodos area. *Geological Survey Department, Cyprus, Memoir 1*, 184pp.
- WOODSIDE, J.M. & BOWIN, C.O., 1970. Gravity anomalies and inferred crustal structure in the eastern Mediterranean sea. *Geological Society of America Bulletin*, v.81, p.1107-1122.
- WOODSIDE, J.M., 1976. Regional vertical tectonics in the Eastern Mediterranean. *Geophysical Journal of the Royal Astronomical Society*, V.47, P.493-514.
- WOOLNOUGH, W.G., 1930. Influence of climate and topography in the formation and distribution of products of weathering. *Geological Magazine*, V.67, p.123-132.
- WRAY, J.L., 1971. Ecology and distribution. in: Ginsburg, R., Rezak, R. & Wray, J.L. (eds.), Geology of calcareous algae (notes for a short course). *Comparative sedimentology laboratory, University of Miami*, 5.1-5.6.
- WRAY, J.L., 1977. Calcareous algae. *Developments in sedimentology and stratigraphy*, v.4, Elsevier, 185pp.
- WRIGHT, V.P., PLATT, N.H. & WIMBLETON, W.A., 1988. Biogenic laminar calcretes: evidence for calcified root mat horizons in palaeosols. *Sedimentology*, v.35, p.603-620.
- WRIGHT, V.P., 1990. Estimating rates of calcrete formation and sediment accretion in ancient alluvial deposits. *Geological Magazine*, v.127, p.273-276.
- YAALON, D.H. & LARONNE, J., 1971. Internal structures in aeolianites and palaeowinds, Mediterranean coast Israel. *Journal of Sedimentary Petrology*, v.41, p.1059-1064.
- YAALON, D.H., 1975. Internal geometry and origin of vegetated coastal sands and dunes. *Journal of Sedimentary Geology*, v.45, p.359.
- ZEUNER, F.E., 1959. The Pleistocene Period. *Hutchinson, London*, 447pp.
- ZIBROWIUS, H., 1980. Les sclérectinaires de la Méditerranée et de l' Atlantique nord-oriental. *Mémoires de l' Institute Océanographique, Monaco*, no.11, p.28-30.
- ZOMENIS, S.L., 1977. Hydrology of the central Mesaoria (Cyprus). *Unpublished Ph.d. thesis, University of London*, 245pp.

**APPENDIX A: SAMPLE COLLECTION IN STORE AT THE DEPARTMENT OF GEOLOGY  
AND GEOPHYSICS, EDINBURGH UNIVERSITY.**

*BOX 1. - Residue from U-series samples.*

Residue from U-series dating (including unpicked coral, picked and ground samples).  
The general samples numbers are:

---

| Speciman No.          | Location               | Grid reference and sheet number |
|-----------------------|------------------------|---------------------------------|
| 200a, 527, 529        | Cape Greco (1-125)     | (985,700) Sh.15                 |
| 336                   | Paphos (2-11)          | (466,465) Sh.16                 |
| 355 (Pliocene)        | Coral Bay (2-22)       | (425,565) Sh.16                 |
| 358 (Pleistocene, F3) | Coral Bay (2-22)       | (425,565) Sh.16                 |
| 425                   | Paphos Airport (2-50)* | (523,413) Sh.22                 |
| 508a                  | Ayia Trias (2-74)*     | (934,795) Sh.15                 |
| 617,021               | Larnaca (1-130)        | (575,610) Sh.21                 |
| 598                   | Dhekelia (2-76)        | (673,713) Sh.21                 |
| Argaka                | Argaka                 | (52,81) Sh.8                    |
| C40/89                | Petounda Point (3-11)  | (455,487) Sh.20                 |
| C68/89                | Akrotiri (3-96)        | (940,255) Sh.23                 |
| C80/89                | Protaras*              | (695,793) Sh.15                 |
| P#/89                 | Paralimni (3-50)       | (976,737) Sh.15                 |

Note: Letters on the sample bags indicate different colony, or location on colony but from the same terrace and same height above sea - level.

All sheet numbers mentioned here (throughout) refer to the Cyprus 1:50,000 map series.

\* - these samples were not used during the U-series work.

*BOX 2. - Borehole and caliche residue; micropalaeo samples.*

i) Residue from borehole samples both crushed and ground and unsampled.

The location of the villages and samples within the borehole can be found in figures in Chapter 5 of the thesis.

ABH - Astromeritis.

MBH - Meniko.

ii) Crushed and ground residue after XRF analysis of caliche samples.

The sample numbers and locations are as follows:

|                           |                     |                 |
|---------------------------|---------------------|-----------------|
| A1 - C20/89, A17 - C22/89 | Ayios Ioannis (1-9) | (180,817) Sh.11 |
| A3 - C13/89, A9 - C33/89  | Ayios Ioannis (3-3) | (157,815) Sh.11 |
| A4 - C58/89, A22 - C59/89 | Episkopi (3-28)     | (922,354) Sh.23 |
| A27 - C61/89              |                     |                 |

|                            |                     |                 |
|----------------------------|---------------------|-----------------|
| A7 - C51/89                | Sophtadhes (3-18)   | (489,549) Sh.21 |
| A8 - C16/89                | Akaki (1-12)        | (111,881) Sh.11 |
| A10 - C81/89               | Pissouri (3-30)     | (753,352) Sh.22 |
| A11 - C25/89               | Aredhiou (1-93)     | (202,786) Sh.11 |
| A12 - C5/89                | Astromeritis (1-16) | (015,879) Sh.11 |
| A13 - C29/89, A15 - C30/89 | Pera (3-6)          | (238,753) Sh.12 |
| A26 - C28/89               |                     |                 |
| A14 - C38/89               | Petounda Pt. (3-10) | (480,503) Sh.20 |
| A16 - C4/89                | Astromeritis (1-27) | (015,879) Sh.11 |
| A19 - C73/89               | Akrotiri (3-97)     | (99,25) Sh.23   |
| A20 - C7/89                | Kato Moni (3-1)     | (083,803) Sh.11 |
| A21 - C97/89               | Tremithousa (3-35)  | (486,516) Sh.16 |
| A23 - C54/89               | Zygi (3-21)         | (295,437) Sh.24 |
| A24 - C64/89               | Maroni (3-31)       | (358,467) Sh.20 |
| A25 - C57/89               | Limassol (3-24)     | (083,408) Sh.23 |
| A28 - C33A/89              | Mazotos (3-9)       | (443,523) Sh.20 |
| A31 - 1                    | Kato Moni           | (08,79) Sh.11   |

iii) Picked micropalaeontology slides (not utilised during the course of this work).

|                         |                    |           |                 |
|-------------------------|--------------------|-----------|-----------------|
| 257, 258                | Limni (1-166)      | F3        | (49,78) Sh.8    |
| 202, 161, 165, 163, 200 | Cape Greco (1-125) | F3-F4     | (985,700) Sh.15 |
| 186, 193, 196           | Ormidhia (1-129)   | F4        | (700,715) Sh.14 |
| 130a                    | Larnaca (1-130)    | F3        | (575,610) Sh.21 |
| 332                     | Paphos (2-11)      | ?Pliocene | (466,463) Sh.16 |

iv) Invertebrate palaeontological samples - refer to Moshkovitz (1968) for details. Sample C93/89 was collected from the grey-green marls of Pliocene age that crop out to the south of Polis close to the Paphos 71 mile post on the old Paphos-Polis road, grid reference (487,758) Sh.8.

*BOXES 3 and 3a. - Thin sections and accompanying hand specimens.*

Thin section chips, hand specimens and thin section.

|                                            |                        |           |                 |
|--------------------------------------------|------------------------|-----------|-----------------|
| 1                                          | Kato Moni              | --        | (08,79) Sh.11   |
| 6                                          | Kato Koutraphas (1-20) | --        | (974,842) Sh.10 |
| 8a, 8b, 617, 618                           | Larnaca (1-130)        | F3        | (575,610) Sh.21 |
| *12, 11, C84/89                            | Pissouri (3-30)        | ?Pliocene | (755,352) Sh.22 |
| 17                                         | Paphos (1-51)          | F4        | (461,475) Sh.16 |
| 21, 22, 312, 313                           | Paphos (2-3)           | F1        | (500,478) Sh.16 |
| 28                                         | Paphos (1-57)          | F4        | (458,472) Sh.16 |
| 65                                         | Peristerona (1-90)     | --        | (076,869) Sh.11 |
| 72                                         | Ayios Ioannis (1-92)   | --        | (177,811) Sh.11 |
| 123, 123b, 137, 138,<br>134, 124, 120, 121 | Paralimni (1-120)      | F4        | (93,79) Sh.15   |
| 140, 145a, 145, 148, 149                   | Ayia Trias (1-121)     | F3        | (930,798) Sh.15 |
| 141, 143, 144, 147                         |                        |           |                 |
| 150                                        | Paralimni (1-123)      | F3        | (97,71) Sh.15   |

|                                                                                                            |                                          |                |                                  |
|------------------------------------------------------------------------------------------------------------|------------------------------------------|----------------|----------------------------------|
| 151, 152, 154, 174,<br>158, 160, 161, 162, 163,<br>165, 168, 197a, 197b, 199,<br>202, 202a, 203, 203a, 172 | Cape Greco (1-124)<br>Cape Greco (1-125) | F3-F4<br>F3-F4 | (99,69) Sh.15<br>(985,700) Sh.15 |
| 27, 357, 358, C100/89<br>173, 169,164, 200                                                                 | Coral Bay (2-24)                         | F3             | (425,568) Sh.16                  |
| 190, 195, 196                                                                                              | Ormidhia (1-129)                         | F4             | (700,715) Sh.14                  |
| 208, 209                                                                                                   | Cape Kiti (1-132)                        | F3             | (554,542) Sh.21                  |
| 213, 214                                                                                                   | Cape Greco (1-135)                       | F2-F3          | (975,698) Sh.15                  |
| 216, 217, 218a, 219,<br>220a, 220b                                                                         | Xylophagou (1-136)                       | F3-F4          | (824,698) Sh.14                  |
| 222                                                                                                        | Xylophagou (1-137)                       | ?F3            | (819,705) Sh.14                  |
| 224                                                                                                        | Cape Greco (1-139)                       | F3-F4          | (985,722) Sh.15                  |
| 228                                                                                                        | Mari (1-141)                             | --             | (265,445) Sh.24                  |
| 229                                                                                                        | Moni (1-142)                             | F3-F4          | (217,405) Sh.24                  |
| 231                                                                                                        | Moni (1-145)                             | Recent         | (162,412) Sh.24                  |
| 244                                                                                                        | Xylophagou (1-150)                       | F3-F4          | (725,713) Sh.14                  |
| 258                                                                                                        | Limni (1-166)                            | F3             | (49,78) Sh.8                     |
| 316, 317, 318, 319                                                                                         | Paphos (2-4)                             | F4             | (454,466) Sh.16                  |
| 322, 323                                                                                                   | Yeroskipos (2-5)                         | F2             | (490,469) Sh.16                  |
| 331, 337                                                                                                   | Paphos (2-10)                            | F2             | (483,473) Sh.16                  |
| 350                                                                                                        | Paphos (2-17)                            | --             | (484,508) Sh.16                  |
| 400                                                                                                        | Lara (2-30)                              | F3             | (382,656) Sh.16                  |
| 522                                                                                                        | Cape Pyla (2-700)                        | F3-F4          | (770,682) Sh.14                  |
| 571                                                                                                        | Ormidhia (2-79)                          | F2-F3          | (705,723) Sh.14                  |
| 600, 601, 603, 604b                                                                                        | Dhekelia (2-84)                          | F4             | (673,713) Sh.21                  |
| 613, 614                                                                                                   | Dhekelia (2-85)                          | F4             | (655,715) Sh.21                  |
| 720, 721, 722, 723, 724                                                                                    | Protaras (2-100)                         | F3-F4          | (965,752) Sh.15                  |
| 3/301, 3/302, 3/303                                                                                        | Argaka (3-109)                           | F3             | (52,81) Sh.8                     |
| B, C, D, E, E1, F                                                                                          | *Cape Greco area                         | --             | (95,71) Sh.15                    |
| X1                                                                                                         | Paphos (2-5b)                            | F2             | (469,483) Sh.16                  |
| C14/89                                                                                                     | Ayios Ioannis (3-3)                      | --             | (157,815) Sh.11                  |
| C18/89                                                                                                     | Perakhorio (3-4)                         | --             | (355,778) Sh.12                  |
| C41/89, C42/89                                                                                             | Petounda Point (3-11)                    | F3             | (455,487) Sh.20                  |
| C48/89                                                                                                     | Tersephanou (3-17)                       | --             | (498,570) Sh.21                  |
| C63-89                                                                                                     | Mazotos (3-13)                           | F3             | (486,549) Sh.21                  |
| C70/89                                                                                                     | Pissouri (3-30a)                         | ?Pliocene      | (73,33) Sh.22                    |
| C93/89                                                                                                     | Polis (3-150)                            | Pliocene       | (487,758) Sh.8                   |
| C96/89                                                                                                     | Tremithousa (3-34)                       | F0             | (486,516) Sh.16                  |
| C110/89, C111/89,<br>C112/89                                                                               | Kato Pyrgos (3-110)                      | F3             | (70,94) Sh.9                     |
| C229/89                                                                                                    | Paphos (2-3)                             | F1             | (500,478) Sh.16                  |
| C230/89                                                                                                    | Paphos (2/50)                            | F2             | (490,469) Sh.16                  |
| F1, F2, F3                                                                                                 | Xylophagou (2-75)                        | --             | (743,703) Sh.14                  |
| Kel                                                                                                        | Kellia                                   | Pliocene       | (588,713) Sh.21                  |
| Mar A, Mar B                                                                                               | Marathounda (2-51)                       | F0             | (538,530) Sh.16                  |
| Mes1                                                                                                       | Mesoyi (2-18)                            | F0             | (506,528) Sh.16                  |

Note: \* - aeolian grainstone collected from the general area to the west of Cape Greco.

*BOX 4. - Miscellaneous hand specimens.*

|                    |                       |       |                 |
|--------------------|-----------------------|-------|-----------------|
| 67                 | Ayios Ioannis (1-91)  | --    | (168,794) Sh.11 |
| 86                 | K. Koutraphas (1-105) | --    | (968,835) Sh.10 |
| 122, 128           | Ayia Trias (1-120)    | F4    | (93,79) Sh.15   |
| 146                | Ayia Trias (1-121)    | F3/F4 | (930,798) Sh.15 |
| 156, 167, 173, 532 | Cape Greco (1-125)    | F3-F4 | (985,700) Sh.15 |
| 175, 177           | Ormidhia (1-128)      | F3    | (705,713) Sh.14 |
| 221                | Xylophagou (1-136)    | ?F4   | (824,698) Sh.14 |
| 223                | Xylophagou (1-138)    | ?F3   | (816,708) Sh.14 |
| 314                | Paphos (2-3)          | F1    | (500,478) Sh.16 |
| 335                | Paphos (2-11)         | ?F4   | (466,463) Sh.16 |
| 402                | Lara Point (2-33)     | F3    | (365,685) Sh.16 |
| 562                | Ormidhia (2-78)       | --    | (715,735) Sh.14 |
| 569                | Ormidhia (2-79)       | --    | (705,723) Sh.14 |
| 590                | Ormidhia (2-82)       | --    | (746,705) Sh.14 |
| 597                | Dhekelia (2-76)       | F4    | (673,713) Sh.21 |
| 606                | Dhekelia (2-83)       | F4    | (660,735) Sh.21 |
| 702                | Kato Pyrgos (3-110)   | F3    | (70,94) Sh.9    |
| 725                | Protaras (2-100)      | F3-F4 | (965,752) Sh.15 |
| 3/308, 3/309       | Vasilikos (3-23)      | ?F1   | (273,429) Sh.24 |
| C34/89             | Petounda Point (3-10) | F3    | (480,503) Sh.20 |
| C76/89             | Ormidhia (2-79a)      | --    | (715,731) Sh.14 |

## **APPENDIX B: LOCATIONS CITED IN THE TEXT.**

Grid references and 1:50,000 ordinance survey sheet number of locations documented in the text.

| Location number | Grid reference   | Location        |
|-----------------|------------------|-----------------|
| 1-7             | (162,775) Sh.11  | Malounda        |
| 1-8             | (163,777) Sh.11  | Malounda        |
| 1-9             | (180,817) Sh.11  | Ayios Ioannis   |
| 1-12            | (111,881) Sh.11  | Akaki           |
| 1-15            | (025,885) Sh.11  | Astromeritis    |
| 1-19            | (017,810) Sh.11  | Vyzekia         |
| 1-20            | (974,843) Sh.11  | Kato Koutraphas |
| 1-23            | (582,613) Sh.21  | Larnaca         |
| 1-27            | (015,879) Sh.11  | Astromeritis    |
| 1-28            | (017,863) Sh.11  | Potami          |
| 1-31a           | (964,828) Sh.10  | Kato Koutraphas |
| 1-57            | (461,475) Sh.16  | Paphos          |
| 1-58            | (013,800) Sh.11  | Astromeritis    |
| 1-59            | (980,848) Sh.10  | Kato Koutraphas |
| 1-67            | (004,861) Sh.11  | Astromeritis    |
| 1-68            | (995,859) Sh.10  | Astromeritis    |
| 1-69            | (990,856) Sh.10  | Astromeritis    |
| 1-70            | (985,852) Sh.10  | Astromeritis    |
| 1-72            | (973,842) Sh.10  | Kato Koutraphas |
| 1-75            | (158,777) Sh.11  | Malounda        |
| 1-76            | (162,771) Sh.11  | Malounda        |
| 1-79            | (167,797) Sh.11  | Ayios Ioannis   |
| 1-81            | (167,801) Sh.11  | Ayios Ioannis   |
| 1-82            | (166,798) Sh.11  | Aredhiou        |
| 1-83            | (167,797) Sh.11  | Aredhiou        |
| 1-84            | (077,843) Sh.11  | Orounda         |
| 1-86            | (074,797) Sh.11  | Kato Moni       |
| 1-87            | (074,798) Sh.11  | Kato Moni       |
| 1-89            | (078,844) Sh.11  | Orounda         |
| 1-90            | (076,8690) Sh.11 | Orounda         |
| 1-91            | (168,794) Sh.11  | Ayios Ioannis   |
| 1-92            | (177,811) Sh.11  | Koraka Hill     |
| 1-93            | (202,786) Sh.11  | Peratis Hill    |
| 1-94            | (195,762) Sh.11  | Politiko        |
| 1-96            | (193,770) Sh.11  | Peratis Hill    |
| 1-97            | (235,778) Sh.12  | Pera            |
| 1-98            | (232,773) Sh.12  | Pera            |
| 1-99            | (203,778) Sh.11  | Peratis Hill    |
| 1-101           | (084,803) Sh.11  | Kato Moni       |
| 1-102           | (025,850) Sh.11  | Potami          |
| 1-104           | (018,864) Sh.11  | Potami          |
| 1-105           | (968,835) Sh.10  | Kato Koutraphas |
| 1-109           | (015,816) Sh.11  | Potami          |
| 1-110           | (010,815) Sh.11  | Vyzakia         |
| 1-113           | (004,827) Sh.11  | Vyzakia         |
| 1-114           | (005,831) Sh.11  | Vyzakia         |
| 1-115           | (005,832) Sh.11  | Vyzakia         |
| 1-117           | (992,841) Sh.10  | Pano Koutraphas |
| 1-118           | (992,838) Sh.10  | Pano Koutraphas |
| 1-119           | (993,832) Sh.10  | Vyzakia         |
| 1-120           | (93,79) Sh.15    | Paralimni       |
| 1-125           | (985,700) Sh.15  | Cape Greco      |
| 1-126           | (987,718) Sh.15  | Cape Greco      |

|        |                  |                  |
|--------|------------------|------------------|
| 1-127  | (985,704) Sh.15  | Cape Greco       |
| 1-128  | (705,713) Sh.14  | Ormidhia         |
| 1-129  | (700,715) Sh.14  | Ormidhia         |
| 1-129a | (690,714) Sh.14  | Ormidhia         |
| 1-130  | (575,610) Sh.21  | Larnaca          |
| 1-136  | (824,698) Sh.14  | Xylophagou       |
| 1-140  | (281,453) Sh.24  | Zyyi             |
| 1-143  | (223,405) Sh.24  | Cape Dolos       |
| 1-148  | (715,717) Sh.14  | Ormidhia         |
| 1-151  | (731,706) Sh.14  | Ormidhia         |
| 1-155  | (378,549) Sh.20  | Alaminos         |
| 1-156  | (39,55) Sh.20    | Menoyia          |
| 1-157  | (398,521) Sh.20  | Alaminos         |
| 1-159  | (346,529) Sh.20  | Ayios Theodhores |
| 1-160  | (354,497) Sh.20  | Ayios Theodhores |
| 1-162  | (338,435) Sh.24  | Zyyi             |
| 1-163  | (325,452) Sh.24  | Maroni           |
| 1-165  | (318,476) Sh.24  | Maroni           |
| 1-166  | (49,78) Sh.8     | Limni            |
| 1-247  | (441,539) Sh.16  | Kissonerga       |
| 2-1    | (497,505) Sh.16  | Anavagos         |
| 2-2    | (495,495) Sh.16  | Paphos           |
| 2-3    | (500,478) Sh.16  | Paphos           |
| 2-4    | (454,466) Sh.16  | Paphos           |
| 2-5    | (490,469) Sh.16  | Yeroskipos       |
| 2-7    | (483,473) Sh.16  | Paphos           |
| 2-10   | (483,473) Sh.16  | Paphos           |
| 2-11   | (466,463) Sh.16  | Paphos           |
| 2-12   | (473,481) Sh.16  | Paphos           |
| 2-13   | (497,465) Sh.16  | Yeroskipos       |
| 2-14   | (465,492) Sh.16  | Paphos           |
| 2-16   | (472,500) Sh.16  | Paphos           |
| 2-17   | (484,508) Sh.16  | Paphos           |
| 2-18   | (506,528) Sh.16  | Mesoyi           |
| 2-19   | (472,500) Sh.16  | Paphos           |
| 2-20   | (445,555) Sh.16  | Kissonerga       |
| 2-22   | (425,565) Sh.16  | Coral Bay        |
| 2-24   | (424,566) Sh.16  | Coral Bay        |
| 2-25   | (402,587) Sh.16  | Coral Bay        |
| 2-27   | (376,624) Sh.16  | Ayios Yeoryios   |
| 2-30   | (382,656) Sh.16  | Lara             |
| 2-32   | (374,670) Sh.16  | Lara             |
| 2-33   | (365,685) Sh.16  | Lara Point       |
| 2-34   | (381,675) Sh.16  | Lara             |
| 2-35   | (385,638) Sh.16  | Ayios Yeoryios   |
| 2-40   | (464,472) Sh.16  | Paphos           |
| 2-41   | (520,443) Sh.22  | Akhelia          |
| 2-42   | (508,429) Sh.22  | Akhelia          |
| 2-43   | (513,438) Sh.22  | Akhelia          |
| 2-44   | (530,451) Sh.22  | Akhelia          |
| 2-45   | (531,452) Sh.22  | Akhelia          |
| 2-46   | (576,427) Sh.22  | Mandria          |
| 2-48   | (588,435) Sh.22  | Anarita          |
| 2-50   | (523,413) Sh.22  | Akhelia          |
| 2-51   | (438,530) Sh.16  | Marathounda      |
| 2-53   | (635,425) Sh.22  | Kouklia          |
| 2-54   | (620,415) Sh.22  | Kouklia          |
| 2-57   | (508,462) Sh.16  | Yeroskipos       |
| 2-57a  | (508,462) Sh.16  | Yeroskipos       |
| 2-59   | (515,4600) Sh.16 | Koloni           |
| 2-63   | (523,462) Sh.16  | Ayia Marathounda |



|       |                  |                        |
|-------|------------------|------------------------|
| 2-63a | (465,593) Sh.16  | Akoursos               |
| 2-70  | (760,692) Sh.14  | Xylophagou             |
| 2-71  | (755,694) Sh.14  | Xylophagou             |
| 2-75  | (743,703) Sh.14  | Xylophagou             |
| 2-76  | (673,713) Sh.21  | Dhekelia               |
| 2-77  | (700,713) Sh.14  | Dhekelia               |
| 2-78  | (715,735) Sh.14  | Ormidhia               |
| 2-79  | (705,723) Sh.14  | Ormidhia               |
| 2-80  | (726,717) Sh.14  | Ormidhia               |
| 2-81  | (748,701) Sh.14  | Xylophagou             |
| 2-82  | (746,705) Sh.14  | Xylophagou             |
| 2-83  | (660,7350) Sh.21 | Dhekelia               |
| 2-84  | (673,715) Sh.21  | Dhekelia               |
| 2-93  | (467,713) Sh.8   | Prodhomi               |
| 2-96  | (700,713) Sh.16  | Skouli                 |
| 2-100 | (655,715) Sh.15  | Protaras               |
| 2-700 | (770,684) Sh.14  | Xylophagou             |
| 3-1   | (083,803) Sh.11  | Kato Moni              |
| 3-2   | (165,815) Sh.11  | Ayios Ioannis          |
| 3-3   | (157,815) Sh.11  | Ayios Ioannis          |
| 3-4   | (355,778) Sh.12  | Perakhorio             |
| 3-6   | (238,7530) Sh.12 | Kambia                 |
| 3-7   | (430,522) Sh.21  | Mazotos                |
| 3-9   | (443,523) Sh.21  | Mazotos                |
| 3-10  | (480,503) Sh.21  | Petounda Point         |
| 3-11  | (455,487) Sh.21  | Petounda Point         |
| 3-12  | (450,500) Sh.21  | Mazotos                |
| 3-13  | (486,549) Sh.21  | Mazotos                |
| 3-14  | (500,580) Sh.21  | Tersephanou            |
| 3-16  | (488,581) Sh.21  | Tersephanou            |
| 3-17  | (498,570) Sh.21  | Tersephanou            |
| 3-18  | (489,549) Sh.21  | Sophtadhes             |
| 3-19  | (313,432) Sh.24  | Zyyi                   |
| 3-20  | (315,449) Sh.24  | Zyyi                   |
| 3-21  | (295,437) Sh.24  | Zyyi                   |
| 3-23  | (273,429) Sh.24  | Vasilikos              |
| 3-26  | (005,405) Sh.23  | Limassol               |
| 3-27  | (924,373) Sh.23  | Erimi                  |
| 3-28  | (922,354) Sh.23  | Episkopi               |
| 3-29  | (943,269) Sh.23  | Akrotiri               |
| 3-30  | (755,352) Sh.22  | Pissouri               |
| 3-31  | (083,408) Sh.23  | Maroni                 |
| 3-32  | (699,715) Sh.14  | Ormidhia               |
| 3-35  | (486,516) Sh.16  | Tremithousa            |
| 3-50  | (976,737) Sh.15  | Paralimni              |
| 3-61  | (914,772) Sh.10  | Tembria                |
| 3-69  | (918,380) Sh.23  | Kouris River           |
| 3-70  | (304,426) Sh.24  | Zyyi                   |
| 3-96  | (942,255) Sh.23  | Cape Zevgari, Akrotiri |
| 3-96a | (985,857) Sh.23  | Akrotiri               |
| 3-97  | (99,25) Sh.23    | Cape Gata, Akrotiri    |
| 3-101 | (446,522) Sh.16  | Lemba                  |
| 3-106 | (49,78) Sh.8     | Limni                  |
| 3-109 | (52,81) Sh.8     | Argaka                 |
| 3-110 | (70,94) Sh.9     | Kato Pyrgos            |
| 3-150 | (487,758) Sh.8   | Polis                  |
| M1    | (305,515) Sh.20  | Khirokitia             |
| M5    | (325,451) Sh.20  | Maroni                 |
| M10   | (318,471) Sh.20  | Maroni                 |

**APPENDIX C: METHOD FOR RADIOCARBON AND URANIUM SERIES DISEQUILIBRIUM  
DATING.**

**1.1. SAMPLE PREPARATION.**

**1.1.1. Radiocarbon method.**

Sample preparation of molluscs for the  $^{14}\text{C}$  method follows that set out by Vita-Finzi (1980). The molluscs were thoroughly cleaned using a dentist drill, a pick and an ultrasound bath. The specimen, once wet, was stored in distilled water to prevent any contamination by atmospheric  $\text{CO}_2$ . The clean mollusc shells were subjected to a series of simple tests (Grant-Taylor, 1972) to ascertain whether any recrystallization of the shells had taken place. Aragonitic shells were used, as aragonite is metastable and will readily recrystallize to calcite. The test used were:

- i) acetate peels and subsequent microscope examination of the shell structures to reveal whether primary aragonite structures were still present (Plate 3.1),
- ii) X-ray diffraction analysis. A comparison of the aragonite versus aragonite and calcite peaks from the sample, with known standards, set on the same machine, allows the proportions of aragonite to calcite to be ascertained (Fig.C.1; Table C.1),
- iii) scanning electron microscope studies to examine the shell structure and locate any impurities in the sample (Plate 3.1).

**Table C.1. Relative aragonite and calcite X-ray diffraction peaks, with the ratio of aragonite to aragonite plus calcite versus percentage aragonite.**

a) Readings taken at aragonite intervals of 10%.

| % Aragonite | Aragonite peak (A) | Calcite. peak (C) | A+C | A/A+C |
|-------------|--------------------|-------------------|-----|-------|
| 0           | 0                  | 154               | 154 | 0.000 |
| 10          | 4                  | 126               | 130 | 0.031 |
| 20          | 8                  | 126               | 134 | 0.060 |
| 30          | 13                 | 127               | 140 | 0.095 |
| 40          | 16                 | 96                | 112 | 0.143 |
| 50          | 19                 | 68                | 87  | 0.218 |
| 60          | 25                 | 66                | 91  | 0.275 |
| 70          | 32                 | 50                | 82  | 0.390 |
| 80          | 36                 | 38                | 74  | 0.486 |
| 90          | 39                 | 20                | 59  | 0.661 |
| 100         | 42                 | 0                 | 42  | 1.000 |

b) Readings taken at aragonite intervals of 2%.

|      |      |     |    |       |
|------|------|-----|----|-------|
| 90   | 49   | 20  | 79 | 0.620 |
| 93   | 51   | 14  | 65 | 0.782 |
| 95   | 52   | 10  | 63 | 0.841 |
| 97   | 54   | 6   | 60 | 0.900 |
| 99   | 61   | 3   | 64 | 0.953 |
| 99.5 | 58.5 | 1.5 | 60 | 0.975 |
| 100  | 50   | 0   | 50 | 1.000 |

Fig.C1. A plot of the primary X-ray diffraction peak height of aragonite versus aragonite divided by aragonite plus calcite.

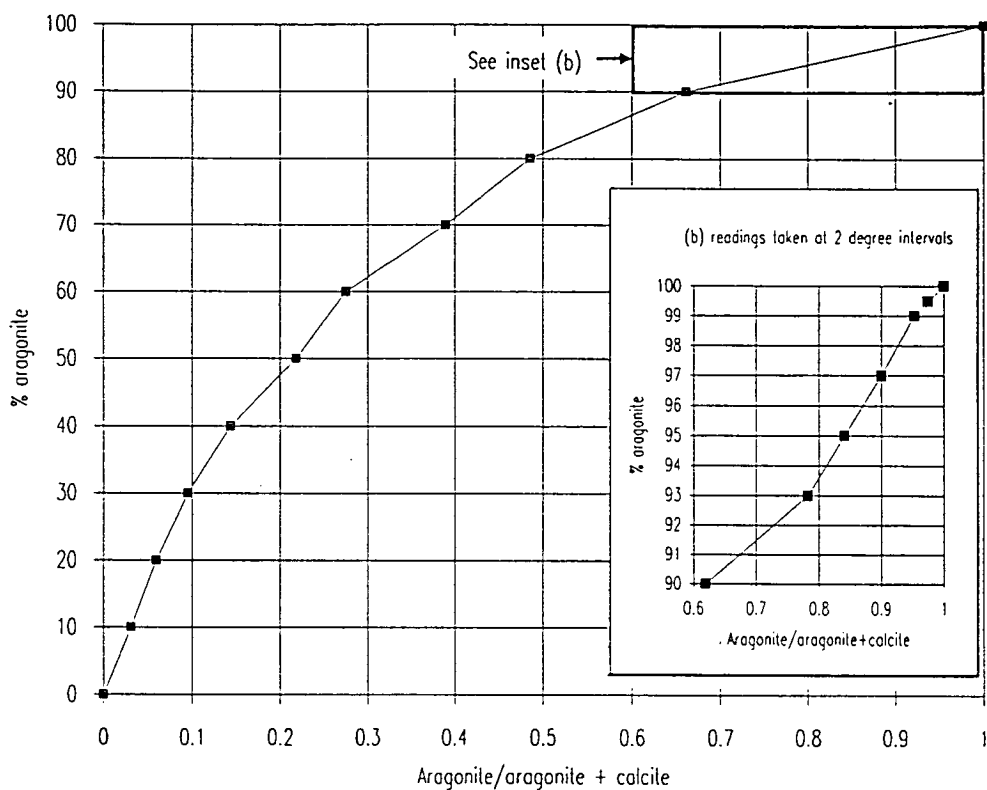
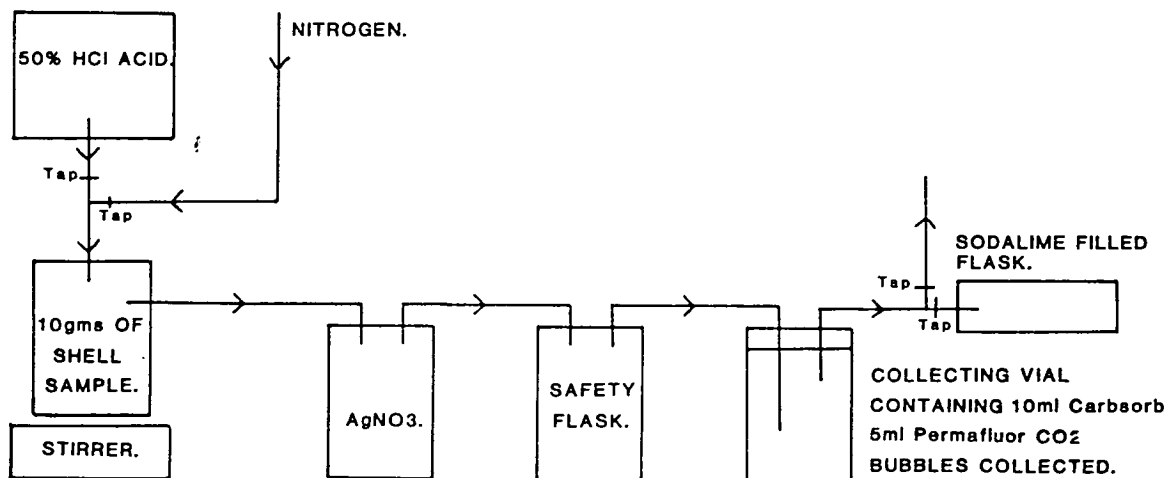


Fig.C2. Diagrammatic representation of the apparatus used for the preparation of mollusc samples for radiocarbon scintillation analyses.



These tests were carried in order from i) to iii), with samples being rejected if evidence of recrystallization or impurities were seen. Samples containing less than 90% aragonite, from the comparison of standard and sample X-ray diffraction peaks, were rejected. Samples were also identified to the generic level (and to the specific level, if possible) before being subjected to the rigorous preparations, outlined above.

### **1.1.2. Uranium series method.**

The uranium series method utilised aragonitic corals. The coral samples were identified to their specific level, where possible. Cleaning of the samples followed the same procedure used during the radiocarbon method, with samples being routinely subject to X-ray diffraction, to deduce the proportion of aragonite to calcite in the coral. Samples containing less than 90% aragonite were not sampled and, where possible, samples with greater than 95% aragonite were utilised.

## **1.2. METHODOLOGY.**

### **1.2.1. Radiocarbon method.**

The sample was broken up and weighed after it had been confirmed that recrystallization had not taken place, and that the sample still possessed its original mineralogy. The following procedure was used (Fig.C.2):

- i) a clean vial filled with  $N_2$  was weighed and the weight was recorded. 10ml of Carbsorb and 5ml of Permaflor were then added to the vial using an Eppendorf pipette. A new tip should be used for each weighing procedure,
- ii) the vial and its metal cap were then weighed and the weight recorded. This is the start weight,
- iii) 10gms of the sample are then introduced to a glass flask (Fig.C.2),
- iv) the neck of the flask is then cleaned and a full bottle containing 50% HCl is then introduced to the system. A firm contact should be made between the flask containing the specimen and the bottle of HCl (all indicator arrows should now point to the output end of the system),
- v) nitrogen is introduced to the system to wash air through. This process is complete when bubbles are seen in the container at the output end of the system which contains 0.1mol  $AgNO_3$  (0.85gms/50ml = 0.1mol),
- vi) the sodalime container is connected to the system once the system is free of air, so preventing air re-entering the system,

vii) the magnetic stirrer is started and the HCl is introduced into the specimen flask at 2 drops per second. A steady stream of CO<sub>2</sub> bubbles should be seen entering the collecting vial,

viii) the apparatus runs for 30 minutes, by which time the majority of the sample should have been digested. During this time the vial should have become quite warm and subsequently have cooled down again. A stream of reasonably vigorous bubbles should have been seen in the system throughout the 30 minute period,

ix) the HCl dropper should be turned off, the specimen vial removed and the sample weighed. 5ml of Permaflor should be added to the sample and the vial should then be weighed again,

x) the sample should now undergo scintillation for 24 hours. Scintillation (in a TriCarb liquid scintillation analyser) should take place as soon as possible after sample preparation.

### **1.2.2. Uranium series disequilibrium method.**

The uranium series dating was carried out in the Department of Geology and Geophysics at Edinburgh University, under the supervision of Dr. Graham Shimmiel. The method utilised  $\alpha$ -spectrometry and made use of a silicon surface barrier detector. The following method was utilised:

i) the samples were cleaned and the mineralogy ascertained (using X-ray diffraction and a comparison with standard aragonite/aragonite + calcite peaks). Samples containing less than 90% calcite were not analysed. Samples for analysis were ground to a fine powder using a pestal and mortar. Samples weighing between 6.0 and 4.5gms were used,

ii) the samples were then dried at 110°C, placed in a crucible and heated to 900°C. Heating enables the CaCO<sub>3</sub> to be converted to CaO and causes decomposition of organic matter. The samples were cooled at room temperature.

N.B. From this point on preparation should take place in a "clean air fume cupboard", with the filter fan on (at position 2).

iii) the sample was saturated with de-ionised water and digested using concentrated HCl, when the digestion reaction had ceased the sample was taken up to a volume of 50ml, using 7.8mol HCl. This procedure left digested CaCO<sub>3</sub> and an insoluble residue. If less than 3 samples from the same locality are available, then both the soluble digest and insoluble residue should be analysed. The analysis of the residue involves the digestion of the insoluble fraction of the sample in a P.T.F.E crucible. The following steps should be followed: a) add 4ml conc HNO<sub>3</sub> and 10ml conc HF to

- digest, b) add 4ml conc  $\text{HNO}_3$  and 5ml conc HF, to achieve complete digestion, c) add 4ml  $\text{HNO}_3$  and fume to dryness, d) add 10ml 9mol HCl, e) warm the sample slowly and cover with a cover glass,
- iv) a mixed 0.05ml (for concentrations of 0 to 10ppm U and Th) spike of  $^{228}\text{Th}$  and  $^{232}\text{U}$  (30 des/min) is added to each sample, using an Eppendorf pipette, to allow the chemical yield to be deduced,
- v) the procedure from here is shown in the flow diagram (Fig.C.3).

The following notes amplify the individual steps of the uranium series disequilibrium method given above:

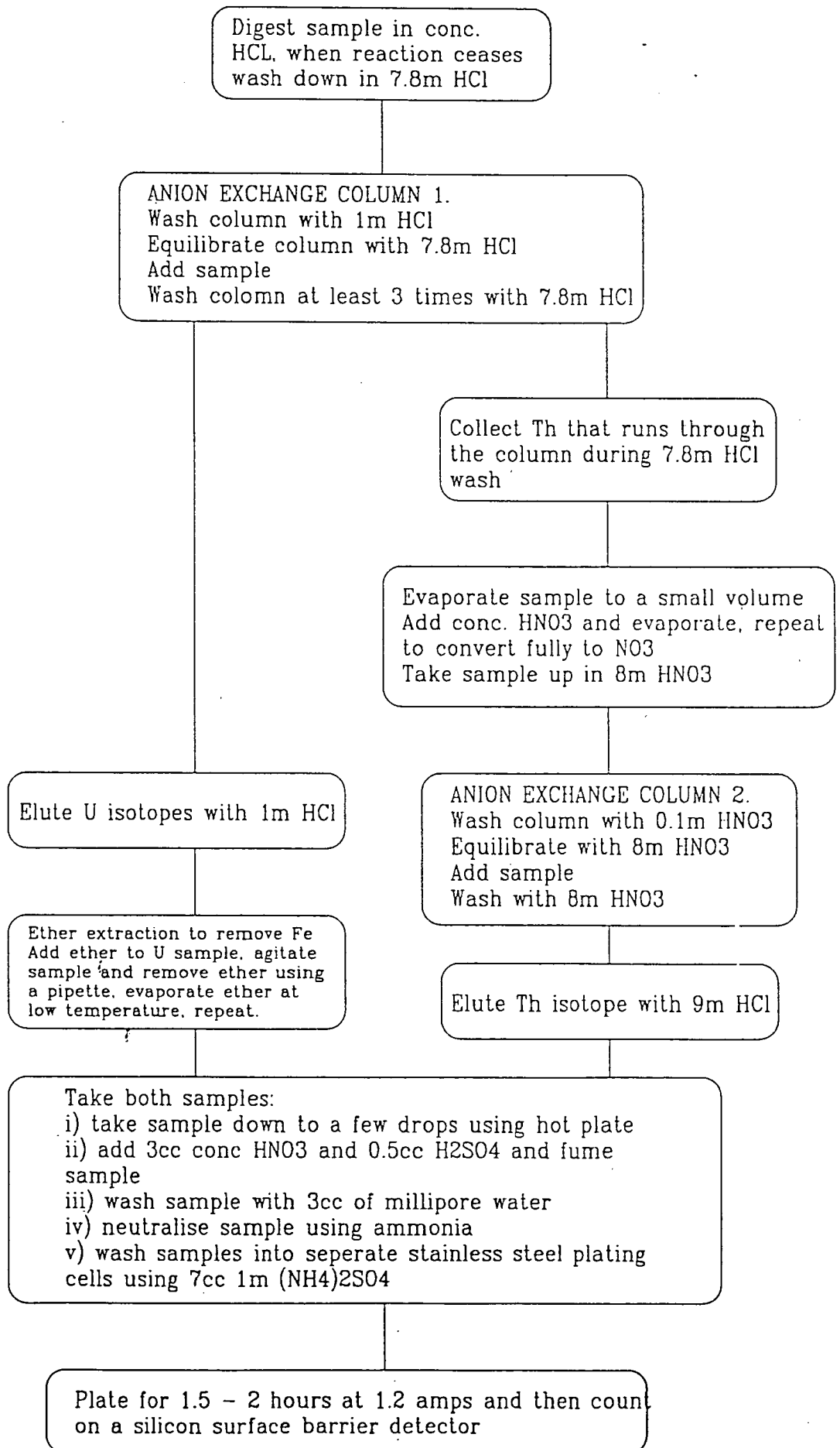
i) the anion exchange column uses a Bio-Rad AG1-X8 resin; 100-200 mesh, chloride form. The diameter of the column is 0.7cm and the resin bed is 6cm long. 50ml (4 column volumes) of solution should be used for each wash of the column, with washes taking place every 30-40 minutes. The columns should be used as soon as possible after they have been set up as organic material could be introduced into the Th system. Care should be taken to prevent the resin being disturbed when the solutions are added. The columns chemically separate the U and Th radionuclides and this allows the  $^{234}\text{U}$  and  $^{230}\text{Th}$  peaks to be distinguished as they have very similar peak  $\alpha$ -particle energies. The anion exchange resin allows selective adsorption and desorption to take place. U is adsorbed by high strength HCl (7.8 mol.), whereas Th is adsorbed by high strength  $\text{HNO}_3$  (8 mol.). The column procedure is outlined in Fig.C.3,

ii)  $^{232}\text{Th}$  activity is a measure of contamination in the sample of the soluble fraction. If the  $^{232}\text{Th}$  count is high the insoluble fraction should also be analysed. This will reveal whether the residue is primary and was deposited at the time of formation of the coral, or whether it is a later feature.  $^{230}\text{Th}/^{234}\text{U}$  and  $^{234}\text{U}/^{238}\text{U}$  ratios for the insoluble residue should be consistent with those obtained when the HCl soluble, i.e.  $\text{CaCO}_3$ , solution was analysed,

iii) an acidic electrolyte solution of  $(\text{NH}_4)_2\text{SO}_4$  is electroplated on to a stainless steel disc to obtain a monoatomic layer suitable for counting. It is common practice (Talvite, 1972) to plate the thorium disc for twice as long as the uranium disc. The plating solution is placed in a P.T.F.E. beaker, mounted on a brass base plate. The base plate acts as the cathode (black, negative), a small coil attached to the P.T.F.E. beaker acting as the anode (red, positive).

iv) samples are counted using  $\alpha$ -spectrometry on a silicon surface barrier counter (Siffet, 1966 for details). Counting usually lasts for  $10^4$  counts, or for a time equivalent to the background count. A count of  $10^4$  enables the counting error due to nuclear statistics to be kept to 1%. A background count on the detectors is taken for two days before the sample is added and is used to correct the data for background

Fig.C3. Flow chart representing the methodology used during anion exchange column work and plating of the uranium series samples.



effects. The background count includes random counts and fixed counts, which usual result from detector contamination,

v) all glassware and P.T.F.E. crucibles should be thoroughly washed and decontaminated after use.

vi) the age of the samples was deduced using: a) an isochron plot (Fig.C.4), b) the Fortran program in Appendix C of Ivanovich and Harmon (1982), or c) the tabulated data (Table C.2; G. Shimmiel, *pers. comm.*, 1989) derived from the following formula:

$$F(t) = -\frac{^{230}\text{Th}}{^{234}\text{U}} + \frac{(1 - e^{-\lambda_{230}\text{Th}t})}{^{234}\text{U}/^{238}\text{U}} + \frac{\lambda_{230}\text{Th}}{\lambda_{230}\text{Th} - \lambda_{234}\text{U}} \left[ 1 - \frac{^{238}\text{U}}{^{234}\text{U}} \right] \left[ 1 - e^{-(\lambda_{230}\text{Th} - \lambda_{234}\text{U})t} \right]$$



Fig.C4. Variation of  $^{234}\text{U}/^{238}\text{U}$  and  $^{230}\text{Th}/^{234}\text{U}$  activity ratios with time in a closed system with no initial  $^{230}\text{Th}$ . The near vertical lines are isochrons, i.e. lines of equal age but different  $^{234}\text{U}/^{238}\text{U}$  activity ratios. The near horizontal lines show change in nuclide activity ratios as age increases for different initial  $^{234}\text{U}/^{238}\text{U}$  activity ratios as indicated (after Schwarcz, 1979).

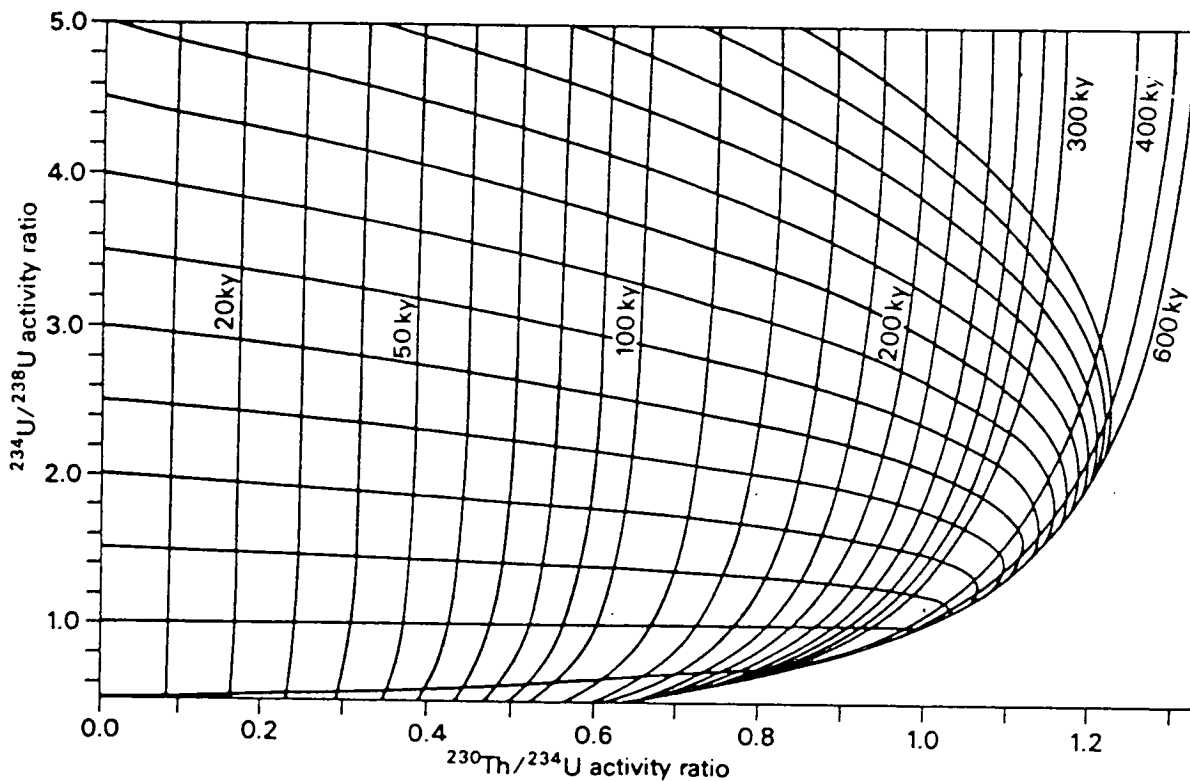


Table C2. Representing a  $^{230}\text{Th}/^{234}\text{U}$  and  $^{234}\text{U}/^{238}\text{U}$  age model for coral samples assuming an initial  $^{234}\text{U}/^{238}\text{U}$  ratio of 1.14 (data after G. Shimmiel, *pers. comm.*, 1988). The  $^{230}\text{Th}/^{234}\text{U}$  ratio represents the age of the sample.

U/Th age model      U/U age model

$^{234}\text{U}/^{238}\text{U} = 1.14$

| Age<br>ky | $^{230}\text{Th}$<br>$^{234}\text{U}$ | $^{234}\text{U}$<br>$^{238}\text{U}$ | Age<br>ky | $^{230}\text{Th}$<br>$^{234}\text{U}$ | $^{234}\text{U}$<br>$^{238}\text{U}$ | Age<br>ky | $^{230}\text{Th}$<br>$^{234}\text{U}$ | $^{234}\text{U}$<br>$^{238}\text{U}$ |
|-----------|---------------------------------------|--------------------------------------|-----------|---------------------------------------|--------------------------------------|-----------|---------------------------------------|--------------------------------------|
| 1         | 0.0092                                | 1.1396                               | 73        | 0.4956                                | 1.1142                               | 145       | 0.7535                                | 1.0934                               |
| 2         | 0.0183                                | 1.1392                               | 74        | 0.5004                                | 1.1138                               | 146       | 0.7560                                | 1.0931                               |
| 3         | 0.0273                                | 1.1388                               | 75        | 0.5051                                | 1.1135                               | 147       | 0.7586                                | 1.0928                               |
| 4         | 0.0362                                | 1.1384                               | 76        | 0.5099                                | 1.1132                               | 148       | 0.7611                                | 1.0926                               |
| 5         | 0.0451                                | 1.1381                               | 77        | 0.5146                                | 1.1129                               | 149       | 0.7636                                | 1.0923                               |
| 6         | 0.0539                                | 1.1377                               | 78        | 0.5192                                | 1.1126                               | 150       | 0.7660                                | 1.0921                               |
| 7         | 0.0626                                | 1.1373                               | 79        | 0.5238                                | 1.1123                               | 151       | 0.7685                                | 1.0918                               |
| 8         | 0.0712                                | 1.1369                               | 80        | 0.5284                                | 1.1119                               | 152       | 0.7709                                | 1.0915                               |
| 9         | 0.0797                                | 1.1365                               | 81        | 0.5329                                | 1.1116                               | 153       | 0.7733                                | 1.0913                               |
| 10        | 0.0882                                | 1.1361                               | 82        | 0.5374                                | 1.1113                               | 154       | 0.7757                                | 1.0910                               |
| 11        | 0.0966                                | 1.1358                               | 83        | 0.5418                                | 1.1110                               | 155       | 0.7781                                | 1.0908                               |
| 12        | 0.1049                                | 1.1354                               | 84        | 0.5462                                | 1.1107                               | 156       | 0.7804                                | 1.0905                               |
| 13        | 0.1132                                | 1.1350                               | 85        | 0.5506                                | 1.1104                               | 157       | 0.7828                                | 1.0903                               |
| 14        | 0.1213                                | 1.1346                               | 86        | 0.5549                                | 1.1101                               | 158       | 0.7851                                | 1.0900                               |
| 15        | 0.1295                                | 1.1343                               | 87        | 0.5592                                | 1.1098                               | 159       | 0.7873                                | 1.0898                               |
| 16        | 0.1375                                | 1.1339                               | 88        | 0.5635                                | 1.1095                               | 160       | 0.7896                                | 1.0895                               |
| 17        | 0.1454                                | 1.1335                               | 89        | 0.5677                                | 1.1092                               | 161       | 0.7919                                | 1.0893                               |
| 18        | 0.1533                                | 1.1331                               | 90        | 0.5719                                | 1.1089                               | 162       | 0.7941                                | 1.0890                               |
| 19        | 0.1612                                | 1.1328                               | 91        | 0.5760                                | 1.1086                               | 163       | 0.7963                                | 1.0888                               |
| 20        | 0.1689                                | 1.1324                               | 92        | 0.5801                                | 1.1083                               | 164       | 0.7985                                | 1.0885                               |
| 21        | 0.1766                                | 1.1320                               | 93        | 0.5842                                | 1.1080                               | 165       | 0.8006                                | 1.0883                               |
| 22        | 0.1842                                | 1.1317                               | 94        | 0.5882                                | 1.1077                               | 166       | 0.8028                                | 1.0880                               |
| 23        | 0.1918                                | 1.1313                               | 95        | 0.5922                                | 1.1074                               | 167       | 0.8049                                | 1.0878                               |
| 24        | 0.1993                                | 1.1309                               | 96        | 0.5962                                | 1.1071                               | 168       | 0.8070                                | 1.0875                               |
| 25        | 0.2067                                | 1.1306                               | 97        | 0.6001                                | 1.1068                               | 169       | 0.8091                                | 1.0873                               |
| 26        | 0.2140                                | 1.1302                               | 98        | 0.6040                                | 1.1065                               | 170       | 0.8112                                | 1.0871                               |
| 27        | 0.2213                                | 1.1298                               | 99        | 0.6079                                | 1.1062                               | 171       | 0.8133                                | 1.0868                               |
| 28        | 0.2285                                | 1.1295                               | 100       | 0.6117                                | 1.1059                               | 172       | 0.8153                                | 1.0866                               |
| 29        | 0.2357                                | 1.1291                               | 101       | 0.6155                                | 1.1056                               | 173       | 0.8173                                | 1.0863                               |
| 30        | 0.2428                                | 1.1287                               | 102       | 0.6193                                | 1.1053                               | 174       | 0.8193                                | 1.0861                               |
| 31        | 0.2498                                | 1.1284                               | 103       | 0.6230                                | 1.1050                               | 175       | 0.8213                                | 1.0858                               |
| 32        | 0.2568                                | 1.1280                               | 104       | 0.6267                                | 1.1047                               | 176       | 0.8233                                | 1.0856                               |
| 33        | 0.2637                                | 1.1277                               | 105       | 0.6304                                | 1.1044                               | 177       | 0.8252                                | 1.0854                               |
| 34        | 0.2706                                | 1.1273                               | 106       | 0.6340                                | 1.1041                               | 178       | 0.8272                                | 1.0851                               |
| 35        | 0.2773                                | 1.1270                               | 107       | 0.6376                                | 1.1038                               | 179       | 0.8291                                | 1.0849                               |
| 36        | 0.2841                                | 1.1266                               | 108       | 0.6412                                | 1.1035                               | 180       | 0.8310                                | 1.0847                               |
| 37        | 0.2907                                | 1.1262                               | 109       | 0.6447                                | 1.1032                               | 181       | 0.8329                                | 1.0844                               |
| 38        | 0.2974                                | 1.1259                               | 110       | 0.6482                                | 1.1029                               | 182       | 0.8348                                | 1.0842                               |
| 39        | 0.3039                                | 1.1255                               | 111       | 0.6517                                | 1.1027                               | 183       | 0.8366                                | 1.0839                               |
| 40        | 0.3104                                | 1.1252                               | 112       | 0.6551                                | 1.1024                               | 184       | 0.8385                                | 1.0837                               |
| 41        | 0.3168                                | 1.1248                               | 113       | 0.6586                                | 1.1021                               | 185       | 0.8403                                | 1.0835                               |
| 42        | 0.3232                                | 1.1245                               | 114       | 0.6619                                | 1.1018                               | 186       | 0.8421                                | 1.0832                               |
| 43        | 0.3296                                | 1.1241                               | 115       | 0.6653                                | 1.1015                               | 187       | 0.8439                                | 1.0830                               |
| 44        | 0.3358                                | 1.1238                               | 116       | 0.6686                                | 1.1012                               | 188       | 0.8457                                | 1.0828                               |
| 45        | 0.3420                                | 1.1235                               | 117       | 0.6719                                | 1.1010                               | 189       | 0.8475                                | 1.0825                               |
| 46        | 0.3482                                | 1.1231                               | 118       | 0.6752                                | 1.1007                               | 190       | 0.8492                                | 1.0823                               |
| 47        | 0.3543                                | 1.1228                               | 119       | 0.6784                                | 1.1004                               | 191       | 0.8509                                | 1.0821                               |
| 48        | 0.3604                                | 1.1224                               | 120       | 0.6816                                | 1.1001                               | 192       | 0.8526                                | 1.0819                               |
| 49        | 0.3664                                | 1.1221                               | 121       | 0.6848                                | 1.0998                               | 193       | 0.8543                                | 1.0816                               |
|           |                                       |                                      | 122       | 0.6880                                | 1.0995                               | 194       | 0.8560                                | 1.0814                               |
| 50        | 0.3723                                | 1.1217                               | 123       | 0.6911                                | 1.0993                               | 195       | 0.8577                                | 1.0812                               |
| 51        | 0.3782                                | 1.1214                               | 124       | 0.6942                                | 1.0990                               | 196       | 0.8593                                | 1.0809                               |
| 52        | 0.3840                                | 1.1211                               | 125       | 0.6973                                | 1.0987                               | 197       | 0.8610                                | 1.0807                               |
| 53        | 0.3898                                | 1.1207                               | 126       | 0.7003                                | 1.0984                               | 198       | 0.8626                                | 1.0805                               |
| 54        | 0.3956                                | 1.1204                               | 127       | 0.7034                                | 1.0982                               | 199       | 0.8642                                | 1.0803                               |
| 55        | 0.4013                                | 1.1201                               | 128       | 0.7064                                | 1.0979                               | 200       | 0.8658                                | 1.0800                               |
| 56        | 0.4069                                | 1.1197                               | 129       | 0.7093                                | 1.0976                               | 201       | 0.8674                                | 1.0798                               |
| 57        | 0.4125                                | 1.1194                               | 130       | 0.7123                                | 1.0973                               | 202       | 0.8690                                | 1.0796                               |
| 58        | 0.4180                                | 1.1190                               | 131       | 0.7152                                | 1.0971                               | 203       | 0.8705                                | 1.0794                               |
| 59        | 0.4235                                | 1.1187                               | 132       | 0.7181                                | 1.0968                               | 204       | 0.8721                                | 1.0792                               |
| 60        | 0.4290                                | 1.1184                               | 133       | 0.7209                                | 1.0965                               | 205       | 0.8736                                | 1.0789                               |
| 61        | 0.4344                                | 1.1181                               | 134       | 0.7238                                | 1.0963                               | 206       | 0.8751                                | 1.0787                               |
| 62        | 0.4397                                | 1.1177                               | 135       | 0.7266                                | 1.0960                               | 207       | 0.8766                                | 1.0785                               |
| 63        | 0.4450                                | 1.1174                               | 136       | 0.7294                                | 1.0957                               | 208       | 0.8781                                | 1.0783                               |
| 64        | 0.4503                                | 1.1171                               | 137       | 0.7322                                | 1.0955                               | 209       | 0.8796                                | 1.0781                               |
| 65        | 0.4555                                | 1.1167                               | 138       | 0.7349                                | 1.0952                               | 210       | 0.8811                                | 1.0778                               |
| 66        | 0.4607                                | 1.1164                               | 139       | 0.7376                                | 1.0949                               | 211       | 0.8825                                | 1.0776                               |
| 67        | 0.4658                                | 1.1161                               | 140       | 0.7403                                | 1.0947                               | 212       | 0.8840                                | 1.0774                               |
| 68        | 0.4708                                | 1.1158                               | 141       | 0.7430                                | 1.0944                               | 213       | 0.8854                                | 1.0772                               |
| 69        | 0.4759                                | 1.1154                               | 142       | 0.7457                                | 1.0941                               | 214       | 0.8868                                | 1.0770                               |
| 70        | 0.4809                                | 1.1151                               | 143       | 0.7483                                | 1.0939                               | 215       | 0.8882                                | 1.0768                               |
| 71        | 0.4858                                | 1.1148                               | 144       | 0.7509                                | 1.0936                               | 216       | 0.8896                                | 1.0765                               |
| 72        | 0.4907                                | 1.1145                               |           |                                       |                                      |           |                                       |                                      |

|     |        |        |     |        |        |     |        |        |
|-----|--------|--------|-----|--------|--------|-----|--------|--------|
| 217 | 0.8910 | 1.0763 | 307 | 0.9771 | 1.0594 | 397 | 1.0171 | 1.0462 |
| 218 | 0.8923 | 1.0761 | 308 | 0.9777 | 1.0592 | 398 | 1.0174 | 1.0460 |
| 219 | 0.8937 | 1.0759 | 309 | 0.9784 | 1.0590 | 399 | 1.0177 | 1.0459 |
| 220 | 0.8951 | 1.0757 | 310 | 0.9790 | 1.0589 | 400 | 1.0179 | 1.0458 |
| 221 | 0.8964 | 1.0755 | 311 | 0.9796 | 1.0587 |     |        |        |
| 222 | 0.8977 | 1.0753 | 312 | 0.9802 | 1.0585 |     |        |        |
| 223 | 0.8990 | 1.0751 | 313 | 0.9808 | 1.0584 |     |        |        |
| 224 | 0.9003 | 1.0749 | 314 | 0.9814 | 1.0582 |     |        |        |
| 225 | 0.9016 | 1.0746 | 315 | 0.9820 | 1.0580 |     |        |        |
| 226 | 0.9029 | 1.0744 | 316 | 0.9826 | 1.0579 |     |        |        |
| 227 | 0.9042 | 1.0742 | 317 | 0.9832 | 1.0577 |     |        |        |
| 228 | 0.9054 | 1.0740 | 318 | 0.9838 | 1.0576 |     |        |        |
| 229 | 0.9067 | 1.0738 | 319 | 0.9843 | 1.0574 |     |        |        |
| 230 | 0.9079 | 1.0736 | 320 | 0.9849 | 1.0572 |     |        |        |
| 231 | 0.9091 | 1.0734 | 321 | 0.9855 | 1.0571 |     |        |        |
| 232 | 0.9103 | 1.0732 | 322 | 0.9860 | 1.0569 |     |        |        |
| 233 | 0.9115 | 1.0730 | 323 | 0.9866 | 1.0568 |     |        |        |
| 234 | 0.9127 | 1.0728 | 324 | 0.9871 | 1.0566 |     |        |        |
| 235 | 0.9139 | 1.0726 | 325 | 0.9877 | 1.0564 |     |        |        |
| 236 | 0.9151 | 1.0724 | 326 | 0.9882 | 1.0563 |     |        |        |
| 237 | 0.9162 | 1.0722 | 327 | 0.9888 | 1.0561 |     |        |        |
| 238 | 0.9174 | 1.0720 | 328 | 0.9893 | 1.0560 |     |        |        |
| 239 | 0.9185 | 1.0718 | 329 | 0.9898 | 1.0558 |     |        |        |
| 240 | 0.9197 | 1.0716 | 330 | 0.9904 | 1.0557 |     |        |        |
| 241 | 0.9208 | 1.0714 | 331 | 0.9909 | 1.0555 |     |        |        |
| 242 | 0.9219 | 1.0712 | 332 | 0.9914 | 1.0554 |     |        |        |
| 243 | 0.9230 | 1.0710 | 333 | 0.9919 | 1.0552 |     |        |        |
| 244 | 0.9241 | 1.0708 | 334 | 0.9924 | 1.0550 |     |        |        |
| 245 | 0.9252 | 1.0706 | 335 | 0.9929 | 1.0549 |     |        |        |
| 246 | 0.9263 | 1.0704 | 336 | 0.9934 | 1.0547 |     |        |        |
| 247 | 0.9273 | 1.0702 | 337 | 0.9939 | 1.0546 |     |        |        |
| 248 | 0.9284 | 1.0700 | 338 | 0.9944 | 1.0544 |     |        |        |
| 249 | 0.9294 | 1.0698 | 339 | 0.9949 | 1.0543 |     |        |        |
| 250 | 0.9305 | 1.0696 | 340 | 0.9954 | 1.0541 |     |        |        |
| 251 | 0.9315 | 1.0694 | 341 | 0.9958 | 1.0540 |     |        |        |
| 252 | 0.9325 | 1.0692 | 342 | 0.9963 | 1.0538 |     |        |        |
| 253 | 0.9335 | 1.0690 | 343 | 0.9968 | 1.0537 |     |        |        |
| 254 | 0.9345 | 1.0688 | 344 | 0.9973 | 1.0535 |     |        |        |
| 255 | 0.9355 | 1.0686 | 345 | 0.9977 | 1.0534 |     |        |        |
| 256 | 0.9365 | 1.0685 | 346 | 0.9982 | 1.0532 |     |        |        |
| 257 | 0.9375 | 1.0683 | 347 | 0.9986 | 1.0531 |     |        |        |
| 258 | 0.9385 | 1.0681 | 348 | 0.9991 | 1.0529 |     |        |        |
| 259 | 0.9394 | 1.0679 | 349 | 0.9995 | 1.0528 |     |        |        |
| 260 | 0.9404 | 1.0677 | 350 | 1.0000 | 1.0526 |     |        |        |
| 261 | 0.9413 | 1.0675 | 351 | 1.0004 | 1.0525 |     |        |        |
| 262 | 0.9423 | 1.0673 | 352 | 1.0008 | 1.0523 |     |        |        |
| 263 | 0.9432 | 1.0671 | 353 | 1.0013 | 1.0522 |     |        |        |
| 264 | 0.9441 | 1.0669 | 354 | 1.0017 | 1.0521 |     |        |        |
| 265 | 0.9450 | 1.0668 | 355 | 1.0021 | 1.0519 |     |        |        |
| 266 | 0.9459 | 1.0666 | 356 | 1.0025 | 1.0518 |     |        |        |
| 267 | 0.9468 | 1.0664 | 357 | 1.0030 | 1.0516 |     |        |        |
| 268 | 0.9477 | 1.0662 | 358 | 1.0034 | 1.0515 |     |        |        |
| 269 | 0.9486 | 1.0660 | 359 | 1.0038 | 1.0513 |     |        |        |
| 270 | 0.9495 | 1.0658 | 360 | 1.0042 | 1.0512 |     |        |        |
| 271 | 0.9503 | 1.0656 | 361 | 1.0046 | 1.0510 |     |        |        |
| 272 | 0.9512 | 1.0655 | 362 | 1.0050 | 1.0509 |     |        |        |
| 273 | 0.9521 | 1.0653 | 363 | 1.0054 | 1.0508 |     |        |        |
| 274 | 0.9529 | 1.0651 | 364 | 1.0058 | 1.0506 |     |        |        |
| 275 | 0.9537 | 1.0649 | 365 | 1.0062 | 1.0505 |     |        |        |
| 276 | 0.9546 | 1.0647 | 366 | 1.0066 | 1.0503 |     |        |        |
| 277 | 0.9554 | 1.0645 | 367 | 1.0069 | 1.0502 |     |        |        |
| 278 | 0.9562 | 1.0644 | 368 | 1.0073 | 1.0501 |     |        |        |
| 279 | 0.9570 | 1.0642 | 369 | 1.0077 | 1.0499 |     |        |        |
| 280 | 0.9578 | 1.0640 | 370 | 1.0081 | 1.0498 |     |        |        |
| 281 | 0.9586 | 1.0638 | 371 | 1.0084 | 1.0496 |     |        |        |
| 282 | 0.9594 | 1.0637 | 372 | 1.0088 | 1.0495 |     |        |        |
| 283 | 0.9602 | 1.0635 | 373 | 1.0092 | 1.0494 |     |        |        |
| 284 | 0.9610 | 1.0633 | 374 | 1.0095 | 1.0492 |     |        |        |
| 285 | 0.9617 | 1.0631 | 375 | 1.0099 | 1.0491 |     |        |        |
| 286 | 0.9625 | 1.0629 | 376 | 1.0103 | 1.0489 |     |        |        |
| 287 | 0.9633 | 1.0628 | 377 | 1.0106 | 1.0488 |     |        |        |
| 288 | 0.9640 | 1.0626 | 378 | 1.0110 | 1.0487 |     |        |        |
| 289 | 0.9647 | 1.0624 | 379 | 1.0113 | 1.0485 |     |        |        |
| 290 | 0.9655 | 1.0622 | 380 | 1.0116 | 1.0484 |     |        |        |
| 291 | 0.9662 | 1.0621 | 381 | 1.0120 | 1.0483 |     |        |        |
| 292 | 0.9669 | 1.0619 | 382 | 1.0123 | 1.0481 |     |        |        |
| 293 | 0.9677 | 1.0617 | 383 | 1.0127 | 1.0480 |     |        |        |
| 294 | 0.9684 | 1.0616 | 384 | 1.0130 | 1.0479 |     |        |        |
| 295 | 0.9691 | 1.0614 | 385 | 1.0133 | 1.0477 |     |        |        |
| 296 | 0.9698 | 1.0612 | 386 | 1.0136 | 1.0476 |     |        |        |
| 297 | 0.9705 | 1.0610 | 387 | 1.0140 | 1.0475 |     |        |        |
| 298 | 0.9712 | 1.0609 | 388 | 1.0143 | 1.0473 |     |        |        |
| 299 | 0.9718 | 1.0607 | 389 | 1.0146 | 1.0472 |     |        |        |
| 300 | 0.9725 | 1.0605 | 390 | 1.0149 | 1.0471 |     |        |        |
| 301 | 0.9732 | 1.0604 | 391 | 1.0152 | 1.0469 |     |        |        |
| 302 | 0.9739 | 1.0602 | 392 | 1.0155 | 1.0468 |     |        |        |
| 303 | 0.9745 | 1.0600 | 393 | 1.0159 | 1.0467 |     |        |        |
| 304 | 0.9752 | 1.0599 | 394 | 1.0162 | 1.0465 |     |        |        |
| 305 | 0.9758 | 1.0597 | 395 | 1.0165 | 1.0464 |     |        |        |
| 306 | 0.9765 | 1.0595 | 396 | 1.0168 | 1.0463 |     |        |        |

| Sample no. | count time | sample wt. | U-238 cnts | U-234 cnts | spike cnts | Th-232 cnts | Th-230 cnts | spike cnts | +/-U-238 | +/-U-234 | +/-Th-232 | +/-Th-230 |
|------------|------------|------------|------------|------------|------------|-------------|-------------|------------|----------|----------|-----------|-----------|
| 021        | 172119     | 3.45191    | 5468       | 6066       | 22112      | 82          | 5140        | 22385      | 0.030    | 0.032    | 0.004     | 0.028     |
| 617a       | 331233     | 5.43868    | 12858      | 14869      | 44482      | 239         | 14004       | 42823      | 0.015    | 0.016    | 0.002     | 0.016     |
| 617b       | 331233     | 4.62565    | 10342      | 11701      | 46802      | 97          | 9744        | 38749      | 0.015    | 0.015    | 0.002     | 0.017     |
| 617c       | 331233     | 5.74586    | 12755      | 14428      | 40555      | 311         | 12163       | 39979      | 0.015    | 0.016    | 0.002     | 0.015     |
| 617d       | 331233     | 6.54999    | 7882       | 8362       | 25999      | 182         | 15182       | 43639      | 0.016    | 0.017    | 0.001     | 0.013     |
| 617e       | 90401      | 6.25983    | 3823       | 4356       | 14252      | 89          | 3562        | 13955      | 0.021    | 0.023    | 0.003     | 0.021     |
| 617f       | 245362     | 6.15361    | 5131       | 5482       | 17298      | 49          | 8269        | 27540      | 0.021    | 0.022    | 0.001     | 0.017     |
| 617g       | 245362     | 5.38296    | 5665       | 6198       | 21663      | 164         | 6337        | 29713      | 0.020    | 0.021    | 0.002     | 0.015     |
| 617ed      | 245362     | 5.26215    | 6307       | 6756       | 28081      | 135         | 6301        | 31901      | 0.017    | 0.017    | 0.002     | 0.015     |
| 358a       | 92646      | 5.79183    | 3889       | 4319       | 11574      | 18          | 2638        | 8841       | 0.029    | 0.030    | 0.003     | 0.031     |
| 358b       | 92646      | 6.42342    | 4535       | 5037       | 14178      | 20          | 2899        | 9766       | 0.023    | 0.024    | 0.002     | 0.027     |
| 358c       | 92646      | 6.86748    | 4110       | 4599       | 10534      | 22          | 3417        | 8301       | 0.027    | 0.029    | 0.002     | 0.030     |
| 358d       | 111371     | 5.48851    | 3473       | 3731       | 13559      | 24          | 2620        | 13614      | 0.025    | 0.025    | 0.002     | 0.021     |
| 358e       | 111371     | 4.80244    | 1538       | 1581       | 6245       | 8           | 2543        | 11974      | 0.041    | 0.041    | 0.002     | 0.027     |
| 200a       | 155889     | 6.33237    | 4664       | 5189       | 18192      | 137         | 6208        | 24829      | 0.018    | 0.019    | 0.002     | 0.016     |
| 527a       | 155889     | 6.16381    | 4180       | 4765       | 14907      | 126         | 4988        | 21650      | 0.022    | 0.023    | 0.003     | 0.016     |
| 527b       | 155889     | 4.34922    | 3309       | 3313       | 19800      | 147         | 4334        | 24420      | 0.021    | 0.021    | 0.004     | 0.019     |
| 529a       | 155889     | 5.85372    | 5012       | 5578       | 21726      | 82          | 6442        | 28530      | 0.017    | 0.018    | 0.002     | 0.015     |
| 336a       | 90401      | 5.64093    | 4366       | 4765       | 12816      | 43          | 3456        | 14566      | 0.028    | 0.030    | 0.002     | 0.022     |
| 336b       | 90401      | 6.24469    | 4718       | 5150       | 13200      | 22          | 3628        | 14575      | 0.026    | 0.027    | 0.002     | 0.021     |
| 336c       | 90401      | 4.57152    | 2867       | 3346       | 12554      | 37          | 2502        | 14957      | 0.029    | 0.031    | 0.003     | 0.023     |
| 336d       | 111371     | 5.55075    | 2757       | 2986       | 7720       | 54          | 3716        | 14621      | 0.038    | 0.040    | 0.003     | 0.023     |
| 336e       | 111371     | 6.00001    | 3599       | 3933       | 9303       | 28          | 3863        | 13421      | 0.033    | 0.035    | 0.002     | 0.024     |
| 598a       | 329369     | 4.44383    | 11620      | 12858      | 51270      | 228         | 9082        | 50830      | 0.015    | 0.015    | 0.002     | 0.013     |
| 598d       | 329369     | 6.40551    | 17032      | 18667      | 47520      | 163         | 12377       | 47145      | 0.013    | 0.014    | 0.001     | 0.011     |
| 598e       | 329369     | 5.38982    | 10445      | 11522      | 37528      | 151         | 11321       | 52209      | 0.016    | 0.016    | 0.001     | 0.012     |
| 598f       | 329369     | 6.69231    | 20222      | 22637      | 52868      | 198         | 16095       | 55918      | 0.012    | 0.013    | 0.001     | 0.011     |
| 598g       | 92646      | 5.29717    | 2928       | 3385       | 11348      | 38          | 2110        | 10154      | 0.028    | 0.030    | 0.004     | 0.026     |
| 598ee      | 91900      | 5.22454    | 3711       | 4236       | 21144      | 57          | 3200        | 24974      | 0.017    |          |           |           |
| 355a       | 245362     | 5.53019    | 5945       | 5410       | 16500      | 44          | 11219       | 25113      | 0.026    | 0.025    | 0.001     | 0.024     |
| P1         | 85513      | 6.48704    | 3408       | 3915       | 11210      | 4           | 14          | 4293       | 0.025    | 0.027    | 0.002     | 0.004     |
| P2         | 85513      | 4.89935    | 2517       | 2910       | 10373      | 0           | 3           | 3255       | 0.031    | 0.033    | 0.000     | 0.003     |
| P3         | 91900      | 4.64522    | 1695       | 1957       | 20574      | 7           | 17          | 16589      | 0.013    | 0.014    | 0.001     | 0.002     |
| c68a/89    | 91900      | 5.04458    | 3703       | 4471       | 22106      | 18          | 4845        | 24696      | 0.017    | 0.019    | 0.001     | 0.017     |
| c68b/89    | 91900      | 5.94272    | 4745       | 5275       | 21281      | 32          | 6649        | 24564      | 0.017    | 0.018    | 0.001     | 0.017     |
| c68c/89    | 87087      | 6.31019    | 3706       | 4125       | 16268      | 11          | 6534        | 23357      | 0.018    | 0.019    | 0.001     | 0.017     |
| c68d/89    | 87087      | 5.07703    | 2342       | 2582       | 13199      | 88          | 4486        | 22869      | 0.022    | 0.024    | 0.003     | 0.018     |
| 40a/89     | 158288     | 4.26748    | 6612       | 7329       | 40752      | 70          | 6338        | 41511      | 0.014    | 0.015    | 0.001     | 0.014     |
| 40d/89     | 87084      | 5.41166    | 3332       | 3685       | 17989      | 32          | 3784        | 21544      | 0.018    | 0.019    | 0.002     | 0.016     |
| P2/89      | 158114     | 5.74998    | 5905       | 6562       | 18757      | 71          | 7400        | 28492      | 0.022    | 0.023    | 0.002     | 0.016     |
| P3/89      | 158114     | 6.34435    | 8001       | 8852       | 27895      | 61          | 6922        | 36672      | 0.016    | 0.016    | 0.001     | 0.013     |
| P4/89      | 93367      | 6.09189    | 1646       | 1832       | 5689       | 93          | 3760        | 17887      | 0.036    | 0.038    | 0.003     | 0.018     |
| P5/89      | 93367      | 6.10951    | 2342       | 2569       | 9639       | 112         | 3760        | 18637      | 0.025    | 0.027    | 0.003     | 0.017     |

Note: sample numbers and locations are quoted in Chapter 3  
sample weights are in grammes and count times in seconds.  
the uranium spike is <sup>232</sup>U and the thorium spike is <sup>228</sup>Th.

Table C3. Raw data from the uranium series disequilibrium studies of Quaternary corals from Cyprus.

**Appendix D: The occurrence of Plio-Pleistocene molluscs from Cyprus, with a comparison of the age ranges of these fauna in the south-east and western Mediterranean (after Moshkovitz, 1968).**

| Species                            | Pliocene |   | Pleistocene |   | Mediterranean stratigraphic range |                     |
|------------------------------------|----------|---|-------------|---|-----------------------------------|---------------------|
|                                    | a        | b | c           | d | S.E. basin                        | Western basin       |
| <b>Pelecypoda</b>                  |          |   |             |   |                                   |                     |
| <i>Nucula nucleus</i> (L.)         |          |   | *           | * | <i>Plio-Rec</i>                   | <i>Mio-Rec</i>      |
| <i>N. sulcata</i> var <i>plana</i> |          |   |             | * | <i>Tyrr-Rec</i>                   | <i>Pleist-Rec</i>   |
| <i>N. sulcata</i>                  |          |   | *           |   | <i>Plio-Rec</i>                   | <i>Mio-Rec</i>      |
| <i>N. placentina</i>               |          | * | *           |   | <i>Mio-Sicil</i>                  | <i>Mio-Sicil</i>    |
| <i>Nuculana pella</i> (L.)         |          | * |             | * | <i>Plio-Rec</i>                   | <i>Mio-Rec</i>      |
| <i>N. fragilis</i>                 |          | * | *           |   | <i>Plio-Rec</i>                   | <i>Mio-Rec</i>      |
| <i>Arca noae</i> (L.)              |          | * |             | * | <i>Mio-Rec</i>                    | <i>Mio-Rec</i>      |
| <i>Barbatia barbata</i> (L.)       |          | * |             | * | <i>Plio-Rec</i>                   | <i>Mio-Rec</i>      |
| <i>B. plicata</i> (L.)             |          |   |             | * | <i>Tyrr</i>                       | <i>Tyrr</i>         |
| <i>Batharca pectunculoides</i>     |          | * |             |   | <i>Plio-Rec</i>                   | <i>Plio-Rec</i>     |
| <i>Galactea lactea</i> (L.)        |          | * | *           | * | <i>Mio-Rec</i>                    | <i>Mio-Rec</i>      |
| <i>Anadara pectinata</i>           | *        | * |             | * | <i>Mio-Calab</i>                  | <i>Mio-Calab</i>    |
| <i>A. diluvii</i>                  |          | * |             |   | <i>Mio-L.Pleist</i>               | <i>Mio-L.Pleist</i> |
| <i>Glycymeris cor.</i> (Lmk.)      |          | * | *           | * | <i>Mio-Rec</i>                    | <i>Mio-Rec</i>      |
| <i>G. bimaculata</i> (Poli)        | *        | * |             | * | <i>Plio-Rec</i>                   | <i>Mio-Rec</i>      |
| <i>G. glycymeris</i> (L.)          |          |   |             | * | <i>Plio-Rec</i>                   | <i>Mio-Rec</i>      |
| <i>G. inflatus</i> (Br.)           |          | * |             | * | <i>Mio-Plio</i>                   | <i>Mio-Plio</i>     |
| <i>Limopsis aurita</i>             |          | * |             |   | <i>Mio-Plio</i>                   | <i>Mio-Rec</i>      |
| <i>L. anomaia</i>                  |          | * |             |   | <i>Mio-Plio</i>                   | <i>Mio-Rec</i>      |
| <i>Pinna nobilis</i>               |          |   |             | * | <i>Tyrr-Rec</i>                   | <i>Plio-Rec</i>     |
| <i>Pecten jacobaeus</i>            | *        | * | *           | * | <i>Plio-Rec</i>                   | <i>Plio-Rec</i>     |
| <i>P. benedictus</i>               |          | * |             |   | <i>Mio-Plio</i>                   | <i>Mio-Plio</i>     |
| <i>P. reghiensis</i>               |          | * |             |   | <i>Plio</i>                       | <i>Mio-Plio</i>     |
| <i>Flabellipecten alessii</i>      |          | * |             |   | <i>Plio</i>                       | <i>Mio-Plio</i>     |
| <i>Amusium cristatum</i>           | *        | * |             |   | <i>Mio-Plio</i>                   | <i>Mio-Plio</i>     |
| <i>Chalmys flexuosus</i>           |          | * | *           | * | <i>Plio-Rec</i>                   | <i>Plio-Rec</i>     |
| <i>Ch. hyalina</i>                 |          |   | *           |   | <i>Plio-Rec</i>                   | <i>Plio-Rec</i>     |
| <i>Ch. clavatus</i>                | *        |   | *           |   | <i>Plio-Rec</i>                   | <i>Plio-Rec</i>     |
| <i>Ch. pesfelis</i>                |          | * |             |   | <i>Plio-Rec</i>                   | <i>Plio-Rec</i>     |
| <i>Ch. varius</i>                  | *        | * |             | * | <i>Mio-Rec</i>                    | <i>Mio-Rec</i>      |
| <i>Ch. multistriatus</i>           |          | * |             | * | <i>Mio-Rec</i>                    | <i>Mio-Rec</i>      |
| <i>Ch. zenonis</i>                 |          | * |             |   | <i>Plio</i>                       | -                   |
| <i>Ch. angelonii</i>               | *        | * |             |   | <i>Plio</i>                       | <i>Mio-Sicil</i>    |
| <i>Ch. opercularis</i>             | *        | * |             |   | <i>Mio-Rec</i>                    | <i>Mio-Rec</i>      |
| <i>Ch. bollenensis</i>             |          | * |             |   | <i>Mio-Pleist</i>                 | <i>Mio-Pleist</i>   |
| <i>Spondylus quaederopus</i>       |          |   |             | * | <i>Plio-Rec</i>                   | <i>Mio-Rec</i>      |
| <i>S. crassicosta</i>              | *        | * |             |   | <i>Mio-Plio</i>                   | <i>Mio-Plio</i>     |
| <i>Plicatula mytilina</i>          |          |   | *           |   | <i>Plio-Sicil</i>                 | <i>Plio-Sicil</i>   |
| <i>Anomia ephippium</i>            | *        | * |             | * | <i>Mio-Rec</i>                    | <i>Mio-Rec</i>      |
| <i>Lima lima</i>                   |          |   |             | * | <i>Plio-Rec</i>                   | <i>Mio-Rec</i>      |
| <i>Ostrea edulis</i>               | *        | * |             | * | <i>Mio-Rec</i>                    | <i>Mio-Rec</i>      |
| <i>O. cucullata</i>                |          | * |             |   | <i>Plio</i>                       | <i>Mio-Plio</i>     |
| <i>Pycndonta cochlear</i>          | *        | * |             |   | <i>Mio-Rec</i>                    | <i>Mio-Rec</i>      |
| <i>Chama gryphina</i>              |          | * |             | * | <i>Plio-Rec</i>                   | <i>Mio-Rec</i>      |
| <i>Ch. gryphoides</i>              | *        | * |             |   | <i>Mio-Rec</i>                    | <i>Mio-Rec</i>      |
| <i>Ch. placentina</i>              |          | * |             |   | <i>Plio</i>                       | <i>Plio-Sicil</i>   |
| <i>Lucina fragilis</i>             |          | * |             | * | <i>Plio-Rec</i>                   | <i>Plio-Rec</i>     |
| <i>Jagonia decussata</i>           |          |   |             | * | <i>Mio-Rec</i>                    | <i>Mio-Rec</i>      |
| <i>Divaricella divaricata</i>      |          | * | *           | * | <i>Plio-Rec</i>                   | <i>Plio-Rec</i>     |
| <i>Loripes lacteus</i>             |          |   | *           | * | <i>Plio-Rec</i>                   | <i>Plio-Rec</i>     |

|                                 |   |   |   |   |                      |                     |
|---------------------------------|---|---|---|---|----------------------|---------------------|
| <i>Megaxinus transversus</i>    |   | * |   |   | <i>Plio-Tyrr</i>     | <i>Mio-Rec</i>      |
| <i>M. ellipticus</i>            | * | * |   |   | <i>Plio</i>          | <i>Mio-Rec</i>      |
| <i>Phacoides orbicularis</i>    |   |   |   | * | <i>Plio</i>          | <i>Mio-Plio</i>     |
| <i>P. borealis</i>              |   | * |   |   | <i>Plio-Pleist</i>   | <i>Mio-Rec</i>      |
| <i>Myrtea spinifera</i>         |   | * | * | * | <i>Mio-Tyrr</i>      | <i>Mio-Rec</i>      |
| <i>Diplodonta rotundata</i>     |   |   |   | * | <i>Plio-Rec</i>      | <i>Plio-Rec</i>     |
| <i>Cardita antiquata</i>        |   | * |   | * | <i>Plio-Rec</i>      | <i>Plio-Rec</i>     |
| <i>C. corbis</i>                |   |   |   | * | <i>L.Pleist-Rec</i>  | <i>Plio-Rec</i>     |
| <i>C. rhomboidea</i>            |   | * |   |   | <i>Plio</i>          | <i>Plio</i>         |
| <i>Begüina trapeza</i>          |   | * |   | * | <i>Plio-Rec</i>      | <i>Plio-Rec</i>     |
| <i>B. calyculata</i>            |   |   |   | * | <i>Plio-Rec</i>      | <i>Mio-Rec</i>      |
| <i>B. intermedia</i>            | * | * |   |   | <i>Plio</i>          | <i>Plio</i>         |
| <i>B. aculeata</i>              |   | * |   |   | <i>Plio-Rec</i>      | <i>Mio-Rec</i>      |
| <i>Astarte fusca</i>            |   | * |   |   | <i>Plio-Rec</i>      | <i>Plio-Rec</i>     |
| <i>Cardium echinatum</i>        | * | * |   | * | <i>Mio-Rec</i>       | <i>Mio-Rec</i>      |
| <i>C. tuberculatum</i>          |   |   | * | * | <i>Plio-Rec</i>      | <i>Mio-Rec</i>      |
| <i>C. edule</i>                 |   |   |   | * | <i>Mio-Rec</i>       | <i>Plio-Rec</i>     |
| <i>C. exiguum</i>               |   |   | * | * | <i>Plio-Rec</i>      | <i>Plio-Rec</i>     |
| <i>C. hians</i>                 |   | * | * |   | <i>Mio-L.Pleist</i>  | <i>Mio-Rec</i>      |
| <i>C. erinaceum</i>             |   | * |   |   | <i>Plio-L.Pleist</i> | <i>Plio-Rec</i>     |
| <i>C. aculeatum</i>             |   | * |   |   | <i>Plio-Rec</i>      | <i>Plio-Rec</i>     |
| <i>Parvicardium papillasum</i>  |   | * | * | * | <i>Mio-Rec</i>       | <i>Mio-Rec</i>      |
| <i>Laevicardium oblongum</i>    |   |   | * | * | <i>Plio-Rec</i>      | <i>Plio-Rec</i>     |
| <i>L. crossum</i>               |   |   |   | * | <i>Plio-Rec</i>      | <i>Plio-Rec</i>     |
| <i>L. cyprium</i>               |   | * |   |   | <i>Mio-Plio</i>      | <i>Mio-Plio</i>     |
| <i>Maetra corallina</i>         |   |   |   | * | <i>Tyrr-Rec</i>      | <i>Plio-Rec</i>     |
| <i>Spisula subtruncata</i>      |   | * | * |   | <i>Plio-Rec</i>      | <i>Mio-Rec</i>      |
| <i>Eastonia rugosa</i>          |   |   |   | * | <i>L.Pleist-Tyrr</i> | <i>Plio-Rec</i>     |
| <i>Donax trunculus</i>          |   |   |   | * | <i>Plio-Rec</i>      | <i>Plio-Rec</i>     |
| <i>Quadrans serratus</i>        |   | * | * |   | <i>Plio-Rec</i>      | <i>Plio-Rec</i>     |
| <i>Gastrana fragilis</i>        |   |   |   | * | <i>Tyrr-Rec</i>      | <i>Plio-Rec</i>     |
| <i>Angulus compressus</i>       |   |   | * |   | <i>Mio-L.Pleist</i>  | <i>Mio-Rec</i>      |
| <i>Arcopagia corbis</i>         |   | * |   |   | <i>Plio-L.Pleist</i> | <i>Mio-Sicil</i>    |
| <i>Solecurtus antiquatus</i>    |   | * |   |   | <i>Plio-Rec</i>      | <i>Plio-Rec</i>     |
| <i>Isocardia humana</i>         |   | * | * |   | <i>Plio-Rec</i>      | <i>Plio-Rec</i>     |
| <i>Venus verrucosa</i>          |   |   |   | * | <i>Plio-Rec</i>      | <i>Mio-Rec</i>      |
| <i>V. multilamella</i>          | * | * | * |   | <i>Mio-L.Pleist</i>  | <i>Mio-Rec</i>      |
| <i>Chione gallina</i>           | * |   |   | * | <i>Plio-Rec</i>      | <i>Mio-Rec</i>      |
| <i>C. fasciata</i>              |   |   |   | * | <i>Plio-Rec</i>      | <i>Mio-Rec</i>      |
| <i>C. ovata</i>                 |   | * | * |   | <i>Plio-Rec</i>      | <i>Mio-Rec</i>      |
| <i>Cordiopsis islandicoides</i> |   | * |   |   | <i>Mio-Plio</i>      | <i>Mio-Plio</i>     |
| <i>Callista chione</i>          |   |   |   | * | <i>Plio-Rec</i>      | <i>Mio-Rec</i>      |
| <i>Corbula gibba</i>            | * | * | * |   | <i>Mio-Rec</i>       | <i>Oligo-Rec</i>    |
| <i>Panopaea faujasi</i>         |   | * |   |   | <i>Mio-L.Pleist</i>  | <i>Mio-L.Pleist</i> |
| <b>Gastropoda</b>               |   |   |   |   |                      |                     |
| <i>Haliotis lamellosa</i>       |   |   |   | * | <i>Tyrr-Rec</i>      | <i>Plio-Rec</i>     |
| <i>Emarginula huzardi</i>       |   |   |   | * | <i>Tyrr-Rec</i>      | <i>Plio-Rec</i>     |
| <i>E. cancellata</i>            |   |   |   | * | <i>Tyrr-Rec</i>      | <i>Mio-Rec</i>      |
| <i>E. elongata</i>              |   |   |   | * | <i>Tyrr-Rec</i>      | <i>Plio-Rec</i>     |
| <i>Diodora italica</i>          |   | * |   | * | <i>Mio-Rec</i>       | <i>Mio-Rec</i>      |
| <i>Patella caerulea</i>         |   |   |   | * | <i>Tyrr-Rec</i>      | <i>Plio-Rec</i>     |
| <i>Gibbula ardens</i>           |   |   |   | * | <i>Tyrr-Rec</i>      | <i>Plio-Rec</i>     |
| <i>G. magus</i>                 |   | * |   |   | <i>Mio-Rec</i>       | <i>Mio-Rec</i>      |
| <i>Monodonta turbinatus</i>     |   |   |   | * | <i>Tyrr-Rec</i>      | <i>Plio-Rec</i>     |
| <i>M. articulata</i>            |   |   |   | * | <i>Tyrr-Rec</i>      | <i>Plio-Rec</i>     |
| <i>Calliastoma exasperatus</i>  |   |   | * | * | <i>L.Pleist-Rec</i>  | <i>Mio-Rec</i>      |
| <i>C. striatus</i>              |   |   | * | * | <i>Plio-Rec</i>      | <i>Plio-Rec</i>     |
| <i>Clanulus corallinus</i>      |   |   |   | * | <i>L.Pleist-Rec</i>  | <i>Mio-Rec</i>      |

|                                      |   |   |     |                      |                   |
|--------------------------------------|---|---|-----|----------------------|-------------------|
| <i>C. cruciatus</i>                  |   |   | *   | <i>Plio-Rec</i>      | <i>Plio-Rec</i>   |
| <i>Homalopoma sanguineum</i>         |   |   | *   | <i>L.Pleist-Rec</i>  | <i>Mio-Rec</i>    |
| <i>Astraea rugosa</i>                | * |   | *   | <i>Mio-Rec</i>       | <i>Mio-Rec</i>    |
| <i>Tricolia pulia</i>                | * |   | * * | <i>Plio-Rec</i>      | <i>Plio-Rec</i>   |
| <i>T. tenuis</i>                     |   |   | *   | <i>Tyrr-Rec</i>      | <i>Pleist-Rec</i> |
| <i>T. speciosa</i>                   |   |   | *   | <i>Tyrr-Rec</i>      | <i>Plio-Rec</i>   |
| <i>Turritella decipiens</i>          |   |   | *   | <i>Pleist-Rec</i>    | <i>Pleist-Rec</i> |
| <i>T. triplicata</i>                 | * |   | * * | <i>Plio-Rec</i>      | <i>Mio-Rec</i>    |
| <i>T. tricarinata</i>                | * |   | *   | <i>Mio-Rec</i>       | <i>Mio-Rec</i>    |
| <i>T. pliorecens</i>                 |   |   | *   | <i>Plio-L.Pleist</i> | <i>Plio-Sicil</i> |
| <i>T. communis</i>                   |   |   | *   | <i>Mio-Rec</i>       | <i>Mio-Rec</i>    |
| <i>T. bicarinata</i>                 |   | * |     | <i>Plio</i>          | <i>Plio</i>       |
| <i>T. subangulata</i>                | * | * |     | <i>Mio-Calab</i>     | <i>Mio-Calab</i>  |
| <i>T. tornata</i>                    |   | * |     | <i>Mio-L.Pleist</i>  | <i>Mio-Calab</i>  |
| <i>Tenagodus anguinus</i>            |   |   | *   | <i>Tyrr-Rec</i>      | <i>Pleist-Rec</i> |
| <i>Bittium latreillei</i>            |   |   | * * | <i>L.Pleist-Rec</i>  | <i>Pleist-Rec</i> |
| <i>B. reticulatum</i>                | * |   | *   | <i>Plio-Rec</i>      | <i>Mio-Rec</i>    |
| <i>Cerithium vulgatum</i>            | * |   | * * | <i>Mio-Rec</i>       | <i>Mio-Rec</i>    |
| <i>C. vulgatum var spinosa</i>       |   |   | *   | <i>Tyrr-Rec</i>      | <i>Pleist-Rec</i> |
| <i>C. varicosum</i>                  | * |   | *   | <i>Mio-Calab</i>     | <i>Mio-Calab</i>  |
| <i>Epitonium pseudoscalaris</i>      |   |   | *   | <i>Plio-L.Pleist</i> | <i>Plio</i>       |
| <i>E. communis</i>                   | * |   |     | <i>Mio-Rec</i>       | <i>Mio-Rec</i>    |
| <i>E. commutata</i>                  | * |   |     | <i>Plio-Rec</i>      | <i>Plio-Rec</i>   |
| <i>Pyramidella plicosa</i>           | * |   |     | <i>Plio</i>          | <i>Mio-Plio</i>   |
| <i>Crepidula crepidula</i>           | * |   |     | <i>Plio-Rec</i>      | <i>Mio-Rec</i>    |
| <i>Xenophora crispa</i>              | * |   | *   | <i>Plio-Sicil</i>    | <i>Plio-Rec</i>   |
| <i>Strombus bubonius</i>             |   |   | *   | <i>Tyrr</i>          | <i>Tyrr</i>       |
| <i>S. coronatus</i>                  | * | * |     | <i>Mio-L.Pleist</i>  | <i>Mio-Plio</i>   |
| <i>Aporrhais pesphcani</i>           |   | * | * * | <i>Plio-Rec</i>      | <i>Plio-Rec</i>   |
| <i>A. uttingerianus</i>              | * | * | *   | <i>Mio-Calab</i>     | <i>Mio-Calab</i>  |
| <i>Polynices lacteus</i>             |   |   | *   | <i>Tyrr</i>          | <i>Calab-Tyrr</i> |
| <i>P. jesephinus</i>                 |   |   | *   | <i>Mio-Rec</i>       | <i>Mio-Rec</i>    |
| <i>P. fusca</i>                      | * | * | *   | <i>Plio-L.Pleist</i> | <i>Mio-Rec</i>    |
| <i>Natica millepunctata</i>          |   |   | *   | <i>Sicil-Rec</i>     | <i>Sicil-Rec</i>  |
| <i>N. figrina</i>                    | * |   | *   | <i>Mio-Calab</i>     | <i>Plio-Calab</i> |
| <i>Cymatium corrugatum</i>           | * |   | *   | <i>Plio-Tyrr</i>     | <i>Plio</i>       |
| <i>Talparia lurida</i>               |   |   | *   | <i>Tyrr-Rec</i>      | <i>Pleist-Rec</i> |
| <i>Murex rudis</i>                   |   |   | * * | <i>Calab-Tyrr</i>    | <i>Mio-Plio</i>   |
| <i>M. trunculus</i>                  |   |   | *   | <i>Plio-Rec</i>      | <i>Plio-Rec</i>   |
| <i>M. brandaris</i>                  |   | * | * * | <i>Plio-Rec</i>      | <i>Plio-Rec</i>   |
| <i>Acamptochetus mitraeformis</i>    | * | * |     | <i>Plio</i>          | <i>Mio-Plio</i>   |
| <i>Euthria cornea</i>                |   | * | *   | <i>Plio-Rec</i>      | <i>Plio-Rec</i>   |
| <i>Columbella rustica</i>            |   |   | *   | <i>Tyrr-Rec</i>      | <i>Plio-Rec</i>   |
| <i>Nassa mutabilis</i>               |   |   | *   | <i>Plio-Rec</i>      | <i>Plio-Rec</i>   |
| <i>N. ferussaci</i>                  |   |   | *   | <i>Tyrr-Rec</i>      | <i>Plio-Rec</i>   |
| <i>N. louisii</i>                    |   |   | *   | <i>Tyrr-Rec</i>      | ?                 |
| <i>N. gibbosula</i>                  |   |   | *   | <i>Tyrr-Rec</i>      | <i>Plio-Rec</i>   |
| <i>N. semistriata var transitans</i> |   | * |     | <i>Plio</i>          | <i>Plio</i>       |
| <i>N. semistriata var gigantula</i>  |   |   | *   | <i>Plio-Rec</i>      | <i>Plio-Rec</i>   |
| <i>N. reticulata</i>                 |   | * |     | <i>Plio-Rec</i>      | <i>Plio-Rec</i>   |
| <i>N. prismatica</i>                 |   | * |     | <i>Calab</i>         | <i>Plio-Calab</i> |
| <i>Fusus syracusanus</i>             |   |   | *   | <i>Tyrr-Rec</i>      | <i>Plio-Rec</i>   |
| <i>F. longiroster</i>                | * | * |     | <i>Plio</i>          | <i>Plio-Calab</i> |
| <i>Cancellaria cancellata</i>        |   |   | *   | <i>Plio-Rec</i>      | <i>Plio-Rec</i>   |
| <i>Conus mediterraneus</i>           |   |   | *   | <i>Plio-Rec</i>      | <i>Plio-Rec</i>   |
| <i>C. testudinarius</i>              |   |   | *   | <i>Tyrr</i>          | <i>Tyrr</i>       |
| <i>C. pelagicus</i>                  |   | * |     | <i>Plio</i>          | <i>Plio</i>       |
| <i>Ringicula auriculata</i>          |   |   | *   | <i>Plio-Rec</i>      | <i>Plio-Rec</i>   |
| <i>R. ventricosa</i>                 |   |   | * * | <i>Plio-Tyrr</i>     | <i>Mio-Pleist</i> |

|                                  |   |     |                     |                   |
|----------------------------------|---|-----|---------------------|-------------------|
| <i>Scaphander lignarius</i>      | * |     | <i>Plio-Rec</i>     | <i>Mio-Rec</i>    |
| <b>Scaphopoda</b>                |   |     |                     |                   |
| <i>Dentalium inaequicostatum</i> |   | * * | <i>L.Pleist-Rec</i> | <i>Plio-Rec</i>   |
| <i>D. vulgare</i>                |   | *   | <i>Plio-Rec</i>     | <i>Plio-Rec</i>   |
| <i>D. rectum</i>                 |   | *   | <i>Mio-Sicil</i>    | <i>Mio-Sicil</i>  |
| <i>D. michelotti</i>             | * |     | <i>Plio</i>         | <i>Mio-Plio</i>   |
| <i>D. sexangulum</i>             | * |     | <i>Mio-Plio</i>     | <i>Mio-Plio</i>   |
| <i>D. novemcostatum</i>          | * |     | <i>Mio-Pleist</i>   | <i>Mio-Rec</i>    |
| <i>Fustiaria jani</i>            |   | *   | <i>Plio</i>         | <i>Mio-Pleist</i> |

a = Lower Pliocene, b = Upper Pliocene, c = Lower Pleistocene (Calabro-Sicilian), d = Middle Pleistocene (Tyrrhenian)

Oligo = Oligocene, Mio = Miocene, Plio = Pliocene, Pleist = Pleistocene, Calab = Calabrian, Sicil = Sicilian, Tyrr = Tyrrhenian, Rec = Recent



## **APPENDIX E: X-RAY FLUORESCENCE AND X-RAY DIFFRACTION DATA.**

The data presented in the following tables have been documented in Chapter 5. X-ray fluorescence and diffraction data comes from the Meniko and Astromeritis boreholes, situated on the north Troodos margin (Fig.5.27). Detailed clay mineralogy is shown in figures in Chapter 5. Reference plots of the mineral phases generated by the X-ray diffraction studies are presented on acetate to ease identification. The reference plots have peak height percentages plotted along the "Y" axis with the  $2\theta$  diffraction angle plotted along the "X" axis. The peak height plots of the borehole data are shown with counts on the "Y" axis versus  $2\theta$  diffraction angles on the "X" axis.

Table E1. Raw X-ray fluorescence data from samples collected within the Meniko borehole

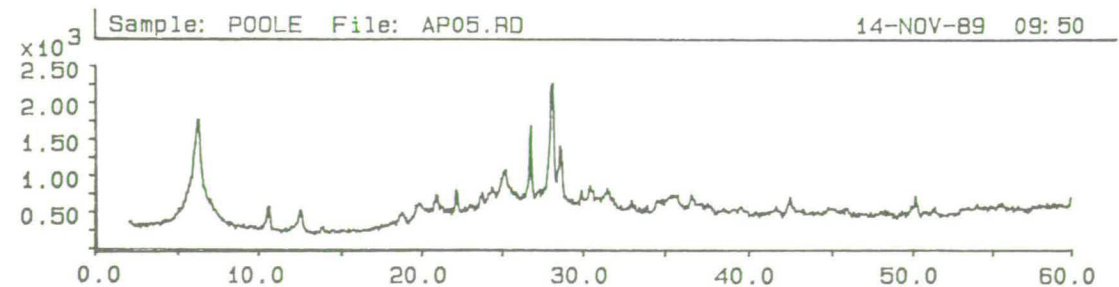
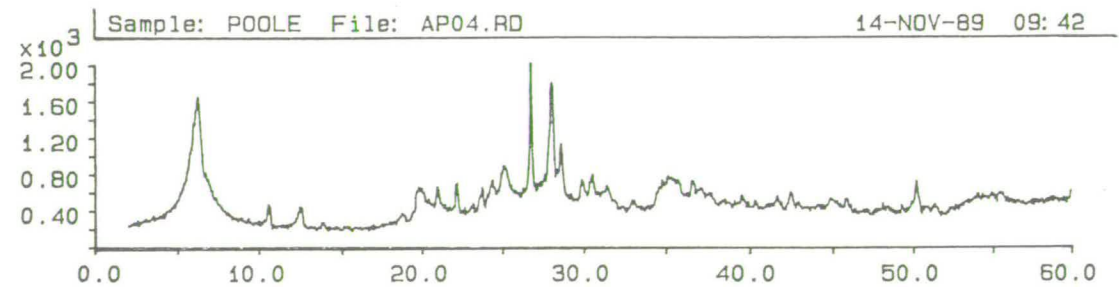
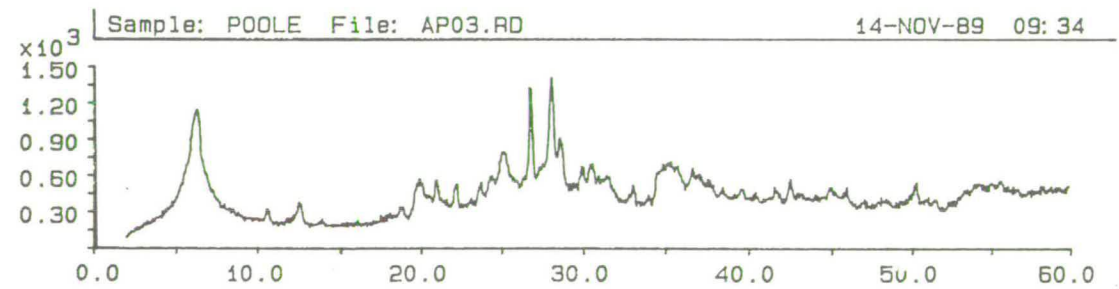
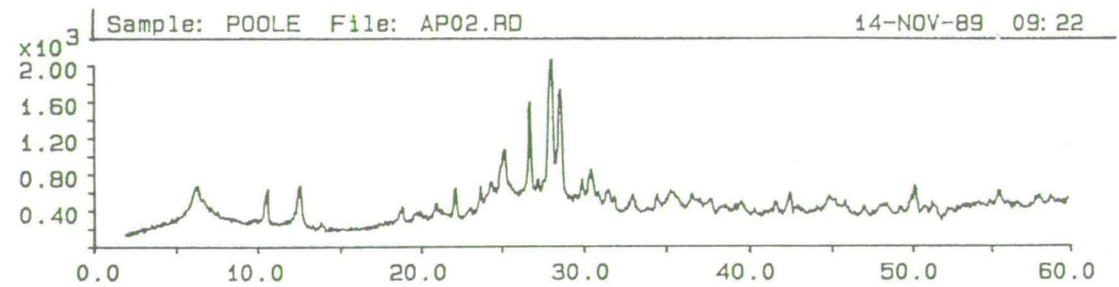
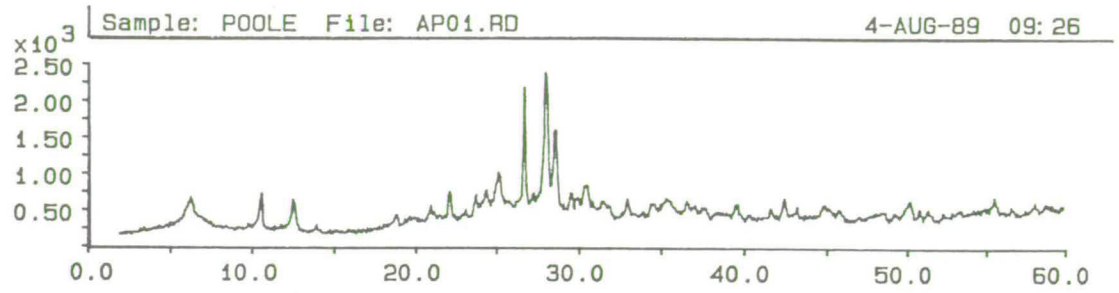
|       | MBH 1                          | MBH 2 | MBH 3  | MBH 4  | MBH 5  | MBH 6 | MBH 7  | MBH 8  | MBH 9  | MBH 10 | MBH 11 | MBH 12 | MBH 13 | MBH 14 | MBH 15 |       |
|-------|--------------------------------|-------|--------|--------|--------|-------|--------|--------|--------|--------|--------|--------|--------|--------|--------|-------|
| %     | SiO <sub>2</sub>               | 56.05 | 56.37  | 55.61  | 55.73  | 57.71 | 58.24  | 60.2   | 60.61  | 61.01  | 59.36  | 59.12  | 56.27  | 56.65  | 57.22  | 57.34 |
|       | Al <sub>2</sub> O <sub>3</sub> | 15.11 | 15.2   | 15.34  | 15.33  | 14.94 | 14.76  | 13.97  | 13.69  | 12.94  | 12.59  | 12.82  | 12.08  | 12.38  | 12.56  | 12.64 |
|       | Fe <sub>2</sub> O <sub>3</sub> | 10.36 | 10.79  | 11.37  | 11.25  | 10.82 | 11.34  | 10.13  | 10.23  | 8.95   | 8.52   | 8.78   | 9.59   | 9.76   | 9.6    | 8.85  |
|       | MgO                            | 3.46  | 4.34   | 4.56   | 4.4    | 3.77  | 3.55   | 3.01   | 3.46   | 3.36   | 3.46   | 3.07   | 3.56   | 3.5    | 3.27   | 5.17  |
|       | CaO                            | 3.46  | 5.76   | 5.61   | 5.5    | 3.75  | 4.16   | 5.23   | 4.83   | 5.2    | 6.04   | 7.19   | 8.61   | 8.13   | 8.19   | 6.16  |
|       | Na <sub>2</sub> O              | 2.13  | 3.71   | 3.57   | 3.49   | 1.99  | 2.44   | 2.7    | 2.71   | 2.98   | 2.89   | 2.96   | 2.72   | 2.74   | 2.55   | 3.04  |
|       | K <sub>2</sub> O               | 1.23  | 0.34   | 0.36   | 0.39   | 0.79  | 0.59   | 0.29   | 0.3    | 0.42   | 0.44   | 0.28   | 0.32   | 0.32   | 0.3    | 0.47  |
|       | TiO <sub>2</sub>               | 1.11  | 0.95   | 0.96   | 0.97   | 0.94  | 1.04   | 0.92   | 1.07   | 0.94   | 0.92   | 0.87   | 1.11   | 1.1    | 1.08   | 1.08  |
|       | MnO                            | 0.2   | 0.16   | 0.17   | 0.17   | 0.17  | 0.21   | 0.16   | 0.15   | 0.14   | 0.12   | 0.11   | 0.13   | 0.13   | 0.13   | 0.12  |
|       | P <sub>2</sub> O <sub>5</sub>  | 0.18  | 0.06   | 0.07   | 0.07   | 0.06  | 0.06   | 0.07   | 0.06   | 0.05   | 0.06   | 0.05   | 0.05   | 0.05   | 0.05   | 0.05  |
|       | LOI                            | 6.54  | 2.78   | 3.02   | 3.21   | 4.75  | 4.25   | 3.77   | 3.55   | 4.35   | 5.23   | 5.07   | 5.97   | 5.51   | 5.17   | 4.87  |
|       | Total                          | 99.83 | 100.46 | 100.64 | 100.51 | 99.69 | 100.63 | 100.43 | 100.65 | 100.32 | 99.63  | 100.32 | 100.42 | 100.25 | 100.12 | 99.79 |
|       | ppm                            | Ba    | 166.5  | 36.5   | 34.3   | 45.6  | 32.9   | 57.4   | 28.7   | 26.3   | 25.6   | 8.4    | 22.7   | 16.3   | 23.2   | 19    |
| La    |                                | 20.5  | 2.5    | 4.4    | 15.2   | 7.8   | 3      | 3      | 6.6    | 6.9    | 4.1    | 2      | 2.2    | 0.3    | 0.4    | 6.8   |
| Ce    |                                | 40.7  | 2.6    | 4.1    | 4.7    | 10.3  | 4.9    | 0.1    | -6.4   | -1.2   | 5.1    | -0.8   | -4.7   | 2.8    | -9.1   | 3.8   |
| Sc    |                                | 37.7  | 41.7   | 42     | 42.5   | 50.2  | 46.3   | 37.7   | 42.9   | 38     | 36.8   | 33.2   | 36.9   | 37.3   | 36.2   | 35.6  |
| V     |                                | 256.8 | 287.2  | 302.2  | 302.4  | 259.2 | 270    | 268.9  | 283.3  | 274.3  | 273.3  | 268.3  | 303.2  | 307.4  | 304.5  | 300.1 |
| Cr    |                                | 160.2 | 51.3   | 50.8   | 60.7   | 246.2 | 263.6  | 176.4  | 290.2  | 345    | 306.3  | 167.9  | 352.5  | 336.4  | 284    | 285.7 |
| Cu    |                                | 86.5  | 83.5   | 89.4   | 83.3   | 115.4 | 96.9   | 72.1   | 63.1   | 52.8   | 51.7   | 47.4   | 42.8   | 44     | 43.2   | 33.6  |
| Ni    |                                | 61.1  | 25.1   | 29.2   | 28.6   | 54.9  | 45.8   | 27.8   | 44     | 66.4   | 67.1   | 38.6   | 61.1   | 60.3   | 50.3   | 84.4  |
| Zn    |                                | 110.5 | 76.3   | 82.1   | 82     | 111.3 | 93.7   | 94     | 79.9   | 76.8   | 78.9   | 63.2   | 64.7   | 78.1   | 67.3   | 73.3  |
| Sr    |                                | 113.4 | 140    | 140.2  | 137.6  | 97.2  | 105    | 122.5  | 111.2  | 144.1  | 163.2  | 162.1  | 136.1  | 135    | 144.2  | 192.4 |
| Rb    |                                | 31.1  | 6.7    | 3.4    | 5.9    | 12.6  | 11.3   | 7      | 6.7    | 11.4   | 7.6    | 9      | 10.1   | 7.2    | 7.9    | 8.8   |
| Ba/Al |                                | 11.02 | 2.4    | 2.24   | 2.97   | 2.2   | 3.89   | 2.05   | 1.92   | 1.98   | 0.67   | 1.77   | 1.35   | 1.87   | 1.51   | 0.6   |
| La/Al |                                | 1.36  | 0.16   | 0.29   | 0.99   | 0.52  | 0.2    | 0.21   | 0.48   | 0.53   | 0.33   | 0.16   | 0.18   | 0.02   | 0.03   | 0.54  |
| Ce/Al |                                | 2.69  | 0.17   | 0.27   | 0.31   | 0.69  | 0.33   | 0.01   | -0.47  | -0.09  | 0.41   | -0.06  | -0.39  | 0.23   | -0.72  | 0.3   |
| Sc/Al |                                | 2.5   | 2.74   | 2.74   | 2.77   | 3.36  | 3.14   | 2.7    | 3.13   | 2.94   | 2.92   | 2.59   | 3.05   | 3.01   | 2.88   | 2.82  |
| V/Al  |                                | 17    | 18.89  | 19.7   | 19.73  | 17.35 | 18.29  | 19.25  | 20.69  | 21.2   | 21.71  | 20.93  | 25.1   | 24.83  | 24.24  | 23.74 |
| Cr/Al |                                | 10.6  | 3.38   | 3.31   | 3.96   | 16.48 | 17.86  | 12.63  | 21.2   | 26.66  | 24.33  | 13.1   | 29.18  | 27.17  | 22.61  | 22.6  |
| Cu/Al | 5.72                           | 5.49  | 5.83   | 5.43   | 7.72   | 6.57  | 5.16   | 4.61   | 4.08   | 4.11   | 3.7    | 3.54   | 3.55   | 3.44   | 2.66   |       |
| Ni/Al | 4.04                           | 1.65  | 1.9    | 1.87   | 3.67   | 3.1   | 1.99   | 3.21   | 5.13   | 5.33   | 3.01   | 5.06   | 4.87   | 4      | 6.68   |       |
| Zn/Al | 7.31                           | 5.02  | 5.35   | 5.35   | 7.45   | 6.35  | 6.73   | 5.84   | 5.94   | 6.27   | 4.93   | 5.36   | 6.31   | 5.36   | 5.8    |       |
| Sr/Al | 7.5                            | 9.21  | 9.14   | 8.98   | 6.51   | 7.11  | 8.77   | 8.12   | 11.14  | 12.96  | 12.64  | 11.27  | 10.9   | 11.48  | 15.22  |       |
| Rb/Al | 2.06                           | 0.44  | 0.22   | 0.38   | 0.84   | 0.77  | 0.5    | 0.49   | 0.88   | 0.6    | 0.7    | 0.84   | 0.58   | 0.63   | 0.7    |       |

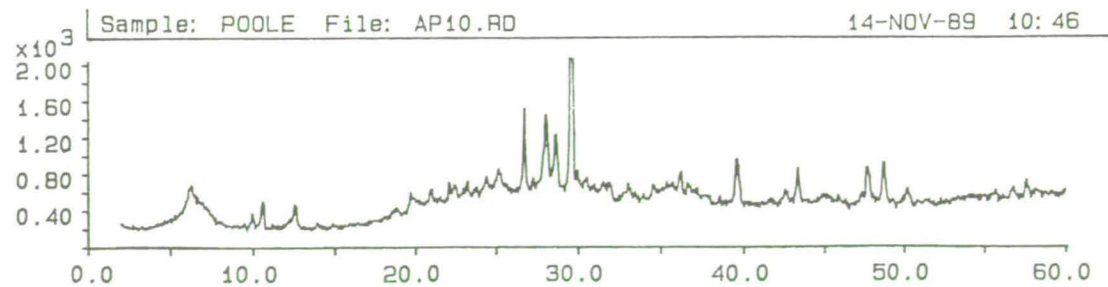
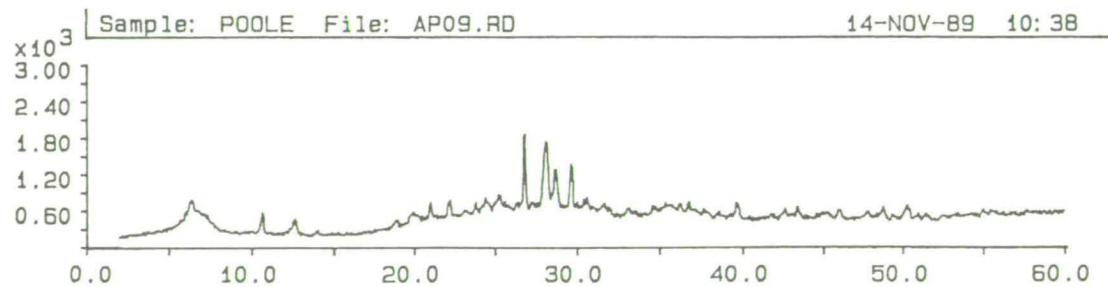
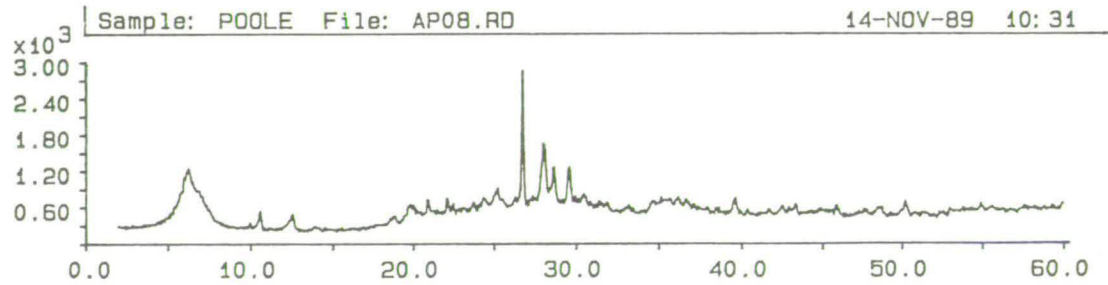
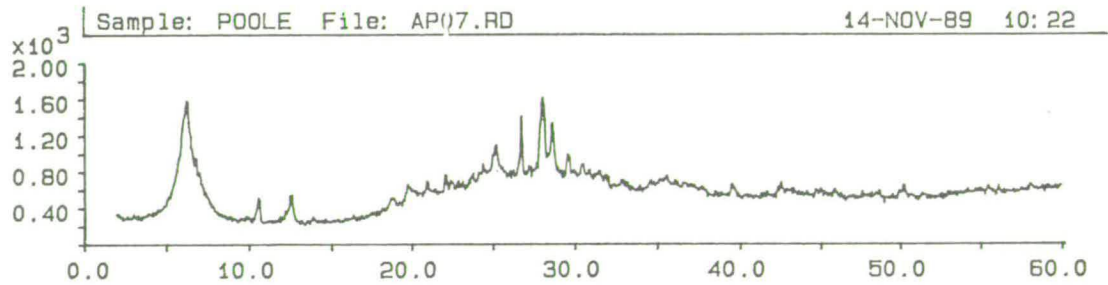
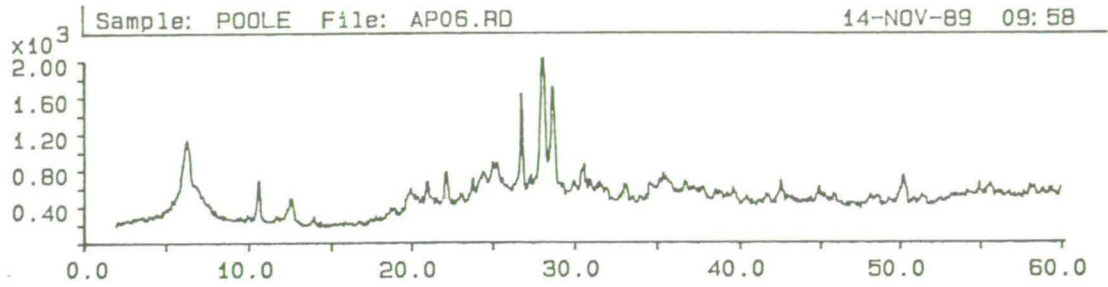
Table E2. Raw X-ray fluorescence data from samples collected within the Astromeritis borehole

|         | ABH 1 | ABH 2 | ABH 3  | ABH 4  | ABH 5  | ABH 6  | ABH 7  | ABH 8  | ABH 9  | ABH 10 | ABH 11 | ABH 12 | ABH 13 | ABH 14 | ABH 15 |
|---------|-------|-------|--------|--------|--------|--------|--------|--------|--------|--------|--------|--------|--------|--------|--------|
| SiO2    | 52.2  | 53.03 | 53.38  | 56.43  | 55.6   | 58.5   | 58.79  | 58.89  | 58.9   | 55.79  | 57.8   | 58.69  | 59.16  | 59.08  | 59.24  |
| Al2O3   | 18.07 | 14.35 | 14.74  | 15     | 15.52  | 13.64  | 14.32  | 13.94  | 14.36  | 15.02  | 14.61  | 13.71  | 13.95  | 13.11  | 13.14  |
| Fe2O3   | 12.6  | 10.48 | 10.84  | 11.47  | 11.61  | 10.23  | 10.68  | 9.98   | 11.18  | 11.58  | 11.11  | 10.21  | 11.09  | 10.7   | 10.95  |
| MgO     | 3.21  | 4.38  | 4.22   | 4.12   | 4.32   | 4.05   | 3.9    | 4.31   | 3.7    | 4.6    | 4.39   | 3.96   | 3.97   | 3.53   | 4.16   |
| CaO     | 2.7   | 6.94  | 6.06   | 5.13   | 3.39   | 5.68   | 4.05   | 4.59   | 3.34   | 3.81   | 4.17   | 5.18   | 3.81   | 5.06   | 4.31   |
| -Na2O   | 2     | 3.19  | 2.99   | 3.65   | 3.31   | 2.73   | 2.67   | 3.05   | 2.89   | 3.46   | 3.44   | 3.03   | 3.04   | 3.05   | 2.84   |
| K2O     | 0.95  | 0.35  | 0.4    | 0.26   | 0.32   | 0.27   | 0.37   | 0.35   | 0.43   | 0.31   | 0.26   | 0.22   | 0.34   | 0.3    | 0.36   |
| TiO2    | 1.09  | 1.02  | 1.06   | 1.11   | 1.13   | 0.87   | 0.99   | 0.96   | 1.23   | 1.09   | 1.03   | 0.96   | 1.24   | 1.25   | 1.31   |
| MnO     | 0.13  | 0.16  | 0.17   | 0.16   | 0.15   | 0.17   | 0.11   | 0.14   | 0.15   | 0.23   | 0.16   | 0.14   | 0.14   | 0.14   | 0.16   |
| P2O5    | 0.07  | 0.05  | 0.05   | 0.06   | 0.06   | 0.06   | 0.05   | 0.05   | 0.05   | 0.09   | 0.08   | 0.07   | 0.05   | 0.06   | 0.06   |
| LOI     | 7.29  | 6.05  | 6.37   | 3.25   | 5.01   | 3.99   | 4.35   | 3.92   | 4.05   | 3.95   | 3.4    | 4.56   | 3.51   | 4.13   | 3.45   |
| Total   | 100.3 | 99.99 | 100.27 | 100.64 | 100.41 | 100.19 | 100.29 | 100.17 | 100.35 | 99.93  | 100.44 | 100.72 | 100.29 | 100.42 | 99.98  |
| Ba      | 88.4  | 29.7  | 38.6   | 31     | 12.9   | 42.3   | 23.6   | 22.9   | 21.8   | 33.5   | 22.6   | 20     | 19.6   | 18.3   | 8.8    |
| La      | 22.3  | 5.2   | 10.6   | 6      | 6.6    | -1.1   | 7.6    | 7.5    | 1.7    | 6.5    | -3.1   | 4.6    | 3.2    | 9.6    | 3.4    |
| Ce      | 28    | 2.3   | 6.9    | -7.7   | 4.3    | -3.7   | 4.3    | 9.5    | 0.6    | 1.3    | 6.5    | 4      | -2.2   | 12.8   | 3.6    |
| Sc      | 49.8  | 39.7  | 42.9   | 43.4   | 48.7   | 42.8   | 44.3   | 45.3   | 44.8   | 48.6   | 42.9   | 38.2   | 41.9   | 39.6   | 45.8   |
| V       | 289.4 | 269.9 | 274.1  | 306.2  | 379.8  | 275.3  | 404.5  | 278.4  | 292.1  | 288    | 286.6  | 248.9  | 309.6  | 292.6  | 327.9  |
| Cr      | 114.9 | 49.6  | 59.4   | 46.3   | 67.4   | 650.6  | 408.4  | 334.7  | 243.2  | 69.2   | 91     | 191.5  | 158.7  | 120.2  | 152    |
| Cu      | 80.2  | 77.6  | 86.7   | 57.1   | 101.1  | 69.5   | 59.7   | 55.8   | 59.7   | 89.5   | 70.8   | 59.3   | 76.4   | 62.7   | 64.8   |
| Ni      | 50.3  | 26    | 30     | 22.5   | 33.3   | 206.6  | 107.2  | 113.6  | 70.8   | 36.2   | 40.1   | 59.7   | 43.4   | 41.6   | 59.6   |
| Zn      | 87.3  | 85.2  | 91.2   | 73.3   | 97.6   | 69.4   | 71.9   | 82.9   | 87.4   | 86.7   | 73.4   | 59.7   | 85.3   | 67.7   | 68     |
| Sr      | 99.3  | 133.4 | 121.5  | 119.9  | 106.6  | 112.1  | 97.8   | 107.7  | 96.5   | 104.7  | 125    | 115.6  | 123.4  | 121.3  | 131.4  |
| Rb      | 29.1  | 7.8   | 9.5    | 4      | 2.8    | 4.8    | 8.7    | 8.1    | 9      | 3.2    | 3.2    | 5.8    | 7.3    | 5.7    | 6      |
| Ba / Al | 4.89  | 2.07  | 2.62   | 2.07   | 0.83   | 3.1    | 1.65   | 1.64   | 1.52   | 2.23   | 1.55   | 1.46   | 1.41   | 1.4    | 0.67   |
| La / Al | 1.23  | 0.36  | 0.72   | 0.4    | 0.43   | -0.08  | 0.53   | 0.54   | 0.12   | 0.43   | -0.21  | 0.34   | 0.23   | 0.73   | 0.26   |
| Ce / Al | 1.55  | 0.16  | 0.47   | -0.51  | 0.28   | -0.27  | 0.3    | 0.68   | 0.04   | 0.09   | 0.44   | 0.29   | -0.16  | 0.98   | 0.27   |
| Sc / Al | 2.76  | 2.77  | 2.91   | 2.89   | 3.14   | 3.14   | 3.09   | 3.25   | 3.12   | 3.24   | 2.94   | 2.79   | 3      | 3.02   | 3.49   |
| V / Al  | 16.02 | 18.81 | 18.6   | 20.41  | 24.47  | 20.18  | 28.25  | 19.97  | 20.34  | 19.17  | 19.62  | 18.15  | 22.19  | 22.32  | 24.95  |
| Cr / Al | 6.36  | 3.46  | 4.03   | 3.09   | 4.34   | 47.7   | 28.52  | 24.01  | 16.94  | 4.61   | 6.23   | 13.97  | 11.38  | 9.17   | 11.57  |
| Cu / Al | 4.44  | 5.41  | 5.88   | 3.81   | 6.51   | 5.1    | 4.17   | 4      | 4.16   | 5.96   | 4.85   | 4.33   | 5.48   | 4.78   | 4.93   |
| Ni / Al | 2.78  | 1.81  | 2.04   | 1.5    | 2.15   | 15.15  | 7.49   | 8.15   | 4.93   | 2.41   | 2.74   | 4.35   | 3.11   | 3.17   | 4.54   |
| Zn / Al | 4.83  | 5.94  | 6.19   | 4.89   | 6.29   | 5.09   | 5.02   | 5.95   | 6.09   | 5.77   | 5.02   | 4.35   | 6.11   | 5.16   | 5.18   |
| Sr / Al | 5.5   | 9.3   | 8.24   | 7.99   | 6.87   | 8.22   | 6.83   | 7.73   | 6.72   | 6.97   | 8.56   | 8.43   | 8.85   | 9.25   | 10     |
| Rb / Al | 1.61  | 0.54  | 0.64   | 0.27   | 0.18   | 0.35   | 0.61   | 0.58   | 0.63   | 0.21   | 0.22   | 0.42   | 0.52   | 0.43   | 0.46   |

Table E3. X-ray diffraction peak plots from the Meniko borehole.

Note: Meniko borehole samples are numbered AP12.





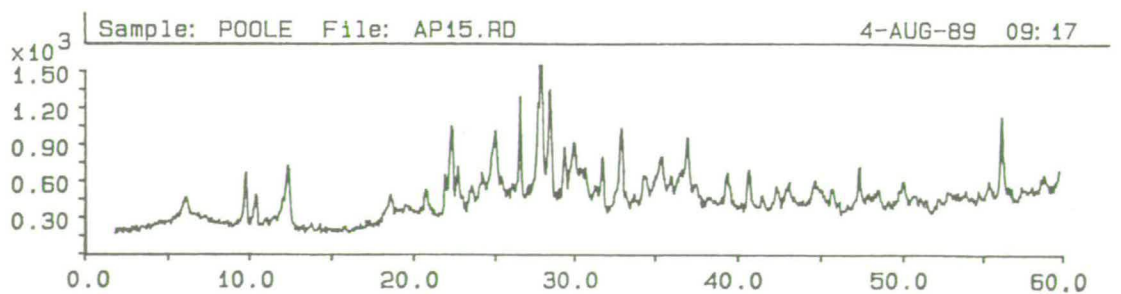
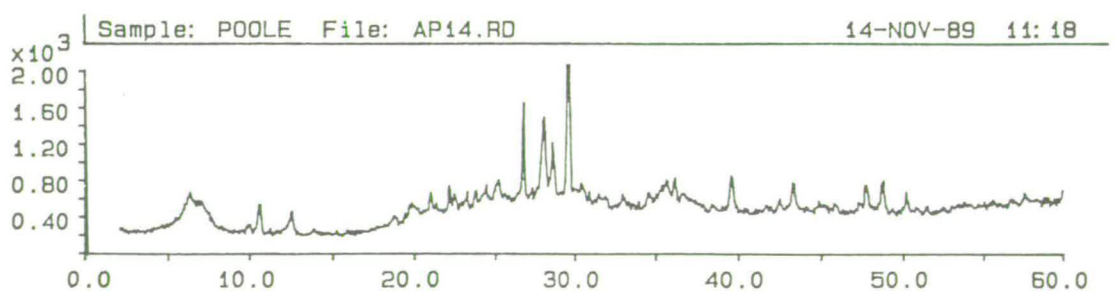
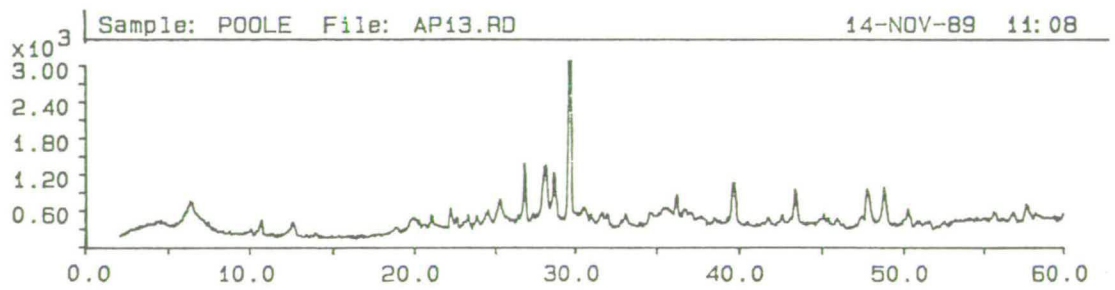
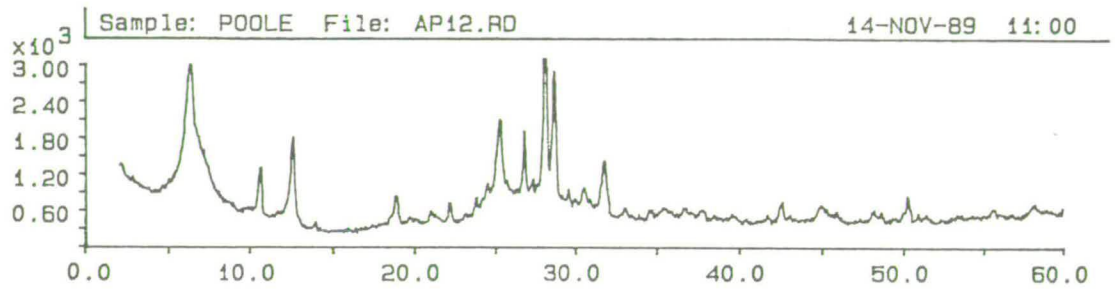
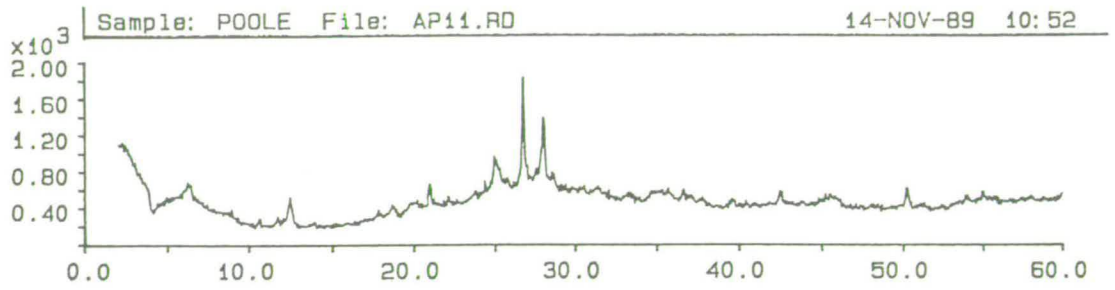
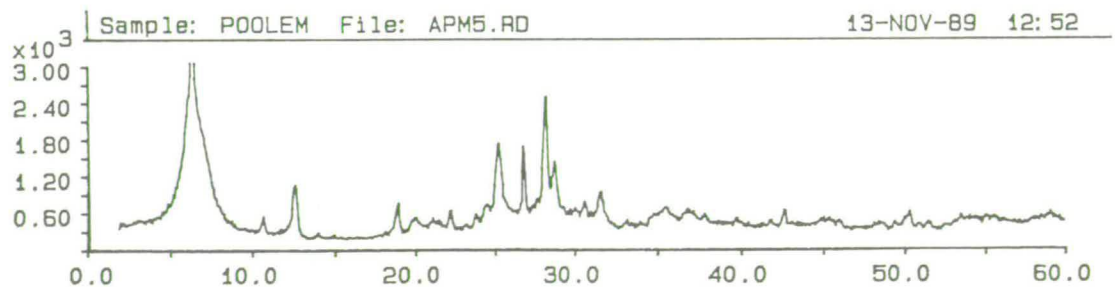
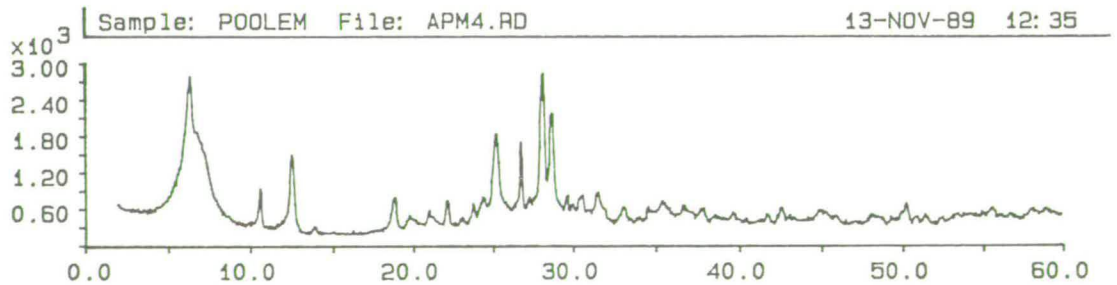
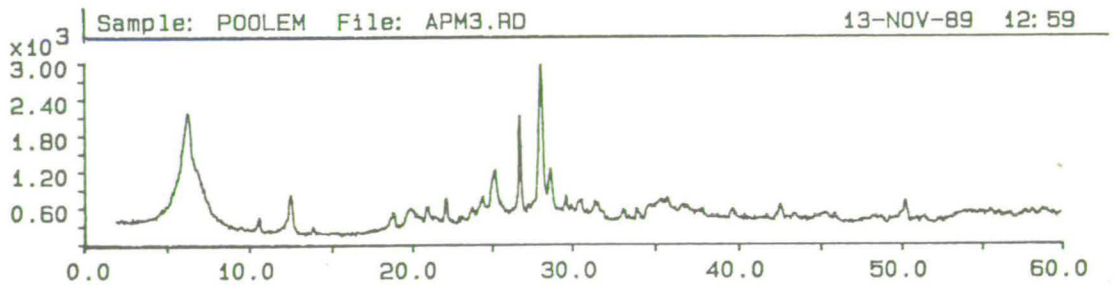
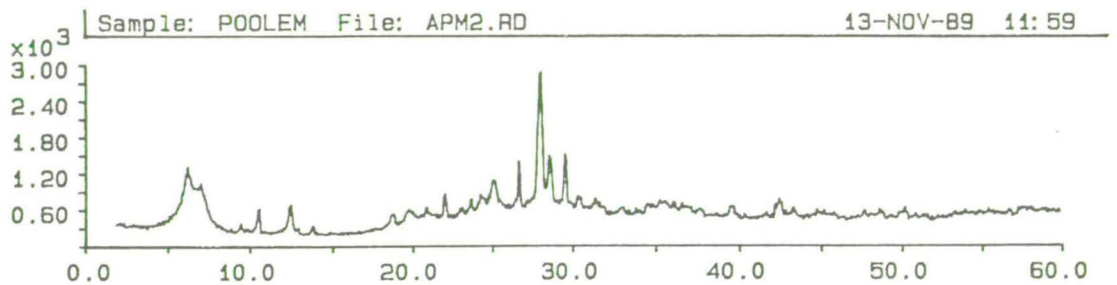
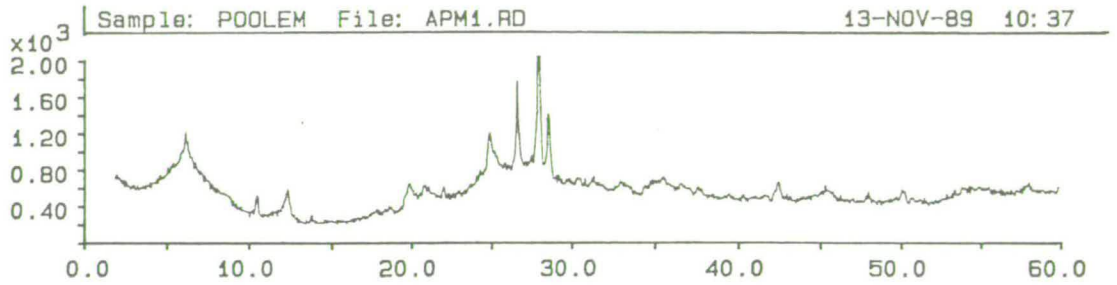
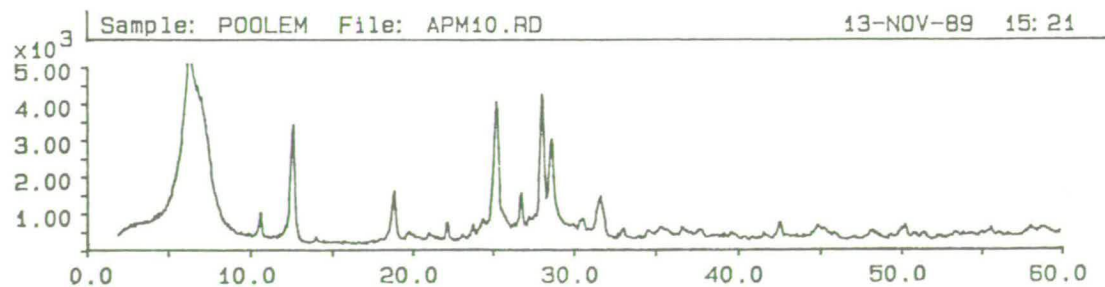
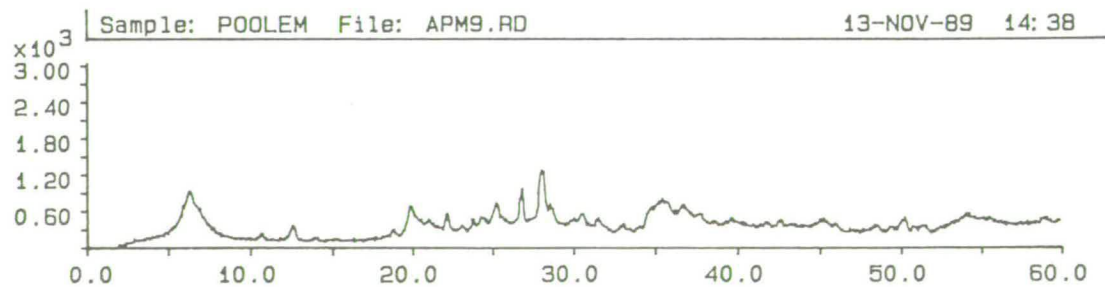
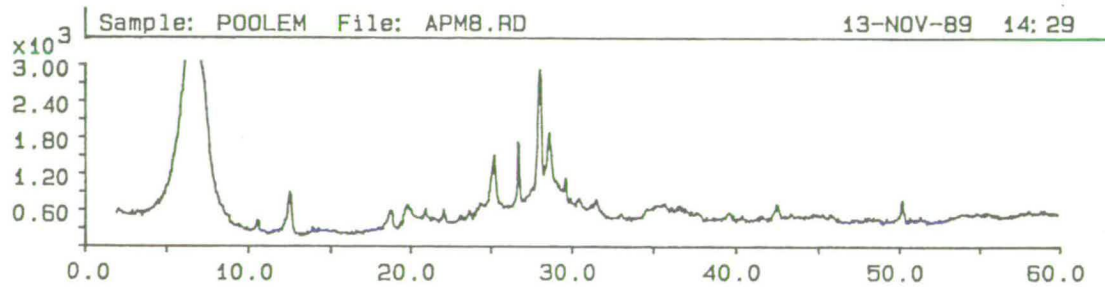
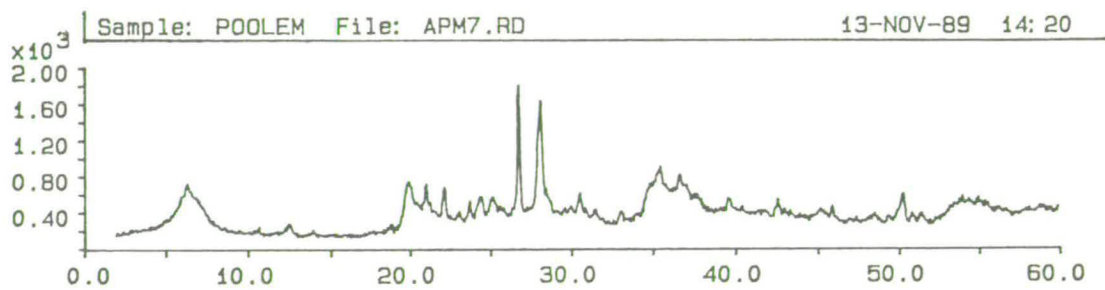
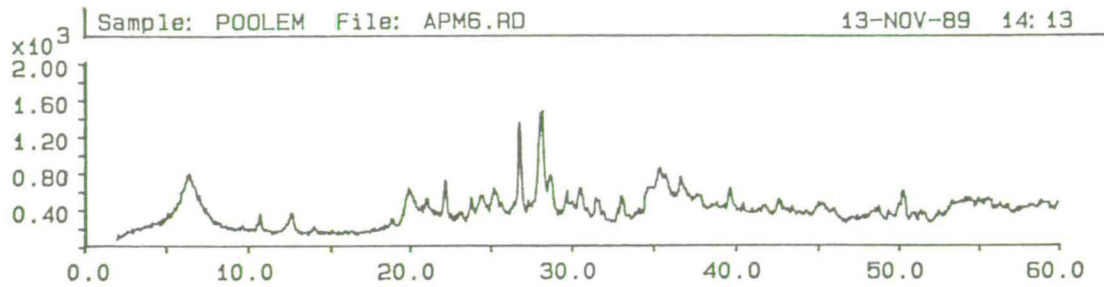


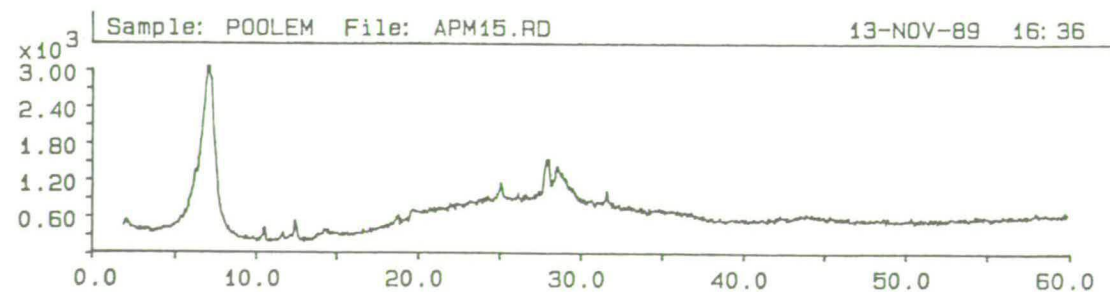
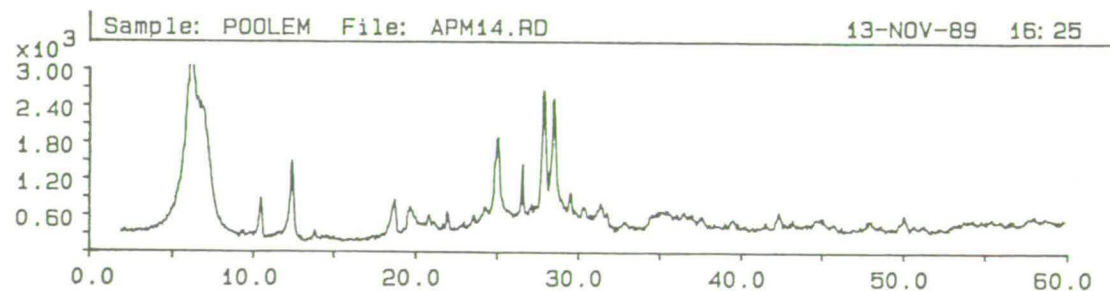
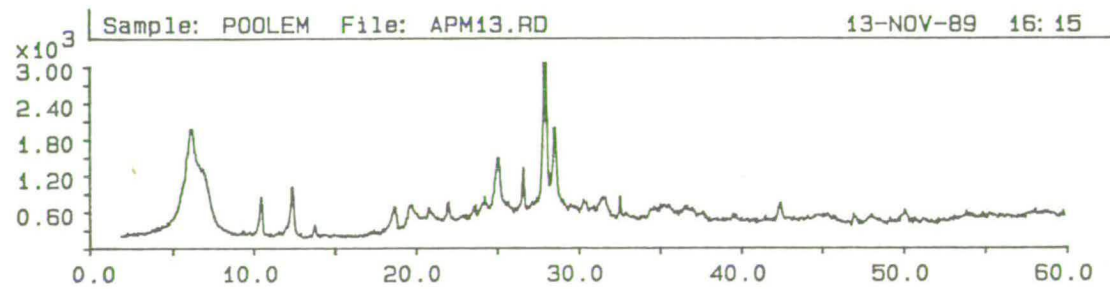
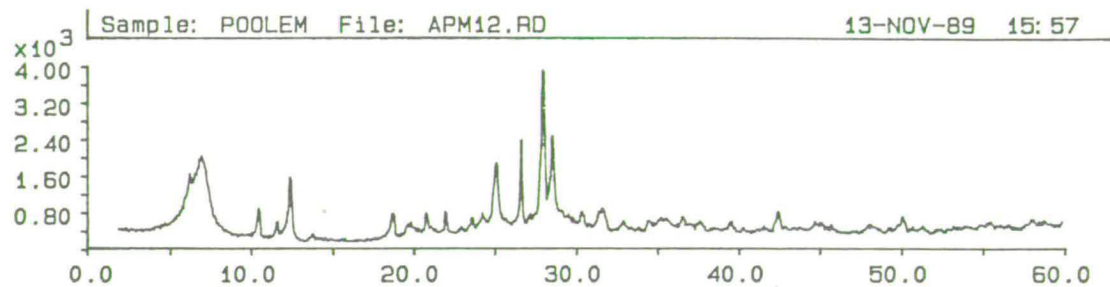
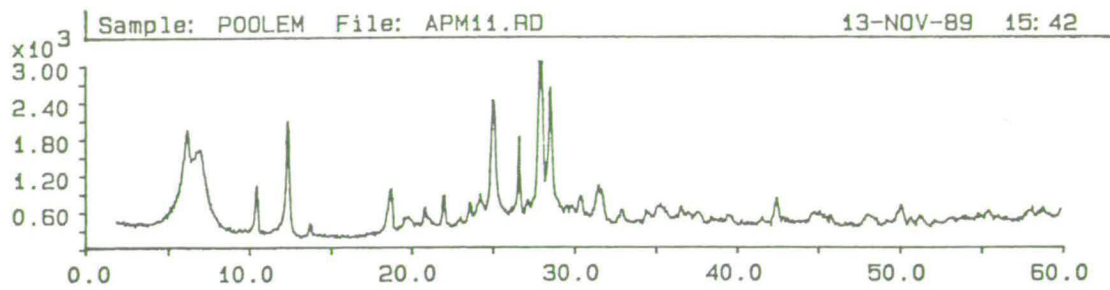
Table E4. X-ray diffraction peak plots from the Astromeritis borehole.

Note: Astromeritis borehole samples are numbered APM12









## **APPENDIX F: PUBLISHED PAPERS.**

Published papers by the author based on this study are:

i) Poole, A.J., Shimmiel, G.B. & Robertson, A.H.F., 1990. Late Quaternary uplift of the Troodos ophiolite, Cyprus: Uranium-series dating of Pleistocene coral. *Geology*, v.18, p.894-897.

ii) Poole, A.J. & Robertson, A.H.F., 1991. Quaternary uplift and sea-level change at an active plate boundary, Cyprus. *Journal of the Geological Society of London*, v.148, p.909-921.

These papers form this appendix.

# Late Quaternary uplift of the Troodos ophiolite, Cyprus: Uranium-series dating of Pleistocene coral

Andrew J. Poole, Graham B. Shimmield, Alastair H.F. Robertson

Department of Geology and Geophysics, University of Edinburgh, West Mains Road, Edinburgh EH9 3JW, Scotland

## ABSTRACT

In an attempt to constrain the timing and mode of tectonic uplift of the classic Troodos ophiolite, colonial corals were collected from Quaternary littoral raised terraces in coastal southern Cyprus and dated using the uranium-series disequilibrium method. A total of 28 samples of *Cladocora caespitosa* were collected at five localities from the 8–11-m-high and <3-m-high marine terraces. The corals yield systematic ages of 185–192 ka ( $ka = 10^3$  yr) and 116–130 ka for the 8–11 m and <3 m terraces, respectively. When correlated with the global oxygen isotope stages, the results suggest that southern Cyprus was uplifted by 18 m during the past 185–192 ka, as a single tectonic entity. Of this uplift, 13 m took place between 130 and 185 ka (at ~24 cm/ka), and a maximum of 6 m of uplift (at 5 cm/ka) took place over the past 116 ka, but with some evidence of coastal subsidence in more recent time. An exception, the extreme southeast of Cyprus (Cape Greco), was perhaps uplifted faster during the past 141 ka, at a rate of 12 cm/ka.

## GEOLOGIC SETTING

The Troodos ophiolite is one of only several examples of oceanic lithosphere in the process of being emplaced onto continental crust (Gass and Masson-Smith, 1963). Available offshore geophysical data indicate that Cyprus is astride an active plate boundary, along which the African plate is being subducted northward beneath the Anatolian microplate (Fig. 1; McKenzie, 1970; Lort, 1971; Kempler and Ben-Avraham, 1987).

Onland geologic evidence indicates that the pulsed uplift of southern Cyprus began in mid-Tertiary time, and then accelerated in the late Pliocene–Quaternary (Robertson, 1977; McCallum and Robertson, 1990).

## STRATIGRAPHY

The corals we dated are from Quaternary raised marine terraces located around the margins of the Troodos ophiolite in southern Cyprus

(Fig. 2). The terraces are present in all areas between 1 and 610 m above present-day sea level (Turner, 1971). During our work we recognized and correlated four distinct marine terraces throughout southern Cyprus (Poole and Robertson, unpublished). Fauna suitable for uranium-series method dating are absent from a 350-m-high Pliocene(?) terrace (W. M. Turner, unpublished; Ducloux, 1965; Dregghorn, 1978) and the highest Quaternary terraces (at ~60 and

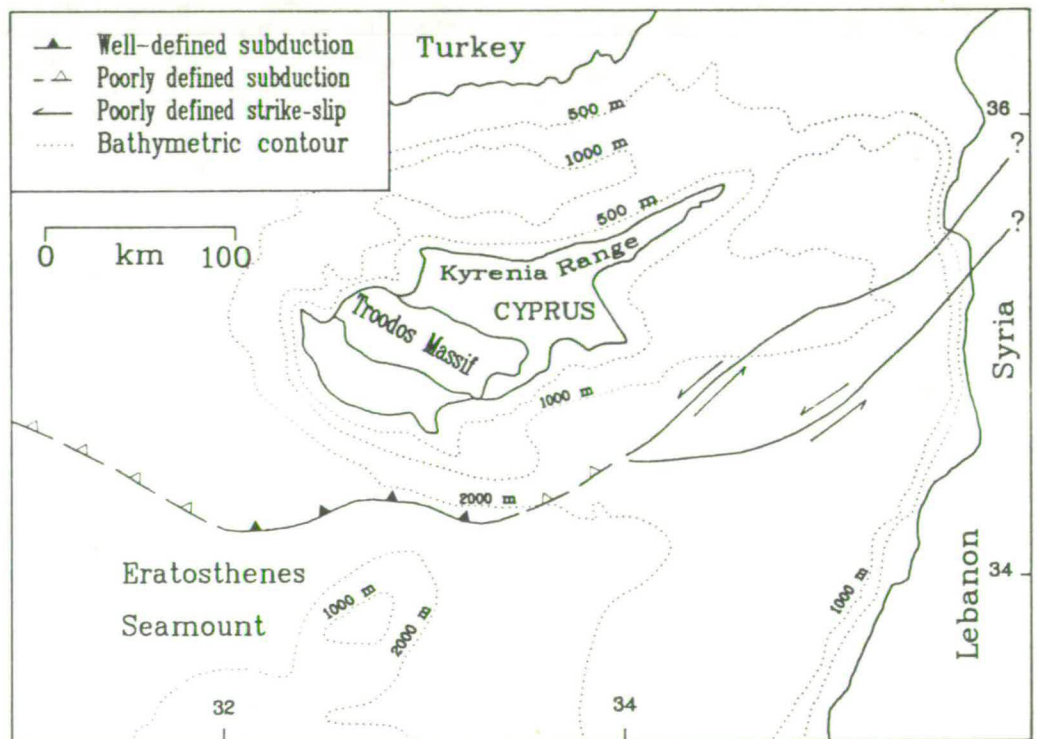


Figure 1. Tectonic setting of Cyprus in northeastern Mediterranean, showing relative motions along Cyprus arc (after McCallum, 1989).

100 m) and are thus not considered further here. However, the cosmopolitan, hematitic Mediterranean scleractinian coral *Cladocora caespitosa* is abundant in the two lower marine terrace levels, located within 8–11 m and <3 m of the present-day sea level. The corals typically form

colonies 1–2 m in diameter and are associated with a diverse mollusk fauna (Moshkovitz, 1968) and a littoral carbonate grainstone facies. The marine coral-bearing terrace sediments display gradational regressive littoral successions (see Fig. 2) and are overlain conformably by

eolianite and karst, as reported elsewhere in the Mediterranean (Butzer, 1975). Sedimentological evidence and the presence of paleo-cliff lines, wave-cut notches, and paleo-shorelines suggest that the *Cladocora caespitosa* colonies grew in shallow water, at depths not exceeding 10 m (Poole and Robertson, unpublished). The majority of the corals sampled were in life position.

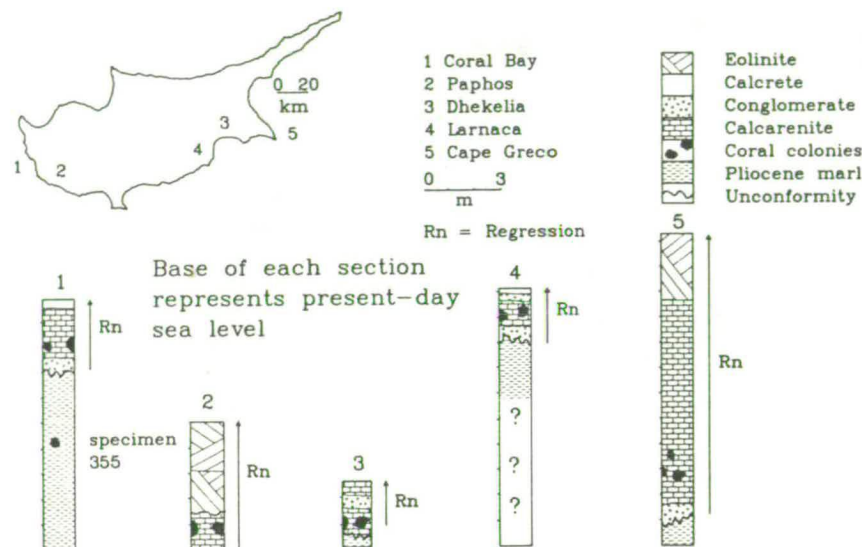


Figure 2. Schematic sedimentary sections and location of sampling sites.

## SAMPLING AND ANALYTICAL TECHNIQUES

*Cladocora caespitosa* coral was collected from the 8–11 m terraces at three localities (Cape Greco, Larnaca, and Coral Bay; Fig. 2) and from the <3 m terrace at two localities (Paphos and Dhekelia; Fig. 2). Samples of unaltered aragonitic coral without signs of calcite replacement (Husseini and Matthews, 1972) were selected for isotopic analysis with optical microscopic examination and X-ray diffraction. Uranium and thorium isotopes were analyzed by alpha spectrometry using silicon surface barrier detectors, following the method of Veeh (1966). Complete dissolution of 4.5–6.0 g of sample, followed by standard ion-exchange separation and electrolysis, prepared the separate U and Th sources. A mixed spike of  $^{232}\text{Th}$  and  $^{228}\text{Th}$  was used to determine the isotopic activities of the  $^{232}\text{Th}$ ,  $^{230}\text{Th}$ ,  $^{238}\text{U}$ , and  $^{234}\text{U}$  isotopes. The samples were counted for two to three days to obtain the requisite counting statistics. Exclusive U and Th isotope detectors were used to minimize the alpha-recoil contamination. Background counts with use of identical conditions were routinely determined prior to the counting of each sample. Two modern samples of *Porites porites*, a Barbados coral (P1, P2), were analyzed as a control (Table 1). The errors quoted here (Table 1) are calculated as one standard deviation (1  $\sigma$ ) of the counting statistics.

## RESULTS OF ANALYSIS

As shown in Table 1, the  $^{232}\text{Th}$  activity is consistently very low (less than 0.004 dpm/g). This indicates that little detrital clay is present as a contaminant and that little or no thorium was introduced after death of the coral. In addition, the initial  $^{230}\text{Th}$  of the control samples (P1, P2) is also extremely low and is therefore consistent with a recent age of formation, ruling out possible analytical contamination during analysis.

The  $^{234}\text{U}/^{238}\text{U}$  ratio of the Barbados samples (1.15  $\pm$  0.03) and younger Cyprus corals corresponds to the expected initial ratio of modern seawater (Bender et al., 1979; Chen et al., 1986; Edwards et al., 1986–1987) following decay correction. Contrasting results were, however, obtained from the older samples collected from Larnaca and Coral Bay (Table 1), which exhibited initial activity ratios greater than 1.14, following decay correction (solid line in Fig. 3).

Some other results also appear to be anomalous.

TABLE 1. U AND Th ISOTOPIC COMPOSITIONS, MINERALOGICAL AND AGE DATA FOR LATE QUATERNARY CYPRUS CORALS

| Sample | Locality   | Terrace height (m) | $^{234}\text{U}/^{238}\text{U}$ | $^{230}\text{Th}/^{232}\text{Th}$ | $^{230}\text{Th}/^{234}\text{U}$ | $^{232}\text{Th}$ (dpm/g) | U (ppm) | Arag. (%) | Age (ka)     |
|--------|------------|--------------------|---------------------------------|-----------------------------------|----------------------------------|---------------------------|---------|-----------|--------------|
| 021    | Larnaca    | 8-11               | 1.10 $\pm$ 0.02                 | 68.67 $\pm$ 8.15                  | 0.84 $\pm$ 0.01                  | 0.03                      | 2.99    | 90        | 183 $\pm$ 2  |
| 617a   | Larnaca    | 8-11               | 1.16 $\pm$ 0.01                 | 63.33 $\pm$ 4.38                  | 1.01 $\pm$ 0.01                  | 0.03                      | 2.19    | 99        | > 300        |
| 617b   | Larnaca    | 8-11               | 1.13 $\pm$ 0.02                 | 85.50 $\pm$ 7.33                  | 1.03 $\pm$ 0.01                  | 0.02                      | 1.97    | 99        | > 300        |
| 617c   | Larnaca    | 8-11               | 1.13 $\pm$ 0.02                 | 41.75 $\pm$ 2.51                  | 0.88 $\pm$ 0.01                  | 0.04                      | 2.25    | 97        | 209 $\pm$ 7  |
| 617d   | Larnaca    | 8-11               | 1.06 $\pm$ 0.02                 | 84.00 $\pm$ 6.18                  | 1.11 $\pm$ 0.02                  | 0.02                      | 1.90    | 98        | > 300        |
| 617e   | Larnaca    | 8-11               | 1.14 $\pm$ 0.02                 | 43.00 $\pm$ 4.85                  | 0.86 $\pm$ 0.02                  | 0.03                      | 1.76    | 98        | 197 $\pm$ 16 |
| 617f   | Larnaca    | 8-11               | 1.07 $\pm$ 0.02                 | 154.0 $\pm$ 19.79                 | 0.97 $\pm$ 0.01                  | 0.01                      | 1.98    | 98        | > 300        |
| 617g   | Larnaca    | 8-11               | 1.09 $\pm$ 0.01                 | 41.67 $\pm$ 3.49                  | 0.77 $\pm$ 0.01                  | 0.03                      | 2.00    | 85        | *            |
| 617ed  | Larnaca    | 8-11               | 1.07 $\pm$ 0.03                 | 39.33 $\pm$ 2.86                  | 0.84 $\pm$ 0.02                  | 0.03                      | 1.76    | 92        | 183 $\pm$ 12 |
| 358a   | Coral Bay  | 8-11               | 1.11 $\pm$ 0.02                 | 163.0 $\pm$ 41.98                 | 0.82 $\pm$ 0.02                  | 0.01                      | 2.39    | 91        | 176 $\pm$ 10 |
| 358b   | Coral Bay  | 8-11               | 1.11 $\pm$ 0.02                 | 146.0 $\pm$ 32.38                 | 0.86 $\pm$ 0.02                  | 0.01                      | 2.05    | 94        | 196 $\pm$ 12 |
| 358c   | Coral Bay  | 8-11               | 1.11 $\pm$ 0.03                 | 176.0 $\pm$ 41.97                 | 0.90 $\pm$ 0.02                  | 0.01                      | 2.34    | 93        | 226 $\pm$ 17 |
| 358d   | Coral Bay  | 8-11               | 1.08 $\pm$ 0.02                 | 111.0 $\pm$ 22.66                 | 0.72 $\pm$ 0.01                  | 0.01                      | 1.92    | 70        | *            |
| 358e   | Coral Bay  | 8-11               | 1.03 $\pm$ 0.03                 | N.a.                              | 0.86 $\pm$ 0.02                  | 0.00                      | 2.11    | 92        | 196 $\pm$ 12 |
| 200a   | Cape Greco | 8-11               | 1.11 $\pm$ 0.02                 | 41.67 $\pm$ 3.25                  | 0.91 $\pm$ 0.02                  | 0.03                      | 1.67    | 91        | 229 $\pm$ 16 |
| 527a   | Cape Greco | 8-11               | 1.14 $\pm$ 0.02                 | 39.33 $\pm$ 3.46                  | 0.74 $\pm$ 0.01                  | 0.03                      | 1.87    | 91        | 141 $\pm$ 4  |
| 527b   | Cape Greco | 8-11               | 1.00 $\pm$ 0.02                 | 32.25 $\pm$ 2.89                  | 1.09 $\pm$ 0.02                  | 0.04                      | 1.58    | 81        | *            |
| 529    | Cape Greco | 8-11               | 1.11 $\pm$ 0.03                 | 61.00 $\pm$ 5.18                  | 0.88 $\pm$ 0.02                  | 0.02                      | 1.67    | 95        | 209 $\pm$ 16 |
| 336a   | Paphos     | < 3                | 1.09 $\pm$ 0.02                 | 66.50 $\pm$ 8.30                  | 0.66 $\pm$ 0.01                  | 0.02                      | 2.49    | 96        | 113 $\pm$ 3  |
| 336b   | Paphos     | < 3                | 1.09 $\pm$ 0.03                 | 126.0 $\pm$ 20.23                 | 0.66 $\pm$ 0.02                  | 0.01                      | 2.36    | 100       | 112 $\pm$ 6  |
| 336c   | Paphos     | < 3                | 1.17 $\pm$ 0.03                 | 57.50 $\pm$ 8.01                  | 0.64 $\pm$ 0.02                  | 0.02                      | 2.06    | 96        | 108 $\pm$ 6  |
| 336d   | Paphos     | < 3                | 1.08 $\pm$ 0.02                 | 72.00 $\pm$ 10.17                 | 0.67 $\pm$ 0.01                  | 0.02                      | 2.65    | 98        | 117 $\pm$ 4  |
| 336e   | Paphos     | < 3                | 1.09 $\pm$ 0.02                 | 151.0 $\pm$ 30.85                 | 0.70 $\pm$ 0.01                  | 0.01                      | 2.65    | 100       | 125 $\pm$ 4  |
| 598a   | Dhekelia   | < 3                | 1.10 $\pm$ 0.01                 | 42.33 $\pm$ 2.96                  | 0.73 $\pm$ 0.01                  | 0.03                      | 2.10    | 95        | 138 $\pm$ 4  |
| 598d   | Dhekelia   | < 3                | 1.09 $\pm$ 0.01                 | 64.50 $\pm$ 4.27                  | 0.69 $\pm$ 0.02                  | 0.02                      | 2.30    | 99        | 122 $\pm$ 3  |
| 598e   | Dhekelia   | < 3                | 1.10 $\pm$ 0.02                 | 63.50 $\pm$ 4.34                  | 0.73 $\pm$ 0.01                  | 0.02                      | 2.13    | 97        | 135 $\pm$ 4  |
| 598f   | Dhekelia   | < 3                | 1.12 $\pm$ 0.01                 | 68.00 $\pm$ 4.00                  | 0.69 $\pm$ 0.01                  | 0.02                      | 2.35    | 98        | 123 $\pm$ 3  |
| 598g   | Dhekelia   | < 3                | 1.15 $\pm$ 0.03                 | 62.00 $\pm$ 11.09                 | 0.72 $\pm$ 0.02                  | 0.02                      | 2.01    | 99        | 132 $\pm$ 7  |
| 355    | Coral Bay  | N.a.               | 0.91 $\pm$ 0.02                 | 255.0 $\pm$ 37.83                 | 1.40 $\pm$ 0.02                  | 0.01                      | 2.68    | 91        | > 300        |
| P1     | Barbados   | N.a.               | 1.15 $\pm$ 0.02                 | N.a.                              | 0.01 $\pm$ 0.00                  | 0.01                      | 1.93    | 93        | Recent       |
| P2     | Barbados   | N.a.               | 1.16 $\pm$ 0.02                 | N.a.                              | 0.01 $\pm$ 0.00                  | 0.00                      | 2.04    | 100       | Recent       |

Note: N.a. = not applicable.

\*Age invalid as the sample contains <90% aragonite.

lous. Specimen 355 from Coral Bay is considered to be unreliable for the following reasons: the  $^{234}\text{U}/^{238}\text{U}$  activity ratios, compared with the theoretical curve (Fig. 3), suggest an age greater than the upper limit of the method, ca. 300 ka (Broecker, 1963). Sedimentological and microfossil evidence (A. Lord and L. Gallagher, 1989, personal commun.) suggest that the terrace containing the coral can be correlated with Pliocene shallow-marine successions found elsewhere in Cyprus (Poole and Robertson, unpublished). Of the coral samples collected from Larnaca, four yield results consistent with the geologic and stratigraphic data, and three other samples give anomalous results. These (617a, 617b, 617d) have  $^{230}\text{Th}/^{234}\text{U}$  ratios greater than 1.01, and it is likely that  $^{230}\text{Th}$  has been added to the system, for the following reasons: (1) results from the control samples P1 and P2 militate against contamination of the analytical equipment; (2) the high  $^{230}\text{Th}/^{232}\text{Th}$  ratios indicate the presence of a closed system; and (3) high initial  $^{234}\text{U}/^{238}\text{U}$  ratios suggest that  $^{234}\text{U}$  has not been lost. Bender et al. (1979) showed that  $^{230}\text{Th}$  enrichment has taken place in corals older than 150 ka from Barbados and that  $^{230}\text{Th}$  could have been released into ground water from dissolving mollusk shells and then scavenged by the coral, increasing the  $^{230}\text{Th}/^{234}\text{U}$  ratio as a consequence. The anomalous spread of ages obtained for the Cape Greco terrace (Fig. 2) could reflect the fact that this is a death assemblage, potentially containing coral of

different ages. In this case, the two older samples (200a, 529) have been reworked into position prior to lithification, while the younger sample (527a) yields an age for the terrace which is consistent with geologic and stratigraphic data.

## DISCUSSION

### Sea-Level Changes

Any interpretation involving tectonic uplift of Cyprus must first take into account Quaternary eustatic sea-level change. Thus, the uranium-series age data (Tables 1 and 2) can be considered in the light of the known chronostratigraphic ages of Quaternary global oxygen isotope stages (Chappell and Shackleton, 1986). On this basis, the 185–192 ka age of the 8–11 m marine terraces suggests a correlation with global oxygen isotope stage 7, and this, in turn, supports the view that no more than 18 m of uplift has taken place since this time, assuming that the corals formed at a maximum water depth of 10 m. Similarly, the lower marine terrace, <3 m above present-day sea level, can be correlated with the sea-level maximum recorded by oxygen isotope substage 5e, 5–8 m higher than the present-day maximum (Mesoletta et al., 1969; Bloom et al., 1974; Chappell, 1974; Stearns, 1976).

### Uplift of the Ophiolite

Sedimentary evidence has established that the Limassol Forest ophiolite of southern Cyprus was wholly emergent and eroding in early Mio-

cene time (Robertson, 1977; Eaton, 1987), while the main Troodos ophiolite to the north remained mainly submerged, with little erosion until early-late Pliocene time (McCallum, 1989; McCallum and Robertson, 1990). Strong uplift of the Troodos ophiolite was delayed until late Pliocene–early Quaternary time, as documented by the ophiolite-derived alluvial conglomerates that radiate from Mount Olympos in the center of the Troodos massif (Robertson, 1977; Poole and Robertson, unpublished). At present the alluvial conglomerates have only been dated using a late Pliocene–early Pleistocene fauna, including ostracods (Kakkaristra Formation; McCallum, 1989). Current work indicates that the alluvial conglomerates can be correlated with the higher, undated, marine terraces, while the 8–11 m and <3 m terraces studied here are distinctly younger and postdate the main phase of uplift (Poole and Robertson, unpublished). Thus, the 185–192 ka age obtained for the 8–11-m-high marine terraces implies that the main phase of tectonic uplift (350 m along the coast) must have taken place earlier. It is unlikely that rapid uplift is still taking place. On the contrary, in some areas of coastal Cyprus (i.e., in the Limassol and Paphos regions) cemented beachrock, littoral terrace deposits, and archaeological sites are now partially submerged (Moshkovitz, 1968; Flemming, 1978; Poole and Robertson, unpublished).

The new uranium-series isotopic age data show that terraces at similar heights over widely spaced areas of coastal Cyprus (8–11 m and <3 m above present-day sea level) are of similar age (192–185 ka and 130–116 ka). Pulsed regional uplift of the whole of southern Cyprus has apparently taken place without the strong differential movement resulting from localized block faulting suggested by other workers (Giangrande et al., 1987) (the terraces correlated by these authors [i.e., at Coral Bay and Paphos] have proved to be of different ages in our study; see Table 2). The terraces along the southern coast

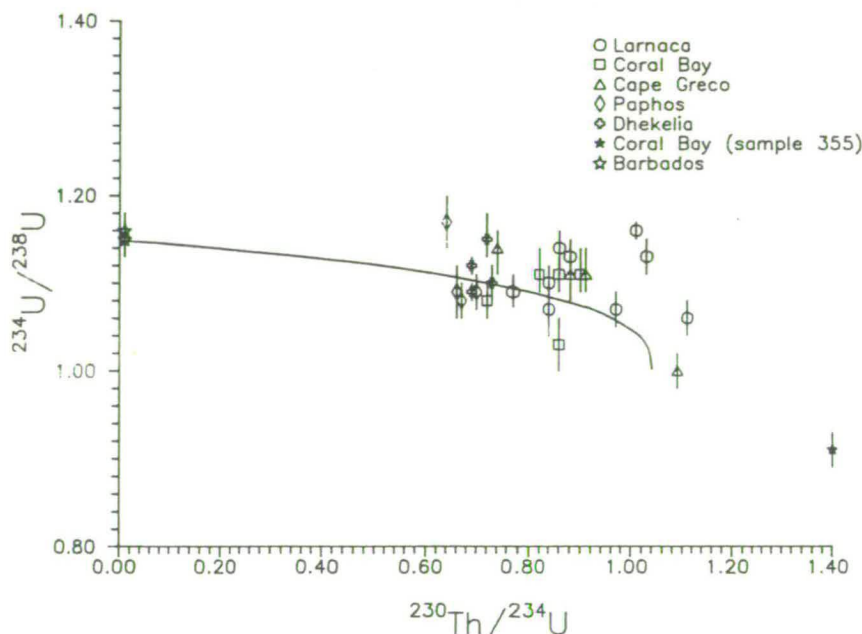


Figure 3. Plot of  $^{234}\text{U}/^{238}\text{U}$  vs.  $^{230}\text{Th}/^{234}\text{U}$  activity ratios. Solid line represents theoretical decay curve. Error bars are indicated by vertical lines and width of symbols.

TABLE 2. WEIGHTED MEAN AGES FOR CYPRUS CORAL SAMPLES

| Location    | Terrace height (m) | Weighted mean age (ka) |
|-------------|--------------------|------------------------|
| Larnaca*    | 8–11               | 185 ± 2                |
| Coral Bay   | 8–11               | 192 ± 6                |
| Cape Greco* | 8–11               | 141 ± 4                |
| Paphos      | <3                 | 130 ± 2                |
| Dhekelia    | <3                 | 116 ± 2                |

\* Not including anomalous data (617a, 617b, 617d) resulting from excess  $^{230}\text{Th}$ , see text.

† Excluding data from reworked corals (200a, 529; see text).

of Cyprus are horizontal, or dip slightly seaward, as reported from other Mediterranean shorelines (Hey, 1978) where vertical displacements are similar over wide areas, only small segments of the coastlines being deformed. The new age data are consistent with regional uplift prior to 116 ka, postdated by reduced uplift and possible submergence of the southern Cyprus region. The plate boundary still appears to be active, as suggested by the presence on Cyprus of episodic large earthquakes of magnitude 6 or greater (A.D. 342, 1189, 1953; Soren and Lane, 1981).

#### Uplift Rates

Average rates of uplift can be inferred, assuming that the coral colonies developed at a depth of 10 m below sea level, as stated above. A maximum of 6 m of uplift would then have occurred over the past 116 ka, assuming that the sea-level maxima during substage 5e were 5–8 m higher than the present-day sea level (Mesolella et al., 1969; Bloom et al., 1974; Chappell, 1974; Stearns, 1976). This would give an average rate of uplift of ~5 cm/ka. It should be noted that in some regions partial submergence has taken place (see above). Thirteen metres of uplift took place between 130 and 185 ka, at an average rate of ~24 cm/ka. An exception is the 10-m-high 141 ka terrace at Cape Greco, which was uplifted at a rate of 12 cm/ka, much quicker than elsewhere, again suggesting regional uplift of southern Cyprus as a whole, as opposed to uplift focused on the Troodos massif. The apparent reduction in rates of uplift over the past 192 ka could reflect either the slowing or cessation of subduction or a switch to strike-slip following collision (Kempfer and Ben-Avraham, 1987; Robertson, 1990).

#### CONCLUSIONS

1. New uranium-series disequilibrium dates from *Cladocora caespitosa* corals from raised marine terraces in southern Cyprus confirm that lithologically correlated terraces are similar in age, ranging from 192–185 ka for the 8–11 m terraces to 130–116 ka for terraces <3 m above the present-day sea level. The two highest raised marine terraces, which are coeval with alluvial conglomerate deposition, are older (>300 ka).

2. The older terraces (8–11 m) record maximum uplift at average rates of 24 cm/ka between 130 and 185 ka. The younger terraces (<3 m) indicate average uplift rates of ~5 cm/ka for 116 ka, with the exception of Cape Greco, which suggests a rate of 12 cm/ka.

3. Correlation with the Quaternary global isotopic stages confirms that maximum uplift has been limited to 18 m during the past 185–192 ka and also suggests that relative subsidence has taken place in some coastal areas over the past 116 ka.

#### REFERENCES CITED

- Bender, M.L., Fairbanks, R.G., Taylor, F.W., Matthews, R.K., Goddard, J.G., and Broecker, W.S., 1979, Uranium series dating of Pleistocene reef tracts of Barbados, West Indies: Geological Society of America Bulletin, v. 90, p. 577–594.
- Bloom, A.L., Broecker, W.S., Chappell, J.M.A., Matthews, R.K., and Mesolella, K.J., 1974, Quaternary sea level fluctuations on a tectonic coast: New  $^{230}\text{Th}/^{234}\text{U}$  dates from the Huon Peninsula, New Guinea: Quaternary Research, v. 4, p. 185–205.
- Broecker, W.S., 1963, A preliminary evaluation of uranium-series inequilibrium as a tool for absolute age measurement on marine carbonates: Journal of Geophysical Research, v. 68, p. 2817–2834.
- Butzer, K.W., 1975, Pleistocene littoral sedimentology cycles of the Mediterranean basin: A Mallorquin view, in Butzer, K.W., and Issac, G.L., eds., After the Australopithecines: Stratigraphy, ecology and culture change in the Middle Pleistocene: The Hague, Mouton Publications, p. 25–71.
- Chappell, J., 1974, Geology of coral terraces, Huon Peninsula, New Guinea: A study of Quaternary movements and sea-level changes: Geological Society of America Bulletin, v. 85, p. 553–570.
- Chappell, J., and Shackleton, N.J., 1986, Oxygen isotopes and sea level: Nature, v. 324, p. 137–140.
- Chen, J.H., Edwards, R.L., and Wasserburg, G.J., 1986,  $^{238}\text{U}$ ,  $^{234}\text{U}$  and  $^{232}\text{Th}$  in seawater: Earth and Planetary Science Letters, v. 80, p. 241–251.
- Dreghorn, W., 1978, Landforms of the Girne Range, northern Cyprus: Ankara, Mineral Research and Exploration Institute of Turkey, No. 172, 222 p.
- Ducloz, C., 1965, Revision of the Pliocene and Quaternary stratigraphy of the Central Mesaoria, in Hadjistavrinou, Y., ed., Annual report of the Geological Survey Department of Cyprus for 1964: Nicosia, Cyprus, p. 31–42.
- Eaton, S., 1987, The sedimentology of Mid to Late Miocene carbonates and evaporites in Southern Cyprus [Ph.D. thesis]: Edinburgh, Scotland, University of Edinburgh, 240 p.
- Edwards, R.L., Chen, J.H., and Wasserburg, G.J., 1986–1987,  $^{238}\text{U}$ ,  $^{234}\text{U}$ ,  $^{230}\text{Th}$ ,  $^{232}\text{Th}$  systematics and the precise measurement of time over the past 500,000 years: Earth and Planetary Science Letters, v. 81, p. 175–192.
- Fleming, N.C., 1978, Holocene eustatic changes and coastal tectonics in the northeastern Mediterranean: Implications for models of crustal consumption: Royal Society of London Philosophical Transactions, ser. A, v. 289, p. 405–458.
- Gass, I.G., and Masson-Smith, D., 1963, The geology and gravity anomalies of the Troodos Massif, Cyprus: Royal Society of London Philosophical Transactions, ser. A, v. 255, p. 417–467.
- Giannandrea, C., Richards, G., Kennet, D., and Adams, J., 1987, Cyprus underwater survey, 1983–1984, A preliminary report, in Karageorghis, V., ed., Report of the Department of Antiquities for 1987: Nicosia, Cyprus, p. 185–197.
- Hey, R.W., 1978, Horizontal Quaternary shorelines of the Mediterranean: Quaternary Research, v. 10, p. 197–203.
- Husseini, S.I., and Matthews, R.K., 1972, Distribution of high-magnesium calcite in lime muds of the Great Bahama Bank—Diagenetic implications: Journal of Sedimentary Petrology, v. 42, p. 179–182.
- Kempfer, D., and Ben-Avraham, Z., 1987, The tectonic evolution of the Cyprian Arc: Annales Tectonicae, v. 1, p. 58–71.
- Lort, J.M., 1971, The tectonics of the Eastern Mediterranean: A geophysical review: Reviews of Geophysics and Space Physics, v. 9, p. 189–216.
- McCallum, J.E., 1989, Sedimentation and tectonics of the Plio-Pleistocene of Cyprus [Ph.D. thesis]: Edinburgh, Scotland, University of Edinburgh, 263 p.
- McCallum, J.E., and Robertson, A.H.F., 1990, Pulsed uplift of the Troodos Massif—Evidence from the Plio-Pleistocene Mesaoria Basin, in Moores, E.M., et al., eds., Ophiolites and oceanic lithosphere: Proceedings of an international symposium: Nicosia, Cyprus (in press).
- McKenzie, D.P., 1970, Plate tectonics of the Mediterranean region: Nature, v. 226, p. 239–243.
- Mesolella, K.J., Matthews, R.K., Broecker, W.S., and Thurber, D.L., 1969, The astronomical theory of climatic change: Barbados data: Journal of Geology, v. 77, p. 250–274.
- Moshkovitz, S., 1968, The mollusca in the marine Pliocene and Pleistocene sediments of the south-eastern Mediterranean basin (Cyprus-Israel) [Ph.D. thesis]: Jerusalem, Hebrew University, 153 p.
- Robertson, A.H.F., 1977, Tertiary uplift of the Troodos Massif, Cyprus: Geological Society of America Bulletin, v. 88, p. 1763–1772.
- 1990, Tectonic evolution of Cyprus, in Moores, E.M., et al., eds., Ophiolites and oceanic lithosphere: Proceedings of an international symposium: Nicosia, Cyprus (in press).
- Soren, D., and Lane, E., 1981, New ideas about the destruction of Paphos, in Karageorghis, V., ed., Report of the Department of Antiquities for 1981: Nicosia, Cyprus, p. 178–183.
- Stearns, C.E., 1976, Estimates of the position of sea level between 140,000 and 75,000 years ago: Quaternary Research, v. 6, p. 443–449.
- Turner, W.M., 1971, Quaternary sea levels of western Cyprus: Quaternaria, v. 15, p. 197–202.
- Veeh, H.H., 1966,  $^{230}\text{Th}/^{234}\text{U}$  and  $^{234}\text{U}/^{238}\text{U}$  ages of Pleistocene high sea-level stand: Journal of Geophysical Research, v. 71, p. 3379–3386.

#### ACKNOWLEDGMENTS

Poole was funded by a Natural Environmental Research Council (NERC) Studentship (GT4/87/GS35). Shimmield was supported by NERC Grant GR3/6175. The Department of Geology and Geophysics, University of Edinburgh partially supported Robertson's field work costs. We thank the reviewers for constructive criticism of earlier drafts of this manuscript; E. Follows, B. Gomez, J. McCallum, S. Moshkovitz, and C. Xenophonos for helpful discussion; and F. Lindsay, S. Mowbray, and M. Saunders for help in analyzing the samples in Edinburgh.

Manuscript received November 10, 1989  
Revised manuscript received April 13, 1990  
Manuscript accepted April 23, 1990

## Quaternary uplift and sea-level change at an active plate boundary, Cyprus

A. J. POOLE<sup>1</sup> & A. H. F. ROBERTSON

Department of Geology and Geophysics, Edinburgh University, West Mains Road, Edinburgh EH9 3JW UK

<sup>1</sup>Present address: MAFF, Fisheries Laboratory, Lowestoft, Suffolk NR33 0HT, UK

**Abstract:** A combination of northward underthrusting of the African plate and serpentinite diapirism resulted in progressive uplift of Cyprus during the Quaternary. The uplift was associated with the development of succession of alluvial fans and marine terraces. Marine terraces in coastal southern Cyprus are developed at 350–360 m, 110–100 m, 60–50 m, 11–8 m and 2–3 m above present sea-level. The terraces display sequences of regressive, deltaic, carbonate and siliciclastic sub-littoral, to littoral and sub-aerial type. Alluvial fans of the Fanglomerate Group crop out on the northern flanks of the Troodos Massif, forming extensive, dissected, peneplaned terraces. Later uplift resulted in the formation of channel fans and river terraces. Proximal sheetflood conglomerates pass distally into channelized braid-plain environments. On the southern margin of the Troodos Massif the Fanglomerate Group comprises braided, channelized and floodplain sequences, which pass laterally into littoral facies. Provenance studies indicate that uplift and resulting erosion of Cyprus was centred on the Troodos Massif (Mount Olympus). Radiometric dates indicate that uplift was rapid in the early and mid-Pleistocene. In the late Pleistocene–Holocene, eustatic sea-level changes and anthropogenic effects dominated, while the rate of uplift was reduced, with local submergence of southern coastal areas.

This paper presents new field data and interpretations on the geomorphology, sedimentology and tectonics, associated with the uplift and unroofing of the Troodos ophiolite, Cyprus. The Troodos Massif (Gass & Masson-Smith 1963; Moores & Vine 1971) is one of the few known examples of actively emplacing oceanic lithosphere, thus an analysis of the Quaternary geology sheds light on the tectonic processes involved and the relative roles of tectonic uplift, versus glacio-eustatic sea-level change. In Cyprus, successively developed geomorphological surfaces, alluvial features and coastal deposits can be stratigraphically correlated, dated and related to the evolution of an active plate boundary (Robertson 1977).

### Quaternary evolution

The neotectonic (i.e. Miocene–Recent) evolution of Cyprus began with the inferred initiation of northwards subduction along the active Cyprus margin (Fig. 1), probably in earliest Miocene (Robertson *et al.* 1990). During the Miocene, compression affected areas of southern Cyprus nearest the trench (Eaton 1987). Extension and subsidence took place in northern and western Cyprus during the Late Miocene and Pliocene (Follows & Robertson 1990; McCallum & Robertson 1990). Uplift, in the Late Pliocene to Early Quaternary, was marked by the deposition of regressive, marine to non-marine sediments in both northern and southern Cyprus (McCallum & Robertson 1990). Combined seismic, stratigraphic and earthquake focal mechanism data indicate that an active margin exists to the south of Cyprus (Kempner & Ben-Avraham 1987). At present there is little activity along the plate boundary to the south of the island, but active convergence is inferred to be taking place beneath SW Cyprus (Kempner & Ben-Avraham 1987).

### Quaternary sedimentation in southern Cyprus

During the Quaternary, rapid tectonic uplift, in combination with eustatic sea-level changes, gave rise to the following

features in southern Cyprus, which can be correlated by satellite imagery, photogrammetry and field survey. (i) *Intermontane fluvial systems*: these are dominated by conglomeratic alluvial and channel fan sequences on the Mesaoria Plain north of the Troodos Massif; proximal debris flow, and sheetflood sediments pass laterally into braid plain deposits; palaeosol and caliche horizons are also seen. (ii) *Conglomeratic channels*: channel fan sequences crop out along the southern flanks of the Troodos Massif; conglomeratic fan systems pass laterally into braid, delta and beach environments; off-shore sand and gravel sequences are also present. (iii) *Coastal settings*: aeolian, shoreface and near shore carbonate sediments crop out in SE Cyprus (e.g. Cape Greco, Dhekelia and Larnaca), S Cyprus (e.g. Petounda Point, Akrotiri), SW Cyprus (e.g. Paphos, Ayios Yeoryios) and east of Polis (e.g. Argaka, Kato Pyrgos). (iv) *Island-wide geomorphological features and erosion surfaces*: pronounced erosional surfaces on the Mesaoria Plain north of the Troodos Massif and to the south, on the coastal plains of southern Cyprus, are an important component of the Quaternary evolution and aid relative correlation; associated geomorphological features include caves, solution hollows and wave-cut platforms in coastal areas and river terraces on the Mesaoria Plain.

### Quaternary stratigraphy of southern Cyprus

Fieldwork and aerial photography show that the terraces occur systematically throughout S Cyprus, with younger units at progressively lower topographical levels (Table 1). Biostratigraphic control (both macro- and micro-) in the Quaternary is sparse, as many species are still living today. Changes in faunal groups may be used with caution. Gross climatic changes allow cold and warm faunas to be distinguished (Issar 1979). Ostracode (McCallum 1989) and nannofossil data (Houghton *et al.* 1990; A. Lord & L. Gallagher pers. comm. 1989) have yielded Upper Pliocene to lower Pleistocene ages. The gastropod *Strombus bubonius*, described from a marine terrace in Larnaca, was

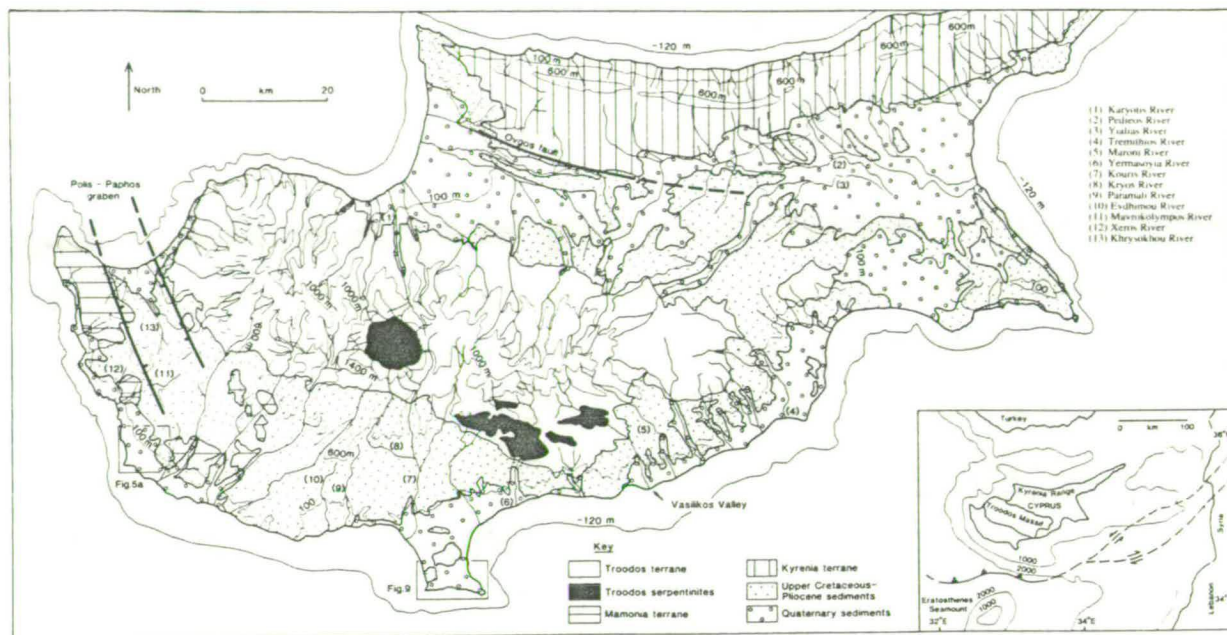


Fig. 1. Geological, topographic and drainage map of Cyprus. The contours heights and bathymetric depth are indicated and the two main active fault lineaments shown. Inset: outline tectonic setting of Cyprus in the Eastern Mediterranean. Note: the location of the areas shown in detail in Figs 5a and 9, and of locations mentioned in the text.

assigned as being Tyrrhenian (Pantazis 1966; Moshkovitz 1968), but this has not been confirmed by subsequent uranium series disequilibrium dating (Poole *et al.* 1990). It is likely that the *Strombus* fauna existed for more than one warm, interglacial phase in the Late Pleistocene (Butzer 1975). Chronostratigraphic methods that have been used to date and correlate marine terrace levels in Cyprus are uranium series disequilibrium dating (Poole *et al.* 1990; this study) and  $^{14}\text{C}$  dating (Vita-Finzi 1990). Correlation of (alluvial and marine) terrace sequences provides a third technique for establishing a relative chronology, as shown by De Vaumas (1960) for the Troodos Massif, Ducloz (1964) for the Mesaoria Plain and Gomez (1987) for the lower Vasilikos Valley.

#### Upper Pliocene–lower Pleistocene: early uplift

The oldest known erosive feature in Cyprus is a mature erosion surface of Mio-Pliocene age, approximately 500 m ASL (above present day sea-level), along the Akamas Peninsula (Fig. 2). A second, distinct terrace at 350–360 m ASL in SW Cyprus dips gently seawards. Overlying bioclastic grainstones are locally preserved in a small cliffline, east of Paphos (Fig. 2).

#### Interpretation

The 350–360 m terrace is correlated with a terrace on the southern flanks of the Kyrenia Range (Ducloz 1967; Dregghorn 1978), from which Upper Pliocene foraminifera were identified (Mantis 1970). The 350–360 m terrace is also correlated with deposition of the Athalassa and Kakkaristra Formations (Table 1) in the Mesaoria Plain (Ducloz 1964; McCallum 1989) and with submarine channels, described

from Khirokitia and Amathus (Fig. 2) (Houghton *et al.* 1990) which contain latest Pliocene (*c.* 2.2–1.8 Ma) nanofossils and planktonic foraminifera. The Kakkaristra Formation is dated by ostracodes as Upper Pliocene to lower Pleistocene (McCallum 1989). The 350–360 m terrace, therefore was established during the earliest Pleistocene, after an early phase of uplift.

#### Lower Pleistocene–middle Pleistocene

##### Intermontane fluvial system

The main phase of uplift was marked by the deposition of the fluvial Fanglomerate Group, which is best exposed along the north margin of the Troodos Massif, where it unconformably overlies the sand and silt dominated Apalos Formation (Table 1), and is locally incised into the Troodos ophiolite (e.g. at Malounda).

The Fanglomerate Group consists mainly of conglomerates, with subordinate sand and silt. Proximal conglomerates are matrix-supported, poorly sorted, weakly consolidated and immature (Fig. 3b). Facies pass distally into channelized units, comprising abundant fine-grained sediments with palaeosols (Fig. 3a). The Fanglomerate Group is generally structureless, but contains locally imbricated clasts and rare cross-bedding in the more distal localities. Previous estimates of thickness of this unit vary from 3–5 m on mesa-type hills in the east (McCallum 1989), to 90 m elsewhere (Zomenis 1977). However, this study has shown that the thickness of the Fanglomerate Group, varies greatly across the Mesaoria Plain, from proximal (pedmont), to distal (braid) localities (south to north), as well as along the axis of the plain (east to west). Provenance studies indicate that the Fanglomerate Group on the northern margin of the



**Table 1.** Summary of the Quaternary stratigraphy and age date from Cyprus

|                                     | Central Mesaoria Plain<br>(Ducloz 1964)        | Central Kyrenia Range<br>(Ducloz 1972) | Lower Vasilikos Valley<br>(Gomez 1987) | S Cyprus correlation*<br>(this paper) |
|-------------------------------------|------------------------------------------------|----------------------------------------|----------------------------------------|---------------------------------------|
| Holocene                            |                                                |                                        |                                        |                                       |
| Late Pleistocene                    | Xeri Alluvium                                  | Kyrenia Terr.                          | Argakitis Kamilas Terr.                | F4                                    |
|                                     | Laxial Gravel                                  | Ayios Epikitos Terr.                   | Kalavastos Terr.                       | F3                                    |
| Mid- to Early Pleistocene           |                                                | Trapeza Terr.                          | Mitsinjites Terr.                      | F2                                    |
|                                     | Kambia Gravel                                  | Klepini Terr.                          | Phalakros Terr.                        | F1                                    |
|                                     | Kantara Gravel                                 |                                        |                                        | F0                                    |
|                                     | Apalos Formation                               |                                        |                                        |                                       |
| Upper Pliocene to Early Pleistocene | Kakkaristra Formation and Athalassa Formation‡ |                                        |                                        |                                       |

**Table 1. cont.**

|                                     | Climate (Issar 1979)                                                 | Inferred Oxygen isotope stage† | Height of marine terrace (m ASL) | Age (ka)     |
|-------------------------------------|----------------------------------------------------------------------|--------------------------------|----------------------------------|--------------|
| Holocene                            | Present day fauna                                                    | 1                              |                                  |              |
| Late Pleistocene                    | Tyrrhenian ( <i>Strombus</i> fauna)                                  | 2                              |                                  |              |
|                                     |                                                                      | 3-4                            |                                  |              |
|                                     |                                                                      | 5                              | <3                               | 116-134 ± 10 |
|                                     |                                                                      | 6                              |                                  |              |
|                                     |                                                                      | 7                              | 8-11                             | 185-204 ± 8  |
| Mid- to Early Pleistocene           | Calabro-Sicilian (cold marine fauna, i.e. <i>Arctica islandica</i> ) | 8-14                           |                                  |              |
|                                     |                                                                      | ?                              | 50-60                            | ?            |
|                                     |                                                                      | ?                              | 100-110                          | ?            |
| Upper Pliocene to Early Pleistocene |                                                                      | ?                              |                                  |              |

\* Note: the numerical F1-F4 nomenclature used in this paper.

† After Shackleton (1975).

‡ After McCallum (1989).

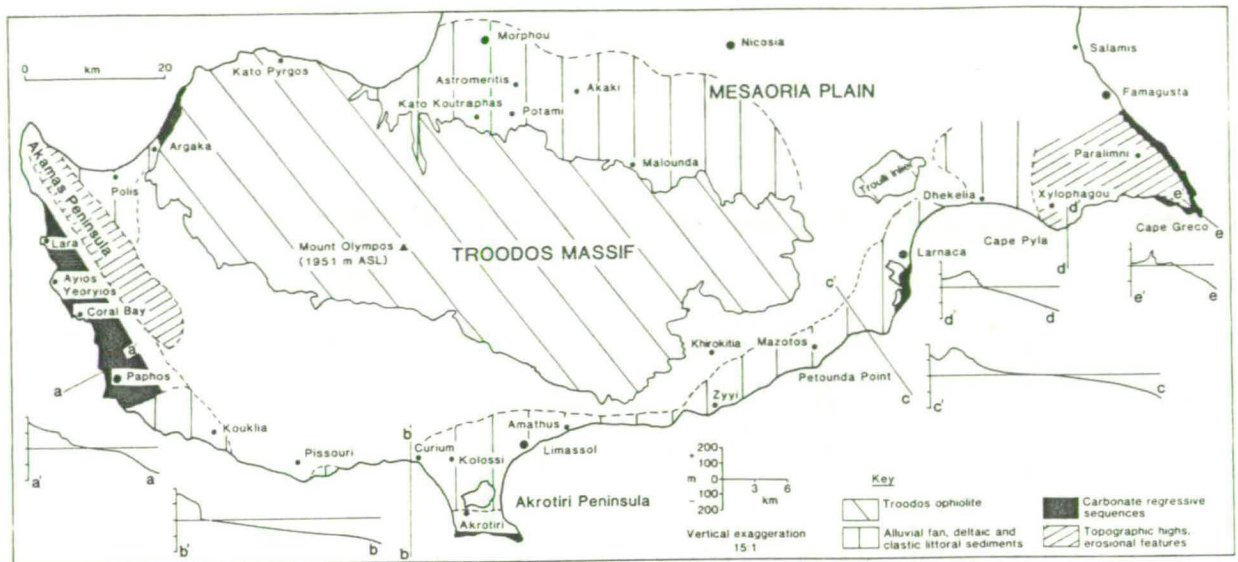


Fig. 2. Outline map of southern Cyprus showing the variation in Quaternary sediments and locations mentioned in the text. Selected topographic sections are shown.

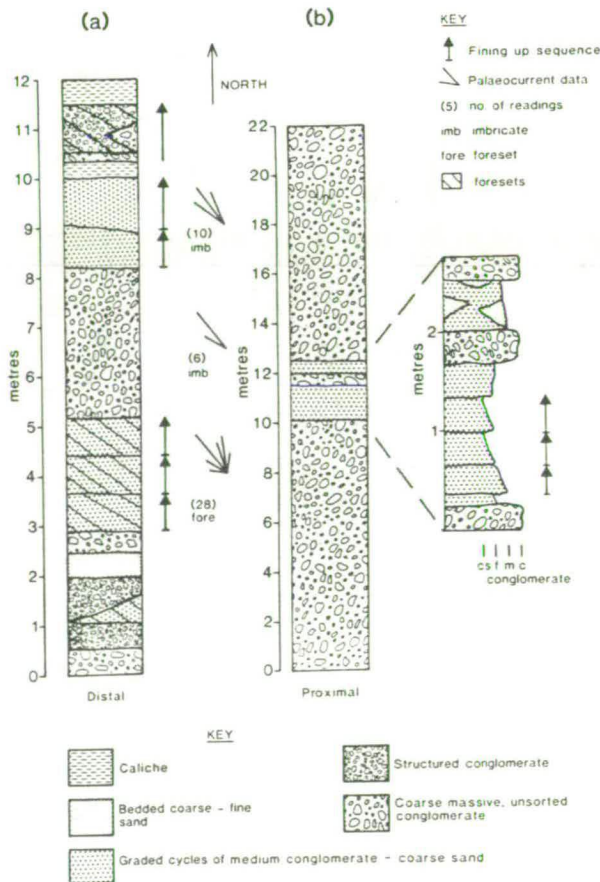


Fig. 3. Sketch logs of the F1 alluvial fan facies from the northern margin of the Troodos Massif: (a) distal, (b) proximal facies. Note the palaeocurrent data.

Troodos Massif differs from the earlier Apalos and Kakkaristra Formations (Fig. 4a-e). There is a greater proportion of diabase and gabbroic clasts in the Faglomerate Group conglomerates in the western and central areas. By contrast, in the eastern area of the Mesaoria Plain, there is a conformable contact between the Faglomerate Group and the Apalos Formation, with the later Faglomerate Group showing an unchanged provenance from the underlying Apalos Formation (Fig. 4k-l). Ultramafic clasts are not seen in the Faglomerate Group along the northern margins of the Troodos Massif, although their occurrence is reported from outcrops of the Faglomerate Group in the north, close to Morphou (Wilson 1958).

Palaeocurrent data and satellite imagery confirm that a series of alluvial fans prograded from the north margin of the Troodos Massif onto the Mesaoria Plain. These fans show a swing in drainage direction from west to east across the Mesaoria Plain.

*Coastal sedimentation*

The first of a series of Quaternary marine terraces is exposed in SW Cyprus at 100-110 m ASL (e.g. near Paphos). This terrace is correlated with the Faglomerate Group (Table 1). We term the successive terrace levels in Cyprus F1 to F4 (Table 1, Fig. 5a). Thus, the Faglomerate Group represents the F1 surface. On the west coast, NW of Paphos, a series of gorges are cut through resistant Miocene limestones and chalks, from the 350-360 m, earliest Pleistocene terrace to the level of the F1 surface. The 100-110 m terrace exposed in the Paphos area unconformably overlies Miocene and Oligocene sediments. A conglomeratic lag of locally derived clasts (e.g. chalks and limestones) is overlain by a coralline algae framework, which in turn passes into a sequence of littoral grainstones, containing abundant molluscs (Fig. 5bA).

At Pissouri, cliffs show ?Pliocene fan-delta sequences

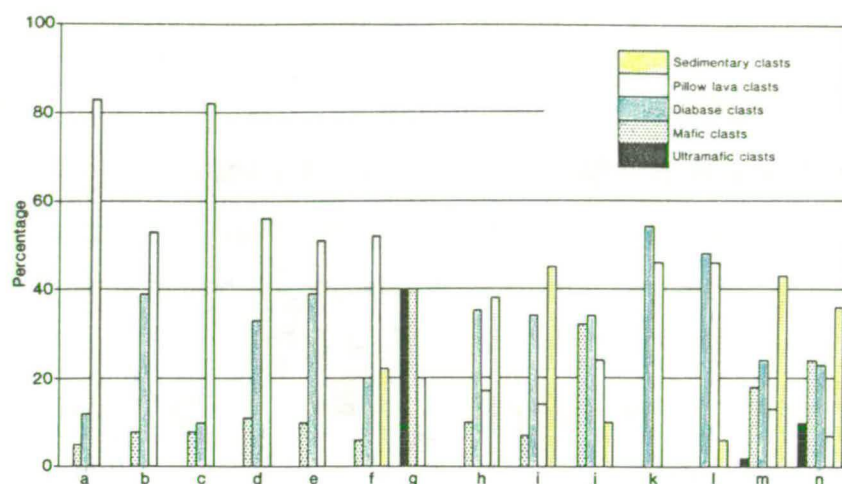


**Fig. 4.** Histograms of clast provenance: (a) and (b) Pliocene fan-delta clasts and Fanglomerate Group clasts from Akaki; (c) and (d) Apalos Formation and Fanglomerate Group clasts, respectively, from Kato Koutraphas; (e) and (f) Fanglomerate Group clast and clast from the Recent sequence, respectively, from Astromeritis; (g) clasts from Recent deposits in the Karyotis river valley; (h) and (i) clasts from the Quaternary Fanglomerate Group and braid-delta sequences, respectively, from Dhekelia; (j) clasts from the Fanglomerate Group cropping out at Pissouri; (k) and (l) Apalos Formation and Fanglomerate Group clasts, respectively, eastern Mesaoria Plain; (m) and (n) Fanglomerate Group and Recent clasts, respectively, from the Kouris River. Note the letters a–n are referenced in the text.

passing unconformably up into the Pleistocene Fanglomerate Group. The Fanglomerate Group crops out at c. 100 m ASL and comprises conglomerates, derived from both the Troodos ophiolite and the local sedimentary sequence (e.g. chalks, cherts and limestones; Fig. 4j). Remnant channelized sequences, up to 5 m thick, after erosion and peneplanation, are overlain by red terra rossa-type palaeosols, with thick sequences of caliche (e.g. 2–3 m thick at Pissouri). The Fanglomerate Group also crops out along the southern coast of Cyprus. Subsequent downcutting of major river channels (e.g. Kouris and Yermasoyia Rivers) has isolated these exposures.

The Fanglomerate Group, additionally, crops out in SE Cyprus, as an easterly extension of the Mesaoria Plain. An extensive erosion surface is present, but associated exposure is restricted. Channelized conglomerates of the Fanglomerate Group unconformably overlie the Pliocene Athalassa Formation (e.g. north of Dhekelia). These conglomerates are again capped by extensive caliche and soil horizons. Provenance studies (Fig. 4h) indicate that the clasts were derived from the Troodos ophiolite, the Troulli Inlier and local sedimentary sources.

#### *Island-wide erosion surfaces*

The F1 surface is exposed, as a plateau in two areas along the northern margin of the Troodos ophiolite (i.e. between Potami and Kato Koutraphas in the west and between Akaki and Malounda in the east). The undissected F1 conglomerate surface is locally covered by terra rossa-type soil and caliche.

#### *Interpretation: main phase of uplift*

The main control on the lower to middle Pleistocene F1 fanglomerate and terrace deposition was tectonic. The large-scale fans relate to drastic uplift and downcutting. However, climatic effects probably largely controlled the architecture of the fans. A similar interplay of processes is

described from the Dead Sea, Israel (Frostrick & Reid 1989) and SE Spain (Harvey & Wells 1987).

The presence of ultramafic clasts (Wilson 1958) in the F1 Fanglomerate Group, transported by the Karyotis River (Fig. 1; Fig. 4g) is evidence of erosion of the ultramafic core of the Troodos Massif in early Pleistocene, yet ultramafic clasts are not found in the F1 Fanglomerate Group deposits away from this fan, a similar pattern to that observed today (Fig. 4f). The implication is that the drainage pattern of the early Pleistocene was similar to the present (Fig. 1). The F1 alluvial fans on the northern margin of the Troodos Massif were deposited as proximal sheetflood deposits and debris flows, passing distally into channelized braided systems. Such a depositional setting would account for the thickness variations in the F1 Fanglomerate unit. A piedmont area bordered the Troodos Massif, with a thicker sedimentary succession to the north. Inter-channel areas were subjected to less incision and survived as thin conglomeratic deposits, lapping onto the Troodos Massif and pre-Quaternary sediments.

Large alluvial fans did not develop during the lower–middle Pleistocene to the south of the Troodos Massif. Instead, large incised channels (e.g. Kouris River) carried sediment from the rising Troodos Massif southwards, to areas close to, or beyond the present coast (e.g. Pissouri). Seismic data suggest that a large proportion of the detritus derived from the Troodos Massif at this time is now located in offshore slope areas (McCallum 1989). Several of the rivers, thus may have already existed in the pre-Pleistocene (e.g. Maroni and Kouris Rivers). In addition, gorges on the west coast of the island reflect rapid relative uplift, similar to that described from the Kyrenia Range, N Cyprus (Dreghorn 1978).

Carbonate littoral and sub-littoral sequences also developed at this time; these crop out in areas away from the influence of the Troodos drainage systems, particularly to the west of the Akamas Peninsula, which was already a topographic high (Fig. 2). The offlap of the carbonate sequence indicates that formation took place during a relative sea-level fall.

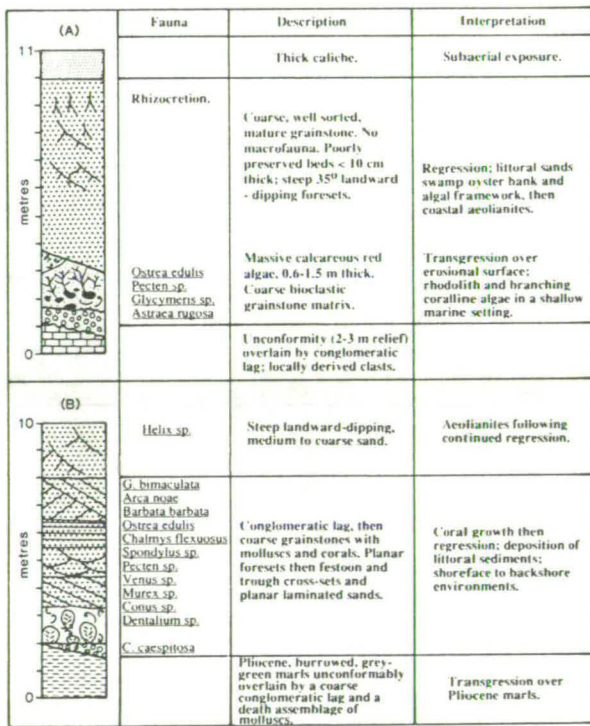
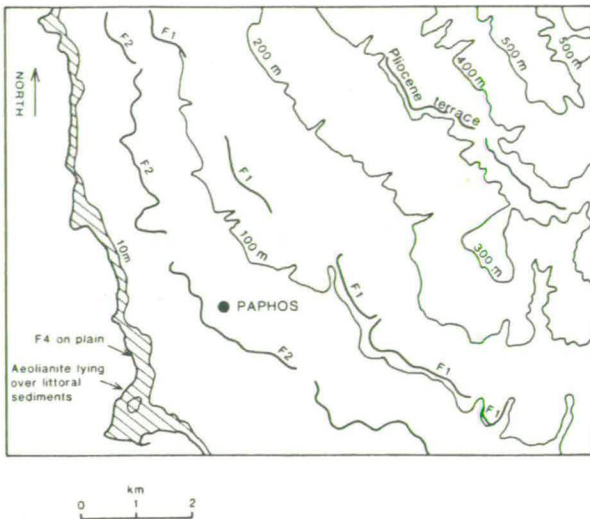


Fig. 5. (a) Contour map of SW Cyprus showing the location of the Pliocene, F1 and F2 terraces and the occurrence of aeolianite in SW Cyprus; (b) composite sedimentary logs of the coastal carbonate facies. The F1 and F2 terrace sequence is shown in 5bA and the F3 and F4 terrace sequence in 5bB. Note: minor colonies of rue coral *Cladocora caespitosa* are present within the F2 terrace.

Middle Pleistocene

Intermontane basin

The second phase of the Faglomerate Group (Fig. 2; Table 1) forms a distinct horizon at topographically lower levels than the F1 surfaces, to the north of the Troodos Massif.

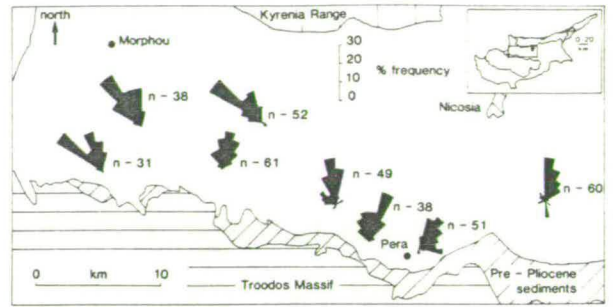


Fig. 6. Palaeocurrent data for the Faglomerate Group sediments cropping out on the Mesaoria Plain; based on clast imbrication.

The peneplaned F1 terrace is incised by F2 channels and smaller distributary streams, reworking the F1 conglomerates into the F2 alluvial system (e.g. Potami). Poorly sorted conglomerates that comprise the F2 channel fill, generally 8-10 m thick, are locally overlain by red terra rossa-type palaeosols and caliche horizons (e.g. Potami and near Astromeritis).

Conglomerate clasts of this age to the north of the Troodos Massif are dominantly gabbro, diabase and pillow lava, but lack ultramafic clasts, similar to the earlier F1 depositional phase. Clast imbrication trends are also similar to the F1 Faglomerate Group; i.e. from N and NW on the western side of the Mesaoria Plain, to N to NE further east (Fig. 6). In proximal localities matrix-supported conglomerates pass upwards into clast-supported, massive conglomerates. Few sedimentary structures exist within proximal areas of the F2 Faglomerate Group. Well bedded, more mature, better sorted and imbricated conglomerates occur in more distal areas.

Coastal settings

The second marine terrace level, at 50-60 m ASL forms an extensive cliffline from south and east of Paphos along the west coast to Lara. This terrace, lying unconformably on earlier Miocene sediments, comprises superbly exposed sequences of sub-aerial, littoral and sub-littoral sediments, very similar to the F1 terrace (Fig. 5bA). To the south and east of Paphos, towards Koukليا, the 50-60 m terrace passes laterally into fluvial sediments that comprise moderately well sorted conglomerates, containing ophiolite-derived clasts, from all but the ultramafic core of the Troodos ophiolite, as well as locally derived sedimentary clasts (e.g. limestone, chert and chalk).

Major rivers (e.g. Xeros, Mavrokolympos), which drained the west flank of the Akamas Peninsula, deposited silts, sands and minor conglomerates. These sediments pass northwards into red, channelized conglomeratic units at lower topographic level than the F1 terrace; this crops out further east. Sediments of F2 age along the south coast are dominated by Troodos-derived, fluvial conglomerates, like those north of the Troodos Massif. A number of exposed units along the south coast can be correlated viz: the Mitsinjites terrace in the Vasilikos Valley (Gomez 1987; Table 1) with areas west of the Vasilikos Valley and sequences from the Akrotiri Peninsula and the Yermasoyia and Kouris river valleys.

In general, an increased proportion of ultramafic and

locally derived sedimentary clasts (e.g. chalk, chert) are seen in the Recent bars of the Kouris River, relative to the F2 Fanglomerate Group flanking the rivers (Fig. 4m-n). This suggests a change in provenance and/or down cutting into the ultramafic core of the Troodos ophiolite. In distal localities (e.g. Kolossi and Zyvi) shallow channels were cut into the F1 Fanglomerate. Still more distal deposits are seen further south on the Akrotiri Peninsula, where the Fanglomerate Group cannot be subdivided due to its patchy outcrop, but borehole records show conglomerates to be at least 70 m thick. The margin of the F2 Fanglomerate channels forms a mature erosion surface that intersects an earlier F1 erosion surface to the north, close to the core of the Troodos Massif.

**Braid-delta and fluvial facies**

Sand and gravel sequences of the F2 stage crop out extensively in quarries between Dhekelia and Xylophagou. These deposits are bounded to the east by an erosion surface in the Xylophagou area, at c. 100 m, which is capped by Miocene limestones. Borehole data reveal sands and gravels up to 40-50 m below the present sea-level. The gravels consist of mixed, Troodos-derived clasts and sediments (e.g. limestones and chalk); these display tabular cross-bedded units containing a marine fauna, including the molluscs *Glycymeris* sp. and *Ostrea edulis*. Texturally mature sediments pass up into immature, poorly sorted sands and gravels (similar to Fig. 7). Provenance studies

show that gabbro, diabase, pillow lava and sedimentary clasts dominate the sequence, suggesting at least partial derivation from the main Troodos Massif (Fig. 4i).

**Island-wide erosion surfaces and river capture**

After deposition of the F2 fanglomerate, horizontal to low-angle sloping surfaces, on the northern flanks of the Troodos Massif, were uplifted in response to a phase of relative uplift. The erosion surface was planated, cut by small channels and capped by red terra rossa-type palaeosols and caliche horizons.

In coastal SW Cyprus, a 'stranded' 100-110 m cliff-line, cut during the F2 phase, forms the upper limit of an extensive coastal plain, extending down to 50 m ASL. A similar palaeo-cliff-line and terrace is also seen in S and SE Cyprus (Fig. 2). In SE Cyprus, non-depositional terraces and cliff-lines are cut into the exposed Miocene limestones, at Cape Pyla and Cape Greco.

**Interpretation: further phase of uplift**

Further relative uplift associated with downcutting of channels on both the north and south margin of the Troodos Massif, resulted in fan valley deposition (cf. Muto 1987), back-cutting of the drainage towards the Troodos Massif and the development of mature erosion surfaces on the now isolated, dissected F1 fan-sheets and terraces. Further uplift also caused greater dissection of the Troodos ophiolite as

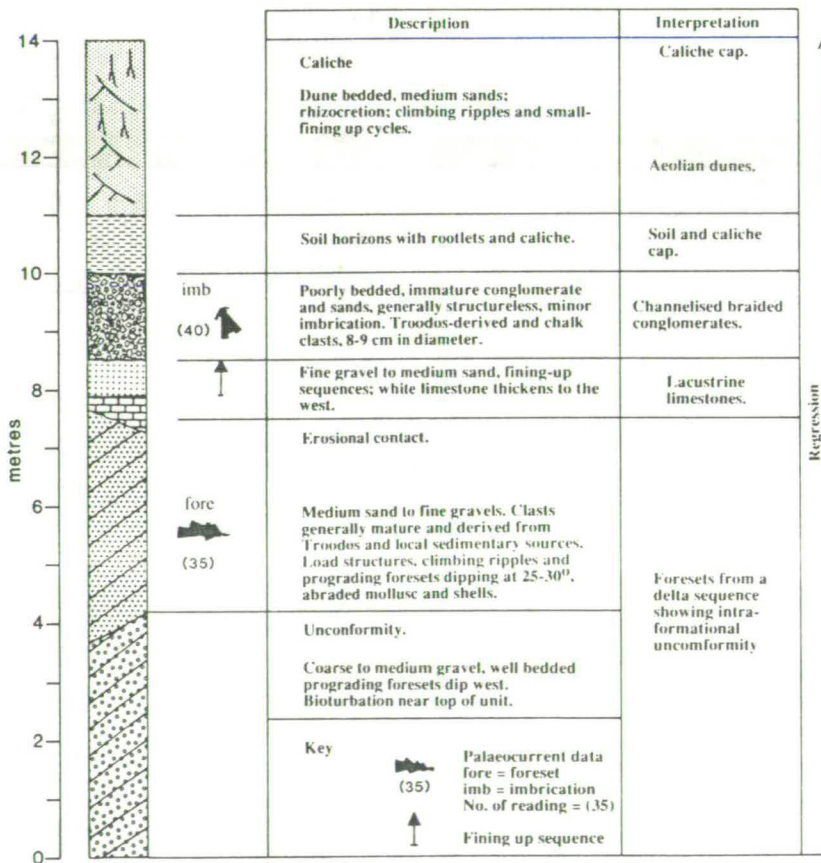


Fig. 7. Composite sedimentary log of the deltaic-fluvial-aeolianite regressive sequence seen in southern Cyprus.

deeper structural levels were exposed. Proximal channelized sequences passed out into braid plain environments (e.g. Kolossi in the south and Astromeritis in the north). The relative uplift also resulted in the formation of a palaeo-cliff-line at 100–110 m ASL, and the deposition of regressive-upwards, sedimentary successions. The quarry sequences in SE Cyprus represent an overall regression from deltaic to fluvial sequences (e.g. Fig. 7). Carbonate sub-littoral and sub-aerial sediments in SW Cyprus are also interpreted as being of regressive origin (Fig. 5bA).

Eustatic sea-level fall and tectonic uplift caused the progradation of fluvial channels and down-cutting into the Pleistocene carbonate sequences in the Kouklia area (Fig. 8). A subsequent rise in sea-level resulted in the formation of the 50–60 m terrace, cutting sediments from marine, fluvial and sub-aerial environments.

Direct evidence of river capture is seen in the Limassol area, where the Kouris River has captured the Kryos River, which can be traced back onto the Troodos Massif. Evidence from the F1 conglomerates at Pissouri, which contain Troodos-derived clasts (Fig. 4j), suggests that the Paramali and Evdhimou Rivers, which now do not rise in the Troodos Massif were also modified by river capture. Similarly, the presence of gabbroic clasts in both deltaic and fluvial deposits (Fig. 4h–i) in SE Cyprus points to the existence of a major drainage system flowing southwards, off the northern margin of the Troodos Massif during the middle Pleistocene. As no major river channels flow in this area today, the suggestion is that river capture has taken place, perhaps reflected in the pattern of drainage seen, with the Pedieos and Yialias Rivers flowing out towards Famagusta Bay today.

### Early Late Pleistocene

#### Coastal settings

A distinctive feature of southern Cyprus is an extensive, flat coastal plain that extends around much of the coast from Larnaca to Paphos and into the Polis region. Sub-littoral and littoral facies crop out below the level of this extensive plain and contain intact specimens of the coral *Cladocora caespitosa* that have yielded uranium series dates of 204 ka, 192 ka, and 185 ka for the time of formation of the terraces, at Petounda Point, Coral Bay and Larnaca, respectively (Poole *et al.* 1990; Table 2).

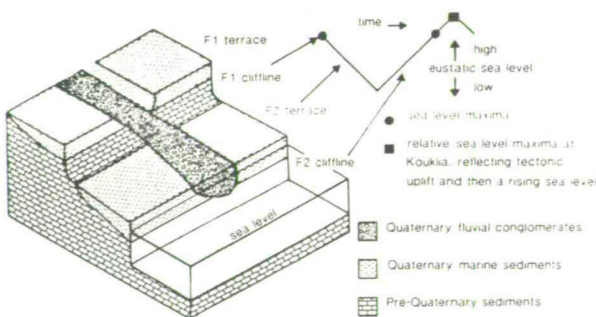


Fig. 8. Block diagram showing the relationship between alluvial downcutting and terrace development during phases of relative uplift. Inset curve represent a single (c. 100 ka) eustatic sea-level cycle.

Table 2. New uranium series age data for Cyprus corals

| Location       | Terrace height ASL (m) | Age (ka) |
|----------------|------------------------|----------|
| Petounda Point | 8–11                   | 203 ± 7  |
|                | 8–11                   | 209 ± 15 |
| Paralimni      | < 3                    | 138 ± 4  |
|                | < 3                    | 129 ± 4  |

Note: more extensive data are published in Poole *et al.* (1990).

#### Littoral sequences

The most extensive carbonate sub-littoral, to littoral sequences, of the early Late Pleistocene, crop out in the Larnaca area, forming a small cliff less than five metres high, unconformably overlying Pliocene marls. The succession (Fig. 5bB) is made up of coarse bioclastic grainstones containing small colonies of the coral *C. caespitosa*, up to one metre in diameter. Minor lenses of Troodos-derived conglomerates are seen within this carbonate facies. Remnants of a once extensive littoral sequence are also seen at Petounda Point, Coral Bay and east of Polis. The littoral sequences form part of an extensive coastal plain. The width of this plain narrows to a few hundred metres on the steeply-rising Akamas Peninsula in NW Cyprus. In the Polis region, mixed carbonate sub-littoral to littoral sequences, containing small colonies of *C. caespitosa* are overlain by clastic detritus (e.g. gabbro, basalt, chert, marl and limestone) transported down the axis of the Polis–Paphos graben by the Khrysoxhou River.

#### Fluvial–deltaic deposits

Early Late Pleistocene fluvial–deltaic deposits contain only minor conglomerates, relative to the scale of deposits associated with earlier uplift. In the Polis–Paphos graben the littoral sequences (see above) pass laterally into conglomerates dominated by ophiolite-derived clasts. The conglomerates contain a marine fauna (i.e. *Glycymeris* sp. and *Ostrea edulis*) and are well bedded, with seawards-dipping foresets. This facies is overlain by a thin, littoral sequence, capped by caliche and soil horizons.

Mature, cross-bedded conglomerates, with interbedded sands, of similar inferred age are seen in quarries along the south coast of the island (i.e. near Mazotos). Although ophiolite-derived clasts dominate, locally-derived sedimentary clasts are also present (e.g. limestones and chalks). The relationship between these deltaic deposits and a discontinuous fluvial sequence is shown in Fig. 7. Conglomerates are also extensively exposed beneath the coastal plains in both the Larnaca and Paphos areas.

Closer to the Troodos Massif pre-existing drainage systems were further incised by rivers, cutting through Pliocene and older sediment, into the Troodos Massif and giving rise to sedimentary and ophiolite-derived clasts.

#### Aeolianites

Cross-bedded aeolianite deposits are widely developed on the coastal plains of west and south Cyprus (e.g. Lara, north of Paphos) as poorly cemented, moderately sorted, buff-coloured bioclastic grainstones. In SW Cyprus, the aeolianites were derived from carbonate littoral sediments, whilst in south Cyprus (e.g. Mazotos) are green, clastic sands dominate. The dune structures are cut by extensive

rhizocretion, penetrating to depths of 3 to 4 m below the palaeo-dune surface. Aeolianites are banked up and over pre-existing cliff-lines on the west coast.

### Erosion surfaces

A major sub-horizontal erosion surface overlies the facies of this age (i.e. littoral, deltaic, fluvial) as well as the Troodos ophiolitic basement and its sedimentary cover. This surface is not clear on the Mesaoria Plain to the north of the Troodos Massif, but is recognized in western and southern Cyprus, with the development of an extensive 8–11 m high coastal terrace. In the south-east, a terrace is not clearly discernable between Dhekelia and Xylophagou, probably because the sediments that crop out there are poorly consolidated sands and gravels. A very distinct terrace and wave cut notch is, however, observed east of Xylophagou, cut on and into resistant Miocene limestones (e.g. Cape Pyla and Cape Greco).

### Interpretation: further uplift

Systematically lowered topographic levels of littoral, deltaic and fluvial deposition, plus the presence of extensive erosion surfaces, together indicate that uplift continued after F2 times (Middle Pleistocene). Littoral deposits were preserved due to this subsequent relative uplift. The emergence allowed unconsolidated littoral sands to be blown onshore to form migrating dunes, that banked up against and over palaeo-cliff-lines.

Up to 12 m of uplift and incision into the pre-existing channel fan system took place on the Mesaoria Plain during this time. Islandwide relative uplift was limited however, with little scope for erosion of the Troodos Massif, but reworking of Troodos-derived clasts continued. Widespread channels tended to be shallow, dominated by sands and gravels. Deltas containing much reworked, mature gravel developed along the axis of the Polis-Paphos graben and around the southern coast of the island. These gravels are interbedded with sands and overlain by thin limestone of probable lacustrine origin. The deltas are locally overlain by thin, discontinuous sequences of littoral sediments (e.g. Polis). The deltaic sequences are also overlain by poorly sorted fluvial conglomerates (e.g. Larnaca area), consistent with overall regression, as also indicated by the presence of sub-littoral to sub-aerial carbonate sequences (e.g. Larnaca). This regression culminated in the formation of an extensive erosional surface.

By the end of the F3 (early Late Pleistocene) phase, an extensive coastal plain had developed, extending out beyond the present coastline, as a result of a eustatic sea-level fall.

## Late Late Pleistocene

### Coastal environments

Littoral and coastal sediments of this age are seen throughout southern Cyprus, at heights of less than 3 m ASL. The pattern of sedimentation is very similar to that of the Quaternary period in general. Carbonate sequences formed in areas away from the major rivers of the Troodos Massif (i.e. west of the Akamas Peninsula; in SE Cyprus, east of the Xylophagou F1 erosion surface). Specimens of the coral *C. caespitosa* from littoral deposits at

Paphos and Dhekelia (Poole *et al.* 1990) and Paralimni (this study; Table 2) were dated using the uranium series method, and the results establish a correlation with the last inter-glacial sea-level high (Table 1).

### Littoral environments

In the Paphos region, littoral deposits crop out along the coast, extending up to 100 m inland. These are similar to those of the older 8–11 m-high terrace (Fig. 5bB). In many areas this terrace lies close to, or just beneath, the present day sea-level, thus good vertical sections are rare. Notable is the presence of solution hollows filled by high abundance-low diversity faunas, consisting primarily of the gastropod *Astraea rugosa*. This infilling may be significantly younger than the primary terrace. *A. rugosa* is not restricted to this lower terrace and is found in all the Quaternary terraces of SW Cyprus; it also ranges from Miocene to Recent throughout the Eastern Mediterranean basin (Moshkovitz 1968). Similar sub-littoral to littoral terrace deposits occur widely at Kato Pyrgos, Paphos, Akrotiri, Dhekelia and in SE Cyprus, to the north and south of Paralimni.

### Alluvial deposits

Alluvial deposits of this age are best developed in the south and south-west of the island. In the north Troodos region, valleys are floored by alluvial conglomerates and sands, with a mixed clastic input. The axis of the Polis-Paphos graben and an embayment near Pissouri are filled with similar deposits. Excavation pits in the Lower Vasilikos Valley (Gomez 1987) show that 3 to 5 units of silts, were deposited at this time, comprising centimetre-sized rhythmic cycles, intercalated with calcareous horizons.

### Aeolianites

Extensive, weakly lithified aeolianites overlie the late Late Pleistocene terraces. Dunes from isolated 'highs' on the terrace relief in both SE and SW Cyprus. They display rhizocretion fabrics and, like the earlier aeolianites (F3) are banked up against palaeo-cliff-lines (e.g. Akrotiri, Fig. 9). In the Cape Greco area of SE Cyprus, the dunes crop out over a low-lying plain. Palaeocurrent data suggest onshore winds in both SW and SE Cyprus at this time, with possible funnelling of sediment through gaps in the low lying Miocene hills in the Cape Greco area (Follows 1990).

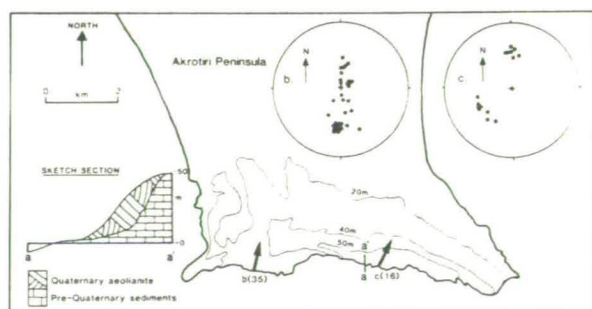


Fig. 9. Aeolianite palaeocurrent date from the Akrotiri Peninsula, showing evidence for onshore wind. Note sketch section showing the banking of the aeolianite over the former cliff.

### Erosion surfaces

A distinct peneplaned surface of this age exists throughout the island (e.g. beneath the high cliffs at Curium, extending across the Akrotiri Peninsula). Erosion of aeolianites (F3) also took place in the Paphos district (e.g. Lara), resulting in small embayments. Sea caves are well preserved in areas of resistant bedrock (e.g. Miocene limestone of Cape Pyla). The erosion surface is overlain by red terra rossa-type palaeosols, locally, several metres thick in the southeast of the island. This soil, however, could be Recent.

### Interpretation: slightly lowered base levels

The coral ages correlate with the Tyrrhenian sea-level (oxygen isotope stage 5e; Shackleton 1975). Widespread littoral deposits in Cyprus apparently relate to this transgressive/regressive event. Uplift in the order of 6 m has taken place since this time (Poole *et al.* 1990), assuming that the Tyrrhenian sea-level high was 5–8 m higher than the present day sea-level (Mesolella *et al.* 1969; Bloom *et al.* 1974; Chappell 1974; Stearns 1976). The high sea-level accounts for the formation of cliffs under which, apparently anomalously wide, low lying beaches are seen today (e.g. below Curium), and the formation and preservation of sea caves 2–3 m ASL (e.g. Cape Pyla). Limited uplift is consistent with the observed minimal downcutting of pre-existing channels and the domination of silt and floodplain deposits to the N and S of the Troodos Massif, in contrast to the older fan sequences. We do not favour the 'transgressive model' for aeolianite formation (Land 1967; Vacher 1973), as the lithified F3 dunes on the west coast appear to have been cut and/or eroded by the 5e sea-level high, and were not formed at that time. The F4 dunes overlie the dated littoral sequence, which is correlated with the 5e sea-level high. The high-angle of repose, lack of capping soils, dominantly onshore palaeocurrent directions and knowledge that a drier climate (Rognon & Williams 1977; Sarnthein 1978) is likely to have existed during a glacial episode, are all consistent with the hypothesis that large-scale onshore migration of aeolianites took place. The available evidence thus points to formation of the dunes during a falling sea-level, in line with evidence from other Mediterranean aeolianites (Hey 1962; Sabaris 1962; Butzer 1975).

### Latest glacial and Holocene period

Clear evidence of the latest glacial event (c. 40–10 ka; Dansgaard *et al.* 1982) comes from shallow offshore seismic data from S Cyprus. The seismic surfaces, cut by inferred channels, can be correlated with fluvial channels onshore (e.g. Zygi; McCallum 1989). These shallow conglomerate-filled channels are incised into floodplain conglomerates. Admiralty charts indicate the presence of a planar offshore surface down to a depth of c. 120 m (Fig. 1), in line with the estimated fall in sea-level during the last glacial (–110 to –120 m; Shackleton *et al.* 1984). Caves found at less than 3 m ASL (e.g. Cape Pyla) were cut during the 5e sea-level high and contain a fauna of dwarf mammals, including hippopotami (Boekschoonten & Sondaar 1972). Other features apparently dating from this time include the formation of the extensive Kouris River braidplain and the Akrotiri and Larnaca salt lakes. Muddy, poorly sorted alluvium was deposited in the Tremithios River, in the

Larnaca lowlands (Gifford 1978) during the latest Pleistocene and early Holocene. The floor of the Vasilikos Valley was downcut by 6 m, followed by a period of aggradation and alluviation between 5540 to 5010 B.C. (Gomez 1987). This preceded a phase of fine-grained overbank sedimentation and subsequent downcutting to form an alluvial terrace within 2 m of the present floodplain, as seen in the Tremithios Valley (Gifford 1978). Incision into this terrace has occurred since Byzantine (c. 330–1190 A.D.) times (Gifford 1978); shards found in this terrace south of Nicosia support this interpretation. Archaeological sites at Paphos, Salamis, Amathus and Larnaca show evidence of Recent submergence (Alexander-son 1972; Flemming 1978; Gifford 1978).

### Interpretation: submergence and anthropogenic influences

Limited relative uplift of the island occurred during the period from the last glacial to the present. The sedimentary sequences and geomorphological changes during the latest Pleistocene and Holocene period reflect anthropogenic, climatic, eustatic and/or continuing minor tectonic effects, in line with the views of Flemming (1978), Gomez (1987) and Poole *et al.* (1990) but contrary to the views of Giangrande *et al.* (1987) and Vita-Finzi (1990) who suggest that rapid uplift and neotectonic faulting took place during this time.

## Discussion

### Tectonic uplift versus sea-level change

The Troodos Massif has been uplifted during a period of glacio-eustatic sea-level change. To what extent can the two processes be disentangled in the Quaternary of southern Cyprus?

During the earliest Pleistocene, both tectonism and sea-level changes influenced erosion and deposition. The highest 350–360 m terrace is preserved only in SW Cyprus, probably because this area was away from the later focus of uplift and thus survived erosion. This terrace is correlated with the earlier pre-F1 Fanglomerate depositional events in the Mesaoria basin, the Upper Pliocene–lower Pleistocene Kakkaristra and Apalos Formations, dated by ostracodes. Correlation can also be extended northwards, via the bioclastic Athalassa Formation of the Mesaoria basin with the ?Upper Pliocene terrace on the southern flanks of the Kyrenia Range (Ducloz 1967). In southern Cyprus, Late Pliocene nannofossil muds and Troodos-derived conglomerates infilled channels (Houghton *et al.* 1990) indicating incision that resulted from a relative fall in sea-level. Latest Pliocene marine muds are also overlain by bioclastic limestones in southern Cyprus (near Amathus; Houghton *et al.* 1990) that are lithologically correlated with the Late Pliocene–earliest Pleistocene Athalassa Formation of the Mesaoria Plain, implying a relative rise in sea-level, that was probably eustatically controlled.

The dominant control on erosion and sedimentation, during the early–mid-Pleistocene, was drastic uplift centred on Mount Olympos, modified by glacio-eustatic effects, as observed in coastal areas. The exact timing of the dominant F1 Fanglomerate remains poorly known, owing to the lack



of datable material in the localized correlative littoral deposits. A late Lower Pleistocene age (i.e. c. 1 Ma.) for the climax of uplift is probable. The record of ultramafic clasts in the alluvial conglomerates mirrors that found today, showing that no substantial unroofing of the Troodos Massif has taken place since that time. Along the north Troodos margin alluvial fan systems infilled the pre-existing Mesaoria basin, whilst along the south margin, most of the detritus bypassed onshore areas, probably within pre-existing channels; deposition then took place offshore, on the narrow continental shelf and slope. Except where river capture has occurred, drainage patterns were established as early as the Late Pliocene and have remained little changed since (itself a strong argument against many major differential tectonic movements in southern Cyprus during the Quaternary). The correlative littoral deposits, preserved only in areas away from the main focus of uplift and erosion of the Troodos Massif (SW Cyprus), indicate that sea-level was relatively high during at least part of the time of F1 deposition (early-mid-Pleistocene), thus further emphasizing the dominant role of tectonic uplift at this time. Regression followed, indicating sea-level fall and/or continued regional uplift, marked by the deposition of the F2 (mid-Pleistocene) sediments. The F2 features mirror those of the F1, with similar fluvial and marine sediments. F2 phase channels cut down into F1 terraces and the pre-Quaternary sediments, suggesting that tectonic uplift took place during the F2 phase. The evidence from the Kouklia area in SW Cyprus (Fig. 8) suggests that this tectonic uplift occurred during a falling, or low eustatic sea-level stand, allowing tectonic uplift and sea-level change to be differentiated for the first time in Cyprus (Fig. 8).

During the early Late Pleistocene, the local lateral passage from fluvial gravels to coral-bearing littoral deposits in NW Cyprus shows that erosion corresponded to a time of relative sea-level fall, thus favouring eustatic sea-level changes as the main control of the F3 (early Late Pleistocene) alluvial system. Dates from corals in these marine terraces correspond to oxygen isotope 7 (Shackleton 1975) and suggest that 13 m of tectonic uplift took place between 130 ka and 192 ka (Poole *et al.* 1990; this paper, Table 2). The later stages of uplift were marked by regressive successions of shallow marine sediments, aeolianite and caliche deposits and the development of palaeo-cliff-lines. Dissection of pre-existing erosion surfaces took place with fluvial channel incision, regressive fan-delta accumulation and the development of erosion surfaces covered with caliche and terra rossa type-palaeosols.

During the F4 phase (latest Pleistocene since c. 130 ka) sea-level change, specifically transgression and regression, associated with the 5e sea-level high, was the dominant control on the erosive and sedimentary features in S Cyprus, although limited uplift may have taken place (Poole *et al.* 1990). Littoral deposits developed on a broad, flooded peneplaned surface, with hinterland raised cliff-lines and caves. Extensive aeolianites migrated onshore as sea-level fell, exposing and reworking large areas of newly formed marine bioclastic sediment. A maximum of 6 m of uplift has taken place in the past 116 ka (Poole *et al.* 1990), confirming that eustatic sea-level change, and not tectonics, has been the dominant control in the latest Pleistocene.

During the Holocene (post-10 ka) glacio-eustatic change has clearly dominated sedimentation, modified by relatively minor tectonic movements, mainly subsidence of some

coastal regions (Flemming 1978). Regression, resulting from an estimated sea-level fall of 110–120 m (Shackleton *et al.* 1984) during the last glacial (40–10 ka), is widely recognizable in the form of offshore and onshore peneplaned surfaces and shallow conglomerate-filled channels.

Anthropogenic influences have apparently dominated sedimentation, related to deforestation and agriculture during the Holocene. Gradual tectonic movements may have been taking place, but are not distinguishable. Silting, flooding and further downcutting to the present level occurred between 5540–5010 BC. Late Holocene alluvial terraces were locally incised between 330–1190 AD (Gomez 1987).

#### *Climatic variation*

The sedimentary environments in all the documented marine terraces of SW Cyprus (i.e. F1–F4) are very similar; yet as Fig. 5b shows there is a distinct change in fauna, with red algal build ups and no coral in the F1 terrace (e.g. above Paphos; Fig. 5a). Colonies of the *C. caespitosa*, however, occur in the F2, F3 and F4 (e.g. Coral Bay and Paphos) terraces, as well as in the Pliocene sediments of the Mesaoria Plain (McCallum 1989). The presence, or absence of coral can be correlated with long term, Quaternary, climatic variations identified in other areas in the Mediterranean (e.g. Israel, Issar 1979; Mallorca, Butzer 1975). These changes resulted in the introduction of a 'cool water' molluscan fauna during the Calabro-Sicilian stage, succeeded by a 'warm water' fauna during the Tyrrhenian stage (Table 1) (Moshkovitz 1968). The F3 terrace at Larnaca, identified as Tyrrhenian in age (Pantazis 1966; Moshkovitz 1968) on the presence of the gastropod, *Strombus bubonius* actually corresponds to oxygen isotope stage 7 (Poole *et al.* 1990), in agreement with the proposal that the 'warm' water Tyrrhenian fauna were present in the Mediterranean from c. 200 ka to 120 ka (Butzer 1975). The occurrence of the 'cool water' molluscan fauna corresponds to the presence of red algal build ups, as seen in the F1 terrace, while the colonies of *C. caespitosa* may relate to warmer periods (e.g. the Late Pliocene and Tyrrhenian). This correlation between the mollusc population and the presence, or lack of hermatypic coral and red algal frameworks suggests that the Quaternary assemblages on Cyprus behaved in a similar manner to the skeletal groups of Lees & Buller (1972). These authors identified two skeletal assemblages: foramol ('temperate water'), where forams, molluscs and calcareous red algae are the dominant grain type; and chlorozoan ('warm water'), where hermatypic corals and/or calcareous green algae are also present. Teichert (1958) also shows that hermatypic corals only exist in 'warm water'. Thus, Quaternary coral and calcareous red algal populations in Cyprus may reflect climatic changes, that were previously only recorded in molluscan populations. Overall, 'cooler waters' existed in the early Pleistocene with warmer conditions in the latest Pliocene, middle and latest Pleistocene.

#### *Nature of tectonic control*

After the inferred initiation of northwards subduction along an active margin south of Cyprus, probably in earliest Miocene, southern Cyprus began to emerge, with localized

compression in the south in the Miocene and extension in the north (Mesaoria basin) in the Late Miocene–Early Pliocene (Robertson *et al.* 1990). Extension in the north was accompanied by uplift of the north Troodos margin areas that flanked the main graben (Mesaoria basin), with accompanying erosion and marine fan delta deposition (Nicosia Formation; McCallum & Robertson 1990). Focussed uplift of the Troodos Massif first became evident in the Late Pliocene–early Pleistocene (Kakkaristra and Apalos Formations), while marine deposition persisted on south Kyrenia flank and probably in the Mesaoria basin into the early Quaternary. One alternative to explain the main tectonic uplift in early to mid-Pleistocene is serpentinite-driven diapiric protrusion of the ultramafic core of the Troodos Massif (Gass & Masson-Smith 1963). Another, is underthrusting of a continental fragment, or seamount northwards beneath Cyprus during the Quaternary. Underthrusting of a seamount (e.g. the Eratosthenes Seamount; Fig. 1) could have triggered serpentinization and thus diapiric uplift of the Troodos Massif (Robertson 1990), combined with regional uplift of the whole of Cyprus (including the Kyrenia Range). It should be noted that southern Cyprus was uplifted as a single structural entity with little evidence of major differential faulting, other than in the Polis graben in SW Cyprus, where extension continued into the Quaternary. This agrees with observations from other tectonically active areas of the Mediterranean (Hey 1978), where large areas have undergone equivalent amounts of uplift with little evidence of active faulting and local differential movement.

One outstanding problem is whether the documented phases of relative uplift represent truly episodic tectonic pulses of uplift, or whether they were the result of superimposition of the glacio-eustatic sea-level changes, on a single cycle of accelerating and then decelerating tectonic uplift. While initially favouring the first (McCallum & Robertson, 1990), we now believe that the second possibility is at least likely. Resolution of this problem is unlikely without absolute ages of the earlier, crustal uplift phases.

In summary, an initial drastic phase of uplift of the Troodos Massif took place in the late early to mid-Quaternary (c. 1.5–1.0 Ma), followed by further less pronounced uplift continuing until the late Pleistocene (c. 130 ka). A maximum of 6 m of uplift has taken place since 116 ka and there is evidence of Holocene submergence of some coastal areas (Flemming 1978). The slowing and/or cessation of tectonic uplift could correspond to the apparent absence of present day subduction beneath southern Cyprus. Similar uplift of 'fore-arc' areas related to the collision of seamounts with trenches is documented elsewhere (Cadet *et al.* 1987).

## Conclusions

The potential to correlate geomorphological terrace surfaces, alluvial systems and coastal marine and non-marine settings throughout southern Cyprus provides an ideal opportunity to assess the importance of tectonic uplift, versus sea-level change in the Quaternary unroofing of the Troodos ophiolite. Following earlier uplift, the Troodos Massif underwent drastic, focussed uplift in the late early to mid-Pleistocene (c. 1.5–1 Ma), with a further weaker phase of uplift continuing into the late Late Pleistocene (c. 130 ka). The uplift corresponded to times of relative high

sea-levels, followed by relative regression. After 130 ka, only a maximum of c. 6 m of further tectonic uplift of coastal areas took place. The dominant control in the late Quaternary was thus eustatic, particularly the Tyrrhenian highstand (c. 130 ka). The overall tectonic setting during the Quaternary involved the overriding plate of a northwards-dipping subduction zone, that was punctured by the diapiric protrusion of serpentinite, possibly associated with the collision of a seamount with the Cyprus trench.

For helpful discussion we thank E. Follows, B. Gomez, J. McCallum, S. Moshkovitz, C. Vita-Finzi and C. Xenophontos. The two reviewers of the paper are thanked for their constructive comments. A. Lord and L. Gallagher are thanked for identifying the nannofossils. D. Baty assisted with drafting. G. Shimmield is thanked for his continued support of uranium series dating of coral samples in the Department of Geology and Geophysics, Edinburgh University. A.P. was funded by a NERC Research Studentship (GT4/87/GS/35) and A.H.F.R. by Edinburgh University.

## References

- ALEXANDERSON, T. 1972. Mediterranean beachrock cementation: marine precipitation of Mg-calcite. In: STANLEY, D. J. (ed.) *The Mediterranean Sea*. Dowden, Hutchinson and Ross, 203–223.
- BLOOM, A. L., BROECKER, W. S., CHAPPELL, J. M. A., MATTHEWS, R. K. & MOSOLELLA, K. J. 1974. Quaternary sea level fluctuations on a tectonic coast: new  $^{230}\text{Th}$ / $^{234}\text{U}$  dates from the Huon Peninsula, New Guinea. *Quaternary Research*, **4**, 185–205.
- BOESCHHOONTEN, G. J. & SONDAAR, P. Y. 1972. On the fossil mammalia of Cyprus, I and II. *Proceedings Series B Koninklijke Nederlandse Akademie van Wetenschappen*, **75**, 306–338.
- BUTZER, K. W. 1975. Pleistocene littoral sedimentology cycles of the Mediterranean basin: a Mallorquin view. In: BUTZER, K. W. & ISSAC, G. L. (eds) *After the Australopithecines: stratigraphy, ecology and culture change in the Middle Pleistocene*. Moulton, The Hague, 25–72.
- CADET, J.-P., KOBAYASHI, K., AUBOUIN, J., BOULEGUE, J., DEPLUS, C., DUBOIS, J., VON HUENE, R., JOLIVET, L., KANAZAWA, T., KASAHARA, J., KOIZUMI, K., LALLEMAND, S., NAKAMURA, Y., PAUTOT, G., SUYEHRO, K., TANI, S., TOKUYAMA, H. & YAMAIZAKI, T. 1987. The Japan Trench and its juncture with the Kuril Trench: cruise results of the Kaiko project, leg 3. *Earth and Planetary Science Letters*, **83**, 267–284.
- CHAPPELL, J. 1974. Geology of coral terraces, Huon Peninsula, New Guinea. A study of Quaternary movements and sea level changes. *Geological Society of America Bulletin*, **85**, 553–570.
- DANSGAARD, W., CLAUSEN, H. B., GUNDESTRUP, N., HAMMER, C. U., JOHNSEN, S. F., KRISTINDOTTIR, P. M. & REEH, N. 1982. A new Greenland deep ice core. *Science*, **218**, 1273–1277.
- DE VAUMAS, E. 1960. The principal geomorphological regions of Cyprus. In: INGHAM, F. (ed.) *Annual Report of the Geological Department, Cyprus*, 38–43.
- DREHORN, W. 1978. *Landforms of the Girne Range, northern Cyprus*. The Mineral Research and Exploration Institute of Turkey Report, 172.
- DULCOZ, C. 1964. Revision of the Pliocene and Quaternary stratigraphy of the central Mesaoria. In: HADJISTAVRINOY, Y. (ed.) *Annual Report of the Geological Survey Department, Cyprus*, 31–42.
- DULCOZ, C. 1967. Les formations quaternaires de la région de Klepini (Chypre) et leur place dans la chronologie du Quaternaire méditerranéen. *Archives des Sciences, Genève*, **20**, 123–198.
- EATON, S. 1987. *The sedimentology of Mid to Late Miocene carbonates and evaporites in southern Cyprus*. PhD Thesis, Edinburgh University.
- FLEMMING, N. C. 1978. Holocene eustatic changes and coastal tectonics in the north eastern Mediterranean: implications for models of crustal consumption. *Philosophical Transactions of the Royal Society of London*, **A289**, 405–458.
- FOLLOWS, E. J. 1990. *Sedimentology and tectonic setting of Miocene reef and related sediments in Cyprus*. PhD Thesis, Edinburgh University.
- & ROBERTSON, A. H. F. 1990. Sedimentology and structural setting of Miocene reefal limestones in Cyprus. In: MALPAS, J., MOORES, E., PANAYIOTOU, A. & XENOPHONTOS, C. (eds) *Ophiolites and Oceanic Lithosphere*. Proceedings of the International Symposium, Nicosia, Cyprus, October 1987, 207–216.
- FROSTRICK, L. E. & REID, I. 1989. Climatic versus tectonic controls on fan

- sequences; lessons from the Dead Sea, Israel. *Journal of the Geological Society, London*, **146**, 527-539.
- GASS, I. G. & MASSON-SMITH, D. 1963. The geology and gravity anomalies of the Troodos Massif, Cyprus. *Philosophical Transactions of the Royal Society of London*, **A255**, 417-467.
- GIANGRANDE, C., RICHARDS, G., KENNET, D. & ADAMS, J. 1987. Cyprus underwater survey, 1983-1984. A preliminary report. In: KARAGEORGHIS, V. (ed.) *Report of the Department of Antiquities, Cyprus*, 185-197.
- GIFFORD, J. A. 1978. *Palaeogeography of archaeological sites of the Larca lowlands, south eastern Cyprus*. PhD Thesis, University of Minnesota.
- GOMEZ, B. 1987. The alluvial terraces and fills of the Lower Vasilikos Valley, in the vicinity of Kalavassos, Cyprus. *Transactions of the Institute of British Geographers*, **12**, 345-359.
- HARVEY, A. M. & WELLS, S. G. 1987. Response of Quaternary fluvial systems to differential epeirogenic uplift: Aguas and Feos river systems, southeast Spain. *Geology*, **15**, 689-693.
- HEY, R. W. 1962. The Quaternary and Palaeolithic of northern Libya. *Quaternaria*, **6**, 435-450.
- 1978. Horizontal Quaternary shorelines of the Mediterranean. *Quaternary Research*, **10**, 197-203.
- HOUGHTON, S. D., JENKINS, D. G., XENOPHONTOS, C. & GASS, I. G. 1990. Microfossil evidence for a late Pliocene age for the Amathus and Khirokitia channel deposits, southern Cyprus and thereby unroofing of the Troodos Massif. In: MALPAS, J., MOORES, E., PANAYIOTOU, A. & XENOPHONTOS, C. (eds) *Ophiolites and Oceanic Lithosphere* Proceedings of the International Symposium, Nicosia, Cyprus, October 1987. 231-234.
- ISSAR, A. 1979. Stratigraphy and palaeoclimates of the Pleistocene of central and northern Israel. *Palaeogeography, Palaeoclimatology, Palaeoecology*, **20**, 261-280.
- KEMPLER, D. & BEN-AVRAHAM, Z. 1987. The tectonic evolution of the Cyprian Arc. *Annales Tectonicae*, **1**, 58-71.
- LAND, L. S. 1967. Diagenesis of skeletal carbonate. *Journal of Sedimentary Petrology*, **37**, 914-930.
- LEES, A. & BULLER, A. T. 1972. Modern temperate-water and warm-water shelf carbonate sediments contrasted. *Marine Geology*, **13**, M67-73.
- MANTIS, N. 1970. Upper Cretaceous-Tertiary foraminiferal-zones in Cyprus. *Epithris, Cyprus Research Centre, Nicosia*, **3**, 227-241.
- MCCALLUM, J. E. 1989. *Sedimentation and tectonics of the Plio-Pleistocene of Cyprus*. PhD Thesis, Edinburgh University.
- & ROBERTSON, A. H. F. 1990. Pulsed Uplift of the Troodos Massif—Evidence from the Plio-Pleistocene Mesaoria Basin. In: MALPAS, J., MOORES, E., PANAYIOTOU, A. & XENOPHONTOS, C. (eds) *Ophiolites and Oceanic Lithosphere*. Proceedings of the International Symposium, Nicosia, Cyprus, October 1987. 217-230.
- MESOLELLA, K. J., MATTHEWS, R. K., BROECKER, W. S. & THURBER, D. L. 1969. The astronomical theory of climatic change: Barbados data. *Journal of Geology*, **77**, 250-274.
- MOORES, E. M. & VINE, F. J. 1971. The Troodos Massif, Cyprus and other ophiolites as oceanic crust: evaluation and implications. *Philosophical Transactions of the Royal Society of London*, **A268**, 433-466.
- MOSHKOVITZ, S. 1968. *The mollusca in the marine Pliocene and Pleistocene sediments of the south eastern Mediterranean basin (Cyprus-Israel)*. PhD Thesis, Hebrew University, Jerusalem.
- MUTO, T. 1987. Coastal fan processes controlled by sea-level changes: a Quaternary example from the Tenryugawa Fan System, Pacific coast of central Japan. *Journal of Geology*, **95**, 716-724.
- PANTAZIS, T. M. 1966. Tyrrhenian terraces of the Larnaca area, south eastern Cyprus. *Annual report of the Geological Department, Cyprus*, 29-34.
- POOLE, A. J., SHIMMIELD, G. B. & ROBERTSON, A. H. F. 1990. Late Quaternary uplift of the Troodos ophiolite, Cyprus: uranium-series dating of Pleistocene coral. *Geology*, **18**, 894-897.
- ROBERTSON, A. H. F. 1977. Tertiary uplift of the Troodos Massif, Cyprus. *Geological Society of America Bulletin*, **88**, 1763-1772.
- 1990. Tectonic evolution of Cyprus. In: MALPAS, J., MOORES, E., PANAYIOTOU, A. & XENOPHONTOS, C. (eds) *Ophiolites and Oceanic Lithosphere*. Proceedings of the International Symposium, Nicosia, Cyprus, October 1987. 235-250.
- , EATON, S., FOLLOWS, E. J. & MCCALLUM, J. E. 1990. Role of tectonics versus sea level change in the Neogene (Miocene-Pliocene) evolution of the Cyprus active margin. In: MACDONALD, D. I. M. (ed.) *Sedimentation, tectonics and eustasy: sea-level change at active plate margins*. Special Publication of the International Association of Sedimentologists, **12**, (in press).
- ROGNON, P. & WILLIAMS, M. A. J. 1977. Late Quaternary climatic changes in Australia and North Africa: a preliminary interpretation. *Palaeogeography, Palaeoclimatology, Palaeoecology*, **21**, 285-327.
- SABARIS, L. S. 1962. Le quaternaire marin des Balears et ses rapports avec les côtes Méditerranéennes de la Péninsule Iberique. *Quaternaria*, **6**, 309-342.
- SARNTHEIN, M. 1978. Sand deserts during glacial maximum and climatic optimum. *Nature*, **272**, 43-46.
- SHACKLETON, J. C., VAN ANDEL, T. H. & RUNNELS, C. N. 1984. Coastal palaeogeography of the central and western Mediterranean during the last 125 000 years and its archaeological implications. *Journal of Field Archaeology*, **4**, 307-314.
- SHACKLETON, N. J. 1975. The stratigraphic record of deep-sea cores and its implications for the assessment of glacial, interglacial and interstadial in the Mid-Pleistocene. In: BUTZER, K. W. & ISSAC, G. LI. (eds) *After the Australopithecines: stratigraphy, ecology and culture change in the Middle Pleistocene*. Moulton, The Hague, 1-24.
- STEARNS, C. E. 1976. Estimates of the position of sea level between 140 000 and 75 000 years ago. *Quaternary Research*, **6**, 443-449.
- TEICHERT, C. 1958. Cold-and deep-water coral banks. *American Association of Petroleum Geologists Bulletin*, **42**, 1064-1082.
- VACHER, L. 1973. Coastal dunes of younger Bermuda In: COATES, D. R. (ed) *Coastal geomorphology*. Publications in geomorphology, State University of New York, 355-391.
- VITA-FINZI, C. 1990. <sup>14</sup>C dating of Late Quaternary uplift in western Cyprus. *Tectonophysics*, **172**, 135-140.
- WILSON, R. A. M. 1958. The Geology of the Xeros-Troodos area. *Memoir 1, Geological Survey Department, Cyprus*, 41-47.
- ZOMENIS, S. L. 1977. *Hydrology of the central Mesaoria (Cyprus)*. PhD Thesis, University of London.

Received 20 August 1990; revised typescript accepted 6 March 1991.

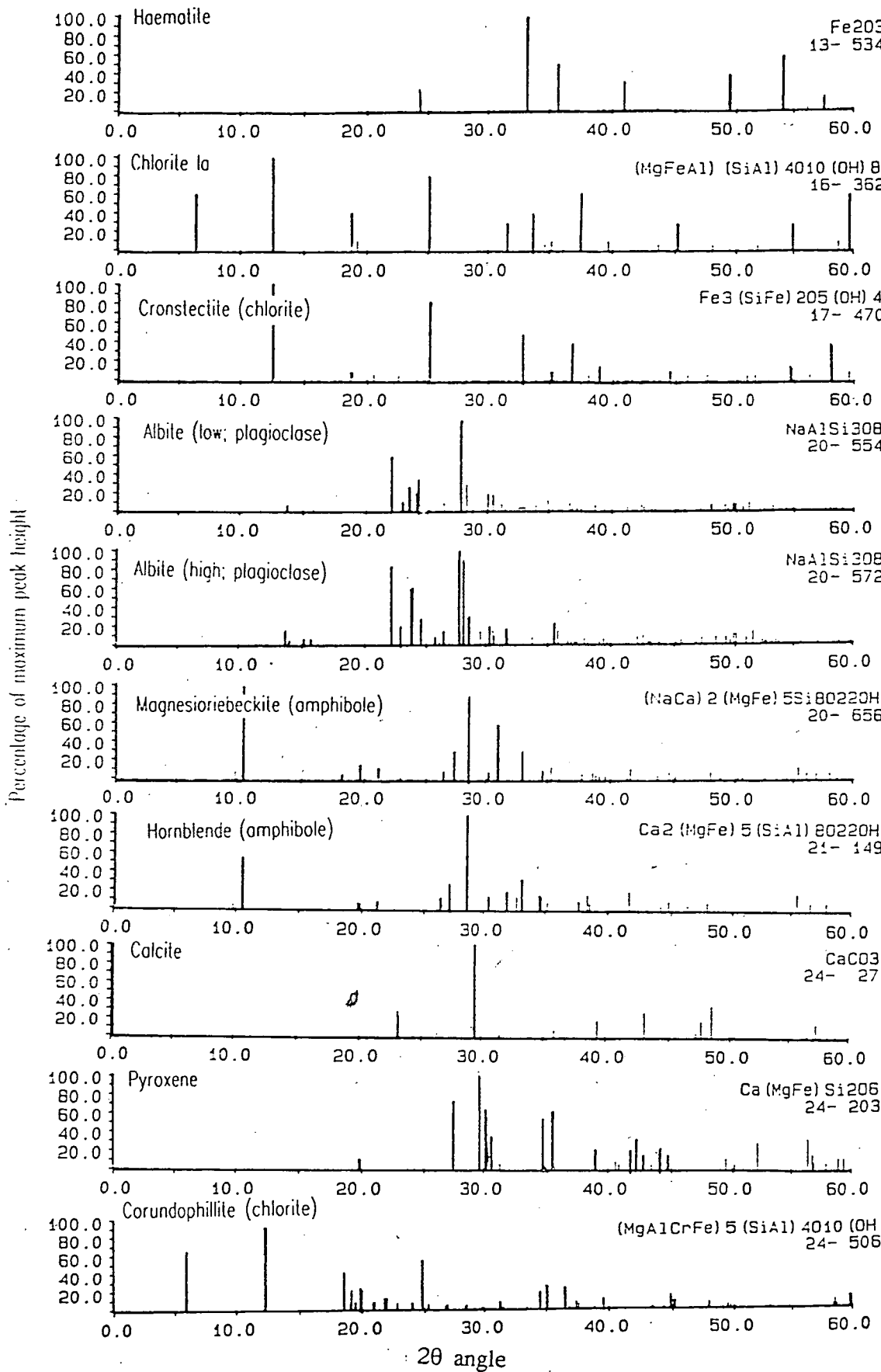


Table E5. X-ray diffraction peak reference plots of the mineral phases present with borehole and other samples analysed during the course of this work.

